Synthesis and Reactivity of New Titanium Hydrazido Complexes

Pei Jen Tiong

Thesis submitted to the University of Oxford for the degree of Doctor of Philosophy, March 2012.

The work described in this Thesis was carried out in the Chemistry Research Laboratory, University of Oxford from October 2008 to March 2012 under the supervision of Professor Philip Mountford. All work is my own unless stated to the contrary, and has not previously been submitted for any degree at this or any other university.

Pei Jen Tiong

March 2012

Abstract

Pei Jen Tiong Hilary 2012

Linacre College D.Phil. Thesis

This Thesis describes the synthesis and characterisation of titanium hydrazido(2-) and alkylidene hydrazido(2-) complexes and their reactivity towards unsaturated molecules. Exploration of the bonding in titanium hydrazido(2-) and alkylidene hydrazido(2-) complexes is performed through structural and computational studies.

Chapter 1 introduces current Group 4 hydrazido chemistry in comparison to Group 4 imido and mid/late metal hydrazido examples. Current Group 4 alkylidene hydrazido chemistry is also described.

Chapter 2 describes the synthesis, bonding and the novel reaction chemistry of titanium hydrazido(2-) half-sandwich complexes. Novel reactivity at the Ti=N_α bond is presented with the mechanisms of some of these transformations probed by Density Functional Theory (DFT) calculations.

Chapter 3 describes the novel reaction chemistry of Cp*Ti{MeC(N^iPr)$_2$}($NNMe_2$) in comparison to its imido and diphenyl hydrazido analogues. Novel reactivity at both Ti=N_α and N_α–N_β bonds is presented with the mechanisms of some of these transformations probed by Density Functional Theory (DFT) calculations.

Chapter 4 describes the synthesis and characterisation of a new titanium alkylidene hydrazido(2-) complex. The bonding of the alkylidene hydrazido(2-) ligand is explored through structural and computational studies. Novel reactivity at Ti=N_α and N_α-N_β bonds is presented.

Chapter 5 presents full experimental procedures and characterising data for the new complexes reported.

CD Appendix contains .cif files for all new crystallographically characterised complexes described.

Contents

	Declaration	i
	Abstract	ii
	Contents	iii
	Acknowledgements	vii
	Abbreviations	viii
	Notes	xiii
Chapter One – Introduction		1
1.1	General Introduction	2
1.2	Group 4 imido chemistry	2
1.3	Metal hydrazido chemistry	7
1.3.1	The hydrazido ligand	7
1.3.2	Bonding in hydrazido complexes	8
1.3.2.1	Hydrazido(2-) *versus* isodiazene	8
1.3.2.2	Bonding in Group 4 hydrazido(2-) complexes compared to imido complexes	11
1.3.3	Metal hydrazido(2-) complexes in the context of nitrogen fixation	12
1.3.4	Group 6 hydrazido chemistry	15
1.3.5	Group 5 hydrazido chemistry	18
1.3.6	Titanium hydrazido chemistry	20
1.3.7	Zirconium and hafnium hydrazido chemistry	31
1.4	Group 4 alkylidene hydrazido chemistry	37
1.5	Summary and objectives	41
1.6	References	42
Chapter Two – Reactions of cyclopentadienyl-amidinate titanium hydrazides with CO_2, CS_2, and isocyanates		51
2.1	Introduction	52
2.2	Improved synthesis and molecular structures of half-sandwich titanium hydrazido complexes	55
2.3	DFT analysis of molecular and electronic structures and imide-hydrazine exchange energies	60

2.4	Reactions of Cp*Ti{MeC(N^iPr)$_2$}(NNR_2) (R = Ph (**2.13**) or Me (**2.15**)) with CO_2 and CS_2	63
2.4.1	Reactions of Cp*Ti{MeC(N^iPr)$_2$}(NNR_2) (R = Ph (**2.13**) or Me (**2.15**)) with CO_2	64
2.4.2	Reactions of Cp*Ti{MeC(N^iPr)$_2$}(NNR_2) (R = Ph (**2.13**) or Me (**2.15**)) with CS_2	69
2.4.3	DFT studies of different reaction pathways	71
2.5	Reactions of Cp*Ti{MeC(N^iPr)$_2$}($NNPh_2$) (**2.13**) with isocyanates, isothiocyanates and CO_2	78
2.6	Reactions of Cp*Ti{MeC(N^iPr)$_2$}($NNMe_2$) (**2.15**) with isocyanates	84
2.7	Reactions of Cp*Ti{MeC(N^iPr)$_2$}($NNMe_2$) (**2.15**) with isothiocyanates	92
2.8	Adduct formation between Cp*Ti{MeC(N^iPr_2)}($NNMe_2$) (**2.15**) and ^{t}BuNC	94
2.9	Thermodynamic considerations	96
2.10	Conclusions	100
2.11	References	101
Chapter Three – Site selectivity and reversibility in the reactions of titanium hydrazides with Si–H, Si–X, C–X and H^+ reagents		106
3.1	Introduction	107
3.2	Reactions with primary silanes and dihydrogen	108
3.3	Reactions of Cp*Ti{MeC(N^iPr)$_2$}($NNMe_2$) (**3.1**) with halosilanes	116
3.3.1	Reactions of Cp*Ti{MeC(N^iPr)$_2$}($NNMe_2$) (**3.1**) with chlorosilanes	116
3.3.2	Reactions of Cp*Ti{MeC(N^iPr)$_2$}($NNMe_2$) (**3.1**) with dichlorosilanes	120
3.3.3	Reaction of Cp*Ti{MeC(N^iPr)$_2$}($NNMe_2$) (**3.1**) with bromosilane	123
3.4	Reactions of Cp*Ti{MeC(N^iPr)$_2$}($NNPh_2$) (**3.2**) with chlorosilanes	124
3.4.1	Reaction of Cp*Ti{MeC(N^iPr)$_2$}($NNPh_2$) (**3.2**) with $PhSiH_2Cl$	125
3.4.2	Reaction of Cp*Ti{MeC(N^iPr)$_2$}($NNPh_2$) (**3.2**) with PhSiH(Me)Cl	125
3.5	Reactions of Cp*Ti{MeC(N^iPr)$_2$}(NTol) (**3.3**) with halosilanes	128
3.6.	DFT study of the mechanism of Si–H and Si–Cl addition	129
3.6.1	Si–H bond addition	131
3.6.2	Si–Cl bond addition	133
3.7	Alkylation and protonation reactions	135
3.7.1	Alkylation reactions	135
3.7.2	Protonation reactions	138

3.8	Conclusions	142
3.9	References	143
Chapter Four – Synthesis and reactivity of Cp*Ti{MeC(N^{i}Pr)$_2$}(NNCPh$_2$) (41)		149
4.1	Introduction	150
4.2	Synthesis and molecular structure of a new titanium alkylidene hydrazido complex	151
4.3	DFT analysis	156
4.4	Reaction of Cp*Ti{MeC(N^{i}Pr)$_2$}(NNCPh$_2$) (**41**) with CO_2	158
4.5	Reaction of Cp*Ti{MeC(N^{i}Pr)$_2$}(NNCPh$_2$) (**41**) with CS_2	164
4.6	Reactions of Cp*Ti{MeC(N^{i}Pr)$_2$}(NNCPh$_2$) (**41**) with isocyanates and isothiocyanates	166
4.6.1	Reaction of Cp*Ti{MeC(N^{i}Pr)$_2$}(NNCPh$_2$) (**41**) with ^{t}BuNCO	166
4.6.2	Reactions of Cp*Ti{MeC(N^{i}Pr)$_2$}(NNCPh$_2$) (**41**) with Ar′NCO (Ar′ = 2,6- C$_6$H$_3$^{i}Pr$_2$)	167
4.6.3	Reaction of Cp*Ti{MeC(N^{i}Pr)$_2$}(NNCPh$_2$) (**41**) with TolNCO	168
4.6.4	Reactions of Cp*Ti{MeC(N^{i}Pr)$_2$}(NNCPh$_2$) (**41**) with isothiocyanates	172
4.6.5	Reaction of Cp*Ti{MeC(N^{i}Pr)$_2$}{N(Tol)C(NNCPh$_2$)S} (**51**) with TolNCO	175
4.7	Adduct formation between Cp*Ti{MeC(N^{i}Pr)$_2$}(NNCPh$_2$) (**41**) and isonitriles	176
4.8	Reactions of Cp*Ti{MeC(N^{i}Pr)$_2$}(NNCPh$_2$) (**41**) with nitriles	179
4.9	Reactions of Cp*Ti{MeC(N^{i}Pr)$_2$}(NNCPh$_2$) (**41**) with alkynes	188
4.10	Reactions of Cp*Ti{MeC(N^{i}Pr)$_2$}(NNCPh$_2$) (**41**) with silanes	191
4.10.1	Reactions of Cp*Ti{MeC(N^{i}Pr)$_2$}(NNCPh$_2$) (**41**) with primary and secondary silanes	191
4.10.2	Reactions of Cp*Ti{MeC(N^{i}Pr)$_2$}(NNCPh$_2$) (**41**) with halosilanes	194
4.11	Conclusions	196
4.12	References	197
Chapter Five – Experimental details and characterising data		202
5.1	General methods and instrumentation	203
5.2	Literature preparations	203
5.3	Experimental details and characterising data for Chapter Two	204

5.4 Experimental details and characterising data for Chapter Three 218
5.5 Experimental details and characterising data for Chapter Four 233
5.6 X-ray data collection and processing parameters for Chapter Two 253
5.7 X-ray data collection and processing parameters for Chapter Three 256
5.8 X-ray data collection and processing parameters for Chapter Four 260
5.9 References 264

CD Appendix

Acknowledgements

Firstly, I would like to express my gratitude to my supervisor Professor Philip Mountford for his endless help, enthusiasm, support and guidance throughout the course of my studies. I thank him for providing me with an interesting and exciting project which has been challenging but ultimately both enjoyable and rewarding.

I would like to thank all members of the Mountford group, both past and present, that I have had the pleasure to work with. Special thanks go to Dr Jonathan Selby for his help and training at the start of my degree, and Dr Andrey Protchenko for his endless help and invaluable advices for the past two years. Thanks in particular to Dr. Andrew Schwarz, Matthew Blake, and Laura Groom for helping to proof read my Chapters and making many useful suggestions. Also, Dr Zengyong Chu, Dr Alex Heath, Dr Michael Cushion, Daniel Schofield, Lawrence Clark, Nigel Yong, Richard Scott, Liban Saleh, Dr Yong Huang, Hannah Morgan, Chee Onn, and Richard Collins for always being available for a chat and just generally as great people to work and socialise with. Laura Groom and Junjuda Unruangsri deserve special mention for being fantastic friends who are always there to share my ups and downs and being supportive at all time.

I am grateful to Daniel Schofield for the collection of X-ray crystallographic data and Professor Philip Mountford and Dr Amber Thompson for the solution of molecular structures. Thanks also go to our collaborators, Dr Ainara Nova and Dr Eric Clot of Université Montpellier, France for DFT calculations. Dr. Nick Rees and Dr Colin Sparrow must be thanked for their help with NMR spectroscopy and mass spectrometry. I would also like to thank all other technical support staff within the Department of Chemistry, and Stephen Boyer at London Metropolitan University and Elemental Microanalysis Ltd for the elemental analyses service.

I would like to take this opportunity to thank Dr Asel Sartbaeva for being such a great college advisor. Her continuous support and advice are highly appreciated.

I would also like to thank all my friends from Oxford for being brilliant over the last three years I've studied here. Finally, and most importantly, I would like to thank my parents, Gaojie, the rest of my family and friends for their continuous support and encouragement. Without you this Thesis would never have been written. Thank you!

Abbreviations

General

Å	Ångstrom
atm	atmosphere(s)
avg.	average
ca.	*circa*, about
calcd.	calculated
cf.	*confer*, compared to
Cp_{cent}	computed cyclopentadienyl ring carbon centroid
CSD	Cambridge Structural Database
°	degrees
℃	degrees Celsius
d	day(s)
fac	facially coordinating
g	grams
h	hour(s)
K	Kelvin
kcal mol^{-1}	kilocalorie(s) per mole
mbar	millibar(s)
min	minute(s)
mL	millilitre(s)
mmol	millimole(s)
rt	room temperature
s	second(s)
vs.	versus

Chemical

acac	acetylacetonate
Ad	adamantyl
$AlNp_3$	trineopentylaluminum
Ar	aryl group
Ar'	2,6- $C_6H_3{}^iPr_2$
Bn_2Cyclam	1,8-dibenzyl-1,4,8,11-tetraazacyclotetradecane
Bu	*n*-butyl
COT	cyclooctatetraene

COT′	η^8-1,4-$C_8H_6(SiMe_3)_2$
Cp	C_5H_5
Cp'	C_5H_4Me
Cp*	C_5Me_5
dap	α-(dimethylaminomethyl)pyrrole)
DEDM	diethyl diazomalonate
DMAP	4-dimethylaminopyridine
dme	1,2-dimethoxyethane
dmpe	$Me_2PCH_2CH_2PMe_2$
dpma	*N*,*N*-di(pyrrolyl-α-methyl)-*N*-methylamine
dppe	$Ph_2PCH_2CH_2PPh_2$
E	generic chalcogen atom
Et	ethyl
H_2enp	N,N'-dimethylethylenediamine-N,N'-bis(2-methylpyrrole)
$H_2N_2N^{C_2,Me}$	$MeN(CH_2CH_2NHSiMe_3)_2$
$H_2N_2N^{C_2,SiMe_3}$	$Me_3SiN(CH_2CH_2NHSiMe_3)_2$
$H_2N_2N^{C_3,Me}$	$MeN(CH_2CH_2CH_2NHSiMe_3)_2$
$H_2N_2N^{py}$	$MeC(2\text{-}C_5H_4N)(CH_2NHSiMe_3)_2$
H_2Me_4taa	tetramethyl dibenzotetraaza[14]annulene
H_2TTP	*meso*-tetra-*p*-tolylporphyrine
HIPT	$3,5\text{-}(2,4,6\text{-}C_6H_2{}^iPr_3)_2C_6H_3$
^{i}Pr	*iso*-propyl
KIE	kinetic isotope effect(s)
L	a supporting ligand (set)
LiHMDS	lithium hexamethyldisilazide
Me	methyl
Me_2Calix	dianion of 1,3-dimethyl ether of *tert*-butyl calix[4]arene
Me_3[6]ane	1,3,5-trimethyltriazacyclohexane
Me_3[9]ane	1,4,7-trimethyltriazacyclononane
Me_2pz	3,5-dimethylpyrazolyl
Mes	$2,4,6\text{-}C_6H_2Me_3$
MOCVD	metal organic chemical vapour deposition
N_2N^R	generic diamidoamine ligand
$N_2{}^{TBS}N^{py}$	$MeC(2\text{-}C_5H_4N)\{CH_2N(Si^tBuMe_2)\}_2$

NS_3	$N(CH_2CH_2S)_3$
$N^{Xyl}N$	2-(3,5-dimethylphenylamino)pyrrolinato
$N_2{}^{Mes}N^{py}$	$MeC(2\text{-}C_5H_4N)\{CH_2N(Mes)\}_2$
$N_2{}^{Xyl}N^{py}$	$MeC(2\text{-}C_5H_4N)\{CH_2N(Xyl)\}_2$
O_2NN^{py}	$(2\text{-}C_5H_4N)CH_2N(CH_2\text{-}2\text{-}O\text{-}3,5\text{-}C_6H_2Me_2)_2$
OTf	$CF_3SO_3^-$
P	generic phosphine ligand
Ph	phenyl
Pr	*n*-propyl
py	pyridine
pz	pyrazolyl
R	generic aryl or alkyl
ROMP	ring opening metathesis polymerisation
^{t}Bu	*tert*-butyl
^{t}Bu-bipy	di-*tert*-butyl bipyridine
THF	tetrahydrofuran
TIP	2-((2-thiolatophenylimino)methylene)phenolate
Tol	$4\text{-}C_6H_4Me$
X	Generic halide
Xyl	$2,6\text{-}C_6H_3Me_2$

Calculations

BDEs	bond dissociation energies
DFT	density functional theory
EHMO	extended Hückel molecular orbital
HOMO	highest occupied molecular orbital
LP	lone pair
LUMO	lowest unoccupied molecular orbital
MO	molecular orbital
NBO	natural bond orbital
TS	transition state(s)

Mass Spectrometry

EI	electron impact
ES	electrospay

FI	field ionisation
HR	high-resolution
m/z	mass to charge ratio
MS	mass spectrometry

Nuclear Magnetic Resonance Spectroscopy

$^{13}C\{^{1}H\}$	proton-decoupled ^{13}C
$^{11}B\{^{1}H\}$	proton-decoupled ^{11}B
app.	apparent
br	broad
COSY	correlation spectrocopy
d	doublet
HMBC	heteronuclear multiple bond correlation
HMQC	heteronuclear single quantum correlation
Hz	Hertz
i	*ipso*
J	coupling constant
m	*meta*
m	multiplet
MHz	Megahertz
NMR	nuclear magnetic resonance
nOe	nuclear Overhauser effect
o	*ortho*
p	*para*
ppm	parts per million
q	quartet
ROESY	rotating-frame nuclear Overhauser Effect spectroscopy
s	singlet
sept	septet
t	triplet
VT	variable temperature
δ	chemical shift in ppm

Infrared Spectroscopy

br	broad

FT-IR	fourier transform infrared red
IR	infrared red
cm^{-1}	wavenumber
m	medium
s	strong
w	weak
ν	frequency

Notes

Literature compounds described in this Thesis are numbered **1.x**, **2.x**, **3.x**, **4.x** according to the Chapter in which they first occur. The new compounds described in this Thesis are numbered **1** – **xx** or as **#**$^{+}$ if the cation alone is being referred to. Model systems used in calculations are denoted by **#Q**. Density functional theory (DFT) calculated compounds are given letters for hypothetical/non-experimentally observed species.

X-ray crystallography (for compounds **3**, **9**, **11**, **15**, **16**, and **2.16**) was performed by Daniel Schofield, and the molecular structures were solved by Professor Phillip Mountford.

DFT calculations were performed in collaboration with Dr Ainara Nova and Dr Eric Clot of Université Montpellier, France.

Chapter One

Introduction

1.1 General Introduction

The chemistry of Group 4 imido complexes (L)M=NR (L = a supporting ligand (set), R = alkyl or aryl) has been extensively studied for more than 20 years.[1-9] In addition to the fundamental studies on their bonding and reactivity, their possible practical applications have also been intensively investigated. Examples include their potential use as catalysts in hydroamination of C–C multiple bonds and olefin polymerisation. In contrast, the chemistry of the related Group 4 terminal hydrazido(2-) complexes (L)M=NNR_2 (R = alkyl or aryl) received little attention until relatively recently.[10-12] Although initial reactivity reports of Group 4 hydrazides appeared some time ago,[13, 14] there has recently been a surge in activity and output in this area,[11, 12, 15-28] with a number of new reactions of the M=NNR_2 functional group having been discovered.

This Thesis describes the synthesis of titanium hydrazido(2-) complexes. The bonding is explored through the use of computational and crystallographic studies and compared with their imido analogues. Their reactivity studies towards small molecules have been investigated, with novel transformations described. The synthesis of new terminal titanium alkylidene hydrazido(2-) complex is also described, and the bonding is explored through the use of computational and crystallographic studies. Reactivity towards small molecules has been carried out and novel transformations are discussed. Parts of this work have been published.[29-32] This Chapter introduces the chemistry of Group 4 hydrazido(2-) and alkylidene hydrazido(2-) complexes, starting with a description of Group 4 imido chemistry, followed by an introduction of the hydrazido ligand. The bonding of hydrazido complexes, including comparison of the bonding of Group 4 hydrazido(2-) complexes with both later metal isodiazene and imido examples is discussed. The relevance of hydrazido complexes towards nitrogen fixation is described, followed by a discussion of later metal hydrazido(2-) chemistry. The examples of Group 4 hydrazido(2-) complexes and the limited number of Group 4 alkylidene hydrazido(2-) complexes are reviewed.

1.2 Group 4 imido chemistry

Although transition metal imido complexes were first reported in the late 1950s,[33, 34] the first Group 4 examples were only reported in 1980s.[35] Early transition metal imido complexes have been intensively studied ever since.[36] The imido ligand can either

function as a spectator ligand or as an active site leading to a wide range of reactivity.[3, 5, 33, 36-40] For example, imido complexes have been shown to be excellent catalysts for hydroamination,[1, 41] carbodiimide metathesis,[1] ROMP (ring opening metathesis polymerisation),[42, 43] Ziegler-Natta catalysis[44-46] and MOCVD (metal organic chemical vapour deposition).[5, 47, 48]

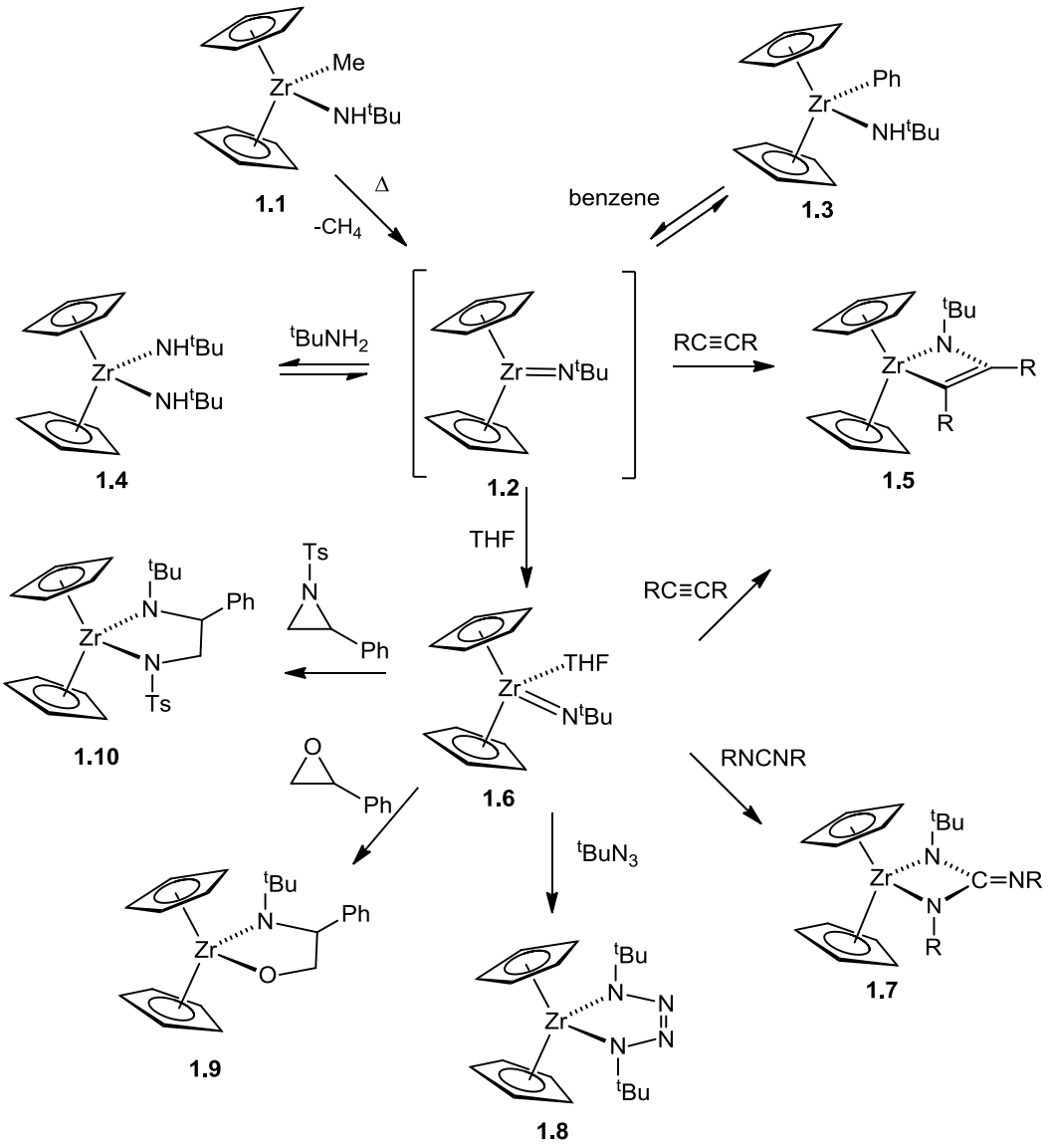

Scheme 1.1. Synthesis and reactivity of the transient $Cp_2Zr(N^tBu)$ (**1.2**) and the THF adduct $Cp_2Zr(N^tBu)(THF)$ (**1.6**).

The first examples of Group 4 imido complexes were reported by Bergman *et al.* in 1988, for the family of complexes, $Cp_2Zr(NR)$ (R = 4-$C_6H_4{}^tBu$, Xyl (Xyl = 2,6-$C_6H_3Me_2$) or ^tBu (**1.2**)).[35] These transient complexes were obtained *via* thermolysis of the corresponding amido compounds $Cp_2Zr(NHR)(R')$ (R′ = alkyl). Interestingly,

thermolysis of the *tert*-butyl amido complex $Cp_2Zr(NH^tBu)(Me)$ (**1.1**) in benzene resulted in solvent activation to give the phenyl amido zirconocene complex $Cp_2Zr(NH^tBu)(Ph)$ (**1.3**) (Scheme 1.1). However, when the aryl amido complex $Cp_2Zr(NHAr)(Me)$ (Ar = 4-$C_6H_4{}^tBu$) was used, spontaneous dimerisation occurred to give the bis(μ-imido) dimer $[Cp_2Zr(\mu\text{-}NAr)]_2$ (**1.11**). An isolable monomeric imido compound $Cp_2Zr(N^tBu)(THF)$ (**1.6**) was successfully obtained through thermolysis in THF. This complex displayed extensive reaction chemistry with various substrates and some of them are shown in Scheme 1.1.[35, 49-53] Complex **1.6** undergoes [2+2] or [2+3] cycloaddition reactions at the Zr=N bond, forming 4- or 5- membered metallacyclic products. Mechanistic studies were carried out to understand the reaction mechanisms and to provide new synthetic strategies to C–N containing organic products.[50, 51, 53]

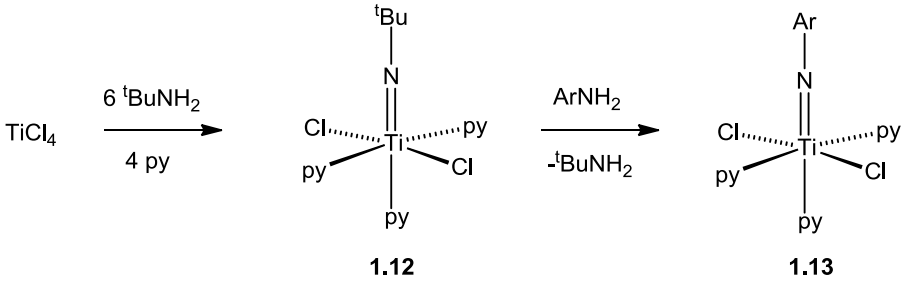

1.12 **1.13**

Scheme 1.2. Synthesis of new titanium imido synthons.

It was not until 1990 that the first examples of terminal titanium imido complexes were reported, by Rothwell *et al.* and Roesky *et al.*.[6, 7] Mountford *et al.* later on reported the synthesis of titanium imido synthons $Ti(NR)Cl_2(py)_3$ (R = akyl (**1.12**) or aryl (**1.13**)) (Scheme 1.2) which served as convenient entry points into a large number of titanium imido compounds with various ancillary ligands (Scheme 1.3) through ligand exchange or/ and salt metathesis reactions.[1, 14, 36, 40, 54-62]

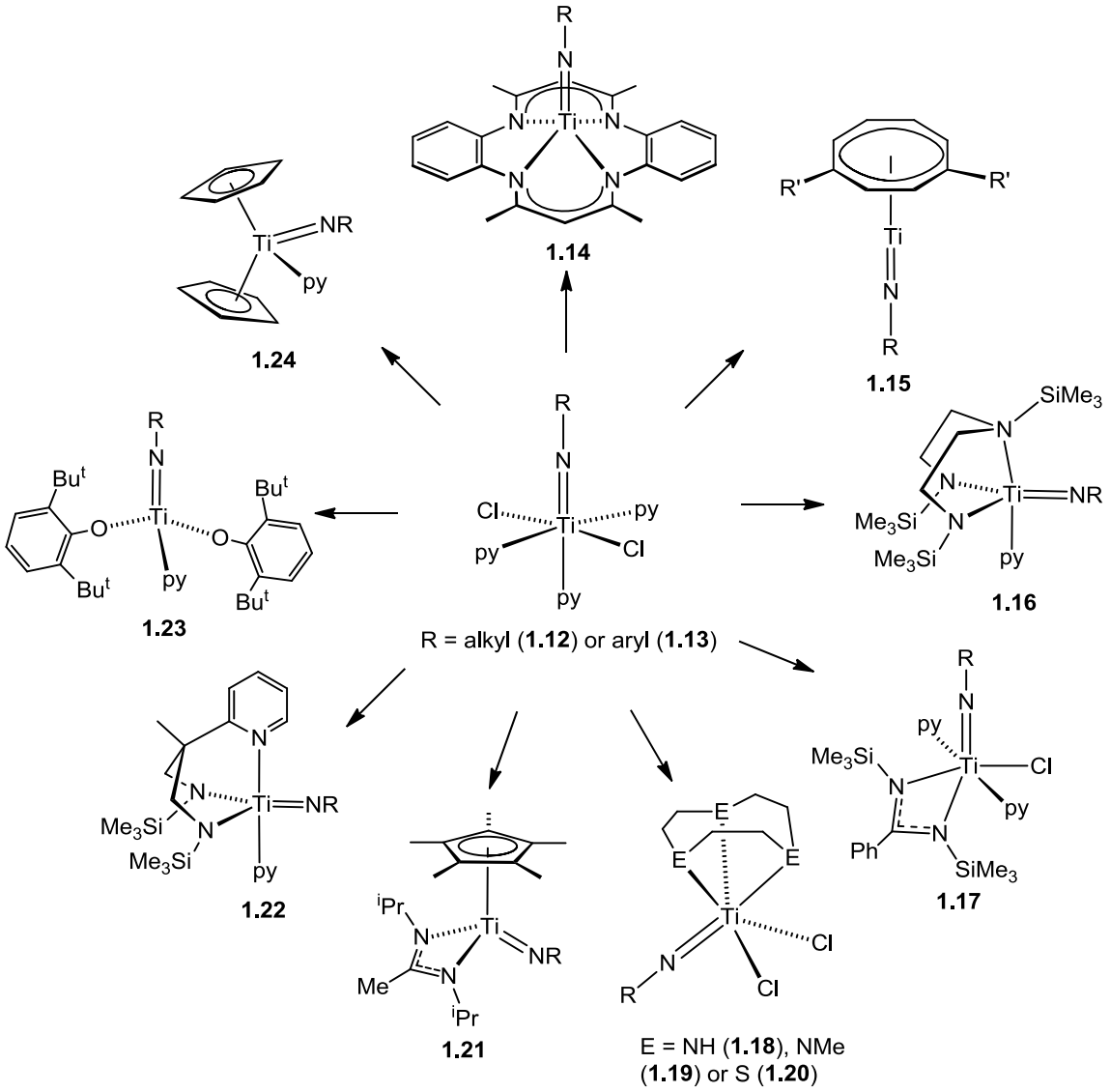

Scheme 1.3. Synthesis of various titanium imido complexes.

The imido complexes obtained demonstrated a wide range of reactivity with various substrates. Both Ti(NR)(Me_4taa) (**1.14**; H_2Me_4taa = tetramethyl dibenzotetraaza[14]-annulene)[14] and Ti(NR)(η^8-COT) (**1.15**; COT = cyclooctatetraene)[62, 63] underwent [2+2] cycloaddition reactions with aryl isocyanates to give four-membered metallacyclic products. Complex **1.15** also reacted with alkyl or aryl isonitriles to yield the corresponding isonitrile adducts.[63] The diamide-amine supported imido complex Ti($N_2N^{C_2,SiMe_3}$)(^{t}NBu)(py) (**1.16**; $N_2N^{C_2,SiMe_3}$ = ($SiMe_3$)N(CH_2CH_2N-$SiMe_3$)$_2$)[58] formed a [2+2] cycloadduct with ^{t}BuCP, and complex **1.17**[56] underwent further metathesis with LiCp* to give Cp*Ti{PhC($NSiMe_3$)$_2$}(N^tBu) (**1.25**). Complexes of the type **1.18** – **1.20** were reported to be highly active precatalysts for ethylene polymerisation.[5, 64] Complexes **1.21** Cp*Ti{MeC(N^iPr)$_2$}(NR) (R = ^{t}Bu or

2,6-$C_6H_3Me_2$) displayed different reactivity depending upon the imido N substituent. Although both underwent initial [2+2] cycloaddition with CO_2, the alkyl derivative underwent further retrocyclization to give ^tBuNCO and an oxo-bridged dimer, whereas the aryl derivative underwent a second CO_2 insertion to give a dicarboxylate species.[1, 65] The tridentate diamide-donor supported imido complex $Ti(N_2N^{py})(N^tBu)(py)$ (**1.22**; $H_2N_2N^{py}$ = $MeC(2\text{-}C_5H_4N)(CH_2NHSiMe_3)_2$) displayed a rich reaction chemistry towards a number of reagents,[1, 40, 66-72] some examples are given in Scheme 1.4.

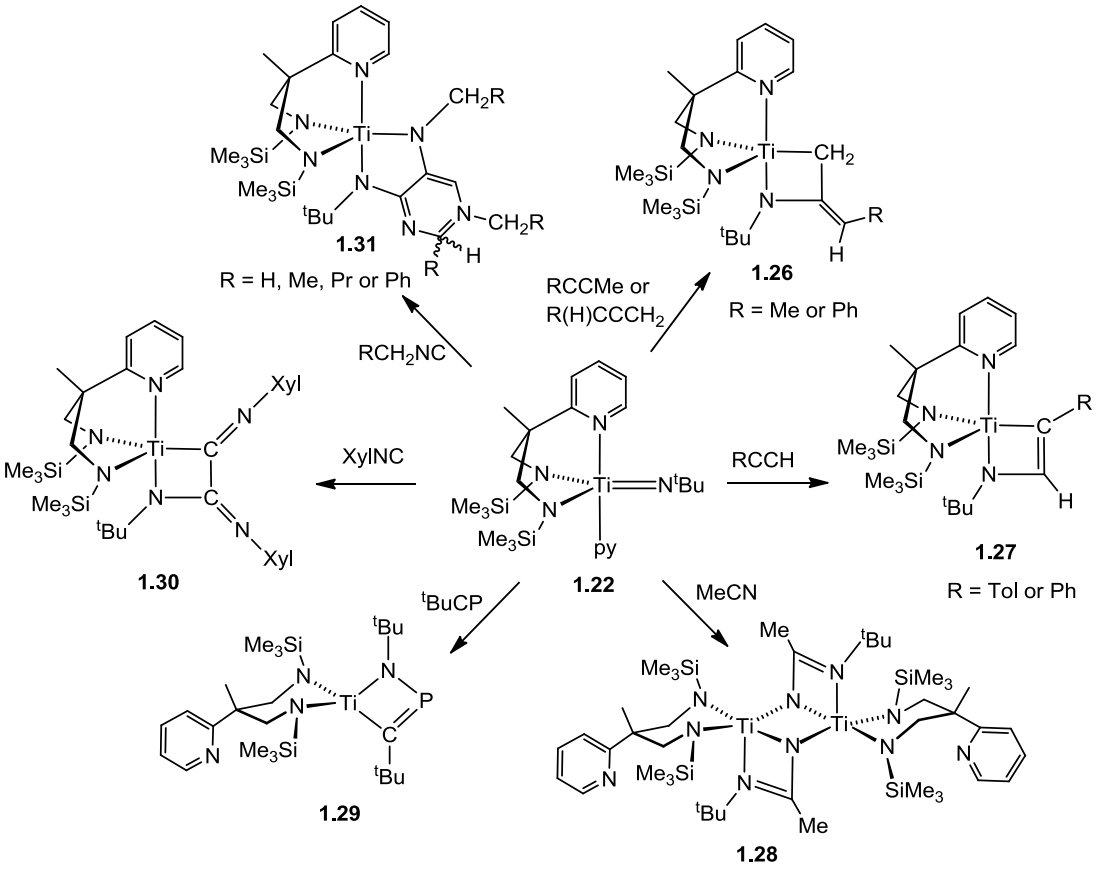

Scheme 1.4. Reactivity of $Ti(N_2N^{py})(N^tBu)(py)$ (**1.22**)

Reaction of **1.22** with internal alkynes (RCCMe, R = Me or Ph) generated titanaazetidines **1.26.** It was proposed that the reaction proceeded *via* initial addition of a C-H bond of the methyl group across the Ti=NR bond followed by H atom transfer, which led to the formation of a π-bonded allene ligand, the final [2+2] cycloaddition gave the titanazetidine products. Interestingly, reaction with selected allenes ($R(H)C=C=CH_2$) (R = H or Ph) also formed titanaazetidines **1.26**. Reaction with terminal alkynes resulted in [2+2] cycloaddition reactions. When phenyl

acetylene was used in the presence of excess *tert*-butylamine, hydroamination occurred regenerating **1.22** whilst forming *trans*-cinnamyl(*tert*-butyl)amine. However, the reaction was limited to a few catalytic cycles due to degradation of the titanium complex. Reaction with acetonitrile resulted in the formation of a dimeric species **1.28**, with a doubly deprotonated *tert*-butylacetamidinate ligand and a κ^2-bound N_2N^{py}. The reaction is thought to proceed through an initial [2+2] cycloaddition followed by a spontaneous dimerisation. Reaction with ^{t}BuCP also led to a doubly deprotonated *tert*-butylacetamidinate ligand and a κ^2-bound N_2N^{py}, but no dimerisation occurs after initial cycloaddition giving a monomeric species **1.29**. In this instance, the cycloaddition occurred in an opposite sense to that seen for **1.28** with an N–P bond favoured over an N–C bond. On reaction with XylNC coupling of two molecules of isonitrile with Ti=N^{t}Bu occurred to form the titanacycle **1.30**. With three equivalents of alkyl isonitriles RCH_2NC (R = H, Me, Pr or Ph) bearing a C-H bond adjacent to the NC group however, complex **1.22** underwent highly selective coupling with the Ti=N^{t}Bu bond, forming complexes of the type **1.31**. Interestingly, reaction of **1.22** with ArNCO (Ar = 2,6-$C_6H_3(^i Pr)_2$) gave complex Ti(N^{t}Bu)(py){MeC(2-C_6H_4N)(CH_2NSiMe_3)(CH_2NC{N(SiMe$_3$)Ar}O} (**1.32**) with attack on the amido ligand while the imido ligand remained intact.

1.3 Metal hydrazido chemistry

1.3.1 The hydrazido ligand

Hydrazido ligands may bind to transition metal centres through several coordination modes.[12, 33] One of the defining features is the formal charge on the hydrazido fragment. Depending on the presence and identity of the substituents at N_α, the formal charge can be −1 or −2. The hapticity with respect to the metal centre can be η^1- or η^2- depending on whether it binds to the metal centre through one or both nitrogen atoms of the ligand. Finally, the ligand can be terminal, bound to one metal, or bridging between to two metal centres, denoted by μ_2.[12] Several potential bonding modes observed for the hydrazido ligand are illustrated in Figure 1.1. From this point onwards, hydrazido(2-) mentioned in this Thesis refers to η^1-hydrazido(2-) of the general type (L)Ti=NNR_2 (where R = alkyl, aryl or mixed alkyl/aryl), and where other bonding modes are reported they are clearly labelled. The nitrogen atoms are described as M=N_α-$N_\beta R_2$ in all cases.

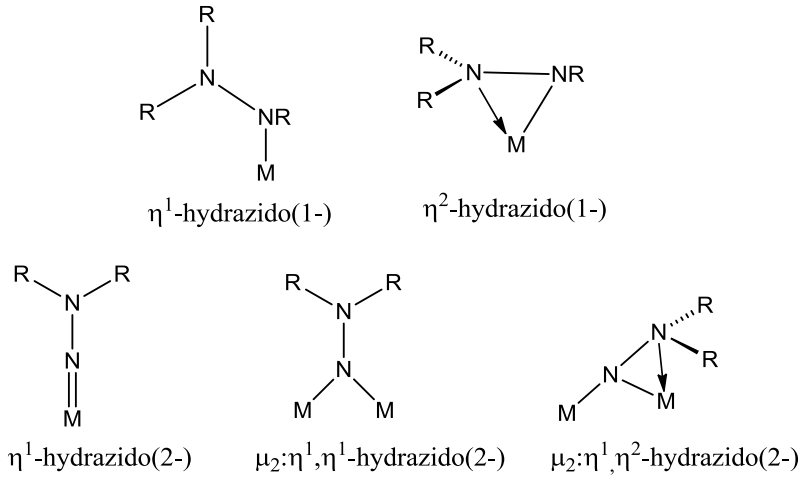

Figure 1.1. A selection of the bonding modes of the hydrazido ligand.

1.3.2 Bonding in hydrazido complexes

1.3.2.1 Hydrazido(2-) *versus* isodiazene

The terminal hydrazido(2-) ligand (NNR_2^{2-}) is an isolobal analogue of the terminal imido ligand (NR^{2-}), in which bonding to the metal centre usually occurs through one σ-bond and two π-bonds. However, the presence of a second nitrogen atom, N_β, alters the structural and electronic properties in the hydrazido analogue.

Due to the potential lone pair donation from N_β, the terminal hydrazido(2-) moiety has two possible resonance forms, namely dianionic hydrazido(2-) and neutral isodiazene (Figure 1.2).[12] In the more reduced hydrazido(2-) form, the N_α–N_β π* molecular orbital is occupied, resulting in a N_α–N_β single bond. However, in the less reduced neutral isodiazene form, the N_α–N_β π* molecular orbital is significantly less occupied and a N_α=N_β double bond is observed. Apart from the difference in N_α-N_β bond distances, the extent of the orbital occupancy can also be reflected in the geometry at N_β. For instance, an isodiazene with a N_α=N_β double bond character will have an sp^2 hybridised N_β atom and a corresponding planar geometry. However, for the hydrazido(2-) canonical, the N_β will be sp^3 hybridised and thus having a pyramidal geometry.[73]

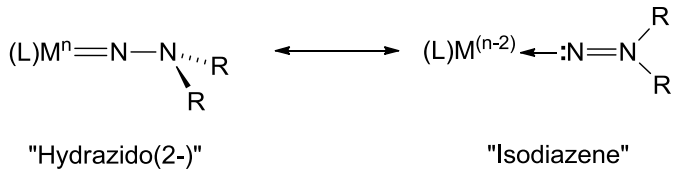

Figure 1.2. The hydrazido(2-) *versus* the neutral isodiazene resonance forms.

A comparison between the structural data for Group 4 – 6 hydrazido complexes is shown in Table 1.1. It can be seen that the average N_α–N_β bond length of Group 6 hydrazido complexes is shorter than that of Group 4, indicative of a greater degree of multiple bonding character and hence a larger contribution from the isodiazene resonance form. This is consistent with the observed geometry at N_β, which is exclusively planar (sp^2 hybridised) for Group 6 complexes, while for Group 4 and 5 complexes, both planar and pyramidal geometries at N_β are observed.[74]

Table 1.1. Comparative structural data for Group 4 – 6 hydrazido complexes.[74]

	N_α–N_β range (Å)	**N_α–N_β avg. (Å)**	**Geometry at N_β**
Group 4	1.344(2) − 1.398(3)	1.380	planar (aryl), pyramidal (alkyl)
Group 5	1.292(3) – 1.338(2)	1.313	planar or pyramidal
Group 6	1.280(6) − 1.375(29)	1.317	planar

The investigation of the bonding in Group 6 and other late metal M=NNR_2 complexes by Carrillo *et al.* using the Extended Hückel Molecular Orbital (EHMO) and *ab initio* calculations[73] suggested that the isodiazene canonical form provided a better bonding match with the metal centre of mid-later metals, and that the 'hydrazido' ligand is best described as (L)M←:N=NR_2. This is consistent with the shorter N_α=N_β bond distance and planar N_β observed in the experimental data. This 'isodiazene' formulation is also supported by the reports of Tuczek *et al.* who studied the mechanism of the Chatt cycle using Density Functional Theory (DFT) calculations.[75, 76]

For Group 4 hydrazido complexes, the experimental data suggest a more reduced hydrazido fragment 'NNR_2^{2-}' with a longer N_α–N_β bond. In principle, N_β should be sp^3 hybridised. However, this is only seen for alkyl substituted hydrazido complexes, whilst planar N_β is seen for aryl substituted hydrazido complexes. It has been suggested that the planar geometry is a result of conjugation of the N_β lone pair with the aryl substituents.[12, 22] Although no computational data has been reported, Group 5

hydrazido complexes seem to have intermediate behaviour between Group 4 and later metal hydrazido complexes, with both planar and pyramidal geometries being observed at N_β. The nature of the hydrazido ligand also affects the $M{=}N_\alpha$ bond distances. For example, a dative bond with longer M←:N bond distance is observed for Group 6 isodiazene complexes while a shorter unsaturated $M{=}N_\alpha$ bond is observed for early metal hydrazido(2-) complexes.

Bonding analyses on the NNR_2 group carried out by Saillard *et al*. and Mountford *et al*. suggested that the behaviour of a hydrazido ligand is comparable to that of a carbene.[11, 25, 77] Fischer carbenes and Schrock alkylidenes (Figure 1.3) are the two extremes with distinctively different interactions between a metal centre and a carbene unit. The level of reduction of the carbene which in turn affects the reactivity of the carbene is dependent on the oxidation state of the metal centre, as well as the identity of the supporting ligand and carbene substituents. Fischer carbenes are normally found for mid-late transition metals with low oxidation states, π-acceptor ligands and heteroatom carbene substituents. The bonding of a carbene to a metal centre is mainly based on σ-electron donation of a filled methylene lone pair orbital to an empty metal d-orbital, with π-back donation from the metal to the empty 2p orbital on the carbon. The reactivity of a Fischer carbene is characterised by nucleophilic attack at the carbon atom or electrophilic attack at the metal centre. Schrock alkylidenes, on the other hand, are often found for early transition metals with higher oxidation states. The Schrock alkylidenes normally contain H or alkyl group substituents, and is considered as a dianionic 4 electron donor ligand.[78] The reactivity of a Schrock alkylidene is characterised by electrophilic attack at the carbon atom and nucleophilic attack at the electron deficient metal centre. Schrock alkylidenes with highly polarised M=CR bond are generally more reactive than Fischer carbenes.

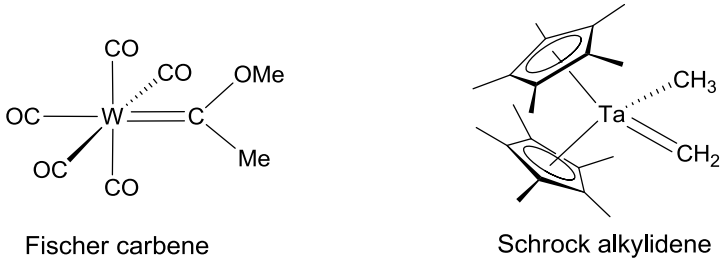

Figure 1.3. Examples of a Fischer carbene and Schrock alkylidene.[79-82]

Direct comparison between hydrazide and carbene suggests that the neutral isodiazene is equivalent to a Fischer carbene, while the hydrazido(2-) is comparable to a Schrock alkylidene. The limited reactivity reported for Group 6 hydrazido complexes can thus be explained by the isodiazene formalism, with transformation only observed at N_β, and not the dative $M{=}N_\alpha$. Typical reactions reported for late metal hydrazido complexes involve N_β protonation or insertion/condensation reactions of $N_\beta{-}H$.[83, 84] The greater multiple bonding nature of $N_\alpha{=}N_\beta$ causes cleavage of the $N_\alpha{-}N_\beta$ bond to be difficult, and is only possible under highly forcing conditions with the presence of external reductants. In contrast, rich reactivity has been reported for the Group 4 $(L)M{=}NNR_2$ complexes, which include reactivity at the unsaturated $Ti{=}N_\alpha$, insertion into the $N_\alpha{-}N_\beta$ bond, and cleavage of the single $N_\alpha{-}N_\beta$ bond (Section 1.3.6).

1.3.2.2 Bonding in Group 4 hydrazido(2-) complexes compared to imido complexes

DFT calculations on the frontier MOs of the model systems of terminal hydrazido complexes performed by Mountford *et al.*[11, 25], Gade *et al.*[20] and Odom *et al.*[16] show the isolobal relationship between hydrazido(2-) and the corresponding imido analogue. The bonding occurs through one σ and two π interactions, forming a $\sigma^2\pi^4$ M≡N formally triple bond. However, the presence of an additional lone pair electrons on N_β of the hydrazido ligand which participates in metal-hydrazide interactions has a substantial effect on the $M{=}N_\alpha$ π-bonding. The presence of an unfavourable $N_\alpha{-}N_\beta$ π* interaction destabilises the $M{=}N_\alpha$ π-bond and raises the energy of one of the $M{=}N_\alpha$ π-bonds relative to the other (Figure 1.4).[11, 21]

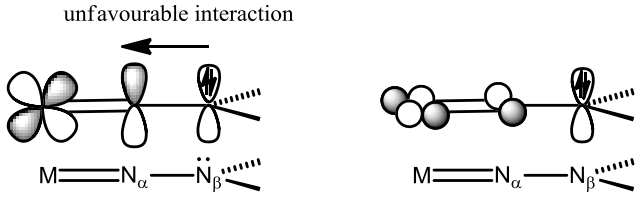

Figure 1.4. Destabilisation of the $Ti{=}N_\alpha$ π bond by N_β lone pair donation.

Figure 1.5 shows the three frontier MOs of the DFT calculated model system $Ti\{HC(pz)_3\}(NNPh_2)Cl_2$ (**1.33Q**)[11] reported by Mountford *et al.*. The $NNPh_2$ ligand binds to the metal centre through one σ and two π interactions, acting as a four electron donor.

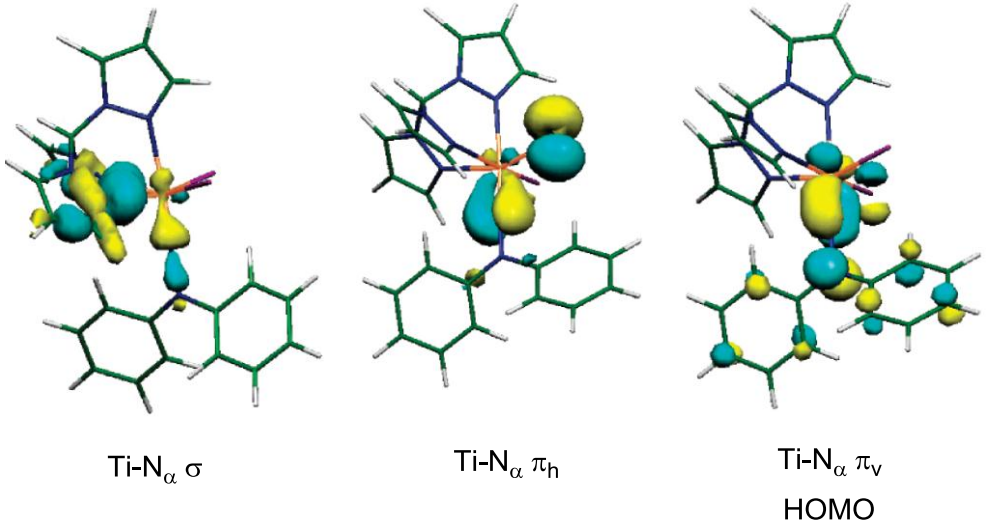

Figure 1.5. Frontier MOs of the model system Ti{HC(pz)$_3$}(NNPh$_2$)Cl$_2$ (**1.33Q**).[11]

The analysis performed for both hydrazido and imido systems shows that the main difference between their orbital interaction diagrams relates to the relative energies of the two Ti=NR π-bonding orbitals. For the alkyl imido model system Ti{HC(pz)$_3$}(NMe)Cl$_2$ (**1.34Q**), both π interactions are degenerate (unfavourable π* interactions with the phenyl ring of the aryl imido model system Ti{HC(pz)$_3$}(NPh)Cl$_2$ (**1.35Q**) causes one of the π orbitals to be slightly destabilised). However, for **1.33Q** the N$_\beta$ π* lone pair destabilises the Ti-N$_\alpha$ π$_v$ bond (HOMO) by 1.38 eV relative to Ti-N$_\alpha$ π$_h$ (Figure 1.5). This destabilisation resulted in lengthening of the Ti=N distance in Ti=NNR$_2$ compared to that in Ti=NR bond. For example, the Ti=N distance in Ti{HC(Me$_2$pz)$_3$}(N^{t}Bu)Cl$_2$ (**1.36**, 1.703(2) Å; Me$_2$pz = 3,5-dimethylpyrazolyl) is shorter than that in Ti{HC(Me$_2$pz)$_3$}(NNPh$_2$)Cl$_2$ (**1.33**, 1.718(2) Å). Likewise, the Ti=N distance in Ti(Me$_2$Calix)(N^{t}Bu) (**1.37**, 1.706(2) Å; Me$_2$Calix = dianion of 1,3-dimethyl ether of *tert*-butyl calix[4]arene) is shorter than that for the hydrazido(2-) complexes Ti(Me$_2$Calix)(NNR^{1}R^2) (R^1 = Ph, R^2 = Ph (**1.38**) or Me (**1.39**); R^1 = R^2 = Me (**1.40**), 1.717(2) – 1.729(4) Å).[11] It is suggested that this destabilisation may affect the reaction chemistry of the Ti=NNR$_2$ functional group, giving rise to interesting reactivity at both the M=N$_\alpha$ and N$_\alpha$–N$_\beta$ bonds.[1, 20]

1.3.3 Metal hydrazido(2-) complexes in the context of nitrogen fixation

Initial investigation of the hydrazido functional group was driven by the study of nitrogen fixation. Nitrogen containing compounds are widely used as precursors in the synthesis of fertilisers, explosives and many physiologically important compounds.

However, due to the inherent stability of dinitrogen, the current synthetic methods for functionalisation of dinitrogen (Figure 1.6) require high temperatures and pressures and are energy intensive whilst the range of products which can be directly synthesised is very limited.[84-87] In contrast, enzymatic processes in biological systems enable the fixation of nitrogen (N_2) under ambient conditions. Thus, extensive studies have been carried out to understand the mechanism involved in the conversion of N_2 to ammonia by nitrogenase, and the search for new catalytic processes for the fixation and functionalisation of dinitrogen has become a topic of on-going interest.[83, 84, 86]

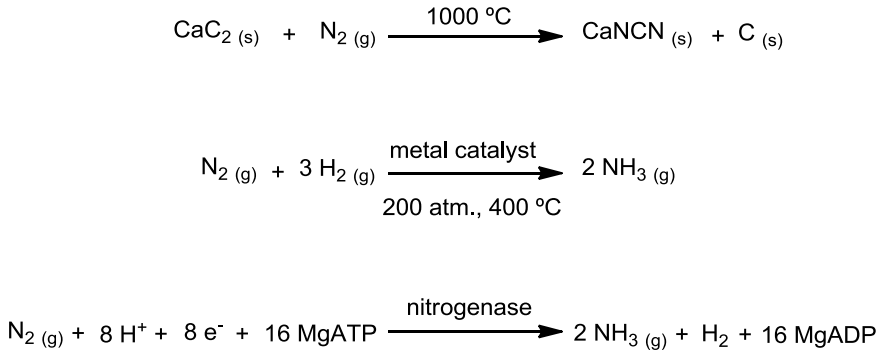

Figure 1.6. Nitrogen fixation through the Frank-Caro cyanamide process (top), Haber-Bosch process (middle) and nitrogenase enzymatic process (bottom).

The most common nitrogenase enzyme contains an iron-molybdenum-sulfur cluster (FeMo-cofactor)[88, 89] at its active site and is the most studied, although nitrogenases with iron-vanadium (FeV)[90, 91] or Fe-only (Fe)[92, 93] cores are also known. Although the X-ray crystal structure of the FeMo nitrogenase enzyme from *Azotobacter vinelandii* was determined in 1992 (Figure 1.7),[94] the binding site or mechanism involved in dinitrogen reduction remain inconclusive.[95]

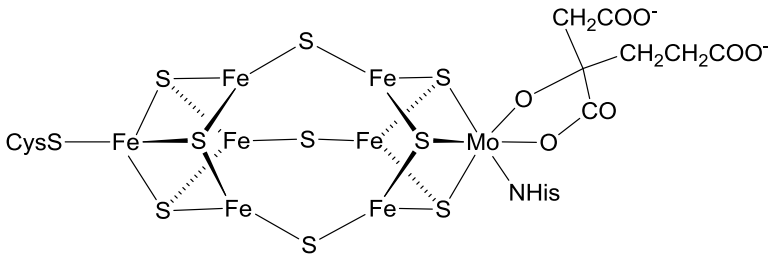

Figure 1.7. FeMo cofactor of FeMo nitrogenase.

Although various models have been developed to propose N_2 coordination at molybdenum or iron centres, one of the most successful models is based on a

monometallic dinitrogen complex of a Group 6 metal with ancillary phosphine ligands $(P)_4M(N_2)L$ (M = Mo or W, P = phosphine ligand, L = a monodentate ligand including N_2) developed by Chatt.[96, 97] It is clear from the Chatt cycle that terminal imide and hydrazide are among the multiple intermediates (Figure 1.8). However, it is to be noted that while most of the intermediates were isolated, catalytic reduction of dinitrogen to ammonia was not achieved.

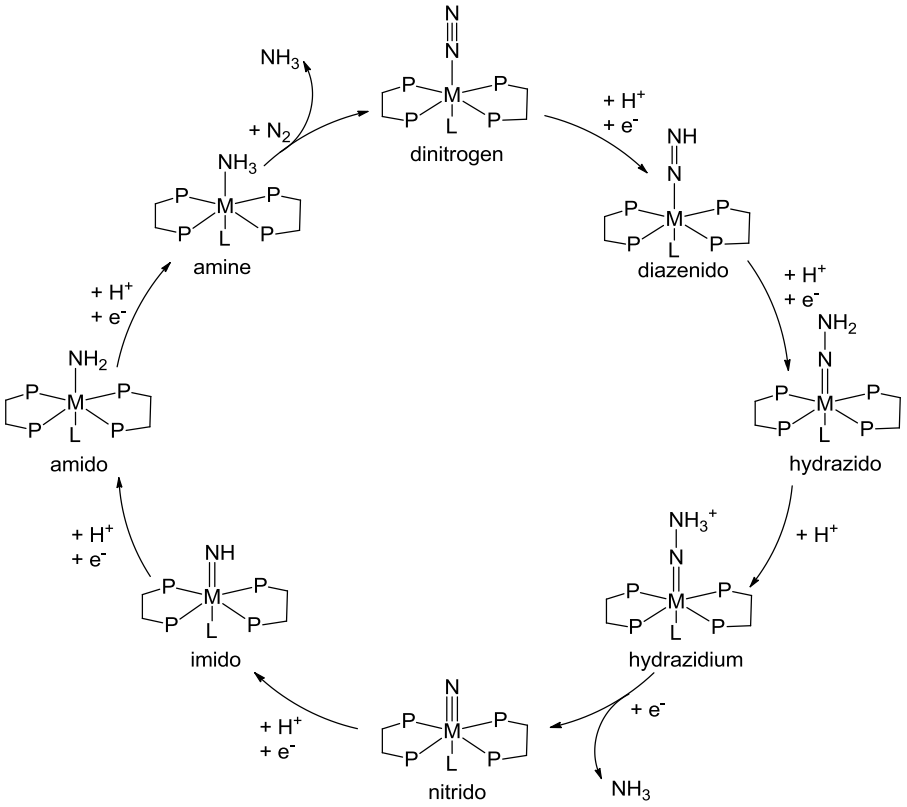

Figure 1.8. The Chatt cycle (M = Mo or W).

The first fully catalytic reduction from dinitrogen to ammonia was reported by Schrock and co-workers employing Mo(HIPTN$_3$N) (**1.41**; HIPT = 3,5-(2,4,6-$C_6H_2{}^iPr_3)_2C_6H_3$) (Figure 1.9).[98-101] The presence of bulky amido substituents suppress the formation of the inert nitrogen bridged dimeric Mo–N=N–Mo species.[98, 99] It was proposed that the mechanism proceeds through a "Chatt-like" cycle. Eight of the proposed intermediates were isolated and characterised. It is apparent that a hydrazido species is also one of the proposed intermediates in the catalytic cycle. The metal-bound N_α of M=N−NH_2 is calculated to be bent, suggesting a possibility of an η^2-coordinated NNH_2 unit.[102]

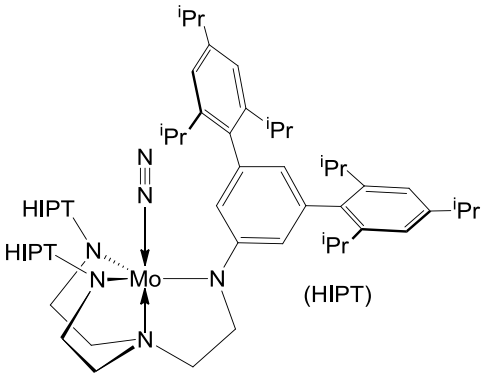

Figure 1.9. Molybdenum complex used for catalytic transformation of N_2 to ammonia.

As various nitrogenous intermediates are involved in the cycles, researchers started to explore the use of these intermediates for reactions which include N atom transfer and N-C bond formation.[83] Among the intermediates involved, imido complexes have been extensively studied on a range of metal centres over the last few decades.[1, 2, 40] The chemistry of the isolobal terminal hydrazido complexes, however, is significantly less well developed, with early work involved mostly Group 6 complexes.[103, 104]

1.3.4 Group 6 hydrazido chemistry

Due to the involvement of hydrazido complexes as intermediates in the Chatt cycle, most of the early work on terminal hydrazido complexes focused on the later metals. One of the early works by Hidai *et al*. featured the synthesis and reactivity of phosphine supported Group 6 hydrazido(2-) complexes $M(NNH_2)F(dppe)_2$ (M = Mo (**1.42**) or W (**1.43**); dppe = $Ph_2PCH_2CH_2PPh_2$).[97, 105-107] Condensation occurred with aldehydes and ketones leading to the formation of alkylidene hydrazides (**1.44**, **1.45**), while reaction with acyl chlorides underwent substitution at N_β through HCl elimination (**1.46**) (Scheme 1.5).

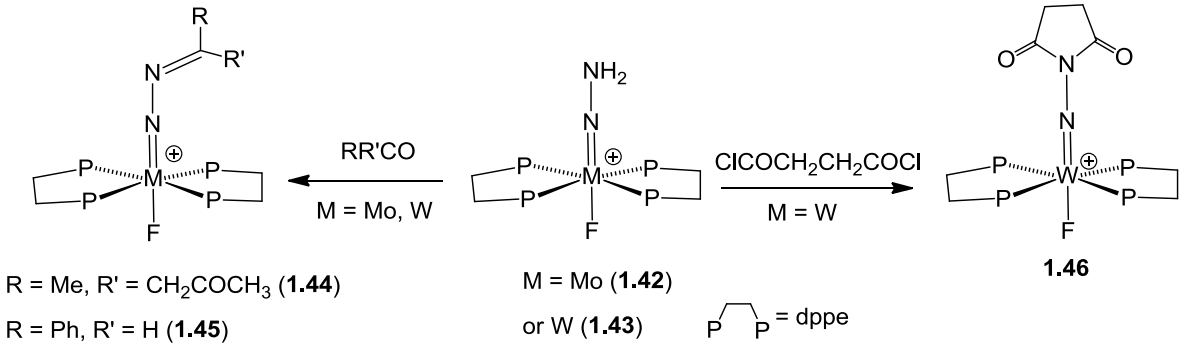

Scheme 1.5. Reactivity of $M(NNH_2)F(dppe)_2$ (M = Mo **1.42** or W **1.43**).

At about the same period of time, McCleverty and co-workers reported the terminal hydrazido(1-) complexes Mo{HB(Me_2pz)$_3$}(NO)I(NHNRR')} (**1.47**) (Figure 1.10).[108, 109] Protonolysis of the hydrazido(1-) ligand upon addition of acid resulted in the elimination of free hydrazine without N_α-N_β bond cleavage. This contrasts with the findings previously reported by Chatt *et al*. on $WX_2(NNH_2)(PMe_2Ph)_2$ (**1.48**; X = halide) in which case protonation resulted in N_α-N_β bond cleavage.[96, 110]

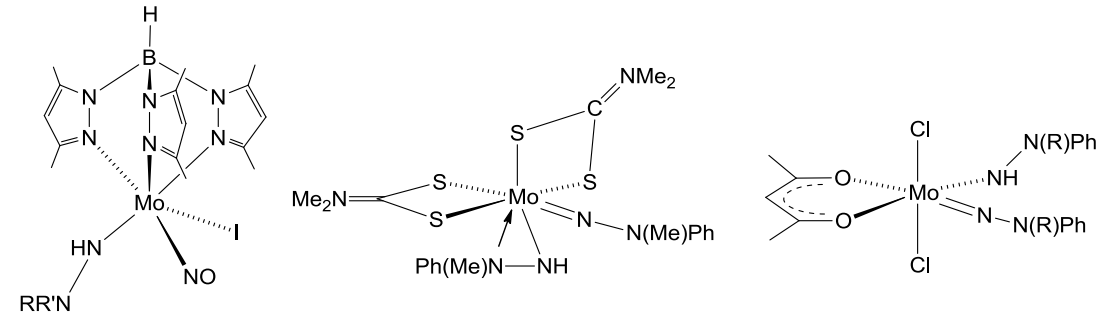

R = Me, R' = Me or Ph (**1.47**) **1.49** R = Me (**1.50**) or Ph (**1.51**)

Figure 1.10. Examples of later metal hydrazido complexes.

Dilworth *et al*. reported an unusual mixed η^2-hydrazido(1-)/η^1-hydrazido(2-) complex of molybdenum (**1.49**) which allowed direct comparison between a terminal hydrazido(2-) and a bent hydrazido(1-) ligand (Figure 1.10).[111] Significant multiple bond character was seen for the terminally bound hydrazido(2-) 1igand, with a short Mo=N_α distance (l.752(1) Å) and almost linear Mo=N–N bond angle of 169.6(7)°. The short N–N distance of 1.285(14) Å suggests significant delocalisation within the Mo=NNR_2 bond. As for the bent hydrazido(1-) ligand, longer Mo=N_α distance of 2.069(8) Å was observed, together with the N–N distance of 1.388(12) Å which is typical for a single bond.

Another example of a mixed η^1-hydrazido(1-)/η^1-hydrazido(2-) complex was reported for Mo(acac){NN(R)Ph}{N(H)N(R)Ph}Cl_2 (R = Me (**1.50**) or Ph (**1.51**); acac = acetylacetonate) (Figure 1.10).[112] In this case however, both hydrazido ligands are coordinated in the 'end-on' fashion, due to steric constraints. Nevertheless, they can be easily distinguished. The hydrazido(2-) ligands display almost linear Mo=N–N bond angles of 173.8(2)° and 171.9(4) respectively, and significant delocalisation is apparent with short Mo=N_α (1.750(2) and 1.752(4) respectively) and N–N distances. The hydrazido(1-) ligands however, are seen with longer Mo=N_α (1.948(5) and 1.948(2) Å respectively) and N–N (1.359(6) and 1.339(3) Å respectively) bond. These

were found to react with tertiary phosphine to generate bis(hydrazido(2-)) phosphine complex.[113]

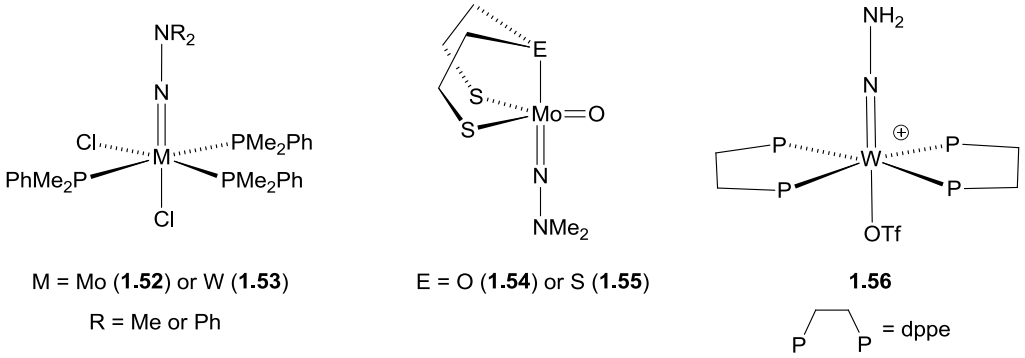

Figure 1.11. Further examples of Group 6 hydrazido compounds.

Some other examples of Group 6 hydrazido(2-) complexes are shown in Figure 1.11. In 1996, Niemoth-Anderson and co-workers reported the syntheses of complexes $M(NNR_2)Cl_2(PMe_2Ph)_3$ (M = Mo (**1.52**) or W (**1.53**); R = Me or Ph). The solid state structure of **1.53** shows short $W{=}N_\alpha$ and $N_\alpha{-}N_\beta$ distances which indicate a high degree of delocalisation and significant multiple bond character, consistent with hydrazido(2-) complexes of tungsten. Reactions with acid in the presence of a labile ligand (PR_3) led to protonation and cleavage of the $N_\alpha{-}N_\beta$ bond, producing ammonia and the corresponding amine.[114] In another report by Janas *et al*., addition of acid to complexes $Mo(NNMe_2)O\{E(CH_2CH_2S)_2\}$ (E = O (**1.54**) or S (**1.55**)) did not protonate the hydrazido(2-) ligands. Instead, attack on the metal centre was observed.[115] The results showing that hydrazido(2-) ligand can be stabilised by ancillary ligands with electron poor sulfur atoms whereas electron rich phosphorus donor ligands promote protonation and $N_\alpha{-}N_\beta$ bond cleavage suggest that the reactivity of the metal hydrazido(2-) bond is dependent on the nature of the ancillary ligands.

Field *et al*. reported the synthesis of complex $[W(NNH_2)(OTf)(dppe)_2][OTf]$ (**1.56**; dppe = $Ph_2PCH_2CH_2PPh_2$; OTf = $CF_3SO_3^-$) which was obtained from the reaction of $W(N_2)_2(dppe)_2$ with trifluoromethanesulfonic acid. The triflate ligand in **1.56** can be easily displaced by acetonitrile to yield $[W(NNH_2)(NCMe)(dppe)_2]^{2+}$ which can then be deprotonated by a variety of bases to give the dinitrogen-acetonitrile complex $W(N_2)(NCMe)(dppe)_2$.[116]

In 2000, Redshaw and Elsegood reported the synthesis and structures of calixarene supported hydrazido(2-) complexes of W and Mo. The W=N distance (1.7523(19) Å)

and N_α–N_β distance (1.333(3) Å), together with the near linear W–N–N angle (170.43(17)°) reported for complex W(NCMe)($NNPh_2$)L (**1.57**; L = *tert*-butylcalix[4]arene) are consistent with a hydrazido(2-) ligand. Interestingly, the molybdenum complex was obtained as an air stable dimer [Mo($NNPh_2$)(L)]$_2$ (**1.58**; L = *tert*-butylcalix[4]arene) with no metal-bound solvent ligand.[117]

1.3.5 Group 5 hydrazido chemistry

The fact that nitrogenases with Fe-V cores are known[91] encouraged the extension of hydrazido chemistry to Group 5 metals,[118] although fewer examples exist compared to that of Group 6. The first Group 5 hydrazido complex $Cp_2V\{NN(SiMe_3)_2\}$ (**1.59**) (Figure 1.12) was reported by Wiberg and coworkers in 1976.[119] The three coordinate complex **1.59** was obtained by reacting Cp_2V with 1,2-bis(trimethylsilyl)diazene, where a silyl-transfer reaction was proposed. In the same year, Veith reported the molecular structure of this complex. The short V–N_α distance of 1.666(6) Å confirmed the presence of a metal-nitrogen multiple bond, and the N_α–N_β distance (1.369(9) Å) is long, showing less double bond character of the N–N linkage.[120]

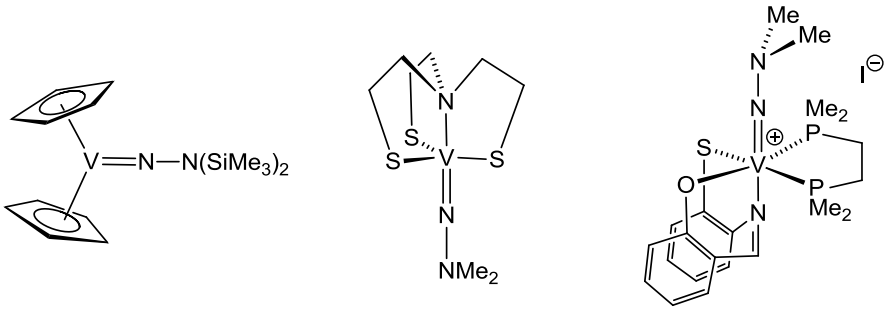

1.59 **1.60** **1.63**

Figure 1.12. Vanadium hydrazido(2-) complexes.

In 1997, Davies *et al*. reported the first vanadium hydrazido complex with sulfur-donor co-ligands V(NS_3)$NNMe_2$ (**1.60**; NS_3 = $N(CH_2CH_2S)_3$) (Figure 1.12), obtained *via* the reaction of V(NS_3)O with $Me_3SiNHNMe_2$. The structural characterisation of this complex showed a V–N_α distance of 1.681(3) Å. The N_α–N_β distance (1.305(5) Å) is shorter than that seen by Veith for complex **1.59**.[121] They later extended the chemistry to form a family of alkyl or aryl substituted vanadium(V) hydrazido(2-) complexes using the same method.[122, 123] These complexes could not be protonated by anhydrous HBr or reduced by Zn/HO-2,6-$C_6H_3{}^iPr_2$.[122]

An example with alkoxide co-ligands $V(NNMe_2)(OAr)_3$ (**1.61**; Ar = 2,6-$C_6H_3{}^iPr_2$) was reported by Sobota *et al*. through the treatment of the dianion $[(VCl_3)_2(\mu\text{-}NNMe_2)_3]^{2-}$ with LiOAr. The solid state structure of **1.61** showed a V–N_α distance of 1.653(3) Å, N_α–N_β distance of 1.311(4) Å and a near linear V=N–N bond angle of 175.8(3) ° comparable to **1.60**. Reaction of **1.61** with H_3NS_3 formed the known complex $V(NS_3)(NNMe_2)$ (**1.60**).[122, 124] In a more recent report, Banerjee and Odom reacted **1.61** with H_2TIP (TIP = 2-((2-thiolatophenylimino)methylene)phenolate) through ligand metathesis to form $V(TIP)(NNMe_2)(OAr)$ (**1.62**). The aryloxide can be easily displaced by Me_3SiI to form $V(NNMe_2)(TIP)(I)$ which reacted with dmpe (dmpe = $Me_2PCH_2CH_2PMe_2$) to give $[V(TIP)(NNMe_2)(dpme)]I$ (**1.63**) (Figure 1.12). The solid state structure of **1.63** shows a V=N_α distance of 1.698(2) Å and N_α–N_β distance of 1.293(3) Å. The V=N_α distance is slightly longer while the N_α–N_β distance is considerably shorter than seen for (**1.60**).[118]

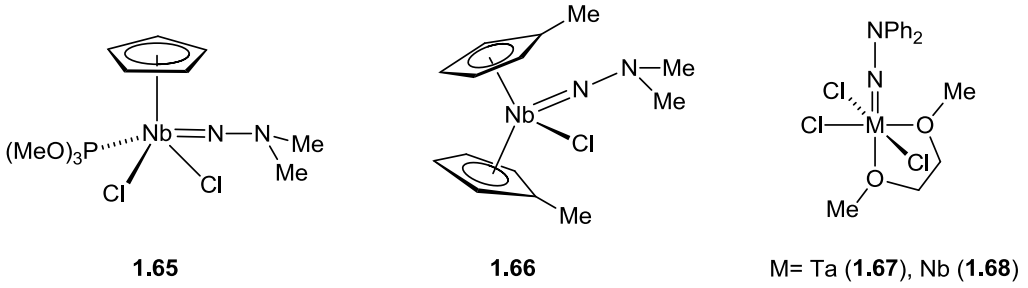

1.65 **1.66** M= Ta (**1.67**), Nb (**1.68**)

Figure 1.13. Niobium and tantalum hydrazido(2-) complexes.

Green and co-workers extended the work to niobium by employing cyclopentadienyl supported system. Reaction between $CpNbCl_4$ and dimethylhydrazine in the presence of triethylamine gave an unusual bridged dimer $Cp_2Nb_2Cl_4(\mu{:}\eta^1,\eta^2\text{-}NNMe_2)(\eta^1\text{-}NNMe_2)$ (**1.64**). However, **1.64** reacted with trimethyl phosphite to give an isolable monomeric adduct (**1.65**) (Figure 1.13). The solid state structure of **1.65** shows that it had a reasonably long Nb=N_α (1.789(2) Å) distance, a short N_α–N_β (1.338(2) Å) distance and a pyramidal N_β.[125] They also reported the synthesis of various hydrazido(2-) complexes of niobocene including $Cp'_2Nb(NNMe_2)Cl$ (**1.66**) (Figure 1.13) which was obtained *via* the treatment of $Cp'NbCl_2(NNMe_2)$ with LiCp' (Cp' = C_5H_4Me). The molecular structure of **1.66** shows that the Nb=N_α and N_α–N_β distances (1.794(2) and 1.340(3) Å respectively) are comparable to those for **1.65**, the N_β is also sp^3 hybridised.[126]

Very recently Bercaw and Tonks reported the synthesis of a tantalum hydrazido synthon $TaCl_3(NNPh_2)(dme)$ (**1.67**; dme = 1,2-dimethoxyethane) (Figure 1.13) which served as an entry point to a series of new tantalum hydrazido complexes upon reactions with a variety of neutral, mono- and dianionic ligands. Complex **1.67** was synthesised *via* a Lewis-acid assisted dehydrohalogenation reaction between MCl_5 and diphenylhydrazine. The solid state structure of **1.67** shows a Ta–N_α distance of 1.773(1) Å, N_α–N_β distance of 1.347(1) Å and Ta–N_α–N_β bond angle of 173.65(8) °. The short Ta–N_α distance which indicates a multiple bond character and the near linear Ta–N_α–N_β bond angle support the hydrazido(2-) resonance form as the major contributor in **1.67**. The same method was used to synthesise the niobium hydrazido complex $NbCl_3(NNPh_2)(dme)$ (**1.68**) (Figure 1.13). [127]

1.3.6 Titanium hydrazido chemistry

Group 4 hydrazido chemistry is not directly relevant to biological nitrogen fixation, and thus the field has remained underdeveloped compared to the later metals until relatively recently. Group 4 hydrazido chemistry became a point of interest as previous studies on the isolobal imido ligand suggested the possibility of a rich reaction chemistry.

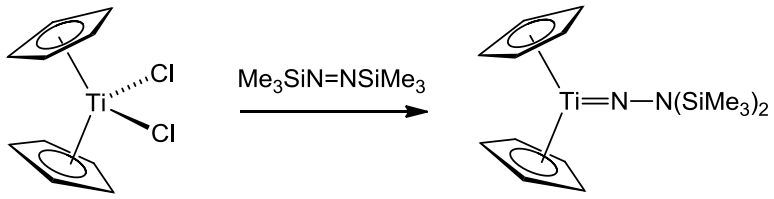

1.69

Equation 1.1

The first terminal titanium hydrazido(2-) complex was reported by Wiberg and co-workers in 1978.[128] They proposed the synthesis of a three-coordinate titanocene complex $Cp_2Ti\{NN(SiMe_3)_2\}$ (**1.69**) through a silyl-transfer reaction between Cp_2TiCl_2 and two equivalents of 1,2-bis(trimethylsilyl)diazene ($Me_3SiN{=}NSiMe_3$) (Equation 1.1). An η^1-bonding mode was assigned by analogy to the structurally characterised complex $Cp_2V\{NN(SiMe_3)_2\}$ (**1.59**).[120] However, insufficient characterising data prevented the confirmation of the monomeric, terminal nature of the hydrazido(2-) ligand in **1.69**. The challenging synthesis and thermally sensitive

nature of $Me_3SiN{=}NSiMe_3$ which decomposes to 1,1,2,2-tetra(trimethylsilyl)-hydrazine above -35 ℃ precluded further structural confirmation of this species.[129]

It was not until 1999 that Mountford and co-workers reported the first fully characterised terminal titanium hydrazido(2-) complex $Ti(NNPh_2)(Me_4taa)$ (**1.70**; H_2Me_4taa = tetramethyl dibenzotetraaza[14]annulene) (Equation 1.2). Complex **1.70** was obtained *via* ligand exchange between the corresponding imido complex $Ti(N^tBu)(Me_4taa)$ and diphenylhydrazine. This was reported as the first example of exchange between an imido ligand with free hydrazine to yield hydrazido complexes. Both reactions of **1.70** with TolNCO and CO_2 resulted in [2+2] cycloaddition yielding products with four-membered metallacycles.[14]

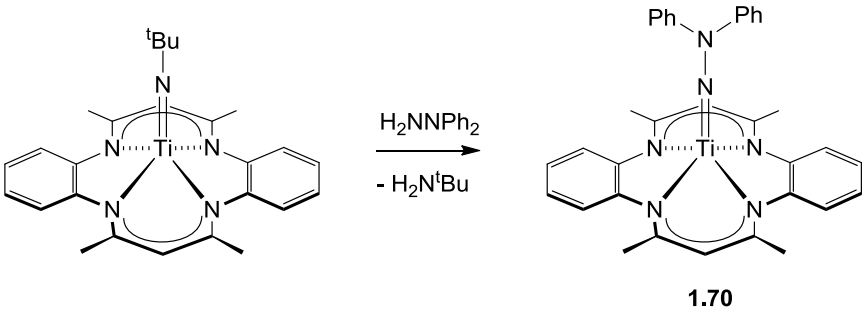

1.70

Equation 1.2

Subsequently, Woo and Thorman synthesised two macrocycle supported titanium hydrazido(2-) complexes of the type $Ti(NNR_2)(TTP)$ (R = Me (**1.71**) or Ph (**1.72**); TTP = *meso*-tetra-*p*-tolylporphyrinato dianion). These were prepared by treating $Ti(TTP)Cl_2$ with 1,1-disubstituted hydrazines in the presence of a base. Both complexes underwent protonolysis with phenol or water, forming either the diphenoxide or the oxo complexes, and free hydrazine. Reaction with 4-chlorobenzaldehyde formed the oxo species Ti(TTP)O and the corresponding hydrazone.[130]

Following the success with imido synthons of the type $Ti(NR)(NHMe_2)_2Cl_2$ (R = alkyl or aryl),[1] Mountford *et al*. synthesised $Ti(NNPh_2)(NHMe_2)_2Cl_2$ (**1.73**) *via* a protonolysis reaction between $Ti(NMe_2)_2Cl_2$ and H_2NNPh_2. This could be converted to $[Ti(NNPh_2)Cl_2(py)_2]_2$ (**1.74**) upon heating in neat pyridine for 16 hours. Both complexes worked as useful synthons for terminal titanium hydrazido(2-) chemistry. Reactions of **1.73** with a selection of neutral tridentate ligands (1,4,7-trimethyl triazacyclononane (Me_3[9]ane), 1,3,5-trimethyl triazacyclohexane (Me_3[6]ane),

tris(3,5-dimethylpyrazolyl)methane ($HC(3,5\text{-}Me_2pz)_3$) and tris(4-^{n}butylpyrazolyl)methane ($HC(4\text{-}^nBupz)_3$)) yielded *fac*-N_3 donor ligand supported titanium η^1-hydrazido(2-) complexes. One of the examples (**1.33**) is shown in Figure 1.14. DFT calculations were carried out using the molecular structure of **1.33** as the basis for investigating the nature of the titanium hydrazido(2-) bond.[11] These are described in Section 1.3.2.2.

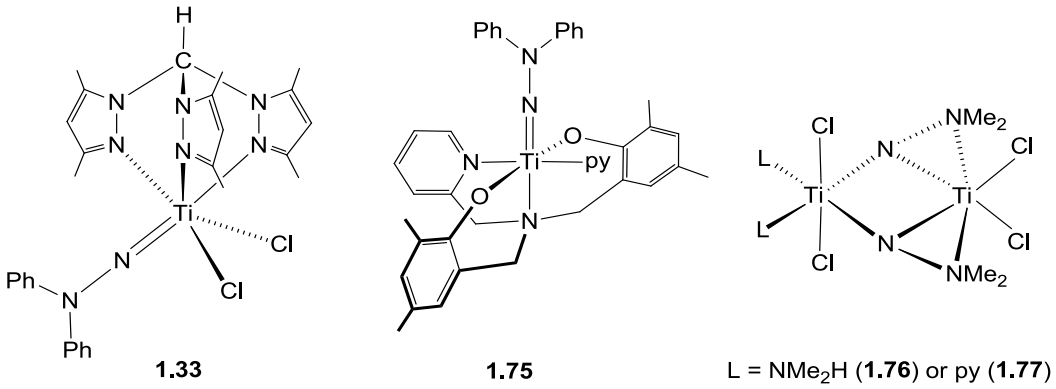

Figure 1.14. Examples of titanium hydrazido(2-) complexes.

The efforts to synthesise hydrazido complexes supported by anionic ligands using **1.73** were unsuccessful due to undesired side-reactions caused by the somewhat acidic N-H groups of the $NHMe_2$ ligands. However, these could be achieved using **1.74** which reacted with various alkali metal dianionic N_4-, O_4- and O_2N_2- donor ligands to give the desired terminal hydrazido(2-) complexes. An example $Ti(O_2NN^{py})(NNPh_2)(py)$ (**1.75**; O_2NN^{py} = $(2\text{-}C_5H_4N)CH_2N(CH_2\text{-}2\text{-}O\text{-}3,5\text{-}C_6H_2Me_2)_2$) is shown in Figure 1.14.[21, 25] The attempts to synthesise dimethyl analogues of **1.73** and **1.74** were unsuccessful due to dimerisation which yielded bridged hydrazido(2-) complexes of the type $[Ti(\mu{:}\eta^2,\eta^1\text{-}NNMe_2)Cl_2(L)_2]_2$ (L = $NHMe_2$ (**1.76**) or py (**1.77**)) (Figure 1.14). Both were found to be unreactive towards further salt metathesis or protonolysis reactions, implying that the $\mu{:}\eta^2,\eta^1$-hydrazido(2-) bridges are not readily cleaved.[11]

Mountford *et al*. later reported the syntheses of new sandwich and half-sandwich titanium hydrazido complexes *via* the *tert*-butyl imido/hydrazine exchange reaction. It was reported that although the reaction of $Cp^*Ti(N^tBu)Cl(py)$ (**1.78**) with Ph_2NNH_2 gave the desired hydrazido(2-) complex $Cp^*Ti(NNPh_2)Cl(py)$ (**1.79**), the corresponding reaction of $CpTi(N^tBu)Cl(py)$ gave the dimer $Cp_2Ti_2(\mu\text{-}\eta^1{:}\eta^1\text{-}$

$NNPh_2)(\mu\text{-}\eta^2\text{:}\eta^1\text{-}NNPh_2)Cl_2$ (**1.80**) (Figure 1.15). The reaction between **1.78** and Me_2NNH_2 also gave the analogous dimer $Cp^*_2Ti_2(\mu\text{-}\eta^1\text{:}\eta^1\text{-}NNMe_2)(\mu\text{-}\eta^2\text{:}\eta^1\text{-}NNMe_2)Cl_2$ (**1.81**) suggesting that suitable supporting ligands and hydrazido substituents are essential in order to supress the formation of a dimer. They also reported the synthesis of the titanocene derivative $Cp_2Ti(NNPh_2)(py)$ (**1.82**) through the reaction of $Cp_2Ti(N^tBu)(py)$ with Ph_2NNH_2.[21, 26] Complex **1.82** was found to undergo [2+2] cycloaddition with ^{t}BuCP (**1.83**), the first reported reactivity of any metal hydrazides with phosphaalkynes (Equation 1.3).[23]

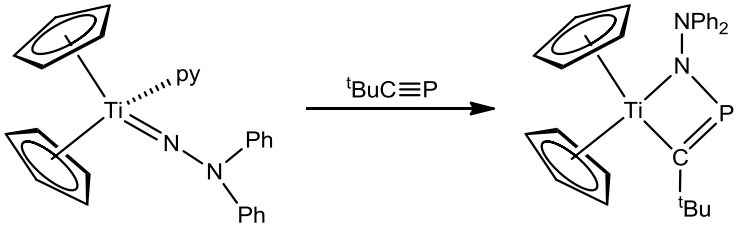

1.82 **1.83**

Equation 1.3

The formation of dimeric hydrazido(2-) complexes with N_β coordination to a metal centre was first reported by Leigh *et al*. in 1983.[131] Complexes with cyclopentadienyl titanium systems of the form $CpTi(\eta^2\text{-}NR'NR_2)Cl_2$ (**1.84**) (Figure 1.15) were synthesised *via* the reaction of $CpTiCl_3$ with lithiated or silylated hydrazines $MNR'NR_2$ (M = Li or $SiMe_3$, R' = H or alkyl and R = H, alkyl or aryl).[131-133] When R' = H, deprotonation occurred with overall loss of HCl yielding the bridging hydrazido(2-) complexes $Cp_2Ti_2(\mu\text{-}NNR_2)_2Cl_2$ (**1.85**)[131, 134] analogous to **1.80**. The solid state structure showed a mixed $[\mu\text{-}\eta^1\eta^1][\mu\text{-}\eta^2\eta^1]$ hydrazido ligands which explained the complicated solution NMR spectrum.[134]

Another example exhibiting the donor properties of N_β was reported by Park *et al*. The *ansa*-cyclopentadienyl hydrazido(1-) complex (**1.86**) (Figure 1.15) was synthesised *via* the reaction of $Ti(NMe_2)_4$ with $(C_5Me_4H)SiMe_2NHNMe_2$. The hydrazido ligand could be tuned between η^1- and η^2-coordination modes by substituting the π-donating amido ligands with electron withdrawing chlorides or alkyl groups. It was suggested that N_β donation was suppressed by an electron rich metal centre.[135, 136]

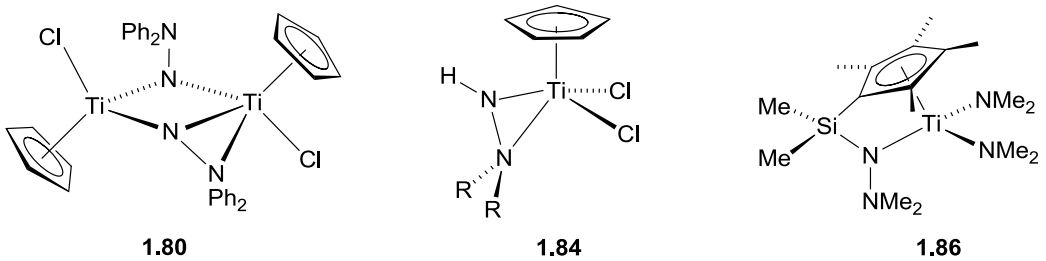

1.80 **1.84** **1.86**

Figure 1.15. Examples of titanium hydrazido complexes

In 2004, Odom and co-workers studied the hydrohydrazination reaction between alkyl hydrazines and substituted alkynes using the proven hydroamination precatalyst Ti(dpma)$(NMe_2)_2$ (**1.87**; dpma = *N*,*N*-di(pyrrolyl-α-methyl)-*N*-methylamine) but found it to be catalytically inactive. They then found out that the reaction of the dimethylamide-precatalyst with an excess of 1,1-dimethylhydrazine yielded a mixture of the bis(hydrazido(1-)) complex Ti(dpma)$(\eta^2\text{-}NHNMe_2)_2$ (**1.88**) and the μ-hydrazido(2-) dimer Ti_2(dpma)$(\mu{:}\eta^2{;}\eta^1\text{-}NNMe_2)$, (**1.89**) with elimination of $HNMe_2$. When only a slight excess (1.2 equiv.) of dimethyl hydrazine was added, pure **1.89** was obtained.[4, 12] In order for catalytic hydroamination to be successful, the titanium catalyst has to access terminal multiple bond species. Presumably the hydrohydrazination reaction follows a similar pathway and thus it is necessary for the amide precursors to form an η^1-hydrazido(2-) species. The efforts to convert dimeric **1.89** to a monomeric η^1-hydrazido(2-) species were, however, unsuccessful. Nevertheless, in the presence of a dative ligand trap (^{t}Bu-bipy), the reaction of Ti(dpma)$(NMe_2)_2$ with dimethyl hydrazine yielded the monomeric Ti(dpma)$(NNMe_2)$(^{t}Bu-bipy) (**1.90**). Complex **1.90** reacted with MeI to form the hydrazidium salt (**1.91**) (Equation 1.4), the first of such example reported for Group 4 metals.[12]

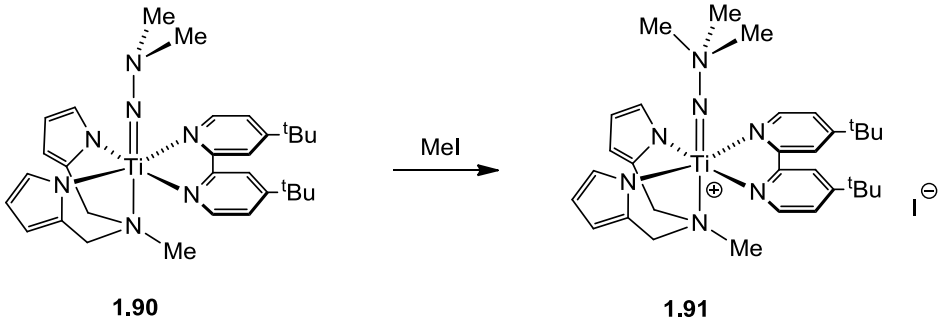

1.90 **1.91**

Equation 1.4

With the results obtained, it was proposed that a successful hydrohydrazination precatalyst could be obtained by suppressing the possible dimerisation pathways, which could be accomplished through a combination of a more electron-rich titanium centre and/or a bulkier ancillary ligand.[4, 12] Thus, the pyrrolyl complex, $Ti(dap)_2(NMe_2)_2$ (**1.92**; dap = α-(dimethylaminomethyl)pyrrole) was then synthesised. This was found to successfully catalyse the reaction between 1,1-dimethyl hydrazine and 1-hexyne at 100 ℃ (10 mol% solution of **1.92**) to give the corresponding hydrazone in *ca*. 80% yield (Scheme 1.6). The reactions with terminal alkynes were more efficient compared to those for internal alkynes. When aryl substituted hydrazines were used in the presence of $ZnCl_2$, Fischer indole synthesis occurred to yield the corresponding indoles. This could also be achieved in a one-pot procedure.[4] If alkyl or aryl isonitriles were added to the reaction mixture, iminohydrazination occurred to yield 1,3-iminohydrazones in 12 – 73% yield depending on the substrates (Scheme 1.6). It was proposed that the hydrohydrazination catalytic cycle proceeded through a [2+2] cycloaddition of a transient terminal titanium hydrazido(2-) intermediate with the alkyne, yielding a four membered metallacycle. The presence of a further equivalent of hydrazine protonated off the ring to yield the corresponding hydrazone, and regenerated the active species. In the presence of an isonitrile, however, insertion into the metallacycle occurred prior to protonolysis by the hydrazine to yield 1,3-iminohydrazones.[137]

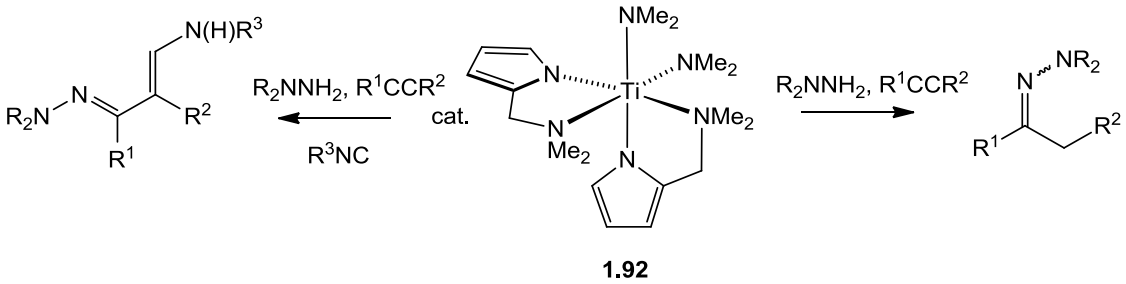

1.92

Scheme 1.6. Catalytic hydrohydrazination and iminohydrazination catalysed by $Ti(dap)_2(NMe_2)_2$ (**1.92**, 10 mol%).

As complex **1.92** was only active with disubstituted hydrazines, Odom *et al.* designed a new catalyst supported by a dipyrrolyl-based tetradentate ligand, namely $Ti(enp)(NMe_2)_2$ (**1.93**; H_2enp = N,N'-dimethylethylenediamine-N,N'-bis(2-methylpyrrole)) in 2008 in an effort to extend the hydrohydrazination reaction to monosubstituted hydrazines. Compound **1.93** worked as an active hydrohydrazination

catalyst for terminal and internal alkynes with both alkyl and aryl substituted hydrazines. Fischer indole cyclisation was achieved through a one-pot procedure yielding *NH*-indoles in 48 – 87% yield depending on the substrates.[138]

Although **1.92** and **1.93** were successful hydrohydrazination catalysts, elevated temperatures (100 ℃ and 80 ℃ respectively) and long reaction times were required. Recently, Gade *et al.* reported a series of compounds supported by a 2-aminopyrrolinato ligand, Cp*Ti($N^{Xyl}N$)(NNR_2)(L) (**1.94** – **1.96**; $N^{Xyl}N$ = 2-(3,5-dimethylphenylamino)pyrrolinato) (Equation 1.5) which showed remarkable catalytic activity towards hydrohydrazination at ambient conditions. These were obtained *via tert*-butyl imido/hydrazine exchange reaction between Cp*Ti($N^{Xyl}N$)(N^tBu)($NH_2{}^tBu$) (**1.97**) and the appropriate hydrazine. For the diphenyl hydrazido(2-) complex **1.94**, heating at 60 ℃ for 72 hours under a high vacuum (10^{-6} mbar) removed the *tert*-butylamine to yield the monomeric Cp*Ti($N^{Xyl}N$)($NNPh_2$) (**1.98**). However, both the methylphenyl (**1.95**) and dimethyl (**1.96**) hydrazido(2-) complexes required the presence of a dative ligand to suppress dimerisation. All these achieved complete conversions of terminal alkynes and diynes to give the hydrazone products with >99% Markovnikov regioselectivities within one hour with a 5 mol % catalyst loading.[17]

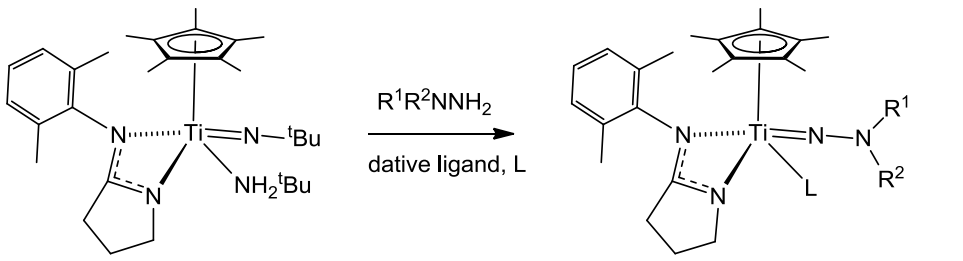

1.97

$R^1 = R^2$ = Ph, L = $NH_2{}^tBu$ or py (**1.94**)
R^1 = Me, R^2 = Ph, L = py or DMAP (**1.95**)
$R^1 = R^2$ = Me, L = DMAP (**1.96**),

Equation 1.5

Further study on the reactions of complexes **1.94** and **1.95** with unsaturated substrates were also reported (Scheme 1.7). Reactions with phenylallene formed a mixture of diasteriomeric cycloaddition products **1.99** and **1.100**. DFT calculations were employed to rationalise the observed product distribution.[139]

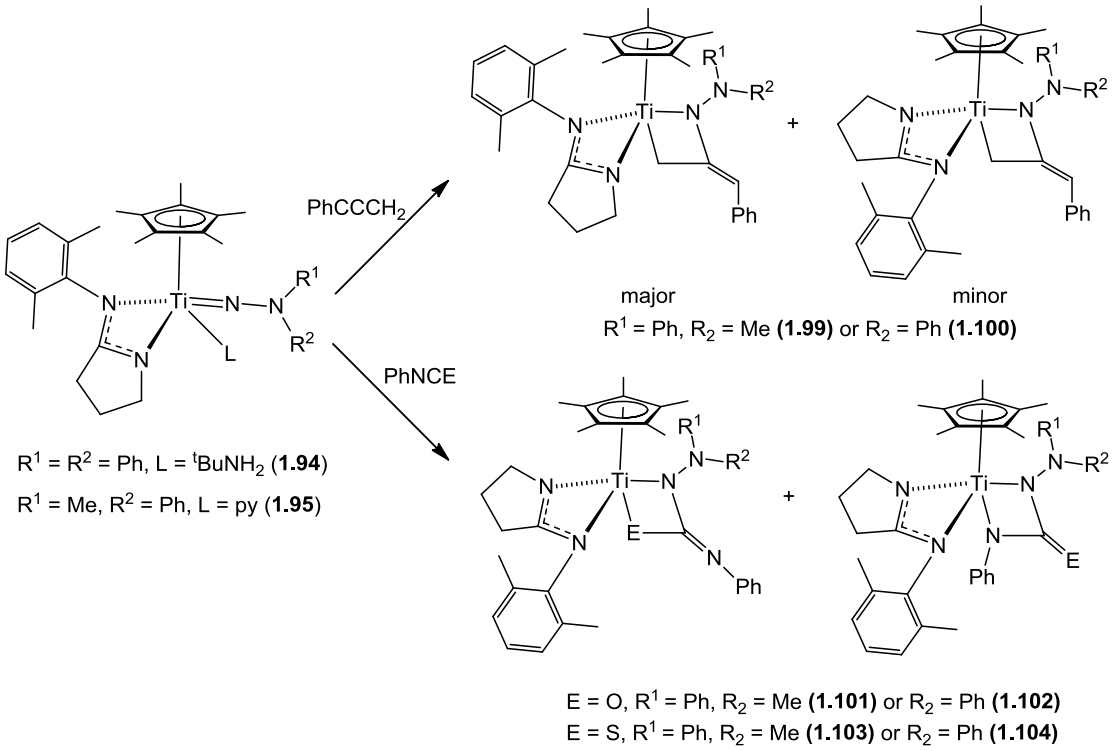

Scheme 1.7. Reactions between Cp*Ti($N^{Xyl}N$)(NNR_2)(L) (**1.94** or **1.95**) and $PhCCCH_2$ (top) or PhNCE (E = O or S) (bottom).

Reactions with phenylisocyanate or phenylisothiocyanate gave mixtures of cycloaddition products with both κ(*N*,*E*)- and κ(*N*,*N*)-coordination modes (**1.101** − **1.104**) (Scheme 1.7). The distribution of κ(*N*,*E*)- and κ(*N*,*N*)-coordinated products were dependent on the hydrazido(2-) substituents and the identity of E. Interestingly, complex **1.96** was reported to react with trimethylsilylazide to yield the N-silylated η^2-hydrazido(1-) titanium azide Cp*Ti($N^{Xyl}N$)(η^2-N($SiMe_3$)NMe_2)(N_3) (**1.105**) with the azide terminally coordinated to the titanium centre.[139]

In 2008, Mountford *et al.* reported the syntheses of a series of terminal titanium hydrazido(2-) complexes Ti(Me_2Calix)(NNR_2) (**1.38** – **1.40**) (Figure 1.16) *via* the reaction of Ti(Me_2Calix)Cl_2 with two equivalents of the appropriate lithiated hydrazine.[22] The series of complexes with diaryl, mixed aryl/alkyl and dialkyl substituted hydrazido(2-) ligands enabled the comparison of the molecular structures to be carried out. All three demonstrated essentially linear Ti=N–N linkages with short Ti=N_α distances (indicative of multiple bonding character) and long N_α–N_β distances (suggestive of a single bond character) consistent with a hydrazido(2-) ligand.

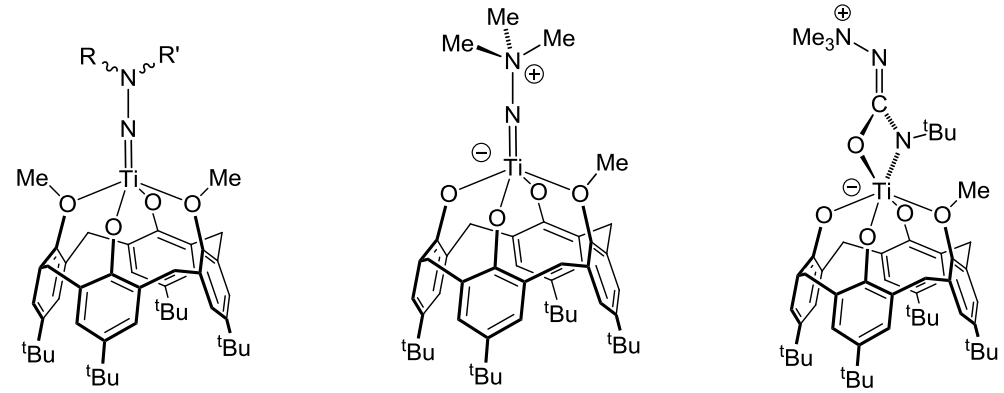

Figure 1.16. Titanium hydrazido(2-) complexes and their reaction products.

Although no well-behaved reactions with small molecules were observed for both complexes **1.38** and **1.39**, the dimethyl complex **1.40** did react with one equivalent of MeI to form an unsymmetrical zwitterionic hydrazidium complex Ti(MeCalix)($NNMe_3$) (**1.106**) (Figure 1.16), a consequence of the chemical activation of the supporting calix[4]arene ligand. This was suggested to occur *via* an initial methylation of N_β followed by demethylation of the supporting ligand by the iodide anion. Interestingly, this reaction was found to be catalytic with methyl iodide. Another successful reaction was reported between **1.40** and ^{t}BuNCO where similar migration of a methyl group to form a hydrazidium complex was observed. It was suggested that the reaction proceeds *via* an initial [2+2] cycloaddition to form a metallacycle with N_β in close proximity to one of the methyl groups on the Me_2Calix[4]arene. Migration of the methyl group onto N_β followed by rearrangement yielded the κ(*N,O*)-coordinated zwitterionic hydrazidium complex **1.107** (Figure 1.16), the first example of an overall insertion into the Ti=N_α hydrazido(2-) bond reported.[22]

In the same year, new terminal hydrazido(2-) complexes with dianionic N_3- donor ligands were synthesised using Ti($NNPh_2$)Cl_2($py)_3$ (**1.108**). Four diamide-amine supported hydrazido(2-) complexes of the type Ti($NNPh_2$)("N_2N")(py) ("N_2N" = $MeN(CH_2CH_2NSiMe_3)_2$ (**1.109**) (Scheme 1.8); $Me_3SiN(CH_2CH_2NSiMe_3)_2$ (**1.110**); $MeN(CH_2CH_2CH_2NSiMe_3)_2$ (**1.111**); (2-NC_5H_4)C(Me)$(CH_2NSiMe_3)_2$ (**1.112**) (Scheme 1.9)) were obtained through salt metathesis reactions between **1.108** and the

lithiated donor ligands.[25] These complexes were found to display a rich chemistry with various unsaturated substrates.

Reaction of **1.109** with MeCCMe and PhCCMe (Scheme 1.8) unexpectedly resulted in net insertion of the alkyne into the cleaved N_α–N_β bond, yielding a vinyl imido species, instead of a [2+2] cycloaddition product. When treated with Ph_2NNH_2, the insertion product with PhCCMe regenerated $Ti(N_2N^{Me})(NNPh_2)(py)$ and released $PhC(NH_2)C(Me)NPh_2$ as the side-product, demonstrating the potential of the hydrazido complex to act as catalyst for 1,2-diamination reactions.[21]

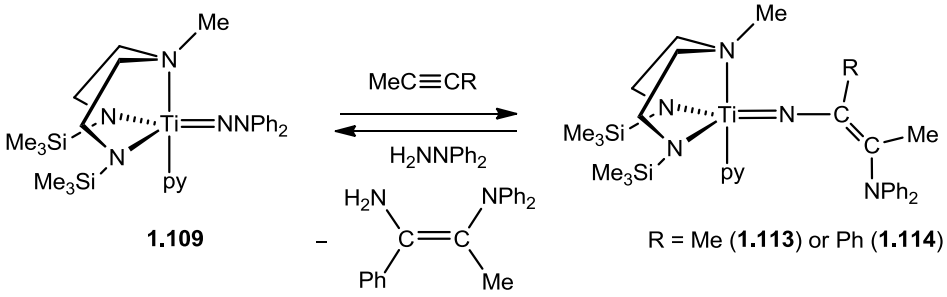

Scheme 1.8. 1,2 diamination reaction of $Ti(N_2N^{Me})(NNPh_2)(py)$ with alkynes.

In contrast to the closely related $Ti(N_2N^{Me})(NNPh_2)(py)$, reaction of **1.112** with PhCCMe allowed isolation of a [2+2] cycloaddition product prior to net insertion with N_α–N_β bond cleavage. The alkyne cycloaddition product was found to have anti-Markovnikov selectivity. Addition of pyridine to the cycloaddition product reformed **1.112** and the corresponding alkyne, showing the reversibility of the cycloaddition process. The results also demonstrated that systems capable of forming azametallacycles can also undergo N_α-N_β bond insertion reactions (Scheme 1.9).[23] In a later publication, they reported that for both **1.109** and **1.112**, internal alkynes with electron-withdrawing aryl groups were found to stabilise the metallacycles (with anti-Markovnikov selectivity), whereas the ones with electron-releasing aryl groups promote insertion (C_{Ti}-N_α bond formation).[27]

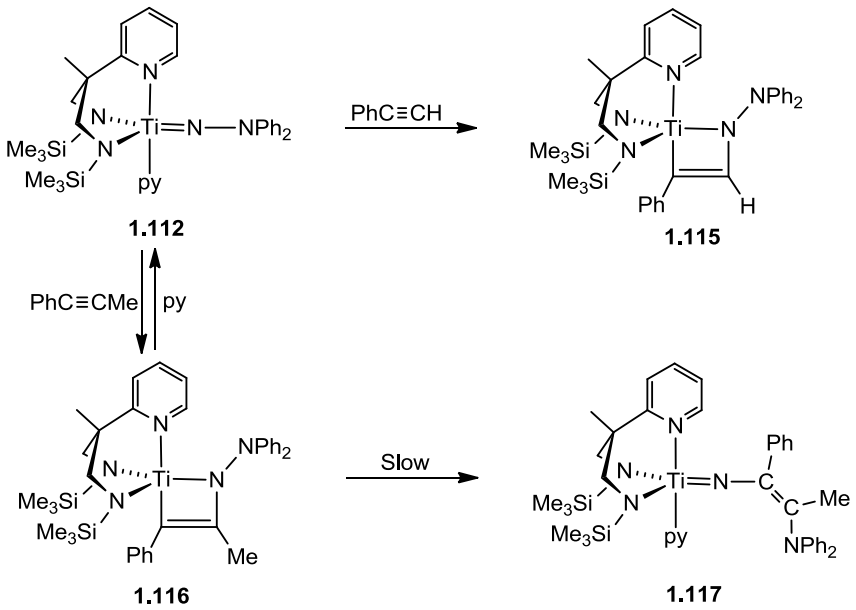

Scheme 1.9. Reactions of $Ti(N_2N^{py})(NNPh_2)(py)$ with alkynes.

Complex **1.112** reacted with MeCN to yield a self-trapped dimer $Ti_2(N_2N^{py})_2\{\mu\text{-}N(NPh_2)C(Me)N\}_2$ (**1.118**) (Figure 1.17) through the transient cycloaddition intermediate $Ti(N_2N^{py})\{N(NPh_2)C(Me)N\}$. This addition of nitrile was the first of its type reported for any metal hydrazides.[23, 28] Reaction of **1.109** or **1.112** with fluorinated benzonitriles however, resulted in the formation of terminal hydrazonamide complexes $Ti(N_2N^{R})\{NC(Ar^{Fx})NNPh_2\}(py)$ (**1.119**; R = py or Me; Ar^{Fx} = 2,6-$C_6H_3F_2$ or C_6F_5) (Figure 1.17). These were proposed to proceed through an overall [2+2] cycloaddition-reverse cycloaddition reaction, with net insertion of $Ar^{Fx}CN$ into the hydrazide $Ti{=}N_\alpha$ bond. Interestingly, addition of a mixture of PhCCMe and MeCN to **1.112** resulted in a sequential coupling of $Ti{=}NNPh_2$ with PhCCMe and MeCN to form the metallacycle $Ti(N_2N^{py})\{NC(Me)C(Ph)C(Me)NNPh_2\}$ (**1.120**) (Figure 1.17).[28]

Reaction of **1.112** with two equivalents of $B(Ar^{F5})_3$ (Ar^{F5} = C_6F_5) resulted in electrophilic attack at N_α to give the zwitterionic borate $Ti(N_2N^{py})\{\eta^2\text{-}N(NPh_2)B(Ar^{F5})_3\}$ (**1.121**). Both **1.109** and **1.112** were found to react with isonitriles (^{t}BuNC and XylNC) to form N_α–N_β bond scission products $Ti(N_2N^{R})(NCNR')(NPh_2)$ (**1.122**; R = py or Me; R′ = ^{t}Bu or Xyl (Figure 1.17)) which contained metallated carbodiimide ligands. Unlike the above mentioned reactions, they found that **1.109** underwent [2+2] cycloaddition reactions with Ar′NCE (E = O, S, Se; Ar′ = 2,6-$C_6H_3{}^iPr_2$) without further transformation, giving $Ti(N_2N^{Me})\{N(NPh_2)C(NAr')O\}(py)$

(**1.123**) (Figure 1.17) and Ti(N_2N^{Me}){N(NPh_2)C(NAr′)E} (**1.124**; E = S or Se) as the stable products.[28]

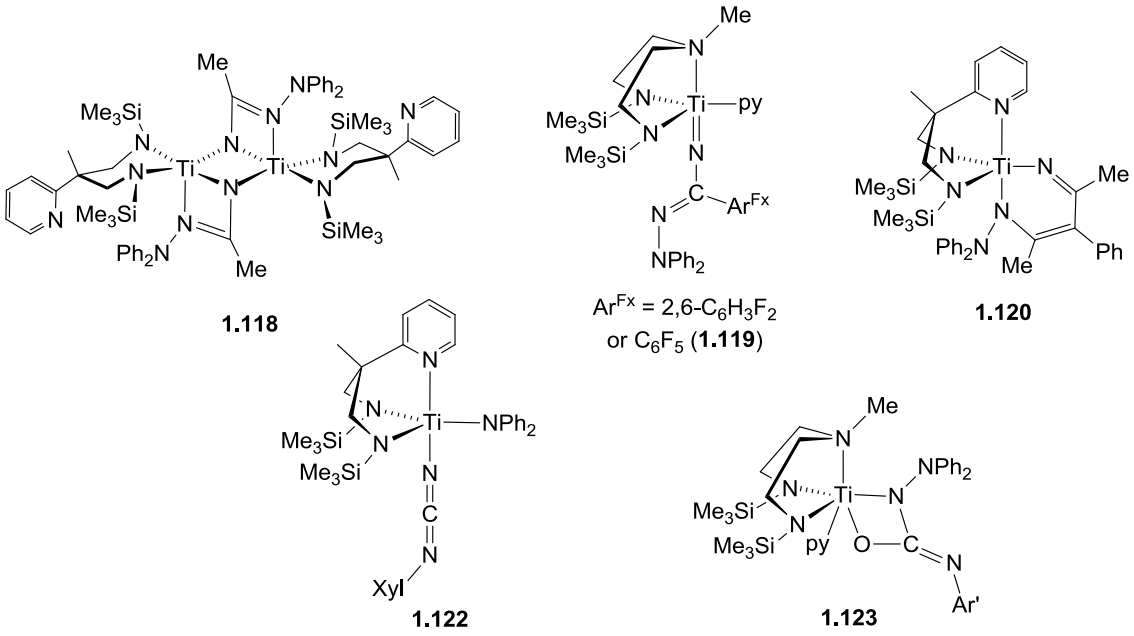

Figure 1.17. Reactivity of titanium hydrazido(2-) complexes.

1.3.7 Zirconium and Hafnium hydrazido chemistry

The first structurally characterised η^1-hydrazido(2-) complex of Group 4 was reported by Bergman *et al.* in 1991.[13] This zirconocene complex $Cp_2Zr(NNPh_2)$(DMAP) (**1.125**; DMAP = 4-dimethylaminopyridine) (Scheme 1.10) was synthesised from thermolysis of the alkyl hydrazido(1-) complex $Cp_2Zr\{N(H)NPh_2\}(CH_2CH_2{}^tBu)$ (**1.126**). In the absence of a dative ligand trap, thermolysis of **1.126** at 110 ℃ for twelve hours formed the transient intermediate $Cp_2Zr(NNPh_2)$ (**1.127**) which spontaneously dimerised to a mixed [μ-$\eta^1\eta^1$][μ-$\eta^2\eta^1$] hydrazido(2-) bridged species (**1.128**) with elimination of 2,2-dimethylbutane. The presence of DMAP in the reaction mixture enabled the isolation of the monomeric species **1.125**. Complex **1.125** could also be obtained by heating dimer **1.128** in the presence of DMAP. This reversible behaviour contrasts with the unreactive dimers of titanium complexes described in Section 1.3.6.

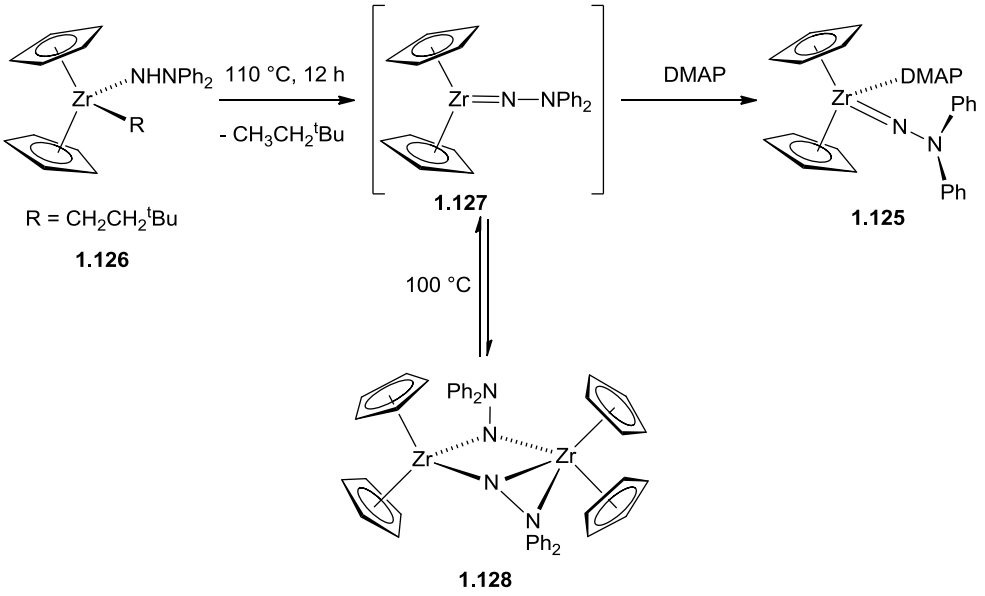

Scheme 1.10. Synthesis of zirconocene hydrazido(2-) complexes.

The monomeric nature of **1.125** was confirmed by X-ray crystallographic analysis. The molecular structure showed a short Zr=N_α bond distance of 1.873(7) Å which is comparable to that reported for the imido species $Cp_2Zr(N^tBu)(THF)$ (**1.129**),[140] and is consistent with a Zr=N_α multiple bond. In addition, the N_α–N_β bond length of 1.364(10) Å is indicative of an N–N single bond.

Heating **1.126** in the presence of an internal alkyne RCCR (R = Et, Ph or Tol) resulted in N_α–N_β bond cleavage to give the seven membered metallacyclic product **1.130** – **1.132** (Scheme 1.11) which upon acid hydrolysis formed the corresponding N-phenylindoles. Reaction with CO (700 torr) also resulted in N_α–N_β bond cleavage, yielding the N-bound cyanate-amide complex **1.133** (Scheme 1.11).[13]

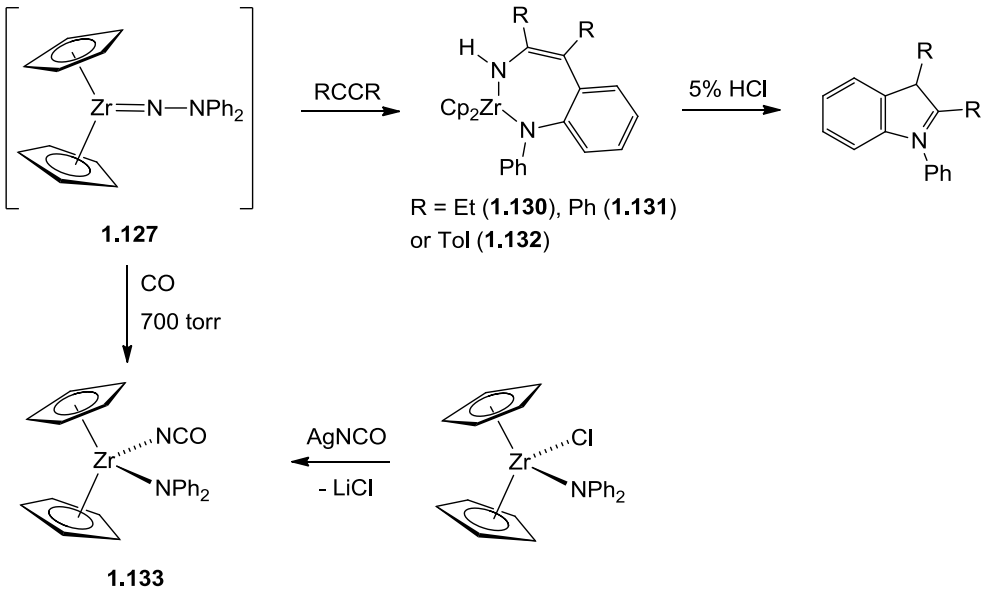

Scheme 1.11. Reactivity of zirconocene hydrazido(2-) complex.

In 2007 and 2008, Gade *et al*. reported the syntheses of zirconium and hafnium hydrazido(2-) complexes supported by a diamido-pyridyl ligand.[10, 20] The dichloro complex $M(N_2^{TBS}N^{py})Cl_2$ (M = Zr (**1.134**) or Hf (**1.135**); $N_2^{TBS}N^{py}$ = MeC(2-C_5H_4N){$CH_2N(Si^tBuMe_2)$}$_2$)) reacted with one equivalent of $LiNHNPh_2$ to form two stereoisomers of mixed chloro-hydrazido(1-) complexes. Dehydrohalogenation with lithium hexamethyldisilazide (LiHMDS) in the presence of pyridine gave hydrazido(2-) complexes $M(N_2^{TBS}N^{py})(NNPh_2)(py)$ (M = Zr (**1.136**) or Hf (**1.137**)) (Scheme 1.12) with pyridine occupying the axial position. A methyl phenyl analogue for zirconium, $Zr(N_2^{TBS}N^{py})(NN(Me)Ph)(DMAP)$ (**1.138**) was also synthesised through the analogous route. However, a stronger Lewis base (DMAP) was needed to get an isolable product in this case. Their attempts to synthesise a dimethyl analogue only led to the formation of an η^2-coordinated hydrazido(1-) complex $Zr(N_2^{TBS}N^{py})(NHNMe_2)Cl$ (**1.139**).[141]

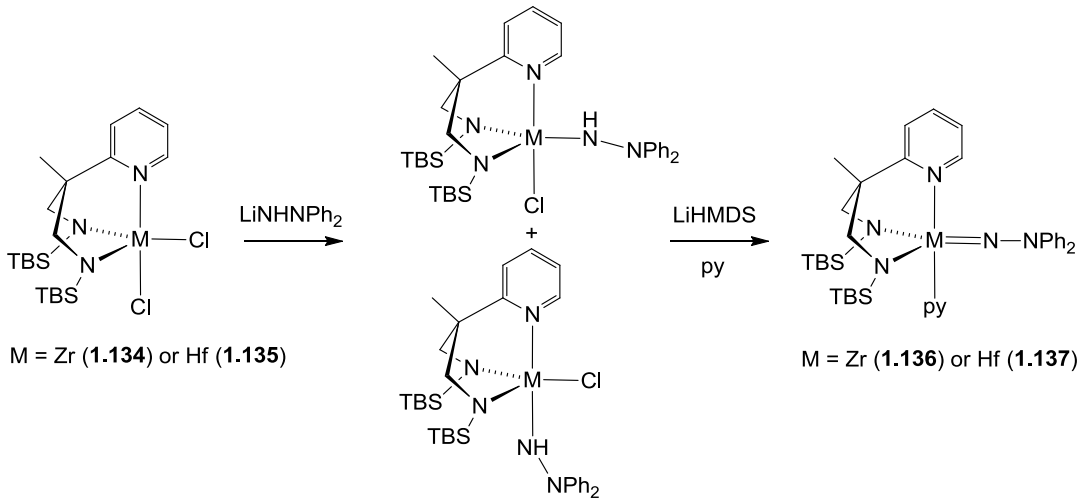

Scheme 1.12. Synthesis of $M(N_2^{TBS}N^{py})(NNPh_2)(py)$ (M = Zr (**1.136**) or Hf (**1.137**)).

Both **1.136** and **1.137** formed Lewis acid adducts with $B(C_6F_5)_3$ (**1.140**) (Scheme 1.13).[20] Complex **1.136** displayed interesting reactivity towards a selection of small unsaturated substrates, with the reactions dominated by facile N_α–N_β bond scission. Reaction with ^{t}BuNC resulted in N_α–N_β bond cleavage to yield the carbodiimido complex **1.141** (Scheme 1.13) while the reaction with chalcogen atom transfer agents (propylene sulphide or Ph_3PSe) gave the chalcogen bridged species $\{Zr(N_2^{TBS}N_{py})(NPh_2)\}_2(\mu\text{-}N_2E)$ (E = S (**1.142**) or Se (**1.143**)) (Scheme 1.13), also with N_α–N_β bond cleavage.[10] Upon the addition of different substituted azides ($SiMe_3$, adamantyl or mesityl), [2+3] cycloaddition occurred to form a five membered metallacyclic complex with a N_5 unit (**1.144**) (Scheme 1.13). Heating liberated dinitrogen followed by N_α–N_β bond cleavage to yield a side-on bound diazenido ligand with a diphenylamido ligand occupying the equatorial site.[18] Interestingly, complex **1.136** reacted with a variety of metal carbonyl complexes to yield a series of heteronuclear complexes $Zr(N_2^{TBS}N^{py})(py)\{\mu\text{-}OCNNPh_2\text{-}1\kappa C\text{:}2\kappa^2NO\}(M(CO)_n)$ (**1.145**; M = Cr, Mo, W (n = 5), Fe (n = 4)) (Scheme 1.13) with [2+2] cycloaddition of the $Zr{=}NNPh_2$ unit and the coordinated CO forming the bridging N-aminoisocyanato ligand.[142]

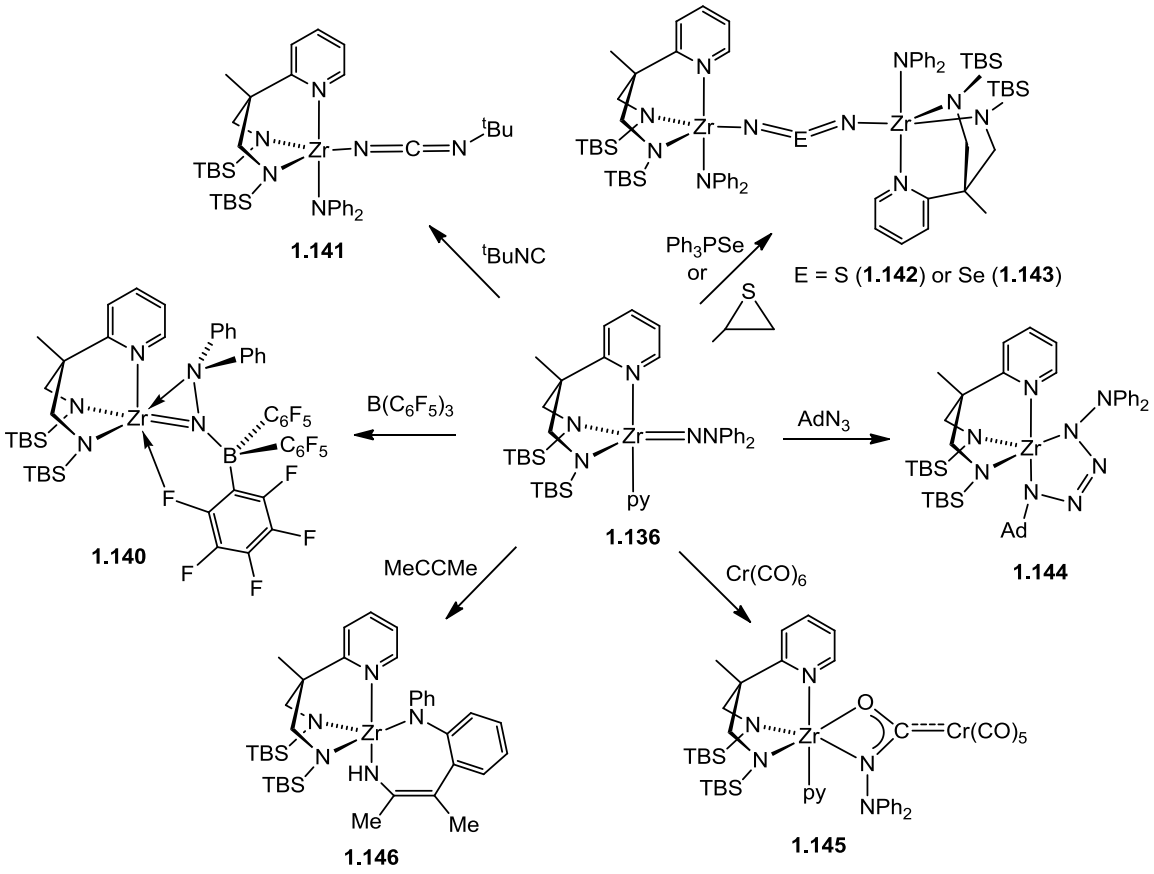

Scheme 1.13. Reactivity of $Zr(N_2{}^{TBS}N^{py})(NNPh_2)(py)$ (**1.136**).

Reaction of **1.136** with internal alkynes (MeCCMe, EtCCEt) underwent N_α–N_β bond cleavage and C–H activation through coupling of the alkyne with one of the phenyl rings to form the seven-membered diazazirconacycles (**1.146**, Scheme 1.13) analogous to those seen by Bergman *et al.* for **1.130** – **1.132**. In this case, addition of diphenylhydrazine also formed the corresponding indoles.[143] In a recent report, Gade *et al.* described the synthesis of two similar zirconium hydrazido(2-) complexes, namely $Zr(N_2{}^{Xyl}N^{py})(NNRPh)(DMAP)_2$ (R = Me (**1.147**) or Ph (**1.148**); $N_2{}^{Xyl}N^{py}$ = $MeC(2\text{-}C_5H_4N)\{CH_2N(Xyl)\}_2$), which were synthesised through the reactions of $Zr(N_2{}^{Xyl}N^{py})(NMe_2)_2$ (**1.149**) with the corresponding disubstituted hydrazines in the presence of an excess of DMAP. However, the reaction of the bis(amido) complex $Zr(N_2{}^{Mes}N^{py})(NMe_2)_2$ (**1.150**; $N_2{}^{Mes}N^{py}$ = $MeC(2\text{-}C_5H_4N)\{CH_2N(Mes)\}_2$) with one or two equivalents of diphenylhydrazine resulted in the formation of the mixed amido/hydrazido(1-) complex $Zr(N_2{}^{Mes}N^{py})(HNNPh_2)(NMe_2)$ and the bis(hydrazido(1-)) complex $Zr(N_2{}^{Mes}N^{py})(HNNPh_2)_2$ respectively. In both cases, thermal induced conversion to the corresponding hydrazido(2-) complexes were

unsuccessful even in the presence of excess donor ligands. The bis(amido) complex **1.150** however, reacted with one molar equivalent of internal alkynes and diphenylhydrazine to form the seven-membered diazazirconacycles analogous to **1.146** and **1.130** – **1.132**. Results for the mechanistic and catalytic studies were reported. The bis(amido) complex **1.149** was found to be an active catalyst for indole synthesis, in which the reaction of 1.2 equivalents of diarylhydrazines with various substituted alkynes in the presence of 10 mol% of **1.149** gave the corresponding indole derivatives either at ambient temperature or at 80 ℃.[144]

The related zirconium and hafnium (1-pyridinio)imido complexes were also reported by Gade *et al.* through the reaction of $M(N_2^{TBS}N_{py})(NMe_2)_2$ (M = Zr (**1.151**) or Hf (**1.152**)) with 1-aminopyridinium triflate in the presence of pyridine (Figure 1.18). The coordinated triflate ligand was easily replaced by anionic ligands such as PhCCLi. Reaction of **1.151** with ^{t}BuNC gave the carbodiimido complex **1.153** with N_α–N_β bond scission (Figure 1.18) and loss of pyridine. Similar behaviour was seen with CO where the loss of pyridine was observed to yield the isocyanato complex **1.154** (Figure 1.18) analogous to that seen by Bergman *et al*. for **1.133** (Scheme 1.11).[145, 146]

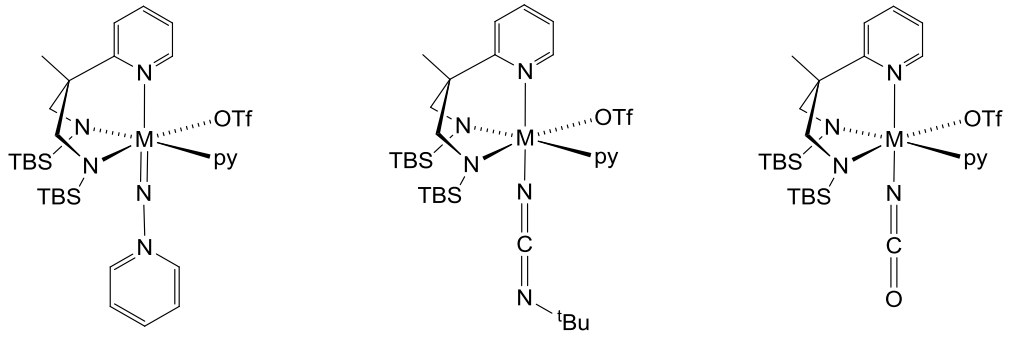

M = Zr (**1.151**) or Hf (**1.152**) **1.153** **1.154**

Figure 1.18. Zirconium and hafnium hydrazido(2-) complexes and their reaction products.

Mountford *et al*. attempted the synthesis of the zirconium analogues of $Ti(Me_2Calix)(NNR_2)$ (**1.38** – **1.40)** by reacting $Zr(Me_2Calix[4]arene)Cl_2$ with $LiNHNR_2$. However, these only led to the formation of bis(hydrazido(1-)) complexes.[22] Martins *et al.* reported a similar reactivity for $Zr(Bn_2Cyclam)Cl_2$ ($Bn_2Cyclam$ = 1,8-dibenzyl-1,4,8,11-tetraazacyclotetradecane) which reacted with $LiNHNPh_2$ to form the bis(hydrazido(1-)) complex $Zr(Bn_2Cyclam)(NHNPh_2)_2$ (**1.155**).[147]

1.4 Group 4 alkylidene hydrazido chemistry

Metal alkylidene hydrazido complexes have been widely studied due to their rich coordination chemistry[148] and also their relevance to the chemistry of dinitrogen fixation.[149, 150] Nevertheless, Group 4 alkylidene hydrazido complexes are rather scarce, with only one example of a monomeric η^1-alkylidene hydrazido(2-) complex reported prior to this study.[74, 151]

Early studies on titanium alkylidene hydrazido(2-) complexes were undertaken by Floriani *et al*. in the early 1980s.[152-154] In 1982, they reported the reaction between titanocene dicarbonyl, $Cp_2Ti(CO)_2$ and diethyl diazomalonate (DEDM) which yielded complex $Cp_2Ti(DEDM)$ (**1.156**) (Figure 1.19) with the loss of CO. The molecular structure of complex **1.156** showed an η^3-N,N,O bonded alkylidene hydrazido ligand.[152] In another report, they discussed the reaction of $(CpTiCl_2)_n$ with Ph_2CN_2 which resulted in the formation of the dimeric species $[CpTiCl(\mu\text{-}NNCPh_2)]_2$ (**1.157**). They proposed that the reaction occurred through an initial formation of $[CpTiCl_2]_2(\mu\text{-}NNCPh_2)$ followed by elimination of $CpTiCl_3$ to give the intermediate $CpTiCl(NNCPh_2)$. Dimerisation of the intermediate afforded **1.157** with two titanium atoms doubly bridged by an alkylidene hydrazido(2-) ligand.[153, 154]

The first authenticated η^1-alkylidene hydrazido(2-) complex of titanium, namely $Cp_2Ti(NNCPh_2)(PMe_3)$ (**1.158**) (Figure 1.19) was reported by Kool *et al*. in 1986 *via* the reactions of $Cp_2Ti(PMe_3)_2$ or $Cp_2Ti(CO)(PMe_3)$ with Ph_2CN_2. X-ray diffraction study confirmed its η^1- bonding mode. The bond lengths and angles of complex **1.158** are discussed in Section 4.2. It was found to be stable towards dimerisation or loss of phosphine or N_2. No reactivity studies were included in the report.[151]

A decade later, Bergman *et al.* reported the synthesis of an η^2-alkylidene hydrazido(2-) complex, namely $Cp^*_2Ti\{NNC(H)SiMe_3\}$ (**1.159**) (Figure 1.19) which was obtained *via* the treatment of $Cp^*_2Ti(C_2H_4)$ with one equivalent of Me_3SiCHN_2. One equivalent of C_2H_4 was produced in the reaction. Unlike **1.158**, complex **1.159** was found to be unstable towards N_2 loss in solution at room temperature to give the fulvene complex $Cp^*FvTiCH_2SiMe_3$. Thermolysis of **1.159** in the presence of α-olefins gave the trans-α,β-disubstituted titanacyclobutane complexes $Cp^*_2Ti\{CH(SiMe_3)CH(R)CH_2\}$ (**1.160**; R = H, Ph, Me, Et) (Figure 1.19). The kinetic study suggested a mechanism with N_2 loss to give a carbene intermediate as the rate-

determining step.[155, 156] Complex **1.159** was found to react with alkynes and allene to form cycloaddition products with retention of N_2. In addition, it reacted with Lewis bases reversibly to form adducts $Cp^*_2Ti\{NNC(H)SiMe_3\}(py)$ (**1.161**) or $Cp^*_2Ti\{NNC(H)SiMe_3\}(DMAP)$ (**1.162**), resulting in end-on coordination of the alkylidene hydrazido ligand. Although not isolable, the adducts were found to slow the formation of the fulvene complex.[156]

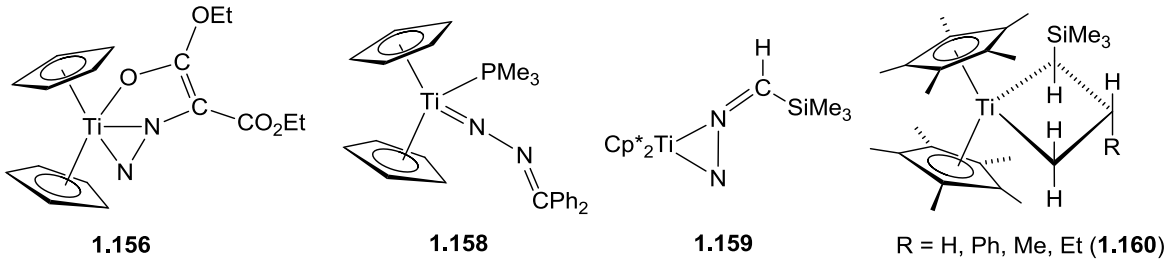

1.156 **1.158** **1.159** R = H, Ph, Me, Et (**1.160**)

Figure 1.19. Titanium alkylidene hydrazido(2-) complexes and the reaction product.

In 1998, Bergman *et al.* reported the syntheses of a series of η^2-alkylidene hydrazido(2-) complexes $Cp^*_2Ti\{NNC(H)Ar\}$ (Ar = 4-$C_6H_4CF_3$ (**1.163**), 4-C_6H_4Cl (**1.164**), 4-$C_6H_4NMe_2$ (**1.165**), Tol (**1.166**), Ph (**1.167**)) analogous to **1.159** using the same route.[157] Unlike **1.159** however, these are stable up to 75 ℃ which allowed the study of their reactivity to be carried out without competitive N_2 loss. Heating all five at 75 ℃ for a day in the presence of styrene gave the α,β-disubstituted titanacyclobutane complexes $Cp^*_2Ti\{CH(Ar)CH(Ph)CH_2\}$ (**1.168**; Ar = 4-$C_6H_4CF_3$, 4-C_6H_4Cl, 4-$C_6H_4NMe_2$, Tol, Ph) analogous to **1.160**.

When treated with CO, complex $Cp^*_2Ti\{NNC(H)Tol\}$ (**1.166**) underwent N_α–N_β bond scission to yield the alkylideneimido isocyanato complex $Cp^*_2Ti\{NC(H)Tol\}(NCO)$ (**1.169**) analogous to $Cp_2Zr(NPh_2)(NCO)$ (**1.133**) observed for the reaction between zirconocene complex $Cp_2Zr(NNPh_2)(DMAP)$ (**1.125**) and CO.[13] Complex **1.166** underwent Si–H addition across the Ti=N_α bond with aryl silanes ($PhSiH_2R$, R = H or Ph) to form kinetic products of the type (*E*)-$Cp^*_2Ti(H)\{N(PhSiHR)NC(H)Tol\}$ (**1.170**) and thermodynamic products of the type (*Z*)-$Cp^*_2Ti(H)\{N(PhSiHR)NC(H)Tol\}$ (**1.171**). Reaction of complex **1.166** with $AlNp_3$ resulted in coordination of the Lewis acid to the N_α forming $Cp^*_2Ti\{N(AlNp_3)NC(H)Tol\}$ (**1.172**). Complex $Cp^*_2Ti\{NNC(H)Ph\}$ (**1.167**) reacted with ^{t}BuNC to form a stable Lewis base adduct $Cp^*_2Ti\{NNC(H)Ph\}(^t$BuNC) (**1.173**)

with an η^1- coordinated alkylidene hydrazido ligand. A summary of the reactivity is shown in Scheme 1.14.

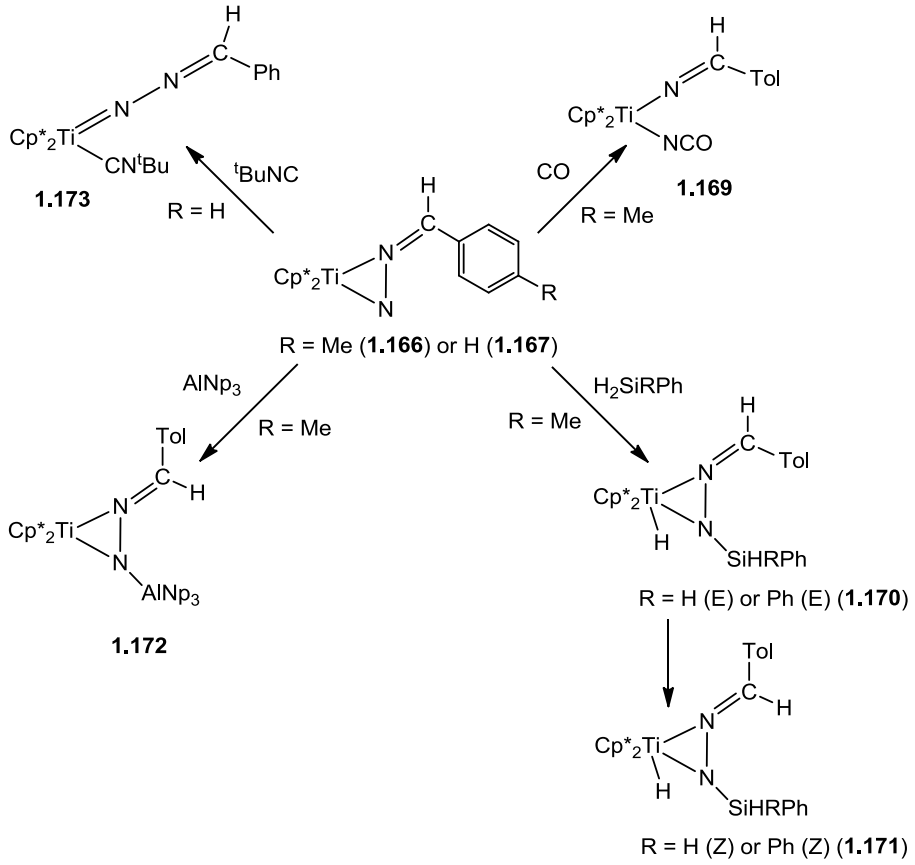

Scheme 1.14. Reactivity of titanium alkylidene hydrazido(2-) complexes.

In 2004, Chirik *et al*. reported the synthesis of $\{\eta^5\text{-}1,3\text{-}C_5H_3(SiMe_3)_2\}_2Ti(NNCPh_2)$ (**1.174**) *via* the reaction of $[\{\eta^5\text{-}1,3\text{-}C_5H_3(SiMe_3)_2\}_2Ti]_2(\mu_2,\eta^1,\eta^1\text{-}N_2)$ with Ph_2CN_2.[158] Complex **1.174** was reported to undergo dynamic interconvertion between η^2- and η^1-isomers in solution. In this case, addition of Lewis base also managed to trap the alkylidene hydrazido adduct. Addition of DMAP to **1.174** formed the terminally bonded alkylidene hydrazido complex $\{\eta^5\text{-}1,3\text{-}C_5H_3(SiMe_3)_2\}_2Ti(NNCPh_2)(DMAP)$ (**1.175**). Interestingly, complex **1.174** reacted with CO to form the adduct $\{\eta^5\text{-}1,3\text{-}C_5H_3(SiMe_3)_2\}_2Ti(NNCPh_2)(CO)$ (**1.176**) instead of N_α–N_β bond cleavage seen by Bergman *et al*. for their permethyltitanocene complex **1.166**.[157] They proposed that the difference in reactivity was caused by the reduced nucleophilicity of N_α in **1.174** due to the relative electron-withdrawing nature of the silylated cyclopentadienyl ligands compared to the permethyltitanocene complex **1.166**, which would have a more nucleophilic N_α to attack the coordinated CO and induce N_α–N_β bond scission.

Although Bergman *et al*. observed only decomposition products upon addition of H_2 to complex **1.166**, treatment of **1.174** or **1.176** with H_2 (1 atm) both yielded the hydrogenation product $\{\eta^5\text{-}1,3\text{-}C_5H_3(SiMe_3)_2\}_2Ti(H)\{N(H)NCPh_2\}$ (**1.177**) (Scheme 1.15).

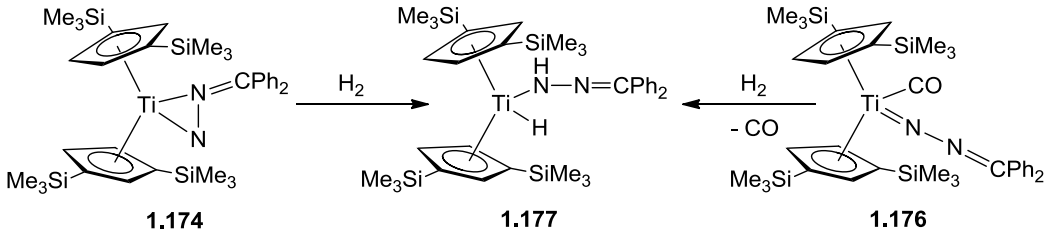

Scheme 1.15. Hydrogenation reaction of complexes **1.174** and **1.176**.

Most of the available examples of alkylidene hydrazido complexes were prepared using diazoalkanes. Only a few examples of Group 4 alkylidene hydrazido complexes reported were synthesised using hydrazones or hydrazone derivatives. These, however, gave either alkylidene hydrazido(1-) complexes or formed dimers. One of the examples was reported by Schwartz and co-workers where they reacted Cp_2ZrCl_2 with lithiated hydrazone, LiNNC(H)Ph in THF at -78 ℃ to yield the dimer $[Cp_2Zr]_2(\mu\text{-}\eta^1\text{:}\eta^1\text{-}NNCHPh)(\mu\text{-}\eta^2\text{:}\eta^1\text{-}NNCHPh)$ (**1.178**). The molecular structure analysis confirmed its dimeric nature. This species was found to react with aldehydes or ketones to yield olefins.[159, 160]

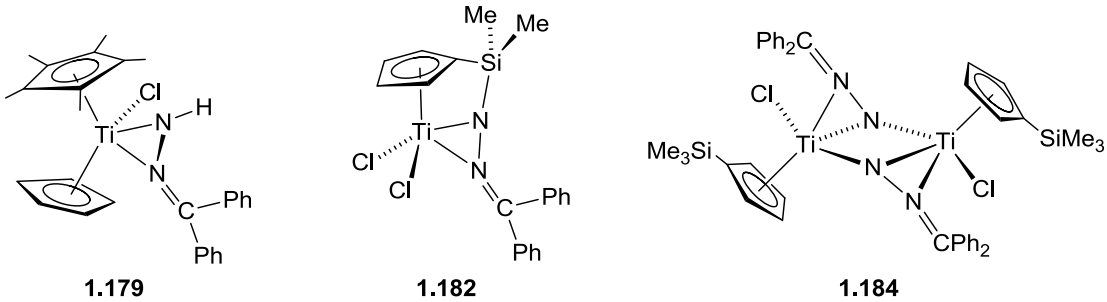

Figure 1.20. Titanium alkylidene hydrazido complexes.

Another report was by Cuenca *et al*. in which they described the syntheses of a series of titanium alkylidene hydrazido complexes using hydrazones or lithiated hydrazones. The reaction of $Cp^*CpTiCl_2$ with one equivalent of $LiN(H)NCPh_2$ in toluene at -78 ℃ yielded $Cp^*CpTiCl\{N(H)NCPh_2\}$ (**1.179**) (Figure 1.20) while $Cp^*CpTi\{N(H)NCPh_2\}_2$ (**1.180**) was formed when two equivalents of the lithiated salt was added. Treatment of $Ti\{\eta^5\text{-}C_5H_4(SiMe_2Cl)\}Cl_3$ with Ph_2CNNH_2 in the

presence of one equivalent of NEt_3 formed the alkylidene hydrazido(1-) complex $Ti\{\eta^5\text{-}C_5H_4(SiMe_2Cl)\}Cl_2\{N(H)NCPh_2\}$ (**1.181**). In the presence of two equivalents of NEt_3, aminolysis occurred forming the cyclopentadienyl-amido derivative $Ti\{\eta^5\text{-}C_5H_4(SiMe_2\text{-}\eta^1\text{-}NNCPh_2)\}Cl_2$ (**1.182**) (Figure 1.20). Reactions of the trichloride complexes $(Cp^R)TiCl_3$ (Cp^R = Cp*, $\eta^5\text{-}C_5H_4(SiMe_3)$) with benzophenone hydrazone in the presence of one equivalent of NEt_3 formed the alkylidene hydrazido(1-) complexes $(Cp^R)TiCl_2\{N(H)NCPh_2\}$ (**1.183**), while the dimer $[Ti\{\eta^5\text{-}C_5H_4(SiMe_3)\}Cl(\mu\text{-}NNCPh_2)]_2$ (**1.184**) (Figure 1.20) could be formed by either reacting $Ti\{\eta^5\text{-}C_5H_4(SiMe_3)\}Cl_2\{N(H)NCPh_2\}$ with NEt_3 or by reacting $Ti\{\eta^5\text{-}C_5H_4(SiMe_3)\}Cl_3$ with Ph_2CNNH_2 in the presence of two equivalents of NEt_3. The molecular structure of complex **1.184** confirmed its dimeric nature and showed that two titanium atoms are doubly bridged by an alkylidene hydrazido(2-) ligand. Reactivity studies showed that these complexes were useful as catalysts for olefin polymerisation.[161]

1.5 Summary and objectives

This Chapter has introduced the chemistry of Group 4 metal hydrazido and alkylidene hydrazido complexes. It has described the chemistry of the related Group 4 imido complexes, Group 5 and Group 6 hydrazido(2-) complexes, and their relevance to nitrogen fixation. Synthetic chemistry of available Group 4 hydrazido(2-) complexes and the bonding are discussed. Previous examples of Group 4 alkylidene hydrazido(2-) complexes are also described. Comparison with Group 4 imido and later metal hydrazido complexes together with previous reports on their chemistry suggests the potential of titanium hydrazido(2-) complexes to display unique structure, bonding and reactivity. Thus, the aim of this Thesis is to explore the chemistry of the $Ti{=}NNR_2$ (hydrazido) and $Ti{=}NNCR_2$ (alkylidene hydrazido) functional groups through a combined synthesis, calculation and reactivity study. The principal aims include (i) to compare the chemistry of Ti=NR (imido), $Ti{=}NNR_2$, and $Ti{=}NNCR_2$ complexes within the same ligand framework, and (ii) to explore similarities or differences between compounds having $Ti{=}NNPh_2$ and $Ti{=}NNMe_2$ functional groups.

1.6 References

1. N. Hazari and P. Mountford, *Acc. Chem. Res.*, 2005, **38**, 839.
2. A. P. Duncan and R. G. Bergman, *The Chemical Record*, 2002, **2**, 431.
3. D. E. Wigley, *Prog. Inorg. Chem.*, 1994, **42**, 239.
4. A. L. Odom, *Dalton Trans.*, 2005, 225.
5. P. D. Bolton and P. Mountford, *Adv. Synth. Catal.*, 2005, **347**, 355.
6. J. E. Hill, R. D. Profilet, P. E. Fanwick and I. P. Rothwell, *Angew. Chem. Int. Ed. Engl.*, 1990, **29**, 664.
7. H. W. Roesky, H. Voelker, M. Witt and M. Noltemeyer, *Angew. Chem. Int. Ed. Engl.*, 1990, **29**, 669.
8. C. C. Cummins, C. P. Schaller, G. D. Van Duyne, P. T. Wolczanski, A. W. E. Chan and R. Hoffmann, *J. Am. Chem. Soc.*, 1991, **113**, 2985.
9. P. L. McGrane, M. Jensen and T. Livinghouse, *J. Am. Chem. Soc.*, 1992, **114**, 5459.
10. H. Herrmann, J. L. Fillol, H. Wadepohl and L. H. Gade, *Angew. Chem. Int. Ed.*, 2007, **46**, 8426.
11. T. B. Parsons, N. Hazari, A. R. Cowley, J. C. Green and P. Mountford, *Inorg. Chem.*, 2005, **44**, 8442.
12. Y. Li, Y. Shi and A. L. Odom, *J. Am. Chem. Soc.*, 2004, **126**, 1794.
13. P. J. Walsh, M. J. Carney and R. G. Bergman, *J. Am. Chem. Soc.*, 1991, **113**, 6343.
14. A. J. Blake, J. M. McInnes, P. Mountford, G. I. Nikonov, D. Swallow and D. J. Watkin, *J. Chem. Soc., Dalton Trans.*, 1999, 379.
15. S. Banerjee and A. L. Odom, *Organometallics*, 2006, **25**, 3099.
16. S. Patel, Y. Li and A. L. Odom, *Inorg. Chem.*, 2007, **46**, 6373.
17. K. Weitershaus, H. Wadepohl and L. H. Gade, *Organometallics*, 2009, **28**, 3381.
18. T. Gehrmann, J. L. Fillol, H. Wadepohl and L. H. Gade, *Angew. Chem. Int. Ed.*, 2009, **48**, 2152.
19. H. Herrmann, J. L. Fillol, H. Wadepohl and L. H. Gade, *Angew. Chem. Int. Ed.*, 2007, **46**, 8426.
20. H. Herrmann, J. L. Fillol, T. Gehrmann, M. Enders, H. Wadepohl and L. H. Gade, *Chem. Eur. J.*, 2008, **14**, 8131.

21. J. D. Selby, C. D. Manley, M. Feliz, A. D. Schwarz, E. Clot and P. Mountford, *Chem. Commun.*, 2007, 4937.
22. A. J. Clulow, J. D. Selby, M. G. Cushion, A. D. Schwarz and P. Mountford, *Inorg. Chem.*, 2008, **47**, 12049.
23. J. D. Selby, C. Schulten, A. D. Schwarz, A. Stasch, E. Clot, C. Jones and P. Mountford, *Chem.Commun.*, 2008, 5101.
24. D. J. Mindiola, *Angew. Chem. Int. Ed.*, 2008, **47**, 1557.
25. J. D. Selby, C. D. Manley, A. D. Schwarz, E. Clot and P. Mountford, *Organometallics*, 2008, **27**, 6479.
26. J. D. Selby, M. Feliz, A. D. Schwarz, E. Clot and P. Mountford, *Organometallics*, 2011, **30**, 2295.
27. A. D. Schofield, A. Nova, J. D. Selby, C. D. Manley, A. D. Schwarz, E. Clot and P. Mountford, *J. Am. Chem. Soc.*, 2010, **132**, 10484.
28. A. D. Schofield, A. Nova, J. D. Selby, A. D. Schwarz, E. Clot and P. Mountford, *Chem. Eur. J.*, 2011, **17**, 265.
29. P. J. Tiong, A. D. Schofield, J. D. Selby, A. Nova, E. Clot and P. Mountford, *Chem. Commun.*, 2010, **46**, 85.
30. P. J. Tiong, A. Nova, L. R. Groom, A. D. Schwarz, J. D. Selby, A. D. Schofield, E. Clot and P. Mountford, *Organometallics*, 2011, **30**, 1182.
31. P. J. Tiong, A. Nova, E. Clot and P. Mountford, *Chem. Commun.*, 2011, **47**, 3147.
32. P. J. Tiong, A. Nova, A. D. Schwarz, J. D. Selby, E. Clot and P. Mountford, *Dalton Trans.*, 2012, **41**, 2277.
33. W. A. Nugent and B. L. Haymore, *Coord. Chem. Rev.*, 1980, **31**, 123.
34. N. A. Milas and M. I. Ilipulos, *J. Am. Chem. Soc.*, 1959, **81**, 6089.
35. P. J. Walsh, F. J. Hollander and R. G. Bergman, *J. Am. Chem. Soc.*, 1988, **110**, 8729.
36. P. Mountford, *Chem. Commun.*, 1997, 2127.
37. M. H. Chisholm and I. P. Rothwell, *Amido and Imido metal Complexes - Comprehensive Coordination Chemistry*, Pergamon Press, Oxford, 1987, vol. 2, p. 162.
38. W. A. Nugent and B. L. Haymore, *Coord. Chem. Rev.*, 1980, **31**, 123.
39. W. A. Nugent and J. M. Mayer, *Metal-Ligand Multiple Bonds*, Wiley-Interscience, New York, 1988.

40. L. H. Gade and P. Mountford, *Coord. Chem. Rev.*, 2001, **216-217**, 65.
41. A. L. Odom, *Dalton Trans.*, 2005, 225.
42. R. R. Schrock, *Acc. Chem. Res.*, 1990, **23**, 158.
43. V. C. Gibson, *Adv. Materials*, 1994, **6**, 37.
44. P. J. Wilson, P. A. Cooke, A. J. Blake, P. Mountford and M. Schröder, *New J. Chem.*, 1999, **23**, 271.
45. M. P. Coles, C. I. Dalby, V. C. Gibson, W. Clegg and M. R. J. Elsegood, *J. Chem. Soc., Chem. Commun.*, 1995, 1709.
46. S. Scheuer, J. Fischer and J. Kress, *Organometallics*, 1995, **14**, 2627.
47. C. H. Winter, P. H. Sheridan, T. S. Lewkebandara, M. J. Heeg and J. W. Proscia, *J. Am. Chem. Soc.*, 1992, **114**, 1095.
48. T. S. Lewkebandra, P. H. Sheridan, M. J. Heeg, A. L. Rheingold and C. H. Winter, *Inorg. Chem.*, 1994, **33**, 5879.
49. P. J. Walsh, F. J. Hollander and R. G. Bergman, *Organometallics*, 1993, **12**, 3705.
50. K. E. Meyer, P. J. Walsh and R. G. Bergman, *J. Am. Chem. Soc.*, 1995, **117**, 974.
51. S. Y. Lee and R. G. Bergman, *Tetrahedron*, 1995, **51**, 4255.
52. S. Y. Lee and R. G. Bergman, *J. Am. Chem. Soc.*, 1995, **117**, 5877.
53. S. A. Blum, V. A. Rivera, R. T. Ruck, F. E. Michael and R. G. Bergman, *Organometallics*, 2005, **24**, 1647.
54. A. J. Blake, P. E. Collier, S. C. Dunn, W.-S. Li, P. Mountford and O. V. Shishkin., *J. Chem. Soc., Dalton Trans.*, 1997, 1549.
55. S. C. Dunn, P. Mountford and D. A. Robson, *J. Chem. Soc., Dalton Trans.*, 1997, 293.
56. P. J. Stewart, A. J. Blake and P. Mountford, *J. Organomet. Chem.*, 1998, **564**, 209.
57. P. J. Stewart, A. J. Blake and P. Mountford, *Organometallics*, 1998, **17**, 3271.
58. F. G. N. Cloke, P. B. Hitchcock, J. F. Nixon, D. J. Wilson and P. Mountford, *Chem. Commun.*, 1999, 661.
59. M. E. G. Skinner, D. A. Cowhig and P. Mountford, *Chem. Commun.*, 2000, 1167.
60. A. J. Blake, P. E. Collier, L. H. Gade, P. Mountford, J. Lloyd, S. M. Pugh, M. Schubart, M. E. G. Skinner and D. J. M. Troesch, *Inorg. Chem.*, 2001, **40**, 870.

61. S. R. Dubberley, A. Friedrich, D. A. Willman, P. Mountford and U. Radius, *Chem. Eur. J.*, 2003, **9**, 3634.

62. S. C. Dunn, N. Hazari, N. M. Jones, A. G. Moody, A. J. Blake, A. R. Cowley, J. C. Green and P. Mountford, *Chem. Eur. J.*, 2005, **11**, 2111.

63. S. C. Dunn, N. Hazari, A. R. Cowley, J. C. Green and P. Mountford, *Organometallics*, 2006, **25**, 1755.

64. N. Adams, H. J. Arts, P. D. Bolton, D. Cowell, S. R. Dubberley, N. Friederichs, C. Grant, M. Kranenburg, A. J. Sealey, B. Wang, P. J. Wilson, A. R. Cowley, P. Mountford and M. Schröder, *Chem. Commun.*, 2004, 434.

65. A. E. Guiducci, A. R. Cowley, M. E. G. Skinner and P. Mountford, *J. Chem. Soc., Dalton Trans.*, 2001, 1392.

66. D. J. M. Trösch, P. E. Collier, A. Bashall, L. H. Gade, M. McPartlin, P. Mountford and S. Radojevic, *Organometallics*, 2001, **20**, 3308.

67. B. D. Ward, A. Maisse-Francois, P. Mountford and L. H. Gade, *Chem. Commun.*, 2004, 704.

68. N. Vujkovic, J. L. Fillol, B. D. Ward, H. Wadepohl, P. Mountford and L. H. Gade, *Organometallics*, 2008, **27**, 2518.

69. A. Bashall, P. E. Collier, L. H. Gade, M. McPartlin, P. Mountford and D. T. Trösch, *Chem. Commun.*, 1998, 2555.

70. A. Bashall, P. E. Collier, L. H. Gade, M. McPartlin, P. Mountford, S. M. Pugh, S. Radojevic, M. Schubart, I. J. Scowen and D. J. M. Trösch, *Organometallics*, 2000, **19**, 4784.

71. S. M. Pugh, D. J. M. Trosch, D. J. Wilson, A. Bashall, F. G. N. Cloke, L. H. Gade, P. B. Hitchcock, M. McPartlin, J. F. Nixon and P. Mountford, *Organometallics*, 2000, **19**, 3205.

72. B. D. Ward, G. Orde, E. Clot, A. R. Cowley, L. H. Gade and P. Mountford, *Organometallics*, 2005, **24**, 2368.

73. S. Kahlal, J.-Y. Saillard, J.-R. Hamon, C. Manzur and D. Carrillo, *New J. Chem.*, 2001, **25**, 231.

74. D. A. Fletcher, R. F. McMeeking and D. Parkin, *J. Chem. Inf. Comput. Sci.*, 1996, **36**, 746 (The UK Chemical Database Service: CSD version 5.32 updated August 2011).

75. F. Studt and F. Tuczek, *Angew. Chem. Int. Ed.*, 2005, **44**, 5639.

76. G. C. Stephan, C. Sivasankar, F. Studt and F. Tuczek, *Chem. Eur. J.*, 2008, **14**, 644.
77. S. Kahlal, J.-Y. Saillard, J.-R. Hamon, C. Manzur and D. Carrillo, *J. Chem. Soc., Dalton Trans.*, 1998, 1229.
78. C. Elschenbroich and A. Salzer, *Organometallics: a concise introduction*, 2nd edn., VCH, Weinheim, 1992.
79. E. O. Fischer and A. Maasböl, *Angew. Chem. Int. Ed. Eng.*, 1964, **3**, 580.
80. K. H. Doetz and E. O. Fischer, *Chem. Ber.*, 1972, **105**, 1356.
81. L. J. Guggenberger and R. R. Schrock, *J. Am. Chem Soc.*, 1975, **97**, 6578.
82. R. R. Schrock and P. R. Sharp, *J. Am. Chem Soc.*, 1978, **100**, 2389.
83. B. A. MacKay and M. D. Fryzuk, *Chem. Rev.*, 2004, **104**, 385.
84. M. Hidai and Y. Mizobe, *Chem. Rev.*, 1995, **95**, 1115.
85. F. A. Cotton, G. Wilkinson, C. A. Murillo and M. Bochmann, *Adv. Inorg. Chem.*, 6th edn., Wiley-Interscience, New York, 1999.
86. M. D. Fryzuk and S. A. Johnson, *Coord. Chem. Rev.*, 2000, **200-202**, 379.
87. V. Smil, *Enriching the Earth: Fritz Haber, Carl Bosch, and the Transformation of World Food Production*,, MIT Press, Cambridge, 2004.
88. B. K. Burgess and D. J. Lowe, *Chemical Reviews*, 1996, **96**, 2983.
89. M. P. Coughlan, *Molybdenum and Molybdenum-Containing Enzymes*, Pergamon, New York, 1980.
90. D. Rehder, *Coord. Chem. Rev.*, 1999, **182**, 297.
91. R. R. Eady, *Coord. Chem. Rev.*, 2003, **237**, 23.
92. S. Stefan, S. Klaus, D. Melanie and M. Achim, *Eur. J. Biochem.*, 2002, **269**, 1650.
93. E. Krahn, B. Weiss, M. Kröckel, J. Groppe, G. Henkel, S. Cramer, A. Trautwein, K. Schneider and A. Müller, *J. Biol. Inorg. Chem.*, 2002, **7**, 37.
94. J. Kim and D. C. Rees, *Science*, 1992, **257**, 1677.
95. L. C. Seefeldt, I. G. Dance and D. R. Dean, *Biochemistry*, 2004, **43**, 1401.
96. J. Chatt, A. J. Pearman and R. L. Richards, *J. Chem. Soc., Dalton Trans.*, 1977, 1852.
97. M. Hidai, *Coord. Chem. Rev.*, 1999, **185-186**, 99.
98. R. R. Schrock, *Angew. Chem. Int. Ed.*, 2008, **47**, 5512.
99. R. R. Schrock, *Acc. Chem. Res.*, 2005, **38**, 955.

100. W. W. Weare, X. Dai, M. J. Byrnes, J. M. Chin, R. R. Schrock and P. Mueller, *Proceedings of the National Academy of Sciences*, 2006, **103**, 17099.
101. D. V. Yandulov and R. R. Schrock, *Inorg. Chem.*, 2005, **44**, 1103.
102. R. R. Schrock, *Angew. Chem. Int. Ed.*, 2008, **47**, 5512.
103. M. Hidai, Y. Mizobe, M. Sato, T. Kodama and Y. Uchida, *J. Am. Chem Soc.*, 1978, **100**, 5740.
104. K. Iwanami, Y. Mizobe, T. Takahashi, T. Kodama, Y. Uchida and M. Hidai, *Bull. Chem. Soc. Jpn.*, 1981, **54**, 1773.
105. M. Hidai, Y. Mizobe, M. Sato, T. Kodama and Y. Uchida, *J. Am. Chem. Soc.*, 1978, **100**, 5740.
106. M. Hidai, T. Kodama, M. Sato, M. Harakawa and Y. Uchida, *Inorg. Chem.*, 1976, **15**, 2694.
107. K. Iwanami, Y. Mizobe, T. Takahashi, T. Kodama, Y. Uchida and M. Hidai, *Bull. Chem. Soc. Jpn.*, 1981, **54**, 1773.
108. J. A. McCleverty, A. E. Rae, I. Wolochowicz, N. A. Bailey and J. M. A. Smith, *J. Organomet. Chem.*, 1979, **168**, C1.
109. J. A. McCleverty, A. E. Rae, I. Wolochowicz, N. A. Bailey and J. M. A. Smith, *J. Chem. Soc., Dalton Trans.*, 1983, 71.
110. J. Chatt, *J. Organomet. Chem.*, 1975, **100**, 17.
111. J. Chatt, P. L. Dahlstrom, J. Zubieta and J. R. Dilworth, *J. Chem. Soc. Chem. Comm.*, 1980, 786.
112. C. Bustos, C. Manzur, D. Carrillo, F. Robert and P. Gouzerh, *Inorg. Chem.*, 1994, **33**, 1427.
113. C. Bustos, C. Manzur, D. Carrillo, F. Robert and P. Gouzerh, *Inorg. Chem.*, 1994, **33**, 4937.
114. J. D. Niemoth-Anderson, J. R. D. Debord, T. A. George, C. R. Li and J. J. Stezowski, *Polyhedron*, 1996, **15**, 4031.
115. Z. Janas, L. B. Jerzykiewicz, R. L. Richards and P. Sobota, *Inorg. Chim. Acta*, 2003, **350**, 379.
116. L. D. Field, N. G. Jones and P. Turner, *Organometallics*, 1998, **17**, 2394.
117. C. Redshaw and M. R. Elsegood, *Inorg. Chem.*, 2000, **39**, 5164.
118. S. Banerjee and A. L. Odom, *Dalton Trans.*, 2008, 2005.
119. N. Wiberg, H. W. Häring and O. Schieda, *Angew. Chem. Int. Ed. Eng.*, 1976, **15**, 386.

120. M. Veith, *Angew. Chem. Int. Ed. Eng.*, 1976, **15**, 387.

121. S. C. Davies, D. L. Hughes, Z. Janas, L. Jerzykiewicz, R. L. Richards, J. R. Sanders and P. Sobota, *Chem. Commun.*, 1997, 1261.

122. S. C. Davies, D. L. Hughes, Z. Janas, L. B. Jerzykiewicz, R. L. Richards, J. R. Sanders, J. E. Silverston and P. Sobota, *Inorg. Chem.*, 2000, **39**, 3485.

123. S. C. Davies, D. L. Hughes, M. Konkol, R. L. Richards, J. R. Sanders and P. Sobota, *J. Chem. Soc., Dalton Trans.*, 2002, 2811.

124. R. A. Henderson, Z. Janas, L. B. Jerzykiewicz, R. L. Richards and P. Sobota, *Inorg. Chim. Acta*, 1999, **285**, 178.

125. M. L. H. Green, J. T. James, J. F. Saunders and J. Souter, *J. Chem. Soc., Dalton Trans.*, 1997, 1281.

126. M. L. H. Green, J. T. James and A. N. Chernega, *J. Chem. Soc., Dalton Trans.*, 1997, 1719.

127. I. A. Tonks and J. E. Bercaw, *Inorg. Chem.*, 2010, **49**, 4648.

128. N. Wiberg, H.-W. Haring, G. Huttner and P. Friedrich, *Chem. Ber.*, 1978, **111**, 2708.

129. N. Wiberg, W. C. Joo and W. Uhlenbrock, *Angew. Chem. Int. Ed. Eng.*, 1968, **7**, 640.

130. J. L. Thorman and L. K. Woo, *Inorg. Chem.*, 2000, **39**, 1301.

131. J. R. Dilworth, I. A. Latham, G. J. Leigh, G. Huttner and I. Jibril, *J. Chem. Soc., Chem. Commun.*, 1983, 1368.

132. I. A. Latham, G. J. Leigh, G. Huttner and I. Jibril, *J. Chem. Soc., Dalton Trans.*, 1986, 385.

133. D. L. Hughes, M. Jimenez-Tenorio, G. J. Leigh and D. G. Walker, *J. Chem. Soc., Dalton Trans.*, 1989, 2389.

134. D. L. Hughes, I. A. Latham and G. J. Leigh, *J. Chem. Soc., Dalton Trans.*, 1986, 393.

135. S. C. Yoon, B.-J. Bae, I.-H. Suh and J. T. Park, *Organometallics*, 1999, **18**, 2049.

136. J. T. Park, S. C. Yoon, B.-J. Bae, W. S. Seo, I.-H. Suh, T. K. Han and J. R. Park, *Organometallics*, 2000, **19**, 1269.

137. S. Banerjee, Y. Shi, C. Cao and A. L. Odom, *J. Organomet. Chem.*, 2005, **690**, 5066.

138. S. Banerjee, E. Barnea and A. L. Odom, *Organometallics*, 2008, **27**, 1005.

139. K. Weitershaus, J. L. Fillol, H. Wadepohl and L. H. Gade, *Organometallics*, 2009, **28**, 4747.

140. P. J. Walsh, F. J. Hollander and R. G. Bergman, *J. Am. Chem. Soc.*, 1988, **110**, 8729.

141. H. Herrmann, H. Wadepohl and L. H. Gade, *Dalton Trans.*, 2008, 2111.

142. T. Gehrmann, J. L. Fillol, H. Wadepohl and L. H. Gade, *Organometallics*, 2010, **29**, 28.

143. T. Gehrmann, J. L. Fillol, S. A. Scholl, H. Wadepohl and L. H. Gade, *Angew. Chem. Int. Ed.*, 2011, **50**, 5757.

144. T. Gehrmann, S. A. Scholl, J. L. Fillol, H. Wadepohl and L. H. Gade, *Chem. Eur. J.*, 2012, **18**, 3925.

145. H. Herrmann, J. L. Fillol, H. Wadepohl and L. H. Gade, *Organometallics*, 2008, **27**, 172.

146. H. Herrmann, T. Gehrmann, H. Wadepohl and L. H. Gade, *Dalton Trans.*, 2008, 6231.

147. R. F. Munha, L. F. Veiros, M. T. Duarte, M. D. Fryzuk and A. M. Martins, *Dalton Trans.*, 2009, 7494.

148. G. Bai, H. W. Roesky, H. Hao, M. Noltemeyer and H.-G. Schmidt, *Inorg. Chem.*, 2001, **40**, 2424.

149. Y. Mizobe, Y. Ishii and M. Hidai, *Coord. Chem. Rev.*, 1995, **139**, 281.

150. M. Dartiguenave, M. Joëlle Menu, E. Deydier, D. Yves and H. Siebald, *Coord. Chem. Rev.*, 1998, **178-180**, 623.

151. L. B. Kool, M. D. Rausch, H. G. Alt, M. Herberhold, A. F. Hill, U. Thewalt and B. Wolf, *J. Chem. Soc., Chem. Commun.*, 1986, 408.

152. S. Gambarotta, C. Floriani, A. Chiesi-Villa and C. Guastini, *J. Am. Chem. Soc.*, 1982, **104**, 1918.

153. S. Gambarotta, C. Floriani, A. Chiesi-Villa and C. Guastini, *J. Chem. Soc., Chem. Commun.*, 1982, 1015.

154. S. Gambarotta, C. Floriani, A. Chiesi-Villa and C. Guastini, *J. Am. Chem. Soc.*, 1983, **105**, 7295.

155. J. L. Polse, R. A. Andersen and R. G. Bergman, *J. Am. Chem. Soc.*, 1996, **118**, 8737.

156. J. L. Polse, A. W. Kaplan, R. A. Andersen and R. G. Bergman, *J. Am. Chem. Soc.*, 1998, **120**, 6316.

157. A. W. Kaplan, J. L. Polse, G. E. Ball, R. A. Andersen and R. G. Bergman, *J. Am. Chem. Soc.*, 1998, **120**, 11649.

158. T. E. Hanna, I. Keresztes, E. Lobkovsky, W. H. Bernskoetter and P. J. Chirik, *Organometallics*, 2004, **23**, 3448.

159. G. M. Arvanitis, J. Schwartz and D. Van Engen, *Organometallics*, 1986, **5**, 2157.

160. G. M. Arvanitis, J. Smegal, I. Meier, A. C. C. Wong, J. Schwartz and D. Van Engen, *Organometallics*, 1989, **8**, 2717.

161. V. Tabernero, T. Cuenca and E. Herdtweck, *J. Organomet. Chem.*, 2002, **663**, 173.

Chapter Two

Reactions of cyclopentadienyl-amidinate titanium hydrazides with CO_2, CS_2, and isocyanates

2.1 Introduction

As mentioned in Section 1.2, the chemistry of terminal titanium imido compounds (L)Ti=NR (R = alkyl or aryl) has advanced enormously since being established more than two decades ago.[1-4] A series of reviews[5-11] on the progress in this area of chemistry have been published, where most of the interest concerns reactions of the polar and unsaturated Ti=NR multiple bond itself (formally a $\sigma^2\pi^4$ triple bond in most instances[12-14]) which can undergo addition or exchange reactions with a range of unsaturated substrates. As a development from titanium imido chemistry, our group became interested in exploring the related hydrazido complexes (L)Ti=NNR_2. Although they had been postulated as intermediates in hydrohydrazination catalysis,[15-21] the chemistry of well-defined examples of these species was hardly developed at all until relatively recently. While the first report of a terminal titanium hydrazide was in 1978,[22] the first structurally characterised examples only appeared in 2004 and 2005.[17, 23] Similarly, the first fully authenticated [2+2] cycloaddition product of any Group 4 hydrazide was only reported in 2008.[24]

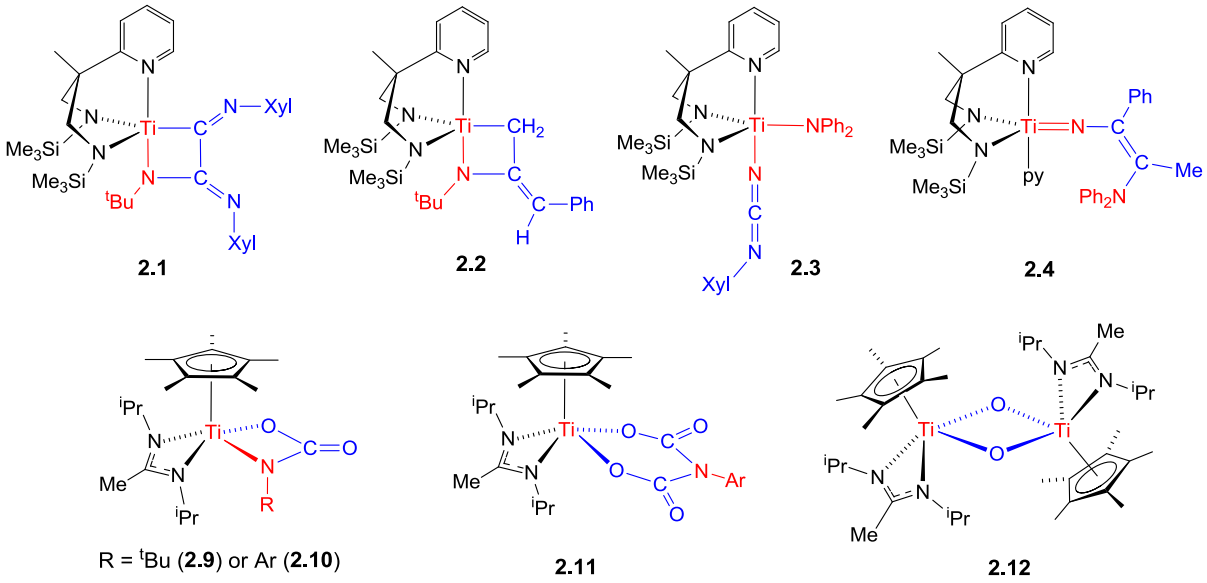

Figure 2.1. Influence of N_α-substituents on reaction outcomes in imido and hydrazido chemistry. Top: for reactions of Ti(N_2N^{py})(NR)(py) (R = ^{t}Bu or NPh_2) with XylNC or PhCCMe.[25, 26] Bottom: for reactions of Cp*Ti{MeC(N^iPr)$_2$}(NR) (R = ^{t}Bu or Ar) with CO_2.[27-29] Atoms derived from the original Ti=NR group are shown in red, while those originating from the organic substrate are shown in blue.

One very distinctive feature of titanium hydrazides and their zirconium congeners is their tendency to undergo facile N_α–N_β bond insertion or cleavage reactions with

substrates such as alkynes, isonitriles, nitriles, CO and heavier chalcogen sources (propylene sulphide or triphenylphosphine selenide), processes that are unavailable to their imido counterparts.[24, 30-35] For example, Ti(N_2N^{py})(N^tBu)(py) reacts with XylNC and PhCCMe to form **2.1** and **2.2** (Figure 2.1) involving coupling or addition reactions across the Ti=N multiple bond.[25, 26] In contrast, Ti(N_2N^{py})($NNPh_2$)(py) forms **2.3** and **2.4** with the same substrates. Mechanistically,[31, 32] these reactions also proceed *via* addition to Ti=N_α, but then lead on to N_α–N_β bond scission. The latter steps formally involve reduction of the nitrogen atoms of the original Ti=N–NPh_2 linkage from -2 in Ti(N_2N^{py})($NNPh_2$)(py) to -3 in the products, and a corresponding net two electron oxidation of the substrates. Accordingly, reactions of Group 4 hydrazides with non-oxidisable substrates such as CO_2, isocyanates and organic nitriles do not give N_α–N_β bond reduction and stop at Ti=N_α cycloaddition or insertion.[24, 32, 36-39]

The main aim of the work described in this Chapter is to gain a better understanding of the reactions of the hydrazide M=N_α bond in both general terms and in comparison with relevant imido counterparts, and also as a function of different β-nitrogen groups which are known to have significant effects on molecular and electronic structure. This aspect of hydrazido chemistry is completely underdeveloped for the following reasons. First, it is only for the recently developed Group 4 systems that any significant M=N_α bond reactivity is seen at all, despite studies of Group 6 hydrazido complexes for many years.[40, 41] The more dative (donor/acceptor) nature of the Group 6 M←:N_α bond and reduced multiple bond character reduces its reactivity. Second, with formally oxidisable substrates, N_α–N_β bond scission readily occurs, effectively masking the initial M=N_α bond reaction. Finally, with regard to comparing different $N_\beta R_2$ groups, there are relatively few homologous pairs or series of complexes of this type.[42-44] A significant cause of this problem is the well-established tendency of Group 4 N_β-dialkyl substituted hydrazides to dimerise forming unreactive $M_2(\mu_2\text{-}NNR_2)_2$ moieties.[17, 23, 44, 45]

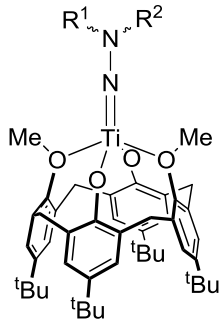

2.5
$R^1 = R^2$ = Ph or Me; R^1 = Ph, R^2 = Me

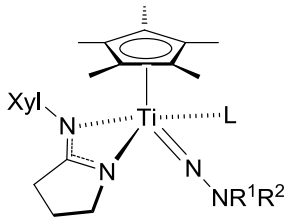

2.6
$R^1 = R^2$ = Ph or Me; R^1 = Ph, R^2 = Me
L = ^{t}BuNH$_2$, py, DMAP or none

Although a series of well-defined terminal hydrazides Ti(Me$_2$Calix)(NNR^{1}R^2) (**2.5**; $R^1 = R^2$ = Ph or Me; R^1 = Ph, R^2 = Me) (Me$_2$Calix = dianion of 1,3-dimethyl ether of *p-tert*-butyl calix[4]arene) had previously been reported by our group with the aim of making a comparative study of the various Ti=NNR^{1}R^2 groups, their negligible intrinsic reactivity caused this approach to fail.[43] Up until 2010, only one other report has appeared describing comparative reactions of different N_β-substituted M=N–NR$_2$ functional groups.[37] In that report, Gade *et al*. found rather similar [2+2] cycloaddition reaction chemistry between Cp*Ti(N^{Xyl}N)(NNR^{1}R^2)(L) (**2.6**; $R^1 = R^2$ = Ph, L = ^{t}BuNH$_2$; R^1 = Ph, R^2 = Me, L = py; Xyl = 3,5-C$_6$H$_3$Me$_2$) and phenyl allene, PhNCO and PhNCS. Reactions of the dimethylhydrazido homologue Cp*Ti(N^{Xyl}N)(NNMe$_2$)(L) (which has a tendency to lose L and dimerise) with these substrates was not reported.

As a renewed attempt to develop the chemistry of the hydrazide Ti=N_α bond, it was decided to target the hydrazido analogues of the *tert*-butyl and aryl imido complexes Cp*Ti{MeC(N^{i}Pr)$_2$}(NR) for several reasons. These undergo a number of different transformations of the Ti=NR bond with a wide range of substrates, namely CO$_2$, CS$_2$, COS, RNCO, RNCS, PhNO, RCONH$_2$, and RCOR′.[27-29, 46, 47] These systems, which have been studied in detail both experimentally and by DFT, are also rather sensitive to the identity of the imido N-substituent, making them good candidates for developing a comparison with hydrazido chemistry. For example, reactions of both Cp*Ti{MeC(N^{i}Pr)$_2$}(N^{t}Bu) (**2.7**) and Cp*Ti{MeC(N^{i}Pr)$_2$}(NAr) (**2.8**, Ar = Tol, 4-C$_6$H$_4$CF$_3$, 4-C$_6$H$_4$NMe$_2$, 2,6-C$_6$H$_3$Me$_2$) with CO$_2$ form [2+2] cycloaddition products **2.9** and **2.10** (Figure 2.1). However, while **2.8** react with a further equivalent of CO$_2$ to form the "double insertion" products **2.11**, the *tert*-butyl homologue does not, giving instead ^{t}BuNCO extrusion and the μ-oxo dimer [Cp*Ti{MeC(N^{i}Pr)$_2$}(μ-O)]$_2$

(**2.12**). In a separate study, it was reported that the reaction of Ti(N^{t}Bu)(COT) (COT = η^8-C_8H_8) with 2 equivalents of ^{t}BuCP generated complex Ti{N(^{t}Bu)PC(^{t}Bu)PC(^{t}Bu)}(COT). However, when the reaction was carried out using Ti(NAr)(COT) (Ar = 2,6-^{i}Pr$_2$C$_6$H$_3$) in the presence of an excess ^{t}BuCP, the organic compound N(Ar)P$_2$C$_2$^{t}Bu$_2$ was the only isolable product, although DFT studies suggest that both reactions proceed through a [2+2] cycloaddition intermediate.[48]

This Chapter includes a combined experimental and DFT investigation of the synthesis, structures and reactivity of cyclopentadienyl-amidinate supported hydrazido complexes. Parts of this work have been communicated.[39, 49] The DFT calculations were performed by our collaborators (Dr. Eric Clot and Dr Ainara Nova) at Université Montpellier.

2.2 Improved synthesis and molecular structures of half-sandwich titanium hydrazido complexes

The previously-reported hydrazido compounds Cp*Ti{MeC(N^{i}Pr)$_2$}(NNR^{1}R^2) (R^1 = Ph, R^2 = Ph (**2.13**) or Me (**2.14**); R^1 = R^2 = Me (**2.15**)) were initially prepared from Cp*Ti{MeC(N^{i}Pr)$_2$}(N^{t}Bu) (**2.7**) and the corresponding hydrazines at room temperature according to Equation 2.1 using the *tert*-butyl imide-hydrazine exchange strategy introduced by our group previously.[36] An analogous approach had also proved successful for preparing the aryl imido complexes Cp*Ti{MeC(N^{i}Pr)$_2$}(NAr) (**2.8**).[29, 47] Initial synthesis of compounds **2.13** – **2.15** gave only *ca*. 35 – 50% isolated yield.[30,50] In this Thesis, optimised syntheses resulted in the isolation of compounds **2.13** and **2.15** as yellow or dark green solids in 83 and 67% yields, respectively.

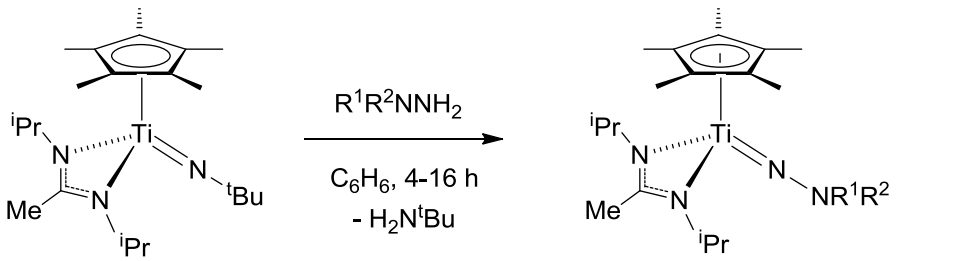

2.7

R^1 = Ph, R^2 = Ph (**2.13**) or Me (**2.14**)
R^1 = R^2 = Me (**2.15**)

Equation 2.1

The attempts to vary the cyclopentadienyl-amidinate supporting ligand set in a way that was successful for the analogous aryl imido systems[47] were unrewarding.[50] For

example, treatment of Cp*Ti{PhC(NSiMe$_3$)$_2$}(N^{t}Bu)[51] with Ph_2NNH_2 in toluene-d_8 at room temperature or 100 ℃ for 3 days gave no reaction. With Me_2NNH_2, no reaction occurred at room temperature while at higher temperatures an unknown mixture of products was formed.[50] Reactions of Cp′Ti{PhC(NSiMe$_3$)$_2$}(N^{t}Bu)[47] (Cp′ = C_5H_4Me) with Ph_2NNH_2 or $PhMeNH_2$ were found to be more promising, but the products were oils which were difficult to manipulate and purify. These suggest that suitable supporting ligand sets play an important role in ensuring the successful synthesis of new half-sandwich titanium hydrazido complexes.

The ^{1}H and ^{13}C{^{1}H} NMR data for **2.13** – **2.15** are analogous to those reported previously and consistent with the C_s symmetric structures depicted in Equation 2.1. The molecular structures were previously determined[50] and are shown in Figures 2.2 and 2.3, and selected distances and angles are listed in Table 2.1. The compounds possess a three-legged piano stool geometry around titanium with η^5-C_5Me_5 and κ^2*N*,*N*′ acetamidinate ligands. The metric parameters associated with the Cp*Ti{MeC(N^{i}Pr)$_2$} fragments are similar in all three and comparable to those reported previously for imido compounds of the type Cp^{R}Ti{R^{1}C(NR^2)$_2$}(NR^3).[29, 47] The main point of interest is the variation in the Ti=NNR^{1}R^2 linkages as a function of the β-N substituents. One such homologous series had been structurally characterised previously, namely Ti(Me$_2$Calix)(NNR^{1}R^2) (**2.5**; R^1 = Ph, R^2 = Ph or Me; R^1 = R^2 = Me). Gade *et al*. has also structurally characterised the series Cp*Ti(N^{Xyl}N)(NNR^{1}R^2)(L) (**2.6**) with the same hydrazide ligands as in **2.13** – **2.15** and **2.5**, but here the donor ligand L (py, DMAP or none) varies in each case making precise comparisons difficult.

In general terms, the Ti=N$_\alpha$ and N$_\alpha$–N$_\beta$ distances, and angles subtended at N$_\alpha$ and N$_\beta$ are all comparable to (L)Ti=NNR^{1}R^2 complexes reported previously (R^1, R^2 = alkyl, aryl, H).[52, 53] The short avg. Ti=N$_\alpha$ bond distance of 1.730 Å and approximately linear Ti=N$_\alpha$–N$_\beta$ angle (avg. 163 °) are consistent with a $\sigma^2\pi^4$ triple bond and formally dianionic [NNR^{1}R^2]$^{2-}$ ligands (see below for a DFT analysis).[23, 42, 54] The N$_\beta$ atoms for the phenyl-substituted compounds **2.13** and **2.14** are planar within error (due to conjugation of the lone pair with the phenyl ring(s)[42, 54]) whereas that of **2.15** is pyramidal. The sum of the angles subtended at N(2) in this case is 334.3(2) °, close to that expected for formal *sp*^{3} hybridisation (328.4 °).

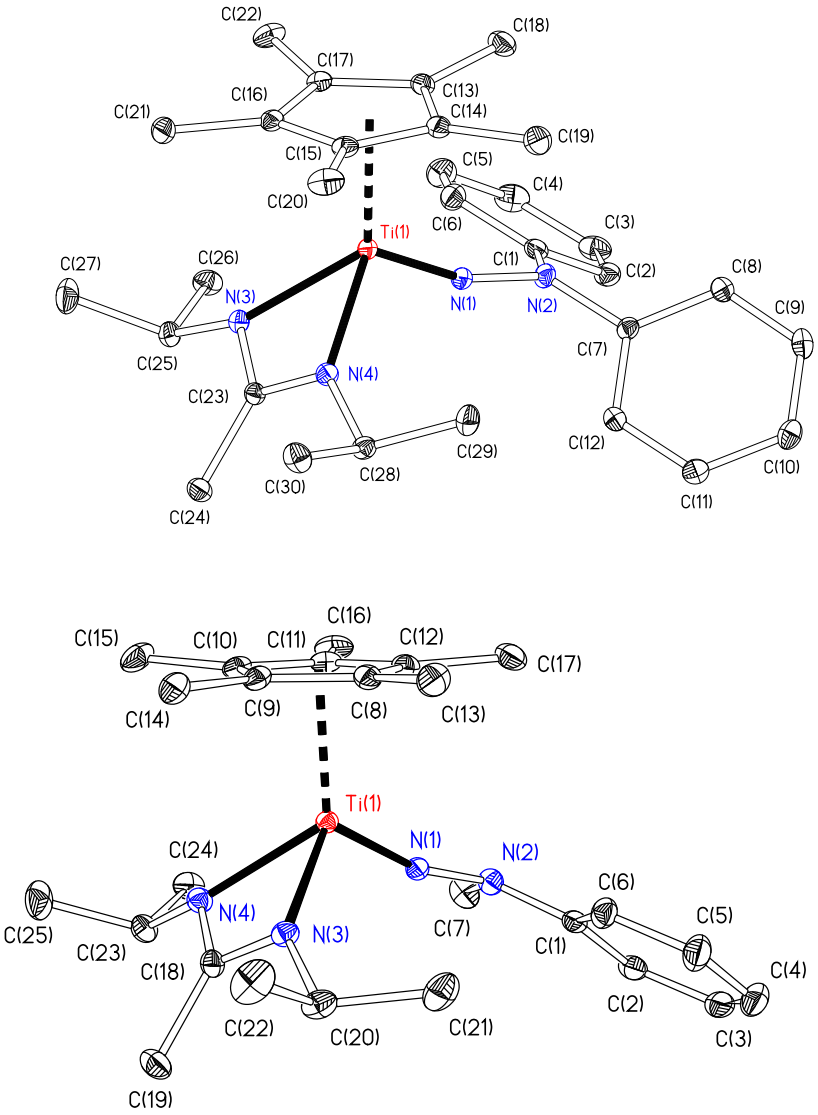

Figure 2.2. Displacement ellipsoid plots (25% probability) of Cp*Ti{MeC(N^{i}Pr)$_2$}(NNPh$_2$) (**2.13**) (top) and Cp*Ti{MeC(N^{i}Pr)$_2$}(NNMePh) (**2.14**) (bottom). H atoms omitted for clarity.[50]

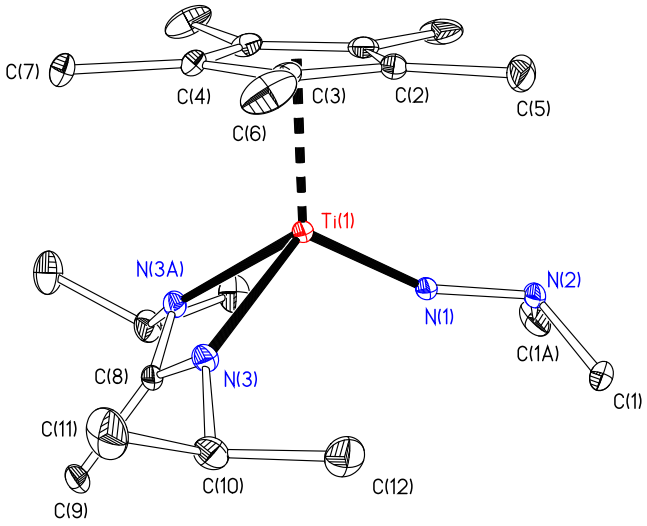

Figure 2.3. Displacement ellipsoid plot (20% probability) of Cp*Ti{MeC(N^{i}Pr)$_2$}(NNMe$_2$) (**2.15**). H atoms omitted for clarity. Atoms carrying the suffix 'A' are related to their counterparts by the symmetry operator *x*, *y*, -*z*+$^{3}/_{2}$).[50]

The Ti=N$_\alpha$ and N$_\alpha$–N$_\beta$ distances for **2.13** and **2.14** are identical within error. Although those for **2.15** are shorter and longer, respectively, the differences are not significant. A similar trend in N$_\alpha$–N$_\beta$ distance was found for the calixarene-supported compounds **2.5**, and Group 4 N$_\beta$-dialkyl substituted hydrazides generally have longer N$_\alpha$–N$_\beta$ distances and pyramidal N$_\beta$ atoms.[52, 53] The N$_\alpha$–N$_\beta$ single bond in free Me$_2$NNH$_2$ (1.436(2) Å, pyramidal N<u>N</u>Me$_2$) is likewise longer than that in Ph$_2$NNH$_2$ (1.418(2) Å, planar N<u>N</u>Ph$_2$), apparently due to N$_\beta$ hybridisation effects.[54, 55]

The Ti=N$_\alpha$ distances for **2.13** and **2.14** are equivalent within error to the value of 1.738(2) Å found for Ti=N in the aryl imide Cp*Ti{MeC(N^{i}Pr)$_2$}(N-2,6-C$_6$H$_3$Me$_2$), while that of **2.15** is slightly shorter.[47] Within the series **2.13** – **2.15** the Ti=N$_\alpha$ bond distances vary in the order Ti=NNPh$_2$ ~ Ti=NNMePh > Ti=NNMe$_2$, with Δ(Ti=N$_\alpha$) = 0.011(3) Å between **2.15** and **2.13** or **2.14**. In contrast, the corresponding distances for Ti(Me$_2$Calix)(NNR^{1}R^2) (**2.5**) vary in the opposite way with Ti=NNPh$_2$ < Ti=NNMePh ~ Ti=NNMe$_2$ (1.717(2), 1.727(3) and 1.729(4) Å, respectively),[43] although all were longer than Ti=N in Ti(Me$_2$Calix)(N^{t}Bu) (1.705(3) Å).[56]

Table 2.1. Selected bond lengths (Å) and angles (°) for Cp*Ti{MeC(N^{i}Pr)$_2$}(NNPh$_2$) (**2.13**), Cp*Ti{MeC(N^{i}Pr)$_2$}(NNMePh) (**2.14**) and Cp*Ti{MeC(N^{i}Pr)$_2$}(NNMe$_2$) (**2.15**). Cp$_{cent}$ is the computed Cp* ring carbon centroid. Atoms carrying the suffix 'A' are related to their counterparts by the symmetry operator *x*, *y*, -*z*+$^3/_2$).[50]

Parameter	**2.13**	**2.14**	**2.15**
Ti(1)-Cp$_{cent}$	2.097	2.067	2.063
Ti(1)-N(1)	1.734(2)	1.734(2)	1.723(2)
Ti(1)-N(3)	2.115(2)	2.110(2)	2.101(1)
Ti(1)-N(4)	2.099(2)	2.090(2)	–
N(1)-N(2)	1.369(2)	1.371(3)	1.386(2)
N(2)-C(1)	1.409(3)	1.396(4)	1.461(2)
N(2)-C(7)	1.425(3)	1.460(4)	–
Cp$_{cent}$-Ti(1)-N(1)	121.4	121.1	119.5
Cp$_{cent}$-Ti(1)-N(3)	120.8	121.8	120.8
Cp$_{cent}$-Ti(1)-N(4)	119.6	119.7	–
N(3)-Ti(1)-N(4)/N(3A)	64.23(7)	64.44(9)	64.45(7)
Ti(1)-N(1)-N(2)	163.9(1)	166.3(2)	159.5(1)
N(1)-N(2)-C(1)	118.9(2)	118.2(2)	110.7(1)
N(1)-N(2)-C(7)/C(1A)	116.7(2)	115.3(2)	110.7(1)
C(1)-N(2)-C(7)/C(1A)	121.5(2)	120.8(2)	112.9(2)

DFT was employed to explore this further by calculating the geometries of the simplified model imido and hydrazido compounds CpTi{MeC(NMe)$_2$}(NR) (R = Me (**1Q_Me**) or Ph (**1Q_Ph**)) and CpTi{MeC(NMe)$_2$}(NNR^{1}R^2) (R^1 = Ph, R^2 = Ph (**1Q_NPh$_2$**) or Me (**1Q_NMePh**); R^1 = R^2 = Me (**1Q_NMe$_2$**)) as illustrated in Figure 2.4. A further model was calculated based on CpTi{MeC(NMe)$_2$}(NNMe$_2$) but this time with a constrained NNMe$_2$ group in which the geometry at N$_\beta$ was forced to be planar (**1Q_NMe$_2$_planar**). Model **1Q_NMe$_2$_planar** was 4.6 kcal mol^{-1} less stable than the fully relaxed **1Q_NMe$_2$**.

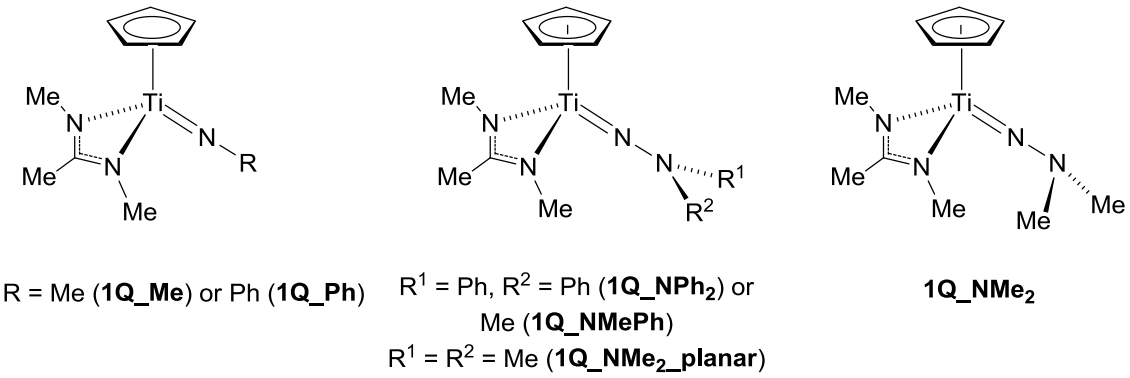

Figure 2.4. Model complexes used in the DFT calculations. Selected distances (Å): Ti=N = 1.688 (**1Q_Me**), 1.709 (**1Q_Ph**), 1.713 (**1Q_NPh$_2$**), 1.714 (**1Q_NMePh**), 1.716 (**1Q_NMe$_2$_planar**) and 1.705 (**1Q_NMe$_2$**); N_α–N_β = 1.345 (**1Q_NPh$_2$**), 1.339 (**1Q_NMePh**), 1.329 (**1Q_NMe$_2$_planar**) and 1.360 (**1Q_NMe$_2$**).

2.3 DFT analysis of molecular and electronic structures and imide-hydrazine exchange energies

The DFT trend in Ti=N_α distances (Ti=NNPh$_2$ ~ Ti=NNMePh > Ti=NNMe$_2$) for the model hydrazides **1Q_NPh$_2$**, **1Q_NMePh**, and **1Q_NMe$_2$** is consistent with that observed experimentally, although the computed distances are systematically shorter due to the reduced bulk of the models. The trends in N_α–N_β distances and angles at N_α and N_β are likewise consistent. In particular, the longest N_α–N_β distance is associated with the shortest Ti=N_α (i.e. **1Q_NMe$_2$**) and *vice versa*. The reason for the longer Ti=N_α distance in **1Q_NPh$_2$** and **1Q_NMePh** is better conjugation of the N_β lone pair denoted (N_β-LP) with the Ti=N_α π^* orbital as a result of the planarity at N_β. Consistent with this, on forcing the N_β atom of **1Q_NMe$_2$** to be planar (giving **1Q_NMe$_2$_planar**) there was a 0.011 Å lengthening of Ti=N_α and a 0.031 Å shortening of N_α–N_β compared to **1Q_NMe$_2$**. The better conjugation of N_β-LP in **1Q_NMe$_2$_planar** is illustrated by a 24 kcal mol^{-1} increase in the donation of N_β-LP into the Ti=N_α π^* orbital as obtained in the NBO (natural bond orbital) second-order perturbation analysis of donor-acceptor interactions.[57] A smaller shortening of the N–Me distances (0.018 Å) was also seen, attributed to the reduction in covalent radius of N_β on going from sp^3 to sp^2 hybridisation.

The Ti=NPh distance in **1Q_Ph** lies between those of **1Q_NPh$_2$** and **1Q_NMe$_2$** which is slightly different from the experimental results for Cp*Ti{MeC(N^{i}Pr)$_2$}(NXyl), but steric effects associated with the xylyl group could lengthen the Ti=NAr bond. The Ti=NMe distance in **1Q_Me** was the shortest of all; consistent with previous structural comparisons of homologous pairs of titanium alkyl and aryl imido complexes.[58-61] The longer Ti=N bond distance in **1Q_Ph** compared to that in **1Q_Me** is due to the π-accepting character of the Ph group as illustrated by the larger donation (by 14 kcal mol^{-1}) from Ti=N π to π* orbital on Ph compared to the reverse donation from π on Ph toward Ti=N π* orbital. Such electron transfer interactions are absent in **1Q_Me**.

Overall, the experimental and DFT results show that while alkyl imides should have the shortest Ti=N$_\alpha$ bonds, those for aryl imide and alkyl or aryl hydrazide ligands are more similar to each other. With respect to the Ti=NNR$_2$ systems, the geometry at N$_\beta$ has the greatest influence on the Ti=N$_\alpha$ and N$_\alpha$–N$_\beta$ bond lengths. For a planar N$_\beta$ the different substituents have a smaller but noticeable (for the DFT models) effect on the Ti=N$_\alpha$ and N$_\alpha$–N$_\beta$ distances.

As mentioned, compounds **2.13** – **2.15** were prepared from **2.7** and the appropriate hydrazine using an exchange strategy well-established for synthesising aryl imido complexes. To gain additional insights into the underlying energetics of these reactions (which experimentally all proceed to completion) the energies of the isodesmic processes were computed (see Figure 2.5) using the model systems in Figure 2.4. The *tert*-butyl imide-hydrazine exchange reactions are all somewhat more favourable than the reaction with PhNH$_2$. Ph$_2$NNH$_2$ is calculated to provide the most energetically favourable exchange reaction, but there is little difference between the three hydrazines studied.

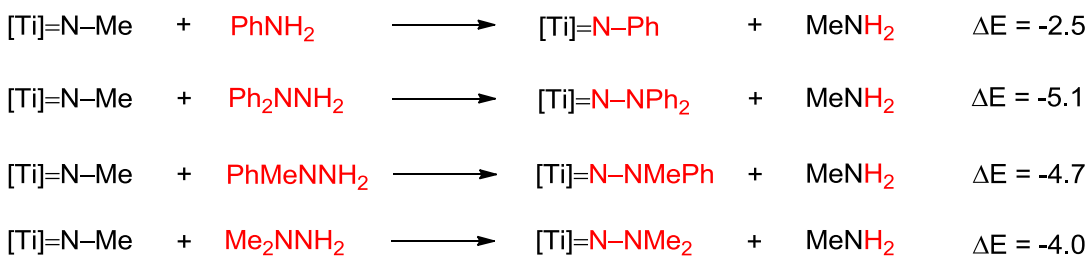

Figure 2.5. DFT computed electronic energies (kcal mol^{-1}) for the isodesmic reactions illustrated. [Ti] represents CpTi{MeC(NMe)$_2$}.

In this study, comparisons of the computed electronic structures of the Ti=NR and Ti=NNR_2 linkages for the model systems **1Q_Me** through **1Q_NMe_2** were also carried out. The electronic structures of titanium imido compounds have been studied in detail,[9, 12-14, 62-65] and a number of DFT investigations of the bonding in hydrazides have also been reported.[23, 42, 54, 66-68] There has been one DFT report comparing the electronic structure of Ti=NMe, Ti=NPh and Ti=$NNPh_2$ ligands within the same supporting ligand framework, namely Ti{$HC(pz)_3$}$(NR)Cl_2$ as models for real systems of the type Ti{$HC(Me_2pz)_3$}$(NR)Cl_2$.[23, 69-72] The effects of varying the N_β substituents or geometry were not assessed.

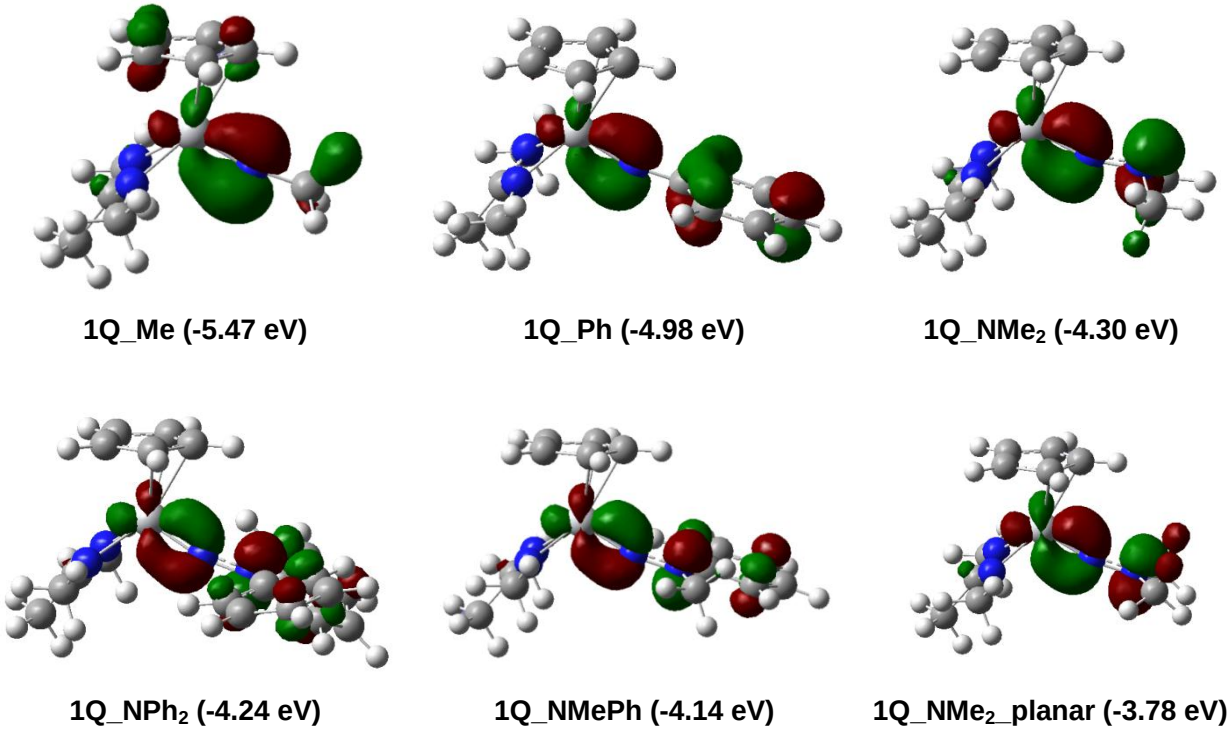

Figure 2.6. Isosurfaces and energies of the π_v MOs of CpTi{$MeC(NMe)_2$}(NR) (R = Me (**1Q_Me**), Ph (**1Q_Ph**), NPh_2 (**1Q_NPh_2**), NMePh (**1Q_NMePh**) or NMe_2 (**1Q_NMe_2** or **1Q_NMe_2_planar**).

All six model systems, **1Q_Me** through to **1Q_NMe_2** and **1Q_NMe_2_planar**, have a formal Ti=N_α triple bond containing two principal d_π-p_π π-bonding molecular orbitals which form, or contribute to, the three highest MOs of the complexes. One MO (denoted π_v) lies in the molecular mirror plane and the other lies perpendicular to it (π_h). The π_h energies are relatively insensitive to the N_α-substituents and vary non-systematically due to different degrees of mixing with the out-of-phase $2p_\pi$

contribution of amidinate N atoms. The π_v MOs do not mix significantly with the supporting ligand orbitals and also interact with the N_α-substituent (Ph, NR_2) orbitals. The π_v MOs for the six models are depicted in Figure 2.6 along with their energies.

Compared to CpTi{MeC(NMe)$_2$}(NMe) (**1Q_Me**), the phenyl substituent in **1Q_Ph** leads to a destabilisation of π_v by +0.49 eV due to a π^* antibonding interaction with one of the occupied ring MOs. This value is within the ranges determined previously by DFT and/or photoelectron spectroscopy.[14, 23] As expected,[23, 42, 54, 67, 68] introduction of $NNPh_2$ in **1Q_NPh$_2$** gives a larger destabilisation (+1.23 eV) due to the N_β atom lone pair. The π_v MO in **1Q_NMePh** is slightly more destabilised compared to **1Q_NPh$_2$** (+0.1 eV) and that in **1Q_NMe$_2$_planar** is the least stable (+0.46 eV *cf.* **1Q_NPh$_2$**; +1.69 eV *cf.* **1Q_Me**). Allowing **1Q_NMe$_2$_planar** to relax to **1Q_NMe$_2$** stabilises π_v by 0.52 eV. The destabilisation along the series **1Q_NPh$_2$**, **1Q_NMePh**, **1Q_NMe$_2$_planar** follows the reduction in delocalisation of the N_β lone pair by the phenyl ring(s) and tracks the changes in Ti=N_α and N_α–N_β noted above. The eventual similarity in energy of π_v (avg. 4.23, range 0.16 eV) for **1Q_NPh$_2$**, **1Q_NMePh** and **1Q_NMe$_2$** arises from two different means of stabilisation: conjugation with the N_β-phenyl group(s) or N_β pyramidalisation.

2.4 Reactions of Cp*Ti{MeC(N^{i}Pr)$_2$}(NNR$_2$) (R = Ph (2.13) or Me (2.15)) with CO$_2$ and CS$_2$

Both **2.13** and **2.15** react with CO_2 and CS_2 rather similarly and so the two systems will be discussed alongside each other in this Section. Their reactions with isocyanates and isothiocyanates on the other hand differed significantly depending upon the β-NR_2 group. These are discussed separately later on. Concurrent with this research, studies on the reactivity of Cp*Ti{MeC(N^{i}Pr)$_2$}(NNMePh) (**2.14**) with small unsaturated molecules were undertaken by an MChem student, Laura Groom, within our group under the author's day-to-day supervision. The reaction outcomes were analogous to those of **2.13** and thus will not be discussed in this thesis.[49] The reactions of **2.13** and **2.15** with CO_2 and CS_2 are summarised in Scheme 2.1. Discussions on DFT studies of these reactions, varying both the Ti=NR group (Ph, NPh_2, NMe_2) and the substrate (CO_2, CS_2, MeNCO) will follow.

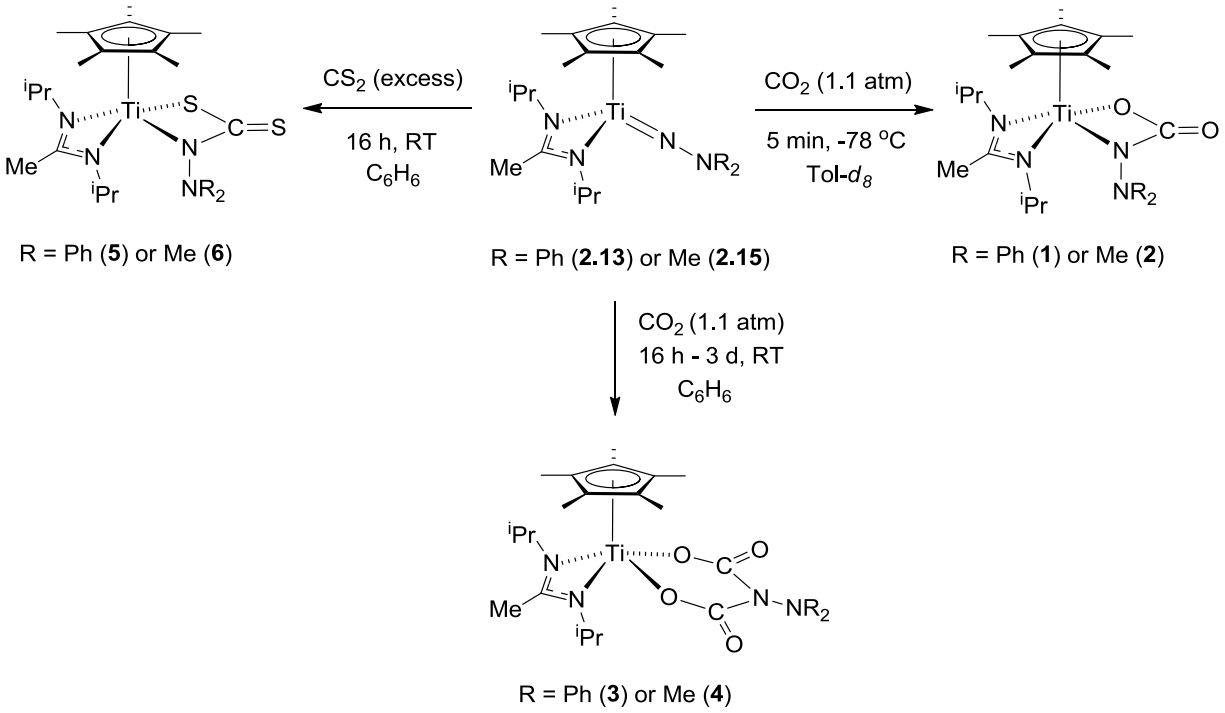

Scheme 2.1. Reactions of Cp*Ti{MeC(N^{i}Pr)$_2$}(NNR$_2$) (R = Ph (**2.13**) or Me (**2.15**)) with CO_2 and CS_2.

2.4.1 Reactions of Cp*Ti{MeC(N^{i}Pr)$_2$}(NNR$_2$) (R = Ph (2.13) or Me (2.15)) with CO_2

When the reactions of **2.13** and **2.15** with CO_2 (excess, 1.1 atm pressure) were followed by ^{1}H NMR in C_6D_6 first-formed intermediates Cp*Ti{MeC(N^{i}Pr)$_2$}{N(NR$_2$)C(O)O} (R = Ph (**1**) or Me (**2**)) were immediately observed. These subsequently converted into the final products Cp*Ti{MeC(N^{i}Pr)$_2$}{OC(O)N(NR$_2$)C(O)O} (R = Ph (**3**) or Me (**4**)) over 3 days and 16 hours, respectively. Under identical conditions, the reaction of **1** with CO_2 was noticeably slower than that of **2** possibly due to the steric bulk of the diphenyl rings. On a preparative scale, **2.13** and **2.15** were reacted with an excess of CO_2 at -78 ℃ for 5 minutes to give compounds **1** and **2** in reasonable isolated yield of *ca.* 60%. Compound **3** was obtained in 70% yield whereas **4** was obtained in 73% isolated yield (Scheme 2.1).

The solution ^{1}H and ^{13}C{^{1}H} NMR data for **1** and **2** are consistent with the C_1 symmetric N,O-bound carbamate-type [2+2] cycloaddition products proposed in Scheme 2.1. The ^{1}H NMR spectrum of **1** shows two apparent septets for the inequivalent *iso*-propyl methine hydrogens, and four doublets for the two pairs of

diastereotopic methyl groups of the amidinate ligand. The IR spectra showed bands at 1684 (**1**) and 1667 cm^{-1} (**2**) which are attributed to ν(C=O) of the carbamate ligands. The observed values are very similar to the corresponding absorption for Ti(Me_4taa){N(NPh_2)C(O)O} (formed from Ti(Me_4taa)($NNPh_2$) and CO_2; H_2Me_4taa = tetramethyl dibenzotetraaza[14]annulene) which appears at 1685 cm^{-1};[36] and those for imide-derived Cp*Ti{MeC(N^iPr)$_2$}{N(R)C(O)O} (R = ^{t}Bu or aryl) which are observed between 1672 and 1655 cm^{-1}.[29] Compounds **1** and **2** are so far only the second reported [2+2] cycloaddition products formed between CO_2 and a transition metal hydrazide.[36] Both **1** and **2** behave like the aryl imido-derived carbamate **2.10** (Figure 2.1). They are stable in solution for days at room temperature without elimination of the corresponding aminoisocyanates R_2NNCO being observed.

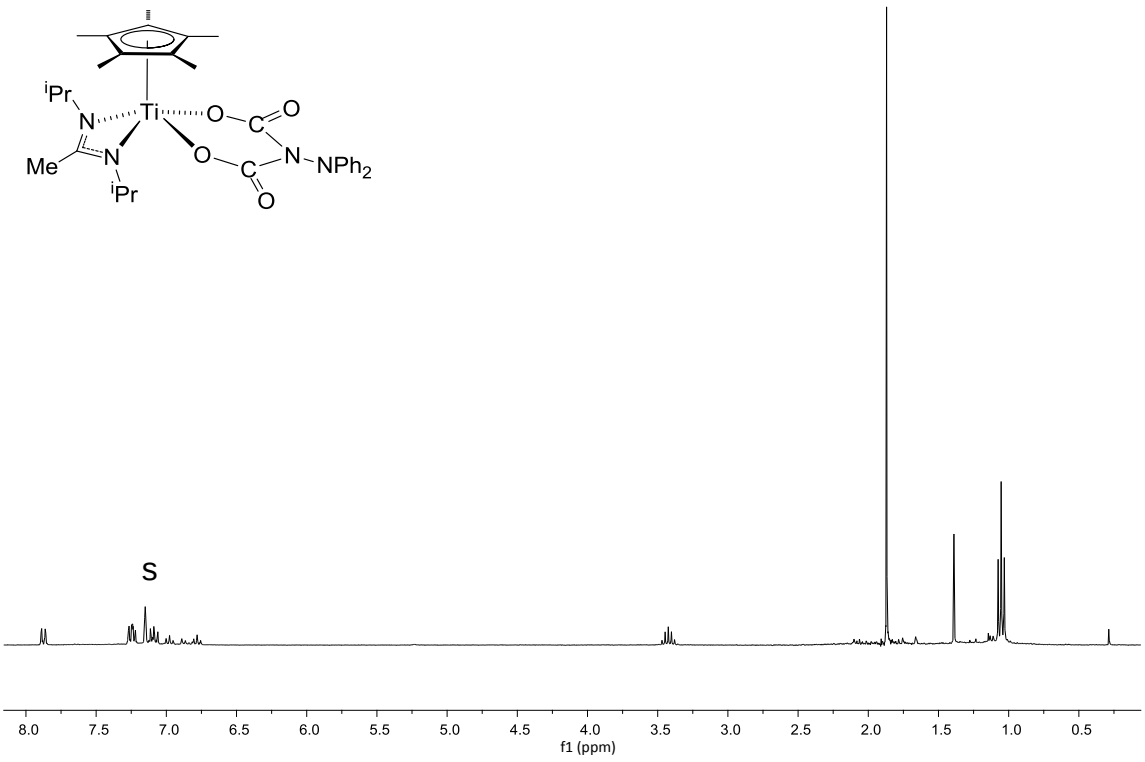

Figure 2.7. ^{1}H NMR spectrum (299.9 MHz) of Cp*Ti{MeC(N^iPr)$_2$}-{OC(O)N(NPh_2)C(O)O} (**3**) in C_6D_6 ("s" denotes residual protio-solvent).

The NMR spectra for **3** and **4** are indicative of C_s symmetric "double insertion" products depicted in Scheme 2.1. The ^{1}H NMR spectrum of **3** is shown in Figure 2.7. It shows one apparent septet for the *iso*-propyl methine hydrogens, and two overlapping doublets for the methyl groups of the amidinate ligand. In addition, their IR spectra show two strong bands at 1715 & 1676 and 1702 & 1655 cm^{-1}, respectively,

consistent with the incorporation of a second CO_2 molecule. The $^{13}C\{^1H\}$ spectra show only one C=O resonance (δ 152.7 and 152.8 ppm respectively) which suggests that these bands are attributed to the symmetric and antisymmetric ν(C=O) modes of a dicarboxylate OC(O)N(NR_2)C(O)O ligand. The corresponding absorptions for the imido-derived compounds **2.11** (Figure 2.1) appear between 1704 – 1694 and 1658 – 1651 cm^{-1}.

Diffraction-quality crystals of both **3** and **4** were grown by slow evaporation of a diethyl ether solution. The molecular structures are shown in Figure 2.8 and selected distances and angles are listed in Table 2.2. Full crystallographic data are given in the CD Appendix. The crystal structures of **3** and **4** confirm that two molecules of CO_2 have been effectively inserted into the Ti=N_α (formally triple[23]) bonds of **2.13** and **2.15**.

The solid state structures of both **3** and **4** confirm the four-legged piano stool geometries around the titanium centre. A second molecule of CO_2 has thus inserted into the Ti=N_α bond of **1** and **2**, expanding the four membered metallacycle to the six membered chelating ring. The distances and angles within the new dicarboxylate ligands are analogous to those reported for **2.11**.[29] The atoms of the {TiOC(O)N(N)C(O)O} moieties are approximately coplanar. For **3** the maximum displacement from the least-squares plane is 0.20 Å, and for **4** it is 0.14 Å. The N_α–N_β distance for **3** is 0.020(4) Å shorter than for **4** reflecting the different N_β hybridisation. The β-NR_2 groups are effectively "locked" between the two adjacent C=O groups, consistent with the NMR data which find two chemically inequivalent N_β substituents.

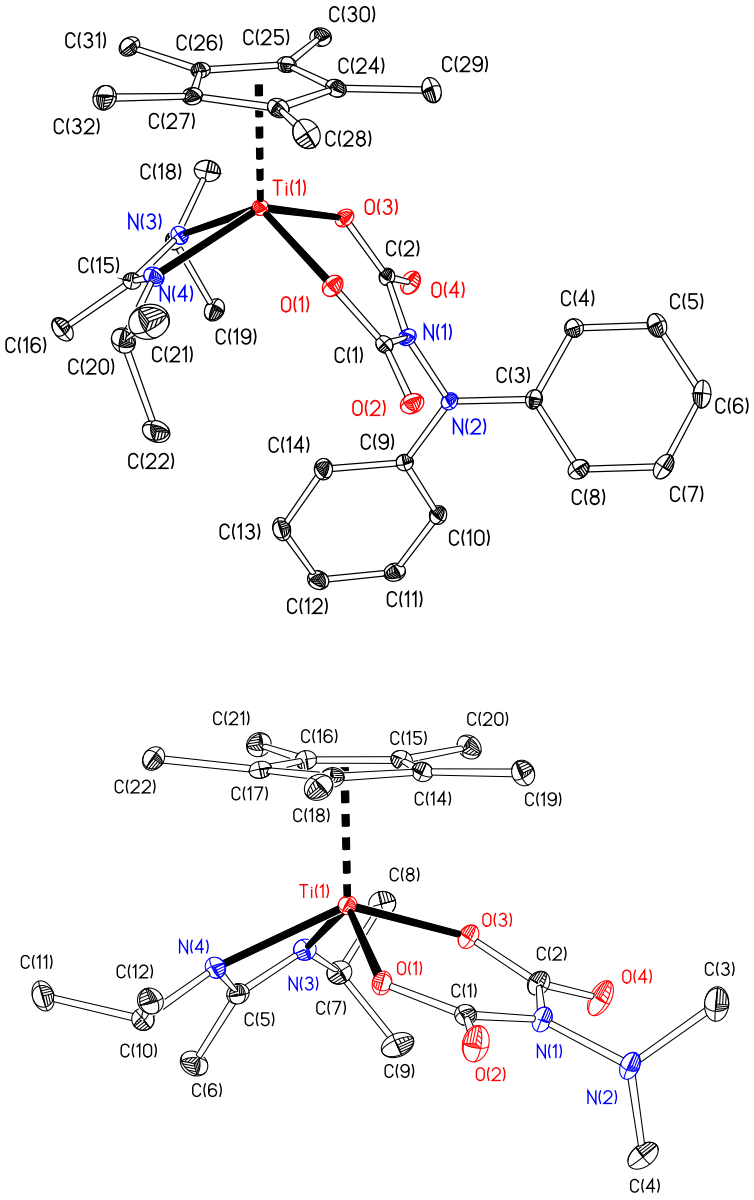

Figure 2.8. Displacement ellipsoid plots (20% probability) of Cp*Ti{MeC(N^{i}Pr)$_2$}-{OC(O)N(NPh$_2$)C(O)O} (**3**) (top) and Cp*Ti{MeC(N^{i}Pr)$_2$}{OC(O)N(NMe$_2$)C(O)O} (**4**) (bottom). H atoms omitted for clarity.

Table 2.2. Selected distances (Å) and angles (°) for Cp*Ti{MeC(N^{i}Pr)$_2$}{OC(O)N(NPh$_2$)C(O)O} (**3**) and Cp*Ti{MeC(N^{i}Pr)$_2$}{OC(O)N-(NMe$_2$)C(O)O} (**4**). Cp$_{cent}$ is the computed Cp* ring carbon centroid.

Parameter	**3**	**4**
Ti(1)-Cp$_{cent}$	2.051	2.053
Ti(1)-O(1)	1.9367(19)	1.9018(18)
Ti(1)-O(3)	1.9512(18)	1.9460(18)
Ti(1)-N(3)	2.059(2)	2.073(2)
Ti(1)-N(4)	2.090(2)	2.123(2)
C(1)-O(2)	1.206(3)	1.209(3)
C(2)-O(4)	1.218(3)	1.213(3)
N(1)-N(2)	1.394(3)	1.414(3)
Cp$_{cent}$-Ti(1)-N(3)	117.3	120.1
Cp$_{cent}$-Ti(1)-N(4)	111.9	114.3
Cp$_{cent}$-Ti(1)-O(1)	114.3	114.5
Cp$_{cent}$-Ti(1)-O(3)	109.5	108.7
N(3)-Ti(1)-N(4)	64.14(9)	63.79(9)
O(1)-Ti(1)-O(3)	82.99(8)	82.63(7)
Ti(1)-O(1)-C(1)	134.43(17)	136.84(16)
Ti(1)-O(3)-C(2)	131.98(16)	136.68(17)
C(1)-N(1)-C(2)	128.3(2)	126.6(2)

The net "double insertion" of two CO_2 molecules into the Ti=N$_\alpha$ bonds of **2.13** – **2.15** is a new transformation for a metal hydrazido compound (mechanistically, a sequential cycloaddition-insertion process). This is also a very unusual process in imido chemistry with the only examples being the insertion of either two CO_2 or two isocyanates into the Ti=NAr bond of **2.8**, or two alkynes into the Ir=N^{t}Bu bond of Cp*Ir(N^{t}Bu).[29, 47, 73] In fact, the OC(O)N(NR$_2$)C(O)O moiety in **3** and **4** is a new structural unit in transition metal chemistry, although Chirik recently reported metal-bound 1,1- or 1,2-NN(CO$_2$)$_2$ ligands prepared from metallocene-N$_2$ complexes and CO_2.[74, 75] The mechanistic studies of this process in the case of **2.11** have been previously reported by our group. Another Ti=N$_\alpha$ bond "insertion", namely the

reaction of $Ti(N_2N^{Me})(NNPh_2)(py)$ (N_2N^{Me} = $MeN(CH_2CH_2NSiMe_3)_2$) with fluorinated benzonitriles to give the hydrazonamide complexes $Ti(N_2N^{Me})\{NC(Ar^F)NNPh_2\}(py)$ (Ar^F = 2,6-$C_6H_3F_2$ or C_6F_5) was recently reported by our group.[32] This reaction proceeds *via* a [2+2] cycloaddition followed by reverse cycloaddition in the opposite sense.

2.4.2 Reactions of Cp*Ti{MeC(N^{i}Pr)$_2$}(NNR$_2$) (R = Ph (2.13) or Me (2.15)) with CS$_2$

Reaction of **2.13** or **2.15** with an excess of CS_2 (3 equivalents) for 16 hours at room temperature afforded the dark brown dithiocarbamates $Cp^*Ti\{MeC(N^iPr)_2\}\{N(NR_2)$-$C(S)S\}$ (R = Ph (**5**) or Me (**6**)). Compound **5** was obtained in a reasonable yield of 71% whereas **6** was obtained in only 42% isolated yield. The relatively high solubility of **6** in hydrocarbon solvents resulted in the disappointing yield. Unfortunately, all attempts to grow diffraction-quality crystals have been unsuccessful. However, spectroscopic and other data are consistent with the C_1 symmetric [2+2] cycloaddition products illustrated in Scheme 2.1.

The ^{1}H NMR spectrum of **5** at room temperature shows very broad signals corresponding to the *iso*-propyl groups of the amidinate ligand, suggesting a fluxional process in the product. This process involves net rotation about the $\{TiN(NPh_2)C(S)S\}$ vector as described previously.[29] Upon cooling to -20 ℃, two apparent septets (3.17 and 3.34 ppm) for the inequivalent *iso*-propyl methine hydrogens, and four doublets (0.86 – 1.10 ppm) for the two pairs of diastereotopic methyl groups of $MeC(N^iPr)_2$ ligand were observed (Figure 2.9). In both cases, further reaction times did not lead to "double-insertion" analogues of **3** and **4**. However, whereas **5** and **6** are stable in solution for days, the corresponding cycloaddition products formed from the imido analogues $Cp^*Ti\{MeC(N^iPr)_2\}(NAr)$ (**2.8**) all eliminate ArNCS forming $[Cp^*Ti\{MeC(N^iPr)_2\}(\mu\text{-}S)]_2$ (**2.16**).[47]

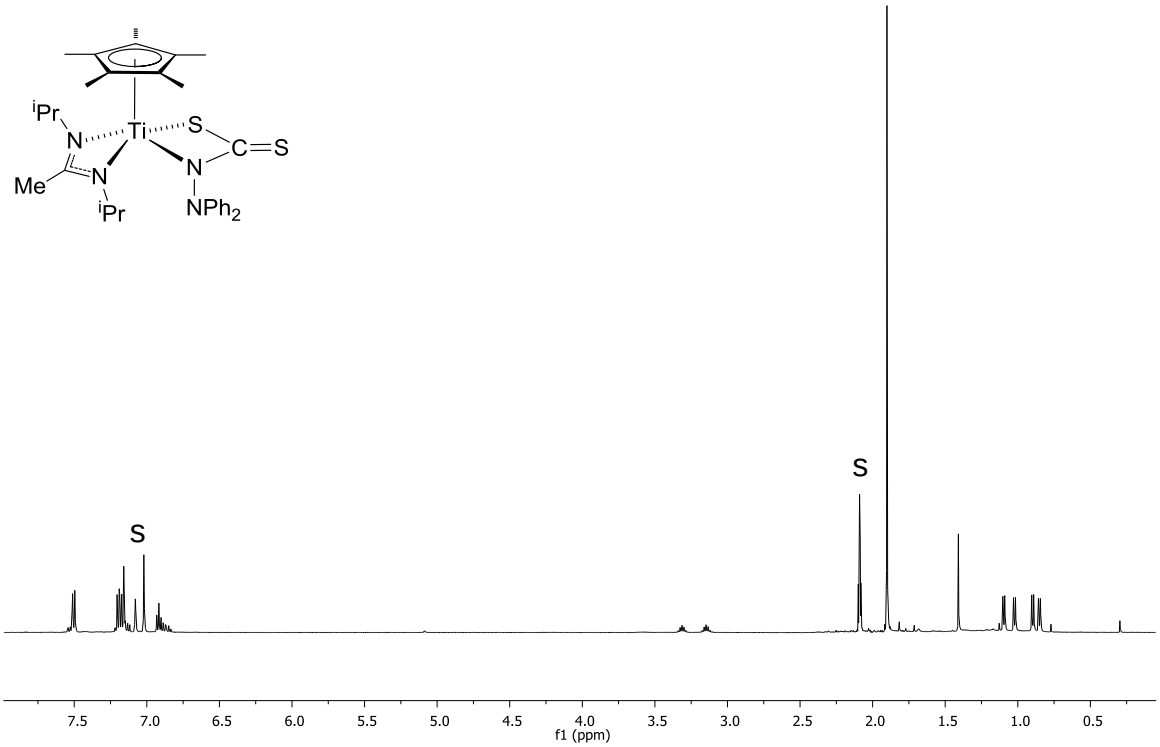

Figure 2.9. ^{1}H NMR spectrum (499.9 MHz) of Cp*Ti{MeC(N^{i}Pr)$_2$}{N(NPh$_2$)C(S)S} (**5**) in toluene-d_8 at -20 ℃ ("ꜱ" denotes residual protio-solvent).

Since CO_2 inserts into the Ti–N bond of **1** to form **3**, the corresponding reaction of CS_2 with **1** was attempted with the hope of forming a mixed CO_2/CS_2 "double insertion" product.

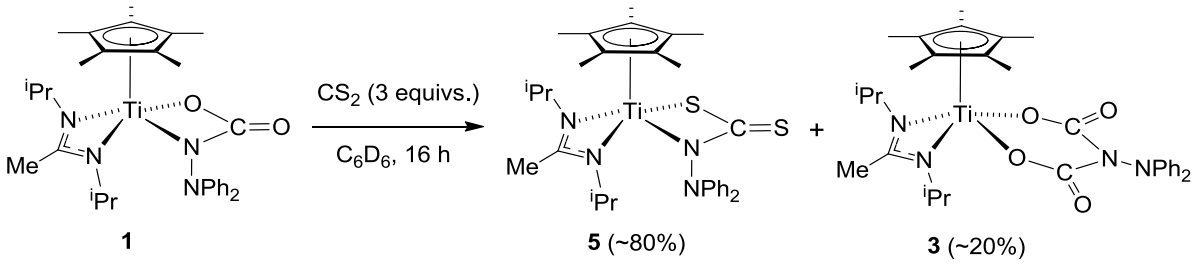

Equation 2.2

Surprisingly, this led to the formation of **5** (major product, *ca.* 80%) along with **3** after 16 hours in C_6D_6 (Equation 2.2). Compound **3** is presumably formed by reaction of **1** with displaced CO_2. In contrast, exposure of **5** to an excess of CO_2 (1.1 atm) for several days gave no reaction. Given the established reversibility of heterocumulene addition to the Ti=NR bonds of **2.7** and **2.8** and other reactions discussed in later Sections, Equation 2.2 probably proceeds *via* a dissociative mechanism transiently

forming **2.13**. Overall these results suggest that [2+2] cycloaddition of CS_2 to the $Ti{=}NNPh_2$ bond of **2.13** is thermodynamically more favourable than addition of CO_2.

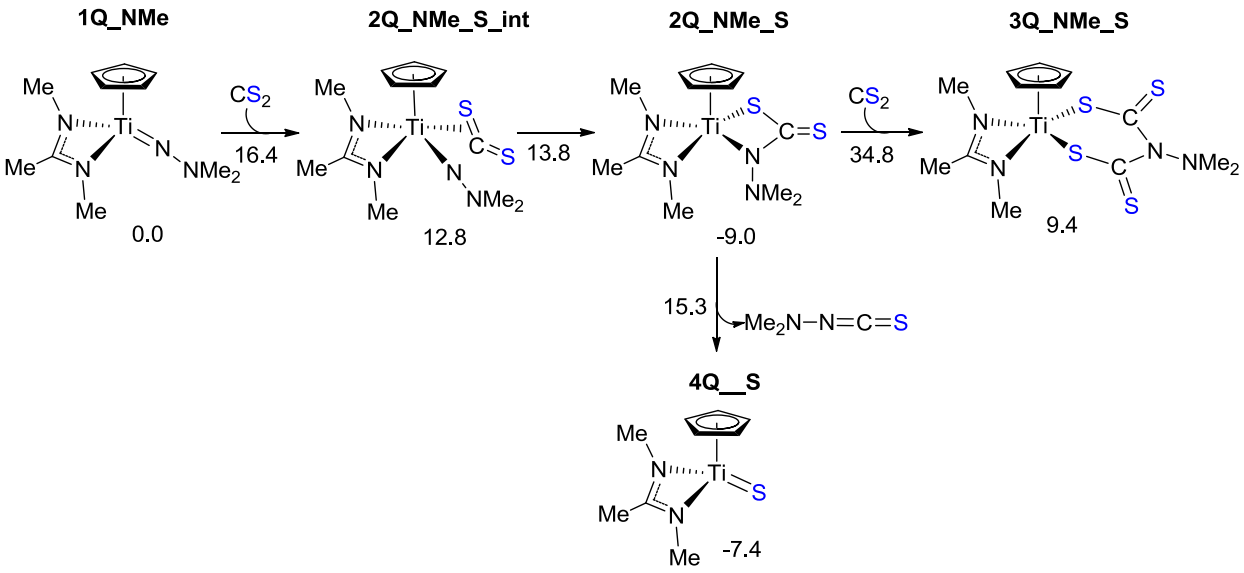

Figure 2.10. DFT mechanism for the reaction of **1Q_NMe$_2$** with CS_2. Values stated are Gibbs free energy (kcal mol^{-1}) at 298 K.

Figure 2.10 shows the DFT proposed mechanism for the reaction of hydrazide with CS_2 using the model system $CpTi\{MeC(NMe)_2\}(NNMe_2)$ (**1Q_NMe$_2$**) and CS_2. This will be discussed in detail in Section 2.4.3.

2.4.3 DFT studies of different reaction pathways

In an effort to gain additional insight into the different intrinsic reactivity patterns of phenyl imido and hydrazido complexes, DFT studies of various reaction pathways were carried out. Figure 2.11 shows the computed reaction profile for $CpTi\{MeC(NMe)_2\}(NNMe_2)$ (**1Q_NMe$_2$**) with the three model substrates CO_2, CS_2 and MeNCO (see Section 2.4 and 2.5 for the corresponding experimental systems), comparing cycloaddition, cycloaddition-insertion and cycloaddition-extrusion possibilities. Examples of all three pathways have been found for the hydrazides **2.13** – **2.15** (Scheme 2.1 and subsequent Sections) and previously for the imido complexes **2.7** and **2.8**.[28, 29, 47] Figure 2.13 compares these same three reaction outcomes for CO_2 with $CpTi\{MeC(NMe)_2\}(NR)$ where R = Ph (**1Q_Ph**), NPh_2 (**1Q_NPh$_2$**) or NMe_2 (**1Q_NMe$_2$**).

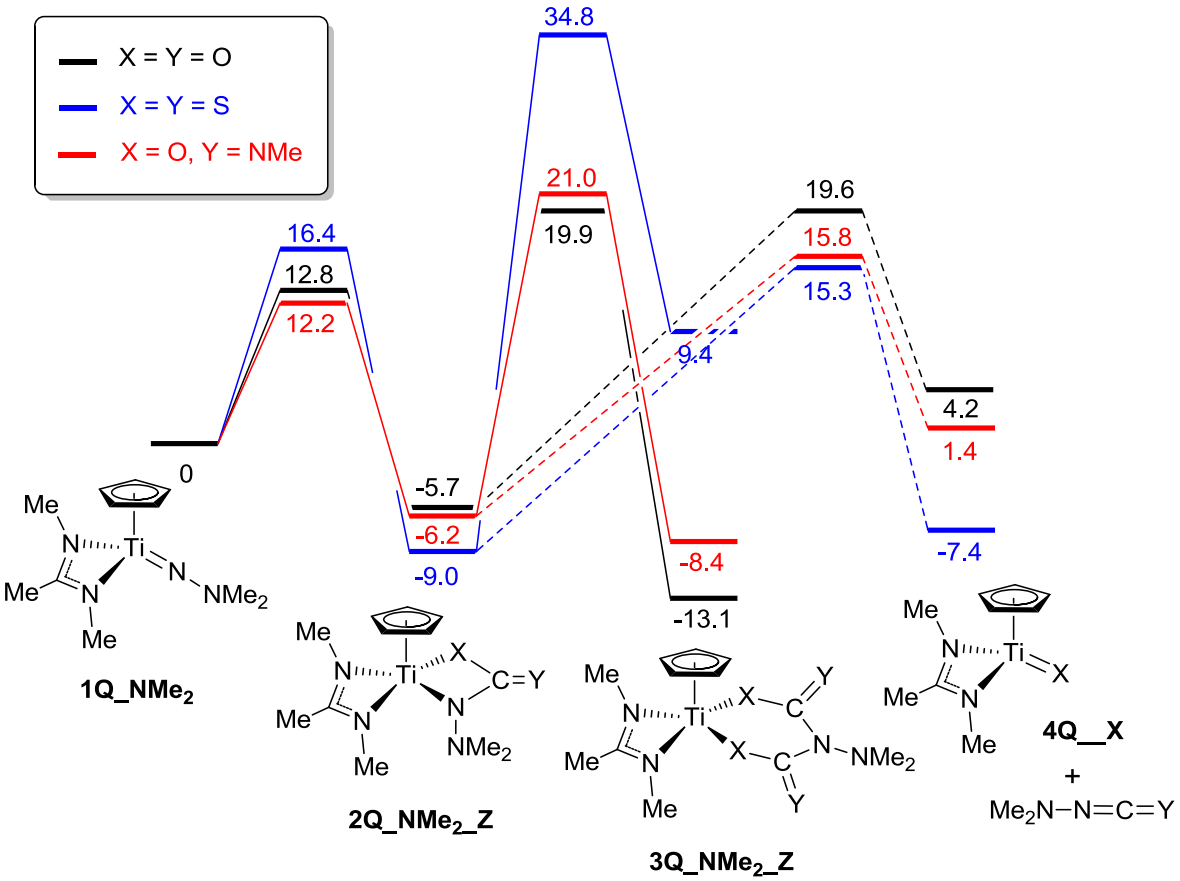

Figure 2.11. Simplified Gibbs free energy diagram (kcal mol^{-1}) at 298 K for the cycloaddition-insertion and cycloaddition-extrusion reactions of CpTi{$MeC(NMe)_2$}-($NNMe_2$) (**1Q_NMe$_2$**) with CO_2, CS_2 and MeNCO. Note that "Z" = O or S in the case of CO_2 or CS_2, respectively, and N in the case of MeNCO. Some intermediates with CS_2 and MeNCO have been omitted to facilitate the comparison between the various substrates (see Figures 2.10 and 2.18).

Figure 2.11 predicts that in the absence of significant steric repulsions, [2+2] cycloaddition products of the type **2Q_NMe$_2$_Z** should be stable for all three substrates, with those formed from CS_2 being the most thermodynamically stable by 2.8 kcal mol^{-1}. This is consistent with Equation 2.2. "Double insertion" products modelled by **3Q_NMe$_2$_Z** are thermodynamically stable with regard to the cycloaddition products for CO_2 and MeNCO, but unstable in the case of CS_2, again consistent with experimental observations. In contrast to **3Q_NMe$_2$_O** and **3Q_NMe$_2$_N** where the {$Ti(OC)_2(N_\alpha)$} ring is almost planar, as in the solid state structures of **3** and **4** (Figure 2.8), the DFT predicted structure of **3Q_NMe$_2$_S** is puckered (Figure 2.12). This prevents electron donation from the sulfur lone pair to

the metal, destabilising the overall molecule. With CO_2 and MeNCO, the activation barrier to the second insertion is 14 kcal mol^{-1} higher than that for the first insertion, explaining the higher temperatures and reaction times required for the second insertion reaction. The barrier to extrusion from **2Q_NMe$_2$_Z** forming **4Q__X** and Me_2NNCO or $Me_2NNCNMe$ is comparable to that for CO_2 or MeNCO insertion in the case of **2Q_NMe$_2$_O** and **2Q_NMe$_2$_NMe**, but the elimination products are +7.6 and +9.9 kcal mol^{-1} less stable thermodynamically. On the other hand, Me_2NNCS elimination from **2Q_NMe$_2$_S** is only slightly thermodynamically unfavourable (+1.6 kcal mol^{-1}) showing the possibility for extrusion in the latter case. Interestingly, while both **2Q_NMe$_2$_O** and **2Q_NMe$_2$_S** are stable to extrusion, loss of CO_2 is the kinetically most accessible and thermodynamically least unfavourable option for **2Q_NMe$_2$_O**, whereas for **2Q_NMe$_2$_S**, Me_2NNCS extrusion is the least unfavoured option and slightly kinetically preferred.

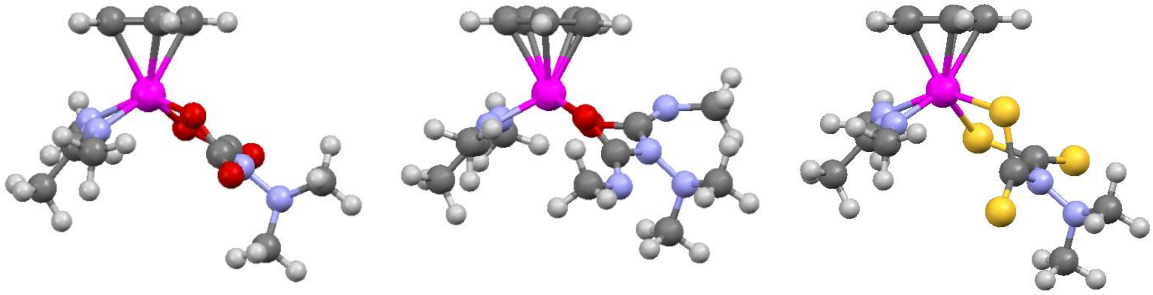

3Q_NMe$_2$_O	**3Q_NMe$_2$_N**	**3Q_NMe$_2$_S**
ΔG = -13.1 kcal mol^{-1}	ΔG = -8.4 kcal mol^{-1}	ΔG = 9.4 kcal mol^{-1}

Figure 2.12. Geometries and energies of **3Q_NMe$_2$_Z** intermediates relative to **1Q_NMe$_2$** and the corresponding heterocumulenes (CO_2, MeNCO, or CS_2, respectively).

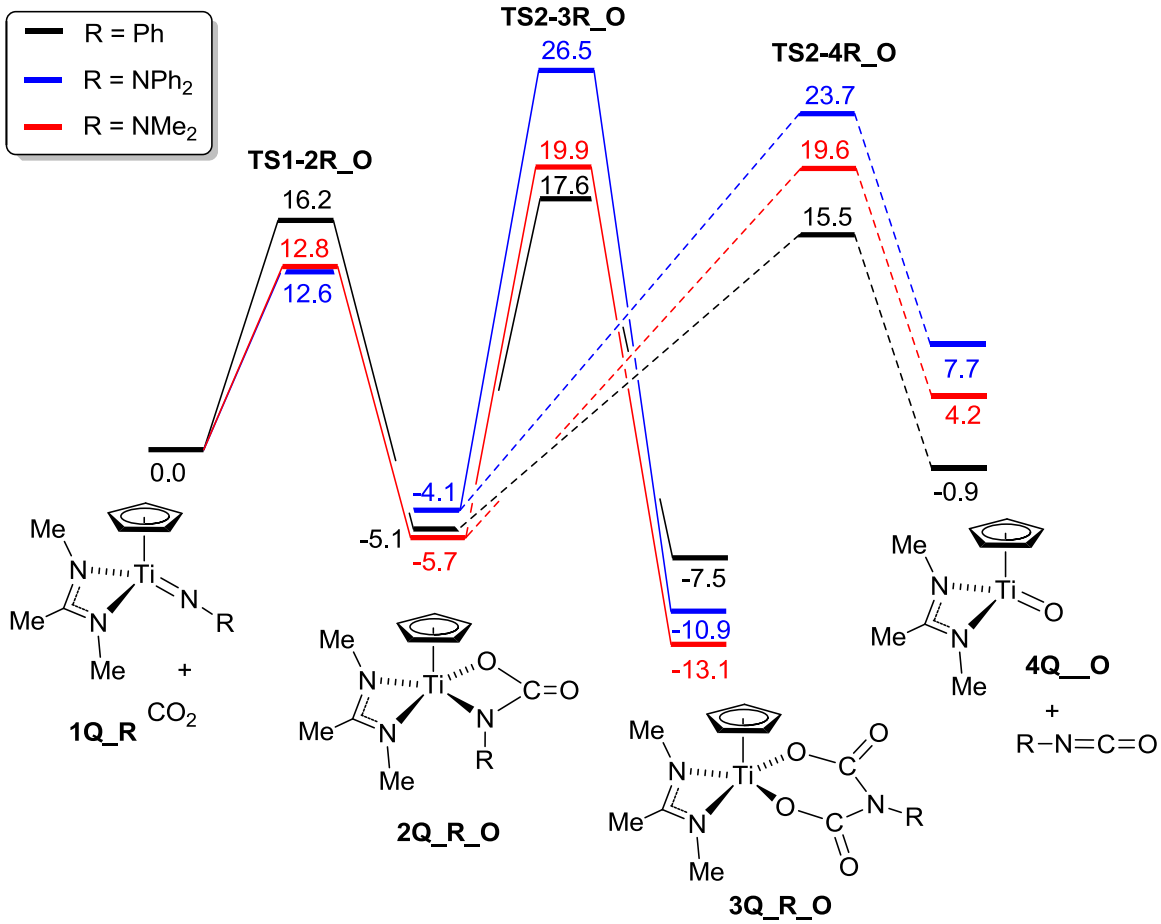

Figure 2.13. Gibbs free energy diagram (kcal mol^{-1}) at 298 K for the CO_2 cycloaddition and second CO_2 insertion (solid lines) or isocyanate extrusion (dotted lines) for the phenyl imido complex **1Q_Ph** (black lines) and its hydrazide analogues **1Q_NPh$_2$** (blue lines) and **1Q_NMe$_2$** (red lines).

Figure 2.13 compares the reaction profiles of the three model systems **1Q_Ph**, **1Q_NMe$_2$** and **1Q_NPh$_2$** with CO_2 as a representative substrate. The profile for **1Q_Ph** (and that of the *tert*-butyl analogue CpTi{MeC(NMe)$_2$}(N^{t}Bu) (**1Q_^{t}Bu**)) has been reported recently by our group as part of a detailed study of the reactions of imido complexes **2.7** and **2.8** with CO_2.[29] Here the main interest is to compare the differences between hydrazides and imides, and the effect of the N_β substitutents.

The cycloaddition products **2Q_R_O** have similar energies for all three systems, with addition to Ti=NNMe$_2$ being the most favourable. A low activation barrier is found for all cases, although that for **1Q_Ph** is somewhat higher than for the hydrazido systems which are effectively identical. The activation barrier for a second CO_2 insertion to form **3Q_R_O** is significantly higher for **2Q_NPh$_2$_O** (30.6 kcal mol^{-1})

compared to the others. This is consistent with the extended reaction times needed to form **3** experimentally. Thermodynamically, insertion is more favoured for the hydrazide-derived systems than for **2Q_Ph_O**. As for **2Q_R_O** hydrazide-derived systems, the most stable **3Q_R_O** complex appears to be for R = NMe_2.

With regard to extrusion of RNCO from **2Q_R_O**, the activation barriers increase in the order R = Ph < NMe_2 < NPh_2. In all cases the process is unfavourable, but is least prohibited for R = Ph and most disfavoured for R = NPh_2. Figure 2.13 suggests that CO_2 loss from the **2Q_R_O** hydrazide-derived systems is less unfavourable both kinetically and thermodynamically than RNCO elimination. In contrast, CO_2 and PhNCO elimination from **2Q_Ph_O** appear to be equally kinetically feasible and thermodynamically disfavoured by a similar amount. Studies in our group have previously shown that the TolNCO moiety in Cp*Ti{MeC(N^iPr)$_2$}{N(Tol)C(O)O} (**2.17**) can be sequestered by adding Ti(Me_4taa)(O) as an isocyanate trap.[29] A comparison of Figures 2.11 and 2.13 offers an explanation for the stability of the CS_2 cycloaddition products Cp*Ti{MeC(N^iPr)$_2$}{N(NR_2)C(S)S} (**5** and **6**) while the imido-derived analogues all eliminate RNCS. The previously reported profile for **1Q_^{t}Bu** was similar to that for **1Q_Ph**, but the barrier to CO_2 insertion from **2Q_^{t}Bu_O** was very high, while ^{t}BuNCO extrusion became thermodynamically favourable by -2.3 kcal mol^{-1} due to steric repulsions within **2Q_^{t}Bu_O**.

Additional NMR tube scale reactions were carried out as a probe of Figures 2.11 and 2.13. Reaction of Cp*Ti{MeC(N^iPr)$_2$}{N(NPh_2)C(O)O} (**1**) with Cp*Ti{MeC(N^iPr)$_2$}(NNMe_2) (**2.15**) in C_6D_6 gave immediate conversion to Cp*Ti{MeC(N^iPr)$_2$}{N(NMe_2)C(O)O} (**2**) and Cp*Ti{MeC(N^iPr)$_2$}(NNPh_2) (**2.13**). This is consistent with the low computed barrier to CO_2 extrusion from **2Q_R_O** and more thermodynamically favourable cycloaddition of CO_2 to Ti=NNMe_2. However, the corresponding reaction of **1** with the tolyl imide Cp*Ti{MeC(N^iPr)$_2$}(NTol) (**2.18**) gave the unexpected outcome summarised in Scheme 2.2 after heating at 60 ℃ (negligible reaction was observed at room temperature). The potential products Cp*Ti{MeC(N^iPr)$_2$}{N(Tol)C(O)O} (**2.17**[47]) and **2.13** were not observed, and instead the μ-oxo dimer **2.12**[29, 47] and the new compound Cp*Ti{MeC-(N^iPr)$_2$}{N(NPh_2)C(NTol)O} (**7**) were formed immediately in quantitative yield. Compound **7** can be prepared independently from **2.13** and TolNCO and is discussed later on in Section 2.5.

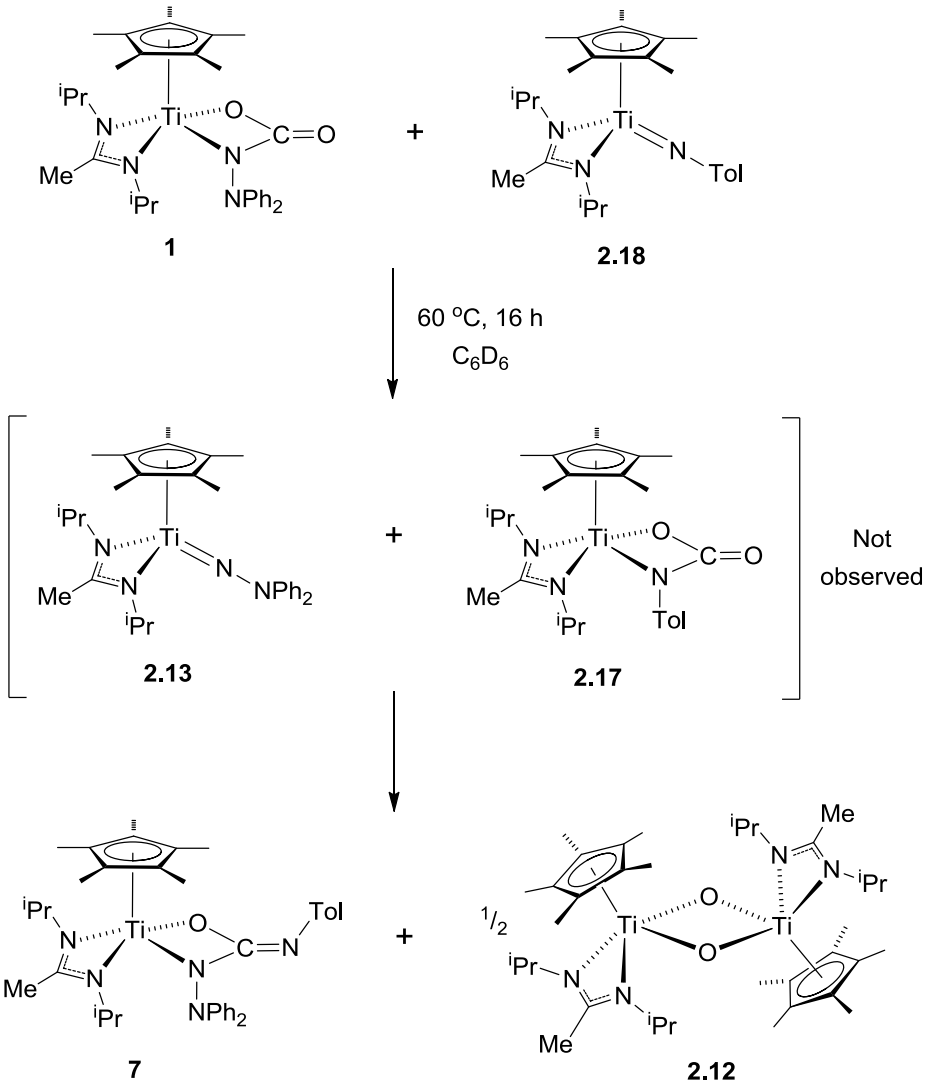

Scheme 2.2. Reaction of Cp*Ti{MeC(N^{i}Pr)$_2$}{N(NPh$_2$)C(O)O} (**1**) with Cp*Ti{MeC-(N^{i}Pr)$_2$}(NTol) (**2.18**).

Given that **7** can be formed from **2.13** and TolNCO, a likely mechanism accounting for the formation of **2.12** and **7** is initial extrusion of CO_2 from **1** to form **2.17** which is not observed but is known to release TolNCO in the presence of a suitable trap (see above[29]). Trapping of the TolNCO released from **2.17** by **2.13** would lead to **7** and monomeric Cp*Ti{MeC(N^{i}Pr)$_2$}(O) which is unstable to dimerisation, forming **2.12**. Consistent with this, it was found that an independently prepared sample of **2.17** reacted immediately with **2.13** in C_6D_6 forming **7** and **2.12** in quantitative yield.

In contrast to the facile transfer of CO_2 from **1** to **2.15**, there was no reaction between Cp*Ti{MeC(N^{i}Pr)$_2$}{N(NPh$_2$)C(S)S} (**5**) and **2.15** at room temperature. Heating to 60 ℃ gave decomposition to a mixture containing the previously reported[47] μ-sulfido

dimer [Cp*Ti{MeC(N^{i}Pr)$_2$}(μ-S)]$_2$ (**2.16**) and a number of unknown products. Although this could mean that addition of CS_2 to Ti=NNPh$_2$ is thermodynamically more favourable than addition to Ti=NNMe$_2$, it could also represent a kinetic limitation since the computed barrier for CS_2 extrusion from **2Q_NMe$_2$_S** (25.4 kcal mol^{-1}) is significantly higher than for CO_2 extrusion from **2Q_NMe2_O** (18.5 kcal mol^{-1}).

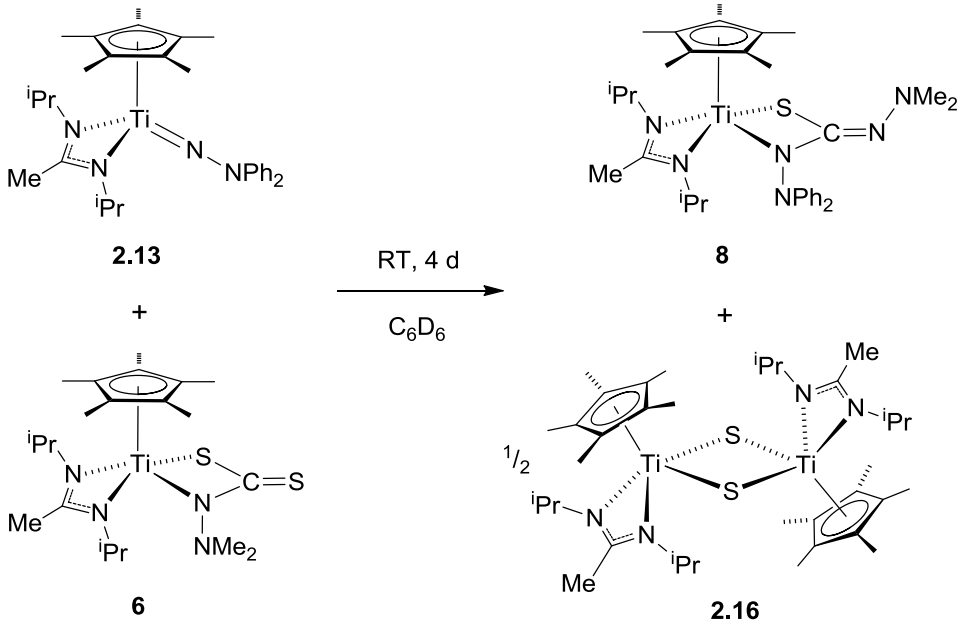

Equation 2.3

The corresponding reaction of **6** and **2.13** was carried out as a further attempt to test the thermodynamic preferences for CS_2 binding experimentally. The reaction formed [Cp*Ti{MeC(N^{i}Pr)$_2$}(μ-S)]$_2$ (**2.16**) and a new compound formulated as Cp*Ti{MeC(N^{i}Pr)$_2$}{N(NPh$_2$)C(NNMe$_2$)S} (**8**) on the basis of its ^{1}H and ^{13}C{^{1}H} NMR spectra (Equation 2.3). Compound **8** is the cycloaddition product of **2.13** and Me$_2$NNCS, and is the analogue of the fully characterised compounds Cp*Ti{MeC(N^{i}Pr)$_2$}{N(NPh$_2$)C(NAr)S} (Ar = Tol or 2,6-C$_6$H$_3$^{i}Pr$_2$) prepared from **2.13** and ArNCS (see Section 2.5). The formation of **8** is consistent with the DFT prediction (Figure 2.11) that Me$_2$NNCS extrusion from **2Q_NMe$_2$_S** is thermodynamically less disfavoured than CS_2 extrusion while being equally kinetically accessible.

2.5 Reactions of Cp*Ti{MeC(N^{i}Pr)$_2$}(NNPh$_2$) (2.13) with isocyanates, isothiocyanates and CO_2

As mentioned earlier, the reactions of Cp*Ti{MeC(N^{i}Pr)$_2$}(NNPh$_2$) (**2.13**) and Cp*Ti{MeC(N^{i}Pr)$_2$}(NNMe$_2$) (**2.15**) with isocyanates differ significantly depending on the individual β-NR$_2$ group and are therefore described in turn.

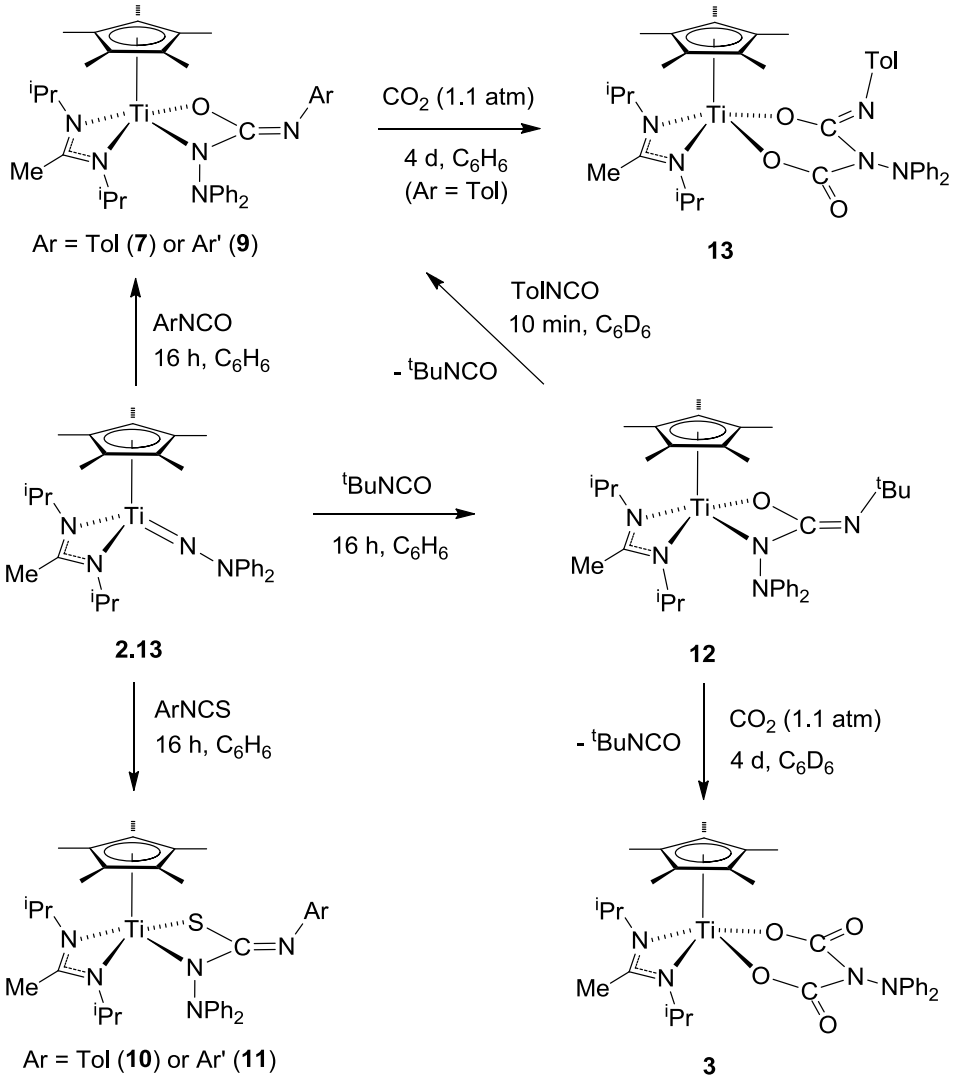

Scheme 2.3. Reactions of Cp*Ti{MeC(N^{i}Pr)$_2$}(NNPh$_2$) (**2.13**) with isocyanates and isothiocyanates. Ar ´= 2,6-C$_6$H$_3$^{i}Pr$_2$.

Scheme 2.3 summarises the reactions of **2.13** with selected isocyanates and isothiocyanates, along with other reactions of the so-formed products. Reaction of **2.13** with TolNCO or Ar′NCO at room temperature in benzene gave the C_1 symmetric ureate-type cycloaddition products Cp*Ti{MeC(N^{i}Pr)$_2$}{N(NPh$_2$)C(NAr)O} (Ar = Tol (**7**) or Ar′ (**9**)) as dark brown solids in *ca*. 70% isolated yield. The corresponding

reactions with ArNCS afforded Cp*Ti{MeC($N^iPr)_2$}{$N(NPh_2)C(NAr)S$} (Ar = Tol (**10**) or Ar′ (**11**)) as dark green solids in slightly lower yields (*ca*. 50%) although the corresponding NMR tube scale experiments for both ArNCO and ArNCS were effectively quantitative. The low isolated yields are attributed to the relatively high solubility of **10** and **11** in hydrocarbon solvents.

Diffraction-quality crystals of **9** and **11** were grown by slow cooling of a hexanes solution and the molecular structures and selected distances and angles are shown in Figure 2.14 and Table 2.3. Full crystallographic data are given in the CD Appendix. The solid state structures for both **9** and **11** confirm the four-legged piano stool geometries around titanium and the κ^2*N,O* or κ^2*N,S* coordination modes for the $N(NPh_2)C(NAr')E$ ligands (E = O or S).

In general, the structural data for **9** and **11** are very similar, except for the significantly longer Ti(1)-S(1) (2.4512(8) Å) and S(1)-C(13) (1.769(2) Å) distances compared to Ti(1)-O(1) (2.0060(14) Å) and O(1)-C(13) (1.337(2) Å). The angles within the metallacycle are very different as well with a smaller bite angle of N(1)-Ti(1)-O(1) (65.60(6)°) compared to N(1)-Ti(1)-S(1) (67.98(6)°), but a larger Ti(1)-O(1)-C(13) angle of 94.72(11)° versus 80.08(8)° for Ti(1)-S(1)-C(13). The Ti(1)-N(1)-C(13) angle of **9** (93.31(11)°) is significantly smaller than that for **11** (105.94(14)°). The differences in bond lengths and bond angles are most probably attributed to the larger size of sulfur compared to oxygen thus causing it to be more sterically demanding. The Ti(1)-N(1) distances of 2.000(15) Å (**9**) and 2.0335(18) (**11**) Å are typical of an amido donor, with an essentially trigonal planar geometry around N(1). The N(1)-N(2) distances for **9** and **11** are 1.400(2) Å and 1.416(3) Å respectively. These are significantly longer than 1.369(2) Å for **2.13**, which indicate a decrease in the bond order from a double bond to a single bond.

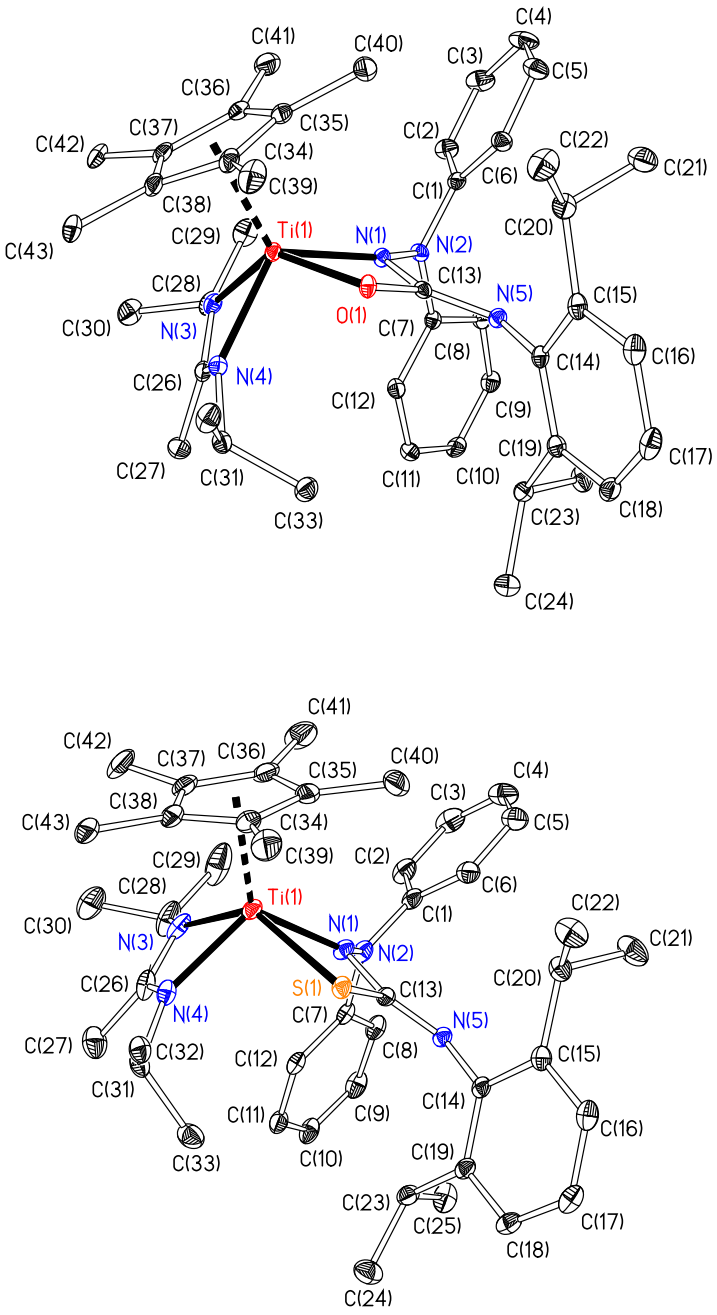

Figure 2.14. Displacement ellipsoid plots (25% probability) of Cp*Ti{MeC(N^{i}Pr)$_2$}{N(NPh$_2$)C(NAr')O} (**9**) (top) and Cp*Ti{MeC(N^{i}Pr)$_2$}{N-(NPh$_2$)C(NAr')S} (**11**) (bottom). H atoms omitted for clarity.

Table 2.3. Selected bond lengths (Å) and angles (°) for Cp*Ti{MeC(N^{i}Pr)$_2$}{N(NPh$_2$)C(NAr′)O} (**9**) and Cp*Ti{MeC(N^{i}Pr)$_2$}{N(NPh$_2$)C(NAr′)S} (**11**). Cp$_{cent}$ is the computed Cp* ring carbon centroid.

Parameter[a]	**9**	**11**
Ti(1)-Cp$_{cent}$	2.065	2.075
Ti(1)-N(1)	2.000(15)	2.0335(18)
Ti(1)-E(1)	2.0060(14)	2.4512(8)
Ti(1)-N(3)	2.1498(17)	2.171(3)
Ti(1)-N(4)	2.0526(18)	2.050(2)
N(1)-N(2)	1.400(2)	1.416(3)
C(13)-N(5)	1.286(3)	1.273(3)
E(1)-C(13)	1.337(2)	1.769(2)
Cp$_{cent}$-Ti(1)-N(1)	126.4	128.3
Cp$_{cent}$-Ti(1)-E(1)	110.5	107.8
Cp$_{cent}$-Ti(1)-N(3)	112.3	111.9
Cp$_{cent}$-Ti(1)-N(4)	119.0	119.6
N(3)-Ti(1)-N(4)	63.46(7)	62.63(10)
N(1)-Ti(1)-E(1)	65.60(6)	67.98(6)
Ti(1)-N(1)-C(13)	93.31(11)	105.94(14)
Ti(1)-E(1)-C(13)	94.72(11)	80.08(8)
N(1)-C(13)-E(1)	105.50(15)	105.58(15)

[a] E = O or S for **9** or **11**, respectively.

The NMR spectra for **7** and **9** – **11** are consistent with the proposed structures. No signals for other isomers of **7** and **9** – **11** (e.g. with a κ^2*N,N′*-N(NPh$_2$)C(E)NAr moiety) were observed in the NMR tube scale experiments or crude reaction products. Although they have not been crystallographically authenticated, the tolyl-substituted analogues Cp*Ti{MeC(N^{i}Pr)$_2$}{N(NPh$_2$)C(NTol)E} (**7** and **10**) are proposed to have analogous structures. For example, very similar ν(C=N) bands for **7** and **9** were observed at 1619 and 1622 cm^{-1}, respectively, which are also comparable to those for the imido-derived products Cp*Ti{MeC(N^{i}Pr)$_2$}{N(Ar^1)C(NAr^2)O} (Ar^1 or Ar^2 = Tol or Xyl, ν(C=N) = 1609 – 1615 cm^{-1}) which possess κ^2*N,O* bound N(Ar^1)C(NAr^2)O

groups.[47] In contrast, the IR spectrum of Ti(Me$_4$taa){N(NPh$_2$)C(O)NTol} possessing a κ^2*N,N′*-N(NPh$_2$)C(O)NTol ligand features a ν(C=O) band at 1656 cm^{-1}.[36]

The metric parameters for the Cp*Ti{MeC(N^{i}Pr)$_2$} moiety in **9** and **11** are within expected ranges, and those for the N(NPh$_2$)C(NAr′)E ligands are comparable to the same groups recently reported in Ti(N$_2$N^{Me}){N(NPh$_2$)C(NAr′)E}(L) (L = py, E = O; L = none, E = S) which also feature κ^2*N,O* or κ^2*N,S* coordination.[32] Interestingly, Gade *et al*. found that Cp*Ti(N^{Xyl}N)(NNRPh)(L) (**2.6**; R = Ph or Me, L = ^{t}BuNH$_2$ or py) reacts with PhNCO or PhNCS to give a mixture of isomers possessing either a κ^2*N,E* or κ^2*N,N′* ureate ligand.[37] An example of each type was crystallographically characterised.

To probe further the coordination mode preferences in **7** and **9** the DFT energies of the model complexes CpTi{MeC(NMe)$_2$}{κ*N,O*-N(NPh$_2$)C(NPh)O} (**κ*N,O*-2Q_NPh$_2$_N**) and CpTi{MeC(NMe)$_2$}{κ*N,N'*-N(NPh$_2$)C(O)NPh} (**κ*N,N′*-2Q_NPh$_2$_N**) were calculated. Results from DFT calculations found that isomer **κ*N,N′*-2Q_NPh$_2$_N** was more stable compared to isomer **κ*N,O*-2Q_NPh$_2$_N**, but only by 1 kcal mol^{-1}. Thus, it is concluded that the preference for isomers with κ^2*N,O* and κ^2*N,S* coordination is due to steric factors. As found in related systems, the κ^2*N,N′*-ureate isomers appear to be electronically preferred, but steric factors can easily overturn this.[32, 47]

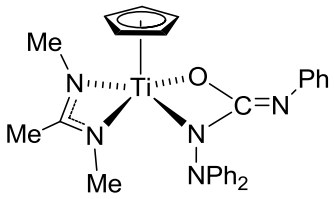

κ*N,O*-2Q_NPh$_2$_N

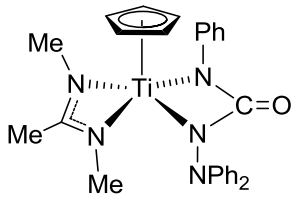

κ*N,N′*-2Q_NPh$_2$_N

Reaction of **2.13** with ^{t}BuNCO gave Cp*Ti{MeC(N^{i}Pr)$_2$}{N(NPh$_2$)C(N^{t}Bu)O} (**12**, Scheme 2.3) through [2+2] cycloaddition. While **12** slowly eliminates ^{t}BuNCNNPh$_2$ forming the oxo-bridged dimer **2.12** (*ca.* 30% conversion after 4 days at room temperature in C$_6$D$_6$), it is significantly more stable than the corresponding products formed from Cp*Ti{MeC(N^{i}Pr)$_2$}(NR) (R = ^{t}Bu (**2.7**) or Tol (**2.18**)) which quantitatively eliminate ^{t}BuNCNR within 2 – 3 hours.[47] These observations are consistent with the DFT calculations in Figure 2.13 for the cycloaddition-isocyanate extrusion reactions of **1Q_Ph** and **1Q_NPh$_2$** with CO$_2$.

Previous studies in our group found that the imide-isocyanate cycloaddition species Cp*Ti{MeC($N^iPr)_2$}{N(Tol)C(NTol)O} could form "double insertion" products on reaction with CO_2 or ArNCO (Ar = Tol or 2,6-$C_6H_3Me_2$). In a similar manner, Cp*Ti{MeC($N^iPr)_2$}{N(Tol)C(O)O} (**2.17**) inserted ArNCO into the Ti–N(Tol) bond to also give a cross-coupled derivative.[47] In contrast, treatment of Cp*Ti{MeC-($N^iPr)_2$}{$N(NPh_2)$C(NTol)O} (**7**) with further TolNCO either at room temperature or at 60 ℃ gave no reaction. The corresponding reaction of **7** with CO_2 successfully but slowly (4 days) formed the mixed TolNCO/CO_2 "double insertion" product Cp*Ti{MeC($N^iPr)_2$}{OC(NTol)$N(NPh_2)$C(O)O} (**13**). Unfortunately, all attempts to grow diffraction quality crystals were unsuccessful. However, other data including the results from elemental analysis are in agreement with the proposed structure. The IR spectrum of **13** shows strong bands at 1699 and 1628 cm^{-1} attributed to ν(C=O) and ν(C=N), consistent with the proposed structure.[47] No reaction was observed between the bulkier **9** and CO_2. Compound **13** is the analogue of the structurally authenticated Cp*Ti{MeC($N^iPr)_2$}{OC(O)$N(NPh_2)$C(O)O} (**3**). Surprisingly, an attempt to form **13** by reaction of Cp*Ti{MeC($N^iPr)_2$}{$N(NPh_2)$C(O)O} (**1**) with TolNCO gave a mixture of **7**, **13**, **3** and unreacted **1**.

Reaction of the bulkier Cp*Ti{MeC($N^iPr)_2$}{$N(NPh_2)$C(N^tBu)O} (**12**) with CO_2 in C_6D_6 slowly led to ^{t}BuNCO extrusion and formation of **3** (Scheme 2.3). This reaction most likely proceeds *via* elimination of the isocyanate to form **2.13**. The reaction of pure **2.13** with CO_2 to form **3** is faster than the reaction with **12** explaining why the cycloaddition intermediate **1** is not observed in the reaction of **12**. Addition of TolNCO to **12** also led to loss of ^{t}BuNCO, immediately forming **7**. Reaction of Cp*Ti{MeC($N^iPr)_2$}($NNMe_2$) (**2.15**) with **12** in C_6D_6 gave quantitative formation of **2.13**, the μ-oxo compound **2.12** and ^{t}BuNCNNMe_2, consistent with the reactions of **2.15** with ^{t}BuNCO and Ar′NCO described below in Section 2.6 (Scheme 2.4).

As mentioned, the reaction of **7** with CO_2 to form **13** requires 4 days for completion (with NMR monitoring) whereas the corresponding reaction for Cp*Ti{MeC($N^iPr)_2$}{N(Tol)C(NTol)O} under comparable conditions was complete within 10 minutes.[47] These differences are again consistent with Figure 2.13 by analogy with the significantly higher TS for **2Q_NPh_2_O** + CO_2 → **3Q_NPh_2_O** compared to **2Q_Ph_O** + CO_2 → **3Q_Ph_O**.

2.6 Reactions of Cp*Ti{MeC(N^{i}Pr)$_2$}(NNMe$_2$) (2.15) with isocyanates

In contrast to the relatively well-behaved cycloaddition chemistry of **2.13** with RNCO and ArNCS, the reactions of **2.15** with these substrates are dominated by cycloaddition-extrusion processes. The reactions of **2.15** with isocyanates are shown in Scheme 2.4.

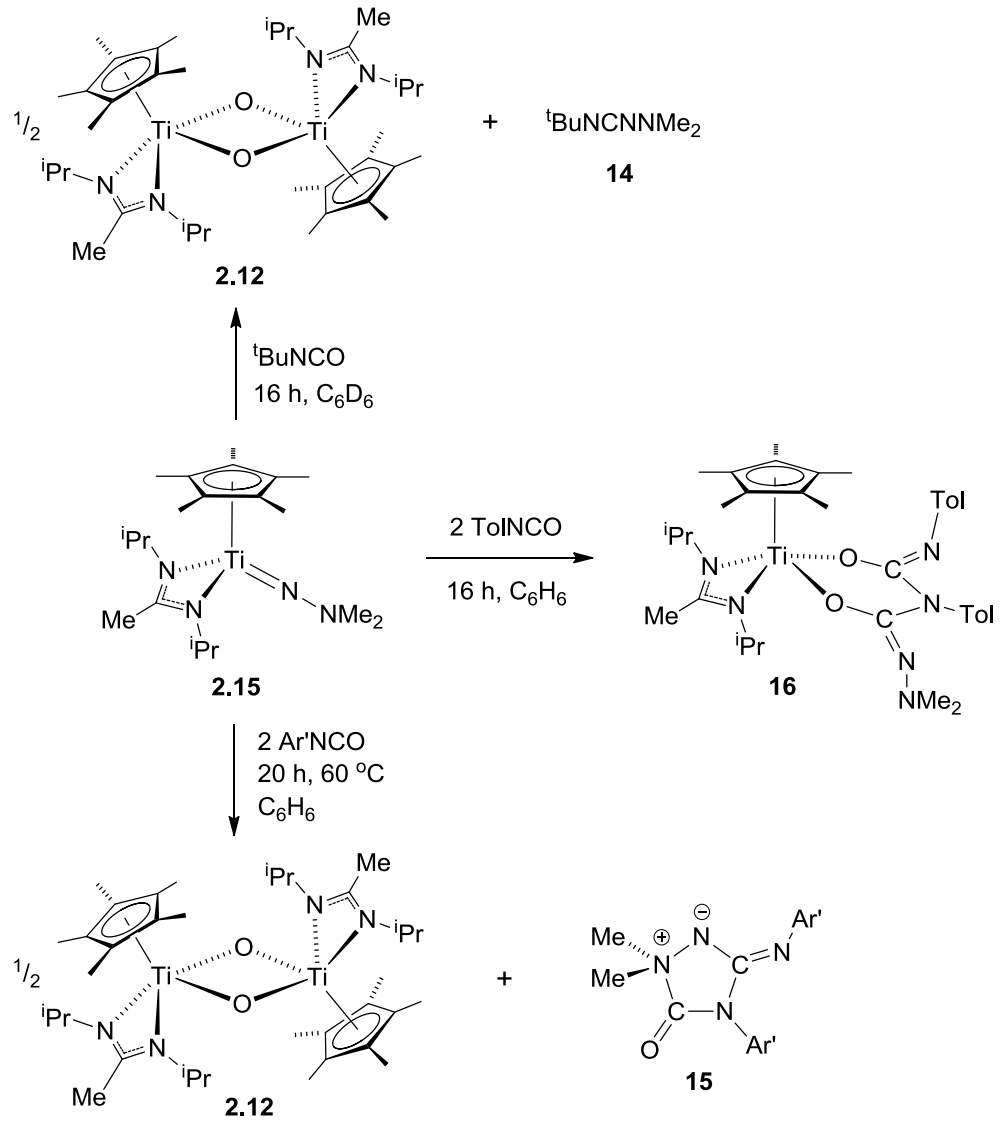

Scheme 2.4. Reactions of Cp*Ti{MeC(N^{i}Pr)$_2$}(NNMe$_2$) (**2.15**) with isocyanates. Ar´ = 2,6-C$_6$H$_3$^{i}Pr$_2$.

Reaction of **2.15** with ^{t}BuNCO in C_6D_6 gave quantitative conversion to the μ-oxo compound **2.12** and the previously reported[76, 77] *N*-dimethylaminocarbodiimide ^{t}BuNCNNMe$_2$ (**14**). Amidocarbodiimides are not stable and are known to dimerise. In the case of **14**, the heterocyclic product N(Me)$_2$NC(N^{t}Bu)N(^{t}Bu)C(NNMe$_2$) (**2.19**) has

been crystallographically characterised.[77] The instability of the presumed cycloaddition intermediate Cp*Ti{MeC(N^{i}Pr)$_2$}{N(NMe$_2$)C(N^{t}Bu)O} to extrusion contrasts strongly with that of **12**, and is reminiscent of the corresponding reactions of Cp*Ti{MeC(N^{i}Pr)$_2$}(NR) (R = ^{t}Bu (**2.7**) or Tol (**2.18**)) mentioned above. The outcomes of these reactions are consistent with the DFT calculations in Figure 2.13 for extrusion of RNCO from **2Q_R_O** which become progressively more favoured (both kinetically and thermodynamically) in the order R = NPh$_2$ < NMe$_2$ < Ph.

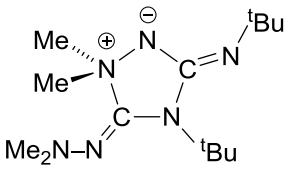

2.19

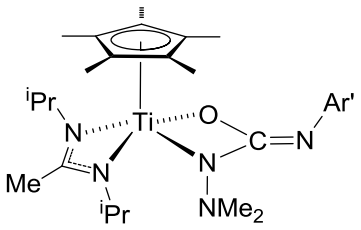

15_int

The stoichiometric reaction of **2.15** with Ar′NCO gave a mixture of products and unreacted hydrazide. Conducting the reaction at 60 ℃ with 2 equivalents of Ar′NCO gave **2.12** and the 1,2,4-triazolidinone N(Me)$_2$NC(NAr′)N(Ar′)C(O) (**15**). When conducted on the NMR tube scale in C_6D_6 the conversion of **2.15** to the products was near-quantitative. On scale-up, the white solid **15** could only be isolated in analytically pure form by high vacuum (5 x 10^{-6} mbar) tube sublimation leading to an overall yield of 15%.

Diffraction-quality crystals of **15** were grown from a concentrated hexanes solution at 4 ℃. The molecular structure is shown in Figure 2.15 and selected distances and angles are given in Table 2.4. Full crystallographic data are given in the CD Appendix. The selected distances and angles are all within normal ranges[78] and comparable to **2.19**.[77] Compound **15** is the apparent product of coupling between Ar′NCO and Ar′NCNNMe$_2$ which is not observed in the reaction mixture but is analogous to ^{t}BuNCNNMe$_2$ formed in the reaction of **2.15** with ^{t}BuNCO. Carbodiimide Ar′NCNNMe$_2$ is probably formed by extrusion from a likely cycloaddition intermediate Cp*Ti{MeC(N^{i}Pr)$_2$}{N(NMe$_2$)C(NAr′)O} (**15_int**), the analogue of the crystallographically characterised **9** (Figure 2.14). The extruded Ar′NCNNMe$_2$ was then trapped by the free Ar′NCO to give **15**. The incorporation of both an Ar′NCO and Ar′NC fragment into **15** accounts for the 1:2 stoichiometry required for this reaction.

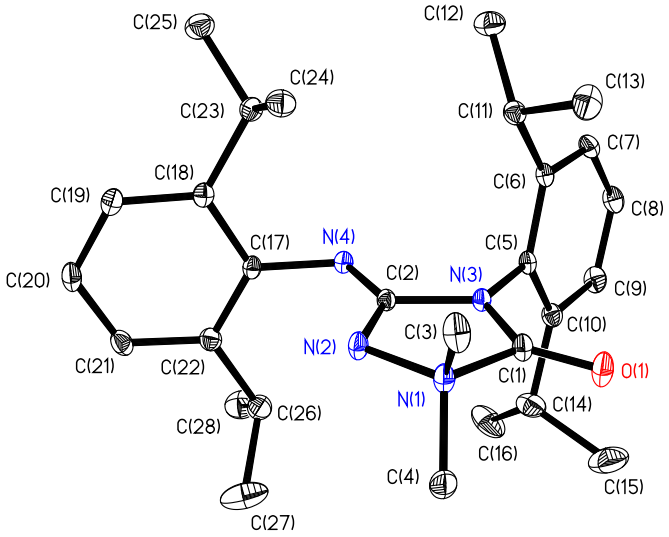

Figure 2.15. Displacement ellipsoid plot (20% probability) of $\overline{N(Me)_2NC(NAr')N(Ar')C}(O)$ (**15**). H atoms omitted for clarity.

Table 2.4. Selected distances (Å) and angles (°) for $\overline{N(Me)_2NC(NAr')N(Ar')C}(O)$ (**15**).

N(1)-N(2)	1.4638(19)	N(1)-C(1)	1.515(2)
N(1)-C(3)	1.497(2)	N(1)-C(4)	1.485(3)
N(2)-C(2)	1.346(2)	C(2)-N(3)	1.4461(19)
C(2)-N(4)	1.278(2)	N(3)-C(1)	1.324(2)
N(3)-C(5)	1.439(2)	C(1)-O(1)	1.204(2)
C(1)-N(1)-N(2)	107.37(12)	C(3)-N(1)-C(4)	109.85(16)
N(1)-N(2)-C(2)	105.74(12)	N(2)-C(2)-N(3)	110.63(13)
C(2)-N(3)-C(1)	111.24(13)	N(3)-C(1)-N(1)	104.82(13)

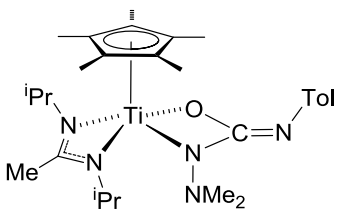

16_int

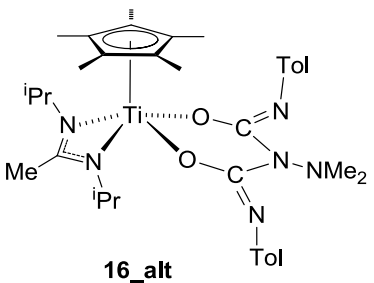

16_alt

The reaction of **2.15** with TolNCO also required 2 equivalents of the isocyanate for complete reaction (Scheme 2.4). However, in this case the single reaction product was the "double-insertion" compound Cp*Ti{MeC(N^{i}Pr)$_2$}{OC(NNMe$_2$)N(Tol)C-(NTol)O} (**16**) isolated in 76% yield. Compound **16** has been crystallographically characterised and the molecular structure is shown in Figure 2.16. Full crystallographic data are given in the CD Appendix. Selected distances and angles are listed in Table 2.5 and are within the expected ranges.

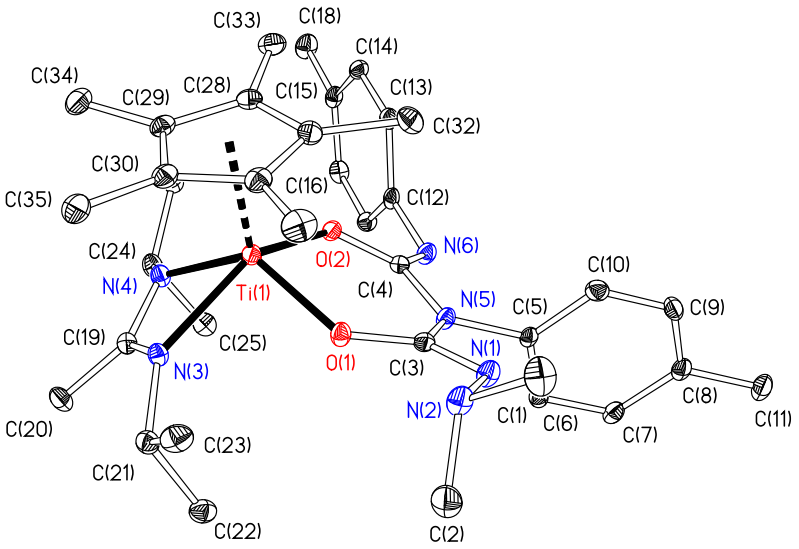

Figure 2.16. Displacement ellipsoid plot (20% probability) of Cp*Ti{MeC(N^{i}Pr)$_2$}{OC(NNMe$_2$)N(Tol)C(NTol)O} (**16**). H atoms omitted for clarity.

The solid state structure of **16** confirms the four-legged piano stool geometries around titanium. The atoms in the six membered metallacycle ring are approximately coplanar. The short C(3)-N(1) distance of 1.289(3) Å is best described as a C=N double bond. The N(1)-N(2) bond length of 1.457(3) Å is indicative of a single bond.

Table 2.5. Selected distances (Å) and angles (°) for Cp*Ti{MeC(N^{i}Pr)$_2$}{OC(NNMe$_2$)N(Tol)C(NTol)O} (**16**). Cp$_{cent}$ is the computed Cp* ring carbon centroid.

Ti(1)-Cp$_{cent}$	2.067	Ti(1)-O(2)	1.9359(17)
Ti(1)-N(3)	2.108(2)	N(5)-C(5)	1.455(3)
Ti(1)-N(4)	2.077(2)	C(3)-N(1)	1.289(3)
Ti(1)-O(1)	1.9065(17)	C(4)-N(6)	1.288(3)
N(1)-N(2)	1.457(3)		
Cp$_{cent}$-Ti(1)-N(3)	110.9	Cp$_{cent}$-Ti(1)-N(4)	114.6
Cp$_{cent}$-Ti(1)-O(1)	116.1	Cp$_{cent}$-Ti(1)-O(2)	111.0
N(3)-Ti(1)-N(4)	63.54(8)	O(1)-Ti(1)-O(2)	83.63(7)
Ti(1)-O(1)-C(3)	134.38(15)	Ti(1)-O(2)-C(4)	135.27(15)
C(3)-N(5)-C(4)	124.5(2)		

The ^{1}H and ^{13}C{^{1}H} NMR spectra of **16** show two sets of *p*-tolyl group resonances and two septets and four doublets corresponding to the inequivalent *iso*-propyl groups for the MeC(N^{i}Pr)$_2$ ligand (Figure 2.17), suggesting the formation of a C_1 symmetric product. The IR spectrum shows two ν(C=N) bands at 1619 and 1599 cm^{-1}. Surprisingly, the product is not the C_s symmetric Cp*Ti{MeC(N^{i}Pr)$_2$}{OC(NTol)N(NNMe$_2$)C(NTol)O} (**16_alt**) which would be expected based on the reactions of Cp*Ti{MeC(N^{i}Pr)$_2$}(NTol) with 2 equivalents of TolNCO or Cp*Ti{MeC(N^{i}Pr)$_2$}(NNR$_2$) with an excess of CO$_2$.[47] The presence of both an exocyclic C=NTol and C=NNMe$_2$ moiety suggests that at least one rearrangement must have taken place between the likely intermediate Cp*Ti{MeC(N^{i}Pr)$_2$}{N(NMe$_2$)C(NTol)O} (**16_int**, the analogue of **7**) and the final product **16**.

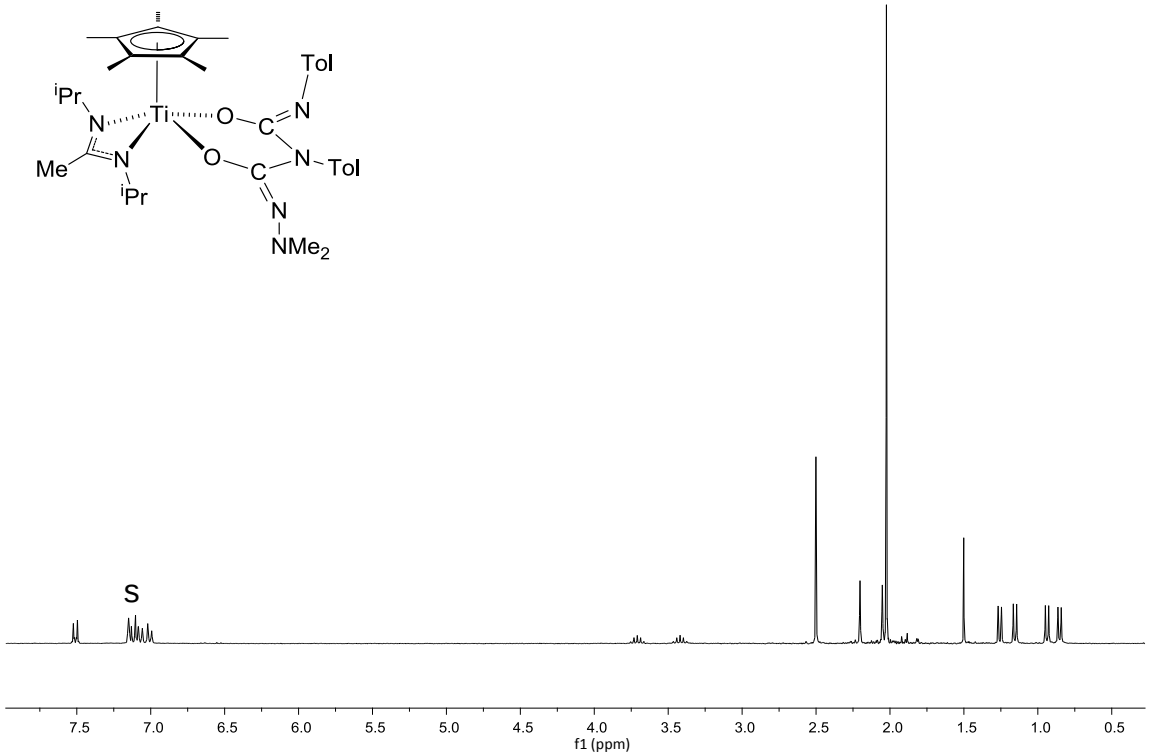

Figure 2.17. ^{1}H NMR spectrum (299.9 MHz) of Cp*Ti{MeC(N^{i}Pr)$_2$}-{OC(NNMe$_2$)N(Tol)C(NTol)O} (**16**) in C_6D_6 ("s" denotes residual protio-solvent).

DFT calculations were carried out to study the mechanism of formation of **16** using the model system CpTi{MeC(NMe)$_2$}(NNMe$_2$) (**1Q_NMe$_2$**) and MeNCO (Figure 2.18). A part of this mechanism was already included in Figure 2.11. Addition of MeNCO forms **2Q_NMe$_2$_N** with a κ*N,O* ureate ligand. Insertion of MeNCO into the Ti–N(NMe$_2$) bond of **2Q_NMe$_2$_N** forms the symmetric "double insertion" product **3Q_NMe$_2$_N** in a slightly exergonic process (ΔG = -2.2 kcal mol^{-1}). The TS for this process lies 27.2 kcal mol^{-1} above **2Q_NMe$_2$_N**. A more accessible second MeNCO insertion was found *via* the alternative *N,O* coordination isomer **2Q_NMe$_2$_N′** with an exocyclic C=NNMe$_2$ group. Direct rearrangement of **2Q_NMe$_2$_N** to **2Q_NMe$_2$_N′** by effective rotation about the O–CN$_2$ bond has a prohibitively high TS of +36.5 kcal mol^{-1} relative to **2Q_NMe$_2$_N**. However, extrusion of MeNCNNMe$_2$ from **2Q_NMe$_2$_N** to form **4Q__O**, followed by recoordination and cycloaddition, presents an alternative route to **2Q_NMe$_2$_N′**. Relative to **2Q_NMe$_2$_N**, the highest TS along this route is 23.5 kcal mol^{-1} (between **2Q_NMe$_2$_N_int** and **2Q_NMe$_2$_N′**) which is lower than the 27.2 kcal mol^{-1} between **2Q_NMe$_2$_N** and **3Q_NMe$_2$_N**. Insertion of MeNCO into the Ti–N(Me) of **2Q_NMe$_2$_N′** forms the desired isomer

3Q_NMe$_2$_N′ (a model of **16**) with an activation free energy barrier of +20.7 kcal mol^{-1} relative to **2Q_NMe$_2$_N′**. Another point to note is that **3Q_NMe$_2$_N′** is -3.1 kcal mol^{-1} more stable than the more symmetrical isomer **3Q_NMe$_2$_N** and so represents both the thermodynamic and kinetically favoured product.

In principle, this model mechanism could apply to reactions with TolNCO, ^{t}BuNCO or Ar′NCO, whereas in practice different outcomes are found for each isocyanate. The reaction outcomes depend not only on the different steric bulk of each of the isocyanates but also their relative rates of trapping RNCNNMe$_2$, whether by Cp*Ti{MeC(N^{i}Pr)$_2$}(O) (seen for R = Tol), free RNCO in the reaction mixture (R = Ar′) or not at all (R′ = ^{t}Bu).

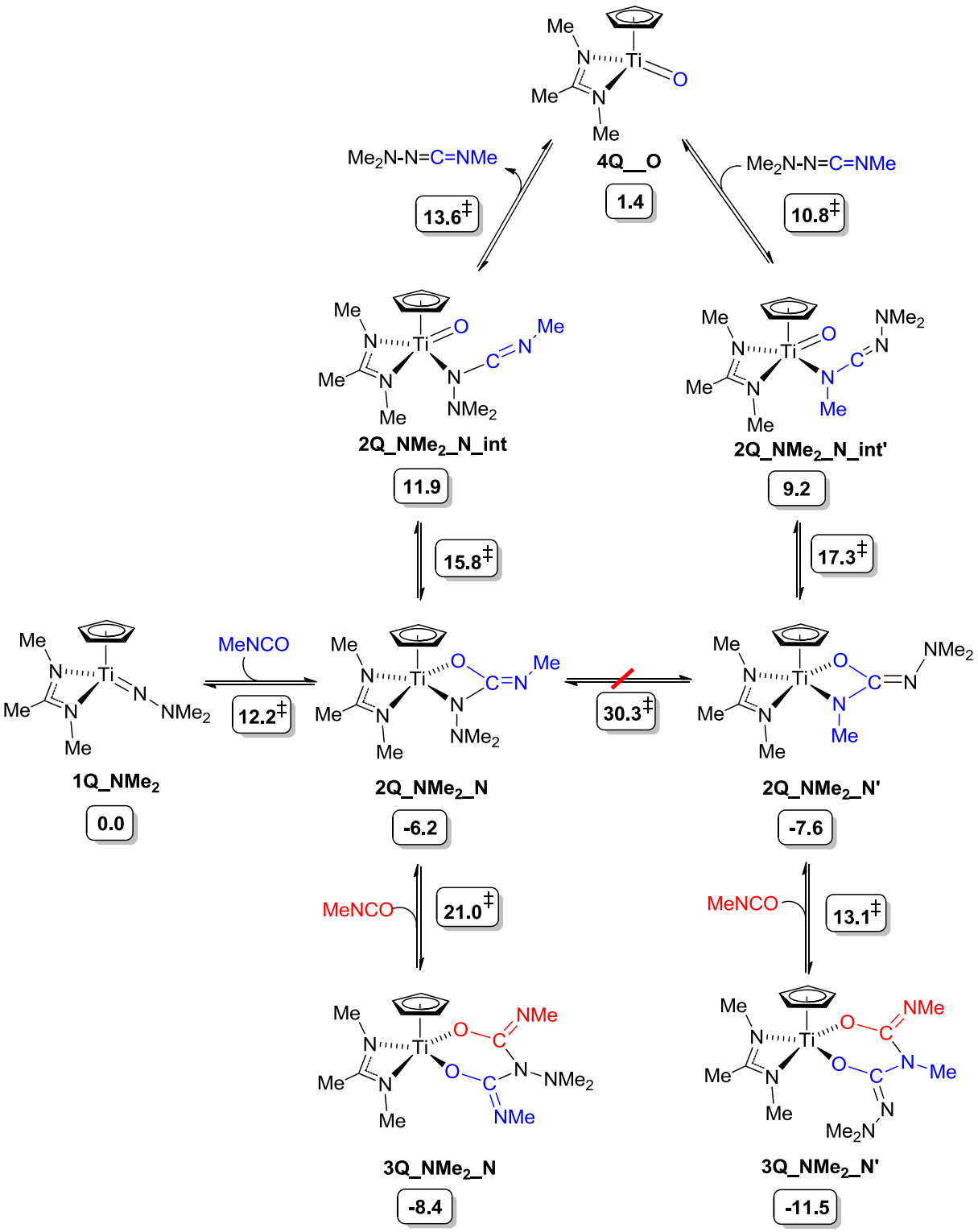

Figure 2.18. DFT mechanism for the formation of CpTi{MeC(NMe)$_2$}{OC(NNMe$_2$)-N(Me)C(NMe)O} (**3Q_NMe$_2$_N´**). Gibbs free energies (298 K) are expressed in kcal mol^{-1} relative to **1Q_NMe$_2$** + 2 MeNCO. The "first" MeNCO is coloured blue and the "second" in red for clarity. All energies are shown in boxes; the values labeled ‡ are transition states.

2.7 Reactions of Cp*Ti{MeC(N^{i}Pr)$_2$}(NNMe$_2$) (2.15) with isothiocyanates

Interestingly, the reaction of **2.15** with Ar′NCS led to the formation of the C_1 symmetric thioureate-type cycloaddition product Cp*Ti{MeC(N^{i}Pr)$_2$}{N(NMe$_2$)-C(NAr′)S} (**17**) with a trace of the μ-sulfido dimer (**2.16**) and Ar′NCNNMe$_2$. The reaction was successfully scaled up in benzene at room temperature yielding **17** as a dark green solid (Scheme 2.5) in 62% yield.

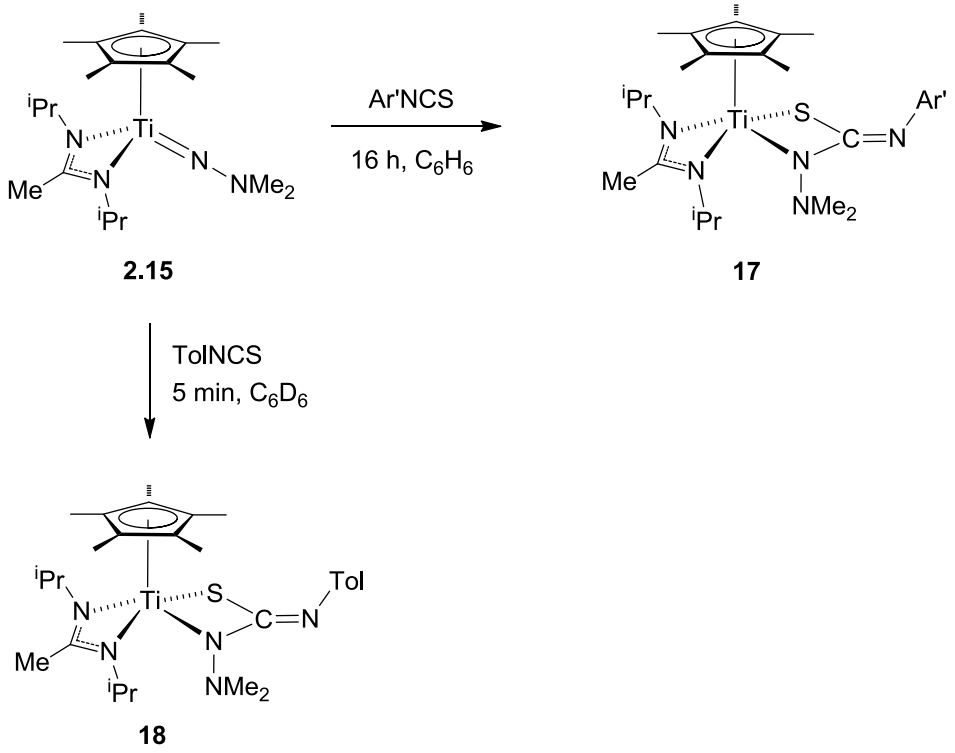

Scheme 2.5. Reactions of Cp*Ti{MeC(N^{i}Pr)$_2$}(NNMe$_2$) (**2.15**) with isothiocyanates. Ar ´= 2,6-C$_6$H$_3$^{i}Pr$_2$.

Unfortunately, all attempts to grow diffraction quality crystals of **17** gave crystals of **2.16**. Although diffraction-quality crystals were not obtained for **17**, other spectroscopic data support the proposed structure shown in Scheme 2.5. The NMR spectra are fully compatible with a cycloaddition product as seen for the reactions between **2.13** with ArNCS. While **2.16** has been reported previously,[47] the solid state structure was not obtained in the previous report. The molecular structure of **2.16** is shown in Figure 2.19. Full crystallographic data are given in the CD Appendix. Selected distances and angles are listed in Table 2.6.

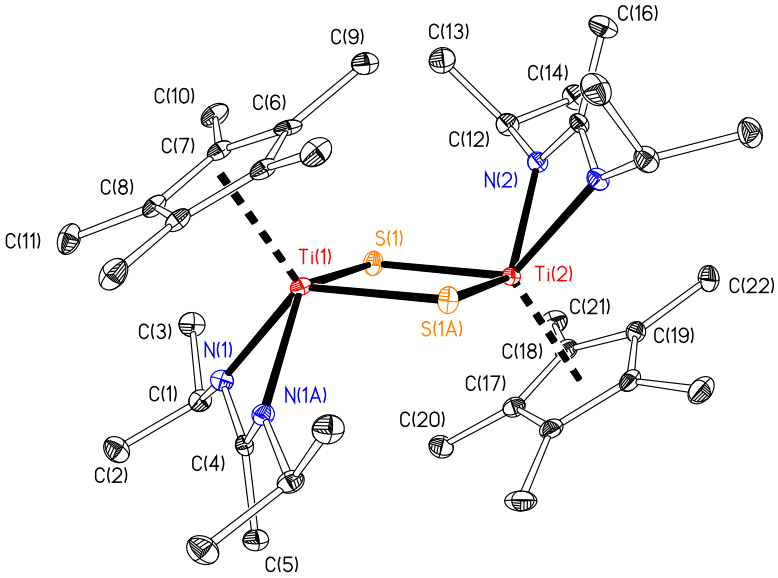

Figure 2.19. Displacement ellipsoid plot (20% probability) of $[Cp^*Ti\{MeC(N^iPr)_2\}(\mu\text{-}S)]_2$ (**2.16**). H atoms and other crystallographically independent molecule omitted for clarity. Atoms carrying the suffix 'A' are related to their counterparts by the symmetry operator *x*, $^1/_2$-*y*, *z*.

Table 2.6. Selected distances (Å) and angles (°) for $[Cp^*Ti\{MeC(N^iPr)_2\}(\mu\text{-}S)]_2$ (**2.16**). Cp_{cent} is the computed Cp* ring carbon centroid. Values in brackets are for the other crystallographically independent molecules.

Ti(1)-$Cp_{cent(1)}$	2.109 [2.093]	Ti(2)-$Cp_{cent(2)}$	2.101 [2.101]
Ti(1)-S(1)	2.3438(9) [2.3145(10)]	Ti(1)-N(1)	2.162(2) [2.135(3)]
$Cp_{cent(1)}$-Ti(1)-S(1)	115.2 [115.2]	$Cp_{cent(1)}$-Ti(1)-N(1)	111.2 [111.3]
$Cp_{cent(2)}$-Ti(2)-S(1)	115.2 [112.9]	$Cp_{cent(2)}$-Ti(2)-N(2)	111.8 [112.5]
Ti(1)-S(1)-Ti(2)	93.29(3) [92.92(3)]	N(1)-Ti(1)-N(1A)	61.71(13) [61.72(14)]
S(1)-Ti(1)-S(1A)	86.28(5) [87.38(5)]		

The molecular structure of **2.16** is very similar to those of the previously reported $[Cp^*Ti\{PhC(NSiMe_3)_2\}(\mu\text{-}S)]_2$ (**2.20**) and $[Cp'Ti\{PhC(NSiMe_3)_2\}(\mu\text{-}S)]_2$ (**2.21**).[47] The structure confirms the dimeric nature of the product, with mutual *trans* arrangement of the cyclopentadienyl rings and may be described as having an edge-shared, four-legged piano stool geometry. The distances and angles are within

expected ranges. The slightly shorter Ti(1)-N(1) bond length compared to **2.20** may be attributed to the sterically less demanding *iso*-propyl groups compared to the $SiMe_3$ groups in **2.20**. The slightly longer Ti-Cp_{cent} and Ti(1)-N(1) distances compared to **2.21** could be due to the greater steric influence of the C_5Me_5 ring in **2.16**.

The presence of Ar′NCNNMe_2 in the product was confirmed by the EI-high resolution mass spectrum obtained, which showed the expected parent ion at *m/z* = 245.1897 with the correct isotope distribution. The ^{1}H NMR data show that both **2.16** and Ar′NCNNMe_2 remained as traces despite repeating the reaction with 2 equivalents of Ar′NCS, or leaving the solution of **17** for 8 days at room temperature. The results obtained suggested that **17** is more stable to extrusion compared to **15_int** which is more susceptible to the lost of Ar′NCNNMe_2 forming **2.12**. This also suggests that both the steric bulk of isothiocyanates and the affinity of NMe_2 fragment towards the metal centre or the organic fragment influence the reaction outcomes.

However, reaction of **2.15** with TolNCS resulted in the formation of an unstable [2+2] cycloaddition product, Cp*Ti{MeC(N^{i}Pr)$_2$}{N(NMe_2)C(NTol)S} (**18**) according to the NMR data. The instability of **18** precludes the scale up reaction. When conducted on the NMR tube scale in toluene-d_8 the conversion of **2.15** to **18** was quantitative. It was thus characterised using NMR spectroscopy at -10 ℃. Unlike the reaction with TolNCO, conducting the reaction with 2 equivalents of TolNCS did not form the "double-insertion" product but instead gave a mixture of unidentified products.

2.8 Adduct formation between Cp*Ti{MeC(N^{i}Pr$_2$)}(NNMe_2) (2.15) and ^{t}BuNC

In Section 2.1, it was mentioned that imides and hydrazides react differently with isonitriles, for example, they can either form a double addition product or result in N_α–N_β bond cleavage. Studies on the reactivity of diamide-pyridyl and diamide-amine supported hydrazides with isonitriles carried out recently also reported the formation of products with N_α–N_β bond scission.[32, 34, 50] However, in this current study, reacting **2.13** with ^{t}BuNC resulted in the formation of a complicated mixture of unidentified products while for **2.15** adduct formation was observed (Equation 2.4).

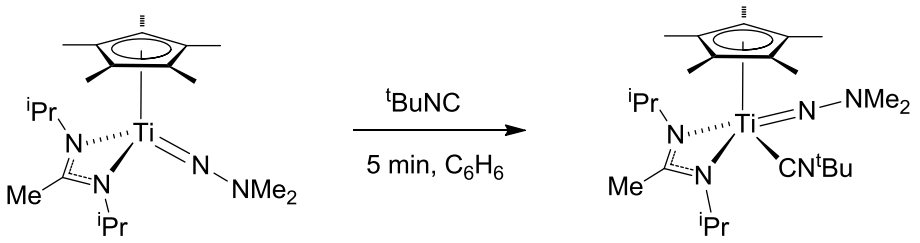

2.15 **19**

Equation 2.4

In the scaled up reaction between **2.15** and ^{t}BuNC, Cp*Ti{MeC(N^{i}Pr)$_2$}{N(NMe$_2$)}(CN^{t}Bu) (**19**) was obtained as a yellow solid with 44% isolated yield. The relatively high solubility of **19** in hydrocarbon solvents contributed to the slightly low yield. Unfortunately, attempts to grow diffraction-quality crystals were unrewarding. However, the ^{1}H and ^{13}C{^{1}H} NMR data support the proposed adduct formation. Room temperature ^{1}H NMR spectrum suggests the formation of a product with a C_s symmetric structure, showing only one septet and a pair of overlapping doublets corresponding to the *iso*-propyl groups of the amidinate ligand. Nevertheless, cooling the sample in the presence of a slight excess of ^{t}BuNC to -60 ℃ in toluene-d_8 resolved the *iso*-propyl groups into two overlapping septets and four doublets, consistent with the proposed adduct with a C_1 symmetric structure (Figure 2.20). The room temperature spectrum can be explained by fast exchange of the two isomers of **19** by isonitrile dissociation which causes the signals to be averaged.

A satisfactory elemental analysis could not be obtained due to the tendency of **19** to lose ^{t}BuNC *in vacuo*. However, the IR spectrum shows a strong band at 2152 cm^{-1}, which is attributed to ν(C≡N) of the isonitrile ligand. This increase in the C–N stretching vibration frequency compared to the uncoordinated ^{t}BuNC (2138 cm^{-1})[79], is consistent with coordination to the electron deficient titanium of **2.15**.[80-82] This type of adduct formation with Lewis bases is not uncommon in Ti=N chemistry. In fact, Lewis bases are sometimes utilised to stabilise the synthesised hydrazido complexes.[33,37,44] Bergman *et al*. previously reported the formation of a similar isonitrile adduct with a strong IR stretch at 2139 cm^{-1} corresponding to the ν(C≡N) of the isonitrile ligand in the adduct.[83] Another example of isonitrile adduct formation was reported by Mountford *et al.* where Ti(N^{t}Bu)(COT′) (COT′ = η^{8}-1,4-

$C_8H_6(SiMe_3)_2$) and Ti(NAr)(COT) (COT = η^8-C_8H_8, Ar = 2,6-^{i}Pr$_2$C$_6$H$_3$) reacted with alkyl or aryl isonitriles to yield the corresponding isonitrile adduct.[84]

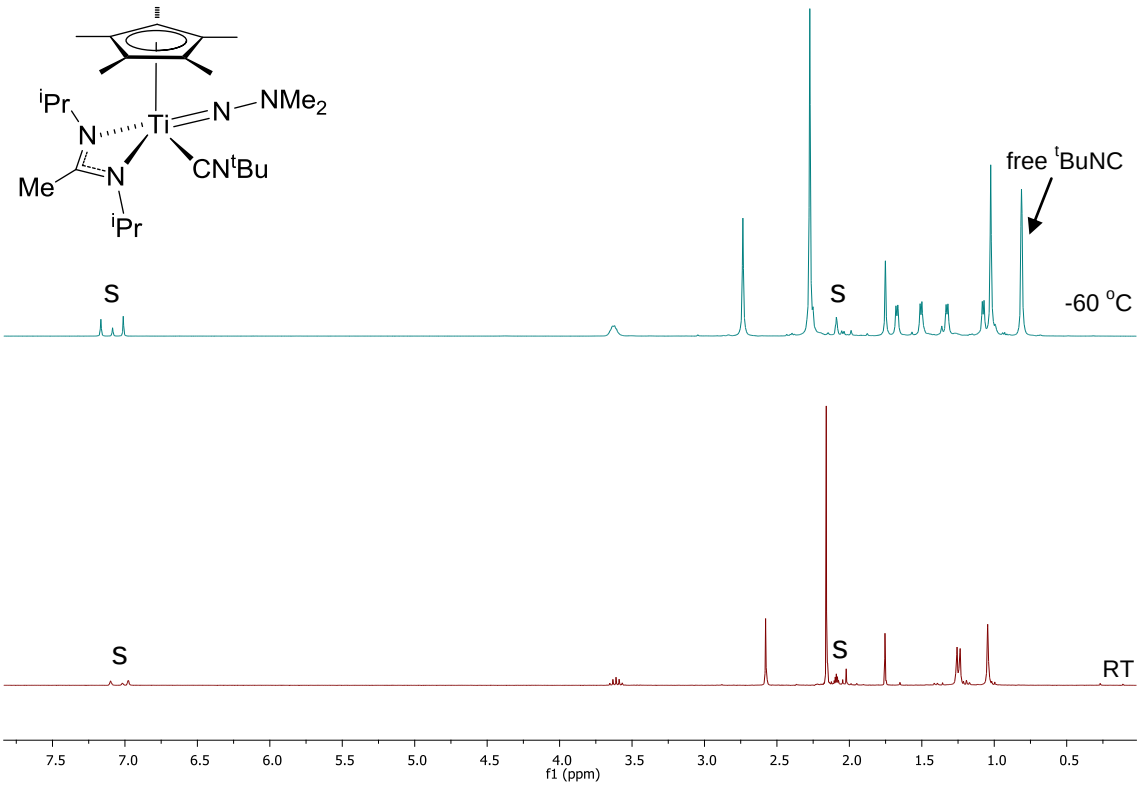

Figure 2.20. ^{1}H NMR spectra of Cp*Ti{MeC(N^{i}Pr)$_2$}{N(NMe$_2$)}(CN^{t}Bu) (**19**) with a slight excess of ^{t}BuNC in toluene-d_8 at room temperature (bottom) and -60 ℃ (top) ("s" denotes residual protio-solvent).

2.9 Thermodynamic considerations

Although many reactions of Cp*Ti{MeC(N^{i}Pr)$_2$}(NR) (R = ^{t}Bu (**2.7**), Tol (**2.18**), NNPh$_2$ (**2.13**) or NNMe$_2$ (**2.15**)) and their homologues with heterocumulenes can result in isolable cycloaddition or "double-insertion" products, there is also a propensity to undergo an overall cycloaddition/extrusion process whereby the "NR" group is transferred to an organic fragment, the NR moiety itself being replaced by O or S. DFT and experimental studies have shown that increasing the steric bulk of the cyclopentadienyl-amidinate ligand set can kinetically stabilise cycloaddition products toward extrusion. It was also reported that the steric demands of the ^{t}Bu group in *tert*-butyl imido complexes leads to extrusion becoming thermodynamically more favourable.[29, 47] The DFT computed reaction of the model imido complex CpTi{MeC(NMe)$_2$}(NMe) (**1Q_Me**) with CO_2 to form CpTi{MeC(NMe)$_2$}(O)

(**4Q__O**) and MeNCO was found to be 5.7 kcal mol^{-1} more favourable (in terms of ΔE) than the corresponding reaction of **1Q_Ph** with CO_2 to form PhNCO, showing a clear underlying preference for NR group transfer to CO in the case of NMe compared to NPh. In this Thesis, the experimental and DFT calculations for this type of reactivity have been extended to include $NNMe_2$ and $NNPh_2$ ligands for the three main substrate classes (CO_2, CS_2 and isocyanates) studied previously with the imido complexes **2.7** and **2.18**. Overall, as demonstrated by experiment and DFT (*cf.* Figure 2.13), the tendency to transfer an imido or hydrazido group from titanium to an organic fragment (CO, CS, CNR) appears to increase in the order $NNPh_2$ < $NNMe_2$ < NTol (< N^tBu). Additionally, taking into account the new results above and those described previously for **2.7** and **2.18**, the imido or hydrazido group exchange with CS_2 is thermodynamically most favourable followed by isocyanates, and least likely with CO_2 to give an overall metathesis reaction (*cf.* Figure 2.11).

To gain further insight into the underlying factors in these metathesis processes we have analysed the model thermodynamic cycle in Figure 2.21 in which the Ti=NR of **1Q_Me**, **1Q_Ph**, **1Q_NPh$_2$** or **1Q_NMe$_2$** exchanges with the C=X (X = O or S) of CO_2, MeNCO or CS_2. The overall energy of this exchange (ΔE_{exch}) can be expressed as the sum of four stepwise bond dissociation energies (BDEs): ΔE_1 (Ti=NR homolysis), ΔE_2 (substrate C=X homolysis), $-\Delta E_3$ (Ti=X formation) and $-\Delta E_4$ (product C=NR bond formation) ($\Delta E_{exch} = \Delta E_1 + \Delta E_2 - \Delta E_3 - \Delta E_4$). This enables the assessment of the effects of the relative affinities of the metal and organic fragment for the NR or X groups and their overall impact on ΔE_{exch}. It should be noted that Figure 2.21 presents electronic energies using 6-311++G** basis sets, whereas Figures 2.11 and 2.13 present Gibbs free energies using a 6-31G** basis set.

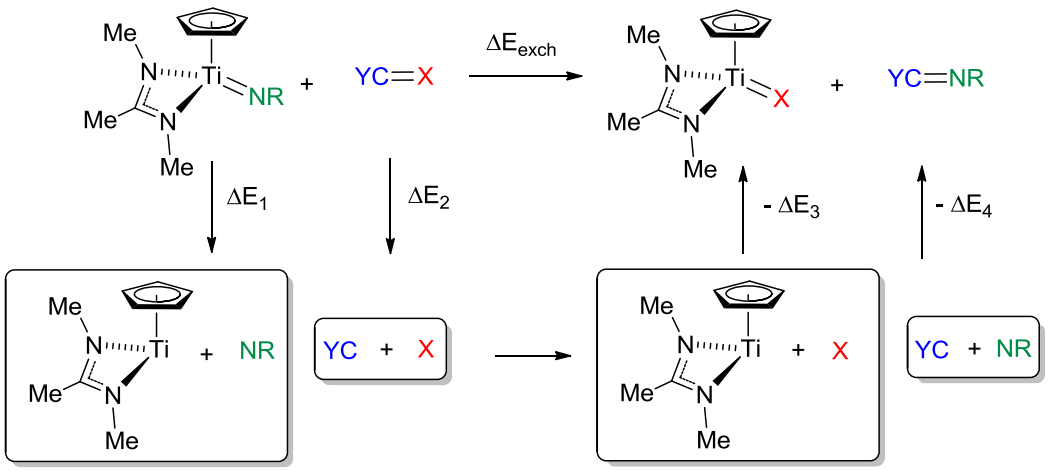

R = Me, Ph, NPh_2, NMe_2; Y = O, S, MeN; X = O, S

Entry	Ti=NR	ΔE_1 (kcal mol^{-1})
1	$TiNNMe_2 \rightarrow Ti + NNMe_2$	59.0
2	$TiNNPh_2 \rightarrow Ti + NNPh_2$	67.7
3	$TiNPh \rightarrow Ti + NPh$	91.6
4	$TiNMe \rightarrow Ti + NMe$	92.1
	YC=X	**ΔE_2 (kcal mol^{-1})**
5	$CO_2 \rightarrow CO + O$	134.0
6	$CS_2 \rightarrow CS + S$	108.8
7	$MeNCO \rightarrow MeNC + O$	133.2
	Ti=X	**ΔE_3 (kcal mol^{-1})**
8	$TiO \rightarrow Ti + O$	148.2
9	$TiS \rightarrow Ti + S$	100.5
	YC=NR	**ΔE_4 (kcal mol^{-1})**
10	$OCNNMe_2 \rightarrow CO + NNMe_2$	36.4
11	$OCNNPh_2 \rightarrow CO + NNPh_2$	39.2
12	$OCNPh \rightarrow CO + NPh$	74.8
13	$OCNMe \rightarrow CO + NMe$	81.7
14	$SCNNMe_2 \rightarrow CS + NNMe_2$	74.6
15	$SCNNPh_2 \rightarrow CS + NNPh_2$	77.7
16	$SCNPh \rightarrow CS + NPh$	111.4
17	$SCNMe \rightarrow CS + NMe$	118.2
18	$MeNCNNMe_2 \rightarrow CNMe + NNMe_2$	41.3
19	$MeNCNNPh_2 \rightarrow CNMe + NNPh_2$	46.0

Figure 2.21. Energy decomposition scheme for selected isodesmic multiple bond exchange reactions of $CpTi\{MeC(NMe)_2\}(NR)$ (R = Me, Ph, NPh_2, NMe_2) with heterocumulenes, and computed bond dissociation energies (ΔE, kcal mol^{-1}). All species are spin state singlets except for the fragments $CpTi\{MeC(NMe)_2\}$, X, NMe and NPh which are spin triplets. $\Delta E_{exch} = \Delta E_1 + \Delta E_2 - \Delta E_3 - \Delta E_4$.

The computed BDEs for the hydrazides **1Q_NMe$_2$** and **1Q_NPh$_2$** (entries 1 and 2) are between 23.9 and 33.1 kcal mol^{-1} less than the imides **1Q_Ph** and **1Q_Me** (entries 3 and 4). The Ti=NNMe$_2$ BDE is somewhat less than that of Ti=NNPh$_2$ (8.7 kcal mol^{-1}). The bond energies of Ti=O and Ti=S (entries 8 and 9) are both greater than any of the Ti=NR systems. Therefore, in terms of titanium-ligand bond strengths, the metathesis reaction is always favourable, and more so for the hydrazides than the imides, and for oxide than sulfide bond formation. However, the experimental results reported above and previously,[29, 47] along with Figures 2.11 and 2.13, are not consistent with these expectations based on titanium-ligand bond strengths *alone*. The substrate and product bond energies also play a key role.

Comparison of entries 1 – 4 (Ti=NR BDEs) with entries 10 – 13 (OC=NR BDEs) or 14 – 17 (SC=NR BDEs) show that all these increase in the order NR = NNMe$_2$ < NNPh$_2$ < NPh < NMe. However, the magnitudes of these changes (i.e. the relative affinities of NR for Ti, CO or CS) differ and this accounts for the different propensities for Ti=NR / C=O or C=S metathesis in the real systems. Consider for example the reactions with CO$_2$. Although the BDE for OC=NNPh$_2$ (entry 11) is 2.8 kcal mol^{-1} greater than for OC=NNMe$_2$ (entry 10), that for Ti=NNPh$_2$ is 8.7 kcal mol^{-1} greater than Ti=NNMe$_2$. Overall, therefore, exchange of Ti=NNR$_2$ and OC=O forming Ti=O and OC=NNR$_2$ is 5.9 kcal mol^{-1} more favourable for NNR$_2$ = NNMe$_2$. Likewise, exchange between Ti=NNR$_2$ and MeNC=O forming Ti=O and MeNC=NNR$_2$ is 4.0 kcal mol^{-1} more favourable for NNR$_2$ = NNMe$_2$ (compare entries 1, 2 and 18, 19) which is consistent with experimental trends.

As for comparison between phenyl imido with the hydrazido systems, entries 2 and 3 show that the Ti=NPh BDE is 23.9 kcal mol^{-1} greater than Ti=NNPh$_2$, but NPh transfer reactions are more favoured experimentally. This can be explained by comparing the BDEs for OC=NNPh$_2$ and OC=NPh (entries 11 and 12) which are greater by 35.6 kcal mol^{-1} for NPh. Thus Ti=NPh / OC=O metathesis is favoured by 11.7 kcal mol^{-1} compared to Ti=NNPh$_2$ because of the greater affinity of NPh for CO. Similarly, Ti=NPh / SC=S metathesis is favoured by 9.8 kcal mol^{-1} compared to the same process for Ti=NNPh$_2$ (compare entries 2, 3 and 15, 16), again consistent with experimental observations of the ready formation of sulfide products in the reactions of aryl imido compounds with CS$_2$, but stable cycloaddition products with **2.13** and **2.15**. Finally, it should be noted that the calculated energy for Ti=NNMe$_2$ + CO$_2$ →

Ti=O + $OCNNMe_2$ (8.4 kcal mol^{-1}) is significantly higher than the corresponding process for MeNCO forming $MeNCNNMe_2$ (2.7 kcal mol^{-1}), consistent with the observed behaviour of the real system **2.15** with CO_2 and isocyanates.

2.10 Conclusions

The cyclopentadienyl-amidinate complexes Cp*Ti{$MeC(N^iPr)_2$}(NNR^1R^2) (R^1 = Ph, R^2 = Ph (**2.13**) or Me (**2.14**); R^1 = R^2 = Me (**2.15**)) have allowed a detailed combined experimental and DFT study of terminal titanium hydrazido complexes as a function of the N_β substituents. DFT studies of the model analogues CpTi{$MeC(NMe)_2$}(NNR^1R^2) confirmed the overall structural trends and an explanation in terms of the effects of the N_β lone pair. A comparison with the corresponding model imido complexes CpTi{$MeC(NMe)_2$}(NR) (R = Me or Ph) completed the bonding picture.

Compounds **2.13** and **2.15** can have different reactivity at the Ti=N_α bond (cycloaddition, cycloaddition-insertion, cycloaddition-elimination) depending on the N_β substituents and the substrates in question. With CO_2 and CS_2, the chemistry is generally rather similar, and reaction products of the type seen previously with imido compounds Cp*Ti{$MeC(N^iPr)_2$}(NR) (R = ^{t}Bu (**2.7**) or Tol (**2.18**)) were observed. The cycloaddition products formed with the hydrazides were, however, more stable with regard to extrusion reactions. In the reactions of **2.13** and **2.15** with ^{t}BuNCO, TolNCO and Ar′NCO there was a more clear-cut difference in reactions. The diphenyl hydrazido compound **2.13** formed quite stable cycloaddition products, which in the case of Cp*Ti{$MeC(N^iPr)_2$}{$N(NPh_2)C(NTol)O$} (**7**), reacted further with CO_2 to give a mixed cycloaddition-insertion product. With **2.15** the chemistry was more dominated by cycloaddition-elimination reactions. Reaction with ^{t}BuNCO or Ar′NCO (2 equivalents) gave *N*-dimethylaminocarbodiimide ^{t}BuNCNNMe$_2$ (**14**) or the heterocycle $\overline{N(Me)_2NC(NAr')N(Ar')}C(O)$ (**15**), respectively, along with [Cp*Ti{$MeC(N^iPr)_2$}(μ-O)]$_2$ (**2.12**). With TolNCO (2 equivalents), Cp*Ti{$MeC(N^iPr)_2$}{$OC(NNMe_2)N(Tol)C(NTol)O$} (**16**) was formed *via* a series of cycloaddition-elimination and cycloaddition-insertion steps. Reaction of **2.13** with ^{t}BuNC formed a complicated mixture of unidentified products but gave a ^{t}BuNC adduct with **2.15**.

The energetics and mechanisms of the cycloaddition, cycloaddition-insertion and cycloaddition-extrusion processes of various model imido and hydrazido complexes were investigated using DFT. In the latter (metathesis) reactions, the reaction outcomes depend on a delicate balance of the relative affinities of NR or NNR_2 for the metal centre or the organic fragment (CO, CS or RNC).

2.11 References

1. J. E. Hill, R. D. Profilet, P. E. Fanwick and I. P. Rothwell, *Angew. Chem. Int. Ed. Engl.*, 1990, **29**, 664.
2. H. W. Roesky, H. Voelker, M. Witt and M. Noltemeyer, *Angew. Chem. Int. Ed. Engl.*, 1990, **29**, 669.
3. C. C. Cummins, C. P. Schaller, G. D. Van Duyne, P. T. Wolczanski, A. W. E. Chan and R. Hoffmann, *J. Am. Chem. Soc.*, 1991, **113**, 2985.
4. P. L. McGrane, M. Jensen and T. Livinghouse, *J. Am. Chem. Soc.*, 1992, **114**, 5459.
5. D. E. Wigley, *Prog. Inorg. Chem.*, 1994, **42**, 239.
6. P. Mountford, *Chem. Commun.*, 1997, 2127.
7. L. H. Gade and P. Mountford, *Coord. Chem. Rev.*, 2001, **216-217**, 65.
8. P. D. Bolton and P. Mountford, *Adv. Synth. Catal.*, 2005, **347**, 355.
9. N. Hazari and P. Mountford, *Acc. Chem. Res.*, 2005, **38**, 839.
10. A. L. Odom, *Dalton Trans.*, 2005, 225.
11. A. R. Fout, U. J. Kilgore and D. J. Mindiola, *Chem. Eur. J.*, 2007, **13**, 9428.
12. T. R. Cundari, *Chem. Rev.*, 2000, **100**, 807.
13. N. Kaltsoyannis and P. Mountford, *J. Chem. Soc., Dalton Trans.*, 1999, 781.
14. S. C. Dunn, N. Hazari, N. M. Jones, A. G. Moody, A. J. Blake, A. R. Cowley, J. C. Green and P. Mountford, *Chem. Eur. J.*, 2005, **11**, 2111.
15. C. Cao, Y. Shi and A. L. Odom, *Org. Lett.*, 2002, **4**, 2853.
16. V. Khedkar, A. Tillack, M. Michalik and M. Beller, *Tet. Letts.*, 2004, **45**, 3123.
17. Y. Li, Y. Shi and A. L. Odom, *J. Am. Chem. Soc.*, 2004, **126**, 1794.
18. A. Tillack, H. Jiao, I. Garcia Castro, C. G. Hartung and M. Beller, *Chem. Eur. J.*, 2004, **10**, 2410.
19. L. Ackermann and R. Born, *Tet. Letts.*, 2004, **45**, 9541.
20. S. Banerjee, E. Barnea and A. L. Odom, *Organometallics*, 2008, **27**, 1005.

21. S. Banerjee and A. L. Odom, *Organometallics*, 2006, **25**, 3099.
22. N. Wiberg, H.-W. Haring, G. Huttner and P. Friedrich, *Chem. Ber.*, 1978, **111**, 2708.
23. T. B. Parsons, N. Hazari, A. R. Cowley, J. C. Green and P. Mountford, *Inorg. Chem.*, 2005, **44**, 8442.
24. J. D. Selby, C. Schulten, A. D. Schwarz, A. Stasch, E. Clot, C. Jones and P. Mountford, *Chem.Commun.*, 2008, 5101.
25. A. Bashall, P. E. Collier, L. H. Gade, M. McPartlin, P. Mountford, S. M. Pugh, S. Radojevic, M. Schubart, I. J. Scowen and D. J. M. Trösch, *Organometallics*, 2000, **19**, 4784.
26. D. J. M. Trösch, P. E. Collier, A. Bashall, L. H. Gade, M. McPartlin, P. Mountford and S. Radojevic, *Organometallics*, 2001, **20**, 3308.
27. A. E. Guiducci, A. R. Cowley, M. E. G. Skinner and P. Mountford, *J. Chem. Soc., Dalton Trans.*, 2001, 1392.
28. C. L. Boyd, E. Clot, A. E. Guiducci and P. Mountford, *Organometallics*, 2005, **24**, 2347.
29. A. E. Guiducci, C. L. Boyd, E. Clot and P. Mountford, *Dalton Trans.*, 2009, 5960.
30. J. D. Selby, C. D. Manley, M. Feliz, A. D. Schwarz, E. Clot and P. Mountford, *Chem. Commun.*, 2007, 4937.
31. A. D. Schofield, A. Nova, J. D. Selby, C. D. Manley, A. D. Schwarz, E. Clot and P. Mountford, *J. Am. Chem. Soc.*, 2010, **132**, 10484.
32. A. D. Schofield, A. Nova, J. D. Selby, A. D. Schwarz, E. Clot and P. Mountford, *Chem. Eur. J.*, 2011, **17**, 265.
33. P. J. Walsh, M. J. Carney and R. G. Bergman, *J. Am. Chem. Soc.*, 1991, **113**, 6343.
34. H. Herrmann, J. L. Fillol, H. Wadepohl and L. H. Gade, *Angew. Chem. Int. Ed.*, 2007, **46**, 8426.
35. T. Gehrmann, J. L. Fillol, H. Wadepohl and L. H. Gade, *Angew. Chem. Int. Ed.*, 2009, **48**, 2152
36. A. J. Blake, J. M. McInnes, P. Mountford, G. I. Nikonov, D. Swallow and D. J. Watkin, *J. Chem. Soc., Dalton Trans.*, 1999, 379.
37. K. Weitershaus, J. L. Fillol, H. Wadepohl and L. H. Gade, *Organometallics*, 2009, **28**, 4747.

38. T. Gehrmann, J. L. Fillol, H. Wadepohl and L. H. Gade, *Organometallics*, 2010, **29**, 28.
39. P. J. Tiong, A. D. Schofield, J. D. Selby, A. Nova, E. Clot and P. Mountford, *Chem. Commun.*, 2010, **46**, 85.
40. M. Hidai, *Chem. Rev.*, 1995, **95**, 1115.
41. M. Hidai, *Coord. Chem. Rev.*, 1999, **185-186**, 99.
42. S. Patel, Y. Li and A. L. Odom, *Inorg. Chem.*, 2007, **46**, 6373.
43. A. J. Clulow, J. D. Selby, M. G. Cushion, A. D. Schwarz and P. Mountford, *Inorg. Chem.*, 2008, **47**, 12049.
44. K. Weitershaus, H. Wadepohl and L. H. Gade, *Organometallics*, 2009, **28**, 3381.
45. J. D. Selby, M. Feliz, A. D. Schwarz, E. Clot and P. Mountford, *Organometallics*, 2011, **30**, 2295.
46. C. L. Boyd, A. E. Guiducci, S. R. Dubberley, B. R. Tyrrell and P. Mountford, *J. Chem. Soc., Dalton Trans.*, 2002, 4175.
47. A. E. Guiducci, C. L. Boyd and P. Mountford, *Organometallics*, 2006, **25**, 1167.
48. F. G. N. Cloke, J. C. Green, N. Hazari, P. B. Hitchcock, P. Mountford, J. F. Nixon and D. J. Wilson, *Organometallics*, 2006, **25**, 3688.
49. P. J. Tiong, A. Nova, L. R. Groom, A. D. Schwarz, J. D. Selby, A. D. Schofield, E. Clot and P. Mountford, *Organometallics*, 2011, **30**, 1182.
50. J. D. Selby, D.Phil Thesis, University of Oxford, 2009.
51. P. J. Stewart, A. J. Blake and P. Mountford, *Organometallics*, 1998, **17**, 3271.
52. F. H. Allen and O. Kennard, *Chemical Design Automation News*, 1993, **8**, 1.
53. D. A. Fletcher, R. F. McMeeking and D. Parkin, *J. Chem. Inf. Comput. Sci.*, 1996, **36**, 746 (The UK Chemical Database Service: CSD version 5.32 updated August 2011).
54. J. D. Selby, C. D. Manley, A. D. Schwarz, E. Clot and P. Mountford, *Organometallics*, 2008, **27**, 6479.
55. O. A. Litvinov, L. V. Ermolaeva, V. V. Zverev and V. A. Naumov, *J. Struct. Chem.*, 1989, **30**, 224.
56. S. R. Dubberley, A. Friedrich, D. A. Willman, P. Mountford and U. Radius, *Chem. Eur. J.*, 2003, **9**, 3634.

57. F. Weinhold and C. R. Landis, *Valency and bonding: a natural bond orbital donor-acceptor perspective*, Cambridge University Press, Cambridge, 2005.
58. A. J. Blake, P. E. Collier, S. C. Dunn, W.-S. Li, P. Mountford and O. V. Shishkin., *J. Chem. Soc., Dalton Trans.*, 1997, 1549.
59. P. E. Collier, S. C. Dunn, P. Mountford, O. V. Shishkin and D. Swallow, *J. Chem. Soc., Dalton Trans.*, 1995, 3743.
60. N. Adams, H. J. Arts, P. D. Bolton, D. Cowell, S. R. Dubberley, N. Friederichs, C. M. Grant, M. Kranenburg, A. J. Sealey, B. Wang, P. J. Wilson, M. A. Zuideveld, A. J. Blake, M. Schröder and P. Mountford, *Organometallics*, 2006, **25**, 3888.
61. N. Adams, H. R. Bigmore, T. L. Blundell, C. L. Boyd, S. R. Dubberley, A. J. Sealey, A. R. Cowley, M. E. G. Skinner and P. Mountford, *Inorg. Chem.*, 2005, **44**, 2882.
62. T. R. Cundari, *J. Am. Chem. Soc.*, 1992, **114**, 7879.
63. P. Mountford and D. Swallow, *J. Chem. Soc., Chem. Commun.*, 1995, 2357.
64. P. D. Bolton, E. Clot, N. Adams, S. R. Dubberley, A. R. Cowley and P. Mountford, *Organometallics*, 2006, **25**, 2806.
65. M. Feliz, P. D. Bolton, E. Clot and P. Mountford, *Organometallics*, 2008, **27**, 6111.
66. H. Herrmann, J. L. Fillol, T. Gehrmann, M. Enders, H. Wadepohl and L. H. Gade, *Chem. Eur. J.*, 2008, **14**, 8131.
67. S. Kahlal, J.-Y. Saillard, J.-R. Hamon, C. Manzur and D. Carrillo, *J. Chem. Soc., Dalton Trans.*, 1998, 1229.
68. N. Lehnert and F. Tuczek, *Inorg. Chem.*, 1999, **38**, 1671.
69. H. R. Bigmore, S. R. Dubberley, M. Kranenburg, S. C. Lawrence, A. J. Sealey, J. D. Selby, M. Zuideveld, A. R. Cowley and P. Mountford, *Chem.Commun.*, 2006, 436.
70. S. C. Lawrence, M. E. G. Skinner, J. C. Green and P. Mountford, *Chem. Commun.*, 2001, 705.
71. S. C. Dunn, P. Mountford and O. V. Shishkin, *Inorg. Chem.*, 1996, **35**, 1006.
72. N. A. H. Male, M. E. G. Skinner, S. Y. Bylikin, P. J. Wilson, P. Mountford and M. Schröder, *Inorg. Chem.*, 2000, **39**, 5483.
73. D. S. Glueck, J. Wu, F. J. Hollander and R. G. Bergman, *J. Am. Chem. Soc.*, 1991, **113**, 2041.

74. W. H. Bernskoetter, E. Lobkovsky and P. J. Chirik, *Angew. Chem. Int. Ed.*, 2007, **46**, 2858.

75. D. J. Knobloch, H. E. Toomey and P. J. Chirik, *J. Am. Chem. Soc.*, 2008, **130**, 4248.

76. J. H. Cooley, E. J. Evain, R. D. Willett and J. T. Blanchette, *J. Org. Chem.*, 1989, **54**, 1048.

77. S. Sarker, J. H. Cooley, R. D. Willett and A. L. Rheingold, *J. Org. Chem.*, 1995, **60**, 476.

78. F. H. Allen, O. Kennard, D. G. Watson, L. Brammer, A. G. Orpen and R. Taylor, *J. Chem. Soc., Perkin Trans. 2*, 1987, S1.

79. T. Carofiglio, C. Floriani, A. Chiesi-Villa and C. Guastini, *Inorg. Chem.*, 1989, **28**, 4417.

80. F. Ekkehardt Hahn and T. Lügger, *J. Organomet. Chem.*, 1995, **501**, 341.

81. T. Carofiglio, P. G. Cozzi, C. Floriani, A. Chiesi-Villa and C. Rizzoli, *Organometallics*, 1993, **12**, 2726.

82. A. Vogler, *Isonitrile Chemistry*, Academic Press, Inc., New York and London, 1971.

83. A. W. Kaplan, J. L. Polse, G. E. Ball, R. A. Andersen and R. G. Bergman, *J. Am. Chem. Soc.*, 1998, **120**, 11649.

84. S. C. Dunn, N. Hazari, A. R. Cowley, J. C. Green and P. Mountford, *Organometallics*, 2006, **25**, 1755.

Chapter Three

Site selectivity and reversibility in the reactions of titanium hydrazides with Si–H, Si–X, C–X and H^+ reagents

3.1 Introduction

Terminal transition metal hydrazide(2-) (L)M=NNR_2 (R = H, alkyl or aryl) have been of ongoing interest for over 30 years.[1-3] Initial studies focused on molybdenum and tungsten derivatives in the context of the biological conversion of dinitrogen to ammonia.[4-6] Both the Chatt type[7-11] and Schrock type[12, 13] model systems proceed mechanistically *via* a series of protonation and electron transfer events. These involve (L)M=NNH_2 intermediates immediately prior to the key N_α–N_β bond cleavage step, in agreement with computational studies.[14-16]

For the earlier transition metals, Fryzuk's landmark report of H_2 and organosilane additions to a μ-η^2:η^2-N_2 ligand bound to a dizirconium platform[17] heralded a series of functionalisation reactions of coordinated N_2 reported during the past 10 – 12 years.[4, 5, 18-22] Among these are Chirik *et al.*'s report of the exhaustive hydrogenation of a similarly coordinated N_2 to form NH_3.[23] Mechanistically distinct from the Chatt-Schrock systems, this proceeds *via* a μ-η^2:η^2-N_2H_2 (diazenido) ligand rather than a terminal NNH_2 (hydrazido) moiety. Other recent work from this group has established the conversion of N_2 to functionalised hydrazide and related groups at zirconium and hafnium centres.[24-28]

Our group and others have recently been developing Group 4 terminal hydrazido(2-) chemistry which has only recently been developed in detail following early reports.[29-32] These compounds show a rich reaction chemistry of both the M=N_α and N_α–N_β bonds. Reactions at the M=N_α bond include cycloaddition, cycloaddition-insertion, cycloaddition-elimination and NNR_2 group transfer with unsaturated substrates such as alkynes, phosphaalkynes, allenes, CO_2, isocyanates, isothiocyanates, nitriles and azides.[31, 33-43] N_α–N_β bond cleavage reactions occur with alkynes, CO and isonitriles as well as with other substrates.[30, 35, 44, 45]

Despite this recent activity, the reactions of terminal Group 4 M=NNR_2 functional groups (in principle also feasible intermediates *en route* to NH_3 or silyl amines) with Si–X (X = H or halogen) or H–H bonds remain unexplored, although there is precedent for their addition to metal-ligand multiple bonds in general.[46-58] Likewise, the chemistry of metal complexes with silanes and silicon-based ligands has been a topic of much interest for many years.[59-64] This Chapter includes a combined experimental and DFT comparative study of the reactions of titanium hydrazido and

imido compounds with silanes, halosilanes and H_2. Alkylation and protonation reactions which have been little studied for group 4 hydrazides are also presented.[65-67] Taken together, these studies provide a detailed picture of the chemistry of the Ti=NNR$_2$ functional group at the interface with N_2 functionalisation chemistry. Parts of this work have been published.[68, 69]

In recent reports[34, 36, 70-74] as well as in the previous Chapter, it was shown that the cyclopentadienyl-amidinate ligand set can support a homologous series of *tert*-butylimido, arylimido, dimethylhydrazido and diphenylhydrazido complexes. Differing only in the nature of the N_α substituent, each of these Ti=NR or Ti=NNR$_2$ linkages can give rise to different reaction outcomes with unsaturated substrates (cycloaddition, cycloaddition-insertion, cycloaddition-elimination). This Chapter focuses on the reactivity of Cp*Ti{MeC(N^{i}Pr)$_2$}(NNR$_2$) [R = Me (**3.1**) or Ph (**3.2**)][34, 75] and Cp*Ti{MeC(N^{i}Pr)$_2$}(NTol) (**3.3**).[73] As discussed in Chapter 2, the N_β atom of **3.1** is strongly pyramidalised, whereas that in **3.2** is planar due to conjugation of the N_β lone pair with the phenyl groups. Compound **3.3** has no NR$_2$ substituent and allows comparison of Ti=N_α bond reactivity without β-NR$_2$ group contributions.

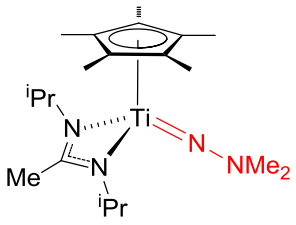

3.1

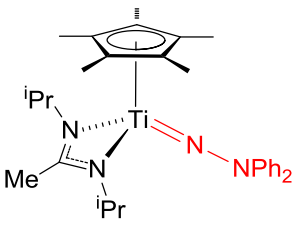

3.2

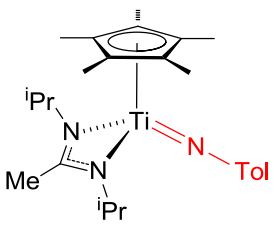

3.3

3.2 Reactions with primary silanes and dihydrogen

This Section will focus on the reactions of **3.1**, **3.2** and **3.3** with primary silanes and H_2. Reaction of **3.1** with $PhSiH_3$ in pentane gave an immediate colour change from dark green to yellow. NMR data shows immediate quantitative conversion to the hydride-hydrazide(1-) complex Cp*Ti{MeC(N^{i}Pr)$_2$}(H){N(NMe$_2$)SiH$_2$Ph} (**20**) *via* net Si–H 1,2-addition to the Ti=N_α bond of **3.1** as shown in Equation 3.1. Compound **20** was isolated as yellow crystals in 58% yield. Diffraction-quality crystals were grown from a concentrated pentane solution at -30 ℃.

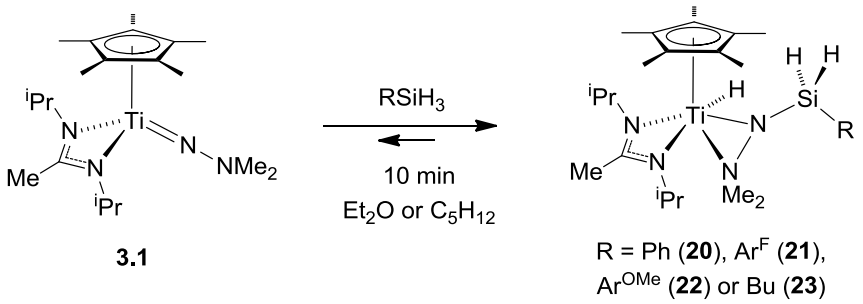

Equation 3.1

To probe the effect of silane electronic factors on the reaction, the same reaction was carried out between **3.1** and different primary aryl and alkyl silanes, namely Ar^FSiH_3, $Ar^{OMe}SiH_3$ (Ar^F = 3,5-$C_6H_3(CF_3)_2$, ArO^{Me} = 4-C_6H_4OMe) and $BuSiH_3$. All three reactions proceed to form the hydride-hydrazide(1-) complexes Cp*Ti{MeC(N^{i}Pr)$_2$}(H){N(NMe$_2$)SiH$_2$R} (R = Ar^F (**21**), Ar^{OMe} (**22**) or Bu (**23**)) *via* net Si–H 1,2-addition to the Ti=N$_\alpha$ bond of **3.1** as shown in Equation 3.1. Both **21** and **22** were isolated as yellow crystals in 76% yield whereas **23** is a very soluble waxy solid which could only be obtained in 22% yield. Diffraction-quality crystals of **21** and **22** were obtained from a concentrated pentane solution at -30 ℃.

Compounds **20** – **23** tend to lose $RSiH_3$ *in vacuo*, particularly in the case of **23**. When followed on the NMR tube scale in C_6D_6 the reactions (1:1 stoichiometry) were essentially quantitative for $ArSiH_3$, whereas with $BuSiH_3$ the conversion of **3.1** to **23** was only *ca*. 85% at room temperature and an equilibrium mixture was formed. All four compounds exhibit temperature-dependent equilibria where exchange between free and coordinated silanes was observed at higher temperatures by NMR. In addition, **20** – **23** are stable for weeks in solution at room temperature, and **20**, **22** and **23** are stable up to 104 ℃ in toluene-d_8 without showing signs of decomposition which is remarkable for titanium-hydride complexes.

As **3.1** reacts cleanly with different primary aryl and alkyl silanes to give hydride-hydrazide(1-) complexes, the corresponding reaction was attempted with the bulkier secondary silane, Ph_2SiH_2. Unfortunately, equilibrium mixtures were formed between **3.1** and Ph_2SiH_2, even when the silane was used in excess. No product could be isolated in this case. When the tertiary silane Et_3SiH was used, no reaction was observed at all, again even in the presence of excess silane. No reaction was observed between **3.2** or **3.3** and any of the aforementioned silanes, and no reaction occured

between **3.1** or **3.2** or **3.3** and H_2 at *ca*. 4 atm pressure and at temperatures down to -70 ℃ (toluene-d_8). Terminal titanium hydride compounds are comparatively uncommon and only a relatively small number have been structurally authenticated.[48, 49, 76-82]

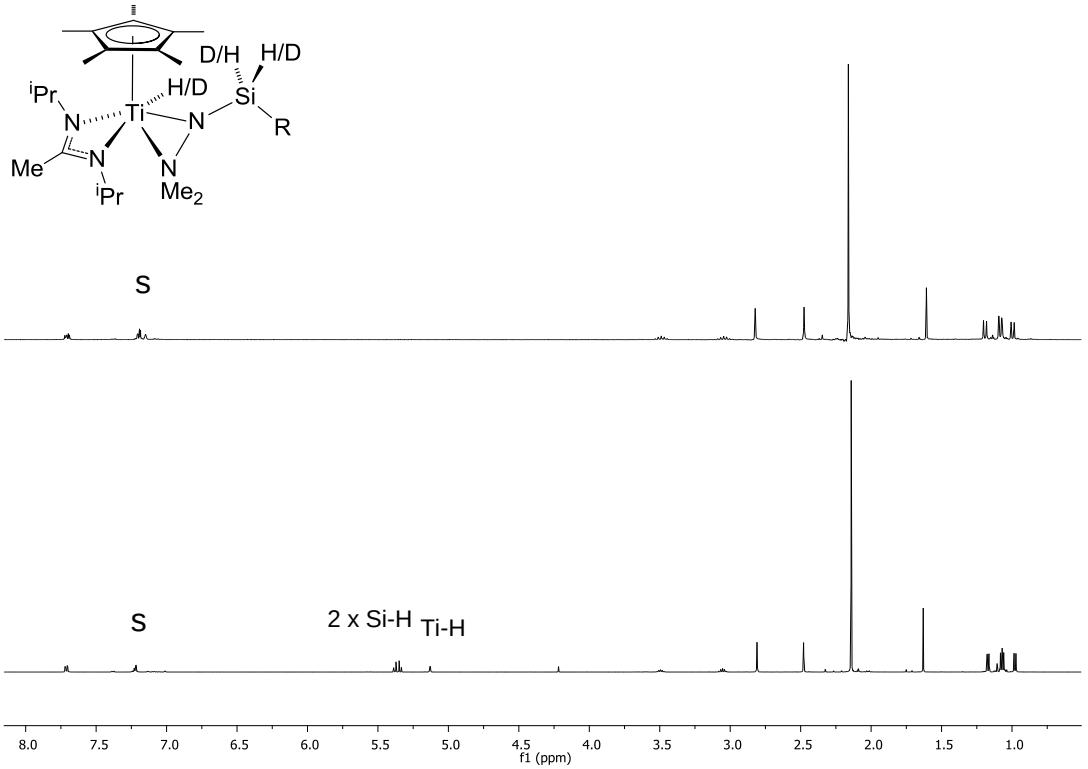

Figure 3.1. ^{1}H NMR spectrum (299.9 MHz) of Cp*Ti{MeC(N^{i}Pr)$_2$}(D)-{N(NMe$_2$)SiD$_2$Ph} (**20-*d*$_3$**) (top) and Cp*Ti{MeC(N^{i}Pr)$_2$}(H){N(NMe$_2$)SiH$_2$Ph} (**20**) (bottom) in C_6D_6 ("s" denotes residual protio-solvent).

To confirm the spectroscopic assignments for Ti–H and Si–H the deuterated compound Cp*Ti{MeC(N^{i}Pr)$_2$}(D){N(NMe$_2$)SiD$_2$Ph} (**20-*d*$_3$**) was prepared from **3.1** and PhSiD$_3$ (Figure 3.1). The ^{1}H, ^{13}C{^{1}H} and ^{29}Si NMR spectra of **20** – **23** are consistent with the proposed structures shown in Equation 3.1 which have been confirmed by X-ray crystallography (*vide infra*). The Ti–*H* NMR resonances appear between 5.05 and 5.19 ppm, and those for the inequivalent Si–*H* atoms between *ca.* 4.8 and 5.5 ppm. A single resonance between -42.1 and -44.3 ppm was observed in the ^{29}Si spectra of **20** – **22**, and at -36.6 ppm for **23**. The ν(Si–H) bands (symmetric and antisymmetric combinations) lie between 2094 and 2195 cm^{-1} in the IR spectra, with ν(Ti–H) appearing between 1558 and 1565 cm^{-1}. These bands, and the corresponding ^{1}H NMR resonances, were absent in **20-*d*$_3$**.

The solid state structure of **20** is shown in Figure 3.2, and that for **21** and **22** are shown in Figure 3.3, and selected distances and angles are given in Table 3.1. Full crystallographic data are given in the CD Appendix. The molecular structures confirm the 1,2-addition of Si–H to Ti=N_α and reveal five-legged piano stool geometries; the distances and angles are within the expected general ranges[76] and there are no significant differences between the three structures.

Figure 3.2 and 3.3 show that N(1), N(3), N(4) and H(1) atoms in **20** – **22** are approximately co-planar. Ti(1) lies *ca.* 0.65 Å above and N(2) *ca.* 1.35 Å below this plane. The new N(NMe_2)SiH_2Ar ligands are κ^2-coordinated as is usually found for titanium hydrazido(1-) complexes,[42, 65, 83-90] except for especially crowded systems[88] or those with β-NPh_2 substituents.[90, 91] The solution NMR data are consistent with this as shown by the inequivalent NMe groups. The Ti(1)-N(1) and N(1)-N(2) distances of *ca.* 1.95 - 1.96 and 1.44 - 1.46 Å are significantly lengthened compared to those of 1.723(3) and 1.386(2) Å, respectively, in **3.1**. These values lie at the longer end of the ranges previously found for κ^2-coordinated hydrazido(1-) complexes (Ti-N_α: 1.832 - 2.005 (mean *ca.* 1.90) Å; N_α-N_β: 1.236 - 1.458 (mean *ca.* 1.41) Å; 14 examples[76]) and are consistent with the disruption of the Ti–N_α triple bond and a change from *sp* hybridisation for N(1) in **3.1** to sp^2 in **20** – **22**. The Ti(1)-N(2) distances (avg. Ti(1)-N(2) = *ca.* 2.21 Å) are only slightly longer than those for the amidinate supporting ligands (avg. Ti-N(3,4) = *ca.* 2.19 Å) and within the usual ranges.

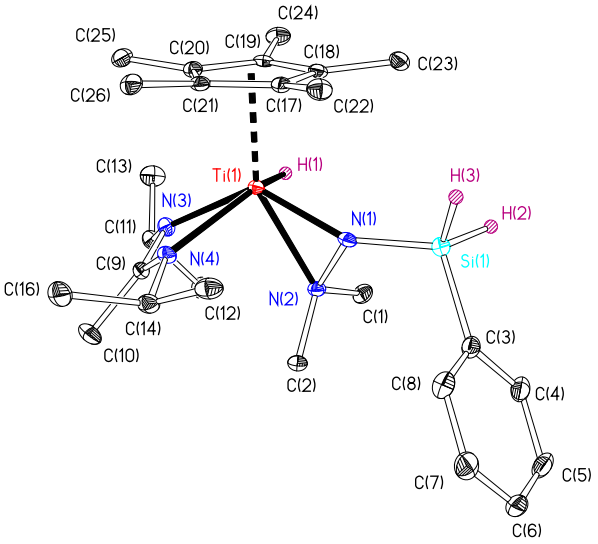

Figure 3.2. Displacement ellipsoid plot (20% probability) of Cp*Ti{$MeC(N^iPr)_2$}(H){N(NMe_2)SiH_2Ph} (**20**). C-bound H atoms omitted for clarity, and other H atoms drawn as spheres of an arbitrary radius.

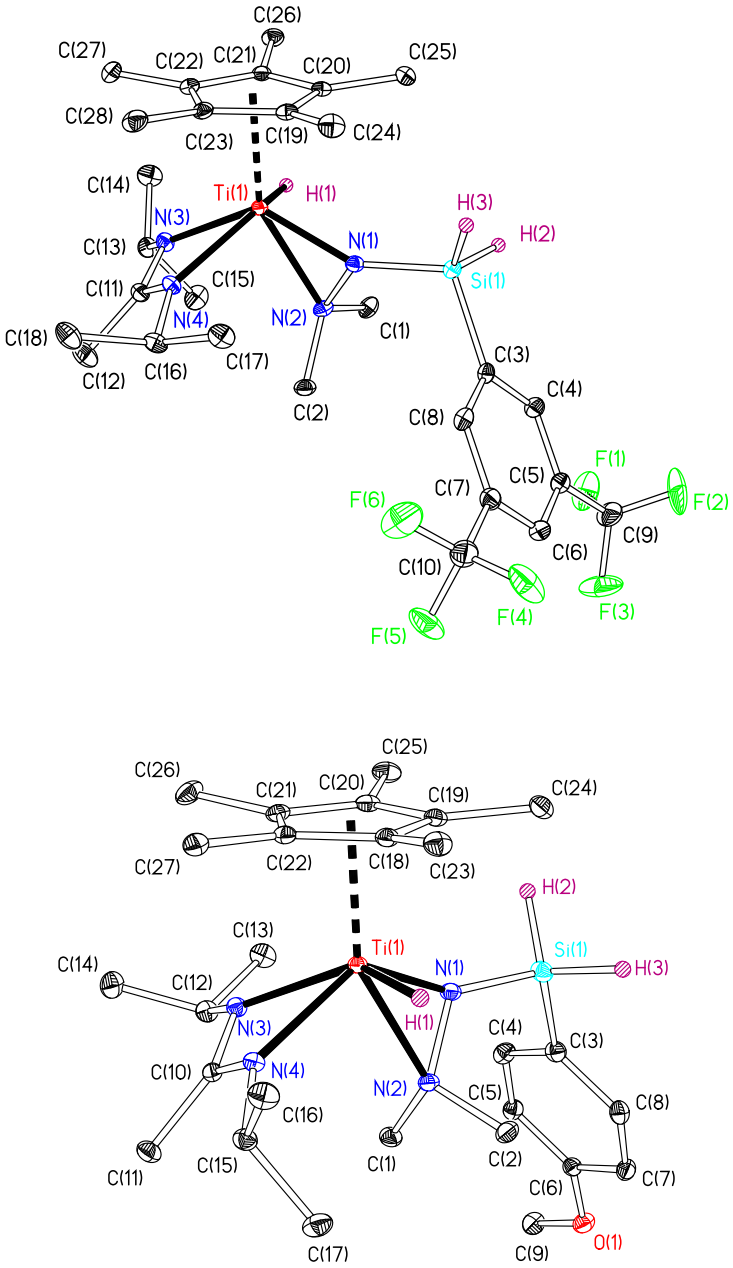

Figure 3.3. Displacement ellipsoid plots (20% probability) of Cp*Ti{MeC(N^{i}Pr)$_2$}-(H){N(NMe$_2$)SiH$_2$R} (R = Ar^{F} (**21**) (top), or Ar^{OMe} (**22**) (bottom)). C-bound H atoms and second orientation of disordered CF_3 groups in **21** omitted for clarity, and other H atoms drawn as spheres of an arbitrary radius.

Table 3.1. Selected bond lengths (Å) and angles (°) for Cp*Ti{MeC(N^{i}Pr)$_2$}(H){N(NMe$_2$)SiH$_2$R} (R = Ph (**20**), Ar^{F} (**21**) or Ar^{OMe} (**22**)). Cp$_{cent}$ refers to the Cp* ring carbon centroid.

Parameter	**20**	**21**	**22**
Ti(1)-Cp$_{cent}$	2.092	2.092	2.093
Ti(1)-N(1)	1.963(3)	1.963(2)	1.952(1)
Ti(1)-N(2)	2.212(3)	2.215(2)	2.201(1)
Ti(1)-N(3)	2.197(3)	2.180(3)	2.190(1)
Ti(1)-N(4)	2.190(3)	2.178(2)	2.194(1)
Ti(1)-H(1)	1.64(4)	1.56(4)	1.63(2)
N(1)-N(2)	1.460(4)	1.441(3)	1.445(1)
N(1)-Si(1)	1.723(3)	1.722(3)	1.735(1)
Si(1)-H(2)	1.38(4)	1.42(4)	1.40(2)
Si(1)-H(3)	1.41(3)	1.40(4)	1.41(2)
Cp$_{cent}$-Ti(1)-N(1)	114.1	114.8	114.4
Cp$_{cent}$-Ti(1)-N(2)	152.0	152.2	152.3
Cp$_{cent}$-Ti(1)-N(3)	116.0	115.6	116.4
Cp$_{cent}$-Ti(1)-N(4)	111.5	111.9	111.9
Cp$_{cent}$-Ti(1)-H(1)	96.2	97.0	94.3
N(1)-Ti(1)-N(2)	40.38(10)	39.77(10)	40.15(4)
Ti(1)-N(1)-Si(1)	155.46(17)	152.92(15)	155.54(6)
N(1)-Si(1)-C(3)	114.02(15)	112.40(13)	113.71(6)

As mentioned, all four compounds **20** – **23** have a tendency to undergo 1,2-elimination of RSiH$_3$ to reform **3.1**. In the cases of **20**, **22** and **23** this process is clean and reversible up to 377 K in toluene-d_8 allowing direct evaluation of the thermodynamic parameters for Equation 3.1 *via* van't Hoff analyses as summarised in Figure 3.4. In the case of **21** an unknown decomposition process set in above *ca.* 313 K and a direct measurement of ΔH and ΔS in this way was not possible.

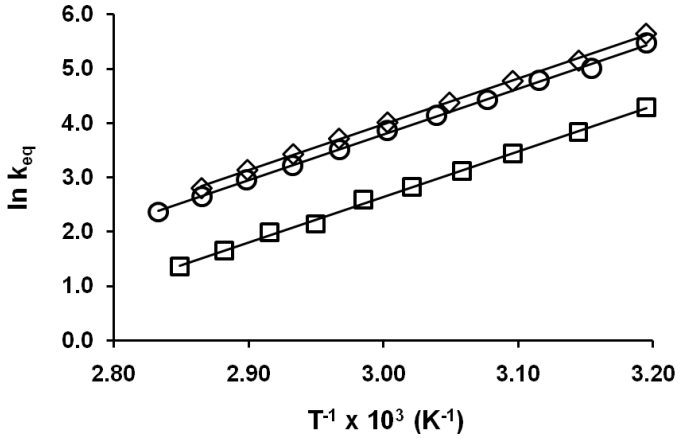

Figure 3.4. van't Hoff plots for the reaction Cp*Ti{MeC(N^{i}Pr)$_2$}(NNMe$_2$) + RSiH$_3$ = Cp*Ti{MeC(N^{i}Pr)$_2$}(H){N(NMe$_2$)SiH$_2$R} (R = Ph (**20**), Ar^{OMe} (**22**) or Bu (**23**) in toluene-d_8). For R = Ph (diamonds): ΔH = -17.1(2) kcal mol^{-1}, ΔS = -43(1) cal mol^{-1} K^{-1}, ΔG_{298} = -4.3(5) kcal mol^{-1} (R^2 = 0.999); for R = Ar^{OMe} (circles): ΔH = -16.9(1) kcal mol^{-1}, ΔS = -43(1) cal mol^{-1} K^{-1}, ΔG_{298} = -4.1(3) kcal mol^{-1} (R^2 = 0.999); for R = Bu (squares): ΔH = -16.6(2) kcal mol^{-1}, ΔS = -45(1) cal mol^{-1} K^{-1}, ΔG_{298} = -3.2(5) kcal mol^{-1} (R^2 = 0.999).

The ΔH values of -17.1(2) and -16.9(1) kcal mol^{-1} are identical within error for **20** and **22**. The ΔH of -16.6(2) kcal mol^{-1} for **23** was also equivalent within error to that of the two aryl systems. However, from the measured ΔG_{298} values (-4.3(5), -4.1(3) and -3.2(5) kcal mol^{-1} for **20**, **22** and **23** respectively), and qualitative observations it is clear that 1,2-addition of BuSiH$_3$ is less favourable than for the aryl silanes. The corresponding ΔH (-17.2(2) kcal mol^{-1}) and ΔG_{298} (-4.4(5) kcal mol^{-1}) values for the formation of **21** were determined indirectly *via* an equilibrium competition experiment between PhSiH$_3$ and Ar^{F}SiH$_3$ for **3.1**, assuming ΔS for 1,2-addition is -43(1) cal mol^{-1} K^{-1} in each case (*cf.* Figure 3.4 caption).

Addition of BuSiH$_3$ (1 equivalent) to a solution of **20-*d*$_3$** in C$_6$D$_6$ or C$_6$H$_6$ immediately formed an equilibrium mixture of BuSiH$_3$, **20-*d*$_3$**, **23** and PhSiD$_3$ (ratio of **20-*d*$_3$**: **23** = *ca.* 3:1 in accordance with the ΔG_{298} values). In addition, after 5 mins, the ^{1}H and ^{2}H NMR spectra also showed incorporation of deuterium into the Ti–H and/or Si–H sites of **23** and BuSiH$_3$. Likewise, hydrogen appeared in the Ti–D and/or Si–D sites of **20-*d*$_3$** and PhSiD$_3$. After 4-5 hours a statistical distribution of H and D into all Si–H/D and Ti–H/D sites was reached.

The implied σ-bond metathesis between Ti–H and Si–D (and Ti–D and Si–H) was also found with H_2 and **20-*d*$_3$** as shown in Equation 3.2 and Figure 3.5. Although H_2 does not form a stable 1,2-addition product with **3.1**, exposure of a solution of **20-*d*$_3$** to H_2 (4 atm) at room temperature led to slow incorporation of hydrogen into the initial Ti–D and Si–D sites of **20-*d*$_3$**. There was *ca*. 30% incorporation of H as judged by integration after 4 days, along with a new 1:1:1 triplet at 4.42 ppm ($^1J_{HD}$ = 43 Hz) for HD.

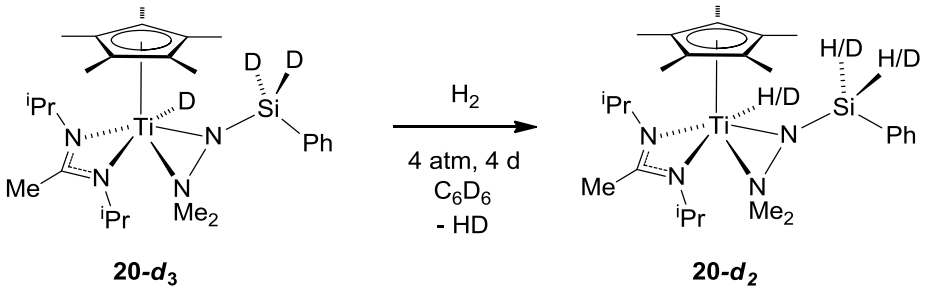

20-*d*$_3$ **20-*d*$_2$**

Equation 3.2

This reaction occurs *via* σ-bond metathesis between Ti–D and H–H followed by 1,2-elimination of $PhSiH_2D$. Subsequent 1,2-addition scrambles the Ti–H and Si–D groups. This latter process is fast compared to the σ-bond metathesis process since H appears in the Ti–D and Si–D sites of **20-*d*$_3$** at the same apparent rate at room temperature.

No Si–H/Si–D exchange was observed between $PhSiD_3$ and the chloride analogue of **20**, namely Cp*Ti{MeC(N^{i}Pr)$_2$}(Cl){N(NMe$_2$)SiH$_2$Ph} (**24**, *vide infra*), establishing the pivotal role of Ti–H in the exchange process as expected. Chirik *et al.* have reported related processes for titanocene imido-derived complexes {η^5-1,3-$C_5H_3(SiMe_3)_2$}$_2$Ti(NRD)D; (R = $SiMe_3$ or 2,4,6-Me_3-C_6H_2) with H_2 where H/D exchange involving σ-bond metathesis and 1,2-addition/ elimination were observed.[57]

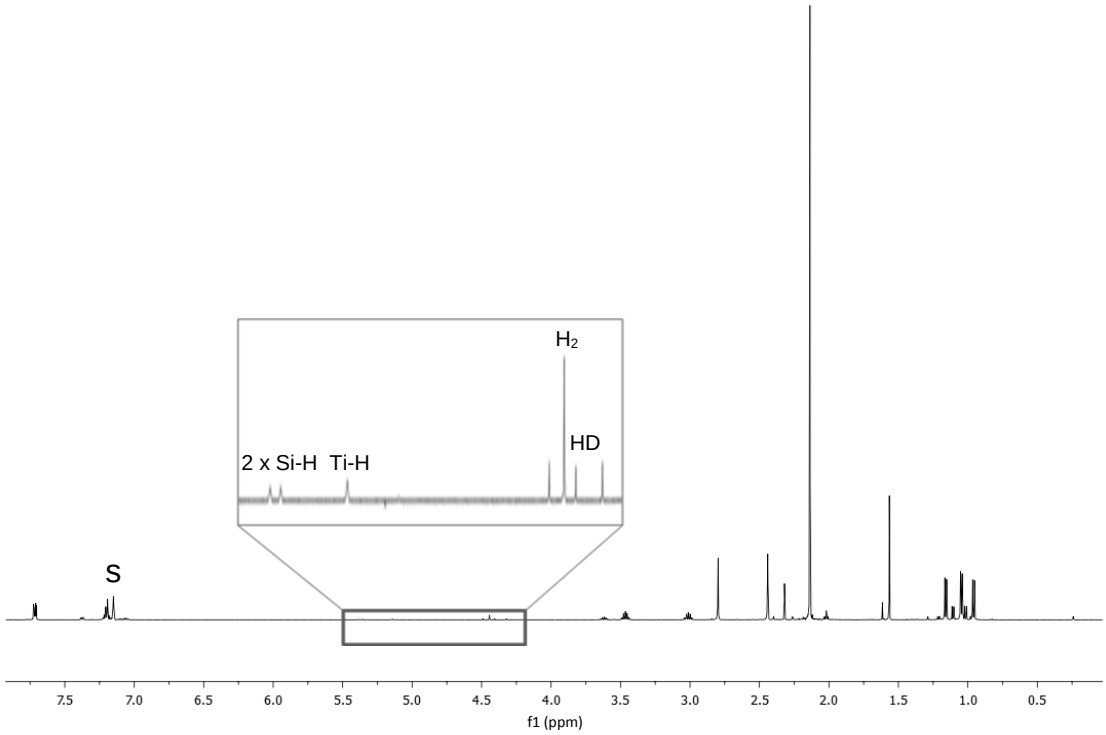

Figure 3.5. ^{1}H NMR spectrum (299.9 MHz) showing H/D exchange between Cp*Ti{MeC(N^{i}Pr)$_2$}(D){N(NMe$_2$)SiD$_2$Ph} (**20-*d*$_3$**) and H_2 in C_6D_6 ("s" denotes residual protio-solvent).

These Si–H addition reactions of silanes with **20** – **23**, and the accompanying σ-bond metathesis reactions, are unique in transition metal dialkylhydrazide chemistry, although it can be compared with other aspects of titanium hydride/silane chemistry[61, 92] and $PhSiH_3$ addition to the alkylidene hydrazide ligand in Cp*$_2$Ti{κ^2-NNC(H)Tol} giving Cp*$_2$Ti(H){N(NC(H)Tol)SiH$_2$Ph}.[48] Although titanium amides can undergo Ti–N/Si–H exchange with silanes,[60, 64, 93] no evidence for hydrazide-to-silicon transfer chemistry was found in our systems.

3.3 Reactions of Cp*Ti{MeC(N^{i}Pr)$_2$}(NNMe$_2$) (3.1) with halosilanes

3.3.1 Reactions of Cp*Ti{MeC(N^{i}Pr)$_2$}(NNMe$_2$) (3.1) with chlorosilanes

Reaction of **3.1** with $PhSiH_2Cl$ gave Cp*Ti{MeC(N^{i}Pr)$_2$}(Cl){N(NMe$_2$)SiH$_2$Ph} (**24**) as an orange solid in 46% isolated yield. The high solubility of **24** in hydrocarbon solvents resulted in the low yield since the reaction was quantitative when followed on the NMR tube scale in C_6D_6. Compound **24** is the chloride analogue of the hydride Cp*Ti{MeC(N^{i}Pr)$_2$}(H){N(NMe$_2$)SiH$_2$Ph} (**20**) and its ^{1}H NMR and IR spectra are

similar to those of **20** except for the absence of the signal attributed to Ti–H. The ^{29}Si NMR resonance for **24** (-45.6 ppm) is very similar to that of **20** (-42.3 ppm). No evidence was found for an alternative titanium-hydride product Cp*Ti{MeC(N^{i}Pr)$_2$}(H){N(NMe$_2$)SiH(Cl)Ph} which would be the product of Si–H activation. Assuming thermodynamic control, this indicates that Si–Cl addition to Ti=NNMe$_2$ is preferred to Si–H addition as has been found for Groups 5 and 6 metal imido compounds.[52-54] Unlike the situation for **20**, the 1,2-addition of Si–Cl to Ti=NNMe$_2$ is irreversible. Compound **24** is reasonably stable in C_6D_6 solution, but after 24 hours at room temperature, a number of unknown decomposition products were observed. Gade *et al.* have observed an apparently related 1,2-addition of Me_3SiN_3 to a Ti=NNMe$_2$ linkage forming a titanium hydrazide(1-) compound.[42]

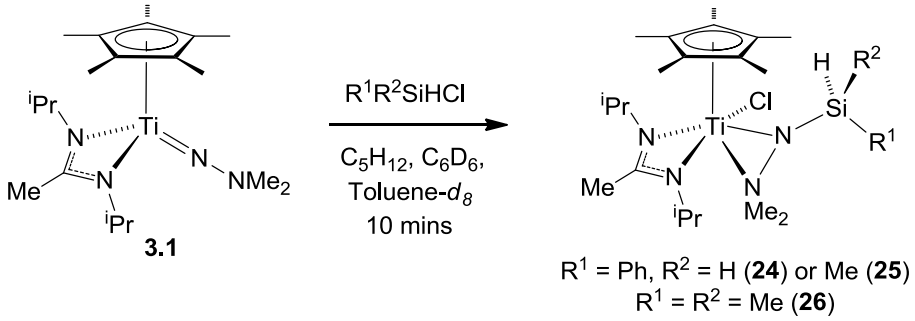

Equation 3.3

Diffraction-quality crystals of **24** were obtained from a saturated toluene solution at -30 ℃. The solid state structure is shown in Figure 3.6 and selected distances and angles are listed in Table 3.2. Full crystallographic data are given in the CD Appendix. The molecular structure for **24** is very similar to those of **20** – **22** (Figure 3.3) and there are few significant differences in the key geometrical features. The Ti–N$_\alpha$ distance in **24** is shorter within error compared to those in its hydride counterparts, but still within the expected ranges;[76] this may be attributed to the higher electronegativity of Cl compared to H. The Ti(1)-N(2) and N$_\alpha$–N$_\beta$ distances are the same within error to those in the hydride analogues. There is a greater asymmetry in the Ti-N(3,4) distances in **24** (Δ(Ti-N(3,4) = 0.089(3) Å) compared to those for **20** – **22** but the origin of this difference is not clear.

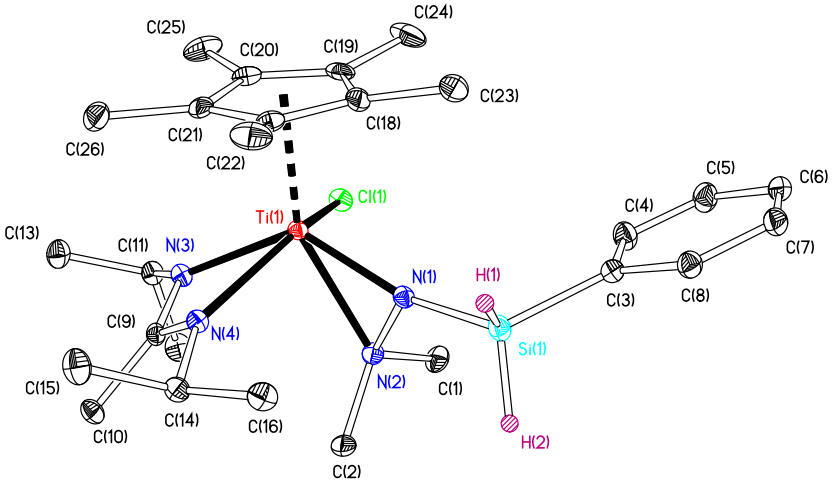

Figure 3.6. Displacement ellipsoid plot (20% probability) of Cp*Ti{MeC(N^{i}Pr)$_2$}(Cl){N(NMe$_2$)SiH$_2$Ph} (**24**). C-bound H atoms omitted for clarity, and Si-bound H atoms drawn as spheres of an arbitrary radius.

Table 3.2. Selected bond lengths (Å) and angles (°) for Cp*Ti{MeC(N^{i}Pr)$_2$}-(Cl){N(NMe$_2$)SiH$_2$Ph} (**24**). Cp$_{cent}$ refers to the Cp* ring carbon centroid.

Ti(1)-Cp$_{cent}$	2.136	Ti(1)-N(1)	1.939(3)
Ti(1)-N(2)	2.223(3)	Ti(1)-N(3)	2.145(2)
Ti(1)-N(4)	2.234(2)	Ti(1)-Cl(1)	2.4463(9)
N(1)-N(2)	1.439(3)	N(1)-Si(1)	1.737(3)
Cp$_{cent}$-Ti(1)-N(1)	114.3	Cp$_{cent}$-Ti(1)-N(2)	153.1
Cp$_{cent}$-Ti(1)-N(3)	112.9	Cp$_{cent}$-Ti(1)-N(4)	106.3
Cp$_{cent}$-Ti(1)-Cl(1)	102.1	N(1)-Ti(1)-N(2)	39.72(9)
Ti(1)-N(1)-Si(1)	156.97(15)	N(1)-Si(1)-C(3)	116.44(13)

As mentioned, formation of **24** was Si–Cl bond selective and irreversible (unlike formation of **20** with PhSiH$_3$), indicating that Si–H addition to Ti=NNMe$_2$ is less favourable than Si–Cl addition. Consistent with this, treatment of **20** with PhSiH$_2$Cl in C$_6$D$_6$ cleanly formed **24** and PhSiH$_3$ immediately and quantitatively (Equation 3.4). In principle,[94] this reaction could proceed *via* direct hydride exchange between **20** and the Si–Cl bond of PhSiH$_2$Cl rather than silane elimination from **20** (forming **3.1**) and then 1,2-addition of PhSiH$_2$Cl. In order to determine the mechanism of the reaction,

the corresponding NMR tube scale reaction was carried out between **20-*d*$_3$** and $PhSiH_2Cl$. The reaction outcome shows exclusive formation of **24** and $PhSiD_3$ with no incorporation of deuterium into the Si–H sites of **24**. This confirms that the reaction proceeded *via* the latter mechanism. Consistent with this, addition of $PhSiD_3$ to a solution of **24** gave no Si–H/ Si–D exchange over several days.

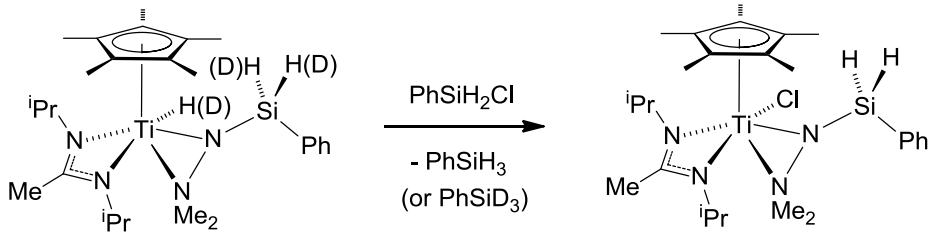

20 (or 20-*d*$_3$) **24**

Equation 3.4

Reaction of **3.1** in toluene-d_8 with disubstituted chlorosilane Ph(Me)SiHCl also led to Si–Cl 1,2-addition giving Cp*Ti{MeC(N^{i}Pr)$_2$}(Cl){N(NMe$_2$)SiH(Me)Ph} (**25)** (Equation 3.3) as judged by ^{1}H, ^{13}C{^{1}H} and ^{29}Si NMR spectroscopy. The reaction also proceeds to completion and is almost instantaneous when followed on the NMR tube scale. Interestingly, the ^{1}H NMR spectrum of **25** shows two sets of signals corresponding to the product which indicates the presence of two different isomers, with one slightly more preferable than the other (ratio *ca*. 1.1:1). The presence of two isomers in this case is most probably due to the different orientation of the methyl group on the silicon, with one isomer having the methyl group pointing upward (towards Cp* ring) while the other having it pointing downward. Unfortunately, the instability of **25**, which developed into unknown mixtures over *ca*. 16 hours, prevents its isolation on the preparative scale and further determination of its molecular structure. However, both isomers of **25** were nonetheless characterised using NMR spectroscopy at -40 ℃.

In another attempt, **3.1** was reacted with Me_2SiHCl in toluene-d_8. The reaction proceeded to completion immediately, forming Cp*Ti{MeC(N^{i}Pr)$_2$}(Cl){N-(NMe$_2$)SiHMe$_2$} (**26**) according to ^{1}H, ^{13}C{^{1}H} and ^{29}Si NMR spectroscopy. Disappointingly, **26** is also unstable, forming a mixture of unidentified products over time which precludes its isolation on the preparative scale. When conducted on the NMR tube scale in toluene-d_8 the conversion of **3.1** to **26** was quantitative. Compound **26** was therefore characterised using ^{1}H, ^{13}C{^{1}H} and ^{29}Si NMR spectroscopy at -50

℃.

Reaction of **3.1** with Me_3SiCl or Ph_2SiCl_2 in C_6D_6 immediately gave a mixture of unknown products. As an indication of the lower stability of these more sterically encumbered products it was found that reaction of **25** with $PhSiH_2Cl$ in C_6D_6 cleanly formed **24** and Ph(Me)SiHCl. However, Ph(Me)SiHCl was nonetheless still able to displace $PhSiH_3$ from **20** forming **25** showing the preference for Si–Cl 1,2-addition over Si-H activation.

3.3.2 Reactions of Cp*Ti{MeC(N^{i}Pr)$_2$}(NNMe$_2$) (3.1) with dichlorosilanes

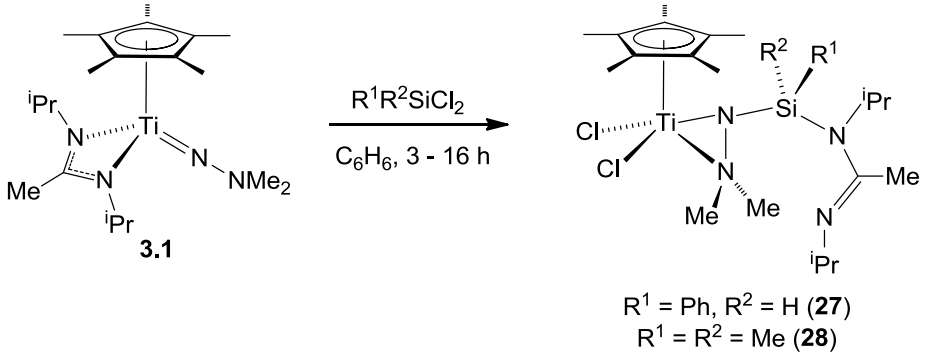

Equation 3.5

In contrast to the unstable products formed with the bulkier monochlorosilanes, reaction of **3.1** with the dichlorosilanes $PhSiHCl_2$ gave the stable hydrazide(1-) product Cp*Ti{N(NMe$_2$)SiH(Ph)N(^{i}Pr)CMeN^{i}Pr}Cl$_2$ (**27**) (Equation 3.5) in which both chlorine atoms of the silane had been transferred to titanium with concomitant transfer of the amidinate ligand to silicon. On the preparative scale, **27** was isolated as a waxy solid which was then washed with cold pentane and dried *in vacuo* to give an orange solid in 58% yield. The high solubility of **27** in hydrocarbon solvents contributed to its low yield. Diffraction-quality crystals of **27** were grown from a saturated diethyl ether solution at -30 ℃.

The reaction of **3.1** with Me_2SiCl_2 also formed a stable hydrazide(1-) product Cp*Ti{N(NMe$_2$)SiMe$_2$N(^{i}Pr)CMeN^{i}Pr}Cl$_2$ (**28**) with both chloride and amidinate ligand transfer. When followed on the NMR tube scale in C_6D_6, **28** (like **27** in the case of $PhSiHCl_2$) was the only product formed. However, on scale up, the isolated yield was only 41% owing to its high solubility. Diffraction quality crystals of **28** were obtained from a saturated diethyl ether solution.

The molecular structures of **27** and **28** are shown in Figure 3.7, and selected distances and angles are presented in Table 3.3. Full crystallographic data are given in the CD Appendix.

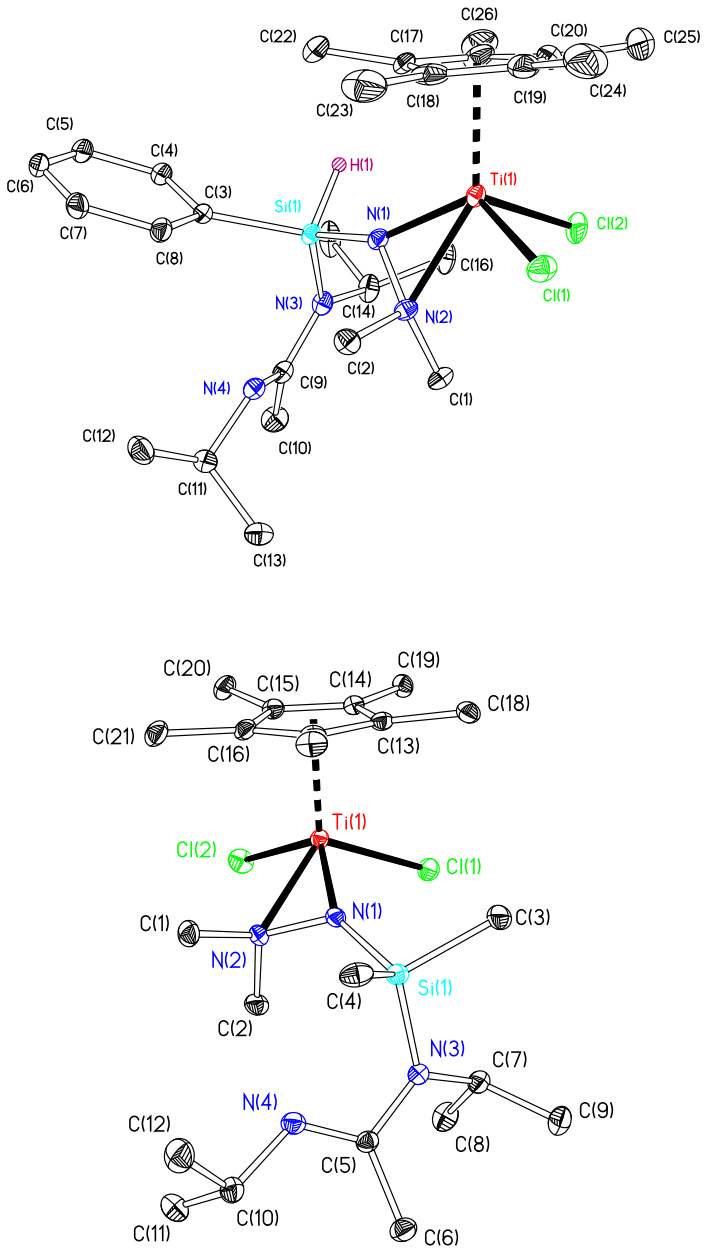

Figure 3.7. Displacement ellipsoid plots (20% probability) of Cp*Ti{N(NMe$_2$)SiH(Ph)N(^{i}Pr)CMeN^{i}Pr}Cl$_2$ (**27**) (top) and Cp*Ti{N(NMe$_2$)-SiMe$_2$N(^{i}Pr)CMeN^{i}Pr}Cl$_2$ (**28**) (bottom). C-bound H atoms omitted for clarity, and Si-bound H atom drawn as a sphere of an arbitrary radius.

Table 3.3. Selected bond lengths (Å) and angles (°) for Cp*Ti{N(NMe$_2$)SiH(Ph)N(^{i}Pr)CMeN^{i}Pr}Cl$_2$ (**27**) and Cp*Ti{N(NMe$_2$)-SiMe$_2$N(^{i}Pr)CMeN^{i}Pr}Cl$_2$ (**28**). Cp$_{cent}$ refers to the Cp* ring carbon centroid.

Parameter	**27**	**28**
Ti(1)-Cp$_{cent}$	2.066	2.083
Ti(1)-N(1)	1.929(2)	1.923(3)
Ti(1)-N(2)	2.109(2)	2.112(3)
Ti(1)-Cl(1)	2.3099(8)	2.3167(12)
Ti(1)-Cl(2)	2.3693(9)	2.3579(12)
N(1)-N(2)	1.406(3)	1.414(4)
N(1)-Si(1)	1.752(2)	1.750(3)
N(3)-C(9/5)	1.392(4)	1.409(4)
N(4)-C(9/5)	1.288(4)	1.273(5)
Cp$_{cent}$-Ti(1)-N(1)	115.7	118.5
Cp$_{cent}$-Ti(1)-N(2)	148.8	127.5
Cp$_{cent}$-Ti(1)-Cl(1)	108.8	112.7
Cp$_{cent}$-Ti(1)-Cl(2)	108.7	108.8
N(1)-Ti(1)-N(2)	40.44(9)	40.68(12)
Ti(1)-N(1)-Si(1)	151.10(14)	153.46(18)
N(1)-Si(1)-N(3)	116.88(11)	114.38(14)
N(3)-Si(9/5)-N(4)	115.4(2)	116.2(3)

The solid state structures of **27** and **28** are very similar. Each features a four-legged piano stool geometry, but with Ti(1) and N(2) lying above and below the plane formed by N(1) and the two Cl atoms. The Ti(1)-N(1) distances are shorter but comparable within error to that in **24**, whereas the Ti-Cl, Ti(1)-N(2) distances are significantly shorter as expected based on the reduced coordination number and decreased donor ability of chloride compared to MeC(N^{i}Pr)$_2$. The N(1)-N(2) distances in **27** and **28** (1.406(3) and 1.414(4) Å respectively) are significantly shorter than in **24** (1.439(3) Å) and **20** – **22** (1.441(3) – 1.460(4) Å) indicative of differing degrees of reduction of this bond in the different complexes.

Compounds **27** and **28** are fluxional on the NMR timescale in a process that

equivalences the two *iso*-propyl groups of the -N(^{i}Pr)CMeN^{i}Pr moiety but not the inequivalent -NMe_2 methyl groups in either case or the $SiMe_2$ methyl groups in **28**. The fluxional process is attributed to rapid 1,3-silicon migration between the amidinate nitrogen atoms. This type of mechanism is well-established for silylated amidines.[95] Cooling an NMR solution of **28** to 223 K freezes out this process, whereas for **27**, which possesses a less sterically crowded silicon, broadening of the *iso*-propyl group resonances was observed but the slow exchange limit could not be reached.

3.3.3 Reaction of Cp*Ti{MeC(N^{i}Pr)$_2$}(NNMe$_2$) (3.1) with bromosilane

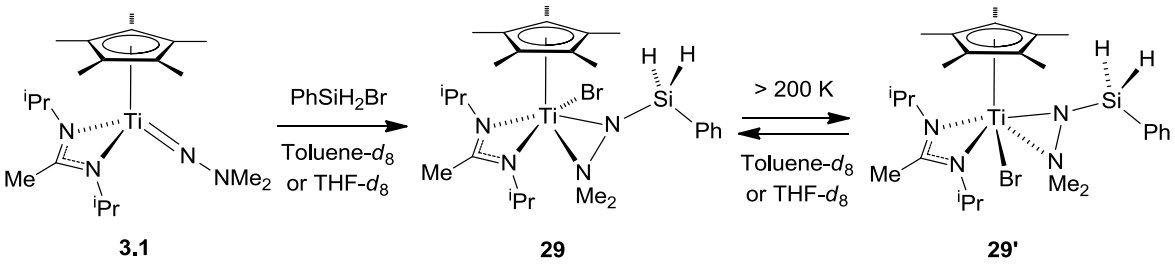

Equation 3.6

Reaction of Cp*Ti{MeC(N^{i}Pr)$_2$}(NNMe$_2$) (**3.1**) with $PhSiH_2Br$ in C_6D_6 gave a single fluxional product in quantitative yield according to the ^{1}H NMR spectrum. Cooling the NMR solution in toluene-d_8 or THF-d_8 to -80 ℃ freezes out the fluxional process suggesting the formation of Cp*Ti{MeC(N^{i}Pr)$_2$}(Br){N(NMe$_2$)SiH_2Ph} (**29**) as a single fluxional product (Equation 3.6). Unfortunately, compound **29** could not be isolated on the preparative scale and solutions show extensive decomposition after only a few hours. At 193 K in toluene-d_8 or THF-d_8 the ^{1}H, ^{13}C{^{1}H} and ^{29}Si NMR data were consistent with the geometry depicted in Equation 3.6 (inequivalent, mutually-coupled SiH_2 hydrogen atoms and inequivalent NMe_2 methyl groups; a single ^{29}Si resonance at -41.7 ppm). Above 220 K the $Si\underline{H}_2$ and $N\underline{Me}_2$ resonances underwent pairwise coalescence consistent with the net fluxional process depicted in Equation 3.6 (interchange of diastereomers **29** and **29′**).

At first sight this fluxional process could proceed *via* elimination of $PhSiH_2Br$ forming **3.1** as an intermediate (as found for **20** – **23**). However, addition of $PhSiH_2Br$ (1 equivalent) to a solution of **29** at room temperature gave no broadening of the free silane resonances whereas those for **29** were indicative of the fast exchange limit. Thus the process interconverting **29** and **29′** does not involve release of $PhSiH_2Br$. Instead a process involving transient Br^- ion elimination *via* [Cp*Ti{MeC(N^{i}Pr)$_2$}-

$\{N(NMe_2)SiH_2Ph\}]^+$ (denoted **[29-Br]$^+$**) is proposed through which chemical exchange of the Si-H and N-Me groups can occur. The cation **[29-Br]$^+$** is the analogue of $[Cp^*Ti\{MeC(N^iPr)_2\}\{N(NMe_2)H\}]^+$ (**38$^+$**, *vide infra*) which has been isolated as its $[BPh_4]^-$ salt and structurally characterised. Direct evidence for **[29-Br]$^+$** was found using positive ion electrospray mass spectrometry for a solution of **29** generated *in situ* in THF. Nevertheless, it is not possible to determine the relative proportions of **29** and [**29-Br**]$^+$ in solution above the fast exchange limit on the available experimental evidence.

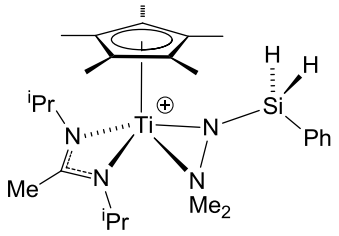

[29–Br]$^+$

As a probe of the energetic preferences of $Ti{=}NNMe_2$ for Si–H, Si–Cl and Si–Br addition further NMR tube scale competition experiments were carried out. Reaction of $Cp^*Ti\{MeC(N^iPr)_2\}(Cl)\{N(NMe_2)SiH(Me)Ph\}$ (**25**) with $PhSiH_2Br$ in C_6D_6 cleanly formed **29** and Ph(Me)SiHCl. Likewise, reaction of **20** with $PhSiH_2Br$ also immediately gave **29** along with $PhSiH_3$. At first sight, these results parallel those found for $PhSiH_2Cl$ and **20** or **25**. However, in contrast to the reaction between **20-*d*$_3$** and $PhSiH_2Cl$ (Equation 3.4), ^1H and ^2H NMR monitoring of that with $PhSiH_2Br$ showed not only the formation of $PhSiD_3$ and $Cp^*Ti\{MeC(N^iPr)_2\}$-$(Br)\{N(NMe_2)SiH_2Ph\}$ (**29**) but also $PhSiH_2D$ and $Cp^*Ti\{MeC(N^iPr)_2\}(Br)$-$\{N(NMe_2)SiD_2Ph\}$ (**29-*d*$_2$**). The ratio of **29** to **29-*d*$_2$** was 5:3 showing that silane elimination from **20** followed by $PhSiH_2Br$ addition is nonetheless kinetically favoured compared to direct Ti–D/Si–Br exchange *via* nucleophilic substitution.[96]

3.4 Reactions of $Cp^*Ti\{MeC(N^iPr)_2\}(NNPh_2)$ (3.2) with chlorosilanes

Equation 3.7 summarises the reactions of the diphenylhydrazido complex $Cp^*Ti\{MeC(N^iPr)_2\}(NNPh_2)$ (**3.2**) with chlorosilanes.

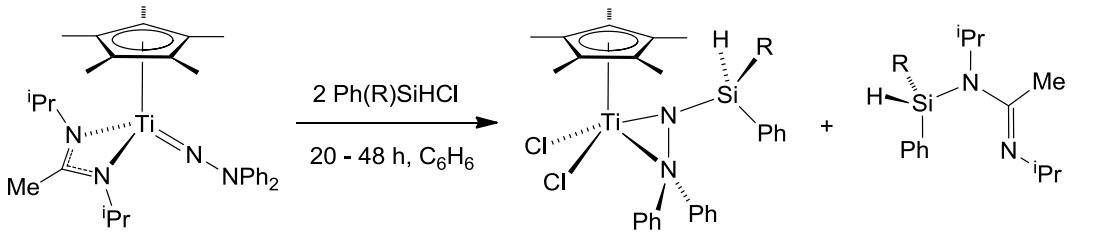

3.2 R = H (**30**) or Me (**32**) R = H (**31**) or Me (**33**)

Equation 3.7

3.4.1 Reaction of Cp*Ti{MeC(N^{i}Pr)$_2$}(NNPh$_2$) (3.2) with PhSiH$_2$Cl

Although **3.2** does not react with $RSiH_3$ (R = aryl, Bu), it does undergo a relatively slow reaction with 2 equivalents of the monochlorosilane $PhSiH_2Cl$ forming dichloride-hydrazide(1-) complex Cp*Ti{N(NPh_2)SiH_2Ph}Cl_2 (**30**) along with the silylated amidine ^{i}PrNC(Me)N(^{i}Pr)SiH_2Ph (**31**). The product mixture of **30** and **31** was obtained as a brown oil which could not be separated. The combined isolated yield was 83%. Although all attempts to grow diffraction-quality crystals were in vain, the proposed reaction products were confirmed in a separate reaction carried out between lithiated amidine with $PhSiH_2Cl$ to generate **31**. The pure **31** generated separately was used to obtain its IR data.

Compound **30** is reminiscent of **27** and **28** formed between **3.1** and dichlorosilanes, but in this case the reaction has involved complete ejection of the amidinate ligand as the silylated amidine **31**. Reaction of **3.2** with 1 equivalent of the monochlorosilane gave a mixture of unreacted **3.2** and the products shown in Equation 3.7. As expected, **31** is fluxional on the NMR timescale and the room temperature spectrum shows equivalent *iso*-propyl resonances, consistent with fast 1,3-shifts of the SiH_2Ph groups between the nitrogen atoms.

The slower rate of reaction and ready loss of the amidinate ligand with **3.2** are attributed to the delocalised nature of the N_β lone pair and the higher steric demands of the β-NPh_2 group (leading to a more sterically crowded metal centre), respectively, compared to **3.1**.

3.4.2 Reaction of Cp*Ti{MeC(N^{i}Pr)$_2$}(NNPh$_2$) (3.2) with PhSiH(Me)Cl

Reaction of **3.2** with 1 equivalent of Ph(Me)SiHCl in C_6D_6 resulted in a mixture of unreacted **3.2** and the products shown in Equation 3.7. Repeating the reaction with 2

equivalents of the halosilane slowly formed the products Cp*Ti{N(NPh_2)-SiH(Me)Ph}Cl_2 (**32**) and the silylated amidine (**33**) cleanly after 48 hours. The mixture of **32** and **33** was isolated as a brown oil. Diffraction-quality crystals of **32** were grown from benzene/hexanes layering at 4 ℃. The high solubility of the brown oil resulted in the disappointing isolated yield of pure **32** (40%). The side product ^{i}PrNC(Me)N(^{i}Pr)SiH(Me)Ph (**33**) could not be isolated in a pure form free from **32** and was characterised by spectroscopic methods.

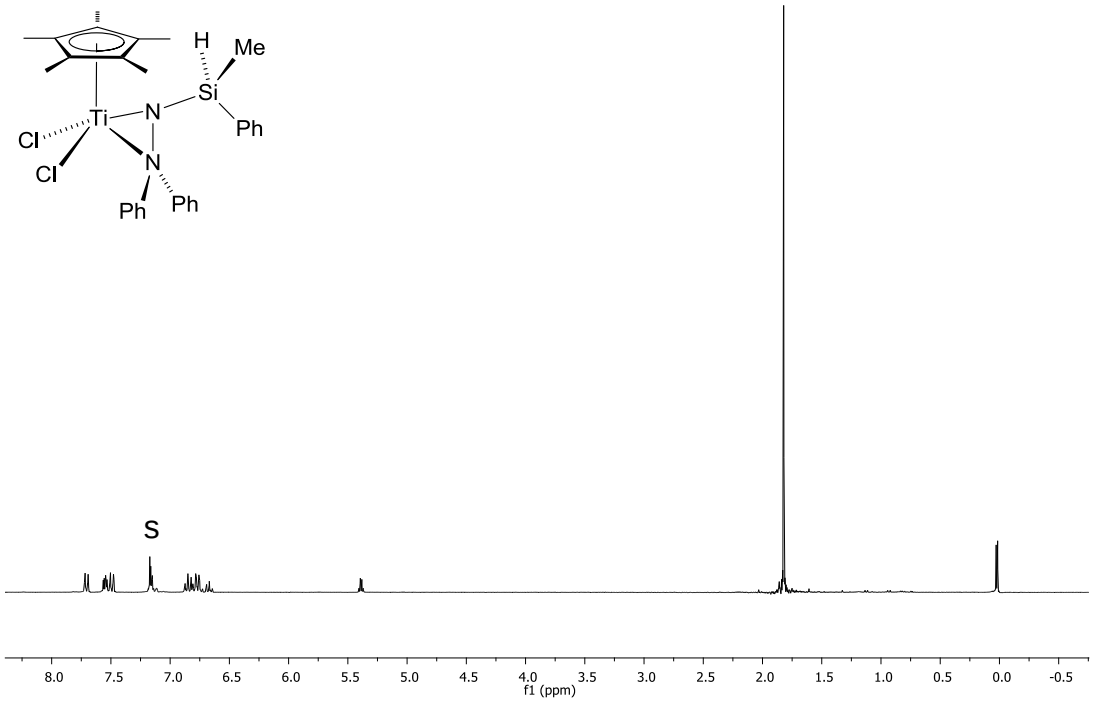

Figure 3.8. ^{1}H NMR spectrum (299.9 MHz) of Cp*Ti{N(NPh_2)SiH(Me)Ph}Cl_2 (**32**) in C_6D_6 ("s" denotes residual protio-solvent).

Compound **32** (Figure 3.8) is analogous to **30**. Like **31**, the amidine **33** is also fluxional on the NMR timescale with equivalent *iso*-propyl resonances being observed at room temperature, consistent with fast 1,3-shifts of the SiH_2Ph groups between the nitrogen atoms.

As mentioned previously in Section 3.4.1, the slower rate of reaction between **3.2** and PhSiH(Me)Cl compared to reaction with **3.1** is due to the delocalised nature of the N_β lone pair and the bulkier β-NPh_2 group compared to NMe_2. The ready loss of amidinate ligand is the result of the higher steric demands of the β-NPh_2 group, which causes the metal centre to be more sterically crowded. The rate of reaction between

3.2 and PhSiH(Me)Cl is even slower compared to reaction with $PhSiH_2Cl$, which is possibly due to the greater steric demand of PhSiH(Me)Cl.

Compound **32** was structurally characterised and the molecular structure is shown in Figure 3.9. Selected distances and angles are given in Table 3.4. Full crystallographic data are given in the CD Appendix. The data for **32** are analogous to those for $Cp^*Ti\{N(NMe_2)SiH(Ph)N(^iPr)CMeN^iPr\}Cl_2$ (**27**) and $Cp^*Ti\{N(NMe_2)SiMe_2N(^iPr)$-$CMeN^iPr\}Cl_2$ (**28**).

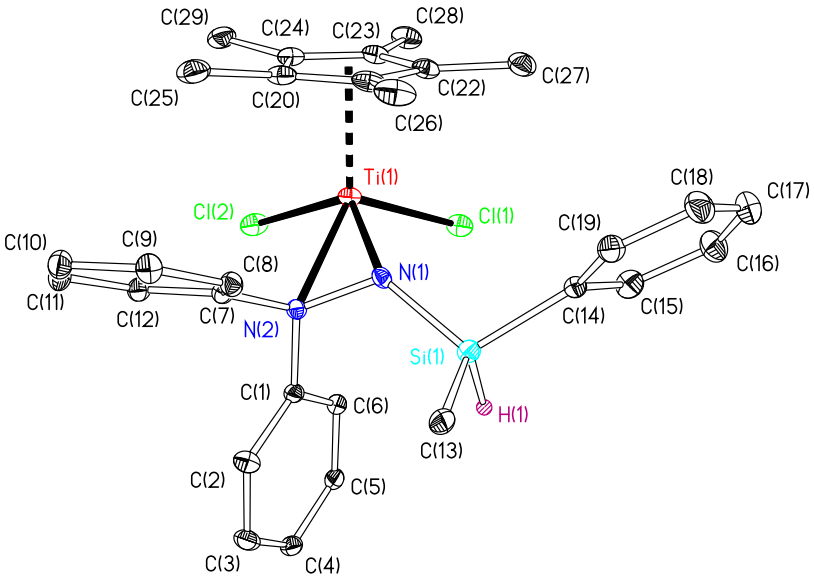

Figure 3.9. Displacement ellipsoid plot (20% probability) of $Cp^*Ti\{N(NPh_2)$-$SiH(Me)Ph\}Cl_2$ (**32**). C-bound H atoms omitted for clarity, and Si-bound H atom drawn as a sphere of an arbitrary radius.

The solid state structure of **32** features a four-legged piano stool geometry around titanium metal centre. Similar to **27** and **28**, the Ti(1) and N(2) of **32** also lie above and below the plane formed by N(1) and the two Cl atoms. The Ti(1)-N(1) distance of 1.932(2) is typical of an amido donor and is comparable within error to that in **27** and **28**. The significantly shorter Ti-Cl distance compared to that of **24** is due to the reduced coordination number and decreased donor ability of chloride compared to $MeC(N^iPr)_2$. The N(1)-N(2) bond length of 1.438(3) Å is significantly longer than those found in **27** and **28** (1.406(3) and 1.414(4) Å respectively). This could be attributed to the steric repulsion between the phenyl rings and the substituents on silicon.

Table 3.4. Selected bond lengths (Å) and angles (°) for Cp*Ti{N(NPh$_2$)SiH(Me)Ph}Cl$_2$ (**32**). Cp$_{cent}$ refers to the Cp* ring carbon centroid.

Ti(1)-Cp$_{cent}$	2.079	Ti(1)-N(1)	1.932(2)
Ti(1)-N(2)	2.197(2)	Ti(1)-Cl(1)	2.3103(10)
Ti(1)-Cl(2)	2.3265(9)	N(1)-N(2)	1.438(3)
N(1)-Si(1)	1.775(2)		
Cp$_{cent}$-Ti(1)-N(1)	116.8	Cp$_{cent}$-Ti(1)-N(2)	130.5
Cp$_{cent}$-Ti(1)-Cl(1)	109.9	Cp$_{cent}$-Ti(1)-Cl(2)	110.6
N(1)-Ti(1)-N(2)	40.13(9)	Ti(1)-N(1)-Si(1)	142.81(15)
N(1)-Si(1)-C(13)	111.07(14)	N(1)-Si(1)-C(14)	109.51(12)

3.5 Reactions of Cp*Ti{MeC(N^{i}Pr)$_2$}(NTol) (3.3) with halosilanes

As an experimental probe of the importance of intramolecular NMe$_2$ chelation in the formation of the products **24** – **26** and **29** the reactions of Cp*Ti{MeC(N^{i}Pr)$_2$}(NTol) (**3.3**) with PhSiH$_2$Cl and PhSiH$_2$Br were carried out as shown in Equation 3.8.

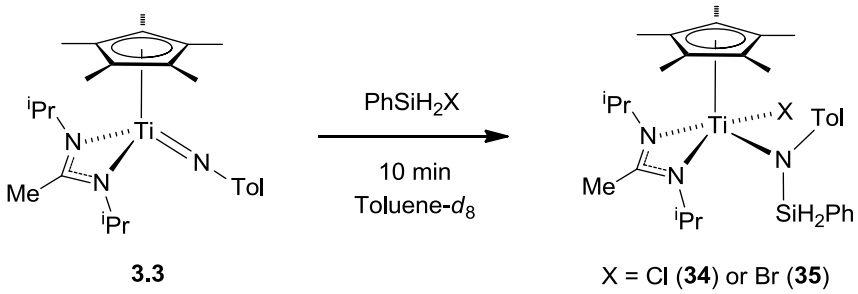

3.3 X = Cl (**34**) or Br (**35**)

Equation 3.8

Reaction of **3.3** with both PhSiH$_2$Cl and PhSiH$_2$Br in C$_6$D$_6$ gave immediate colour change from dark green to brown. When followed by ^{1}H NMR in toluene-d_8, the reactions completed almost immediately and quantitative conversion to the silylamido-chloride or bromide complexes Cp*Ti{MeC(N^{i}Pr)$_2$}(X){N(Tol)SiH$_2$Ph} (X = Cl (**34**) or Br (**35**) (Figure 3.10)) was observed. The NMR spectra are consistent with the proposed structures, featuring inequivalent amidinate *iso*-propyl groups (4 different methyl group environments), a pair of mutually coupled doublets for the diastereotopic SiH$_2$ groups, and a ^{29}Si resonance at *ca.* -36 ppm. The reactions of Group 5 and 6 imido compounds with halosilanes to form silylamido products have

been studied in detail previously.[52-54] The reverse process, namely formation of imido compounds by halosilane elimination, is a well-established synthetic strategy.[97-100]

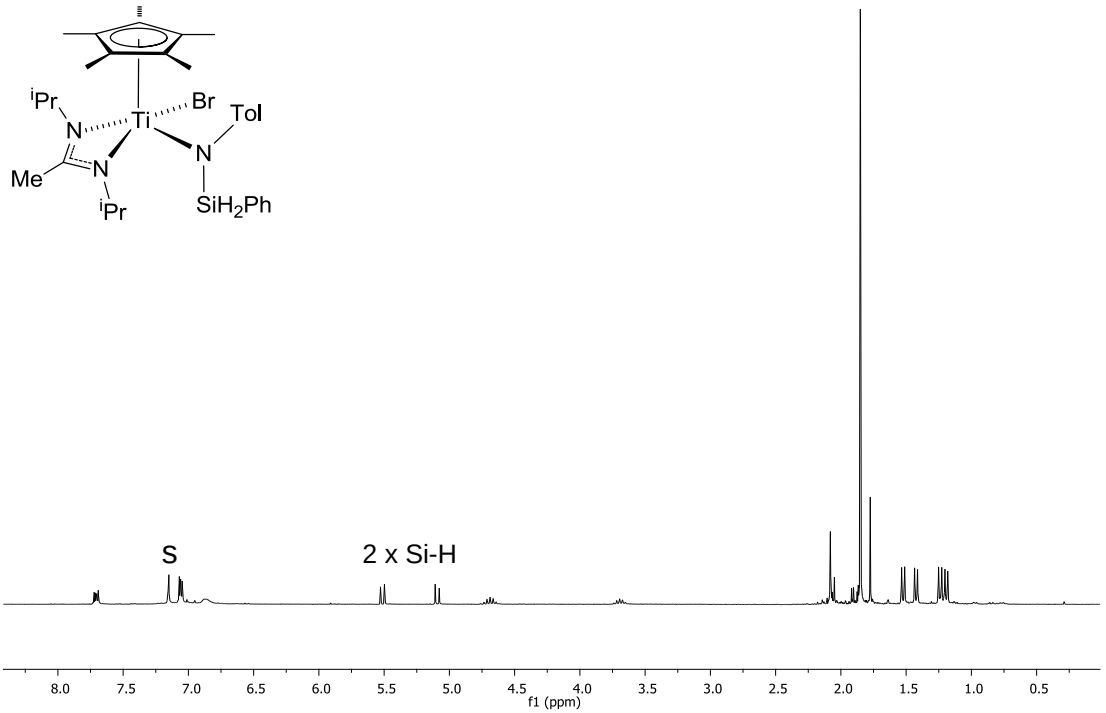

Figure 3.10. ^{1}H NMR spectrum (299.9 MHz) of Cp*Ti{MeC(N^{i}Pr)$_2$}(Br){N(Tol)SiH$_2$Ph} (**35**) in C_6D_6 ("s" denotes residual protio-solvent).

Both **34** and **35** are unstable in solution, fully decomposing to unknown products after 16 hours, and they could not be isolated on the preparative scale. A DFT model of **34** (*vide infra*), CpTi{MeC(NMe)$_2$}(Cl){N(Tol)SiH$_2$Me} (**Q_8Cl**), found the expected four legged piano stool geometry and a *sp*^{2} hybridised N$_\alpha$ for the new silylamido ligand. No β-agostic Si–H ···Ti interactions were found in this 16 valence electron compound. These have often been reported for silylamido ligands and the early transition and rare earth metals.[52-54, 94, 101] Given the unstable nature of **34** and **35**, no further reactions of **3.3** with other halosilanes were carried out.

3.6 DFT study of the mechanism of Si–H and Si–Cl addition

Kinetic or/and computational studies of the mechanism of Si–H and Si–Cl bond addition to the M=E multiple bond of imido, sulfido, and oxo complexes have been reported by the groups of Tilley,[46] Bergman and Andersen,[49] and Chirik,[50] as well as by Nikonov and Mountford.[53] Primary KIEs (kinetic isotope effects) greater than 1 for

Si–H addition to titanocene Ti=S or Ti=O bonds suggested a concerted addition.[49, 50] For Tilley's highly bent tantalum imido system,[46] or Nikonov and Mountford's 18 valence electron Group 5 imides,[53] an inverse KIE or other kinetic data suggested a stepwise process whereby R_3SiX adds first to the N_α atom forming an intermediate with a pentacoordinate silicon centre, followed by Si–H or Si–Cl bond addition to $M=N_\alpha$ (1,2-addition) or the metal centre (oxidative addition). Bergman and Andersen proposed a similar stepwise mechanism for silane Si–H addition across the Ti–NN bond of $Cp^*_2Ti\{\kappa^2\text{-NNC(H)Tol}\}$ (forming alkylidene hydrazide(1-)-hydride products reminiscent of **20** – **23**),[48] but without experimental or other support.

Nothing is known regarding the mechanism of Si–X (X = H, halogen) bond addition to transition metal hydrazide complexes. In particular it is not clear what mechanistic or other role(s) β-NMe_2 chelation plays in the formation of the silane or halo-silane 1,2-addition products described for **3.1** above. The lack of formation of any product between **3.3** and $PhSiH_3$ and poor stability of the product (**34**) formed with $PhSiH_2Cl$ suggest an important thermodynamic contribution.

Attempts to gain experimental mechanistic insight for the reaction of **3.1** with $PhSiH_3$ or $PhSiD_3$ through KIE experiments were unsuccessful, the reason being that the reactions proceed to completion within seconds even at 203 K in toluene-d_8. Likewise, the rapid equilibrium between **20** and free silane (even at 203 K on the chemical timescale) prevented the indirect measurement of any KIE by analysis of the **20**/**20**-$\boldsymbol{d_3}$ product distribution formed in a competition reaction between **3.1** and $PhSiH_3$ and $PhSiD_3$.

In an effort to determine the reaction mechanism(s) and other factors underpinning this chemistry, DFT(M06) calculations[102] using $CpTi\{MeC(NMe)_2\}(NNMe_2)$ (**1Q**, model for **3.1**) and $CpTi\{MeC(NMe)_2\}(NPh)$ (**7Q**, a model for **3.3**) and the silanes $MeSiH_3$ and $MeSiH_2Cl$ were carried out, again in collaboration with the group of Dr. Eric Clot at Université Montpellier. The main results with **1Q** are summarised in Figure 3.11 where, for each silane, Si–X addition to either a terminal ("Path 1") or a κ^2-coordinated ("Path 2") hydrazide ligand were considered.

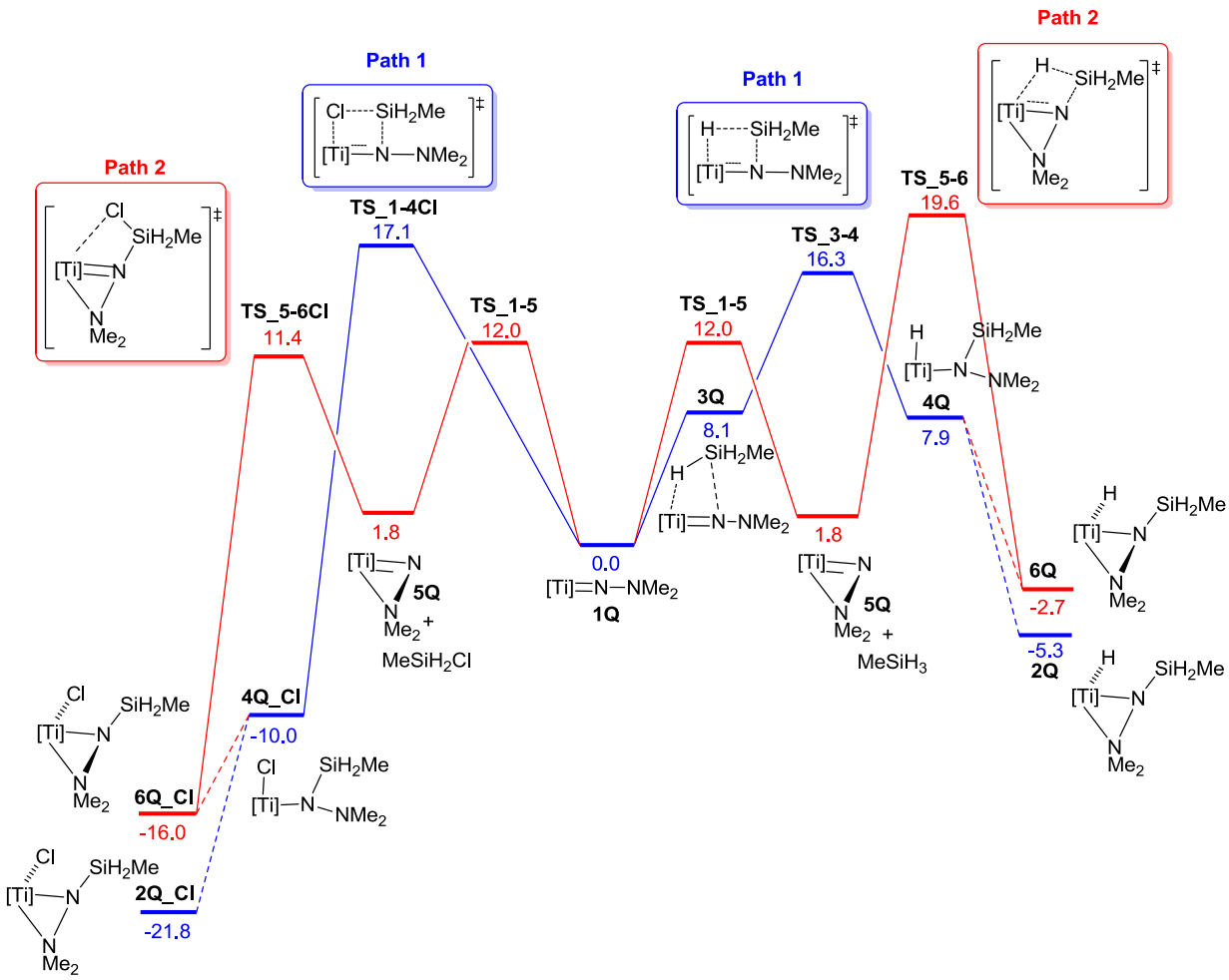

Figure 3.11. Energy profiles for the reaction of CpTi{MeC(NMe)$_2$}(NNMe$_2$) (**1Q**) with MeSiH$_3$ (right) and MeSiH$_2$Cl (left). All energies are ΔG_{sol} in kcal mol^{-1} at 298 K. [Ti] = CpTi{MeC(NMe)$_2$}.

3.6.1 Si–H bond addition

Overall, the calculated thermodynamic parameters for the reaction **1Q** + MeSiH$_3$ → **2Q** (a model for the real complexes **20** – **23**) are in good agreement with the experimental results (DFT: ΔH = -22.5 kcal mol^{-1}, ΔS = -53 cal mol^{-1} K^{-1}; experiment: ΔH = -16.6(2) to -17.2(2) kcal mol^{-1}, ΔS = -43(2) to -45(2) cal mol^{-1} K^{-1}). The calculated values for the full experimental system **3.1** + PhSiH$_3$ → **20** showed even better agreement (DFT: ΔH = -18.9 kcal mol^{-1}, ΔS = -49 cal mol^{-1} K^{-1}; experiment: ΔH = -17.1(2) kcal mol^{-1}, ΔS = -43(2) cal mol^{-1} K^{-1}). Given the good agreement with the small model **1Q**, this was generally selected for further studies so as to improve computational efficiency.

ΔG_{sol} for the formation of the 2,1-addition product CpTi{MeC(NMe)$_2$}-

(SiH_2Me){$N(NMe_2)H$} (**2′Q**) was +6.5 kcal mol^{-1} (*cf.* -5.3 kcal mol^{-1} for forming **2Q**) in agreement with this isomer not being observed experimentally (note that C–H activation at Ti=NR bonds invariably gives 2,1-addition products[103, 104]). ΔH for H_2 addition to the Ti=N_α bond of either **1Q** or the full experimental system **3.1** was calculated to be energetically less favourable relative to Si–H 1,2-addition by *ca.* 9 kcal mol^{-1}, whereas the activation barrier was only 20.0 kcal mol^{-1} *via* Path 1 (Figure 3.11). This shows that the lack of observation of H_2 addition to **3.1** is thermodynamic rather than kinetic in origin. Although ΔG_{sol} for H_2 addition to **3.1** was calculated to be -0.5 kcal mol^{-1}, this slightly negative value is at the limits of the DFT method, especially considering the intrinsic inaccuracy of estimating ΔS using this method.

As shown in Figure 3.11, addition of $MeSiH_3$ is predicted to proceed *via* Path 1 (i.e. without initial β-NMe_2 coordination). The first-formed adduct **3Q** features the necessary interactions between Ti and H (Ti ··H = 1.990 Å), and Si and N_α (Si ··N_α = 2.854 Å), to proceed to the 1,2-addition product **4Q** (Ti–H = 1.707 Å; N_α–Si = 1.775 Å) *via* the transition state (TS) **TS_3-4**. This lies 16.3 kcal mol^{-1} above the separated reactants and is thus readily accessible, consistent with the rapid reaction of **3.1** with silanes. The concerted nature of this TS is illustrated by the almost identical values for the Ti ··H and Si ··H distances (1.765 and 1.760 Å). Intermediate **4Q** is itself not stable, but chelation of the β-NMe_2 forms **2Q** with an overall reaction ΔG_{sol} of -5.3 kcal mol^{-1}.

Path 2 in Figure 3.11 is also accessible but is not kinetically preferred compared to Path 1. Chelation of the β-NMe_2 of **1Q** is facile and forms **5Q** which lies only +1.8 kcal mol^{-1} above **1Q**. Bending takes place along a direction roughly parallel to the N ··N vector of the amidinate ligand and increases the nucleophilicity of N_α as shown by an increase in natural charge from -0.45 to -0.53. Si-H addition to Ti=N_α forms **6Q** (N_α–Si = 1.758 Å) *via* the TS **TS_5-6** with an activation barrier of 17.8 kcal mol^{-1} relative to **5Q**. Isomerisation *via* **4Q** finally gives the more stable isomer **2Q** with coordination of N_β approximately *trans* to the Cp ring. Whereas the new N_α–Si bond is more developed in **TS_5-6** than in **TS_3-4** (N ··Si = 2.099 and 2.119 Å, respectively), hydrogen transfer to Ti is not as advanced as illustrated by Si ··H = 1.594 Å (*cf.* 1.491 Å in $MeSiH_3$) and Ti ··H = 1.878 Å (*cf.* 1.701 Å in **6Q**). Thus Path 2 resembles slightly more a nucleophilic attack of N_α on silicon, followed by

hydrogen transfer to titanium, as proposed previously by Tilley for Si–H addition to a highly bent tantalum imido complex.[46] Note also that κ^2-hydrazido moieties can sometimes be trapped using the strong Lewis acid $B(C_6F_5)_3$ which coordinates strongly to N_α.[35, 105] In both **TS_3-4** and **TS_5-6**, the silicon is 5-coordinate with a trigonal bipyramidal geometry. N_α occupies one of the axial positions and the migrating H atom and Me group lie in the equatorial plane.

The additional stabilisation gained upon coordination of β-NMe_2 (**4Q** → **2Q**, ΔG = -13.2 kcal mol^{-1}) moves the system thermodynamically towards the Si–H activation product. This stabilising effect is not available to imido complexes which explains the lack of reaction between Cp*Ti{$MeC(N^iPr)_2$}(NTol) (**3.3**) and silanes. Calculations on CpTi{$MeC(NMe)_2$}(NPh) (**7Q**) and $MeSiH_3$ show that the energy barrier for the 1,2 addition is accessible ($\Delta G_{sol}^{\#}$ = 19.4 kcal mol^{-1}) and proceeds through a similar TS (**TS_7-8**; Ti ··H = 1.802 Å; Si ··H = 1.699 Å) to **TS_3-4**. However, although formation of CpTi{$MeC(NMe)_2$}(H){$N(Ph)SiH_2Me$} (**8Q**) is 4.0 kcal mol^{-1} more favourable than formation of **4Q**, the reaction is still endothermic by +3.9 kcal mol^{-1}.

3.6.2 Si–Cl bond addition

As summarised in Figure 3.11, Si–Cl addition to the Ti=$NNMe_2$ bond of **1Q** can also, in principle, proceed *via* either direct addition (Path 1) or *via* the β-NMe_2 chelated isomer **5Q**. The final product **2Q_Cl** (model for **24**) is 16.5 kcal mol^{-1} more stable with respect to the separated reactants than **2Q** (overall ΔG_{sol} = -21.8 kcal mol^{-1}), consistent with experimental observations of the irreversible addition of $PhSiH_2Cl$ to **3.1**. The high barrier to elimination of $MeSiH_2Cl$ from **2Q_Cl** *via* **TS_1-4Cl** (38.9 kcal mol^{-1}, *cf.* 21.6 kcal mol^{-1} for elimination of $MeSiH_3$ from **2Q**) is consistent with the absence of detectable exchange between **24** and free $PhSiH_2Cl$ on the NMR timescale.

The energy of the TS **TS_1-4Cl** (17.1 kcal mol^{-1}) is similar to that of **TS_3-4** (16.3 kcal mol^{-1}) for Si–H addition. Comparison of the Si ··Cl (2.312 Å) and Ti ··Cl (2.586 Å) distances in **TS_1-4Cl** with those of $MeSiH_2Cl$ (Si–Cl = 2.100 Å) and the first-formed product **4Q_Cl** (Ti–Cl = 2.373 Å), respectively, confirm the concerted nature of the process. β-NMe_2 chelation (**4Q_Cl** → **2Q_Cl**) brings a further stabilisation of -11.8 kcal mol^{-1} (*cf.* -13.2 kcal mol^{-1} for **4Q** → **2Q**). Unlike **4Q**, however, the chloride analogue **4Q_Cl** is predicted to be stable even without β-NMe_2 coordination,

in agreement with the observable 1,2-addition product **34** formed from Cp*Ti{MeC(N^iPr)$_2$}(NTol) (**3.3**) and $PhSiH_2Cl$ (Equation 3.8). Consistent with this, calculations on CpTi{MeC(NMe)$_2$}(NPh) (**7Q**) and $MeSiH_2Cl$ found a thermodynamically stable product CpTi{MeC(NMe)$_2$}(Cl){N(Ph)SiH_2Me} (**8Q_Cl**, ΔG_{sol} = -12.8 kcal mol^{-1}). The transition state from **7Q** to **8Q_Cl** lies at 17.5 kcal mol^{-1} above the reaction partners (*cf.* 17.1 kcal mol^{-1} for **TS_1-4Cl**) with Si ··Cl and Ti ··Cl distances (2.325 and 2.583 Å, respectively) that are comparable to those of **TS_1-4Cl**.

The formation of **2Q_Cl** *via* $MeSiH_2Cl$ addition to β-NMe_2 chelated **5Q** (Path 2) resembles in general terms that discussed above for $MeSiH_3$ addition. However, it is now the kinetically favoured route with **TS_5-6Cl** lying only 9.6 kcal mol^{-1} above **5Q** (*cf.* $\Delta G^{\#}$ = 17.8 kcal mol^{-1} for **TS_5-6**) and 5.7 kcal mol^{-1} below **TS_1-4Cl**. The geometry of **TS_5-6Cl** is also different to those of **TS_5-6** and **TS_1-4Cl**, and is much better described as a pentacoordinate silicon adduct on N_α with little transfer yet of Cl to titanium (Si–Cl = 2.193 Å; Ti ··Cl = 3.247 Å). This difference is attributed to the electron-withdrawing chloride ligand in $MeSiH_2Cl$ compared to hydride in $MeSiH_3$ and is the origin of the lower energy of **TS_5-6Cl** compared to **TS_5-6**. From **TS_5-6Cl** the hydrazide(1-) product **6Q_Cl** is formed with all 4 nitrogens and the Cl atom lying in an approximate plane. Rearrangement proceeds *via* **4Q_Cl** to place β-NMe_2 approximately *trans* to Cp and below this plane, forming **2Q_Cl** as the final product.

The possibility of silicon addition to the N_β of **1Q** *via* a charge-separated intermediate species [CpTi{MeC(NMe)$_2$}($NNMe_2SiH_2$Me)]Cl or the neutral analogue CpTi{MeC(NMe)$_2$}(Cl)($NNMe_2SiH_2$Me) (with subsequent 1,2-migration of SiH_2Me from N_β to N_α) were also considered. However, both of these species were found to lie above the energy of transition state **TS_5-6Cl** and so this potential pathway was not explored further.

Overall the calculations find a key role for the β-NMe_2 group in the reactions with silanes from both a kinetic and thermodynamic point of view. Furthermore, the effect on selecting the final reaction pathway depends also on whether the substrate is a silane or chlorosilane.

3.7 Alkylation and protonation reactions

While silane addition to metal hydrazides has been hitherto unexplored, alkylation and protonation reactions have been extensively studied for Group 6 compounds in particular in the context of understanding the key N_α–N_β bond cleavage steps in the Chatt and Schrock cycles. Reaction of terminal hydrazides with alkyl halides or triflates invariably occurs at N_β and three examples of the so-formed hydrazidium complexes $[(L)M(NNMe_3)]^+$ have been structurally characterised for titanium[65, 67] and molybdenum.[106] The situation regarding protonation is less clear-cut. Both N_α- and N_β-protonated complexes have been structurally authenticated for Group 6.[107-109] For molybdenum, Tuczek *et al.* have shown through stopped-flow experiments and DFT that protonation at N_β can be kinetically preferred but that a rapid 1,2-proton shift can occur to form the N_α-protonated counterpart which is thermodynamically more stable.[110] DFT studies by Reiher *et al.*,[111] and by Guha and Phukan,[112] support this view.

A number of charge-neutral Group 4 hydrazide(1-) complexes possessing either a κ^1- or κ^2-N(NRR′)H ligand have been reported,[65, 83, 85, 86, 90, 105] suggesting (assuming thermodynamic control) that N_α-protonated tautomers are preferred to the N_β-protonated ones. None of these were prepared by protonation of a hydrazide(2-) precursor. The only such reaction of a terminal group 4 hydrazide was reported by Odom to result in N_β-protonation, albeit without structural characterisation.[66] Two complexes containing a κ^2-$N(NPh_2)B(C_6F_5)_3$ ligand have been reported, prepared by reaction of terminal Group 4 hydrazides with $B(C_6F_5)_3$ at the N_α atom.[35, 105]

To clarify this site-selectivity issue, the thermodynamic preferences involved, and to compare the outcomes of protonation and alkylation with the N_α-silylation found exclusively above a series of further reactions with **3.1**, **3.2** and **3.3** along with DFT studies of model compounds were carried out.

3.7.1 Alkylation reactions

The reactions of $Cp^*Ti\{MeC(N^iPr)_2\}(NNMe_2)$ (**3.1**) with EtBr and $PhCH_2Br$ are summarised in Equation 3.9. In each case, N–C bond formation occurs exclusively at N_β to form the hydrazidium cations $[Cp^*Ti\{MeC(N^iPr)_2\}(NNMe_2R)]^+$ (R = Et (**36**$^+$) or CH_2Ph (**37**$^+$)) and corresponding non-coordinated anion as determined by X-ray

crystallography (*vide infra*).

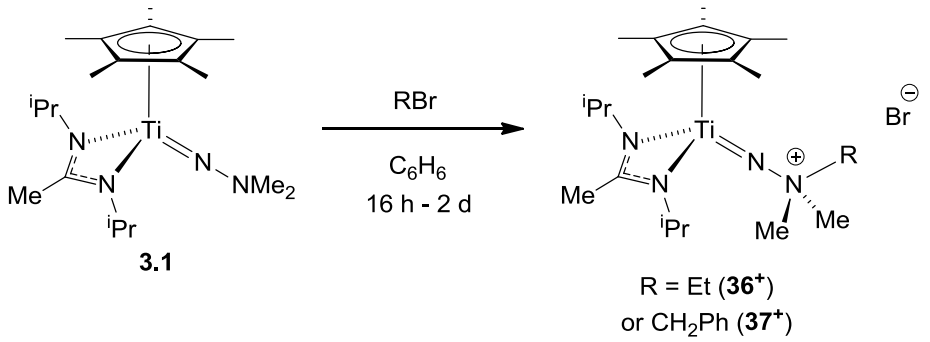

3.1

Equation 3.9

The results obtained are analogous to the previously reported hydrazidium cation $[Cp^*Ti\{MeC(N^iPr)_2\}(NNMe_3)]^+$ (**3.4**$^+$) formed between **3.1** and MeI which is accompanied by non-coordinated I^-.[75] No reaction occurred between **3.1** and PrCl, and with $PhCH_2Cl$ a mixture of unknown products was formed. There was no reaction of MeI, EtBr or $PhCH_2Br$ with either $Cp^*Ti\{MeC(N^iPr)_2\}(NNPh_2)$ (**3.2**) or $Cp^*Ti\{MeC(N^iPr)_2\}(NTol)$ (**3.3**). The same reaction outcomes were found in both benzene and THF in all instances.

When followed in C_6D_6 or THF-d_8 the reactions of **3.3** with MeI, $PhCH_2Br$ or EtBr were considerably slower than for $PhSiH_2X$ (X = H, Cl or Br) which reacted immediately under the same conditions. The reaction with MeI was complete only after 2 hours,[75] and those with $PhCH_2Br$ and EtBr required up to 16 hours and 2 days, respectively. Despite these slow rates, reaction of $PhCH_2Br$ with $Cp^*Ti\{MeC(N^iPr)_2\}(H)\{N(NMe_2)SiH_2Ph\}$ (**20**) formed exclusively **37-Br** and $PhSiH_3$ indicating that N_β-alkylation is thermodynamically prefered to 1,2-addition of Si–H to Ti=N_α. No evidence for direct Ti–H/C–Br exchange was found, in contrast to the reaction between **20** with $PhSiH_2Br$. The absence of any Ti–D/C–Br exchange was confirmed by ^1H and ^2H NMR spectra of the corresponding reaction using **20-*d*$_3$**.

Diffraction-quality crystals of **36-Br** were grown from THF/pentane layering at 4 ℃. The X-ray structure of **36-Br** has been determined. A view of the cation **36**$^+$ is given in Figure 3.12. Selected distances and angles are given in Table 3.5 along with those of **3.1** and **3.4-I** for comparison. Full crystallographic data are given in the CD Appendix. The structure unambigously confirms that the alkyl halide leads to N_β quaterisation as expected.[65, 67]

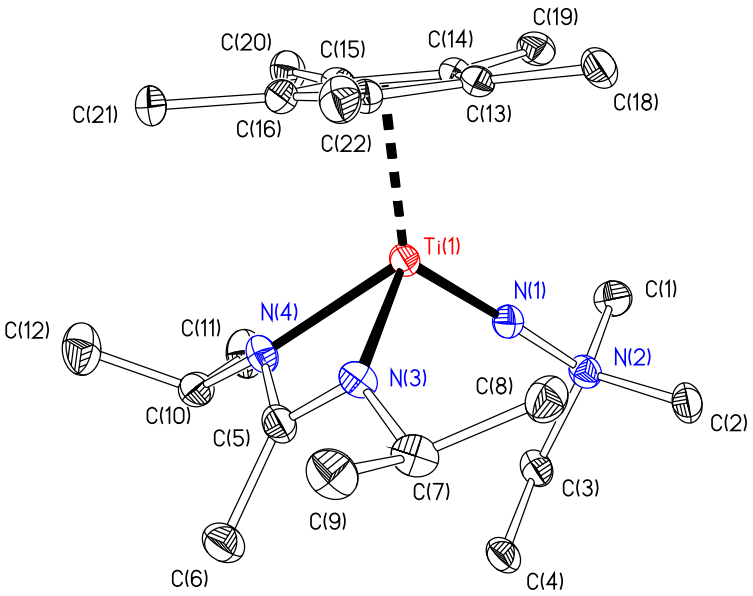

Figure 3.12. Displacement ellipsoid plot (20% probability) of $[Cp^*Ti\{MeC(N^iPr)_2\}(NNMe_2Et)]^+$ (**36**$^+$). H atoms and bromide counter-ion omitted for clarity.

Table 3.5. Selected bond lengths (Å) and angles (°) for $[Cp^*Ti\{MeC(N^iPr)_2\}(NNMe_2Et)]Br$ (**36-Br**) and the corresponding values for the previously reported $[Cp^*Ti\{MeC(N^iPr)_2\}(NNMe_3)]I$ (**3.4-I**)[75] and $Cp^*Ti\{MeC(N^iPr)_2\}(NNMe_2)$ (**3.1**).[34, 75] Cp_{cent} refers to the Cp* ring carbon centroid.

Parameter	**36-Br**	**3.4-I**	**3.1**
Ti(1)-Cp_{cent}	2.074	2.064	2.063
Ti(1)-N(1)	1.717(5)	1.728(3)	1.723(2)
Ti(1)-N(3)	2.083(6)	2.090(3)	2.101(1)
Ti(1)-N(4)	2.085(5)	2.078(3)	2.101(1)
N(1)-N(2)	1.426(7)	1.419(4)	1.386(2)
Cp_{cent}-Ti(1)-N(1)	127.5	125.1	119.5
Cp_{cent}-Ti(1)-N(3)	117.5	118.6	120.8
Cp_{cent}-Ti(1)-N(4)	117.7	118.7	120.8
Ti(1)-N(1)-N(2)	177.5(5)	173.5(3)	159.5(1)

In general terms, **36**$^+$ and **3.4**$^+$ have comparable geometries to that of **3.1** and also to that of the isoelectronic, neutral imido complexes Cp*Ti{RC(NR′)$_2$}(NXyl) (R = Me or Ph; R′ = ^{i}Pr or SiMe$_3$; Xyl = 2,6-C$_6$H$_3$Me$_2$).[73, 74] The molecular structure features a three-legged piano stool geometry. The Ti–N$_\alpha$ distances in the cations are comparable within error to that in **3.1** whereas the N$_\alpha$–N$_\beta$ distance is significantly longer in each case. This is attributed in part to the loss of residual π-bonding[34] between these atoms on quaternarisation. The short Ti–N$_\alpha$ distances are consistent with triple bonds as found in **3.1** and their imido counterparts.[34, 72]

3.7.2 Protonation reactions

Equation 3.10 shows the reaction of Cp*Ti{MeC(N^{i}Pr)$_2$}(NNMe$_2$) (**3.1**) with [Et$_3$NH][BPh$_4$]. Reaction of **3.1** with [Et$_3$NH][BPh$_4$] occurred immediately in THF to form **38-BPh$_4$** which contains the base-free, N$_\alpha$-protonated cation [Cp*Ti{MeC(N^{i}Pr)$_2$}{N(NMe$_2$)H}]$^+$. When followed by ^{1}H NMR spectroscopy in THF-d_8, **38-BPh$_4$** was the only product observed (along with the Et$_3$N side-product).

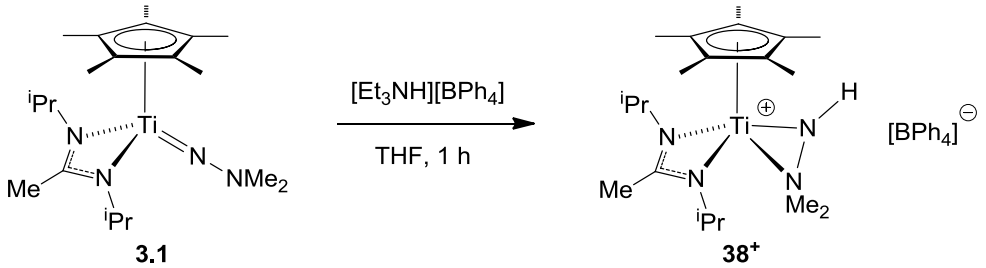

3.1 **38$^+$**

Equation 3.10

Compounds **3.2** and **3.3** also reacted with [Et$_3$NH][BPh$_4$] in THF-d_8 but required an excess of the ammonium salt to drive the first-formed equilibrium mixtures to completion. The products **39-BPh$_4$** and **40-BPh$_4$** are tentatively assigned as the analogues of **38-BPh$_4$** but definitive structural or other analytical data could not be obtained. Both were characterised *in situ* using NMR spectroscopy. Bearing in mind that certain hydrazido compounds are known to form N$_\alpha$-coordinated adducts with B(C$_6$F$_5$)$_3$,[35, 105] analogous reactions of **3.1** were carried out. However, no reaction was observed with either B(C$_6$F$_5$)$_3$ or Me$_3$N·BH$_3$, whereas with MeH$_2$N·BH$_3$ unknown mixtures were formed with complex ^{1}H and ^{11}B NMR spectra.

In order to clearly establish the site of protonation in **38-BPh$_4$** the X-ray structure has been determined. Full crystallographic data are given in the CD Appendix. Selected

distances and angles are listed in Table 3.6 and a view of the cation is given in Figure 3.13 which confirms that N_α carries the added H^+.

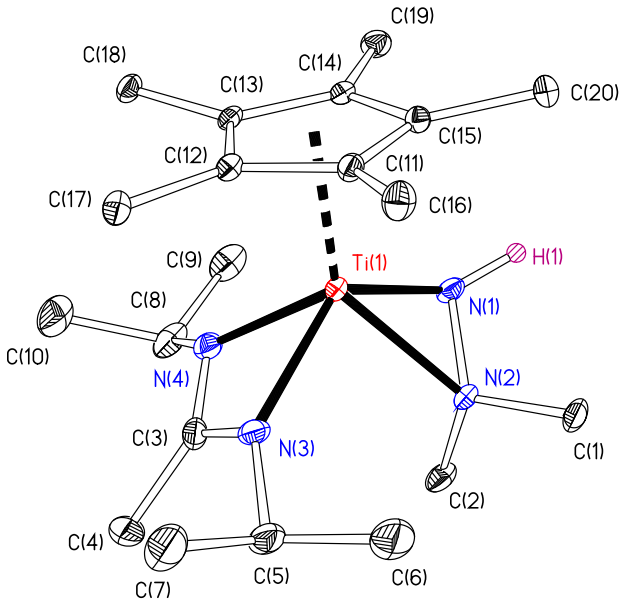

Figure 3.13. Displacement ellipsoid plot (20% probability) of the cation $[Cp^*Ti\{MeC(N^iPr)_2\}\{N(NMe_2)H\}]^+$ (**38**$^+$). C-bound H atoms and $[BPh_4]^-$ counter-ion omitted for clarity. H(1) is drawn as a sphere of arbitrary radius.

Table 3.6. Selected bond lengths (Å) and angles (°) for $[Cp^*Ti\{MeC(N^iPr)_2\}\{N(NMe_2)H\}][BPh_4]$ (**38-BPh$_4$**). Cp_{cent} refers to the Cp* ring carbon centroid.

Ti(1)-Cp_{cent}	2.035	Ti(1)-N(1)	1.889(3)
Ti(1)-N(2)	2.176(2)	Ti(1)-N(3)	2.024(3)
Ti(1)-N(4)	2.098(3)	N(1)-N(2)	1.432(3)
N(1)-H(1)	1.02(6)		
Cp_{cent}-Ti(1)-N(1)	112.8	Cp_{cent}-Ti(1)-N(2)	140.2
Cp_{cent}-Ti(1)-N(3)	115.7	Cp_{cent}-Ti(1)-N(4)	117.3
N(1)-Ti(1)-N(2)	40.49(9)	Ti(1)-N(1)-H(1)	146(3)

The Ti–N_α and Ti–N_β distances to the $N(NMe_2)H$ ligand in **38**$^+$ are significantly shorter than those for the $N(NMe_2)SiH_2Ar$ ligands in **20** – **22** and **24** which is mainly attributed to the higher formal charge and lower coordination number in the cation. The N_α–N_β distance is in general equivalent within error to those in these neutral complexes. While titanium and zirconium compounds containing the κ^2-$N(NMe_2)H$ ligand have been reported previously, none were prepared by protonation of a hydrazide(2-) precursor. [83, 90, 113] The observation that **3.1** undergoes protonation at N_α differs from Odom's report of N_β protonation in $[Ti(dpma)(^tBu\text{-}bipy)(NNH_2Ph)]^+$ based on spectroscopic data.[66]

The lack of any reaction between **3.3** and alkyl halides, and the observation that **3.1** reacts with these substrates only at N_β, shows that N_α alkylation is kinetically and/or thermodynamically disfavoured. The absence of any reaction for **3.2** compared with **3.1** is consistent with the less accessible N_β lone pair in the former due to conjugation with the phenyl rings. On the other hand, all three react with $[Et_3NH]^+$ giving N_α–H bond formation as confirmed by the X-ray structure of **38-[BPh$_4$]**. Likewise, all three give only N_α–Si bond formation with silanes and halosilanes. A precise comparison of C–X *vs.* Si–X reactivity is the slow reaction of **3.1** with $PhCH_2Br$ to form **37-Br** (N_β–C bond) but the immediate reaction with $PhSiH_2Br$ to form **29** (N_α-Si bond). In addition, DFT found that ΔG_{sol} for the reaction of $CpTi\{MeC(NMe)_2\}(NNMe_2)$ (**1Q**) with EtBr to form $CpTi\{MeC(NMe)_2\}(Br)\{N(NMe_2)Et\}$ (**9Q**) was favoured by -30.6 kcal mol^{-1}. This can be compared, for example, with ΔG_{sol} = -21.8 kcal mol^{-1} for **1Q** + $MeSiH_2Cl$ → **2Q_Cl** (Figure 3.11) and shows that C–Br addition across Ti=N_α is thermodynamically viable.

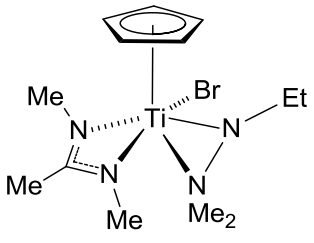

9Q

To test the intrinsic thermodynamic preferences for N_α- and N_β-bond formation with H, alkyl or silyl groups, DFT calculations were carried out on the isomeric model species $[CpTi\{MeC(NMe_2)_2\}\{\kappa^1\text{-}N(NMe_2)R\}]^+$ (**10Q_R**$^+$), $[CpTi\{MeC(NMe_2)_2\}\text{-}\{\kappa^2\text{-}N(NMe_2)R\}]^+$ (**11Q_R**$^+$) and $[CpTi\{MeC(NMe_2)_2\}(NNMe_2R)]^+$ (**12Q_R**$^+$) for R

= H, Me or SiH_2Me. The results are summarised in Figure 3.14 in terms of their free energies relative to that of **12Q_R$^+$**.

In all cases the κ^2-N(NMe_2)R isomer **11Q_R$^+$** is by far the most thermodynamically stable one. As found in Figure 3.11, chelation of the β-NMe_2 group in **10Q_R$^+$** to form **11Q_R$^+$** is very favourable. Figure 3.14 also shows that N_α-bond formation, even without β-NMe_2 coordination, remains thermodynamically preferred. This is consistent with previous DFT calculations on Group 5 and 6 metals.[110-112]

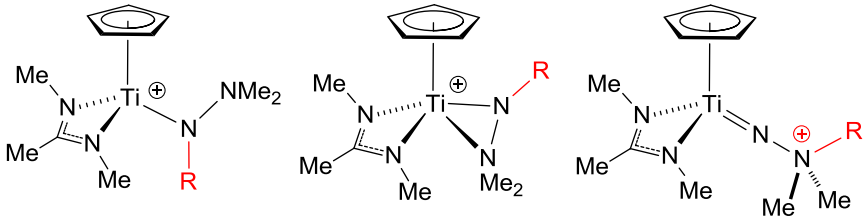

	10Q_R$^+$	**11Q_R$^+$**	**12Q_R$^+$**
R = H	-7.5	-21.3	0
R = Me	-3.3	-22.6	0
R = SiH_2Me	-2.6	-23.1	0

Figure 3.14. Model complexes used in the DFT calculations and their relative energies (ΔG_{sol}, kcal mol^{-1} at 298 K). Representative selected distances (Å) and angles (°): for **10Q_H**, Ti–N_α = 1.851, N_α–N_β = 1.393, Ti–N_α–N_β = 141.0; for **11Q_H**, Ti–N_α = 1.869, N_α–N_β = 1.394, Ti–N_α–N_β = 79.4; for **12Q_H**, Ti–N_α = 1.740, N_α–N_β = 1.400, Ti–N_α–N_β = 156.8.

These results establish that Si–X and H^+ addition reactions to **3.1** are under thermodynamic control, whereas those for C–X are apparently under kinetic control. For both of the low energy pathways for Si–X 1,2-addition, Figure 3.11 shows the importance of accessing a hypercoordinate silicon centre. Therefore carbon's considerably reduced tendency to form 5-coordinate species makes these types of pathways kinetically less accessible. In confirmation of this, the transition state (**TS_5-9Br**) linking EtBr + model **5Q** (*cf.* Figure 3.11) and **9Q** *via* a C–Br 1,2-addition process was found at ΔG_{sol} = 48.9 kcal mol^{-1} relative to **1Q** and EtBr. This confirms that addition to N_α by the 1,2-addition route is indeed kinetically inaccessible.

Electrophilic attack by alkyl halides at N_β in kinetic preference to N_α can be explained

by examination of the HOMO of **3.1** (modelled by **1Q**) which has *ca.* 20% N_α and 35% N_β character.[34] In addition, consideration of a space-filling model for **3.1** shows that N_α is much less sterically accessible than the pyramidalised N_β atom. Thus both frontier orbital and steric control appear to direct the outcome of alkylation reactions whose rates are moderated by the leaving group ability of the halide. Once the new N_β–C bond has formed it is kinetically impossible to rearrange to the N_α-alkylated isomer. In contrast, as shown experimentally by Tuczek *et al.*,[110] N_β could be the kinetically preferred site for protonation, with migration to N_α being fast and facile through a 1,2-shift between the N atoms (mediated in principle by the THF solvent or liberated Et_3N) to form the thermodynamic product.

3.8 Conclusions

The different reaction outcomes of Cp*Ti{MeC(N^iPr)$_2$}($NNMe_2$) (**3.1**), Cp*Ti{MeC(N^iPr)$_2$}($NNPh_2$) (**3.2**) and Cp*Ti{MeC(N^iPr)$_2$}(NTol) (**3.3**) with silanes, halosilanes, alkyl halides and [Et_3NH][BPh_4] represent a unique comparison in transition metal hydrazide chemistry. Reversible 1,2-addition of Si–H to Ti=$NNMe_2$ allows an experimental determination of the energetics of this process which DFT shows proceeds preferentially *via* a non-chelated (κ^1) hydrazide group. However, β-NMe_2 coordination is essential to stabilise the hydride-hydrazide(1-) product. According to DFT, H–H addition to Ti=N_α is less favoured compared to Si–H by *ca.* 9 kcal mol^{-1} and is not observed experimentally. However, net Si–H/Ti–H/H–H exchange does occur *via* a series of σ-bond metathesis and 1,2-addition/elimination steps, as established by labelling experiments.

Addition of primary halosilanes to Ti=$NNMe_2$ is irreversible and proceeds preferentially *via* a κ^2-coordinated hydrazide ligand and nucleophilic attack at silicon by N_α due to the higher Lewis acidity of silicon in these substrates. With secondary chlorosilanes the addition is reversible but still more favourable than for Si–H. Reaction of dichlorosilanes with **3.1** results in double Si–Cl activation and transfer of the amidinate ligand to silicon.

The hydrazidium products (N_β-alkylation in contrast to N_α-silylation) formed with alkyl halides are kinetic rather than thermodynamic products and arise because the HOMO of **3.1** is predominantly based on N_β and carbon is less readily able to adopt

the hypercoordinate, low energy transition states that silicon can access to achieve 1,2-addition to Ti=N_α. Protonation occurs at N_α in terms of thermodynamic preference in either the κ^1- or κ^2-coordinated forms, but mechanistically may proceed *via* initial attack at N_β as proposed for other hydrazides, followed by a 1,2-shift to N_α.

3.9 References

1. B. F. G. Johnson, B. L. Haymore and J. D. Dilworth, in *Comprehensive Coordination Chemistry*, eds. G. Wilkinson, R. D. Gillard and J. A. McCleverty, Pergamon Press, Oxford, Editon edn., 1987, vol. 2, p. 100.
2. W. A. Nugent and J. M. Mayer, *Metal-Ligand Multiple Bonds*, Wiley-Interscience, New York, 1988.
3. D. J. Mindiola, *Angew. Chem. Int. Ed.*, 2008, **47**, 1557.
4. M. D. Fryzuk, *The Chemical Record*, 2003, **3**, 2.
5. B. A. MacKay and M. D. Fryzuk, *Chem. Rev.*, 2004, **104**, 385.
6. C. M. Kozak and P. Mountford, *Angew. Chem. Int. Ed.*, 2004, **43**, 1186.
7. J. Chatt, A. J. Pearman and R. L. Richards, *Nature*, 1975, **253**, 39.
8. C. J. Pickett and G. J. Leigh, *J. Chem. Soc., Chem. Commun.*, 1981, 1033.
9. W. Hussain, G. J. Leigh and C. J. Pickett, *J. Chem. Soc., Chem. Commun.*, 1982, 747.
10. C. J. Pickett and J. Talamarin, *Nature*, 1985, **317**, 652.
11. K. Arashiba, Y. Miyake and Y. Nishibayashi, *Nature. Chem.*, 2011, **3**, 120.
12. D. V. Yandulov and R. R. Schrock, *Science*, 2003, 76.
13. R. R. Schrock, *Acc. Chem. Res.*, 2005, **38**, 955.
14. G. C. Stephan, C. Sivasankar, F. Studt and F. Tuczek, *Chem. Eur. J.*, 2008, **14**, 644.
15. F. Studt and F. Tuczek, *Angew. Chem. Int. Ed.*, 2005, **44**, 5639.
16. R. R. Schrock, *Angew. Chem. Int. Ed.*, 2008, **47**, 5512.
17. M. D. Fryzuk, J. B. Love, S. J. Rettig and V. G. Young, *Science*, 1998, **275**, 1445.
18. Y. Ohki and M. D. Fryzuk, *Angew. Chem. Int. Ed.*, 2007, **46**, 3180.
19. M. P. Shaver and M. D. Fryzuk, *Adv. Synth. Catal.*, 2003, **345**, 1061.
20. B. A. MacKay, R. F. Munha and M. D. Fryzuk, *J. Am. Chem. Soc.*, 2006, **128**, 9472.

21. G. B. Nikiforov, I. Vidyarante, S. Gambarotta and I. Korobkov, *Angew. Chem. Int. Ed.*, 2009, **48**, 7415.
22. H. Tanaka, A. Sasada, T. Kouno, M. Yuki, Y. Miyake, H. Nakanishi, Y. Nishibayashi and K. Yoshizawa, *J. Am. Chem. Soc.*, 2011, **133**, 3498.
23. J. A. Pool, E. Lobkovsky and P. J. Chirik, *Nature*, 2004, **427**, 527.
24. P. J. Chirik, *Dalton Trans.*, 2007, 16.
25. W. H. Bernskoetter, E. Lobkovsky and P. J. Chirik, *Angew. Chem. Int. Ed.*, 2007, **46**, 2858.
26. D. J. Knobloch, H. E. Toomey and P. J. Chirik, *J. Am. Chem. Soc.*, 2008, **130**, 4248.
27. D. J. Knobloch, D. Benito-Garagorri, W. H. Bernskoetter, I. Keresztes, E. Lobkovsky, H. Toomey and P. J. Chirik, *J. Am. Chem. Soc.*, 2009, **131**, 14903.
28. S. P. Semproni, E. Lobkovsky and P. J. Chirik, *J. Am. Chem. Soc.*, 2011, **133**, 10406.
29. N. Wiberg, H.-W. Haring, G. Huttner and P. Friedrich, *Chem. Ber.*, 1978, **111**, 2708.
30. P. J. Walsh, M. J. Carney and R. G. Bergman, *J. Am. Chem. Soc.*, 1991, **113**, 6343.
31. A. J. Blake, J. M. McInnes, P. Mountford, G. I. Nikonov, D. Swallow and D. J. Watkin, *J. Chem. Soc., Dalton Trans.*, 1999, 379.
32. J. L. Thorman and L. K. Woo, *Inorg. Chem.*, 2000, **39**, 1301.
33. S. Banerjee and A. L. Odom, *Organometallics*, 2006, **25**, 3099.
34. P. J. Tiong, A. Nova, L. R. Groom, A. D. Schwarz, J. D. Selby, A. D. Schofield, E. Clot and P. Mountford, *Organometallics*, 2011, **30**, 1182.
35. A. D. Schofield, A. Nova, J. D. Selby, A. D. Schwarz, E. Clot and P. Mountford, *Chem. Eur. J.*, 2011, **17**, 265.
36. P. J. Tiong, A. D. Schofield, J. D. Selby, A. Nova, E. Clot and P. Mountford, *Chem. Commun.*, 2010, **46**, 85.
37. A. D. Schofield, A. Nova, J. D. Selby, C. D. Manley, A. D. Schwarz, E. Clot and P. Mountford, *J. Am. Chem. Soc.*, 2010, **132**, 10484.
38. J. D. Selby, C. Schulten, A. D. Schwarz, A. Stasch, E. Clot, C. Jones and P. Mountford, *Chem.Commun.*, 2008, 5101.
39. J. D. Selby, C. D. Manley, M. Feliz, A. D. Schwarz, E. Clot and P. Mountford, *Chem. Commun.*, 2007, 4937.

40. T. Gehrmann, J. L. Fillol, H. Wadepohl and L. H. Gade, *Organometallics*, 2010, **29**, 28.
41. K. Weitershaus, H. Wadepohl and L. H. Gade, *Organometallics*, 2009, **28**, 3381.
42. K. Weitershaus, J. L. Fillol, H. Wadepohl and L. H. Gade, *Organometallics*, 2009, **28**, 4747.
43. T. Gehrmann, J. L. Fillol, H. Wadepohl and L. H. Gade, *Angew. Chem. Int. Ed.*, 2009, **48**, 2152.
44. H. Herrmann, J. L. Fillol, H. Wadepohl and L. H. Gade, *Angew. Chem. Int. Ed.*, 2007, **46**, 8426.
45. T. Gehrmann, J. L. Fillol, S. A. Scholl, H. Wadepohl and L. H. Gade, *Angew. Chem. Int. Ed.*, 2011, **50**, 5757.
46. T. I. Gountchev and T. D. Tilley, *J. Am. Chem. Soc.*, 1997, **119**, 12831.
47. C. C. Cummins, S. M. Baxter and P. T. Wolczanski, *J. Am. Chem. Soc.*, 1988, **110**, 8731.
48. A. W. Kaplan, J. L. Polse, G. E. Ball, R. A. Andersen and R. G. Bergman, *J. Am. Chem. Soc.*, 1998, **120**, 11649.
49. Z. K. Sweeny, J. L. Polse, R. G. Bergman and R. A. Andersen, *Organometallics*, 1999, **18**, 5502.
50. T. E. Hanna, E. Lobkovsky and P. J. Chirik, *Inorg. Chem.*, 2007, **46**, 2359.
51. D. Sieh, J. Schoffel and P. Burger, *Dalton Trans.*, 2011, **40**, 9512.
52. G. I. Nikonov, P. Mountford, S. K. Ignatov, J. C. Green, P. A. Cooke, M. A. Leech, L. G. Kuzmina, A. G. Razuvaev, N. H. Rees, A. J. Blake, J. A. K. Howard and D. A. Lemenovskii, *J. Chem. Soc., Dalton Trans.*, 2001, 2903.
53. S. K. Ignatov, A. A. Merkoulov, N. H. Rees, S. R. Dubberley, A. G. Razuvaev, P. Mountford and G. I. Nikonov, *Chem. Eur. J.*, 2008, **14**, 296.
54. S. K. Ignatov, A. Y. Khalimon, N. H. Rees, A. G. Razuvaev, P. Mountford and G. I. Nikonov, *Inorg. Chem.*, 2009, **48**, 9605.
55. U. Burckhardt, G. L. Casty, T. D. Tilley, T. K. Woo and U. Rothlisberger, *Organometallics*, 2000, **19**, 3830.
56. J. B. Diminnie and Z. Xue, *J. Am. Chem. Soc.*, 1997, **119**, 12657.
57. T. E. Hanna, I. Keresztes, E. Lobkovsky, W. H. Bernskoetter and P. J. Chirik, *Organometallics*, 2004, **23**, 3448.

58. J. L. Polse, R. A. Andersen and R. G. Bergman, *J. Am. Chem. Soc.*, 1998, **120**, 13405.
59. H. K. Sharma and K. H. Pannell, *Chem. Rev.*, 1995, **95**, 1351.
60. J. Y. Corey and J. Braddock-Wilking, *Chem. Rev.*, 1999, **99**, 175.
61. J. F. Harrod, *Coord. Chem. Rev.*, 2000, **206-207**, 493.
62. G. I. Nikonov, *J. Organomet. Chem.*, 2001, **635**, 24.
63. R. Waterman, P. G. Hayes and T. D. Tilley, *Acc. Chem. Res.*, 2007, **40**, 712.
64. J. Y. Corey, *Chem. Rev.*, 2011, **111**, 863.
65. Y. Li, Y. Shi and A. L. Odom, *J. Am. Chem. Soc.*, 2004, **126**, 1794.
66. S. Patel, Y. Li and A. L. Odom, *Inorg. Chem.*, 2007, **46**, 6373.
67. A. J. Clulow, J. D. Selby, M. G. Cushion, A. D. Schwarz and P. Mountford, *Inorg. Chem.*, 2008, **47**, 12049.
68. P. J. Tiong, A. Nova, E. Clot and P. Mountford, *Chem. Commun.*, 2011, **47**, 3147.
69. P. J. Tiong, A. Nova, A. D. Schwarz, J. D. Selby, E. Clot and P. Mountford, *Dalton Trans.*, 2012, **41**, 2277.
70. A. E. Guiducci, A. R. Cowley, M. E. G. Skinner and P. Mountford, *J. Chem. Soc., Dalton Trans.*, 2001, 1392.
71. C. L. Boyd, A. E. Guiducci, S. R. Dubberley, B. R. Tyrrell and P. Mountford, *J. Chem. Soc., Dalton Trans.*, 2002, 4175.
72. C. L. Boyd, E. Clot, A. E. Guiducci and P. Mountford, *Organometallics*, 2005, **24**, 2347.
73. A. E. Guiducci, C. L. Boyd and P. Mountford, *Organometallics*, 2006, **25**, 1167.
74. A. E. Guiducci, C. L. Boyd, E. Clot and P. Mountford, *Dalton Trans.*, 2009, 5960.
75. J. D. Selby, D.Phil Thesis, University of Oxford, 2009.
76. D. A. Fletcher, R. F. McMeeking and D. Parkin, *J. Chem. Inf. Comput. Sci.*, 1996, **36**, 746 (The UK Chemical Database Service: CSD version 5.32 updated August 2011).
77. S. K. Ignatov, N. H. Rees, B. R. Tyrrell, S. R. Dubberley, A. G. Razuvaev, P. Mountford and G. I. Nikonov, *Chem. Eur. J.*, 2004, **10**, 4991.
78. W. W. Lukens, P. T. Matsunaga and R. A. Andersen, *Organometallics*, 1998, **17**, 5240.

79. M. D. Walter, C. D. Sofield and R. A. Andersen, *Organometallics*, 2008, **27**, 2959.
80. J. M. de Wolf, A. Meetsma and J. H. Teuben, *Organometallics*, 1995, **14**, 5466.
81. Y. You and G. S. Girolami, *Organometallics*, 2008, **27**, 3172.
82. H. Noth and M. Schmidt, *Organometallics*, 1995, **14**, 4601.
83. I. A. Latham, G. J. Leigh, G. Huttner and I. Jibril, *J. Chem. Soc., Dalton Trans.*, 1986, 385.
84. R. Hemmer, U. Thewalt, D. L. Hughes, G. J. Leigh and D. G. Walker, *J. Organomet. Chem.*, 1987, **323**, C29.
85. D. L. Hughes, G. J. Leigh and D. G. Walker, *J. Chem. Soc., Dalton Trans.*, 1989, 1413.
86. D. L. Hughes, M. Jimenez-Tenorio, G. J. Leigh and D. G. Walker, *J. Chem. Soc., Dalton Trans.*, 1989, 2389.
87. B. Goetze, J. Knizek, H. Noth and W. Schnick, *Eur. J. Inorg. Chem.*, 2000, 1849.
88. J.-S. M. Lehn and D. M. Hoffman, *Inorg. Chim. Acta*, 2003, **345**, 327.
89. J. M. Pietryga, J. N. Jones, C. L. B. Macdonald, J. A. Moore and A. H. Cowley, *Polyhedron*, 2006, **25**, 259.
90. J. D. Selby, M. Feliz, A. D. Schwarz, E. Clot and P. Mountford, *Organometallics*, 2011, **30**, 2295.
91. T. Janssen, R. Severin, M. Diekmann, M. Friedemann, D. Haase, Saak, W., S. Doye and R. Beckhaus, *Organometallics*, 2010, **29**, 1806.
92. A. J. Hoskin and D. W. Stephan, *Coord. Chem. Rev.*, 2002, **233-234**, 107.
93. X. Liu, Z. i. Wu, H. Cai, Y. Yang, T. Chen, C. E. Vallet, R. A. Zuhr, D. B. Beach, Z.-H. Peng, Y.-D. Wu, T. E. Concolino, A. L. Rheingold and Z. Xue, *J. Am. Chem. Soc.*, 2001, **123**, 8011.
94. L. J. Procopio, P. J. Carroll and D. H. Berry, *J. Am. Chem. Soc.*, 1994, **116**, 177.
95. M. P. Coles, *Dalton Trans.*, 2006, 985.
96. K. Y. Dorogov, A. V. Churakov, L. G. Kuzmina, J. A. K. Howard and G. I. Nikonov, *Eur. J. Inorg. Chem.*, 2004, 771.
97. P. Mountford, *Chem. Commun.*, 1997, 2127.
98. N. Hazari and P. Mountford, *Acc. Chem. Res.*, 2005, **38**, 839.

99. A. R. Fout, U. J. Kilgore and D. J. Mindiola, *Chem. Eur. J.*, 2007, **13**, 9428.
100. D. E. Wigley, *Prog. Inorg. Chem.*, 1994, **42**, 239.
101. M. F. Lappert, A. V. Protchenko, P. P. Power and A. Seeber, *Metal Amide Chemistry*, Wiley, Chichester, 2009.
102. Y. Zhao and D. G. Truhlar, *Theor. Chem. Acc.*, 2008, **120**, 215.
103. J. L. Bennett and P. T. Wolczanski, *J. Am. Chem. Soc.*, 1997, **119**, 10696.
104. C. C. Cummins, C. P. Schaller, G. D. Van Duyne, P. T. Wolczanski, A. W. E. Chan and R. Hoffmann, *J. Am. Chem. Soc.*, 1991, **113**, 2985.
105. H. Herrmann, J. L. Fillol, T. Gehrmann, M. Enders, H. Wadepohl and L. H. Gade, *Chem. Eur. J.*, 2008, **14**, 8131.
106. M. G. Vale and R. R. Schrock, *Inorg. Chem.*, 1993, **32**, 2767.
107. T. Takahashi, Y. Mizobe, M. Sato, Y. Uchida and M. Hidai, *J. Am. Chem. Soc.*, 1979, **101**, 3405.
108. J. R. Dilworth, R. A. Henderson, P. Dahlstrom, T. Nicholson and J. A. Zubieta, *J. Chem. Soc., Dalton Trans.*, 1987, 529.
109. A. Galindo, A. Hills, D. L. Hughes, R. L. Richards, M. Hughes and J. Mason, *J. Chem. Soc., Dalton Trans.*, 1990, 283.
110. A. Dreher, K. Mersmann, C. Nather, I. Ivanovic-Burmazovic, R. van Eldik and F. Tuczek, *Inorg. Chem.*, 2009, **48**, 2078.
111. S. Schenk, B. Le Guennic, B. Kirchner and M. Reiher, *Inorg. Chem.*, 2008, **47**, 3634.
112. A. K. Guha and A. K. Phukan, *Inorg. Chem.*, 2011, **50**, 8826.
113. H. Herrmann, H. Wadepohl and L. H. Gade, *Dalton Trans.*, 2008, 2111.

Chapter Four

Synthesis and reactivity of

$Cp^*Ti\{MeC(N^iPr)_2\}(NNCPh_2)$ (41)

4.1 Introduction

Alkylidene hydrazido complexes (more commonly known as diazoalkane or hydrazonido complexes) are complexes which possess a NNCRR' ligand. Research on these complexes spans across a range of transition metals as well as some lanthanides and actinides.[1-21] However, the chemistry of titanium alkylidene hydrazido complexes is still relatively underdeveloped. The first structurally characterised terminal η^1-alkylidene hydrazido(2-) complex of titanium was reported by Kool *et al*. in 1986. However, the reactivity of the compound was not studied.[6] Apart from that, only a few studies on titanium alkylidene hydrazido complexes have been reported.[1, 3-5, 10, 13, 19, 20]

As an extension to its work on titanium hydrazide chemistry, our research group became interested in exploring the apparently related alkylidene hydrazido complexes of titanium $(L)_nTi{=}NNCRR'$. Previous studies have demonstrated that the alkylidene hydrazide ligand can have a variety of bonding modes when coordinating to a metal. As shown in Figure 4.1, the alkylidene hydrazide ligand can be σ- and π- bonded through the terminal (N_α) nitrogen atom (i), or coordinated side-on *via* a π-interaction with the N=N bond (ii). Unlike dialkyl or diaryl hydrazido complexes, there is also the possibility of forming a complex through a π-interaction with the C=N bond (iii), or by formation of cycloadduct at the N_α and C_γ atoms (iv).[7, 8]

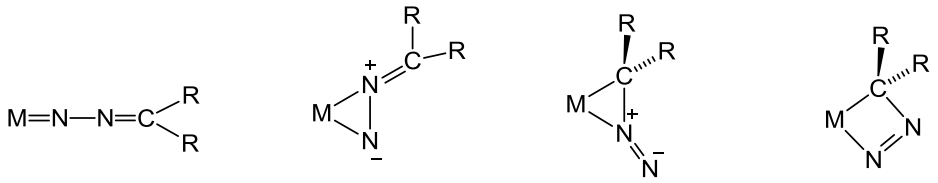

Figure 4.1. Possible bonding modes for alkylidene hydrazido ligand coordinated to a metal.

Monomeric η^1-alkylidene hydrazido(2-) complexes of titanium are not as common compared to their bridging or η^2-coordinated counterparts. In fact, only one example of a monomeric η^1-alkylidene hydrazido(2-) complex of titanium has been structurally characterised prior to this study, namely $Cp_2Ti(NNCPh_2)(PMe_3)$.[6]

Although it is possible to synthesise alkylidene hydrazido complexes from azines, hydrazones or even coordinated dinitrogen, most of the reported complexes are

derived from free diazoalkanes.[7] As free diazoalkanes can be explosive due to the facile loss of N_2 and therefore difficult to handle, it was decided to synthesise the desired complexes using hydrazones which are thermodynamically more stable. In the first attempt to develop the chemistry of $(L)_nTi{=}NNCR_2$, it was decided to target the synthesis of the alkylidene hydrazido analogue of the *tert*-butyl imido complex $Cp^*Ti\{MeC(N^iPr)_2\}(N^tBu)$ through an imido/hydrazone exchange route (a similar strategy proved successful for the synthesis of its dialkyl and diphenyl hydrazide analogues). This Chapter describes the successful synthesis of the terminal titanium η^1-alkylidene hydrazido(2-) complex $Cp^*Ti\{MeC(N^iPr)_2\}(NNCPh_2)$ (**41**), its structural analysis and reactivity towards a variety of substrates.

4.2 Synthesis and molecular structure of a new titanium alkylidene hydrazido complex

The new titanium alkylidene hydrazido complex $Cp^*Ti\{MeC(N^iPr)_2\}(NNCPh_2)$ (**41**) was successfully prepared from $Cp^*Ti\{MeC(N^iPr)_2\}(N^tBu)$ (**4.1**) and benzophenone hydrazone at room temperature according to Equation 4.1 using a *tert*-butyl imido/hydrazone exchange strategy.[22] This analogous approach had proved successful in the preparation of the hydrazido compounds $Cp^*Ti\{MeC(N^iPr)_2\}(NNR^1R^2)$ (R^1 = Ph, R^2 = Ph (**4.2**) or Me (**4.3**); $R^1 = R^2$ = Me (**4.4**))[23-25] mentioned in Chapter Two and Three, and also the aryl imido complexes $Cp^*Ti\{MeC(N^iPr)_2\}(NAr)$ (**4.5**, Ar = Tol, 4-$C_6H_4CF_3$, 4-$C_6H_4NMe_2$, 2,6-$C_6H_3Me_2$).[23, 25-27]

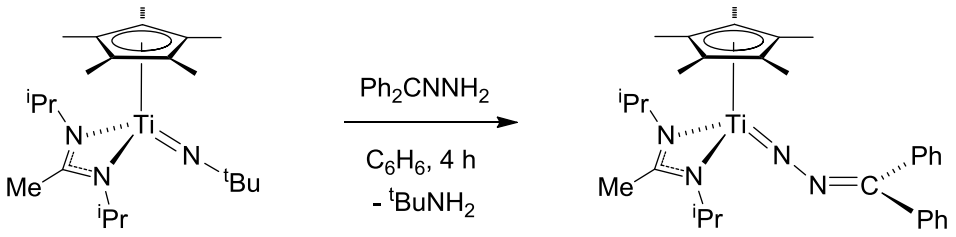

4.1 **41**

Equation 4.1

Reaction of $Cp^*Ti\{MeC(N^iPr)_2\}(N^tBu)$ (**4.1**) with benzophenone hydrazone in benzene gave an immediate colour change from dark red to dark yellow. The reaction was complete after 4 hours at room temperature giving a crude brown oil. Trituration with pentane gave **41** as brown powder in 76% isolated yield. The solution ^1H and $^{13}C\{^1H\}$ NMR data are consistent with the C_s symmetric products illustrated in

Equation 4.1. The ^{1}H NMR spectrum of **41** shows one apparent septet and a pair of doublets corresponding to the *iso*-propyl groups of the amidinate ligand (Figure 4.2). The IR spectrum of **41** shows a ν(C=N) band at 1595 cm^{-1}, which is higher than that for Ph_2CNNH_2 (*ca*. 1568 cm^{-1}). This value is consistent with ν(C=N) bands reported for alkylidene hydrazido complexes of Mo and W which appear in the region between 1510 and 1590 cm^{-1}.[7]

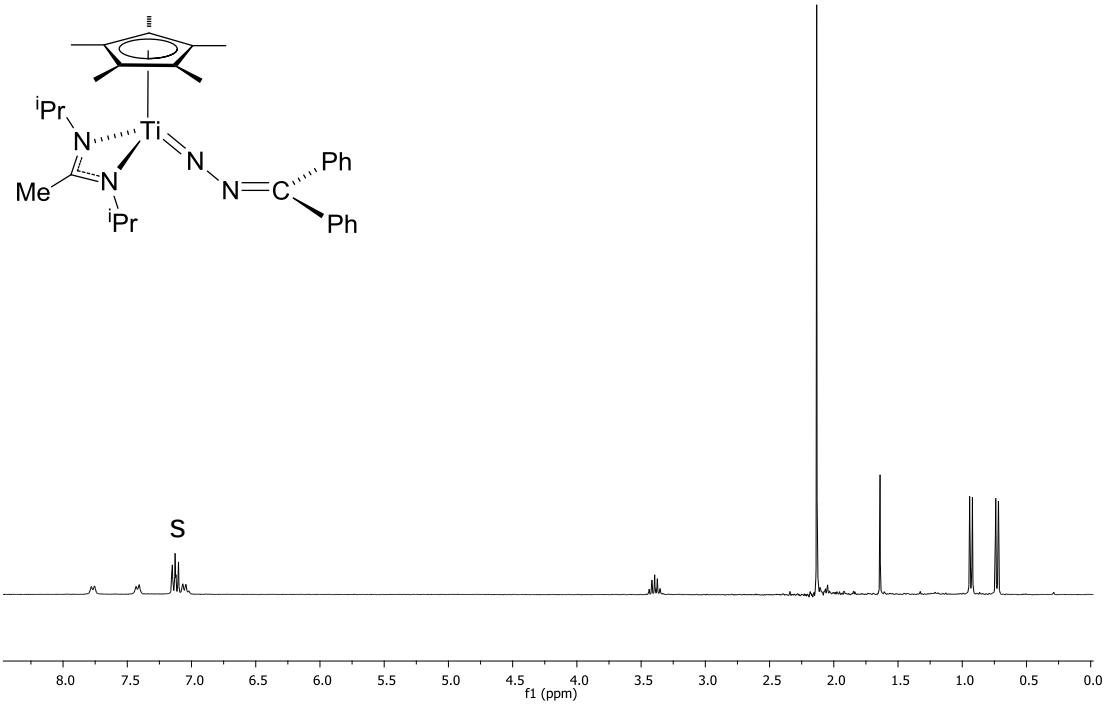

Figure 4.2. ^{1}H NMR spectrum (299.9 MHz) of Cp*Ti{MeC(N^{i}Pr)$_2$}(NNCPh$_2$) (**41**) in C_6D_6 ("S" denotes residual protio-solvent which overlaps with certain Ph resonances).

Compound **41** is stable indefinitely under an inert atmosphere at room temperature, and when heated to 70 ℃ in C_6D_6 for 7 days, with no tendency of dimerisation or loss of dinitrogen. It is the first monomeric η^1-alkylidene hydrazido(2-) complex of titanium formed *via* a protonolysis route. Previously reported alkylidene hydrazido complexes are mostly generated using diazoalkanes.[7, 28] There are only four other examples in literature which described the syntheses of alkylidene hydrazido complexes through the use of hydrazones. Among the four examples, only one successfully synthesised an η^1-alkylidene hydrazido(2-) complex V(NS$_3$)NNCPh$_2$ (NS$_3$ = N(CH$_2$CH$_2$S)$_3$) through the reaction of V(NS$_3$)O with Ph_2CNNH_2.[29] The other three formed either η^2-alkylidene hydrazido(1-) complexes or dimers.[11, 13, 30, 31]

Diffraction-quality crystals of **41** were grown from the slow evaporation of pentane. The molecular structure is shown in Figure 4.3 and selected distances and angles are listed in Table 4.1. Full crystallographic data are given in the CD Appendix. The molecular structure of **41** confirms its monomeric nature with η^1- coordination of the alkylidene hydrazide fragment to the metal. As shown in Figure 4.3, compound **41** features a three-legged piano stool geometry around titanium with η^5-C_5Me_5 and κ^2*N*,*N*′ acetamidinate ligands, similar to that found for its hydrazide analogues.

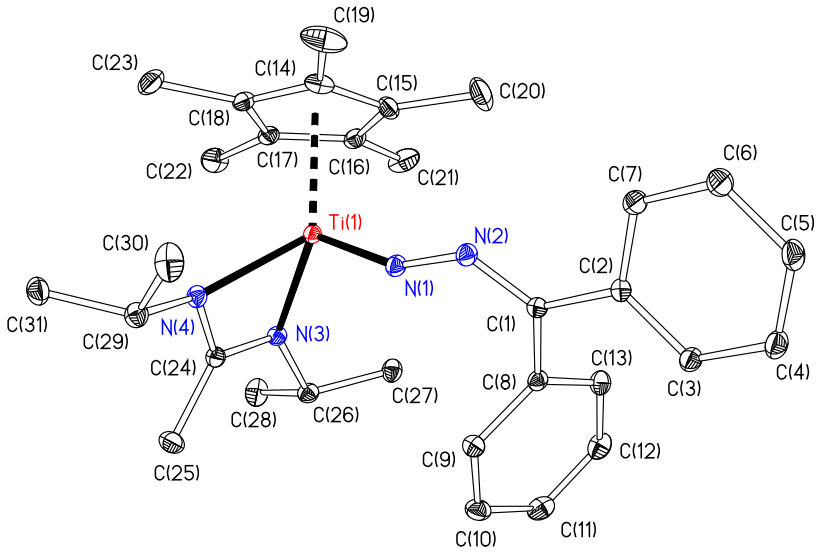

Figure 4.3. Displacement ellipsoid plot (20% probability) of Cp*Ti{MeC(N^{i}Pr)$_2$}(NNCPh$_2$) (**41**). H atoms omitted for clarity.

Table 4.1. Selected distances (Å) and angles (°) for Cp*Ti{MeC(N^{i}Pr)$_2$}(NNCPh$_2$) (**41**). Cp$_{cent}$ refers to the Cp* ring carbon centroid.

Ti(1)-Cp$_{cent}$	2.052	Ti(1)-N(1)	1.7508(16)
Ti(1)-N(3)	2.1093(15)	Ti(1)-N(4)	2.0925(16)
N(1)-N(2)	1.329(2)	N(2)-C(1)	1.304(2)
C(1)-C(2)	1.479(3)	C(1)-C(8)	1.489(3)
Cp$_{cent}$-Ti(1)-N(1)	117.7	Cp$_{cent}$-Ti(1)-N(3)	123.0
Cp$_{cent}$-Ti(1)-N(4)	122.8	Ti(1)-N(1)-N(2)	156.56(14)
N(1)-N(2)-C(1)	120.22(16)	N(2)-C(1)-C(2)	116.87(16)
N(2)-C(1)-C(8)	123.22(17)	C(2)-C(1)-C(8)	119.90(16)

The Ti=N_α distance of **41** (1.751(2) Å) is longer compared to those for its hydrazide analogues Cp*Ti{MeC(N^iPr)$_2$}(NNR^1R^2) (R^1 = Ph, R^2 = Ph (**4.2**) or Me (**4.3**); R^1 = R^2 = Me (**4.4**)) (1.723(2) – 1.734(2) Å). The results of Natural Bond Orbital (NBO) analysis suggested that the longer Ti=N_α bond length in **41** is due to the antibonding interaction between the π_h-type Ti=N_α bonding orbital and the N_β=CPh_2 π-bonding orbital which are not available for its hydrazide analogues. When compared to Ti–NR multiple bonds in general (imides, dialkyl hydrazides) it lies at the long end of the range known, 1.68 – 1.76 Å.[28] The N_α–N_β (1.329(2) Å) bond distance however, is shorter compared to those for its hydrazide analogues (1.369 (2) – 1.386(2) Å).

In general, the selected bond lengths and angles of **41** are comparable with the only other reported monomeric η^1-coordinated alkylidene hydrazido complex of titanium $Cp_2Ti(NNCPh_2)(PMe_3)$ (**4.6**) obtained *via* reactions of the Ti(II) complexes $Cp_2Ti(PMe_3)_2$ or $Cp_2Ti(CO)(PMe_3)$ with diphenyldiazomethane.[6]

When coordinated to a single metal in an η^1-fashion, alkylidene hydrazide ligand can act either as a two electron donor by forming a dative bond to the metal centre formally being a neutral ligand (**A**), or act as a four electron donor forming a $\sigma^2\pi^4$ triple bond as shown in **B**, formally being a dianionic ligand analogous to early transition metal imido or hydrazido complexes.[8] Structurally characterised alkylidene hydrazido complexes found in the Cambridge Structural Database (CSD) (42 examples)[28] show N_α–N_β bond distances in the range 1.264 – 1.368 Å, and N_β–C_γ bond lengths in the range 1.270 – 1.322 Å, suggesting the complexes with more of a type **B** resonance contribution. The M–N–N bond angles are found to be in the range of *ca*. 155 – 177 ° with a mean value of *ca*. 165 °. The N–N–C bond angles lie in the range of *ca*. 117 – 136 ° with a mean value of *ca*. 121 °. In general, no relationship is found between the N_α–N_β and N_β–C_γ bond distances. No relationship is found between N_α–N_β bond lengths and M–N–N, or N–N–C bond angles generally. Larger

N–N–C bond angles are associated with longer N_β–C_γ bond distances while no relationship is found between M–N–N and N–N–C bond angles.

Another small cluster of 8 compounds with shorter N_α–N_β bond distances of 1.144 – 1.206 Å were also found in the CSD.[28] These complexes have longer N_β–C_γ bond lengths (1.326 – 1.372 Å), suggesting more of a type **A** resonance contribution. They are also found to possess smaller M–N–N bond angles (*ca*.144 – 153 °) and larger N–N–C bond angles (*ca*. 150 – 176.5 °).

The N(1)-N(2) (1.329(2) Å) and N(2)-C(1) (1.304(2) Å) bond lengths of **41** lie within the normal ranges reported[28] for alkylidene hydrazido complexes (1.264 – 1.368 Å and 1.270 – 1.322 Å, respectively), and are both intermediate between single and double N–N and N–C bond ranges, respectively. The Ti(1)-N(1)-N(2) bond angle of 156.56(14) ° is distorted from linear, and lies at the lower end of the reported range[28] (*ca*. 150 – 177 °). The value is similar to 156.8(9) ° reported for **4.6** and 152.8(2) ° reported for $\{(Me_3Si)_2N\}_2VCl(N_2CPh_2)$ (**4.7**)[32]. In the case of **4.7**, the alkylidene hydrazide ligand was reported to act as a two electron donor, while that in **4.6** was reported to be a four electron donor. DFT calculations suggest that the alkylidene hydrazide ligand in **41** acts as a four electron donor (*vide infra*). The N–N–C bond is bent with a N(1)-N(2)-C(1) bond angle of 120.22(16) °. This lies in the normal range (*ca*. 117 – 136 °) reported[28] and is as expected for a sp^2 hybridised N_β atom. The phenyl rings are rotated 18.7 ° and 55.8 ° out of the $NNC(C_{ipso})_2$ plane due to steric interactions. The C–C_{ipso} distances (1.48 – 1.49 Å) are intermediate between single and double C–C bonds suggesting partial delocalisation of electron density from C(1) into the phenyl ring π-system.

A comparison between compound **41** and **4.6** shows that **41** has a shorter Ti(1)-N(1) distance of 1.751(2) Å compared to **4.6** (1.829(11) Å) but the N(1)-N(2) bond length in **41** (1.329(2) Å) is longer than that for **4.6** (1.262(15) Å). This suggests that the alkylidene hydrazide fragment in **4.6** is less reduced compared to that in **41**, and that the alkylidene hydrazide ligand in **41** acts as a formal four-electron donor as represented in **B**. In addition, the N(1)-N(2)-C(1) bond angle value of 120.22(16) ° in **41** is smaller than 126.0(9) ° in **4.6**. This is consistent with the report by Dartiguenave *et al*. which states that shortening of the N_α–N_β bond is correlated to the increase in the N(1)-N(2)-C(1) bond angle.[8]

4.3 DFT analysis

DFT calculations have been carried out to compare the computed electronic structures of the Ti=NR, Ti=NNR_2 and Ti=$NNCR_2$ linkages for the model systems **1Q_Me** through **1Q_NCPh$_2$**. The four model systems as shown in Figure 4.4 all have a formal Ti=N_α triple bond with two principal $d_\pi - p_\pi$ molecular orbitals contributing to the three highest MOs of the complexes. The MO which lies in the molecular mirror plane is denoted as π_v and the other which lies perpendicular to it is denoted as π_h. The π_v and π_h MOs for the four models along with their energies are depicted in Figure 4.4. The π_v MOs for **1Q_Me**, **1Q_Ph** and **1Q_NMe$_2$** were discussed in Section 2.3.

The DFT trend in Ti=N_α distances (Ti=$NNCPh_2$ > Ti=$NNMe_2$) for the models **1Q_NCPh$_2$** (1.728 Å) and **1Q_NMe$_2$** (1.705 Å) is consistent with that observed experimentally (1.7508(16) Å and 1.723(2) Å respectively), although the computed distances are systematically shorter due to the reduced bulk of the models. The trend in N_α–N_β distances (N_α–$N_\beta CPh_2$ < N_α–$N_\beta Me_2$) are likewise consistent, with calculated distances of 1.308 Å (**1Q_NCPh$_2$**) and 1.360 Å (**1Q_NMe$_2$**) versus 1.329(2) Å (Ti=$NNCPh_2$) and 1.386(2) Å (Ti=$NNMe_2$) observed experimentally.

In comparison to CpTi{$MeC(NMe)_2$}(NMe) (**1Q_Me**), the π_v orbital energy of **1Q_Ph** with a phenyl substituent is destabilised by +0.49 eV due to a π* antibonding interaction with one of the occupied ring MOs. This value is within the ranges previously obtained through DFT and/or photoelectron spectroscopy.[33, 34] As expected,[34-38] introduction of $NNMe_2$ in **1Q_NMe$_2$** resulted in an even larger destabilisation (+1.17 eV) due to the presence of the N_β atom lone pair. The π_v orbital energy of **1Q_NCPh$_2$** (-4.9 eV) is destabilised by +0.57 eV compared to **1Q_Me**. This destabilisation is comparable to that of **1Q_Ph** (-4.98 eV) but not as destabilised as **1Q_NMe$_2$** (-4.30 eV). The destabilisation in **1Q_NCPh$_2$** arises due to the presence of N_β atom lone pair, somewhat analogous to **1Q_NMe$_2$** but less substantial in the former case. In both cases, the systems are stabilised through N_β pyramidalisation.

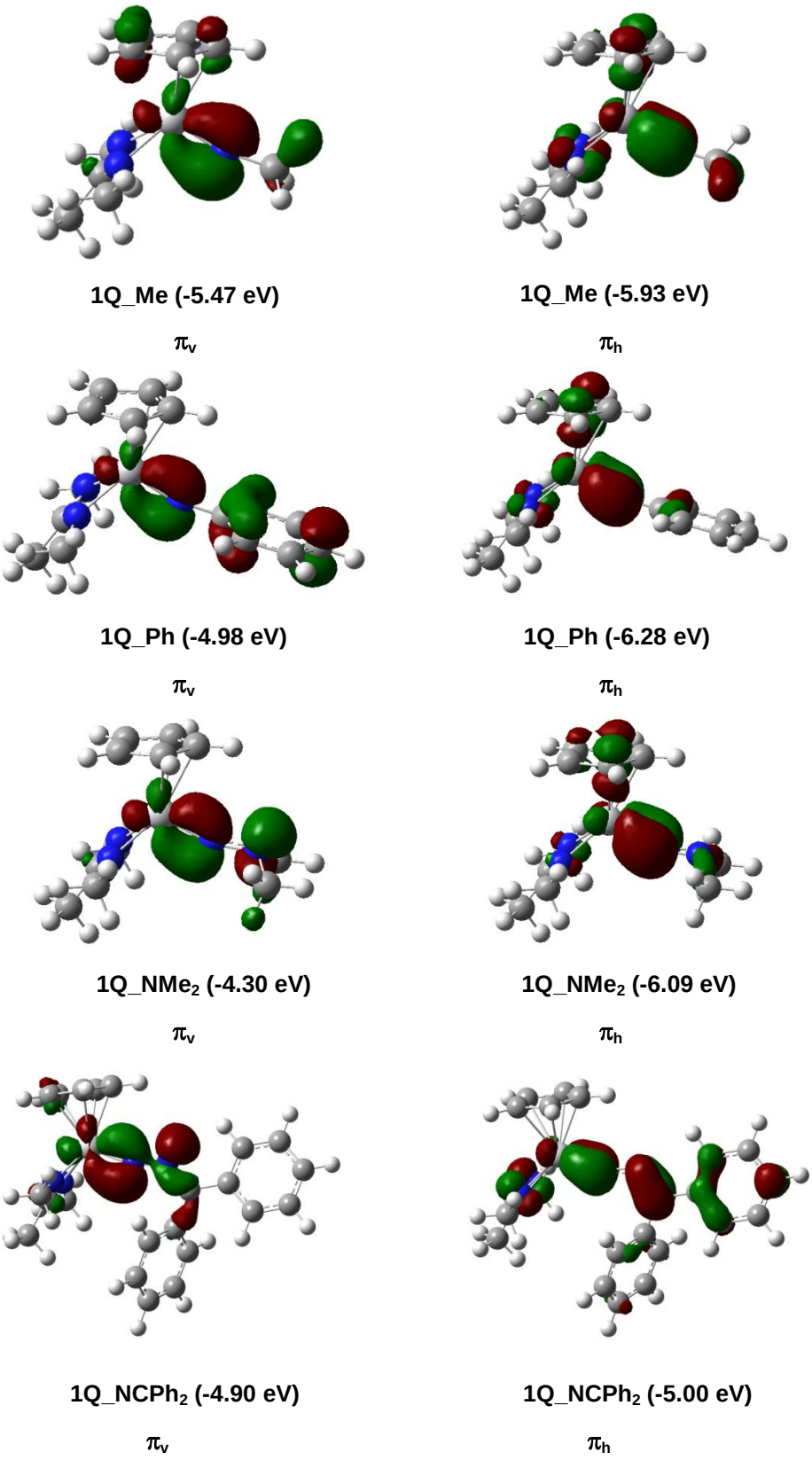

Figure 4.4. Isosurfaces and energies of the π_v and π_h MOs of CpTi{MeC(NMe)$_2$}(NR) (R = Me (**1Q_Me**), Ph (**1Q_Ph**), NMe$_2$ (**1Q_NMe$_2$**) or NCPh$_2$ (**1Q_NCPh$_2$**).

Interestingly, the π_h orbital energy of **1Q_NCPh$_2$** is comparable to its π_v value in contrast to **1Q_Me**, **1Q_Ph** and **1Q_NMe$_2$**. There is no systematic difference between the π_h values of **1Q_Me**, **1Q_Ph** and **1Q_NMe$_2$**. However, the π_h of **1Q_NCPh$_2$** is destabilised by +0.93 eV compared to **1Q_Me**. The destabilisation is due to the antibonding interaction between the π_h-type Ti=N$_\alpha$ bonding orbital and the N$_\beta$=CPh$_2$ π-bonding orbital. This type of interaction is absent in **1Q_Me** – **1Q_NMe$_2$**. Thus both the π_v and π_h MOs of **1Q_NCPh$_2$** (and the real compound **41**) are destabilised by additional antibonding interaction with orbitals of the –NCPh$_2$ substituent.

4.4 Reaction of Cp*Ti{MeC(N^{i}Pr)$_2$}(NNCPh$_2$) (41) with CO$_2$

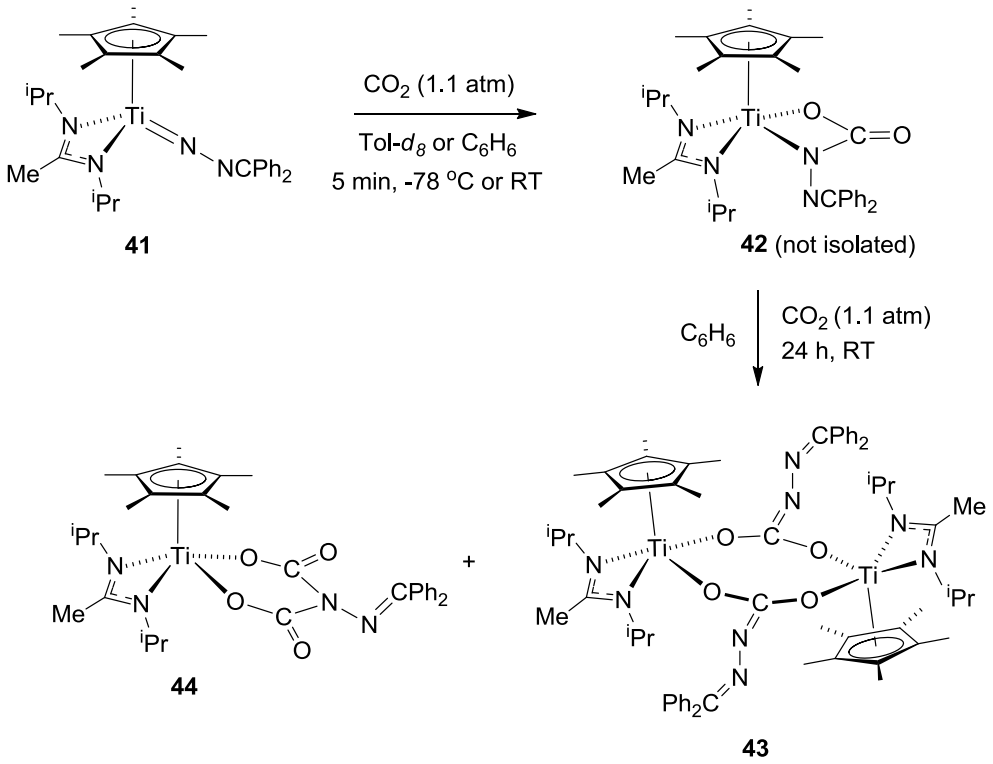

Scheme 4.1. Reaction of Cp*Ti{MeC(N^{i}Pr)$_2$}(NNCPh$_2$) (**41**) with CO$_2$.

The reaction of **41** with CO$_2$ is summarised in Scheme 4.1. When followed by ^{1}H NMR in toluene-d_8 in a low temperature experiment (-78 ℃), the reaction of **41** with CO$_2$ (excess, 1.1 atm pressure) immediately formed the [2+2] cycloaddition intermediate Cp*Ti{MeC(N^{i}Pr)$_2$}{N(NCPh$_2$)C(O)O} (**42**). When approaching room temperature (0 – 20 ℃), a second set of resonances were observed, while at room temperature a third set of broad resonances slowly appeared. After 24 hours, an orange precipitate was observed in the reaction mixture and the ^{1}H NMR spectrum showed a mixture of two products. On the preparative scale, the precipitate (**43**) was

separated from the solution and its ^{1}H NMR spectrum (Figure 4.5) suggested an unsymmetrical structure with two apparent septets for the inequivalent *iso*-propyl methine hydrogens, and four doublets for the two pairs of diastereotopic methyl groups of the amidinate ligand. Diffraction-quality crystals were grown from a saturated diethyl ether solution at 4 ℃. The crystal structure (*vide infra*) obtained shows the product as a dimer [Cp*Ti{MeC(N^{i}Pr)$_2$}{μ-OC(NNCPh$_2$)O}]$_2$ (**43**). Although the bridging Ph$_2$CNNCO$_2$ ligand in **43** is related to a μ-carbonate, this is the first authenticated example of this structural type in transition metal chemistry.

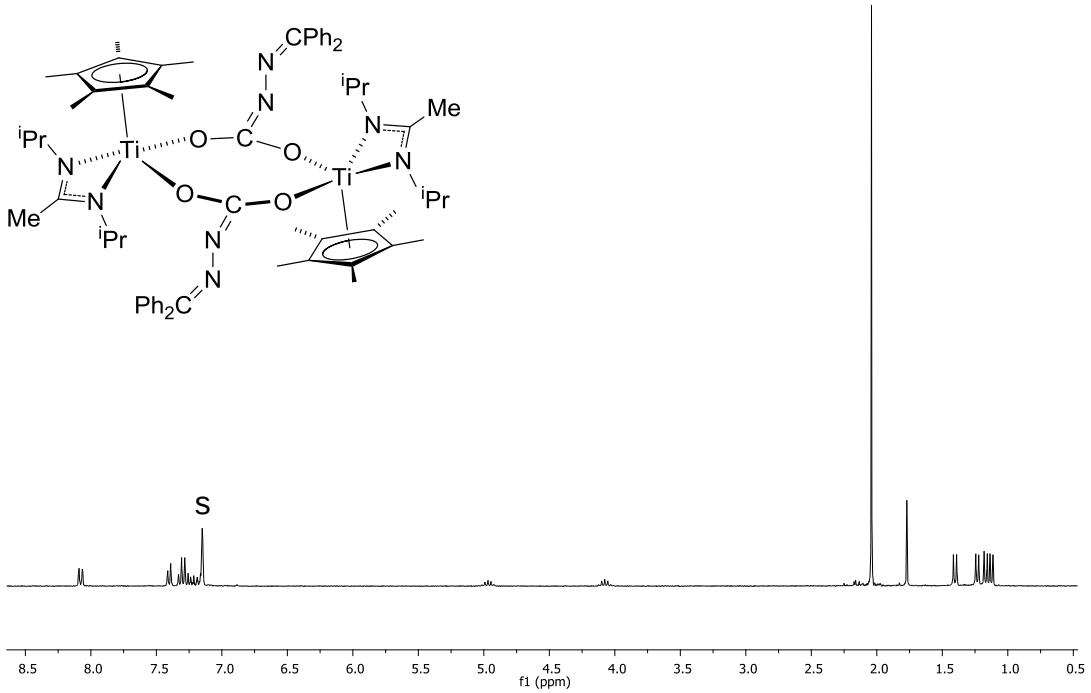

Figure 4.5. ^{1}H NMR spectrum (299.9 MHz) of [Cp*Ti{MeC(N^{i}Pr)$_2$}{μ-OC(NNCPh$_2$)O}]$_2$ (**43**) in C$_6$D$_6$ ("s" denotes residual protio-solvent).

The propensity of the proposed intermediate (**42**) to dimerise into **43** precludes its isolation on preparative scale. Therefore **42** was characterised *in situ* using ^{1}H and ^{13}C{^{1}H} NMR spectroscopy at 248 K. The assignment of **42** as a [2+2] cycloaddition product is supported by the ^{1}H and ^{13}C{^{1}H} NMR data and by analogy to its imido and hydrazido analogues. While **43** can be separated with high purity from the reaction mixture through filtration, its partial solubility in benzene resulted in the low isolated yield of 29%. As the remaining solution of the reaction was still contaminated with **43**, the other fluxional product Cp*Ti{MeC(N^{i}Pr)$_2$}{OC(O)N(NCPh$_2$)C(O)O} (**44**) was obtained through crystallisation of a saturated benzene solution of the

mixture at 4 ℃, which resulted in the very low overall yield of 13%. The solid state structure obtained shows the fluxional species to be the double insertion product Cp*Ti{MeC(N^{i}Pr)$_2$}{OC(O)N(NCPh$_2$)C(O)O} (**44**). When the reaction between **41** and CO_2 is followed by ^{1}H NMR all of **41** is converted, with **43** and **44** formed in 76% and 24% yield, respectively.

Upon cooling to -10 ℃, the broad signals of **44** in the ^{1}H NMR spectrum resolved into two sets of very similar resonances suggesting the presence of two isomers with *ca*. 1:1 ratio. It is proposed that one of the isomers has the N_β pointing "downwards", away from the Cp* ring while the other has the N_β pointing "upwards", towards the Cp* ring (as illustrated in Scheme 4.1). The elemental analysis data are consistent with the molecular formula expected for **44**. Dissolving the crystals of **44** in C_6D_6 instantly restores the fluxionality according to ^{1}H NMR spectroscopy, suggesting that the isomers interconvert in solution *via* rotation about the N_α–N_β bond.

The IR spectrum of **44** shows two strong bands at 1701 and 1656 cm^{-1}, consistent with incorporation of a second CO_2 molecule. The ^{13}C{^{1}H} NMR spectrum shows that each isomer of **44** only has one C=O resonance (δ 154.5 and 154.7 ppm respectively) which suggests that these bands are attributed to the symmetric and antisymmetric ν(C=O) modes of the dicarboxylate OC(O)N(NCPh$_2$)C(O)O ligand. The corresponding absorptions for the hydrazido-derived compounds **3** and **4** (Scheme 2.1) appear at 1715 & 1676 and 1702 & 1655 cm^{-1}, respectively.

It is suggested that the first-formed cycloaddition intermediate **42** is thermally unstable and reactive. When approaching room temperature, it dimerises to give **43** or another CO_2 molecule is inserted into the Ti–N_α bond to form **44**. A possible reason for the formation of dimer **43** could be due to extra conjugation allowed by the rearrangements. Once formed, **43** and **44** are very stable and will not undergo further reaction. Pure **43** does not react with CO_2, so **44** comes from non-rearranged **42** as expected.

The molecular structure of **43** is shown in Figure 4.6 and selected distances and angles are listed in Table 4.2. Full crystallographic data are given in the CD Appendix. The solid state structure of **43** confirms the dimeric nature of [Cp*Ti{MeC(N^{i}Pr)$_2$}-{μ-OC(NNCPh$_2$)O}]$_2$ (**43**) and the *anti* conformation shown in Scheme 4.1. The dimeric species **43** comprises two Cp*Ti{MeC(N^{i}Pr)$_2$}{μ-OC(NNCPh$_2$)O} fragments

linked *via* bridging CO_2 to form the eight-membered chelate ring with the ligands κ^2-coordinated. The Ti–N_α bond has been cleaved in this case.

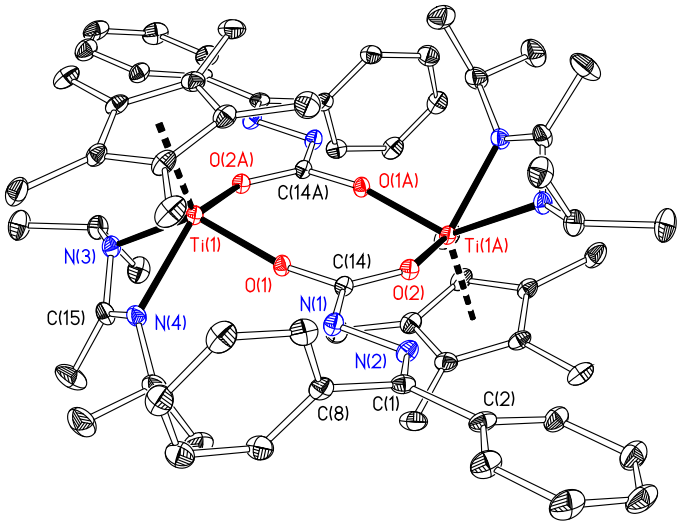

Figure 4.6. Displacement ellipsoid plot (20% probability) of [Cp*Ti{MeC(N^{i}Pr)$_2$}{μ-OC(NNCPh$_2$)O}]$_2$ (**43**). H atoms omitted for clarity. Atoms carrying the suffix 'A' are related to their couterparts by the symmetry operator 1-*x*, 1-*y*, 1-*z*.

The molecule possesses crystallographic inversion symmetry and the geometry about each titanium atom is a four-legged piano stool. The Cp* rings and the amidinate ligands lie on opposite sides of the molecule with an *anti* conformation with respect to Ti(1)···Ti(1A) and are related by an inversion centre. This symmetric nature of the molecule is consistent with the NMR data. The N(1)-N(2) distance of 1.396(4) Å is significantly elongated from that of **41** (1.329(2) Å) showing a decrease in its multiple bond character. However, it still lies in the region between N=N double (*ca*. 1.22 – 1.26 Å) and N–N single (*ca*. 1.40 – 1.45 Å) bonds.[39, 40] The lengthening of the N(1)-N(2) bond in **43** as compared to **41** can be explained as a consequence of the change in N_α hybridisation from *sp* to *sp*^{2}. This can also be observed in the C(14)-N(1)-N(2) bond angle of 111.4(3)° in **43** which is significantly bent compared to the Ti(1)-N(1)-N(2) bond angle of 156.56(14)° in **41**. The bonding of the μ-OC(NNCPh$_2$)O moieties is not quite symmetrical. For example Ti(1)-O(1) (1.876(2) Å) and O(1)-C(14) (1.318(4) Å) are slightly shorter and longer, respectively, than Ti(1)-O(2A) (1.932(2) Å) and O(2)-C(14) (1.294(4) Å). The Ti(1)-O(1)-C(14) angle of 162.1(2)° is somewhat more linear than Ti(1)-O(2A)-C(14A) (140.2(2)°). The Ti–O distances are

nonetheless consistent with single bonds and comparable to those in **44** (see below, 1.9264(11) and 1.9252(12) Å).

Table 4.2. Selected bond lengths (Å) and angles (°) for [Cp*Ti{MeC(N^{i}Pr)$_2$}{μ-OC(NNCPh$_2$)O}]$_2$ (**43**). Cp$_{cent}$ refers to the Cp* ring carbon centroid.

Ti(1)-Cp$_{cent}$	2.049	Ti(1)-N(3)	2.121(3)
Ti(1)-N(4)	2.085(3)	Ti(1)-O(1)	1.876(2)
Ti(1)-O(2A)	1.932(2)	O(1)-C(14)	1.318(4)
O(2)-C(14)	1.294(4)	C(14)-N(1)	1.316(4)
N(1)-N(2)	1.396(4)	N(2)-C(1)	1.304(4)
Cp$_{cent}$-Ti(1)-N(3)	113.8	Cp$_{cent}$-Ti(1)-N(4)	110.7
Cp$_{cent}$-Ti(1)-O(1)	111.9	Cp$_{cent}$-Ti(1)-O(2A)	114.9
O(1)-Ti(1)-O(2A)	93.33(9)	Ti(1)-O(1)-C(14)	162.1(2)
Ti(1)-O(2A)-C(14A)	140.2(2)	O(1)-C(14)-O(2)	117.9(3)
O(1)-C(14)-N(1)	116.8(3)	O(2)-C(14)-N(1)	125.3(3)
C(14)-N(1)-N(2)	111.4(3)	N(1)-N(2)-C(1)	113.5(3)

Diffraction-quality crystals of **44** were obtained from a saturated benzene solution at 4 ℃. The molecular structure of **44** is shown in Figure 4.7 and selected distances and angles are listed in Table 4.3. Full crystallographic data are given in the CD Appendix.

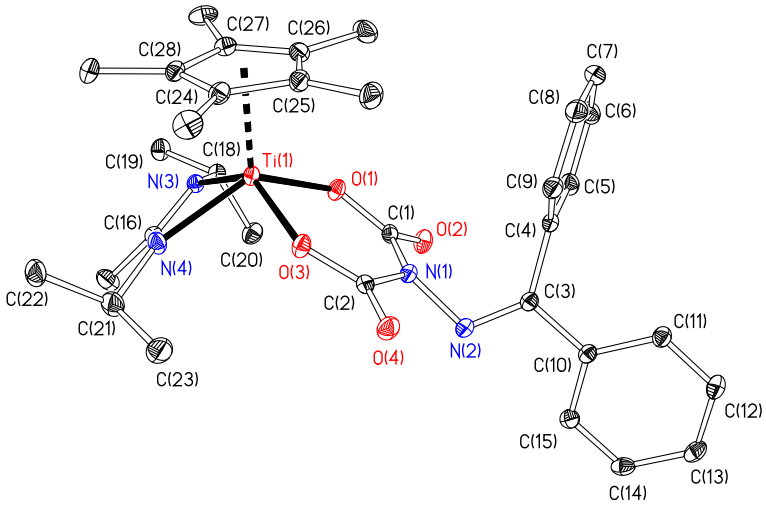

Figure 4.7. Displacement ellipsoid plot (25% probability) of Cp*Ti{MeC(N^{i}Pr)$_2$}{OC(O)N(NCPh$_2$)C(O)O} (**44**). H atoms omitted for clarity.

Table 4.3. Selected bond lengths (Å) and angles (°) for $Cp^*Ti\{MeC(N^iPr)_2\}\{OC(O)N(NCPh_2)C(O)O\}$ (**44**). Cp_{cent} refers to the Cp* ring carbon centroid.

Ti(1)-Cp_{cent}	2.049	Ti(1)-N(3)	2.0830(14)
Ti(1)-N(4)	2.0825(15)	Ti(1)-O(1)	1.9264(11)
Ti(1)-O(3)	1.9252(12)	O(1)-C(1)	1.303(2)
C(1)-N(1)	1.414(2)	O(3)-C(2)	1.299(2)
C(2)-N(1)	1.414(2)	C(1)-O(2)	1.211(2)
C(2)-O(4)	1.212(2)	N(1)-N(2)	1.4364(19)
N(2)-C(3)	1.279(2)		
Cp_{cent}-Ti(1)-N(3)	111.3	Cp_{cent}-Ti(1)-N(4)	118.7
Cp_{cent}-Ti(1)-O(1)	112.8	Cp_{cent}-Ti(1)-O(3)	111.9
O(1)-Ti(1)-O(3)	83.43(5)	Ti(1)-O(1)-C(1)	136.52(11)
Ti(1)-O(3)-C(2)	137.95(11)	O(1)-C(1)-N(1)	115.85(14)
O(3)-C(2)-N(1)	116.07(14)	C(1)-N(1)-C(2)	127.87(13)
N(1)-N(2)-C(3)	114.18(14)		

The crystal structure of **44** confirms the insertion of two molecules of CO_2 into the $Ti{=}N_\alpha$ bonds (formally triple)[23] of **41**. This type of transformation is without precedent in metal alkylidene hydrazide chemistry. In fact, the cycloaddition intermediate **42** and dimer **43** are also the first of their type being reported. The solid state structure of **44** confirms the four-legged piano stool geometry around the titanium centre. Two molecule of CO_2 are inserted into the $Ti{=}N_\alpha$ bond forming a six membered chelating ring.

The distances and angles within the new dicarboxylate ligands are comparable to those for **3** and **4**. The atoms of the {TiOC(O)N(N)C(O)O} moieties are approximately coplanar, with the maximum displacement from the least-squares plane of 0.08 Å. The N(1)-N(2) bond length of **44** (1.4364(19) Å) is significantly elongated from **41** (1.329(2) Å). This long distance can be best described as a single bond. There is no significant difference between N(2)-C(1) distances of **41** and **44**.

4.5 Reaction of Cp*Ti{MeC(N^{i}Pr)$_2$}(NNCPh$_2$) (41) with CS$_2$

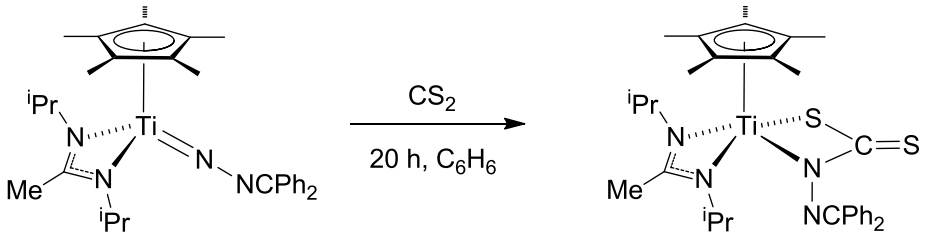

41 **45**

Equation 4.2

Reaction of **41** with 2 equivalents of CS_2 for 20 hours at room temperature afforded Cp*Ti{MeC(N^{i}Pr)$_2$}{N(NCPh$_2$)C(S)S} (**45**) as a dark brown solid. Compound **45** was obtained in a reasonable yield of 60%. All attempts to grow diffraction-quality crystals have been fruitless. However, spectroscopic data and the result obtained in a molecular weight determination experiment using the Signer Method (see below) are consistent with the C_1 symmetric [2+2] cycloaddition product illustrated in Equation 4.2. Compound **45** is the analogue of the unstable **42**.

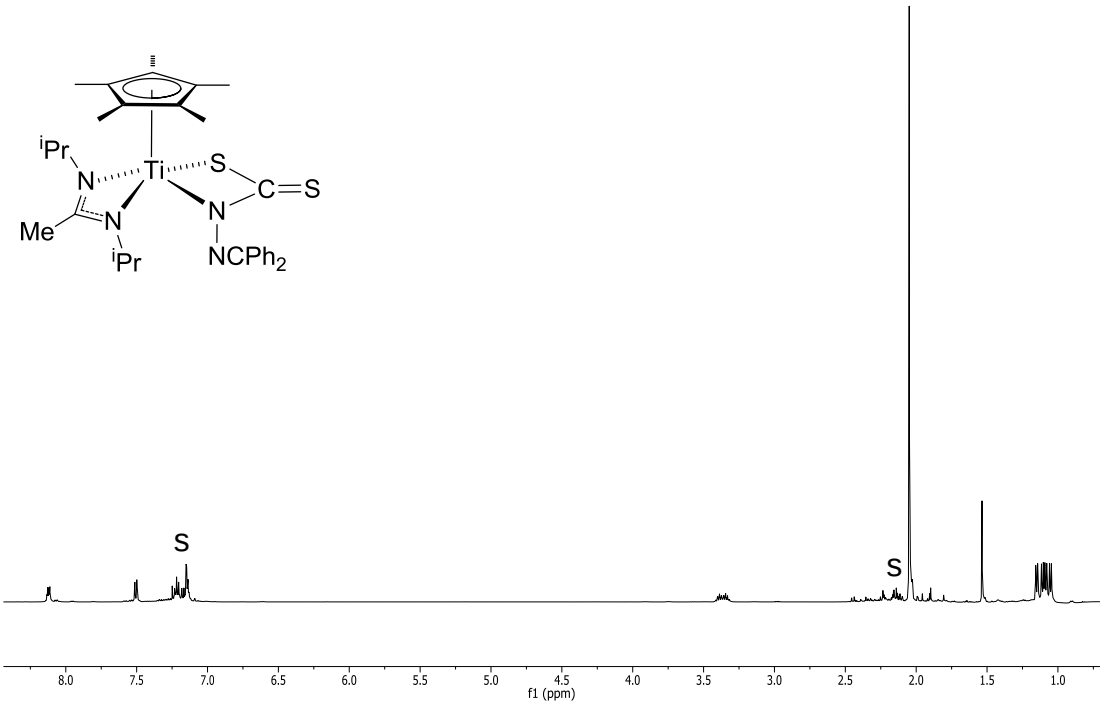

Figure 4.8. ^{1}H NMR spectrum (499.9 MHz) of Cp*Ti{MeC(N^{i}Pr)$_2$}{N(NCPh$_2$)C(S)S} (**45**) in toluene-d_8 at -20 ℃ ("s" denotes residual protio-solvent which overlaps with certain Ph resonances).

The ^{1}H NMR spectrum of **45** at room temperature shows very broad signals corresponding to the *iso*-propyl groups of the amidinate ligand, suggesting involvement of a fluxional process. This process involves net rotation about the {TiN(NCPh$_2$)C(S)S} vector as discussed previously.[26] At 253 K this process is frozen out and the ^{1}H NMR spectrum (toluene-d_8) shows two apparent septets for the inequivalent *iso*-propyl methine hydrogens and four doublets for the two pairs of diastereotopic methyl groups (Figure 4.8). Analogous to its diphenyl hydrazide counterparts, further reaction time did not lead to the "double-insertion" product. As previously mentioned in Section 2.4.3, DFT calculations for its hydrazide analogues predicted that the structure of the "double-insertion" product is puckered, preventing electron donation from the sulfur lone pair to the metal, causing the overall molecule to be destabilised.

As the reaction of **41** with CO_2 led to formation of dimer **43** following initial formation of the cycloaddition product **42**, along with the double insertion product **44**, there is a possibility that the reaction product with CS_2 is actually a dimer analogous to **43**. A solution molecular weight determination experiment was thus carried out in benzene using a Signer apparatus with Cp*$_2$Fe as the standard. The result obtained (536 gmol^{-1}) is consistent with the molecular weight calculated for **45** (594.7 gmol^{-1}) confirming that the [2+2] cycloaddition product in this instance is more stable and not susceptible to dimerisation. Compound **45** is stable in solution for days, and similar observations were made for the hydrazide derivatives **5** and **6**. This contrasts with the corresponding cycloaddition product formed from the imido analogues Cp*Ti{MeC(N^{i}Pr)$_2$}(NAr) (**4.5**, Ar = Tol or 2,6-C$_6$H$_3$Me$_2$) which tend to eliminate ^{t}BuNCS forming [Cp*Ti{MeC(N^{i}Pr)$_2$}(μ-S)]$_2$ (**4.8**).[27] No reaction was observed when **45** was exposed to an atmosphere of CO_2 at *ca*. 1.1 atm pressure at room temperature, and heating the reaction mixture at 60 ℃ resulted in a complicated mixture of unknown products.

4.6 Reactions of Cp*Ti{MeC(N^{i}Pr)$_2$}(NNCPh$_2$) (41) with isocyanates and isothiocyanates

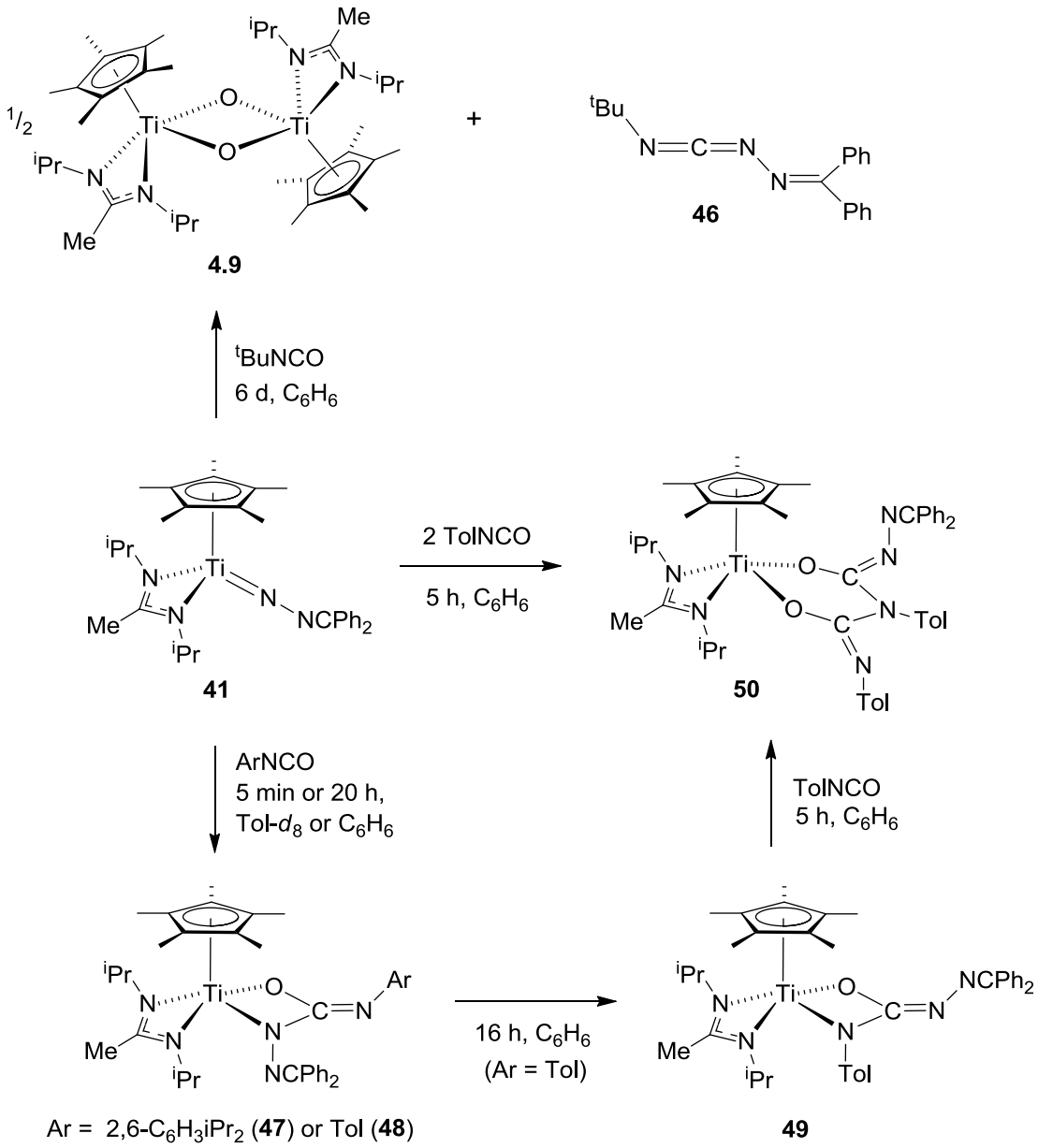

Scheme 4.2. Reactions of Cp*Ti{MeC(N^{i}Pr)$_2$}(NNCPh$_2$) (**41**) with isocyanates.

4.6.1 Reaction of Cp*Ti{MeC(N^{i}Pr)$_2$}(NNCPh$_2$) (41) with ^{t}BuNCO

The reactions of **41** with isocyanates are summarised in Scheme 4.2. Reaction with ^{t}BuNCO in benzene gave quantitative conversion to the μ-oxo compound **4.9** and ^{t}BuNCNNCPh$_2$ (**46**) which is analogous to the previously reported[41, 42] *N*-dimethylaminocarbodiimide ^{t}BuNCNNMe$_2$ (**14**). The reaction is very slow in this case though, taking up to 6 days to reach completion, whereas the reaction between

Cp*Ti{MeC(N^{i}Pr)$_2$}(NNMe$_2$) (**4.4**) and ^{t}BuNCO was complete after 16 hours. This could be due to the greater steric bulk of **41** compared to **4.4**. The instability of the presumed cycloaddition intermediate Cp*Ti{MeC(N^{i}Pr)$_2$}{N(NCPh$_2$)C(N^{t}Bu)O} to extrusion is reminiscent of the corresponding reactions of Cp*Ti{MeC(N^{i}Pr)$_2$}(NR) (R = NMe$_2$ (**4.4**), ^{t}Bu (**4.1**) or Tol (**4.5**)) but contrasts strongly with that of Cp*Ti{MeC(N^{i}Pr)$_2$}{N(NPh$_2$)C(N^{t}Bu)O}(**12**) as mentioned in Section 2.5.

When conducted on the NMR tube scale in C_6D_6 the conversion of **41** to the products was near-quantitative. On the preparative scale however, the white solid **46** could only be isolated in analytically pure form by high vacuum (85-90 ℃, 5 x 10^{-6} mbar) tube sublimation. Prolong heating during sublimation led to contamination by some decomposition product and thus pure **46** can only be obtained at a very low overall yield of 22%. Data obtained by NMR and high resolution mass spectroscopy are consistent with the proposed structure of **46** as shown in Scheme 4.2. The ^{1}H NMR spectrum shows a singlet at 1.07 ppm corresponding to the *tert*-butyl group and resonances corresponding to two different phenyl rings in the range between 7.05 – 7.78 ppm.

4.6.2 Reaction of Cp*Ti{MeC(N^{i}Pr)$_2$}(NNCPh$_2$) (41) with Ar′NCO (Ar′ = 2,6-C$_6$H$_3$^{i}Pr$_2$)

Reaction of **41** with Ar′NCO at room temperature in benzene gave the C_1 symmetric cycloaddition product Cp*Ti{MeC(N^{i}Pr)$_2$}{N(NCPh$_2$)C(NAr')O} (**47**) as a dark brown solid with 72% isolated yield. The NMR data for **47** are consistent with the proposed structure shown in Scheme 4.2. In the reaction, **47** appeared to be the sole product. No signals for the other isomer of **47** (e.g. with a κ^2*N,N′*-N(NCPh$_2$)C(O)NAr moiety) were observed in the NMR tube scale experiment or crude reaction product. All attempts to grow diffraction-quality crystals were in vain.

Although it has not been crystallographically authenticated, it is proposed to have κ^2*N,O* coordination mode analogous to Cp*Ti{MeC(N^{i}Pr)$_2$}{N(NPh$_2$)C(NAr′)O} (**9**), as for its hydrazido and arylimido analogues. This is supported by the ROESY 2-D NMR measurements and also by the very similar ν(C=N) bands for **47** and **9** which were observed at 1618 and 1622 cm^{-1}, respectively. These values are also comparable to those for the imido-derived products Cp*Ti{MeC(N^{i}Pr)$_2$}{N(Ar^1)C(NAr^2)O} (Ar^1 or Ar^2 = Tol or 2,6-C$_6$H$_3$Me$_2$, ν(C=N) = 1609 – 1615 cm^{-1}) which possess κ^2*N,O*

bound $N(Ar^1)C(NAr^2)O$ groups.[27] In addition, the IR spectrum of $Ti(Me_4taa)\{N(NPh_2)C(O)NTol\}$ which possesses a κ^2*N,N'*-$N(NPh_2)C(O)NTol$ ligand features a ν(C=O) band at 1656 cm^{-1}.[22] In lanthanide chemistry, it has been reported that reactions between lanthanide hydrazonido(1-) complexes with PhNCO form cycloaddition products with κ^2*N,O* coordination mode and 1,3-H migration.[11]

4.6.3 Reaction of Cp*Ti{MeC(N^{i}Pr)$_2$}(NNCPh$_2$) (41) with TolNCO

The reactions of **41** with TolNCO are also summarised in Scheme 4.2. Reaction of **41** with one equivalent of TolNCO at room temperature gave a mixture of three different products. When the reaction was followed by ^{1}H NMR in toluene-d_8 in a variable temperature experiment, the first-formed intermediate postulated to be the [2+2] cycloaddition product Cp*Ti{MeC(N^{i}Pr)$_2$}{N(NCPh$_2$)C(NTol)O} (**48**) was immediately observed at -60 ℃. When approaching room temperature, two other products grew in which are proposed to be the rearranged cycloaddition product Cp*Ti{MeC(N^{i}Pr)$_2$}{N(Tol)C(NNCPh$_2$)O} (**49**) and a small amount of the "double insertion" product Cp*Ti{MeC(N^{i}Pr)$_2$}{OC(NNCPh$_2$)N(Tol)C(NTol)O} (**50**) formed due to the presence of a small excess of TolNCO. As **48** is unstable towards rearrangement to **49**, it was characterised *in situ* using NMR spectroscopy at 253 K. The NMR data obtained is consistent with the proposed C_1 symmetric cycloaddition intermediate **48** as shown in Scheme 4.2. The ^{1}H NMR spectrum of **48** shows a singlet corresponding to the *p*-tolyl group, as well as two overlapping apparent septets and four doublets corresponding to the *iso*-propyl groups on the amidinate ligand. This is consistent with its hydrazide analogue **7**.

In order to suppress the competing reaction of **49** with TolNCO to form **50**, the scale up reaction with **41** was carried out at -78 ℃ and all the volatiles were removed after 30 minutes. As the ^{1}H NMR spectrum of the crude showed a mixture of **48** and **49**, this was then redissolved in benzene and left stirring for 16 hours at room temperature. Upon removal of volatiles, **49** was obtained as a brown solid with 93% yield. Unfortunately, all attempts to grow diffraction-quality crystals have been unsuccessful. Nevertheless, the NMR data obtained which include ROESY 2-D NMR are consistent with the proposed C_1 symmetric cycloaddition product **49** as shown in Scheme 4.2. This is also consistent with the intermediate proposed by DFT calculations computed for its dimethyl hydrazide analogue **4.4** (Figure 2.18). In addition, the IR spectrum

shows a ν(C=N) band at 1592 cm^{-1} which is similar to those observed for Cp*Ti{MeC(N^{i}Pr)$_2$}{N(NPh$_2$)C(NTol)O} (**7**, ν(C=N) = 1619 cm^{-1}) and the imido-derived products Cp*Ti{MeC(N^{i}Pr)$_2$}{N(Ar^1)C(NAr^2)O} (Ar^1 or Ar^2 = Tol or Xyl, ν(C=N) = 1609 – 1615 cm^{-1}).[27]

When another equivalent of TolNCO was added to **49**, this inserted into the Ti–N bond to give the "double insertion" product Cp*Ti{MeC(N^{i}Pr)$_2$}{OC(NNCPh$_2$)N-(Tol)C(NTol)O} (**50**). This is analogous to its dimethyl hydrazide counterpart Cp*Ti{MeC(N^{i}Pr)$_2$}{OC(NNMe$_2$)N(Tol)C(NTol)O} (**16**). Compound **50** can also be formed directly with two equivalents of TolNCO. Reaction of **41** with 2 equivalents of TolNCO formed **50** cleanly (Scheme 4.2) as a brown solid in 72% yield after 5 hours. Diffraction-quality crystals of **50** were grown from a saturated benzene solution at 4 ℃. Compound **50** has been crystallographically characterised and the molecular structure is shown in Figure 4.9. Full crystallographic data are given in the CD Appendix. Selected distances and angles are listed in Table 4.4.

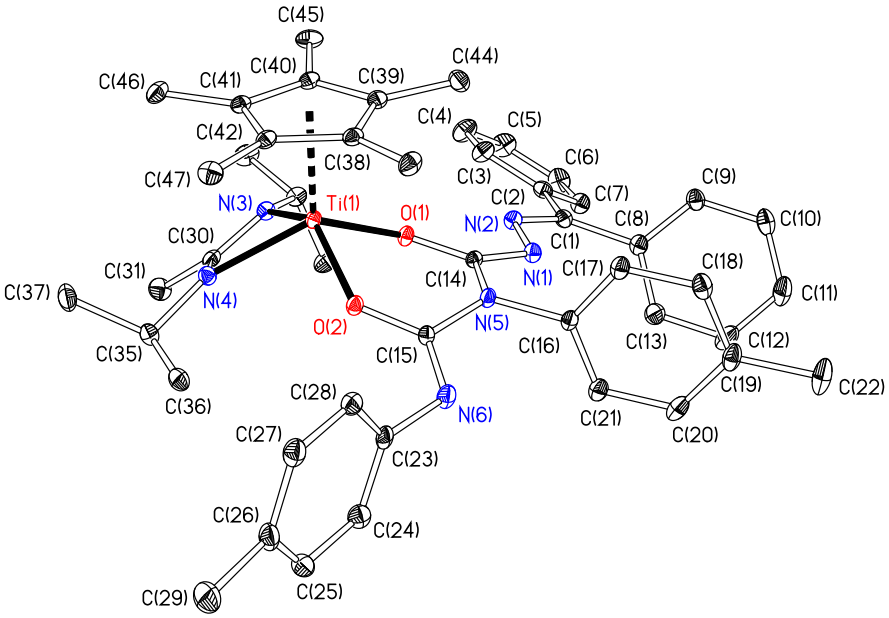

Figure 4.9. Displacement ellipsoid plot (20% probability) of Cp*Ti{MeC(N^{i}Pr)$_2$}-{OC(NNCPh$_2$)N(Tol)C(NTol)O} (**50**). H atoms omitted for clarity.

The selected distances and angles are within expected ranges. The solid state structure of **50** confirms the four-legged piano stool geometries around titanium. A second molecule of TolNCO has inserted into the Ti–N bond of **49**, expanding the four

membered metallacycle to the six membered chelating ring. The atoms in the six membered metallacycle ring are approximately coplanar with the maximum displacement from the least-squares plane of 0.19 Å. The N(1)-N(2) bond length of 1.397(3) Å is significantly longer than that in **41** (1.329(2) Å). This shows a decrease in the multiple bond character between N_α–N_β bond in **50**. However, it is still intermediate between N–N single (*ca*. 1.40 – 1.45 Å) and N=N double (*ca*. 1.22 – 1.26 Å) bonds.[39, 40] This lengthening of the N(1)-N(2) bond can be explained as a consequence of the change in N_α hybridisation from *sp* to sp^2 which can also be observed in the difference in bond angles. While **50** has C(14)-N(1)-N(2) bond angle of 111.5(2)° which is similar to that found in **43** (111.4(3)°), they are significantly bent compared to the Ti(1)-N(1)-N(2) bond angle of 156.56(14)° in **41**. In addition, it is also very similar to the N(1)-N(2)-C(1) bond angle (114.6(2)°) suggesting the same hybridisation for both N(1) and N(2).

Table 4.4. Selected bond lengths (Å) and angles (°) for Cp*Ti{MeC(N^iPr)$_2$}{OC(NNCPh$_2$)N(Tol)C(NTol)O} (**50**). Cp_{cent} refers to the Cp* ring carbon centroid.

Ti(1)-Cp_{cent}	2.051	Ti(1)-N(3)	2.084(2)
Ti(1)-N(4)	2.090(2)	Ti(1)-O(1)	1.9296(19)
Ti(1)-O(2)	1.9234(19)	O(1)-C(14)	1.299(3)
C(14)-N(1)	1.303(4)	C(14)-N(5)	1.406(4)
O(2)-C(15)	1.304(3)	C(15)-N(5)	1.421(4)
C(15)-N(6)	1.274(4)	N(1)-N(2)	1.397(3)
N(2)-C(1)	1.294(4)		
Cp_{cent}-Ti(1)-O(1)	113.8	Cp_{cent}-Ti(1)-N(3)	110.8
Cp_{cent}-Ti(1)-N(4)	116.4	Cp_{cent}-Ti(1)-O(2)	112.7
O(1)-Ti(1)-O(2)	82.98(8)	Ti(1)-O(1)-C(14)	132.86(18)
Ti(1)-O(2)-C(15)	134.45(18)	O(1)-C(14)-N(5)	118.0(2)
O(2)-C(15)-N(5)	116.9(2)	C(14)-N(5)-C(15)	123.3(2)
C(14)-N(1)-N(2)	111.5(2)	N(1)-N(2)-C(1)	114.6(2)

Despite the different substituents at C(14) and C(15) the Ti(1)-O(1) and Ti(1)-O(2) distances are equivalent within error, as are the O(1)-C(14) (1.299(3) Å) and O(2)-C(15) (1.304(3) Å) distances. In contrast, C(14)-N(1) is significantly longer than C(15)-N(6) by 0.029(6) Å while C(14)-N(5) is apparently shorter than C(15)-N(5) by 0.015(6) Å. While the latter is not significant within 3 standard deviations (0.018 Å), the combined data suggest a slightly greater delocalisation of the trigonal planar N(5) lone pair towards the more conjugated C=NNCPh$_2$ moiety.

The ^{1}H and ^{13}C{^{1}H} NMR spectra of **50** show two sets of *p*-tolyl group resonances, and the ^{1}H NMR spectrum shows a pair of apparent septets and two pairs of doublets corresponding to the inequivalent *iso*-propyl groups for the MeC(N^{i}Pr)$_2$ ligand, suggesting the formation of a C_1 symmetric product. The IR spectrum shows two ν(C=N) bands at 1623 and 1604 cm^{-1} which is similar to 1619 and 1599 cm^{-1} reported for Cp*Ti{MeC(N^{i}Pr)$_2$}{OC(NNMe$_2$)N(Tol)C(NTol)O} (**16**).

As seen for **16**, the product is not the C_s symmetric Cp*Ti{MeC(N^{i}Pr)$_2$}{OC(NTol)N(NNCPh$_2$)C(NTol)O} (**50_alt**) which would be expected based on the reported observation between Cp*Ti{MeC(N^{i}Pr)$_2$}(NTol) (**4.5**) and 2 equivalents of TolNCO[27] or Cp*Ti{MeC(N^{i}Pr)$_2$}(NNR$_2$) (R = Ph (**4.2**) or Me (**4.4**)) with an excess of CO$_2$.[25, 43] The presence of the exocyclic C=NTol and C=NNCPh$_2$ moiety suggests that at least one rearrangement must have taken place between the intermediate Cp*Ti{MeC(N^{i}Pr)$_2$}{N(NCPh$_2$)C(NTol)O} (**48**) (the analogue of **7**), and the final product **50**. This further supports the proposed structure for **49** which is the cycloaddition product with rearrangement. This also agrees well with the DFT proposed mechanism for the formation of **16** (Figure 2.18).

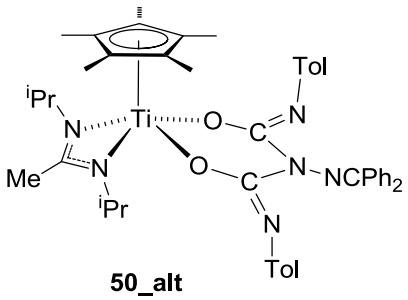

50_alt

It appears that the reaction outcomes between **41** and different isocyanates varies depending on the different steric bulk of the isocyanates. It is interesting that **41** has an intermediate behaviour between dimethyl hydrazide **4.4** and diphenyl hydrazide **4.2**. One of the reasons could be that the diphenyl rings on alkylidene hydrazide

ligand of **41** is quite distant from the active site (N_α–N_β), releasing steric pressure around the active site, hence the different behaviour observed.

4.6.4 Reactions of Cp*Ti{MeC(N^{i}Pr)$_2$}(NNCPh$_2$) (41) with isothiocyanates

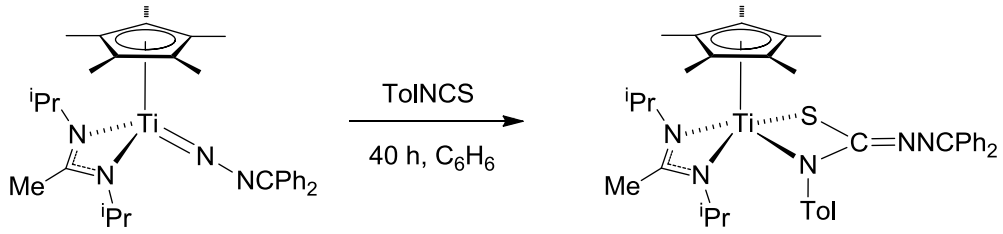

41 **51**

Equation 4.3

No reaction was observed between **41** and Ar′NCS (Ar′ = 2,6-$C_6H_3{}^iPr_2$) at room temperature, and heating to 60 ℃ formed a mixture of unidentified products. Reaction of **41** with TolNCS, however, reacted cleanly but slowly at room temperature in benzene over 40 hours to give the C_1 symmetric thioureate-type cycloaddition product Cp*Ti{MeC(N^{i}Pr)$_2$}{N(Tol)C(NNCPh$_2$)S} (**51**) as a dark brown solid in *ca*. 59% isolated yield (Equation 4.3). The ^{1}H NMR spectrum of **51** shows two apparent septets for the inequivalent *iso*-propyl methine hydrogens, and four doublets for the two pairs of diastereotopic methyl groups of MeC(N^{i}Pr)$_2$ consistent with the proposed C_1 symmetric structure (Figure 4.10). The corresponding NMR tube scale experiment for TolNCS was effectively quantitative. The low yield is attributed to the relatively high solubility of **51** in hydrocarbon solvents.

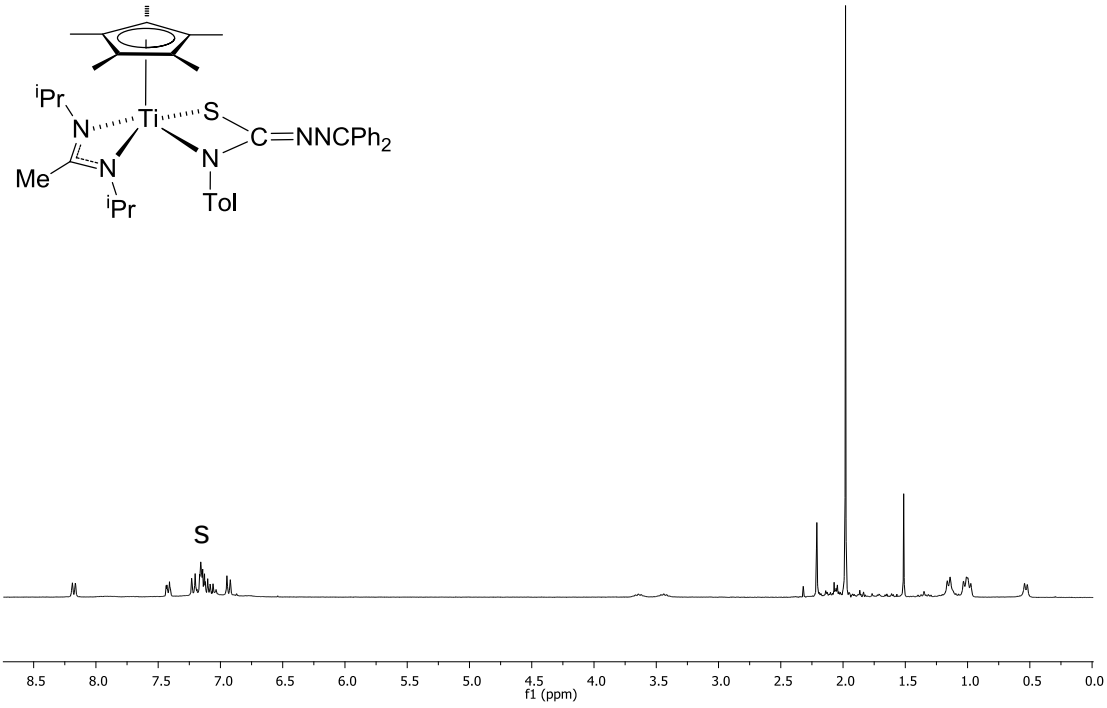

Figure 4.10. ^{1}H NMR spectrum (299.9 MHz) of Cp*Ti{MeC(N^{i}Pr)$_2$}-{N(Tol)C(NNCPh$_2$)S} (**51**) in C_6D_6 ("S" denotes residual protio-solvent which overlaps with certain Ph and Tol resonances).

Diffraction-quality crystals of **51** were grown from a saturated mixture of diethyl ether and pentane at 4 ℃. The molecular structure and selected distances and angles are shown in Figure 4.11 and Table 4.5. Full crystallographic data are given in the CD Appendix. The solid state structure for **51** confirms the four-legged piano stool geometry around titanium and the κ^2*N,S* coordination mode for the N(Tol)C(NNCPh$_2$)S ligand. However, the observed cycloaddition product is not the first-formed product Cp*Ti{MeC(N^{i}Pr)$_2$}{N(NCPh$_2$)C(NTol)S} (**51_int**) but has undergone some rearrangement and the Ti–N$_\alpha$ bond has been cleaved.

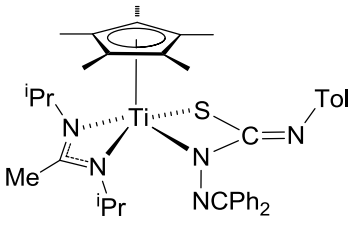

51_int

The proposed intermediate **51_int** was not observed in the reaction suggesting that the transformation of **51_int** to **51** is fast on NMR time scale. It is also suggested that

similar to **48**, the first-formed intermediate in this case is also thermodynamically unstable and undergoes rearrangement to give the final product **51**, analogous to **49**. In fact, the IR spectrum of **51** shows ν(C=N) band at 1606 cm^{-1} which is comparable to that for **49** (1592 cm^{-1}). Nevertheless, **51** does not react with a second molecule of TolNCS to form a "double-insertion" product analogous to **50** and **16**. It is probably because forming a "double-insertion" product would mean forming two Ti–S bonds which is not as favourable as Ti–S + Ti–N bonds in the cycloaddition product. Another possibility could be that the structure for the "double-insertion" product would have a puckered ring as previously described for reactions with CS_2 (Sections 2.4.3 and 4.5).

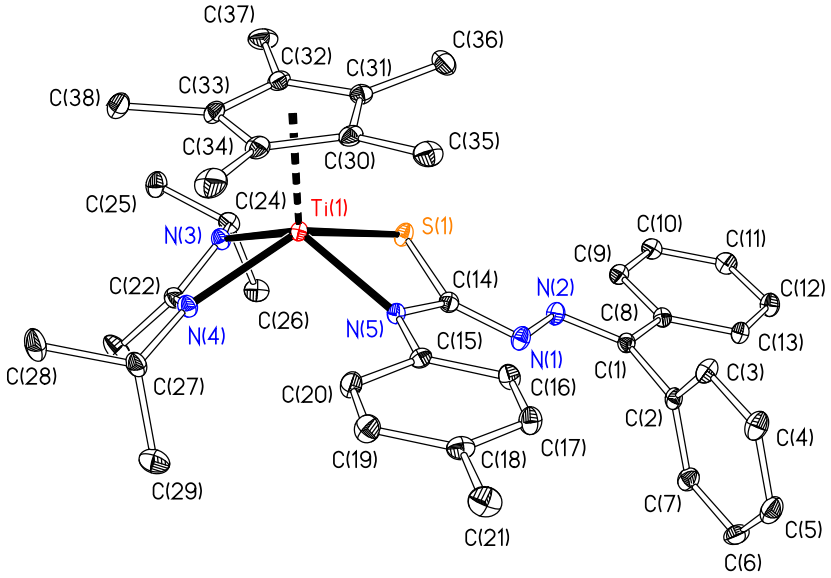

Figure 4.11. Displacement ellipsoid plot (20% probability) of Cp*Ti{MeC(N^{i}Pr)$_2$}{N(Tol)C(NNCPh$_2$)S} (**51**). H atoms omitted for clarity.

A comparison of the structural data between compound **51** and Cp*Ti{MeC(N^{i}Pr)$_2$}{N(NPh$_2$)C(NAr′)S} (**11**) shows that the N–C (1.370(3) Å) and C=N (1.301(3) Å) distances are shorter and longer, respectively in **51** compared to 1.396(3) Å (N–C) and 1.273(3) Å (C=N) observed for **11**. This could be due to extra conjugation allowed by the arrangement of **51**. The C(14)-N(1) bond length of 1.301(3) Å is intermediate between single N–C and double N=C bonds. Although the N(1)-N(2) distance of 1.388(3) Å for **51** is still intermediate between single and double N–N bonds, it is significantly longer than that for **41** (1.329(2) Å) reflecting a change of hybridisation at N_α.

The NMR data for **51** which include nOe measurements through ROESY 2-D NMR are consistent with the proposed structure. No signals for other isomers of **51** (e.g. with a κ^2*N,S*-N(NCPh$_2$)C(NTol)S or κ^2*N,N′*-N(NCPh$_2$)C(S)NTol moieties) were observed in the NMR tube scale experiments or the crude reaction product. The literature example of reactions between lanthanide benzophenone hydrazonido(1-) complexes and PhNCS also reported the formation of cycloaddition products with a κ^2*N,S* coordination mode and M–N$_\alpha$ bond cleavage.[11]

Table 4.5. Selected bond lengths (Å) and angles (°) for Cp*Ti{MeC(N^{i}Pr)$_2$}{N(Tol)C(NNCPh$_2$)S} (**51**). Cp$_{cent}$ refers to the Cp* ring carbon centroid.

Ti(1)-Cp$_{cent}$	2.063	Ti(1)-N(3)	2.110(2)
Ti(1)-N(4)	2.103(2)	Ti(1)-N(5)	2.049(2)
Ti(1)-S(1)	2.4246(8)	S(1)-C(14)	1.765(3)
N(5)-C(14)	1.370(3)	C(14)-N(1)	1.301(3)
N(1)-N(2)	1.388(3)	N(2)-C(1)	1.294(3)
Cp$_{cent}$-Ti(1)-N(3)	114.5	Cp$_{cent}$-Ti(1)-N(4)	113.5
Cp$_{cent}$-Ti(1)-N(5)	116.3	Cp$_{cent}$-Ti(1)-S(1)	113.4
N(5)-Ti(1)-S(1)	69.80(6)	Ti(1)-N(5)-C(14)	101.96(15)
Ti(1)-S(1)-C(14)	78.14(9)	C(14)-N(1)-N(2)	111.5(2)
N(1)-N(2)-C(1)	114.8(2)		

4.6.5 Reaction of Cp*Ti{MeC(N^{i}Pr)$_2$}{N(Tol)C(NNCPh$_2$)S} (51) with TolNCO

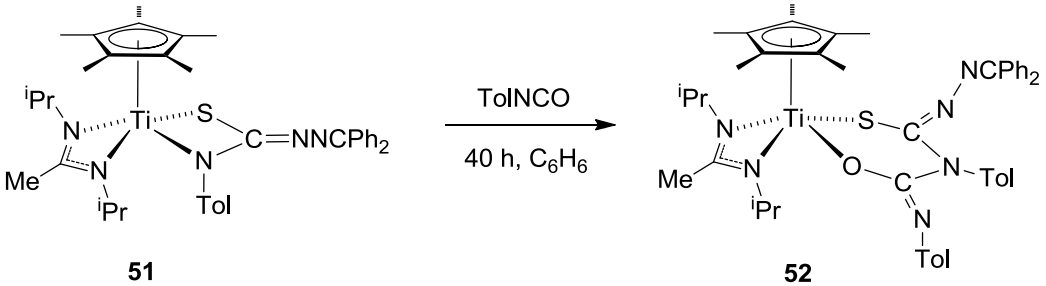

Equation 4.4

Although **51** does not react further with a second equivalent of TolNCS to give the "double-insertion" product analogous to **50**, it does react with TolNCO to form the

mixed "double-insertion" product Cp*Ti{MeC(N^iPr)$_2$}{SC(NNCPh$_2$)N(Tol)C-(NTol)O} (**52**) as shown in Equation 4.4. Another similar cross-coupled derivative of its hydrazide analogue Cp*Ti{MeC(N^iPr)$_2$}{OC(NTol)N(NPh$_2$)C(O)O} (**13**) has been previously discussed in Section 2.5. It is suggested that the difference in the Ti–S and Ti–O bond energy results in the observed reactivity. The reaction with TolNCS is considered to be similar to that calculated for CS_2 (Figure 2.11) where the first addition is exothermic but the second addition is endothermic and has a rather high activation barrier. However, with TolNCO, both first and second additions are calculated to be exothermic, consistent with the observed "double-insertion" products **50** and **52**. Nevertheless, the reaction in forming **52** is rather slow, requiring 40 hours to reach completion compared to 5 hours needed for the formation of **50**.

In the scaled up reaction, a stoichiometric amount of TolNCO was added to **51** in benzene at room temperature and left to react for 40 hours. **52** was obtained as a red brown solid in reasonable yield (79%). Even though all attempts to grow diffraction-quality crystals were unsuccessful, other data including the results from elemental analysis are consistent with the proposed structure (Equation 4.4). The ^{1}H and ^{13}C{^{1}H} NMR spectra of **52** show two sets of *p*-tolyl group resonances and the ^{1}H NMR spectrum shows two apparent septets and four doublets corresponding to the inequivalent *iso*-propyl groups of the amidinate ligand, in agreement with the proposed C_1 symmetric structure. In addition, the IR spectrum shows two ν(C=N) bands at 1614 and 1589 cm^{-1} which is similar to 1619 and 1599 cm^{-1} found for Cp*Ti{MeC(N^iPr)$_2$}{OC(NNMe$_2$)N(Tol)C(NTol)O} (**16**).

4.7 Adduct formation between Cp*Ti{MeC(N^iPr)$_2$}(NNCPh$_2$) (41) and isonitriles

Equation 4.5 summarises the reactions of **41** with selected isonitriles. When followed by ^{1}H NMR, reactions of **41** with ^{t}BuNC and XylNC in C_6D_6 immediately form the Lewis base adducts Cp*Ti{MeC(N^iPr)$_2$}{NNCPh$_2$}(CN^tBu) (**53**) and Cp*Ti{MeC(N^iPr)$_2$}{NNCPh$_2$}(CNXyl) (**54**), respectively, as shown in Equation 4.5.

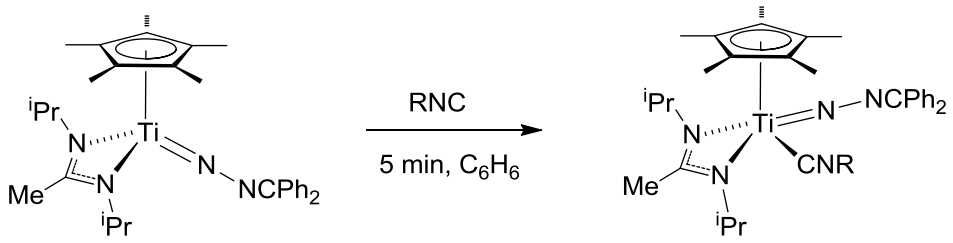

41

Equation 4.5

On the preparative scale, **53** was isolated as a waxy brown solid in 74% yield while **54** was obtained as a dark brown solid with 88% isolated yield. The ^{1}H and ^{13}C{^{1}H} NMR data supported the proposed structures in Equation 4.5. Room temperature ^{1}H NMR spectra suggest the formation of C_s symmetric products with one apparent septet and two overlapping doublets corresponding to the *iso*-propyl groups of the amidinate ligand for each **53** and **54**. Nevertheless, cooling the samples to -70 ℃ in toluene-d_8 resolved the *iso*-propyl groups into two apparent septets and four doublets, consistent with the proposed adduct with C_1 symmetric structures. The room temperature spectra can be explained by fast exchange of the two isomers of **53** and **54** by isonitrile dissociation which causes the signals to be averaged. This is similar to the adduct **19** formed between its hydrazide analogue **4.4** and ^{t}BuNC as reported in Section 2.8 but different to the reactivity previously reported for imides and some hydrazides, which either formed double addition products or underwent N_α–N_β bond cleavage.[24, 44, 45]

Diffraction-quality crystals of **54** were grown from saturated benzene solution at 4 ℃. Its molecular structure is shown in Figure 4.12 and selected distances and angles are shown in Table 4.6. Full crystallographic data are given in the CD Appendix. The solid state structure of **54** features a four-legged piano stool geometry around titanium and confirms the structure proposed in Equation 4.5.

In general, the selected distances and angles of **54** are similar to that in **41**. Ti(1)-N(1) (1.7793(17) Å) of **54** is slightly longer than 1.7508(16) Å for **41**. The Ti(1)-N(3) and Ti-N(4) distances for **54** are also elongated compared to **41**, with bond lengths of 2.1483(18) Å and 2.1841(18) Å compared to 2.1093(15) Å and 2.0925(16) Å, respectively. The lengthening in Ti–N distances is mainly attributed to the steric hindrance caused by the higher coordination number in **54**. Ti(1)-C(14) distance of

2.232(2) Å lies on the shorter end of the corresponding distances reported (2.235(6) – 2.256(6) Å) for Ti(IV) isonitrile adducts.[46-48]

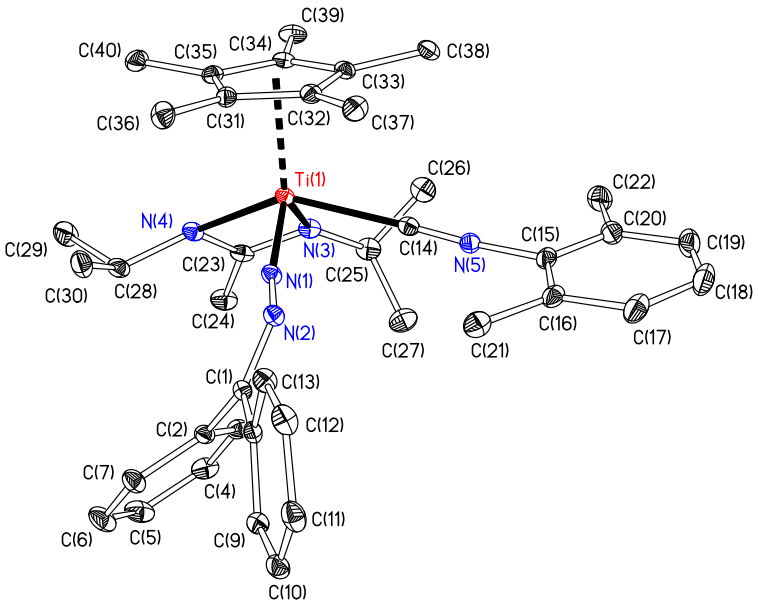

Figure 4.12. Displacement ellipsoid plot (20% probability) of Cp*Ti{MeC(N^{i}Pr)$_2$}{NNCPh$_2$}(CNXyl) (**54**). H atoms omitted for clarity.

Table 4.6. Selected bond lengths (Å) and angles (°) for Cp*Ti{MeC(N^{i}Pr)$_2$}{NNCPh$_2$}(CNXyl) (**54**). Cp$_{cent}$ refers to the Cp* ring carbon centroid.

Ti(1)-Cp$_{cent}$	2.096	Ti(1)-N(1)	1.7793(17)
Ti(1)-N(3)	2.1483(18)	Ti(1)-N(4)	2.1841(18)
Ti(1)-C(14)	2.232(2)	C(14)-N(5)	1.160(3)
N(1)-N(2)	1.313(2)	N(2)-C(1)	1.314(3)
C(1)-C(2)	1.491(3)	C(1)-C(8)	1.479(3)
Cp$_{cent}$-Ti(1)-N(1)	119.6	Cp$_{cent}$-Ti(1)-N(3)	123.4
Cp$_{cent}$-Ti(1)-N(4)	113.2	Cp$_{cent}$-Ti(1)-C(14)	102.8
Ti(1)-N(1)-N(2)	158.66(15)	Ti(1)-C(14)-N(5)	167.03(18)
C(14)-N(5)-C(15)	174.9(2)	N(1)-N(2)-C(1)	123.32(18)
N(2)-C(1)-C(2)	124.85(19)	N(2)-C(1)-C(8)	114.12(18)
C(2)-C(1)-C(8)	120.96(18)		

It is suggested that the isonitrile ligands in **53** and **54** act as simple neutral donors, as no back-bonding is possible for the d^0 metal complex in contrast to low-valent Ti (or other electron rich transition metal) complexes.[48] This is supported by the C(14)-N(5)-C(15) angle of 174.9(2) ° which deviates only slightly from linearity. In an example reported for a Ti(II) isonitrile complex ($Cp_2Ti(CO)(CN^tBu)$), the Ti–CN bond is shortened to 2.112(9) Å, and the C–N–C angle deviates further from linearity (159.8(10) °) due to the Ti–C ($d_\pi \rightarrow p_\pi$) π backbonding that alters the hybridisation of the N atom.[48-50]

The fact that the isonitriles in **53** and **54** acted as pure σ-donors is also reflected in their C–N stretching vibration frequency. The IR spectrum for **53** shows a strong band at 2164 cm^{-1} which is attributed to ν(C≡N) of the isonitrile ligand, similar to 2152 cm^{-1} observed for **19**. The ν(C≡N) for **54** was found at 2124 cm^{-1}. These values are higher than those for the free ligands (^{t}BuNC,[46] ν = 2138 cm^{-1}; XylNC,[49] ν = 2110 cm^{-1}).[48] The increased ν(C≡N) in **53** and **54** compared to the uncoordinated isonitriles is consistent with coordination to the electron deficient titanium in **41**.[47, 50] Bergman *et al*. reported another example of isonitrile adduct formation for an alkylidene hydrazido complex in 1998 where they observed a strong IR stretch corresponding to the ν(C≡N) in the isonitrile ligand of the adduct at 2139 cm^{-1}.[19] One other example of adduct formation for alkylidene hydrazide was reported by Chirik *et al*. where they found that $\{\eta^5\text{-}1,3\text{-}C_5H_3(SiMe_3)_2\}_2Ti(NNCPh_2)$ reacted with CO to form the adduct $\{\eta^5\text{-}1,3\text{-}C_5H_3(SiMe_3)_2\}_2Ti(NNCPh_2)(CO)$.[10] Reaction of **41** with CO however, gave a complicated mixture of unknown products.

4.8 Reactions of Cp*Ti{MeC(N^{i}Pr)$_2$}(NNCPh$_2$) (41) with nitriles

Initial NMR tube scale experiments showed that the reaction of **41** with PhCN required 3 equivalents of the nitrile for complete conversion of **41** to Cp*Ti{MeC(N^{i}Pr)$_2$}{N(NCPh$_2$)C(Ph)NC(Ph)N} (**55**) (Equation 4.6). When a stoichiometric amount of the nitrile was used, an equilibrium mixture of **41** and **55** was observed in the ^{1}H NMR spectrum. The presence of an excess amount of nitrile in the reaction mixture led to the shift of equilibrium towards the formation of the desired product **55**. No cycloaddition (or other) intermediate was observed in the reaction.

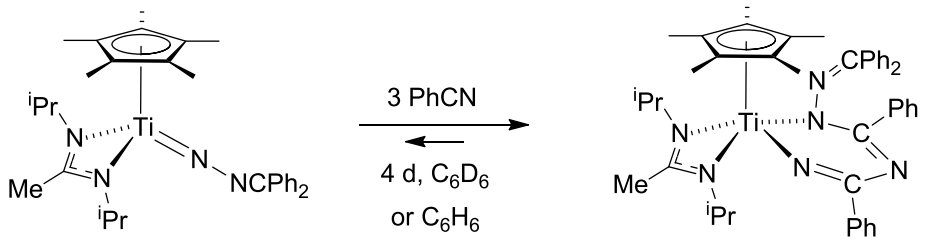

Equation 4.6

When carried out in a benzene solution, the reaction proceeded slowly at room temperature over 4 days to give **55** as a sticky yellow oil which upon washing with cold pentane, filtered, and dried *in vacuo* gave **55** as a yellow solid in 69% yield. However, when the pure **55** was redissolved in C_6D_6, the mixture of starting materials (**41** and PhCN) and product **55** appeared in equilibrium after 5 days with an integrated ratio of *ca*. 1:3, suggesting a reversible reaction.

From the NMR data, it seems that only 2 equivalents of the PhCN are incorporated into the six-membered metallacycle **55**. The ^{1}H and $^{13}C\{^{1}H\}$ NMR spectra of **55** are consistent with the presence of two inequivalent phenyl rings derived from the nitrile (Equation 4.6). X-ray structure analysis confirms the proposed connectivity. Diffraction-quality crystals of **55** were grown from a saturated benzene solution at 4 ℃. The molecular structure is shown in Figure 4.14 and selected distances and angles are listed in Table 4.7. Full crystallographic data are given in the CD Appendix.

Electron withdrawing aryl groups have previously been reported to be able to stabilise the cycloaddition products in the reactions between hydrazides and alkynes.[51] It was thus hoped that addition of an electron withdrawing nitrile to **41** will result in a more stable product. An NMR tube scale reaction between **41** and one equivalent of $Ar^{F5}CN$ (Ar^{F5} = C_6F_5) in C_6D_6 resulted in a 1:1 mixture of **41** and a single product, $Cp^*Ti\{MeC(N^iPr)_2\}\{N(NCPh_2)C(Ar^{F5})NC(Ar^{F5})N\}$ (**56**). The reaction was then repeated with 2 equivalents of the nitrile to give a clean conversion of **41** to **56** as shown in Equation 4.7. This reaction is considerably faster than that for **55**, requiring only less than 16 hours to reach completion, giving **56** as a yellow solid in 46% isolated yield on scale up. The relatively high solubility of **56** in hydrocarbon solvents resulted in the slightly low yield.

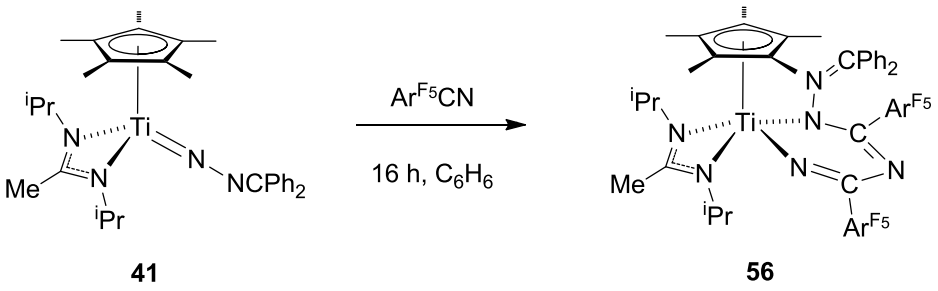

41 **56**

Equation 4.7

The ^{1}H NMR spectrum of **56** (Figure 4.13) shows two apparent septets (3.61 and 3.81 ppm) for the inequivalent *iso*-propyl methine hydrogens, and four doublets (0.86 – 1.32 ppm) for the two pairs of diastereotopic methyl groups of MeC(N^{i}Pr)$_2$ consistent with the C_1 symmetric structure illustrated in Equation 4.7.

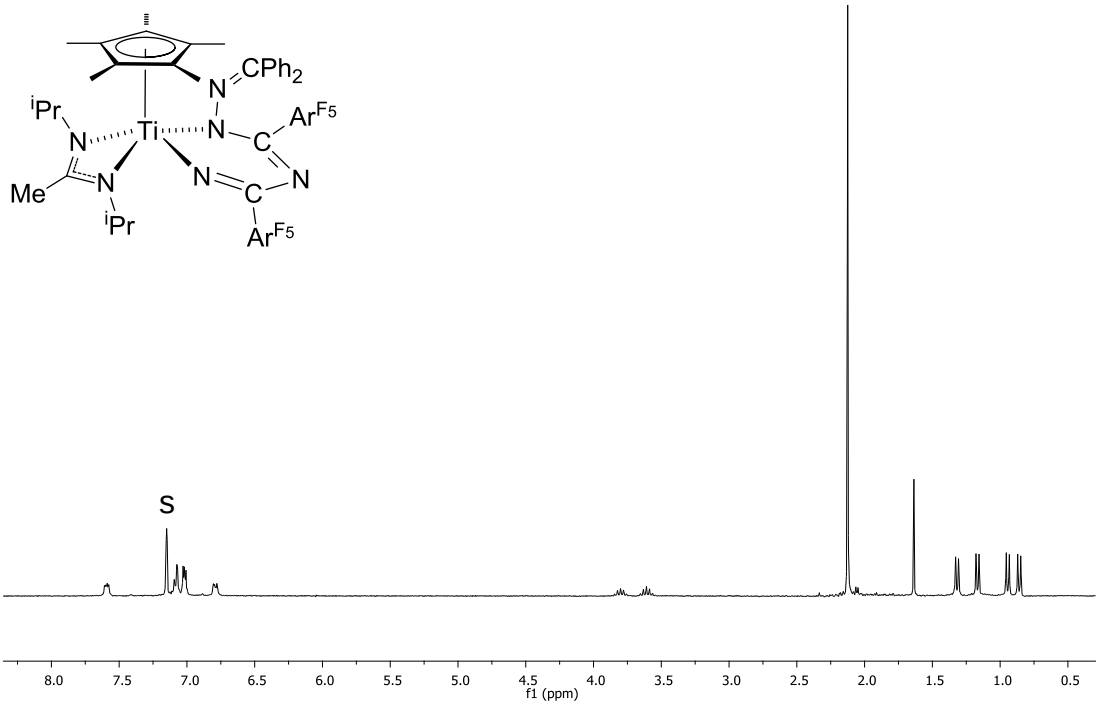

Figure 4.13. ^{1}H NMR spectrum (299.9 MHz) of Cp*Ti{MeC(N^{i}Pr)$_2$}-{N(NCPh$_2$)C(Ar^{F5})NC(Ar^{F5})N} (**56**) in C_6D_6 ("s" denotes residual protio-solvent).

The ^{19}F NMR spectrum shows two different sets of resonances for the two different Ar^{F5} rings, one with free rotation (2:2:1 ratio) while the other has a restricted rotation with two different *ortho*-fluorine environment (possibly due to the proximity of the phenyl rings on the alkylidene hydrazide ligand). The addition reaction is irreversible in this case, with no formation of an equilibrium mixture when **56** was redissolved in

benzene. This shows that the presence of an electron withdrawing group in the nitrile did indeed stabilise the double addition product **56**.

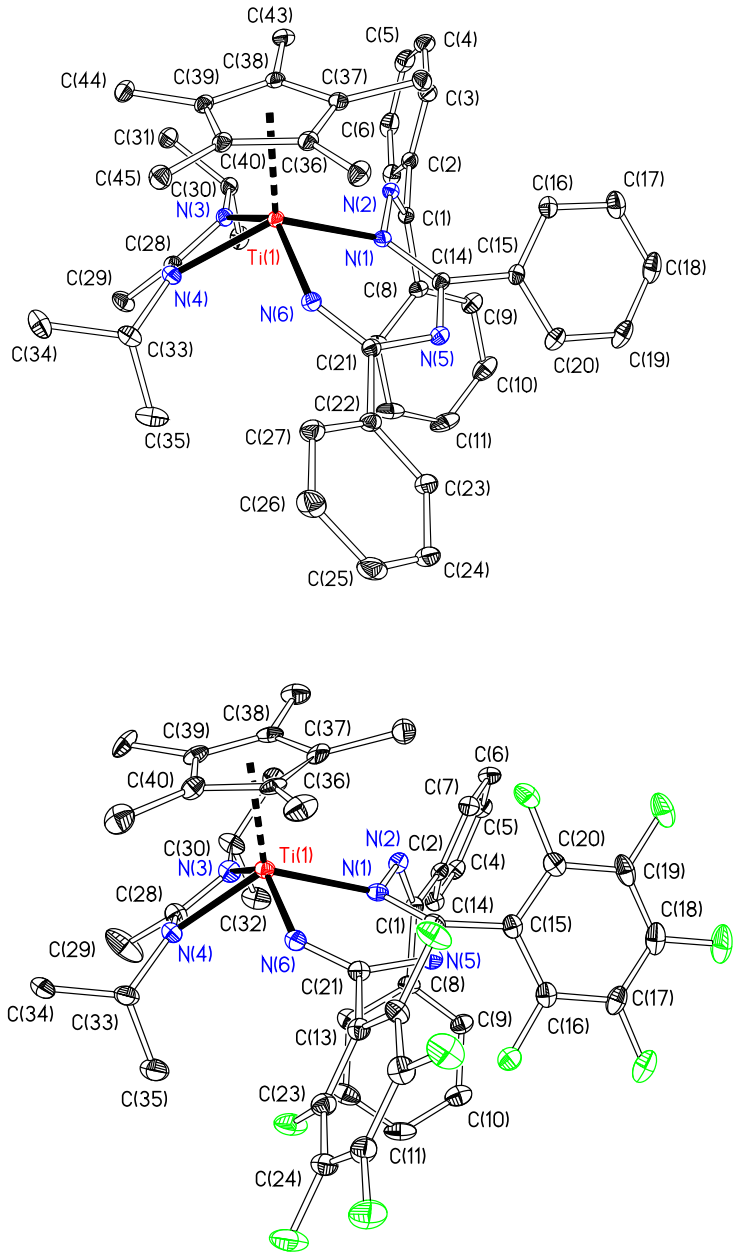

Figure. 4.14. Displacement ellipsoid plots (20% probability) of Cp*Ti{MeC(N^{i}Pr)$_2$}-{N(NCPh$_2$)C(Ph)NC(Ph)N} (**55**, top) and Cp*Ti{MeC(N^{i}Pr)$_2$}{N(NCPh$_2$)C(Ar^{F5})NC-(Ar^{F5})N} (**56**, bottom). H atoms and disorder in the Cp* and ^{i}Pr groups and C_6H_6 of crystallisation of **56** omitted for clarity.

Compound **56** crystallises easily from benzene and diffraction-quality crystals were obtained from a saturated benzene solution at 4 ℃. The solid state structure of **56** is shown in Figure 4.14 and selected distances and angles are listed in Table 4.7. Full

crystallographic data are given in the CD Appendix. In general, the structural data for **55** and **56** are very similar. The solid state structures for **55** and **56** (Figure 4.14) confirm that in both cases, two molecules of nitriles have effectively added into the Ti=N_α bond, forming a six-membered metallacycle. The structures of both **55** and **56** also confirm the four-legged piano stool geometries around the titanium metal centre.

The six-membered metallacycles are approximately planar. For **55** the maximum displacement from the least-squares {Ti(1), N(1), C(14), N(5), C(21), N(6)} plane is 0.096 Å, and for **56** it is 0.126 Å. The Ti(1)-N(1) distances of 2.1306(14) Å and 2.147(3) Å for **55** and **56** respectively are significantly lengthened compared to that of 1.751(16) Å in **41**. However, Ti(1)-N(6) distances for both **55** and **56** (1.8505(15) Å and 1.868(4) Å respectively) are significantly shorter than those for Ti(1)-N(1). The N(1)–N(2) bond lengths of 1.4049(19) Å and 1.428(4) Å for **55** and **56** respectively are significantly elongated from 1.329(2) Å in **41**. This suggests a significant reduction in the multiple bond character, with no significant interaction between N_α and N_β. The metallacycles are completed through donation of N(6) to the titanium centre.

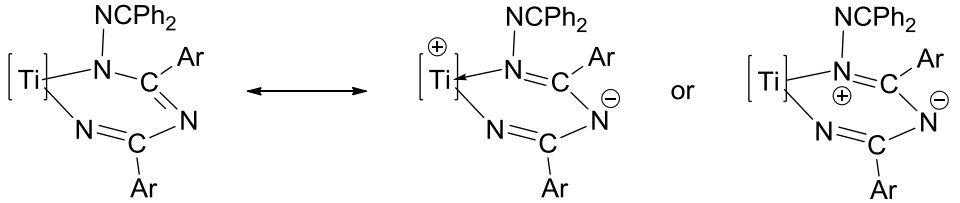

There are two possible resonance forms for **55** and **56**. The resonance form **A** with two amide type donor would maybe suggest similar bond distances for Ti(1)-N(1) and Ti(1)-N(6). However, Ti(1)-N(6) bond distances for both **55** and **56** are short and more like a Ti–N=CNR whereas Ti(1)-N(1) distances are longer and intermediate between Ti–NR_2 and Ti–N^{py}, and similar to those for Ti(1)-N(3) and Ti(1)-N(4) in the delocalised amidinate ligand. The N(6)-C(21) bond distances of 1.284(2) Å and 1.281(5) Å respectively are short compared to N(1)-C(14) (1.347(2) Å and 1.341(5) Å respectively) and N(5)-C(14) (1.332(2) Å and 1.335(5) Å respectively) which are similar. The Ti(1)-N(3) (2.1967(14) Å and 2.231(3) Å respectively) which are situated trans to N(6) have longer bond lengths compared to those for Ti(1)-N(4) (2.0882(15) Å and 2.069(3) Å) consistent with different donor ability of Ti(1)-N(1) and Ti(1)-N(6).

Overall, these suggest that resonance forms **B** or **B′** play an important role in the structures of both **55** and **56**. In addition, both Ti(1)-N(1) and Ti(1)-N(6) in **56** are longer than those for **55** possibly due to the electron withdrawing effect of the Ar^{F5} group in **56**.

Table 4.7. Selected bond lengths (Å) and angles (°) for Cp*Ti{MeC(N^iPr)$_2$}{N(NCPh$_2$)C(Ar)NC(Ar)N} (Ar = Ph (**55**) or Ar^{F5} (**56**)). Cp_{cent} refers to the Cp* ring carbon centroid.

Parameter	**55**	**56**
Ti(1)-Cp_{cent}	2.073	2.050
Ti(1)-N(1)	2.1306(14)	2.147(3)
Ti(1)-N(3)	2.1967(14)	2.231(3)
Ti(1)-N(4)	2.0882(15)	2.069(3)
Ti(1)-N(6)	1.8505(15)	1.868(4)
N(1)-N(2)	1.4049(19)	1.428(4)
N(2)-C(1)	1.293(2)	1.294(5)
N(1)-C(14)	1.347(2)	1.341(5)
N(5)-C(14)	1.332(2)	1.335(5)
N(5)-C(21)	1.369(2)	1.361(5)
N(6)-C(21)	1.284(2)	1.281(5)
Cp_{cent}-Ti(1)-N(1)	113.3	113.8
Cp_{cent}-Ti(1)-N(3)	115.1	113.2
Cp_{cent}-Ti(1)-N(4)	115.1	119.6
Cp_{cent}-Ti(1)-N(6)	112.4	107.8
N(1)-Ti(1)-N(6)	79.41(6)	78.74(13)
Ti(1)-N(1)-C(14)	128.61(11)	127.5(3)
Ti(1)-N(6)-C(21)	141.08(13)	140.1(3)
N(1)-C(14)-N(5)	125.08(15)	126.5(4)
N(6)-C(21)-N(5)	124.59(16)	125.6(4)
C(14)-N(5)-C(21)	119.12(14)	118.0(3)
N(1)-N(2)-C(1)	121.40(14)	118.7(3)

As shown in Figure 4.15, there are two possible mechanisms for the addition reactions to occur (denoted "Path A" and "Path B"). Both Path A and B start with a [2+2] cycloaddition. While Path A proceeds with a direct insertion of a second molecule of nitrile into the new Ti–N bond, Path B undergoes reverse cycloaddition followed by a further cycloaddition, ring opening and then ring closure to go from a four-membered metallacycle to the stable six-membered chelating ring. The reverse cycloaddition intermediate in Path B has been reported previously for the reactions of hydrazides with nitriles.[44] On the other hand, the insertion of nitriles into hydrazide-derived metallacycles to give six-membered rings is also known.[44] There are also literature examples on nitrile insertion into M–NR_2 bonds in general.[52, 53]

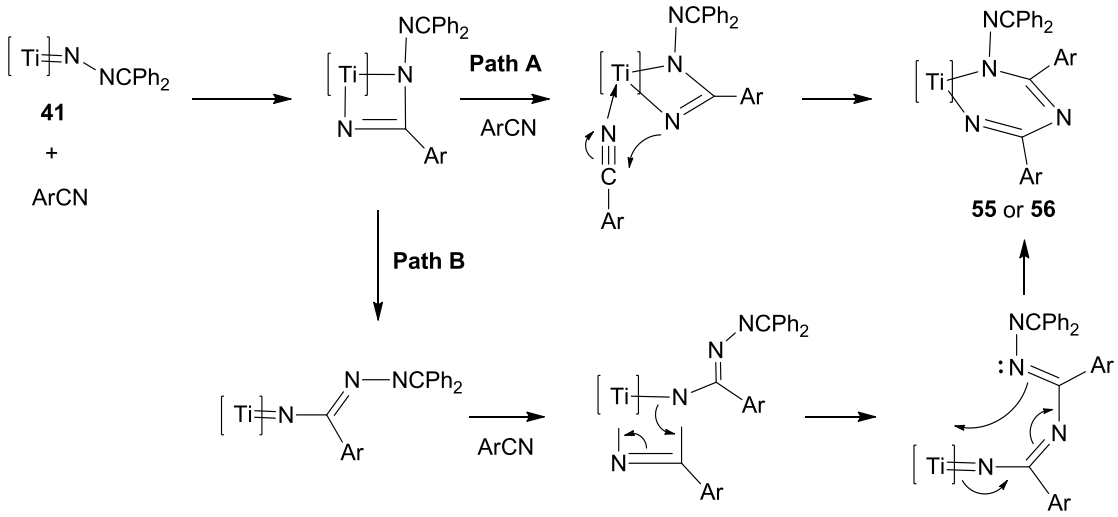

Figure 4.15. Two possible mechanisms for nitrile addition reaction. [Ti] = Cp*Ti{MeC(N^iPr)$_2$}.

The labile nature of **55** in solution suggested that $Ar^{F5}CN$ might be able to replace the PhCN in **55**, generating **56**. A competition experiment was thus carried out by adding 2 equivalents of $Ar^{F5}CN$ to a solution of **55** in C_6D_6. Surprisingly, the ^1H NMR spectrum shows a new set of signals suggesting the formation of a different product instead of **56**. It is proposed to be a mixed double addition product Cp*Ti{MeC(N^iPr)$_2$}{N($NCPh_2$)C(Ph)NC(Ar^{F5})N} (**57**) as shown in Equation 4.8.

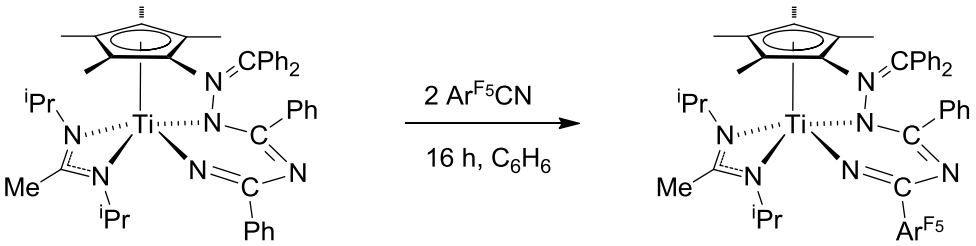

55 **57**

Equation 4.8

The NMR data are consistent with the C_1 symmetric structure proposed, and show only one set of signals corresponding to the phenyl ring on the nitrile and a set of signals corresponding to the $Ar^{F5}CN$ group. The ^{19}F NMR spectrum shows the resonances for the Ar^{F5} ring in 2:2:1 ratio, suggesting free rotation of the ring consistent with the proposed structure shown in Equation 4.8. In principle, there could be another isomer with $Ar^{F5}CN$ bound to the alkylidene hydrazide ligand and PhCN bound to the titanium centre. This second isomer, however, was not observed. The connectivity is further confirmed through the molecular structure obtained which will be discussed in detail later.

When **56** was reacted with an excess amount of PhCN, no reaction was observed suggesting that the double addition reaction with $Ar^{F5}CN$ is more favourable than with PhCN. This is consistent with the reported findings that electron withdrawing aryl groups can help to increase the stability of certain reaction products.[51] When the reaction was carried out by adding 1 equivalent of each nitrile to **41**, a mixture of **56** and unidentified products were obtained. The fact that **57** can only be obtained through a step wise reaction of **41** with PhCN followed by $Ar^{F5}CN$ suggests that the reaction proceeded *via* the loss of one of the two benzonitriles to give the cycloaddition intermediate which then reacted with the added $Ar^{F5}CN$ to afford **57** as the final product.

Several attempts to grow diffraction-quality crystals all ended up giving crystals of the hydrolysed product $Ph_2CNNC(Ph)NC(Ar^{F5})NH_2$ (**58**). The crystals of **58** were grown by slow evaporation of a diethyl ether solution of **57**. Although diffraction-quality crystals of **57** could not be obtained, the structural data for **58** helps establish the connectivity of **57**. The solid state structure of **58** is shown in Figure 4.16 and selected distances and angles are listed in Table 4.8. Full crystallographic data are given in the CD Appendix. The selected distances and angles are all within normal

ranges.[54] The molecular structure of **58** shows that it contains one molecule of each PhCN and $Ar^{F5}CN$, with PhCN bound to the alkylidene hydrazide, confirming the proposed structure of **57**.

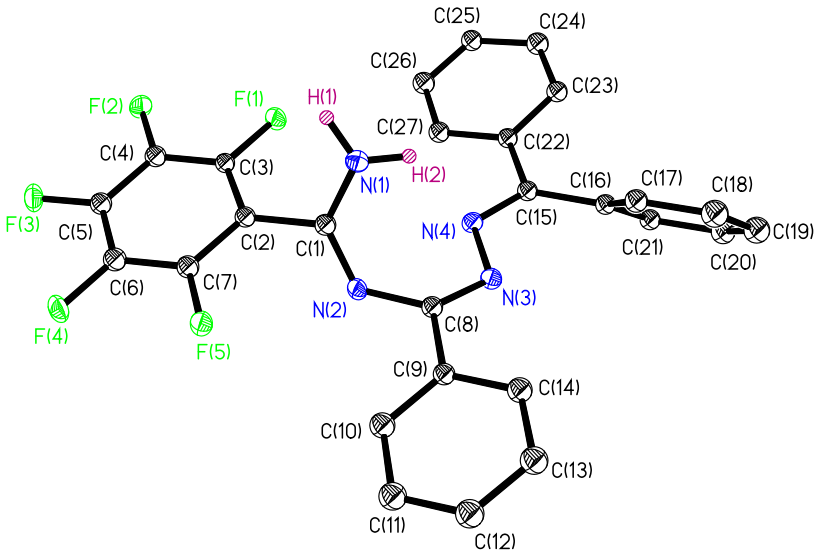

Figure 4.16. Displacement ellipsoid plot (20% probability) of $Ph_2CNNC(Ph)NC(Ar^{F5})NH_2$ (**58**). C-bound H atoms omitted for clarity, other H atoms drawn as spheres of an arbitrary radius.

Table 4.8. Selected distances (Å) and angles (°) for $Ph_2CNNC(Ph)NC(Ar^{F5})NH_2$ (**58**).

N(1)-H(1)	0.915(10)	N(1)-H(2)	0.914(10)
N(1)-C(1)	1.361(7)	C(1)-C(2)	1.488(7)
C(1)-N(2)	1.279(6)	N(2)-C(8)	1.392(7)
C(8)-C(9)	1.487(7)	C(8)-N(3)	1.297(6)
N(3)-N(4)	1.402(6)	N(4)-C(15)	1.307(6)
C(15)-C(16)	1.480(7)	C(15)-C(22)	1.486(7)
H(1)-N(1)-C(1)	117(4)	H(2)-N(1)-C(1)	115(4)
N(1)-C(1)-N(2)	126.4(5)	C(1)-N(2)-C(8)	124.6(5)
N(2)-C(8)-N(3)	126.0(5)	C(8)-N(3)-N(4)	112.7(4)
N(3)-N(4)-C(15)	115.1(5)	N(4)-C(15)-C(16)	125.0(5)
N(4)-C(15)-C(22)	115.3(5)		

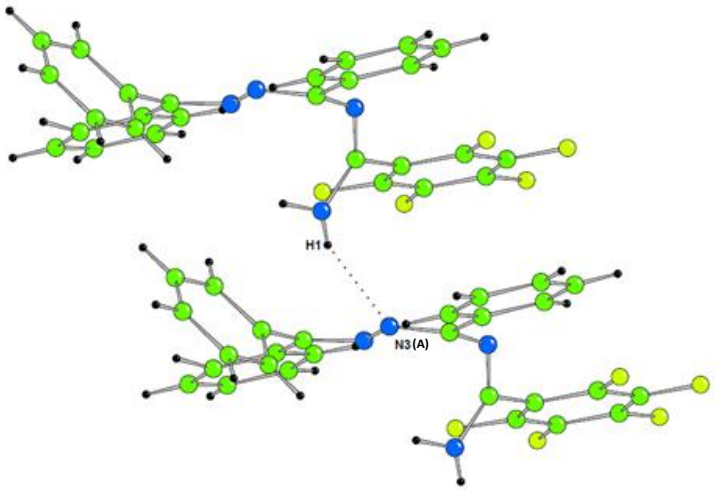

Figure 4.17. H-bonding in $Ph_2CNNC(Ph)NC(Ar^{F5})NH_2$ (**58**). Atoms carrying suffix 'A' are related to their counterparts by the operator 1-*x*, *y*, *z*.

Figure 4.17 shows a N(3A)-H(1) bond distance of 2.64(2) Å and N(3A)-H(1)-N(1) bond angle of 158(5)^o which indicates the presence of hydrogen bonding in **58**. The H-bonded chains run along the a-axis direction with *x*+1, *y*, *z* as the operation relating H(1) to N(3A). The crystal structure also shows that there is no π-stacking between C_6H_5 and C_6F_5 rings of **58** and there are no close C ··C interactions between these planes.

These double addition reactions between nitriles and **41** are the first of their kind reported. There is also no precedent of any double addition of nitriles for its hydrazido or imido analogues in the literature. One related example of a similar double addition of nitriles was reported for an oxo complex [Cp^*_2Zr=O] and its sulfido analogue [Cp^*_2Zr=S] where reactions in the presence of an excess benzonitrile yielded $Cp^*_2Zr\{OC(Ph)NC(Ph)N\}$ and $Cp^*_2Zr\{SC(Ph)NC(Ph)N\}$ respectively.[55] No mechanism was proposed in these instances.

4.9 Reactions of $Cp^*Ti\{MeC(N^iPr)_2\}(NNCPh_2)$ (41) with alkynes

As shown in Equation 4.9, the NMR tube scale reaction of **41** with the terminal alkyne $Ar^{F5}CCH$ gave quantitative conversion to the Markovnikov type cycloaddition product $Cp^*Ti\{MeC(N^iPr)_2\}\{N(NCPh_2)C(Ar^{F5})C(H)\}$ (**59**). On the preparative scale, the reaction in benzene gave a brown solution from which the metallacyclobutene **59** was isolated as a brown solid in 63% yield.

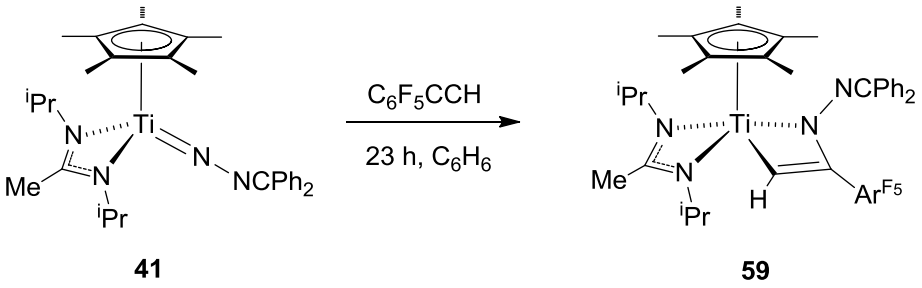

41 **59**

Equation 4.9

Unfortunately, all attempts to grow diffraction-quality crystals were unsuccessful. However, spectroscopic and other data are consistent with the proposed C_1 symmetric [2+2] cycloaddition product proposed in Equation 4.9. The ^{1}H NMR spectrum of **59** shows a singlet at 9.19 ppm which is attributed to the methine proton on the metallacycle, at a characteristically low field resonance. It also shows two apparent septets for the inequivalent *iso*-propyl methine hydrogens, and four doublets for the two pairs of diastereotopic methyl groups of the amidinate ligand (Figure 4.18).

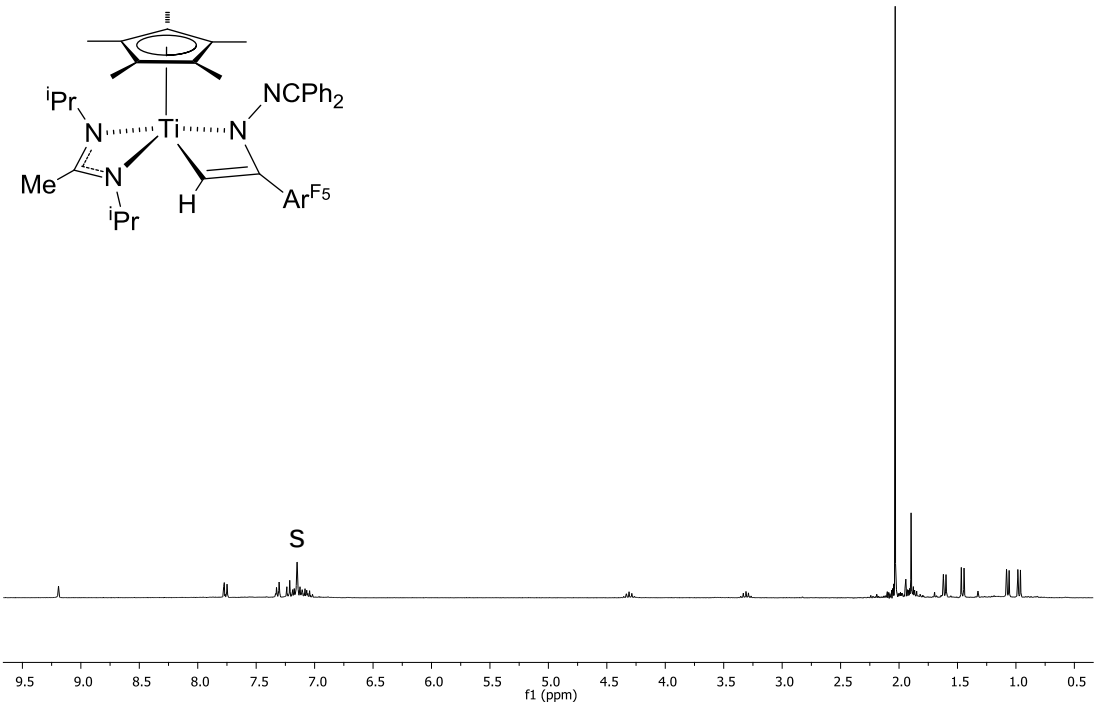

Figure 4.18. ^{1}H NMR spectrum (299.9 MHz) of Cp*Ti{MeC(N^{i}Pr)$_2$}-{N(NCPh$_2$)C(Ar^{F5})C(H)} (**59**) in C_6D_6 ("s" denotes residual protio-solvent).

The Ar^{F5}***C*****C**H carbons, which were observed at 167.8 (C=***C***H) and 140.3 (***C***=CH) ppm in the ^{13}C{^{1}H} spectrum, are also typical for such metallacycles. These values

are in fact comparable to the values reported by Gade *et al*. for a similar metallacyclic product Cp*Ti(N^{Xyl}N){N(NMe_2)C(Ph)C(H)} with C=***C***H and ***C***=CH of 167.3 and 138.2 ppm, respectively.[56]

There are two possible regio-isomers designated as Markovnikov or anti-Markovnikov (Figure 4.19) depending on the position of the alkyne in the cycloaddition product. According to the ^{1}H NMR data, one regio-isomer is formed exclusively in this case, as indicated by the single set of resonances observed. The connectivity of the four-membered metallacycle was confirmed through a combination of 1-D and 2-D NMR experiments. HMBC 2-D NMR spectrum demonstrated that **59** is the Markovnikov regio-isomer with C=C***H*** coupled to ***C***=CH at 140.3 ppm.

Markovnikov **Anti-Markovnikov**

Figure 4.19. The two possible cycloaddition regio-isomers of **59**. [Ti] = Cp*Ti{MeC(N^iPr)$_2$}.

In addition, while the ^{13}C{^{1}H} NMR data of **59** has similar ***C***=***C***H resonances as the Markovnikov product reported by Gade *et al*.,[56] they are very different from the anti-Markovnikov products observed by Mountford and coworkers[51] where they reported more down field ***C***=CH shifts of 181.2 – 215.5 ppm for diamido-amine supporting ligand system. Bergman *et al*. have also reported a similar metallacycle with a Markovnikov type isomer in the reaction of Cp*$_2$Ti{NNC(H)$SiMe_3$} with phenylacetylene.[1]

Reactions were also attempted between **41** and PhCCH and Ar^FCCH (Ar^F = 4-$C_6H_4CF_3$). With PhCCH, an equilibrium mixture of the starting materials and product was observed. Addition of 4 equivalents of alkyne did not shift the equilibrium towards the desired product entirely thus precluding isolation of the product. The reaction between **41** and Ar^FCCH gave mixtures such that isolation of pure product was not possible. In both cases, heating the reaction mixture to 60 ℃ resulted in the formation of an unidentified mixture of products. All the results obtained are consistent with the previous report which through DFT calculations suggest that

reactions with electron-withdrawing terminal alkynes tend to form more stable metallacycles.[51] In fact, Gade *et al.* also could not isolate the metallacyclic product obtained with PhCCH.[56]

Attempted reactions with internal alkynes were all unrewarding. No reactivity was observed between **41** and ArCCMe (Ar = C_6F_5, 4-$C_6H_4CF_3$ or Tol) despite heating at 60 ℃. This is consistent with findings by Bergman *et al*. where no reactions were observed between Cp*$_2$Ti{NNC(H)SiMe$_3$} and internal alkynes.[1] The observed reactivity of **41** with terminal alkynes but not internal alkynes and the formation of more stable products with more electron-withdrawing alkynes are consistent with the reported reactivity of hydrazides.[51]

4.10 Reactions of Cp*Ti{MeC(N^{i}Pr)$_2$}(NNCPh$_2$) (41) with silanes

Inspired by the encouraging 1,2-addition reactions between silanes and hydrazide reported in Chapter Three, reactions between **41** and various silanes were carried out.

4.10.1 Reactions of Cp*Ti{MeC(N^{i}Pr)$_2$}(NNCPh$_2$) (41) with primary and secondary silanes

The reaction between **41** and $PhSiH_3$ proceeded slowly in C_6D_6 at room temperature and reached completion after 16 hours to give Cp*Ti{MeC(N^{i}Pr)$_2$}{N-(PhSiH$_2$)N(CHPh$_2$)} (**60**) (Equation 4.10). This is a much slower reaction compared to those between its hydrazide analogue **4.4** and silanes which completed almost immediately to give hydride-hydrazide(1-) products.

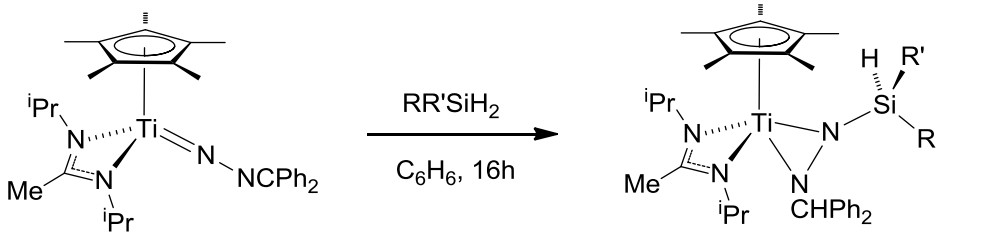

41

R = H, R' = Ph (**60**), Ar^F (**61**), Ar^{OMe} (**62**) or Bu (**63**); R = R' = Ph (**64**)

Equation 4.10

Surprisingly, the ^{1}H NMR spectrum of **60** suggests a C_s symmetric product rather than the C_1 symmetric product which would be expected based on the reactions of Cp*Ti{MeC(N^{i}Pr)$_2$}(NNMe$_2$) (**4.4**) with $PhSiH_3$.[57] Apart from that, it also shows a

singlet rather than a pair of mutually coupled doublets corresponding to Si$\underline{H}_2$ at 5.28 ppm. These observations suggest that the reaction product is different from the hydride-hydrazide(1-) complex (**20**) observed for its hydrazide analogue.

Also unlike the hydride-hydrazide(1-) complexes, the reaction to form **60** is irreversible. On preparative scale, **60** was isolated as a grey green oil in 89% yield. Unfortunately, all attempts to grow diffraction-quality crystals were unsuccessful. Nevertheless, spectroscopic and other data are consistent with the proposed structure **60** in Equation 4.10. The IR spectrum of **60** shows two bands corresponding to ν(Si–H) (symmetric and antisymmetric combinations) at 2119 and 2157 cm^{-1}.

A single resonance was observed at -30.0 ppm in the ^{29}Si spectra of **60**. The $^{13}C\{^1H\}$ NMR spectrum of **60** shows that the resonance corresponding to the carbon on the alkylidene hydrazide ligand has shifted substantially from 140 ppm to 70.3 ppm. A 2-D HMQC spectrum showed coupling between the carbon signal at 70.3 ppm and a proton signal at 5.23 ppm, consistent with the proposed structure. The reaction between **41** and $PhSiD_3$ was then carried out to further confirm the assignment. As expected, the reaction product Cp*Ti{MeC(N^iPr)$_2$}{N($PhSiD_2$)N($CDPh_2$)} (**60-*d*$_3$**) shows a 1:1:1 triplet ($^1J_{CD}$ = 82 Hz) at 70.0 ppm in its $^{13}C\{^1H\}$ NMR spectrum as a result of coupling with deuterium.

Since **60** was an oil and did not form crystals, the same reaction was carried out between **41** and different silanes, namely Ar^FSiH_3, $Ar^{OMe}SiH_3$ (Ar^F = 3,5-$C_6H_3(CF_3)_2$, ArO^{Me} = 4-C_6H_4OMe), $BuSiH_3$ and Ph_2SiH_2 with the hope that more crystalline products and/ or reaction intermediates could be obtained. All four reactions proceeded to form Cp*Ti{MeC(N^iPr)$_2$}{N(RR′SiH)N($CHPh_2$)} (R = H, R′ = Ar^F (**61**), Ar^{OMe} (**62**) or Bu (**63**); R = R′ = Ph (**64**)) in 86 – 96% yield. Unfortunately, **61** – **64** were isolated as oils and all attempts to grow diffraction-quality crystals were unsuccessful. However, their spectroscopic data are consistent with the C_s symmetric structures illustrated in Equation 4.10. The ^1H NMR spectra show resonances corresponding to Si$\underline{H}$ between 4.71 – 5.81 ppm, while those corresponding to C$\underline{H}Ph_2$ were found at 5.16 – 5.99 ppm. The $^{13}C\{^1H\}$ spectra show $\underline{C}HPh_2$ in the range 69.6 – 78.7 ppm and their IR spectra show bands corresponding to ν(Si–H) (symmetric and antisymmetric combinations) between 2148 – 2165 cm^{-1} and 2109 – 2119 cm^{-1}, respectively.

Interestingly, the ^{1}H NMR spectra for all **60** – **64** show the presence of a minor isomer in each case. The minor isomer of **61** (denoted **61_alt**) has been assigned accordingly by NMR spectroscopy. However, for **60** and **62** – **64**, the low percentages of the minor isomers in the product mixtures prevent their proper assignments. Based on the ^{1}H NMR data, only the singlets corresponding to their Cp* ring, and singlets and doublets corresponding to the methyl groups on their amidinate ligands are visible. Figure 4.20 shows the two possible isomers for **60** – **64**. ROESY 2-D NMR spectra demonstrated that the Cp* of major isomers are adjacent to SiH suggesting that **60** – **64** are the major isomers while **60_alt** – **64_alt** are the minor isomers.

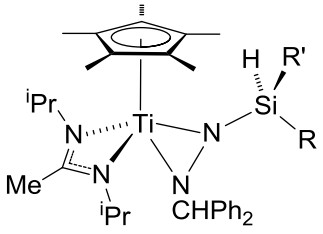

R = H, R' = Ph (**60**),
Ar^F (**61**), Ar^{OMe} (**62**) or
Bu (**63**); R = R' = Ph (**64**)

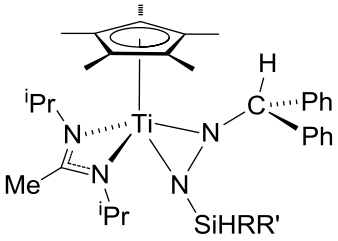

R = H, R' = Ph (**60_alt**),
Ar^F (**61_alt**), Ar^{OMe} (**62_alt**) or
Bu (**63_alt**); R = R' = Ph (**64_alt**)

Figure 4.20. The two possible regio-isomers of **60 – 64**.

Bergman *et al*. previously reported Si-H 1,2-addition reactions between Cp*$_2$Ti{NNC(H)Tol} with $PhSiH_3$ and Ph_2SiH_2 to give hydride-alkylidene hydrazide(1-) products analogous to **20** – **23** formed from Cp*Ti{MeC(N^{i}Pr)$_2$}(NNMe$_2$) (**4.4**).[19] In their reactions, the first formed isomers had to undergo rotation of the tolyl group on the alkylidene hydrazide fragment to form the sterically less congested stable isomers.

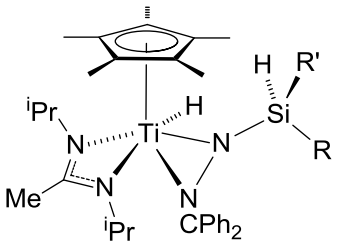

R = H, R' = Ph (**60_int**),
Ar^F (**61_int**), Ar^{OMe} (**62_int**) or
Bu (**63_int**); R = R' = Ph (**64_int**)

It is thus proposed that the reactions between **41** and the above mentioned silanes proceeded through initial Si-H 1,2-addition reactions to form hydride-alkylidene hydrazide(1-) intermediates **60_int** – **64_int** analogous to those reported by Bergman *et al*. and to **20** formed by its hydrazide counterpart. The intermediates then undergo hydride transfer to form the finally observed products **60** – **64**. The instability of the proposed hydride-alkylidene hydrazide(1-) intermediates towards hydride transfer could be due to the greater steric demand of the phenyl groups on the alkylidene hydrazide ligand itself, causing the intermediates to be very congested.

Interestingly, the reaction of **41** with silanes can be related to hydrosilylation in general where Si–H adds to unsaturated substrates with the aid of metal catalysts. The alkylidene hydrazide ligand can be viewed as the unsaturated substrate, and 1,2-Si–H addition followed by hydride transfer formed the hydrosilylation product. However, this is different in the sense that the product does not dissociate from the metal complex.[58-69]

4.10.2 Reactions of Cp*Ti{MeC(N^{i}Pr)$_2$}(NNCPh$_2$) (41) with halosilanes

Reactions of **41** with both $PhSiH_2Cl$ and $PhSiH_2Br$ resulted in an immediate colour change from dark yellow to red. The ^{1}H NMR spectra show complete reactions almost immediately with quantitative conversion to the silylamido-chloride or silylamido-bromide complexes Cp*Ti{MeC(N^{i}Pr)$_2$}(X){N(NCPh$_2$)SiH$_2$Ph} (X = Cl (**65**) or Br (**66**)). This Si–X 1,2-addition reaction is analogous to that found for the hydrazide analogue **4.4**.[57, 70]

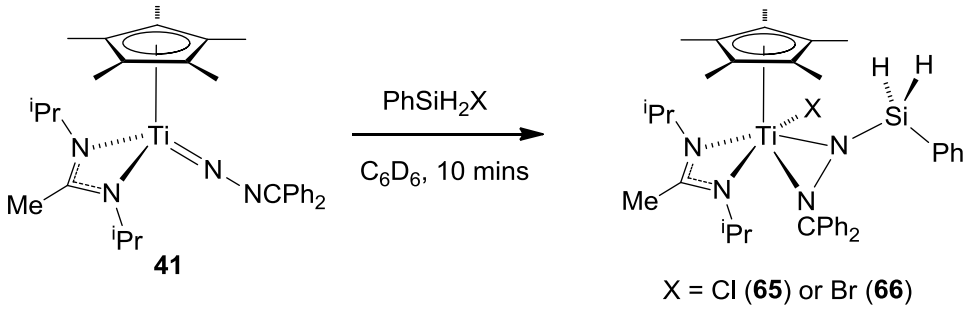

Equation 4.11

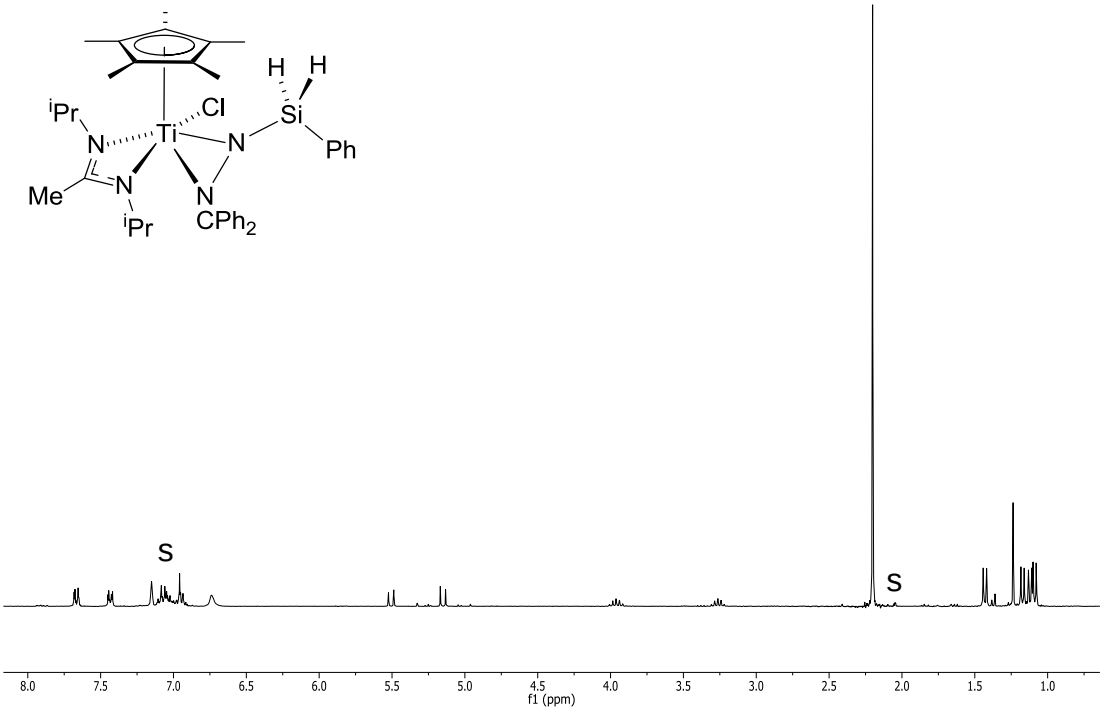

Figure 4.21. ^{1}H NMR spectrum (299.9 MHz) of Cp*Ti{MeC(N^{i}Pr)$_2$}(Cl){N(NCPh$_2$)SiH$_2$Ph} (**65**) in toluene-d_8 at -20 ℃ ("s" denotes residual protio-solvent which overlaps with certain Ph resonances).

The NMR spectra are consistent with the formation of the Si–X 1,2-addition products as shown in Equation 4.11, with both **65** (Figure 4.21) and **66** featuring inequivalent amidinate *iso*-propyl groups with four different methyl group environments, a pair of mutually coupled doublets for the diastereotopic SiH$_2$ groups, and a ^{29}Si resonance at -32.1 and -31.2 ppm, respectively. As for their hydrazide analogue **4.4**, no evidence was found for the alternative titanium-hydride products Cp*Ti{MeC(N^{i}Pr)$_2$}(H){N-(NCPh$_2$)SiH(X)Ph} which would be the products of Si–H activation in both cases. Both **65** and **66** are unstable in solution, fully decomposing into an unknown mixtures after 16 hours, precluding their isolation on the preparative scales. Given the unstable nature of **65** and **66**, both were characterised *in situ* using NMR spectroscopy at 253 K. The formation of **65** and **66** support compounds of the type **60_int** – **64_int** as viable intermediates in the formation of **60** – **64**.

4.11. Conclusions

This Chapter has described the synthesis of the monomeric η^1-alkylidene hydrazido(2-) complex Cp*Ti{MeC(N^{i}Pr)$_2$}(NNCPh$_2$) (**41**) through a *tert*-butyl imido/hydrazone exchange methodology. The study on the reactivity of **41** shows that the Ti=NNCPh$_2$ functional group has rich reactivity patterns towards a wide range of substrates. In general, the reaction of **41** with CO_2 and CS_2 yielded similar products as its diphenyl and dimethyl hydrazide analogues Cp*Ti{MeC(N^{i}Pr)$_2$}(NNR$_2$) (R = Ph (**4.2**) or Me (**4.4**)). However, in the reaction with CO_2, a dimer of the cycloaddition product [Cp*Ti{MeC(N^{i}Pr)$_2$}{μ-OC(NNCPh$_2$)O}]$_2$ (**43**) was observed in addition to the cycloaddition and "double insertion" products.

Compound **41** shows behaviour in-between **4.2** and **4.4** in its reactions with isocyanates. Reaction with Ar'NCO forms Cp*Ti{MeC(N^{i}Pr)$_2$}{N(NCPh$_2$)C(NAr')O} (**47**) through a cycloaddition reaction as seen for **4.2**. However, reactions with ^{t}BuNCO and TolNCO (2 equivalents) gave ^{t}BuNCNNCPh$_2$ (**46**) and Cp*Ti{MeC(N^{i}Pr)$_2$}{OC(NNCPh$_2$)N(Tol)C(NTol)O} (**50**) respectively as shown for **4.4** through cycloaddition-elimination and/or cycloaddition-insertion reactions. Reaction with TolNCS gave a rearranged cycloaddition product Cp*Ti{MeC(N^{i}Pr)$_2$}{N(Tol)C(NNCPh$_2$)S} (**51**) which reacted further with TolNCO to form a mixed cycloaddition-insertion product. Reactions with isonitriles resulted in adduct formation similar to that seen for **4.4**.

In addition to reactivity previously observed for its hydrazide analogues (**4.2** and **4.4**), **41** reacted with nitriles to form double addition products Cp*Ti{MeC(N^{i}Pr)$_2$}-{N(NCPh$_2$)C(Ph)NC(Ph)N} (**55**) and Cp*Ti{MeC(N^{i}Pr)$_2$}{N(NCPh$_2$)C(Ar^{F5})-NC(Ar^{F5})N} (**56**) which are not produced for its hydrazido or imido counterparts. Compound **55** reacted with Ar^{F5}CN to give a mixed double addition product Cp*Ti{MeC(N^{i}Pr)$_2$}{N(NCPh$_2$)C(Ph)NC(Ar^{F5})N} (**57**). Reaction with terminal alkyne Ar^{F5}CCH gave the [2+2] cycloaddition product Cp*Ti{MeC(N^{i}Pr)$_2$}-{N(NCPh$_2$)C(Ar^{F5})C(H)} (**59**). Compound **41** reacted with primary and secondary silanes through initial Si-H 1,2-addition followed by hydride transfer to give Cp*Ti{MeC(N^{i}Pr)$_2$}{N(RR′SiH)N(CHPh$_2$)} (R = H, R′ = Ph (**60**), Ar^F (**61**), Ar^{OMe} (**62**) or Bu (**63**); R = R′ = Ph (**64**)). Reactions of **41** with halosilanes formed Cp*Ti{MeC(N^{i}Pr)$_2$}(X){N(NCPh$_2$)SiH$_2$Ph} (X = Cl (**65**) or Br (**66**)) analogous to those seen for **4.4** and Cp*Ti{MeC(N^{i}Pr)$_2$}(NTol) (**4.5**).

A comparison between the reactivity of compound **41** and $Cp^*_2Ti\{NNC(H)Ar\}$[19] reported by Bergman *et al*. shows that while both formed Markovnikov type cycloaddition product with terminal alkyne, and gave Lewis base adducts with isonitriles, they behave differently with silanes and CO. Compound **41** reacted with silanes to form hydride-alkylidene hydrazide(1-) intermediates *via* Si-H 1,2-addition followed by hydride migration whereas $Cp^*_2Ti\{NNC(H)Tol\}$ reacted with silanes to give stable hydride-alkylidene hydrazide(1-) products. Although $Cp^*_2Ti\{NNC(H)Tol\}$ reacted with CO to form an alkylideneimido isocyanato complex with N–N bond cleavage, the reaction of **41** and CO resulted in a complicated mixture of unknown products. Chirik *et al.* observed a different reactivity between $\{\eta^5\text{-}1,3\text{-}C_5H_3(SiMe_3)_2\}_2Ti(NNCPh_2)$[10] with CO where they reported the formation of a CO adduct. Apart from that, they observed rapid hydrogenation with H_2 to form $\{\eta^5\text{-}1,3\text{-}C_5H_3(SiMe_3)_2\}_2Ti(H)(NHNCPh_2)$ which was not observed for **41**. Interestingly, Bergman *et al.* observed N_2 loss for $Cp^*_2Ti\{NNC(H)SiMe_3\}$[1, 20] to give $Ti{=}CHSiMe_3$ or carbene-like chemistry which was not observed for **41**. Future work would be to explore the effects of changing CRR′ substituents of the alkylidene hydrazido ligand to see if reactions more like the permethyltitanocene (Cp^*_2Ti) system might be induced.

4.12. References

1. J. L. Polse, A. W. Kaplan, R. A. Andersen and R. G. Bergman, *J. Am. Chem. Soc.*, 1998, **120**, 6316.
2. M. H. Chisholm, K. Folting, J. C. Huffman and A. L. Ratermann, *J. Chem. Soc., Chem. Commun.*, 1981, 1229.
3. S. Gambarotta, C. Floriani, A. Chiesi-Villa and C. Guastini, *J. Chem. Soc., Chem. Commun.*, 1982, 1015.
4. S. Gambarotta, C. Floriani, A. Chiesi-Villa and C. Guastini, *J. Am. Chem. Soc.*, 1982, **104**, 1918.
5. S. Gambarotta, C. Floriani, A. Chiesi-Villa and C. Guastini, *J. Am. Chem. Soc.*, 1983, **105**, 7295.
6. L. B. Kool, M. D. Rausch, H. G. Alt, M. Herberhold, A. F. Hill, U. Thewalt and B. Wolf, *J. Chem. Soc., Chem. Commun.*, 1986, 408.
7. Y. Mizobe, Y. Ishii and M. Hidai, *Coord. Chem. Rev.*, 1995, **139**, 281.

8. M. Dartiguenave, M. Jo ëlle Menu, E. Deydier, D. Yves and H. Siebald, *Coord. Chem. Rev.*, 1998, **178-180**, 623.
9. H. Werner, M. E. Schneider, M. Bosch, J. Wolf, J. H. Teuben, A. Meetsma and S. I. Troyanov, *Chem. Eur. J.*, 2000, **6**, 3052.
10. T. E. Hanna, I. Keresztes, E. Lobkovsky, W. H. Bernskoetter and P. J. Chirik, *Organometallics*, 2004, **23**, 3448.
11. Y. Han, J. Zhang, F. Han, Z. Zhang, L. Weng and X. Zhou, *Organometallics*, 2009, **28**, 3916.
12. T. Cantat, C. R. Graves, B. L. Scott and J. L. Kiplinger, *Angew. Chem. Int. Ed.*, 2009, **48**, 3681.
13. V. Tabernero, T. Cuenca and E. Herdtweck, *J. Organomet. Chem.*, 2002, **663**, 173.
14. B. D. Santarsiero and E. J. Moore, *Acta Cryst.*, 1988, **C44**, 433.
15. G. Bai, H. W. Roesky, H. Hao, M. Noltemeyer and H.-G. Schmidt, *Inorg. Chem.*, 2001, **40**, 2424.
16. D. A. Lemenovskii, M. Putala, G. I. Nikonov, N. B. Kazennova, D. S. Yufit and Y. T. Struchkov, *J. Organomet. Chem.*, 1993, **454**, 123.
17. T. Cantat, C. R. Graves, K. C. Jantunen, C. J. Burns, B. L. Scott, E. J. Schelter, D. E. Morris, P. J. Hay and J. L. Kiplinger, *J. Am. Chem. Soc.*, 2008, **130**, 17537.
18. S. Javed and D. M. Hoffman, *Inorg. Chem.*, 2008, **47**, 11984.
19. A. W. Kaplan, J. L. Polse, G. E. Ball, R. A. Andersen and R. G. Bergman, *J. Am. Chem. Soc.*, 1998, **120**, 11649.
20. J. L. Polse, R. A. Andersen and R. G. Bergman, *J. Am. Chem. Soc.*, 1996, **118**, 8737.
21. S. Gambarotta, C. Floriani, A. Chiesi-Villa and C. Guastini, *Inorg. Chem.*, 1983, **22**, 2029.
22. A. J. Blake, J. M. McInnes, P. Mountford, G. I. Nikonov, D. Swallow and D. J. Watkin, *J. Chem. Soc., Dalton Trans.*, 1999, 379.
23. J. D. Selby, C. D. Manley, M. Feliz, A. D. Schwarz, E. Clot and P. Mountford, *Chem. Commun.*, 2007, 4937.
24. J. D. Selby, D.Phil Thesis, University of Oxford, 2009.
25. P. J. Tiong, A. Nova, L. R. Groom, A. D. Schwarz, J. D. Selby, A. D. Schofield, E. Clot and P. Mountford, *Organometallics*, 2011, **30**, 1182.

26. A. E. Guiducci, C. L. Boyd, E. Clot and P. Mountford, *Dalton Trans.*, 2009, 5960.
27. A. E. Guiducci, C. L. Boyd and P. Mountford, *Organometallics*, 2006, **25**, 1167.
28. D. A. Fletcher, R. F. McMeeking and D. Parkin, *J. Chem. Inf. Comput. Sci.*, 1996, **36**, 746 (The UK Chemical Database Service: CSD version 5.32 updated August 2011).
29. S. C. Davies, D. L. Hughes, M. Konkol, R. L. Richards, J. R. Sanders and P. Sobota, *J. Chem. Soc., Dalton Trans.*, 2002, 2811.
30. G. M. Arvanitis, J. Schwartz and D. Van Engen, *Organometallics*, 1986, **5**, 2157.
31. G. M. Arvanitis, J. Smegal, I. Meier, A. C. C. Wong, J. Schwartz and D. Van Engen, *Organometallics*, 1989, **8**, 2717.
32. C. P. Gerlach, *Organometallics,* 1997, **16**, 5148.
33. S. C. Dunn, N. Hazari, N. M. Jones, A. G. Moody, A. J. Blake, A. R. Cowley, J. C. Green and P. Mountford, *Chem. Eur. J.*, 2005, **11**, 2111.
34. T. B. Parsons, N. Hazari, A. R. Cowley, J. C. Green and P. Mountford, *Inorg. Chem.*, 2005, **44**, 8442.
35. S. Patel, Y. Li and A. L. Odom, *Inorg. Chem.*, 2007, **46**, 6373.
36. J. D. Selby, C. D. Manley, A. D. Schwarz, E. Clot and P. Mountford, *Organometallics*, 2008, **27**, 6479.
37. S. Kahlal, J.-Y. Saillard, J.-R. Hamon, C. Manzur and D. Carrillo, *J. Chem. Soc., Dalton Trans.*, 1998, 1229.
38. N. Lehnert and F. Tuczek, *Inorg. Chem.*, 1999, **38**, 1671.
39. Y. Bai, M. Noltemeyer and H. W. Roesky, *Z. Naturforsch.*, 1991, **46b**, 1357.
40. Y. Li, Y. Shi and A. L. Odom, *J. Am. Chem. Soc.*, 2004, **126**, 1794.
41. J. H. Cooley, E. J. Evain, R. D. Willett and J. T. Blanchette, *J. Org. Chem.*, 1989, **54**, 1048.
42. S. Sarker, J. H. Cooley, R. D. Willett and A. L. Rheingold, *J. Org. Chem.*, 1995, **60**, 476.
43. P. J. Tiong, A. D. Schofield, J. D. Selby, A. Nova, E. Clot and P. Mountford, *Chem. Commun.*, 2010, **46**, 85.
44. A. D. Schofield, A. Nova, J. D. Selby, A. D. Schwarz, E. Clot and P. Mountford, *Chem. Eur. J.*, 2011, **17**, 265.

45. H. Herrmann, J. L. Fillol, H. Wadepohl and L. H. Gade, *Angew. Chem. Int. Ed.*, 2007, **46**, 8426.
46. T. Carofiglio, C. Floriani, A. Chiesi-Villa and C. Guastini, *Inorg. Chem.*, 1989, **28**, 4417.
47. T. Carofiglio, P. G. Cozzi, C. Floriani, A. Chiesi-Villa and C. Rizzoli, *Organometallics*, 1993, **12**, 2726.
48. F. Ekkehardt Hahn and T. Lügger, *J. Organomet. Chem.*, 1995, **501**, 341.
49. L. B. Kool, M. D. Rausch, M. Herberhold, H. G. Alt, U. Thewalt and B. Honold, *Organometallics*, 1986, **5**, 2465.
50. A. Vogler, *Isonitrile Chemistry*, Academic Press, Inc., New York and London, 1971.
51. A. D. Schofield, A. Nova, J. D. Selby, C. D. Manley, A. D. Schwarz, E. Clot and P. Mountford, *J. Am. Chem. Soc.*, 2010, **132**, 10484.
52. D. C. Bradley and M. C. Ganorkar, *Chem. Ind.*, 1968, **44**, 1521.
53. G. Chandra, A. D. Jenkins, M. F. Lappert and R. C. Srivastava, *J. Chem. Soc., Sec. A*, 1970, **15**, 2550.
54. F. H. Allen, O. Kennard, D. G. Watson, L. Brammer, A. G. Orpen and R. Taylor, *J. Chem. Soc., Perkin Trans. 2*, 1987, S1.
55. M. J. Carney, P. J. Walsh, F. J. Hollander and R. G. Bergman, *Organometallics*, 1992, **11**, 761.
56. K. Weitershaus, H. Wadepohl and L. H. Gade, *Organometallics*, 2009, **28**, 3381.
57. P. J. Tiong, A. Nova, A. D. Schwarz, J. D. Selby, E. Clot and P. Mountford, *Dalton Trans.*, 2012, **41**, 2277.
58. G. Du, P. E. Fanwick and M. M. Abu-Omar, *J. Am. Chem. Soc.*, 2007, **129**, 5180.
59. A. J. Chalk and J. F. Harrod, *J. Am. Chem. Soc.*, 1965, **87**, 16.
60. N. Schneider, M. Finger, C. Haferkemper, S. Bellemin-Laponnaz, P. Hofmann and L. H. Gade, *Angew. Chem. Int. Ed.*, 2009, **48**, 1609.
61. N. Schneider, M. Finger, C. Haferkemper, S. Bellemin-Laponnaz, P. Hofmann and L. H. Gade, *Chem. Eur. J.*, 2009, **15**, 11515.
62. O. G. Shirobokov, S. I. Gorelsky, R. Simionescu, L. G. Kuzminac and G. I. Nikonov, *Chem. Commun.*, 2010, **46**, 7831.

63. E. Peterson, A. Y. Khalimon, R. Simionescu, L. G. Kuzmina, J. A. K. Howard and G. I. Nikonov, *J. Am. Chem. Soc.*, 2009, **131**, 908.

64. O. G. Shirobokov, L. G. Kuzmina and G. I. Nikonov, *J. Am. Chem. Soc.*, 2011, **133**, 6487.

65. A. Millan, E. Towns and P. M. Maitlis, *J. Chem. Soc. Chem. Comm.*, 1981, 673.

66. I. Ojima and M. Nihonyanagi, *J. Chem. Soc. Chem. Comm.*, 1972, 938.

67. I. Ojima, T. Kogure, M. Kumagai, S. Horiuchi and T. Sato, *J. Organomet. Chem.*, 1976, **122**, 83.

68. R. N. Perutz and S. B. Duckett, *Organometallics*, 1992, **11**, 90.

69. K. A. Nolin, J. R. Krumper, M. D. Pluth, R. G. Bergman and F. D. Toste, *J. Am. Chem. Soc.*, 2007, **129**, 14684.

70. P. J. Tiong, A. Nova, E. Clot and P. Mountford, *Chem. Commun.*, 2011, **47**, 3147.

Chapter Five

Experimental details and characterising data

5.1 General methods and instrumentation

All manipulations were carried out using standard Schlenk line or dry-box techniques under an atmosphere of argon or dinitrogen. Solvents were predried over activated 4 Å molecular sieves and refluxed over sodium (toluene), sodium/potassium alloy (pentane, diethyl ether), potassium (tetrahydrofuran), or calcium hydride (bromobenzene) under a dinitrogen atmosphere and collected by distillation. Alternatively, solvents were degassed by sparging with dinitrogen and dried by passing through a column of the appropriate drying agent.[1] Deuterated solvents were refluxed over the appropriate drying agent, distilled and stored under dinitrogen in Teflon valve ampoules.

Solution NMR samples were prepared under a dinitrogen atmosphere in 5 mm Wilmad 507-PP tubes fitted with J. Young Teflon valves. ^{1}H, ^{13}C{^{1}H}, ^{11}B, ^{19}F, ^{29}Si and ^{2}H NMR spectra were recorded on Varian Mercury-VX 300 or Varian Unity Plus 500 spectrometers. ^{13}C spectra were recorded on a Bruker AVC 500 spectrometer fitted with a ^{13}C cryoprobe. ^{1}H and ^{13}C{^{1}H} spectra are referenced internally to residual protio-solvent (^{1}H) or solvent (^{13}C) resonances, and are reported relative to tetramethylsilane (δ = 0 ppm). ^{2}H NMR spectra were referenced to the natural abundance deuterium resonance of the protio solvent. ^{19}F, ^{29}Si and ^{11}B spectra were referenced externally to $CFCl_3$, $SiMe_4$ and $Et_2O \cdot BF_3$, respectively. Assignments were confirmed as necessary with the use of DEPT-135, DEPT-90, and two dimensional ^{1}H-^{1}H and ^{13}C-^{1}H NMR correlation experiments. Chemical shifts are quoted in δ (ppm) and coupling constants in Hz. IR spectra were recorded on a Perkin Elmer Paragon 1000 FTIR or Nicolet Magna 560 E.S.P. FTIR spectrometer. Samples were prepared in a dry-box as Nujol mulls between NaCl plates, and the data are quoted in wavenumbers (cm^{-1}). Mass spectra were recorded by the mass spectrometry service of Oxford University's Department of Chemistry. Elemental analyses were carried out by Elemental Microanalysis Ltd, Devon or by the Elemental Analysis Service at the London Metropolitan University.

5.2 Literature preparations

Cp*Ti{MeC(N^{i}Pr)$_2$}(N^{t}Bu),[2] Cp*Ti{MeC(N^{i}Pr)$_2$}(NTol),[2] Cp*Ti{MeC(N^{i}Pr)$_2$}{N-(Tol)C(O)O},[2] Cp*Ti{MeC(N^{i}Pr)$_2$}(NNPh$_2$),[3, 4] Cp*Ti{MeC(N^{i}Pr)$_2$}(NNMe$_2$),[3, 4] $PhSiD_3$,[5, 6] Ar^FSiH_3 (Ar^F = 3,5-$C_6H_3(CF_3)_2$),[7] $Ar^{OMe}SiH_3$ (Ar^{OMe} = 4-C_6H_4OMe),[8]

$PhSiH_2Br$,[9] $[Et_3NH][BPh_4]$,[10] and $Ar^{F5}CCH$ (Ar^{F5} = C_6F_5)[11, 12] were prepared according to the literature methods. 1,1-diphenylhydrazine was obtained from Sigma-Aldrich as the hydrogen chloride salt, from which the free hydrazine was obtained by basification, drying and removal of residual solvent, followed by distillation under inert atmospheric conditions. 1,1-dimethylhydrazine and pyridine were dried over freshly ground CaH_2 and distilled before use. $B(C_6F_5)_3$ and the amine-boranes were kindly donated by LANXESS Elastomers BV and Professor S. Aldridge, respectively. Other reagents were obtained commercially and used as received.

5.3 Experimental details and characterising data for Chapter Two

Improved synthesis of Cp*Ti{MeC(N^{i}Pr)$_2$}(NNPh$_2$). To a stirred red solution of Cp*Ti{MeC(N^{i}Pr)$_2$}(N^{t}Bu) (1.70 g, 4.30 mmol) in benzene (10 mL) was added Ph_2NNH_2 (0.140 g, 0.760 mmol) in benzene (10 mL). The solution darkened and after 16 h the volatiles were removed under reduced pressure. The resultant solid was extracted into pentane (3 x 10 mL), filtered, and the volatiles were removed under reduced pressure to give Cp*Ti{MeC(N^{i}Pr)$_2$}(NNPh$_2$) as a dark yellow solid. Yield: 1.81 g (83%). The characterising data obtained are the same as previously reported in literature.

Improved synthesis of Cp*Ti{MeC(N^{i}Pr)$_2$}(NNMe$_2$). To a stirred solution of Cp*Ti{MeC(N^{i}Pr)$_2$}(N^{t}Bu) (1.12 g, 2.83 mmol) in benzene (10 mL) was added Me_2NNH_2 (0.216 mL, 2.83 mmol) in benzene (5 mL). The colour changed from red to dark green, and after 6 h the volatiles were removed under reduced pressure. The resultant waxy oil was recrystallised from pentane at -80 ℃. The solution was filtered, and the product was dried under reduced pressure to give Cp*Ti{MeC(N^{i}Pr)$_2$}(NNMe$_2$) as a dark green solid. Yield: 0.73 g (67%). The characterising data obtained are the same as previously reported in literature.

Cp*Ti{MeC(N^{i}Pr)$_2$}{N(NPh$_2$)C(O)O} (1). A solution of Cp*Ti{MeC(N^{i}Pr)$_2$}(NNPh$_2$) (0.300 g, 0.590 mmol) in toluene (20 mL) was freeze-pump-thawed three times. The solution was then exposed to CO_2 at a pressure of *ca.* 1.1 atm at -78 ℃. Immediately after the colour changed from dark yellow to dark brown (5 min), excess CO_2 and the other volatiles were removed under reduced pressure to afford **1** as a dark brown solid. The resultant dark brown solid was washed with cold pentane (3 × 5 mL) cooled to -78 ℃, filtered, and dried *in vacuo*. Yield:

0.175 g (54%). ^{1}H NMR (toluene-d_8, 499.9 MHz, 293 K): δ 7.51 (2 H, d, ^{3}J = 7.0 Hz, o_a-C_6H_5), 7.19 (2 H, m, m_a-C_6H_5), 6.95 (4 H, m, overlapping o_b-C_6H_5 and m_b-C_6H_5), 6.91 (1 H, t, ^{3}J = 7.0 Hz, p_a-C_6H_5), 6.73 (1 H, t, ^{3}J = 7.0 Hz, p_b-C_6H_5), 3.31 (1 H, app. sept., app. ^{3}J = 6.5 Hz, NC$\underline{H}_a$MeMe), 2.83 (1 H, app. sept., app. ^{3}J = 6.5 Hz, NC$\underline{H}_b$MeMe), 1.95 (15 H, s, C_5Me_5), 1.46 (3 H, s, $MeCN_2$), 1.16 (3 H, d, ^{3}J = 6.5 Hz, NCH$_a$Me$\underline{Me}$), 1.11 (3 H, d, ^{3}J = 6.5 Hz, NCH$_b$Me$\underline{Me}$), 1.09 (3 H, d, ^{3}J = 6.5 Hz, NCH$_a\underline{Me}$Me), 0.93 (3 H, d, ^{3}J = 6.5 Hz, NCH$_b\underline{Me}$Me). ^{13}C{^{1}H} NMR (toluene-d_8, 125.7 MHz, 293 K): δ 170.3 (Me$\underline{C}N_2$), 160.6 (OC(O)N), 147.9 (i_a-C_6H_5), 147.9 (i_b-C_6H_5), 130.4 ($\underline{C}_5Me_5$), 128.5 (m_a-C_6H_5, m_b-C_6H_5), 122.8 (p_a-C_6H_5), 122.4 (o_a-C_6H_5), 119.6 (p_b-C_6H_5), 117.0 (o_b-C_6H_5), 51.2 (N$\underline{C}$H$_a$MeMe), 50.2 (N$\underline{C}$H$_b$MeMe), 26.3 (NCH$_b$Me$\underline{Me}$), 24.6 (NCH$_b\underline{Me}$Me), 24.2 (NCH$_a$Me$\underline{Me}$), 24.1 (NCH$_a\underline{Me}$Me), 12.9 ($C_5\underline{Me}_5$), 12.6 ($\underline{Me}CN_2$). IR (NaCl plates, Nujol mull, cm^{-1}): 1684 (s), 1589 (m), 1492 (s), 1338 (m), 1206 (w), 1026 (w), 744 (m), 691 (m). EI-MS: *m/z* = 233 [*M* – Cp* – N(NPh$_2$)]$^{+}$ (30%), Anal. found (calcd. for $C_{31}H_{42}N_4O_2Ti$): C, 67.61 (67.63); H, 7.78 (7.69); N, 10.11 (10.18)%.

Cp*Ti{MeC(N^{i}Pr)$_2$}{N(NMe$_2$)C(O)O} (2). A solution of Cp*Ti{MeC(N^{i}Pr)$_2$}(NNMe$_2$) (0.250 g, 0.650 mmol) in toluene (15 mL) was freeze-pump-thawed three times. The solution was then exposed to CO_2 at a pressure of *ca.* 1.1 atm at -78 ℃. An immediate colour change from dark green to red was observed. Excess CO_2 and other volatiles were then removed under reduced pressure to afford **2** as a red-brown solid which was then washed with cold pentane (3 × 5 mL) cooled to -78 ℃, filtered, and dried *in vacuo*. Yield: 0.169 g (60%). ^{1}H NMR (toluene-d_8, 499.9 MHz, 263 K): δ 3.33 (1 H, app. sept., app. ^{3}J = 6.5 Hz, NC$\underline{H}_a$MeMe), 3.14 (1 H, app. sept., app. ^{3}J = 6.5 Hz, NC$\underline{H}_b$MeMe), 2.75 (6 H, s, NNMe$_2$), 2.02 (15 H, s, C_5Me_5), 1.47 (3 H, d, ^{3}J = 6.5 Hz, NCH$_a\underline{Me}$Me), 1.44 (3 H, s, $MeCN_2$), 1.12 (3 H, d, ^{3}J = 6.5 Hz, NCH$_a$Me$\underline{Me}$), 1.07 (6 H, overlapping 2 × d, ^{3}J = 6.5 Hz, overlapping NCH$_b\underline{Me}$Me and NCH$_b$Me$\underline{Me}$). ^{13}C{^{1}H} NMR (toluene-d_8, 125.7 MHz, 263 K): δ 170.4 (Me$\underline{C}N_2$), 158.1 (OC(O)N), 128.2 ($\underline{C}_5Me_5$), 50.9 (N$\underline{C}$H$_a$MeMe), 50.7 (N$\underline{C}$H$_b$MeMe), 46.1 (NNMe$_2$), 26.6 (NCH$_a\underline{Me}$Me), 24.1 (NCH$_a$Me$\underline{Me}$), 23.7 (NCH$_b\underline{Me}$Me), 23.3 (NCH$_b$Me$\underline{Me}$), 12.7 ($C_5\underline{Me}_5$), 11.4 ($\underline{Me}CN_2$). IR (NaCl plates, Nujol mull, cm^{-1}): 1667 (s), 1457 (s), 1341 (m), 1314 (m), 1204 (m), 1174 (w), 1126 (m), 1092 (m), 1015 (m), 973 (w), 888 (m), 789 (m), 721 (m). EI-MS: *m/z* = 426 [*M*]$^{+}$

(20%), 324 [M – OC(O)N(NMe_2)]$^+$ (80%). Anal. found (calcd. for $C_{21}H_{38}N_4O_2Ti$): C, 59.10 (59.15); H, 8.90 (8.98); N, 13.08 (13.14)%.

Cp*Ti{MeC(N^{i}Pr)$_2$}{OC(O)N(NPh$_2$)C(O)O} (3). A solution of Cp*Ti{MeC(N^{i}Pr)$_2$}($NNPh_2$) (0.300 g, 0.590 mmol) in toluene (20 mL) was freeze-pump-thawed three times. The solution was then exposed to CO_2 at a pressure of *ca.* 1.1 atm at RT. An immediate colour change from dark yellow to dark brown was observed. After 3 d, excess CO_2 and the other volatiles were removed under reduced pressure to afford **3** as a dark brown solid which was then washed with cold pentane (3 × 5 mL) cooled to -78 ℃, filtered, and dried *in vacuo*. Yield: 0.247 g (70%). Diffraction-quality crystals were grown by slow evaporation of a diethyl ether solution. ^{1}H NMR (C_6D_6, 299.9 MHz, 293 K): δ 7.88 (2 H, d, ^3J = 7.2 Hz, o_a-C_6H_5), 7.27 (2H, m, o_b-C_6H_5), 7.24 (2 H, m, m_a-C_6H_5), 7.09 (2 H, m, m_b-C_6H_5), 6.98 (1 H, t, ^3J = 7.2 Hz, p_b-C_6H_5), 6.78 (1 H, t, ^3J = 7.2 Hz, p_a-C_6H_5), 3.42 (2 H, app. sept., app. ^3J = 6.6 Hz, NC<u>H</u>MeMe), 1.87 (15 H, s, C_5Me_5), 1.39 (3 H, s, MeCN_2), 1.05 (12 H, overlapping 2 × d, ^3J = 6.6 Hz, NCH<u>Me</u>Me, NCHMe<u>Me</u>). ^{13}C{^{1}H} NMR (C_6D_6, 75.4 MHz, 293 K): δ 169.5 (Me<u>C</u>N_2), 152.7 (OC(O)N), 146.7 (i_b-C_6H_5), 146.0 (i_a-C_6H_5), 131.6 (<u>C</u>$_5$Me$_5$), 129.2 (m_a-C_6H_5), 129.0 (m_b-C_6H_5), 123.9 (p_a-C_6H_5), 123.5 (o_a-C_6H_5), 120.9 (p_b-C_6H_5), 117.4 (o_b-C_6H_5), 50.6 (N<u>C</u>HMeMe), 24.1 (NCH<u>Me</u>Me), 23.5 (NCHMe<u>Me</u>), 14.3 (<u>Me</u>CN_2), 12.7 (C_5<u>Me</u>$_5$). IR (NaCl plates, Nujol mull, cm^{-1}): 2205 (w), 1715 (s), 1676 (s), 1590 (m), 1496 (s), 1365(s), 1330 (s), 1209 (m), 1174 (m), 1122 (m), 1030 (w), 925 (w), 794(m), 745 (m), 691(m), 671 (w), 623 (w). EI-MS: *m/z* = 459 [M – Cp*]$^+$ (10%), 426 [M – NPh_2]$^+$ (10%). Anal. found (calcd. for $C_{32}H_{42}N_4O_4Ti$): C, 64.58 (64.64); H, 7.14 (7.12); N, 9.37 (9.42)%.

Cp*Ti{MeC(N^{i}Pr)$_2$}{OC(O)N(NMe$_2$)C(O)O} (4). A solution of Cp*Ti{MeC(N^{i}Pr)$_2$}($NNMe_2$) (0.300 g, 0.590 mmol) in toluene (20 mL) was freeze-pump-thawed three times. The solution was then exposed to CO_2 at a pressure of *ca.* 1.1 atm at RT. An immediate colour change from dark green to red was observed. After 16 h, the excess CO_2 and the other volatiles were removed under reduced pressure to afford **4** as a light brown solid. The solid was washed with cold pentane (3 × 5 mL) cooled to -78 ℃, filtered, and dried *in vacuo*. Yield: 0.268 g (73%). Diffraction-quality crystals were grown by slow evaporation of a diethyl ether solution. ^{1}H NMR (toluene-d_8, 499.9 MHz, 253 K): δ 3.35 (2 H, app. sept., app. ^3J = 7.0 Hz, NC<u>H</u>MeMe), 3.13 (3 H, s, NN<u>Me</u>Me), 3.01 (3 H, s, NNMe<u>Me</u>), 1.91 (15 H, s,

C_5Me_5), 1.29 (3 H, s, $MeCN_2$), 1.10 (6 H, d, ^3J = 7.0 Hz, NCH<u>Me</u>Me), 1.08 (6 H, d, ^3J = 7.0 Hz, NCHMe<u>Me</u>). $^{13}C\{^1H\}$ NMR (toluene-d_8, 125.7 MHz, 253 K): δ 169.2 ($Me\underline{C}N_2$), 152.8 (OC(O)N), 130.5 ($\underline{C}_5Me_5$), 50.4 (N<u>C</u>HMeMe), 43.3 (NNMe<u>Me</u>), 43.0 (NN<u>Me</u>Me), 23.8 (NCH<u>Me</u>Me), 23.7 (NCHMe<u>Me</u>), 13.5 ($\underline{Me}CN_2$), 12.6 ($C_5\underline{Me}_5$). IR (NaCl plates, Nujol mull, cm^{-1}): 1702 (s), 1655 (s), 1458(s), 1360 (s), 1204 (m), 1170 (m), 1113 (m), 1023 (w), 796 (m), 772 (m), 668 (w). EI-MS: *m/z* = 324 $[M - OC(O)N(NMe_2)C(O)O]^+$ (100%), 412 $[M - NNMe_2]^+$ (80%). Anal. found (calcd. for $C_{22}H_{38}N_4O_4Ti$): C, 56.07 (56.17); H, 8.22 (8.14); N, 11.83 (11.91)%.

NMR tube scale reaction of Cp*Ti{MeC(N^{i}Pr)$_2$}{N(NPh$_2$)C(O)O} (1) with CO_2. 10.0 mg (0.018 mmol) Cp*Ti{MeC(N^{i}Pr)$_2$}{N(NPh$_2$)C(O)O} (**1**) was dissolved in C_6D_6 (0.6 mL), and freeze-pump-thawed three times. The solution was then exposed to CO_2 at a pressure of *ca.* 1.1 atm at RT. The reaction was monitored by ^1H NMR spectroscopy. The ^1H NMR spectrum recorded after 3 d showed quantitative formation of Cp*Ti{MeC(N^{i}Pr)$_2$}{OC(O)N(NPh$_2$)C(O)O} (**3**).

Cp*Ti{MeC(N^{i}Pr)$_2$}{N(NPh$_2$)C(S)S} (5). To a solution of Cp*Ti{MeC(N^{i}Pr)$_2$}(NNPh$_2$) (0.300 g, 0.590 mmol) in benzene (20 mL) was added an excess of CS_2 (0.107 mL, 1.78 mmol) all at RT. The resulting dark brown solution was stirred for 16 h. Volatiles were then removed under reduced pressure to afford **5** as a dark brown solid. The solid was washed with cold pentane (3 × 5 mL) cooled to -78 ℃, filtered, and dried *in vacuo*. Yield: 0.245 g (71%). ^1H NMR (toluene-d_8, 499.9 MHz, 263 K): δ 7.47 (4 H, d, ^3J = 6.5 Hz, *o*-C_6H_5), 7.18 (4 H, t, ^3J = 6.5 Hz, *m*-C_6H_5), 6.90 (2 H, t, ^3J = 6.5 Hz, *p*-C_6H_5), 3.34 (1 H, app. sept., app. ^3J = 6.5 Hz, NC<u>H</u>$_a$MeMe), 3.17 (1 H, app. sept., app. ^3J = 6.5 Hz, NC<u>H</u>$_b$MeMe), 1.91 (15 H, s, C_5Me_5), 1.46 (3 H, s, $MeCN_2$), 1.10 (3 H, d, ^3J = 6.5 Hz, NCH$_a$<u>Me</u>Me), 1.04 (3 H, d, ^3J = 6.5 Hz, NCH$_a$Me<u>Me</u>), 0.90 (3 H, d, ^3J = 6.5 Hz, NCH$_b$<u>Me</u>Me), 0.86 (3 H, d, ^3J = 6.5 Hz, NCH$_b$Me<u>Me</u>). $^{13}C\{^1H\}$ NMR (toluene-d_8, 125.7 MHz, 263 K): δ 166.3 ($Me\underline{C}N_2$), 149.1 (overlapping *i*-C_6H_5 and SC(S)N), 131.0 ($\underline{C}_5Me_5$), 128.6 (*m*-C_6H_5), 121.6 (overlapping *o*- and *p*-C_6H_5), 50.9 (overlapping N<u>C</u>H$_a$MeMe and N<u>C</u>H$_b$MeMe), 24.7 (NCH$_a$<u>Me</u>Me), 24.2 (overlapping NCH$_a$Me<u>Me</u> and <u>N</u>CH$_b$<u>Me</u>Me), 24.0 (NCH$_b$Me<u>Me</u>), 13.8 ($C_5\underline{Me}_5$), 13.3 ($\underline{Me}CN_2$). IR (NaCl plates, Nujol mull, cm^{-1}): 1587 (s), 1491 (s), 1401 (m), 1333(m), 1310 (m), 1276 (m), 1203 (s), 750 (m), 603 (m). EI-MS: *m/z* = 279 $[M - Cp^* - NPh_2]^+$ (10%). Anal. found (calcd. for $C_{31}H_{42}N_4S_2Ti$): C, 63.88 (63.90); H, 7.40 (7.27); N, 9.55 (9.62)%.

Cp*Ti{MeC(N^{i}Pr)$_2$}{N(NMe$_2$)C(S)S} (6). To a solution of Cp*Ti{MeC(N^{i}Pr)$_2$}(NNMe$_2$) (0.300 g, 0.780 mmol) in benzene (20 mL) was added an excess of CS_2 (0.142 mL, 2.35 mmol) all at RT. The resulting dark brown solution was stirred for 16 h. Volatiles were then removed under reduced pressure to afford **6** as a dark brown solid. The solid was washed with cold pentane (3 × 5 mL) cooled to -78 ℃, filtered, and dried *in vacuo*. Yield: 0.150 g (42%). ^{1}H NMR (toluene-d_8, 499.9 MHz, 263 K): δ 3.34 (1 H, app. sept., app. ^3J = 6.5 Hz, NC$\underline{H}_a$MeMe), 3.33 (1 H, app. sept., app. ^3J = 6.5 Hz, NC$\underline{H}_b$MeMe), 2.78 (6 H, s, NNMe$_2$), 1.99 (15 H, s, C_5Me_5), 1.48 (3 H, s, MeCN$_2$), 1.09 (3 H, d, ^3J = 6.5 Hz, NCH$_a\underline{Me}$Me), 1.08 (3 H, d, ^3J = 6.5 Hz, NCH$_b\underline{Me}$Me), 1.04 (3 H, d, ^3J = 6.5 Hz, NCH$_a$Me$\underline{Me}$), 1.03 (3 H, d, ^3J = 6.5 Hz, NCH$_b$Me$\underline{Me}$). ^{13}C{^{1}H} NMR (toluene-d_8, 125.7 MHz, 263 K): δ 166.1 (Me$\underline{C}$N$_2$), 156.5 (SC(S)N), 130.3 ($\underline{C}_5$Me$_5$), 50.8 (overlapping N$\underline{C}$H$_a$MeMe and N$\underline{C}$H$_b$MeMe), 47.7 (NNMe$_2$), 24.6 (NCH$_a\underline{Me}$Me), 24.6 (NCH$_b\underline{Me}$Me), 24.4 (NCH$_a$Me$\underline{Me}$), 24.3 (NCH$_b$Me$\underline{Me}$), 13.9 ($C_5\underline{Me}_5$), 13.5 ($\underline{Me}$CN$_2$). IR (NaCl plates, Nujol mull, cm^{-1}): 2805 (m), 2759(w), 1507 (s), 1457 (s), 1399 (w), 1338 (m), 1309 (w), 1205 (s), 1173 (w), 1155 (w), 1117 (m), 1017 (m), 968 (m), 928 (m), 817 (m). EI-MS: *m/z* = 324 [*M* – SC(S)N(NMe$_2$)]$^+$ (10%), 273 [*M* – MeC(N^{i}Pr)$_2$]$^+$ (30%), 182 [Ti{SC(S)N(NMe$_2$)}]$^+$ (20%). Anal. found (calcd. for $C_{21}H_{38}N_4S_2Ti$): C, 54.90 (55.00); H, 8.27 (8.35); N, 12.15 (12.22)%.

NMR tube scale reaction of Cp*Ti{MeC(N^{i}Pr)$_2$}{N(NPh$_2$)C(O)O} (1) with CS$_2$. To a solution of Cp*Ti{MeC(N^{i}Pr)$_2$}{N(NPh$_2$)C(O)O} (**1**, 10.0 mg, 0.018 mmol) in C_6D_6 (0.6 mL) in an NMR tube equipped with a J. Young Teflon valve was added CS_2 (3.30 μL, 0.055 mmol) all at RT. The ^{1}H NMR spectrum recorded after 16 h contained resonances attributed to Cp*Ti{MeC(N^{i}Pr)$_2$}{OC(O)N(NPh$_2$)C(O)O} (**3**) and Cp*Ti{MeC(N^{i}Pr)$_2$}{N(NPh$_2$)C(S)S} (**5**).

NMR tube scale reaction of Cp*Ti{MeC(N^{i}Pr)$_2$}(NNMe$_2$) with Cp*Ti{MeC(N^{i}Pr)$_2$}{N(NPh$_2$)C(O)O} (1). To a solution of Cp*Ti{MeC(N^{i}Pr)$_2$}(NNMe$_2$) (6.95 mg, 0.018 mmol) in C_6D_6 (0.3 mL) in an NMR tube equipped with a J. Young Teflon valve was added Cp*Ti{MeC(N^{i}Pr)$_2$}{N(NPh$_2$)C(O)O} (**1**, 10.0 mg, 0.018 mmol) in C_6D_6 (0.3 mL) all at RT. The ^{1}H NMR spectrum recorded immediately contained resonances attributed to Cp*Ti{MeC(N^{i}Pr)$_2$}{N(NMe$_2$)C(O)O} (**2**) and Cp*Ti{MeC(N^{i}Pr)$_2$}(NNPh$_2$).

NMR tube scale reaction of Cp*Ti{MeC(N^{i}Pr)$_2$}{N(NPh$_2$)C(O)O} (1) with Cp*Ti{MeC(N^{i}Pr)$_2$}(NTol). To a solution of Cp*Ti{MeC(N^{i}Pr)$_2$}{N(NPh$_2$)C(O)O} (**1**, 10.0 mg, 0.018 mmol) in C_6D_6 (0.3 mL) in an NMR tube equipped with a J. Young Teflon valve was added Cp*Ti{MeC(N^{i}Pr)$_2$}(NTol) (7.80 mg, 0.018 mmol) in C_6D_6 (0.3 mL) all at RT. The ^{1}H NMR spectrum recorded after 3 d at RT and then heating at 60 ℃ for a further 16 h contained resonances attributed to Cp*Ti{MeC(N^{i}Pr)$_2$}{N(NPh$_2$)C(NTol)O} (**7**) and [Cp*Ti{MeC(N^{i}Pr)$_2$}(μ-O)]$_2$.

NMR tube scale reaction of Cp*Ti{MeC(N^{i}Pr)$_2$}(NNPh$_2$) with Cp*Ti{MeC(N^{i}Pr)$_2$}{N(Tol)C(O)O}. To a solution of Cp*Ti{MeC(N^{i}Pr)$_2$}(NNPh$_2$) (14.6 mg, 0.029 mmol) in C_6D_6 (0.3 mL) in an NMR tube equipped with a J. Young Teflon valve was added Cp*Ti{MeC(N^{i}Pr)$_2$}{N(Tol)C(O)O} (13.6 mg, 0.029 mmol) in C_6D_6 (0.3 mL) all at RT. The ^{1}H NMR spectrum recorded after 16 h contained resonances attributed to Cp*Ti{MeC(N^{i}Pr)$_2$}{N(NPh$_2$)C(NTol)O} (**7**) and [Cp*Ti{MeC(N^{i}Pr)$_2$}(μ-O)]$_2$.

NMR tube scale reaction of Cp*Ti{MeC(N^{i}Pr)$_2$}(NNPh$_2$) with Cp*Ti{MeC(N^{i}Pr)$_2$}{N(NMe$_2$)C(S)S} (6). To a solution of Cp*Ti{MeC(N^{i}Pr)$_2$}{N(NMe$_2$)C(S)S} (**6**, 12.0 mg, 0.026 mmol) in C_6D_6 (0.3 mL) in an NMR tube equipped with a J. Young Teflon valve was added Cp*Ti{MeC(N^{i}Pr)$_2$}(NNPh$_2$) (13.0 mg, 0.026 mmol) in C_6D_6 (0.3 mL) at RT. The reaction was monitored by ^{1}H NMR spectroscopy. [Cp*Ti{MeC(N^{i}Pr)$_2$}(μ-S)]$_2$ and Cp*Ti{MeC(N^{i}Pr)$_2$}{N(NPh$_2$)C(NNMe$_2$)S} (**8**) were formed quantitatively after 4 d. **8** was characterised by NMR spectroscopy. ^{1}H NMR data (C_6D_6, 499.9 MHz, 293 K): δ 7.52 (1 H, d, ^3J = 7.5 Hz, o_a-C$_6$H$_5$), 7.30 (1 H, d, ^3J = 7.5 Hz, o_b-C$_6$H$_5$), 7.21 (2 H, app. t, app. ^3J = 7.5 Hz, m_a-C$_6$H$_5$), 7.10 (2 H, app. t, app. ^3J = 7.5 Hz, m_b-C$_6$H$_5$), 6.88 (2 H, t, ^3J = 7.5 Hz, p_a-C$_6$H$_5$), 6.79 (2 H, t, ^3J = 7.5 Hz, p_b-C$_6$H$_5$), 3.29 (1 H, app. sept., app. ^3J = 6.5 Hz, NC<u>H</u>$_a$MeMe), 2.97 (1 H, app. sept., app. ^3J = 6.5 Hz, NC<u>H</u>$_b$MeMe), 2.51 (6 H, s, NNMe$_2$), 1.96 (15 H, s, C$_5$Me$_5$), 1.50 (3 H, s, MeCN$_2$), 1.20 (6 H, overlapping 2 × d, ^3J = 6.5 Hz, overlapping NCH$_a$<u>Me</u>Me and NCH$_b$<u>Me</u>Me), 1.17 (3 H, d, ^3J = 6.5 Hz, NCH$_a$Me<u>Me</u>), 0.83 (3 H, d, ^3J = 6.5 Hz, NCH$_b$Me<u>Me</u>). ^{13}C{^{1}H} NMR (C_6D_6, 125.7 MHz, 293 K): δ 168.7 (Me<u>C</u>N$_2$), 156.0 (SC(N)N), 147.4 (i_a-C$_6$H$_5$) 147.4 (i_b-C$_6$H$_5$), 129.2 (<u>C</u>$_5$Me$_5$), 128.3 (m_a-C$_6$H$_5$), 128.1 (m_b-C$_6$H$_5$), 121.7 (p_a-C$_6$H$_5$), 121.3 (o_a-C$_6$H$_5$), 119.4 (p_b-C$_6$H$_5$), 117.7 (o_b-C$_6$H$_5$), 51.6

(N<u>C</u>H$_a$MeMe), 49.4 (N<u>C</u>H$_b$MeMe), 48.7 (NNMe$_2$), 26.3 (NCH$_b$<u>Me</u>Me), 25.5 (NCH$_b$Me<u>Me</u>), 24.6 (NCH$_a$Me<u>Me</u>), 23.5 (NCH$_a$<u>Me</u>Me), 14.2 (<u>Me</u>CN$_2$), 13.5 (C$_5$<u>Me</u>$_5$).

Cp*Ti{MeC(N^{i}Pr)$_2$}{N(NPh$_2$)C(NTol)O} (7). To a solution of Cp*Ti{MeC(N^{i}Pr)$_2$}(NNPh$_2$) (0.400 g, 0.790 mmol) in benzene (20 mL) was added TolNCO (0.100 mL, 0.790 mmol) all at RT. An immediate colour change from dark yellow to dark brown was observed. After 16 h, the volatiles were removed under reduced pressure to afford **7** as a dark brown solid which was then washed with cold pentane (3 × 5 mL) cooled to -78 ℃, filtered, and dried *in vacuo*. Yield: 0.342 g (68%). ^{1}H NMR (C$_6$D$_6$, 299.9 MHz, 293 K): δ 7.71 (2 H, d, ^3J = 7.5 Hz, *o*$_a$-C$_6$H$_5$), 7.65 (2 H, d, ^3J = 7.5 Hz, *o*-C$_6$<u>H</u>$_4$Me), 7.20 (2 H, t, ^3J = 7.5 Hz, *m*$_a$-C$_6$H$_5$), 7.10 (4 H, m, overlapping *o*$_b$-C$_6$H$_5$ and *m*-C$_6$<u>H</u>$_4$Me), 7.02 (2 H, t, ^3J = 7.5 Hz, *m*$_b$-C$_6$H$_5$), 6.90 (1 H, t, ^3J = 7.5 Hz, *p*$_a$-C$_6$H$_5$), 6.74 (1 H, t, ^3J = 7.5 Hz, *p*$_b$-C$_6$H$_5$), 3.29 (1 H, app. sept., app. ^3J = 6.5 Hz, NC<u>H</u>$_a$MeMe), 2.82 (1 H, app. sept., app. ^3J = 6.5 Hz, NC<u>H</u>$_b$MeMe), 2.18 (3 H, s, C$_6$H$_4$<u>Me</u>), 1.96 (15 H, s, C$_5$Me$_5$), 1.40 (3 H, s, MeCN$_2$), 1.17 (3 H, d, ^3J = 6.5 Hz, NCH$_b$<u>Me</u>Me), 1.11 (6 H, overlapping 2 × d, ^3J = 6.5 Hz, overlapping NCH$_a$<u>Me</u>Me and NCH$_a$Me<u>Me</u>), 0.93 (3 H, d, ^3J = 6.5 Hz, NCH$_b$Me<u>Me</u>). ^{13}C{^{1}H} NMR (C$_6$D$_6$, 75.4 MHz, 293 K): δ 169.4 (Me<u>C</u>N$_2$), 155.9 (OC(N)N), 147.7 (overlapping *i*$_a$-C$_6$H$_5$ and *i*$_b$-C$_6$H$_5$), 147.2 (*i*-<u>C</u>$_6$H$_4$Me), 129.7 (*p*-<u>C</u>$_6$H$_4$Me), 129.6 (<u>C</u>$_5$Me$_5$), 129.0 (*m*-<u>C</u>$_6$H$_4$Me), 128.7 (*m*$_a$-C$_6$H$_5$), 128.4 (*m*$_b$-C$_6$H$_5$), 125.8 (*o*-<u>C</u>$_6$H$_4$Me), 122.41 (*p*$_a$-C$_6$H$_5$), 122.2 (*o*$_a$-C$_6$H$_5$), 119.3 (*p*$_b$-C$_6$H$_5$), 117.2 (*o*$_b$-C$_6$H$_5$), 50.9 (N<u>C</u>H$_a$MeMe), 49.9 (N<u>C</u>H$_b$MeMe), 26.3 (NCH$_b$Me<u>Me</u>), 24.8 (NCH$_b$<u>Me</u>Me), 24.4 (NCH$_a$Me<u>Me</u>), 24.2 (NCH$_a$<u>Me</u>Me), 21.0 (C$_6$H$_4$<u>Me</u>), 12.9 (C$_5$<u>Me</u>$_5$), 12.7 (<u>Me</u>CN$_2$). IR (NaCl plates, Nujol mull, cm^{-1}): 1619 (m), 1587 (s), 1491 (s), 1336 (m), 1315 (m), 1206 (m), 1173 (w), 1124 (w), 1027 (w), 982 (w), 811 (w), 743 (m), 691 (w). EI-MS: *m/z* = 506 [*M* – OC(NTol)]$^+$ (20%). A satisfactory elemental analysis could not be obtained.

Cp*Ti{MeC(N^{i}Pr)$_2$}{N(NPh$_2$)C(NAr´)O} (Ar´ = 2,6-C$_6$H$_3$^{i}Pr$_2$) (9). To a solution of Cp*Ti{MeC(N^{i}Pr)$_2$}(NNPh$_2$) (0.300 g, 0.590 mmol) in benzene (20 mL) was added Ar´NCO (0.127 mL, 0.590 mmol) all at RT. The resulting dark green-brown solution was stirred for 16 h. Volatiles were then removed under reduced pressure to afford **9** as a dark green-brown solid. The solid was washed with cold pentane (3 × 5 mL) cooled to -78 ℃, filtered, and dried *in vacuo*. Yield: 0.298 g (71%). Diffraction-quality crystals were grown by slow cooling of a saturated hexanes solution. ^{1}H NMR

(C_6D_6, 299.9 MHz, 293 K): δ 7.69 (2 H, d, ^3J = 7.6 Hz, o_a-C_6H_5), 7.26 (2 H, d, ^3J = 7.6 Hz, o_b-C_6H_5), 7.24 (2 H, t, ^3J = 7.6 Hz, m_a-C_6H_5), 7.04 (4 H, m, overlapping m_b-C_6H_5 and m-$C_6\underline{H}_3(^i Pr_2)$), 6.92 (1 H, t, ^3J = 7.6 Hz, p_a-C_6H_5), 6.83 (1 H, t, ^3J = 7.6 Hz, p_b-C_6H_5), 6.75 (1 H, t, ^3J = 7.6 Hz, p-$C_6\underline{H}_3{}^i Pr_2$), 3.44 (2 H, app. sept., app. ^3J = 6.9 Hz, $C_6H_3(C\underline{H}MeMe)_2$), 3.32 (1 H, app. sept., app. ^3J = 6.6 Hz, $NC\underline{H}_aMeMe$ *trans* to N), 2.87 (1 H, app. sept., app. ^3J = 6.6 Hz, $NC\underline{H}_bMeMe$ *trans* to O), 1.93 (15 H, s, C_5Me_5), 1.49 (3 H, s, $MeCN_2$), 1.32 (3 H, d, ^3J = 6.9 Hz, $C_6H_3(CH\underline{Me}Me)_2$), 1.26 (3 H, d, ^3J = 6.9 Hz, $C_6H_3(CHMe\underline{Me})_2$), 1.16 (3 H, d, ^3J = 6.6 Hz, $NCH_bMe\underline{Me}$), 1.06 (3 H, d, ^3J = 6.6 Hz, $NCH_aMe\underline{Me}$), 0.88 (6 H, overlapping 2 × d, ^3J = 6.6 Hz, overlapping $NCH_a\underline{Me}Me$ and $NCH_b\underline{Me}Me$). $^{13}C\{^1H\}$ NMR (C_6D_6, 75.4 MHz, 293 K): δ 168.2 ($Me\underline{C}N_2$), 152.2 (OC(N)N), 148.1 (i_a-C_6H_5), 147.7 (i_b-C_6H_5), 144.7 (i-$\underline{C}_6H_3(^i Pr_2)$), 140.2 ($o$-$\underline{C}_6H_3(^i Pr_2)$), 129.7 ($\underline{C}_5Me_5$), 128.7 (overlapping m_a-C_6H_5 and m_b-C_6H_5), 122.6 (overlapping o_a-C_6H_5, p_a-C_6H_5 and p_b-C_6H_5), 122.1 (o_b-C_6H_5), 119.1 (p-$\underline{C}_6H_3(^i Pr_2)$), 116.8 ($m$-$\underline{C}_6H_3(^i Pr_2)$), 50.5 ($N\underline{C}H_aMeMe$), 49.8 ($N\underline{C}H_bMeMe$), 29.0 ($C_6H_3(\underline{C}HMeMe)_2$), 26.1 ($NCH_bMe\underline{Me}$), 25.0 ($NCH_aMe\underline{Me}$), 24.7 ($NCH_b\underline{Me}Me$), 24.4 ($NCH_a\underline{Me}Me$), 23.2 (overlapping $C_6H_3(CH\underline{MeMe})_2$), 13.6 ($\underline{Me}CN_2$), 13.1 ($C_5\underline{Me}_5$). IR (NaCl plates, Nujol mull, cm^{-1}): 1622 (s), 1583 (s), 1460 (s), 1318 (s), 1274 (m), 1208 (s), 1176 (m), 1128 (m), 1027 (w), 979 (s), 815 (m), 756 (m), 742 (s), 715 (w), 692 (w), 551(w). EI-MS: *m/z* = 506 $[M - OC(NAr')]^+$ (10%), 369 $[N(NPh_2)C(NAr')]^+$ (40%). Anal. found (calcd. for $C_{43}H_{59}N_5OTi$): C, 72.64 (72.76); H, 8.47 (8.38); N, 9.93 (9.87)%.

Cp*Ti{MeC(N^{i}Pr)$_2$}{N(NPh$_2$)C(NTol)S} (10). To a solution of Cp*Ti{MeC(N^{i}Pr)$_2$}(NNPh$_2$) (0.300 g, 0.590 mmol) in benzene (15 mL) was added TolNCS (88.0 mg, 0.590 mmol) in benzene (15 mL) all at RT. The resulting dark green solution was stirred for 16 h. Volatiles were then removed under reduced pressure to afford **10** as a dark green solid. The solid was washed with cold pentane (3 × 5 mL) cooled to -78 ℃, filtered, and dried *in vacuo*. Yield: 0.210 g (54%). ^1H NMR (C_6D_6, 299.9 MHz, 293 K): δ 7.57 (2 H, d, ^3J = 7.5 Hz, o_a-C_6H_5), 7.36 (2 H, d, ^3J = 7.5 Hz, o_b-C_6H_5), 7.21 (2H, t, ^3J = 7.5 Hz, m_a-C_6H_5), 7.12 (4 H, m, overlapping m_b-C_6H_5 and m-$C_6\underline{H}_4Me$), 6.97 (2 H, d, ^3J = 8.4 Hz, o-$C_6\underline{H}_4Me$,), 6.89 (1 H, t, ^3J = 7.5 Hz, p_a-C_6H_5), 6.79 (1 H, t, ^3J = 7.5 Hz, p_b-C_6H_5), 3.25 (1 H, app. sept., app. ^3J = 6.6 Hz, $NC\underline{H}_aMeMe$), 2.98 (1 H, app. sept., app. ^3J = 6.6 Hz, $NC\underline{H}_bMeMe$), 2.08 (3 H, s, $C_6H_4\underline{Me}$), 1.94 (15 H, s, C_5Me_5), 1.51 (3 H, s, $MeCN_2$), 1.21 (6 H, overlapping 2 × d,

^3J = 6.6 Hz, overlapping NCH$_a$MeMe and NCH$_b$MeMe), 1.10 (3 H, d, ^3J = 6.6 Hz, NCH$_a$MeMe), 0.97 (3 H, d, ^3J = 6.6 Hz, NCH$_b$MeMe). ^{13}C{^{1}H} NMR (C_6D_6, 75.4 MHz, 293 K): δ 169.1 (MeCN$_2$), 154.7 (SC(N)N), 147.5 (overlapping i_a-C_6H_5, i_b-C_6H_5 and i-C_6H_4Me), 130.9 (p-C_6H_4Me), 129.8 (C_5Me_5), 129.0 (o-C_6H_4Me), 128.5 (m_a-C_6H_5), 123.7 (overlapping m-C_6H_4Me and m_b-C_6H_5), 121.9 (p_a-C_6H_5), 121.4 (o_a-C_6H_5), 119.5 (p_b-C_6H_5), 117.7 (o_b-C_6H_5), 51.9 (NCH$_a$MeMe), 49.6 (NCH$_b$MeMe), 26.3 (NCH$_b$MeMe), 25.5 (NCH$_b$MeMe), 24.6 (NCH$_a$MeMe), 23.5 (NCH$_a$MeMe), 20.9 (C_6H_4 Me), 14.2 (MeCN$_2$), 13.6 (C_5Me_5). IR (NaCl plates, Nujol mull, cm^{-1}): 1577 (s), 1490 (s), 1412 (m), 1327 (m), 1313 (m), 1278 (m), 1204 (m), 1167 (m), 1153 (m), 1104 (m), 1042 (m), 1020 (m), 944 (w), 810 (m), 763 (w), 740 (m), 690 (m), 649 (w). EI-MS: *m/z* = 338 [*M* – TolNCS – NPh$_2$]$^+$ (20%). Anal. found (calcd. for $C_{38}H_{49}N_5STi$): C, 69.63 (69.60); H, 7.60 (7.53); N, 10.63 (10.68)%.

Cp*Ti{MeC(N^{i}Pr)$_2$}{N(NPh$_2$)C(NAr′)S} (Ar′ = 2,6-C$_6$H$_3$^{i}Pr$_2$) (11). To a solution of Cp*Ti{MeC(N^{i}Pr)$_2$}(NNPh$_2$) (0.300 g, 0.590 mmol) in benzene (20 mL) was added Ar′NCS (0.129 mL, 0.590 mmol) all at RT. The resulting dark green solution was stirred for 16 h. Volatiles were then removed under reduced pressure to afford **11** as a dark green solid. The resultant solid was washed with cold pentane (3 × 5 mL) cooled to -78 ℃, filtered, and dried *in vacuo*. Yield: 0.215 g (50%). Diffraction-quality crystals were grown by slow cooling of a saturated hexanes solution. ^{1}H NMR (C_6D_6, 299.9 MHz, 293 K): δ 7.57 (2 H, d, ^3J = 7.8 Hz, o_a-C_6H_5), 7.36 (2 H, d, ^3J = 7.8 Hz, o_b-C_6H_5), 7.23 (2 H, t, ^3J = 7.8 Hz, m_a-C_6H_5), 7.19 (2 H, m, m-C_6H_3(^{i}Pr$_2$)), 7.10 (2 H, t, ^3J = 7.8 Hz, m_b-C_6H_5), 7.07 (1 H, m, p-C_6H_3(^{i}Pr$_2$)), 6.88 (1 H, t, ^3J = 7.8 Hz, p_a-C_6H_5), 6.79 (1 H, t, ^3J = 7.8 Hz, p_b-C_6H_5), 3.19 (1 H, m, C_6H_3(CH$_a$MeMe)), 3.17 (1 H, m, NCH$_a$MeMe), 3.14 (1 H, m, C_6H_3(CH$_b$MeMe)), 3.06 (1 H, m, NCH$_b$MeMe), 1.92 (15 H, s, C_5Me_5), 1.59 (3 H, d, ^3J = 6.9 Hz, C_6H_3(CH$_a$MeMe)), 1.55 (3 H, s, MeCN$_2$), 1.34 (3 H, d, ^3J = 6.9 Hz, C_6H_3(CH$_b$MeMe)), 1.18 (3 H, d, ^3J = 6.6 Hz, NCH$_b$MeMe), 1.12 (3 H, d, ^3J = 6.6 Hz, NCH$_a$MeMe), 1.08 (3 H, d, ^3J = 6.9 Hz, C_6H_3(CH$_a$MeMe)), 1.03 (3 H, d, ^3J = 6.6 Hz, NCH$_a$MeMe), 0.98 (3 H, d, ^3J = 6.6 Hz, NCH$_b$MeMe), 0.93 (3 H, d, ^3J = 6.9 Hz, C_6H_3(CH$_b$MeMe)). ^{13}C{^{1}H} NMR (C_6D_6, 75.4 MHz, 293 K): δ 168.4 (MeCN$_2$), 154.7 (SC(N)N), 147.6 (i_b-C_6H_5), 147.5 (i_a-C_6H_5), 144.6 (i-C_6H_3(^{i}Pr$_2$)), 140.5 (o_a-C_6H_3(^{i}Pr$_2$)), 139.8 (o_b-C_6H_3(^{i}Pr$_2$)), 129.8 (C_5Me_5), 128.4 (m_a-C_6H_5), 128.2 (m_b-C_6H_5), 122.8 (m-C_6H_3(^{i}Pr$_2$)), 122.4 (p-C_6H_3(^{i}Pr$_2$)), 121.8 (p_a-C_6H_5), 121.4 (o_a-C_6H_5), 119.6 (p_b-C_6H_5), 117.6 (o_b-C_6H_5), 51.4

(N<u>C</u>H$_a$MeMe), 49.6 (N<u>C</u>H$_b$MeMe), 28.5 (C$_6$H$_3$(<u>C</u>H$_a$MeMe)), 28.4 (C$_6$H$_3$(<u>C</u>H$_b$MeMe)), 26.2 (NCH$_b$Me<u>Me</u>), 25.5 (NCH$_b$<u>Me</u>Me), 24.7 (NCH$_a$Me<u>Me</u>), 24.5 (C$_6$H$_3$(CH$_a$Me<u>Me</u>)), 24.0 (C$_6$H$_3$(CH$_b$Me<u>Me</u>)), 23.9 (C$_6$H$_3$(CH$_a$<u>Me</u>Me)), 23.6 (C$_6$H$_3$(CH$_b$<u>Me</u>Me)), 23.4 (NCH$_a$<u>Me</u>Me), 14.4 (<u>Me</u>CN$_2$), 13.5 (C$_5$<u>Me</u>$_5$). IR (NaCl plates, Nujol mull, cm^{-1}): 2099 (w), 1589 (m), 1566 (s), 1492 (s), 1313 (w), 1277 (w), 1202 (m), 1175 (w), 1154 (w), 1022 (m), 941 (w), 803 (w), 759 (w), 745 (m), 692 (w), 646 (m). EI-MS: *m/z* = 682 [*M* – (^{i}Pr)]$^+$ (10%), 584 [*M* – {MeC(N^{i}Pr)$_2$}]$^+$ (30%), 429 [*M* – Cp* – 2,6-C$_6$H$_3$(^{i}Pr$_2$)]$^+$ (50%). Anal. found (calcd. for C$_{43}$H$_{59}$N$_5$STi): C, 71.06 (71.15); H, 8.10 (8.19); N, 9.63 (9.65)%.

Cp*Ti{MeC(N^{i}Pr)$_2$}{N(NPh$_2$)C(N^{t}Bu)O} (12). To a solution of Cp*Ti{MeC(N^{i}Pr)$_2$}(NNPh$_2$) (0.300 g, 0.590 mmol) in benzene (20 mL) was added ^{t}BuNCO (67.6 μL, 0.590 mmol) all at RT. An immediate colour change from dark yellow to dark brown was observed. After 16 h, the volatiles were removed under reduced pressure to afford **12** as a dark brown solid. The resultant dark brown solid was washed with cold pentane (3 × 5 mL) cooled to -78 ℃, filtered, and dried *in vacuo*. Yield: 0.184 g (51%). ^{1}H NMR (C$_6$D$_6$, 299.9 MHz, 293 K): δ 7.62 (2 H, d, ^3J = 6.5 Hz, *o*$_a$-C$_6$H$_5$), 7.22 (2 H, t, ^3J = 6.5 Hz, *m*$_a$-C$_6$H$_5$), 7.09 (2 H, d, ^3J = 6.5 Hz, *o*$_b$-C$_6$H$_5$), 7.01 (2 H, t, ^3J = 6.5 Hz, *m*$_b$-C$_6$H$_5$), 6.88 (1 H, t, ^3J = 6.5 Hz, *p*$_a$-C$_6$H$_5$), 6.71 (1 H, t, ^3J = 6.5 Hz, *p*$_b$-C$_6$H$_5$), 3.34 (1 H, app. sept., app. ^3J = 6.5 Hz, NC<u>H</u>$_a$MeMe), 2.80 (1 H, app. sept., app. ^3J = 6.5 Hz, NC<u>H</u>$_b$MeMe), 1.96 (15 H, s, C$_5$Me$_5$), 1.56 (9 H, s, ^{t}Bu), 1.39 (3 H, s, MeCN$_2$), 1.17 (3 H, d, ^3J = 6.5 Hz, NCH$_a$<u>Me</u>Me), 1.14 (3 H, d, ^3J = 6.5 Hz, NCH$_a$Me<u>Me</u>), 1.09 (3 H, d, ^3J = 6.5 Hz, NCH$_b$<u>Me</u>Me), 0.92 (3 H, d, ^3J = 6.5 Hz, NCH$_b$Me<u>Me</u>). ^{13}C{^{1}H} NMR (C$_6$D$_6$, 75.4 MHz, 293 K): δ 168.5 (Me<u>C</u>N$_2$), 152.4 (OC(N)N), 148.1 (*i*$_a$-C$_6$H$_5$), 147.8 (*i*$_b$-C$_6$H$_5$), 128.4 (<u>C</u>$_5$Me$_5$), 128.3 (*m*$_a$-C$_6$H$_5$), 128.1 (*m*$_b$-C$_6$H$_5$), 121.7 (*p*$_a$-C$_6$H$_5$), 121.6 (*o*$_a$-C$_6$H$_5$), 119.3 (*p*$_b$-C$_6$H$_5$), 117.7 (*o*$_b$-C$_6$H$_5$), 51.90 (N<u>C</u>Me$_3$), 50.4 (N<u>C</u>H$_a$MeMe), 49.5 (N<u>C</u>H$_b$MeMe), 32.9 (NC<u>Me</u>$_3$), 26.2 (NCH$_b$<u>Me</u>Me), 25.1 (NCH$_b$Me<u>Me</u>), 25.0 (NCH$_a$<u>Me</u>Me), 24.35 (NCH$_a$Me<u>Me</u>), 13.0 (<u>Me</u>CN$_2$), 12.9 (C$_5$<u>Me</u>$_5$). IR (NaCl plates, Nujol mull, cm^{-1}): 1653 (m), 1636 (w), 1589 (w), 1559 (w), 1540 (w), 1521 (w), 1506 (w), 1490 (m), 1458 (s), 1335 (w), 1313 (w), 1207 (w), 1175 (w), 1019 (w), 793 (w), 744 (w), 691 (w), 668 (m). Anal. found (calcd. for C$_{35}$H$_{51}$N$_5$OTi): C, 69.52 (69.41); H, 8.42 (8.49); N, 11.48 (11.56)%.

Cp*Ti{MeC(N^{i}Pr)$_2$}{OC(NTol)N(NPh$_2$)C(O)O} (13). A solution of Cp*Ti{MeC(N^{i}Pr)$_2$}{N(NPh$_2$)C(NTol)O} (**7**, 0.450 g, 0.700 mmol) in toluene (20 mL) was freeze-pump-thawed three times. The solution was then exposed to CO_2 at a pressure of *ca.* 1.1 atm at RT. After 4 d, the volatiles were removed under reduced pressure to afford **13** as a dark brown solid. The resultant dark brown solid was washed with cold pentane (3 × 5 mL) cooled to -78 ℃, filtered, and dried *in vacuo*. Yield: 0.178 g (37%). ^{1}H NMR (C_6D_6, 299.9 MHz, 293 K): δ 7.95 (2 H, d, ^3J = 6.0 Hz, *o*$_a$-C_6H_5), 7.40 (2 H, d, ^3J = 6.0 Hz, *o*$_b$-C_6H_5), 7.29 (2H, t, ^3J = 6.0 Hz, *m*$_a$-C_6H_5), 7.10 (2 H, m, *m*$_b$-C_6H_5), 7.00 (4 H, m, overlapping *o*- and *m*-$C_6\underline{H}_4$Me), 6.98 (1 H, m, *p*$_a$-C_6H_5), 6.82 (1 H, t, ^3J = 6.0 Hz, *p*$_b$-C_6H_5), 3.47 (1 H, app. sept., app. ^3J = 6.0 Hz, NC$\underline{H}_a$MeMe), 3.35 (1 H, app. sept., app. ^3J = 6.0 Hz, NC$\underline{H}_b$MeMe), 2.19 (3 H, s, $C_6H_4\underline{Me}$), 1.83 (15 H, s, C_5Me_5), 1.44 (3 H, s, $MeCN_2$), 1.13 (3 H, d, ^3J = 6.0 Hz, NCH$_a\underline{Me}$Me), 1.09 (3 H, d, ^3J = 6.0 Hz, NCH$_a$Me$\underline{Me}$), 0.88 (6 H, overlapping 2 × d, ^3J = 6.0 Hz, overlapping NCH$_b\underline{Me}$Me and NCH$_b$Me$\underline{Me}$). ^{13}C{^{1}H} NMR (C_6D_6, 75.4 MHz, 293 K): δ 169.6 (Me$\underline{C}N_2$), 152.8 (OC(O)N), 149.9 (OC(N)N), 147.1 (*i*-$\underline{C}_6H_4$Me), 146.6 (*i*$_b$-C_6H_5), 146.2 (*i*$_a$-C_6H_5), 130.9 ($\underline{C}_5Me_5$), 130.4 (*p*-$\underline{C}_6H_4$Me), 128.9 (*m*$_a$-C_6H_5), 128.8 (overlapping *m*-$\underline{C}_6H_4$Me and *m*$_b$-C_6H_5), 123.9 (*o*-$\underline{C}_6H_4$Me), 123.1 (*p*$_a$-C_6H_5), 122.5 (*o*$_a$-C_6H_5), 121.0 (*p*$_b$-C_6H_5), 118.2 (*o*$_b$-C_6H_5), 50.5 (N$\underline{C}$H$_a$MeMe), 50.0 (N$\underline{C}$H$_b$MeMe), 24.3 (NCH$_a$Me$\underline{Me}$), 23.9 (NCH$_b$Me$\underline{Me}$), 23.5 (overlapping NCH$_a\underline{Me}$Me and NCH$_b\underline{Me}$Me), 21.0 ($C_6H_4\underline{Me}$), 14.9 ($\underline{Me}CN_2$), 12.6 ($C_5\underline{Me}_5$). IR (NaCl plates, Nujol mull, cm^{-1}): 1699 (s), 1628 (s), 1592 (s), 1496 (s), 1336 (s), 1207 (m), 1180 (m), 1101 (m), 1017 (w), 862 (w), 794 (m), 746 (m), 690 (w). EI-MS: *m/z* = 424 [*M* – NPh_2 – Tol]$^+$ (30%). Anal. found (calcd. for $C_{39}H_{49}N_5O_3Ti$): C, 68.55 (68.51); H, 7.15 (7.22); N, 10.18 (10.24)%.

NMR tube scale reaction of Cp*Ti{MeC(N^{i}Pr)$_2$}{N(NPh$_2$)C(N^{t}Bu)O} (12) with CO_2. 20.0 mg (0.033 mmol) Cp*Ti{MeC(N^{i}Pr)$_2$}{N(NPh$_2$)C(N^{t}Bu)O} (**12**) was dissolved in C_6D_6 (0.6 mL), and freeze-pump-thawed three times. The solution was then exposed to CO_2 at a pressure of *ca.* 1.1 atm at RT. The reaction was monitored by ^{1}H NMR spectroscopy. The ^{1}H NMR spectrum recorded after 4 d showed quantitative formation of Cp*Ti{MeC(N^{i}Pr)$_2$}{OC(O)N(NPh$_2$)C(O)O} (**3**) and free ^{t}BuNCO.

NMR tube scale reaction of Cp*Ti{MeC(N^{i}Pr)$_2$}{N(NPh$_2$)C(N^{t}Bu)O} (12) with TolNCO. To a solution of Cp*Ti{MeC(N^{i}Pr)$_2$}{N(NPh$_2$)C(N^{t}Bu)O} (**12**, 13.8 mg, 0.023 mmol) in C_6D_6 (0.6 mL) in an NMR tube equipped with a J. Young Teflon valve was added TolNCO (2.90 μL, 0.023 mmol) at RT. The ^{1}H NMR spectrum recorded after 10 min contained resonances attributed to Cp*Ti{MeC(N^{i}Pr)$_2$}{N(NPh$_2$)C(NTol)O} (**7**) and ^{t}BuNCO.

NMR tube scale reaction of Cp*Ti{MeC(N^{i}Pr)$_2$}(NNMe$_2$) with ^{t}BuNCO. To a solution of Cp*Ti{MeC(N^{i}Pr)$_2$}(NNMe$_2$) (10.0 mg, 0.026 mmol) in C_6D_6 (0.6 mL) in an NMR tube equipped with a J. Young Teflon valve was added ^{t}BuNCO (3.00 μL, 0.026 mmol) at RT. Immediate colour change from dark green to yellow was observed. The ^{1}H NMR spectrum recorded after 16 h showed quantitative formation of [Cp*Ti{MeC(N^{i}Pr)$_2$}(μ-O)]$_2$ and ^{t}BuNCNNMe$_2$ (**14**).

Reaction of Cp*Ti{MeC(N^{i}Pr)$_2$}(NNMe$_2$) with Ar^{F}NCO. To a solution of Cp*Ti{MeC(N^{i}Pr)$_2$}(NNMe$_2$) (0.417 g, 1.09 mmol) in benzene (20 mL) was added Ar^{F}NCO (467 μL, 2.18 mmol) all at RT. The resulting yellow solution was stirred for 20 h at 60 °C. Volatiles were then removed under reduced pressure to afford [Cp*Ti{MeC(N^{i}Pr)$_2$}(μ-O)]$_2$ and N(Me)$_2$NC(NAr^F)N(Ar^F)C(O) (**15**). Sublimation (65-75 °C, 5 × 10^{-6} mbar) afforded **15** as a white solid. Yield: 76.0 mg (15%). Diffraction-quality crystals were grown from a concentrated hexanes solution at 4 °C. ^{1}H NMR (C_6D_6, 499.9 MHz, 293 K): δ 7.25 (1 H, t, ^3J = 7.5 Hz, p_a-C$_6$H$_3$(^{i}Pr$_2$)), 7.14 (2 H, d, ^3J = 7.5 Hz, m_a-C$_6$H$_3$(^{i}Pr$_2$)), 7.09 (2 H, d, ^3J = 7.5 Hz, m_b-C$_6$H$_3$(^{i}Pr$_2$)), 7.00 (1 H, t, ^3J = 7.5 Hz, p_b-C$_6$H$_3$(^{i}Pr$_2$)), 3.43 (2 H, app. sept., app. ^3J = 7.0 Hz, NCH$_b$MeMe), 3.20 (2 H, app. sept., app. ^3J = 7.0 Hz, NCH$_a$MeMe), 2.66 (6 H, s, NNMe$_2$), 1.32 (6 H, d, ^3J = 7.0 Hz, NCH$_a$MeMe), 1.21 (18 H, m, overlapping NCH$_a$MeMe, NCH$_b$MeMe and NCH$_b$MeMe). ^{13}C{^{1}H} NMR (C_6D_6, 125.7 MHz, 293 K): δ 159.7 (NC(O)N), 152.9 (NC(N)N), 147.2 (o_a-C$_6$H$_3$(^{i}Pr$_2$)), 146.4 (i_b-C$_6$H$_3$(^{i}Pr$_2$)), 140.4 (o_b-C$_6$H$_3$(^{i}Pr$_2$)), 130.5 (p_a-C$_6$H$_3$(^{i}Pr$_2$)), 128.3 (i_a-C$_6$H$_3$(^{i}Pr$_2$)), 124.1 (m_a-C$_6$H$_3$(^{i}Pr$_2$)), 122.7 (m_b-C$_6$H$_3$(^{i}Pr$_2$)), 122.2 (p_b-C$_6$H$_3$(^{i}Pr$_2$)), 53.5 (NNMe$_2$), 29.5 (CH$_a$MeMe) 28.3 (CH$_b$MeMe), 25.0 (CH$_a$MeMe), 24.3 (overlapping CH$_b$MeMe and CH$_b$MeMe), 22.9 (CH$_a$MeMe). IR (NaCl plates, Nujol mull, cm^{-1}): 2289 (w), 2169 (w), 1808 (s), 1646 (s), 1586 (m), 1465 (s), 1393 (s), 1365 (m), 1356 (w), 1290 (w), 1237 (m), 1207 (w), 1172 (w), 1114 (w), 1063 (m), 1041 (w), 965 (m), 936 (w), 908 (w), 862 (w), 810 (w), 801 (m), 777 (m), 754 (w), 725 (s), 706 (m), 690 (m), 640 (m). EI-MS: *m/z* = 448

$[M]^+$ (100%), 245 $[M - ArNCO]^+$ (80%). Anal. found (calcd. for $C_{64}H_{104}N_8O_3Ti_2$): C, 67.99 (68.07); H, 9.20 (9.28); N, 10.02 (9.92)%.

Cp*Ti{MeC(N^{i}Pr)$_2$}{OC(NNMe$_2$)N(Tol)C(NTol)O} (16). To a solution of Cp*Ti{MeC(N^{i}Pr)$_2$}(NNMe$_2$) (0.300 g, 0.780 mmol) in benzene (20 mL) was added TolNCO (0.198 mL, 1.57 mmol) all at RT. An immediate colour change from dark green to brown was observed and the solution left to stand for 16 h. Volatiles were then removed under reduced pressure to afford **16** as a brown solid. The resultant brown solid was washed with cold pentane (3 × 5 mL) cooled to -78 ℃, filtered, and dried *in vacuo*. Yield: 0.308 g (76%). Diffraction-quality crystals were grown by slow cooling of a saturated hexanes solution. ^{1}H NMR (C_6D_6, 299.9 MHz, 293 K): δ 7.51 (2 H, d, ^3J = 8.4 Hz, o_b-C$_6$H$_4$Me), 7.12 (2 H, d, ^3J = 8.4 Hz, o_a-C$_6$H$_4$Me), 7.07 (2 H, d, ^3J = 8.4 Hz, m_b-C$_6$H$_4$Me), 7.01 (2 H, d, ^3J = 8.4 Hz, m_a-C$_6$H$_4$Me), 3.71 (1 H, app. sept., app. ^3J = 6.6 Hz, NCH$_a$MeMe), 3.42 (1 H, app. sept., app. ^3J = 6.6 Hz, NCH$_b$MeMe), 2.50 (6H, s, NNMe$_2$), 2.20 (3 H, s, C$_6$H$_4$Me$_a$), 2.05 (3 H, s, C$_6$H$_4$Me$_b$), 2.02 (15 H, s, C$_5$Me$_5$), 1.50 (3 H, s, MeCN$_2$), 1.26 (3 H, d, ^3J = 6.6 Hz, NCH$_a$MeMe), 1.15 (3 H, d, ^3J = 6.6 Hz, NCH$_a$MeMe), 0.94 (3 H, d, ^3J = 6.6 Hz, NCH$_b$MeMe), 0.85 (3 H, d, ^3J = 6.6 Hz, NCH$_b$MeMe). ^{13}C{^{1}H} NMR (C_6D_6, 75.4 MHz, 293 K): δ 169.7 (MeCN$_2$), 157.6 (OC(NNMe$_2$)N), 153.2 (OC(NTol)N), 148.1 (i_a-C$_6$H$_4$Me), 142.1 (i_b-C$_6$H$_4$Me), 134.9 (p_b-C$_6$H$_4$Me), 130.1 (o_b-C$_6$H$_4$Me), 129.7 (C$_5$Me$_5$), 129.2 (m_a-C$_6$H$_4$Me), 128.6 (overlapping p_a- and o_a-C$_6$H$_4$Me), 124.3 (m_b-C$_6$H$_4$Me), 50.1 (NCH$_a$MeMe), 49.7 (NCH$_b$MeMe), 48.5 (NNMe$_2$), 24.1 (NCH$_a$MeMe), 24.1 (NCH$_b$MeMe), 23.8 (NCH$_a$MeMe), 23.5 (NCH$_b$MeMe), 21.1 (C$_6$H$_4$Me$_b$), 21.0 (C$_6$H$_4$Me$_a$), 15.5 (MeCN$_2$), 12.5 (C$_5$Me$_5$). IR (NaCl plates, Nujol mull, cm^{-1}): 2805 (m), 2757 (w), 1619 (s), 1599 (s), 1568 (s), 1508 (s), 1458 (s), 1416 (w), 1366 (s), 1340 (m), 1311 (m), 1279 (w), 1255 (m), 1227 (m), 1204 (s), 1171 (w), 1158 (w), 1119 (m), 1105 (m), 1024 (w), 1005 (s), 933 (w), 899 (m), 884 (m), 810 (s), 780 (m), 725 (m), 718 (m), 688 (w), 605 (m). Anal. found (calcd. for $C_{36}H_{52}N_6O_2Ti$): C, 66.73 (66.65); H, 7.98 (8.08); N, 12.95 (12.96)%.

Cp*Ti{MeC(N^{i}Pr)$_2$}{N(NMe$_2$)C(NAr′)S} (17). To a solution of Cp*Ti{MeC(N^{i}Pr)$_2$}(NNMe$_2$) (0.295 g, 0.77 mmol) in benzene (10 mL) was added Ar′NCS (167 μL, 0.77 mmol) all at RT. The resulting dark green solution was stirred for 16 h. Volatiles were then removed under reduced pressure to afford **17** as a dark green solid. Yield: 0.286 g (62%). ^{1}H NMR (toluene-d_8, 499.9 MHz, 253 K): δ 7.28

(1 H, d, ^3J = 7.5 Hz, m_a-2,6-C_6H_3(CHMeMe)$_2$), 7.24 (1 H, d, ^3J = 7.5 Hz, m_b-2,6-C_6H_3(CHMeMe)$_2$), 7.15 (1 H, t, ^3J = 7.5 Hz, *p*-2,6-C_6H_3(CHMeMe)$_2$), 3.55 (1 H, app. sept., app. ^3J = 6.5 Hz, NC$\underline{H}_a$MeMe), 3.42 (2 H, m, overlapping o_a-2,6-C_6H_3(C$\underline{H}$MeMe) and o_b-2,6-C_6H_3(C$\underline{H}$MeMe)), 3.17 (1 H, app. sept., app. ^3J = 6.5 Hz, NC$\underline{H}_b$MeMe), 3.05 (6 H, s, NN$\underline{Me}_2$), 2.00 (15 H, s, $C_5\underline{Me}_5$), 1.64 (3 H, d, ^3J = 6.5 Hz, o_a-2,6-C_6H_3(CH$\underline{Me}$Me)), 1.59 (3H, s, $\underline{Me}CN_2$), 1.48 (3 H, d, ^3J = 6.0 Hz, NCH$_a\underline{Me}$Me), 1.42 (3 H, d, ^3J = 6.5 Hz, o_b-2,6-C_6H_3(CH$\underline{Me}$Me)), 1.34 (6 H, overlapping 2 × d, 2 × ^3J = 6.5 Hz, overlapping o_a-2,6-C_6H_3(CHMe$\underline{Me}$) and o_b-2,6-C_6H_3(CHMe$\underline{Me}$), 1.24 (3 H, d, ^3J = 6.0 Hz, NCH$_a$Me$\underline{Me}$), 1.07 (3 H, d, ^3J = 6.0 Hz, NCH$_b\underline{Me}$Me), 0.88 (3 H, d, ^3J = 6.0 Hz, NCH$_b$Me$\underline{Me}$). $^{13}C\{^1H\}$ NMR (toluene-d_8, 125.7 MHz, 253 K): δ 168.47 (Me$\underline{C}N_2$), 152.03 (S$\underline{C}$(N)N), 145.05 (*i*-2,6-C_6H_3(CHMeMe)$_2$), 140.17 (o_b-2,6-C_6H_3(CHMeMe)$_2$), 139.88 (o_a-2,6-C_6H_3(CHMeMe)$_2$), 128.19 ($\underline{C}_5Me_5$), 122.75 (m_a-2,6-C_6H_3(CHMeMe)$_2$), 122.53 (*p*-2,6-C_6H_3(CHMeMe)$_2$), 122.17 (m_b-2,6-C_6H_3(CHMeMe)$_2$), 50.90 (N$\underline{C}$H$_b$MeMe), 50.41 (N$\underline{C}$H$_a$MeMe), 45.60 (NN$\underline{Me}_2$), 28.67 (*o*-2,6-C_6H_3($\underline{C}$HMeMe)), 28.44 (*o*-2,6-C_6H_3($\underline{C}$HMeMe)), 26.52 (NCH$_a$Me$\underline{Me}$), 24.56 (*o*-2,6-C_6H_3(CHMe$\underline{Me}$))), 24.51 (*o*-2,6-C_6H_3(CHMe$\underline{Me}$)),), 24.44 (NCH$_a\underline{Me}$Me) 24.30 (NCH$_b\underline{Me}$Me), 23.79 (o_a-2,6-C_6H_3(CH$\underline{Me}$Me)), 23.58 (NCH$_b$Me$\underline{Me}$), 22.91 (o_b-2,6-C_6H_3(CH$\underline{Me}$Me)), 13.38 ($C_5\underline{Me}_5$), 12.92 ($\underline{Me}CN_2$). IR (NaCl plates, Nujol mull, cm^{-1}): 2123 (w), 1653 (w), 1591 (m), 1560 (s), 1457 (s), 1332 (s), 1310 (m), 1237 (w), 1204 (s), 1174 (m), 1139 (w), 1114 (m), 1062 (w), 1010 (s), 936 (s), 884 (w), 834 (m), 819 (m) 797 (m) 770 (w) 755 (s) 633 (w). EI-MS: *m/z* = 356 [Cp*Ti{MeCN(^{i}Pr)$_2$}S]$^+$ (50%), 325 [*M* – Cp*Ti{MeCN(^{i}Pr)$_2$}]$^+$ (5%). A satisfactory elemental analysis could not be obtained.

NMR tube scale reaction of Cp*Ti{MeC(N^{i}Pr)$_2$}(NNMe$_2$) with TolNCS. To a solution of Cp*Ti{MeC(N^{i}Pr)$_2$}(NNMe$_2$) (10.0 mg, 0.03 mmol) in toluene-d_8 (0.6 mL) in an NMR tube equipped with a J. Young Teflon valve was added TolNCS (3.9 mg, 0.03 mmol) all at RT. An immediate colour change from dark green to brown green was observed. The product Cp*Ti{MeC(N^{i}Pr)$_2$}{N(NMe$_2$)C(NTol)S} (**18**) formed quantitatively and was characterised by NMR spectroscopy. ^1H NMR (toluene-d_8, 499.9 MHz, 263 K): δ 7.35 (2 H, d, ^3J = 6.5 Hz, *o*-4-C_6H_4Me,), 7.09 (2 H, d, ^3J = 6.5 Hz, *m*-4-C_6H_4Me), 3.51 (1 H, app. sept., app. ^3J = 6.5 Hz, NC$\underline{H}_a$MeMe), 3.20 (1 H, app. sept., app. ^3J = 6.5 Hz, NC$\underline{H}_b$MeMe), 3.03 (6 H, s, NNMe$_2$), 2.22 (3 H, s, 4-$C_6H_4\underline{Me}$), 2.02 (15 H, s, $C_5\underline{Me}_5$), 1.58 (3 H, s, $\underline{Me}CN_2$), 1.52 (3 H, d, ^3J = 6.5 Hz,

NCH_aMeMe), 1.22 (3 H, d, ^3J = 6.5 Hz, NCH_aMeMe), 1.15 (3 H, d, ^3J = 6.5 Hz, NCH_bMeMe), 0.99 (3 H, d, ^3J = 6.5 Hz, NCH_bMeMe). $^{13}C\{^1H\}$ NMR (toluene-d_8, 125.7 MHz, 263 K): δ 169.00 ($MeCN_2$), 152.57 (SC(N)N), 147.38 (*i*-4-C_6H_4Me), 130.33 (C_5Me_5), 128.94 (*m*-4-C_6H_4Me), 128.42 (*p*-4-C_6H_4Me), 124.08 (*o*-4-C_6H_4Me), 51.16 (NCH_bMeMe), 50.53 (NCH_aMeMe), 45.45 ($NNMe_2$), 26.76 (NCH_aMeMe), 24.30 (NCH_aMeMe), 24.07 (NCH_bMeMe), 23.49 (NCH_bMeMe), 21.01 (4-C_6H_4Me), 13.38 (C_5Me_5), 12.65 ($MeCN_2$).

Cp*Ti{MeC(N^{i}Pr)$_2$}{N(NMe$_2$)}{C(N^{t}Bu)} (19). To a solution of Cp*Ti{MeC(N^{i}Pr)$_2$}($NNMe_2$) (0.435 g, 1.14 mmol) in benzene (10 mL) was added a solution of ^{t}BuNC (129 μL, 1.14 mmol) in benzene (10 mL) all at RT. The resulting yellow solution was stirred for 16 h, after which the volatiles were removed under reduced pressure. The solid was then washed with cold pentane (3 × 10 mL) cooled to -78 ℃, filtered, and dried *in vacuo* to afford **19** as a yellow solid. Yield: 0.234 mg (44%). ^1H NMR (toluene-d_8, 299.9 MHz, 223 K): δ 3.65 (1 H, app. sept., app. ^3J = 6.0 Hz, NCH_aMeMe), 3.63 (1 H, app. sept., app. ^3J = 6.0 Hz, NCH_bMeMe), 2.76 (6 H, s, $NNMe_2$), 2.32 (15 H, s, C_5Me_5), 1.76 (3 H, s, $MeCN_2$), 1.73 (3 H, d, ^3J = 6.0 Hz, NCH_aMeMe), 1.55 (3 H, d, ^3J = 6.0 Hz, NCH_aMeMe), 1.36 (3 H, d, ^3J = 6.0 Hz, NCH_bMeMe), 1.09 (3 H, d, ^3J = 6.0 Hz, NCH_bMeMe), 0.99 (9 H, s, ^{t}Bu). $^{13}C\{^1H\}$ NMR (toluene-d_8, 75.4 MHz, 223 K): δ 166.5 ($MeCN_2$), 164.4 ($CNCMe_3$), 113.5 (C_5Me_5), 55.2 ($NCMe_3$), 49.7 (NCH_aMeMe), 49.5 ($NNMe_2$), 48.0 (NCH_bMeMe), 29.1 ($NCMe_3$) 27.4 (NCH_aMeMe), 26.0 (NCH_aMeMe), 25.3 (NCH_bMeMe), 24.7 (NCH_bMeMe), 13.3 (C_5Me_5), 11.5 ($MeCN_2$). IR (NaCl plates, Nujol mull, cm^{-1}): 2805 (s), 2757 (m), 2721 (w), 2152 (s), 2086 (w), 1458 (s, b), 1357 (s), 1340 (s), 1312 (m), 1213 (s), 1173 (s), 1113 (s), 1049 (w), 1017 (m), 897 (w), 881 (m), 809 (m). EI-MS: *m/z* = 324 [M – MeC(N^{i}Pr)$_2$]$^+$ (100%). A satisfactory elemental analysis could not be obtained due to the lability of the ^{t}BuNC ligand *in vacuo*.

5.4 Experimental details and characterising data for Chapter Three

Cp*Ti{MeC(N^{i}Pr)$_2$}(H){N(NMe$_2$)SiH$_2$Ph} (20). To a stirred solution of Cp*Ti{MeC(N^{i}Pr)$_2$}($NNMe_2$) (0.300 g, 0.780 mmol) in pentane (10 mL) was added $PhSiH_3$ (0.194 mL, 0.780 mmol) all at RT. An immediate colour change from dark green to yellow was observed. The solution was concentrated and put into the freezer (-30 ℃) for crystallisation. Yellow crystals were obtained after 2 d. The solution was then filtered, and the product (**20**) washed with pentane and dried *in vacuo*. Yield:

0.223 g (58%). Diffraction-quality crystals were grown from a concentrated pentane solution at -30 ℃. ^{1}H NMR (C_6D_6, 499.9 MHz, 293 K): δ 7.71 (2 H, d, ^{3}J = 7.5 Hz, *o*-C_6H_5), 7.20 (3 H, m, overlapping *m*- and *p*-C_6H_5), 5.41 (1 H, d, ^{2}J = 8.0 Hz, Si$\underline{H}_a$H), 5.37 (1 H, d, ^{2}J = 8.0 Hz, SiH$\underline{H}_b$), 5.16 (1 H, s, Ti-H), 3.49 (1 H, app. sept., app. ^{3}J = 6.5 Hz, NC$\underline{H}_a$MeMe), 3.04 (1 H, app. sept., app. ^{3}J = 6.5 Hz, NC$\underline{H}_b$MeMe), 2.83 (3 H, s, NN$\underline{Me}$Me), 2.48 (3 H, s, NNMe$\underline{Me}$), 2.17 (15 H, s, $C_5\underline{Me}_5$), 1.61 (3 H, s, Me$\underline{C}N_2$), 1.20 (3 H, d, ^{3}J = 6.5 Hz, NCH$_a\underline{Me}$Me), 1.09 (6 H, overlapping 2 × d, 2 × ^{3}J = 6.5 Hz, overlapping NCH$_a$Me$\underline{Me}$ and NCH$_b\underline{Me}$Me), 1.00 (3 H, d, ^{3}J = 6.5 Hz, NCH$_b$Me$\underline{Me}$). ^{13}C{^{1}H} NMR (C_6D_6, 125.7 MHz, 293 K): δ 171.6 (Me$\underline{C}N_2$), 137.3 (*i*-C_6H_5), 136.1 (*o*-C_6H_5), 130.0 (*p*-C_6H_5), 129.9 (*m*-C_6H_5), 118.8 ($\underline{C}_5Me_5$), 60.3 (NN$\underline{Me}$Me), 50.8 (NNMe$\underline{Me}$), 48.3 (N$\underline{C}$H$_a$MeMe), 47.2 (N$\underline{C}$H$_b$MeMe), 27.0 (NCH$_b\underline{Me}$Me), 26.5 (NCH$_a$Me$\underline{Me}$), 25.6 (NCH$_a\underline{Me}$Me), 24.6 (NCH$_b$Me$\underline{Me}$), 13.9 ($C_5\underline{Me}_5$), 12.4 ($\underline{Me}CN_2$). ^{29}Si NMR (HMQC ^{1}H-observed, C_6D_6, 299.9 MHz, 293 K): δ -42.3 (SiH_2Ph). IR (NaCl plates, Nujol mull, cm^{-1}): 2180 (s), 2125 (s), 1558 (s), 1506 (m), 1457 (s), 1428 (s), 1387 (m), 1367 (m), 1339 (m), 1327(m), 1310 (w), 1244 (w), 1220 (w), 1199 (s), 1174 (w), 1140 (w), 1121 (m), 1112 (m), 1065 (w), 1049 (w), 1018 (s), 939 (s), 919 (w), 875 (s), 742 (s), 719 (m), 701 (s), 621 (w), 614 (s). EI-MS: *m/z* = 490 $[M]^+$ (100%). Anal. found (calcd. for $C_{26}H_{46}N_4SiTi$): C, 62.91 (63.65); H, 9.68 (9.45); N, 10.48 (11.42)%. The poor agreement between the found and calculated values is attributed to the lability of the compound (which has been crystallographically characterised) *in vacuo*. Note that the corresponding compound **24** prepared from Cp*Ti{MeC(N^{i}Pr)$_2$}(NNMe$_2$) and $PhSiH_2Cl$ was not labile and gave a CHN combustion analysis within the accepted ranges.

Cp*Ti{MeC(N^{i}Pr)$_2$}(D){N(NMe$_2$)SiD$_2$Ph} (20-*d*$_3$). To a stirred solution of Cp*Ti{MeC(N^{i}Pr)$_2$}(NNMe$_2$) (50.0 mg, 0.13 mmol) in benzene (5 mL) was added $PhSiD_3$ (15.0 mg, 0.13 mmol) all at RT. An immediate colour change from dark green to yellow was observed. After 1 h, the volatiles were removed under reduced pressure to afford **20-*d*$_3$** as a yellow solid in quantitative yield. ^{2}H NMR (C_6H_6, 76.7 MHz, 293 K): δ 5.39 (br. s, SiD_2), 5.14 (br s, Ti-D). IR (NaCl plates, Nujol mull, cm^{-1}): 1586 (w), 1576 (w), 1559 (w), 1544 (w), 1507 (m), 1457 (s), 1339 (m), 1327 (m), 1219 (w), 1199 (m), 1174 (w), 1122 (m), 1112 (m), 1018 (s), 890 (m), 757 (s), 742 (w), 701 (s), 681 (m), 640 (s).

Cp*Ti{MeC(N^{i}Pr)$_2$}(H){N(NMe$_2$)SiH$_2$Ar^F} (21). To a stirred solution of Cp*Ti{MeC(N^{i}Pr)$_2$}(NNMe$_2$) (0.100 g, 0.26 mmol) in pentane (2 mL) was added Ar^{F}SiH$_3$ (Ar^F = 3,5-C$_6$H$_3$(CF$_3$)$_2$) (0.064 g, 0.26 mmol) all at RT. An immediate colour change from dark green to yellow was observed. The solution was concentrated and put into the freezer (-30 ℃) for crystallisation. Yellow crystals were obtained after 2 d. The solution was then filtered, and the yellow crystals (**21**) were dried *in vacuo*. Yield: 0.125 g (76%). Diffraction-quality crystals were grown from a saturated pentane solution at -30 ℃. ^{1}H NMR (C$_6$D$_6$, 299.9 MHz, 293 K): δ 8.09 (2 H, s, *o*-C$_6$H$_3$(CF$_3$)$_2$), 7.80 (1 H, s, *p*-C$_6$H$_3$(CF$_3$)$_2$), 5.19 (1 H, s, Ti-H), 5.18 (1 H, d, ^2J = 8.1 Hz, SiH$_a$H), 5.12 (1 H, d, ^2J = 8.1 Hz, SiHH$_b$), 3.45 (1 H, app. sept, app. ^3J = 6.3 Hz, NCH$_a$MeMe), 3.01 (1 H, app. sept, app. ^3J = 6.3 Hz, NCH$_b$MeMe), 2.65 (3 H, s, NNMeMe), 2.33 (3 H, s, NNMeMe), 2.07 (15 H, s, C$_5$Me$_5$), 1.56 (3 H, s, MeCN$_2$), 1.15 (3 H, d, ^3J = 6.3 Hz, NCH$_a$MeMe), 1.03 (3 H, d, ^3J = 6.3 Hz, NCH$_a$MeMe), 1.02 (3H, d, ^3J = 6.3 Hz, NCH$_b$MeMe), 0.90 (3 H, d, ^3J = 6.3 Hz, NCH$_b$MeMe). ^{13}C{^{1}H} NMR (C$_6$D$_6$, 75.4 MHz, 293 K): δ 171.9 (MeCN$_2$), 141.5 (*m*-C$_6$H$_3$(CF$_3$)$_2$), 135.2 (*o*-C$_6$H$_3$(CF$_3$)$_2$), 131.1 (CF$_3$), 125.9 (*i*-C$_6$H$_3$(CF$_3$)$_2$), 123.4 (*p*-C$_6$H$_3$(CF$_3$)$_2$), 119.2 (C$_5$Me$_5$), 60.6 (NNMeMe), 50.9 (NNMeMe), 48.3 (NCH$_a$MeMe), 47.1 (NCH$_b$MeMe), 26.9 (NCH$_b$MeMe), 26.3 (NCH$_a$MeMe), 25.5 (NCH$_a$MeMe), 24.4 (NCH$_b$MeMe), 13.8 (C$_5$Me$_5$), 12.5 (MeCN$_2$). ^{19}F NMR (C$_6$D$_6$, 282.1 MHz, 293 K): δ -62.7 (6 F, s, CF$_3$). ^{29}Si NMR (HMQC ^{1}H-observed, C$_6$D$_6$, 299.9 MHz, 293 K): δ -44.3 (SiH$_2$Ar^F). IR (NaCl plates, Nujol mull, cm^{-1}): 2195 (w), 2137 (w), 1565 (w), 1506 (w), 1365 (m), 1358 (m), 1340 (w), 1279 (s), 1203 (w), 1178 (m), 1141 (s), 1104 (m), 1024 (m), 940 (w), 902 (m), 878 (s), 843 (w), 799 (w), 727 (m), 707 (m), 682 (m), 500 (s). EI-MS: *m/z* = 626 [*M*]$^+$ (90%), 579 [*M* – NMe$_2$ – 3 H]$^+$ (100%), 412 [*M* – Ar^F – H]$^+$ (40%). Anal. found (calcd. for C$_{28}$H$_{44}$F$_6$N$_4$SiTi): C, 53.85 (53.67); H, 6.89 (7.08); N, 8.81 (8.94)%.

Cp*Ti{MeC(N^{i}Pr)$_2$}(H){N(NMe$_2$)SiH$_2$Ar^{OMe}} (22). To a stirred solution of Cp*Ti{MeC(N^{i}Pr)$_2$}(NNMe$_2$) (0.110 g, 0.29 mmol) in pentane (2 mL) was added Ar^{OMe}SiH$_3$ (Ar^{OMe} = 4-C$_6$H$_4$OMe) (0.040 g, 0.29 mmol) all at RT. An immediate colour change from dark green to yellow was observed. The solution was concentrated and put into the freezer (-30 ℃) for crystallisation. Yellow crystals were obtained after 2 d. The solution was then filtered, and the product (**22**) dried *in vacuo*. Yield: 0.114 g (76%). Diffraction-quality crystals were grown from a saturated

pentane solution at -30 ℃. ^{1}H NMR (C_6D_6, 299.9 MHz, 293 K): δ 7.65 (2 H, d, ^{3}J = 8.7 Hz, *o*-C_6H_4OMe), 6.84 (2 H, d, ^{3}J = 8.7 Hz, *m*-C_6H_4OMe), 5.46 (1 H, d, ^{2}J = 8.1 Hz, Si$\underline{H}_a$H), 5.41 (1 H, d, ^{2}J = 8.1 Hz, SiH$\underline{H}_b$), 5.16 (1 H, s, Ti-H), 3.51 (1 H, app. sept, app. ^{3}J = 6.6 Hz, NC$\underline{H}_a$MeMe), 3.28 (3 H, s, OMe), 3.07 (1 H, app. sept, app. ^{3}J = 6.6 Hz, NC$\underline{H}_b$MeMe), 2.88 (3 H, s, NN$\underline{Me}$Me), 2.52 (3 H, s, NNMe$\underline{Me}$), 2.19 (15 H, s, $C_5\underline{Me}_5$), 1.62 (3 H, s, $\underline{Me}CN_2$), 1.21 (3 H, d, ^{3}J = 6.6 Hz, NCH$_a\underline{Me}$Me), 1.10 (6 H, overlapping 2 × d, 2 × ^{3}J = 6.6 Hz, overlapping NCH$_a$Me$\underline{Me}$ and NCH$_b\underline{Me}$Me), 1.03 (3 H, d, ^{3}J = 6.6 Hz, NCH$_b$Me$\underline{Me}$). ^{13}C{^{1}H} NMR (C_6D_6, 75.4 MHz, 293 K): δ 171.6 (Me$\underline{C}N_2$), 161.6 (*p*-C_6H_4OMe), 137.6 (*i*-C_6H_4OMe), 137.3 (*o*-C_6H_4OMe), 118.8 ($\underline{C}_5Me_5$), 114.1 (*m*-C_6H_4OMe), 61.0 (NN$\underline{Me}$Me), 54.5 (OMe), 50.8 (NNMe$\underline{Me}$), 48.3 (N$\underline{C}$H$_a$MeMe), 47.2 (N$\underline{C}$H$_b$MeMe), 27.0 (NCH$_b$Me$\underline{Me}$), 26.5 (NCH$_a\underline{Me}$Me), 25.6 (NCH$_a$Me$\underline{Me}$), 24.6 (NCH$_b\underline{Me}$Me), 14.0 ($C_5\underline{Me}_5$), 12.4 ($\underline{Me}CN_2$). ^{29}Si NMR (HMQC ^{1}H-observed, C_6D_6, 299.9 MHz, 293 K): δ -42.1 (SiH_2Ar^{OMe}). IR (NaCl plates, Nujol mull, cm^{-1}): 2188 (m), 2094 (m), 1594 (m), 1558 (m), 1501 (s), 1399 (w), 1336 (w), 1328 (w), 1280 (m), 1248 (m), 1224 (w), 1200 (m), 1180 (m), 1113 (s), 1024 (s), 939 (s), 880 (s), 826 (m), 812 (m), 730 (m), 639 (w), 608 (m), 497 (s). Anal. found (calcd. for $C_{27}H_{48}N_4OSiTi$): C, 62.63 (62.29); H, 9.46 (9.29); N, 10.32 (10.76)%

Cp*Ti{MeC(N^{i}Pr)$_2$}(H){N(NMe$_2$)SiH$_2$Bu} (23). To a solution of Cp*Ti{MeC(N^{i}Pr)$_2$}(NNMe$_2$) (0.200 g, 0.52 mmol) in diethyl ether (3 mL) was added BuSiH$_3$ (67.9 μL, 0.52 mmol) all at RT. An immediate colour change from dark green to yellow was observed. After 1 h, volatiles were removed under reduced pressure to afford **23** as a yellow waxy solid which was washed with cold pentane (3 × 5 mL) cooled to -78 ℃, filtered, and dried carefully *in vacuo*. Compound **23** rapidly lost BuSiH$_3$ *in vacuo* and a satisfactory elemental analysis could not be obtained. Yield: 0.053 g (22%). ^{1}H NMR (C_6D_6, 499.9 MHz, 293 K): δ 5.05 (1 H, s, Ti-H), 4.84 (2 H, m, SiH$_2$), 3.53 (1 H, app. sept., app. ^{3}J = 6.5 Hz, NC$\underline{H}_a$MeMe), 3.08 (1 H, app. sept., app. ^{3}J = 6.5 Hz, NC$\underline{H}_b$MeMe), 2.84 (3 H, s, NN$\underline{Me}$Me), 2.56 (3 H, s, NNMe$\underline{Me}$), 2.17 (15 H, s, $C_5\underline{Me}_5$), 1.64 (3 H, s, $\underline{Me}CN_2$), 1.38 (4 H, m, overlapping SiCH$_2$C$\underline{H}_2$CH$_2$CH$_3$ and SiCH$_2$CH$_2$C$\underline{H}_2$CH$_3$), 1.23 (3 H, d, ^{3}J = 6.5 Hz, NCH$_a\underline{Me}$Me), 1.13 (3 H, d, ^{3}J = 6.5 Hz, NCH$_a$Me$\underline{Me}$), 1.09 (3 H, d, ^{3}J = 6.5 Hz, NCH$_b\underline{Me}$Me), 0.98 (3 H, d, ^{3}J = 6.5 Hz, NCH$_b$Me$\underline{Me}$), 0.91 (3 H, t, ^{3}J = 7.0 Hz, SiCH$_2$CH$_2$CH$_2$C$\underline{H}_3$), 0.81 (2 H, m, SiC$\underline{H}_2$CH$_2$CH$_2$CH$_3$). ^{13}C{^{1}H} NMR (C_6D_6, 125.7 MHz, 293 K): δ 171.5 (Me$\underline{C}N_2$), 118.5 ($\underline{C}_5Me_5$), 60.8 (NN$\underline{Me}$Me), 50.4 (NNMe$\underline{Me}$), 48.3 (N$\underline{C}$H$_a$MeMe),

47.2 (N<u>C</u>H$_b$MeMe), 27.1 (NCH$_b$<u>Me</u>Me), 26.7 (SiCH$_2$<u>C</u>H$_2$CH$_2$CH$_3$), 26.5 (NCH$_a$Me<u>Me</u>), 26.2 (SiCH$_2$CH$_2$<u>C</u>H$_2$CH$_3$), 25.6 (NCH$_a$<u>Me</u>Me), 24.5 (NCH$_b$Me<u>Me</u>), 16.3 (Si<u>C</u>H$_2$CH$_2$CH$_2$CH$_3$), 14.0 (SiCH$_2$CH$_2$CH$_2$<u>C</u>H$_3$), 13.8 (C$_5$<u>Me</u>$_5$), 12.4 (<u>Me</u>CN$_2$). ^{29}Si NMR (HMQC ^{1}H-observed, C$_6$D$_6$, 299.9 MHz, 293 K): δ -36.6 (SiH$_2$Bu). IR (NaCl plates, Nujol mull, cm^{-1}): 2165 (w), 2106 (m), 1559 (m), 1506 (m), 1457 (s), 1339 (m), 1201 (s), 1174 (m), 1122 (w), 1079 (w), 1021 (s), 944 (m), 891 (s), 667 (m). EI-MS: *m/z* = 427 [*M* – CH$_2$CH$_2$CH$_3$]$^+$ (100%). A satisfactory elemental analysis could not be obtained due to the lability of the compound *in vacuo*.

NMR tube scale reaction of Cp*Ti{MeC(N^{i}Pr)$_2$}(D){N(NMe$_2$)SiD$_2$Ph} (20-*d*$_3$) with H$_2$. A solution of Cp*Ti{MeC(N^{i}Pr)$_2$}(D){N(NMe$_2$)SiD$_2$Ph} **(20-*d*$_3$**, 14.2 mg, 0.029 mmol) in C$_6$D$_6$ (0.6 mL) in an NMR tube equipped with a J. Young Teflon valve was freeze-pump-thawed three times. The solution was then exposed to H$_2$ at a pressure of *ca.* 4 bar at RT and was monitored using ^{1}H NMR spectroscopy for 4 d. A separate, parallel reaction was carried out in C$_6$H$_6$ and monitored using ^{2}H NMR spectroscopy.

NMR tube scale reaction of Cp*Ti{MeC(N^{i}Pr)$_2$}(D){N(NMe$_2$)SiD$_2$Ph} (20-*d*$_3$) with BuSiH$_3$. To a solution of Cp*Ti{MeC(N^{i}Pr)$_2$}(D){N(NMe$_2$)SiD$_2$Ph} **(20-*d*$_3$**, 13.5 mg, 0.027 mmol) in C$_6$D$_6$ (0.6 mL) in an NMR tube equipped with a J. Young Teflon valve was added BuSiH$_3$ (3.55 μL, 0.52 mmol) all at RT. The solution was then monitored using ^{1}H NMR spectroscopy for 2 d. A separate, parallel reaction was carried out in C$_6$H$_6$ and monitored using ^{2}H NMR spectroscopy.

Cp*Ti{MeC(N^{i}Pr)$_2$}(Cl){N(NMe$_2$)SiH$_2$Ph} (24). To a solution of Cp*Ti{MeC(N^{i}Pr)$_2$}(NNMe$_2$) (0.100 g, 0.260 mmol) in pentane (5 mL) was added PhSiH$_2$Cl (35.0 μL, 0.260 mmol) all at RT. The volatiles were removed under reduced pressure after 10 min following a colour change (from dark green to orange) and precipitation to afford **24** as an orange solid which was then washed with cold pentane (3 × 5 mL) cooled to -78 ℃, filtered, and dried *in vacuo*. Yield: 0.063 mg (46%). Diffraction-quality crystals were grown from a saturated toluene solution at -30 ℃. ^{1}H NMR (toluene-*d*$_8$, 499.9 MHz, 253 K): δ 7.61 (2 H, d, ^3J = 7.5 Hz, *o*-C$_6$H$_5$), 7.17 (2 H, t, ^3J = 7.5 Hz, *m*-C$_6$H$_5$), 7.13 (1 H, t, ^3J = 7.5 Hz, *p*-C$_6$H$_5$), 5.30 (1 H, d, ^2J = 6.5 Hz, Si<u>H</u>$_a$H), 5.25 (1 H, d, ^2J = 6.5 Hz, SiH<u>H</u>$_b$), 4.34 (1 H, app. sept., app. ^3J = 7.0 Hz, NC<u>H</u>$_a$MeMe), 3.00 (1 H, app. sept., app. ^3J = 7.0 Hz, NC<u>H</u>$_b$MeMe), 2.98 (3 H, s, NN<u>Me</u>Me), 2.47 (3 H, s, NNMe<u>Me</u>), 2.12 (15 H, s, C$_5$Me$_5$), 1.55 (3 H, s,

$MeCN_2$), 1.32 (6 H, overlapping 2 × d, 2 × ^3J = 7.0 Hz, overlapping $NCH_a\underline{MeMe}$), 1.07 (6 H, overlapping 2 × d, 2 × ^3J = 7.0 Hz, overlapping $NCH_b\underline{MeMe}$). $^{13}C\{^1H\}$ NMR (toluene-d_8, 125.7 MHz, 253 K): δ 170.3 ($Me\underline{C}N_2$), 136.0 (*i*-C_6H_5), 134.7 (*o*-C_6H_5), 130.0 (*p*-C_6H_5), 128.2 (*m*-C_6H_5), 125.1 ($\underline{C}_5Me_5$), 54.8 (NN$\underline{Me}$Me), 49.7 ($N\underline{C}H_aMeMe$), 48.5 ($N\underline{C}H_bMeMe$), 48.3 (NNMe$\underline{Me}$), 27.1 ($NCH_bMe\underline{Me}$), 23.9 ($NCH_aMe\underline{Me}$), 22.9 ($NCH_b\underline{Me}Me$), 22.8 ($NCH_a\underline{Me}Me$), 15.3 ($\underline{Me}CN_2$), 13.9 ($C_5\underline{Me}_5$). ^{29}Si NMR (HMQC ^1H-observed, C_6D_6, 299.9 MHz, 293 K): δ -45.6 (SiH_2Ph). IR (NaCl plates, Nujol mull, cm^{-1}): 2155 (s), 2127 (s), 1519 (s), 1457 (s), 1429 (s), 1391 (m), 1356 (m), 1340 (m), 1198 (s), 1168(m), 1110 (m), 1084 (w), 1067 (w), 1015 (s), 989 (m), 948 (s), 923 (w), 902 (m), 868 (s), 810 (s), 786 (w), 756 (w), 719 (s), 700 (m), 690 (w), 680 (w), 622 (w), 613 (m), 580 (m). EI-MS: *m/z* = 165 [*M* – $Cp^*Ti\{MeC(N^iPr)_2\}Cl]^+$ (25%), 213 $[Ti\{N(NMe_2)Si(H_2)Ph\}]^+$ (30%), 276 $[Cp^*Ti(NNMe_2)Cl]^+$ (15%), 359 $[Cp^*Ti\{MeC(N^iPr)_2\}Cl]^+$ (100%). Anal. found (calcd. for $C_{26}H_{45}ClN_4SiTi$): C, 59.28 (59.47); H, 8.37 (8.64); N, 10.38 (10.67)%.

NMR tube scale reaction of $Cp^*Ti\{MeC(N^iPr)_2\}(H)\{N(NMe_2)SiH_2Ph\}$ (20) or $Cp^*Ti\{MeC(N^iPr)_2\}(D)\{N(NMe_2)SiD_2Ph\}$ (20-*d*$_3$) with $PhSiH_2Cl$. To a solution of $Cp^*Ti\{MeC(N^iPr)_2\}(H)\{N(NMe_2)SiH_2Ph\}$ (**20**, 15.0 mg, 0.030 mmol) in C_6D_6 (0.6 mL) in an NMR tube equipped with a J. Young Teflon valve was added $PhSiH_2Cl$ (4.10 μL, 0.030 mmol) all at RT. The ^1H NMR spectrum recorded immediately contained resonances attributed to $Cp^*Ti\{MeC(N^iPr)_2\}(Cl)\{N(NMe_2)SiH_2Ph\}$ (**24**) and $PhSiH_3$. The same reaction was repeated using **20-*d*$_3$** and monitored using ^2H NMR spectroscopy.

NMR tube scale synthesis of $Cp^*Ti\{MeC(N^iPr)_2\}(Cl)\{N(NMe_2)SiH(Me)Ph\}$ (25). To a solution of $Cp^*Ti\{MeC(N^iPr)_2\}(NNMe_2)$ (20.0 mg, 0.052 mmol) in C_6D_6 (0.6 mL) in an NMR tube equipped with a J. Young Teflon valve was added Ph(Me)SiHCl (7.90 μL, 0.052 mmol) all at RT. An immediate colour change from dark green to orange was observed and the ^1H NMR spectrum recorded immediately showed complete conversion to **25**. The volatiles were removed under reduced pressure and the product **25** was characterised by NMR spectroscopy.

Major isomer: ^1H NMR (toluene-d_8, 299.9 MHz, 253 K): δ 7.61 (2 H, d, ^3J = 7.5 Hz, *o*-C_6H_5), 7.25 (2 H, app. t, app. ^3J = 7.5 Hz, *m*-C_6H_5), 7.18 (1 H, app. t, app. ^3J = 7.5 Hz, *p*-C_6H_5), 5.52 (1 H, q, ^3J = 3.6 Hz, SiH), 4.40 (1 H, app. sept, app. ^3J = 6.9 Hz, $NC\underline{H}_aMeMe$), 3.00 (3 H, s, NN$\underline{Me}$Me), 2.97 (1 H, app. sept, app. ^3J = 6.9 Hz,

NC$\underline{H}_b$MeMe), 2.48 (3 H, s, NNMe$\underline{Me}$), 2.14 (15 H, s, C_5Me_5), 1.59 (3 H, s, $MeCN_2$), 1.33 (6 H, m, overlapping NC$H_a$$\underline{MeMe}$), 1.09 (6 H, m, overlapping NC$H_b$$\underline{MeMe}$), 0.47 (3 H, d, ^3J = 3.6 Hz, SiMe). $^{13}C\{^1H\}$ NMR (toluene-d_8, 75.4 MHz, 253 K): δ 169.8 (Me$\underline{C}N_2$), 139.6 (*i*-C_6H_5), 135.4 (*o*-C_6H_5), 129.6 (*p*-C_6H_5), 127.9 (*m*-C_6H_5), 125.0 ($\underline{C}_5Me_5$), 54.7 (NN$\underline{Me}$Me), 51.0 (NNMe$\underline{Me}$), 49.4 (N$\underline{C}H_a$MeMe), 48.3 (N$\underline{C}H_b$MeMe), 27.1 (overlapping NC$H_b$$\underline{MeMe}$), 22.7 (overlapping NC$H_a$$\underline{MeMe}$), 15.6 ($\underline{Me}CN_2$), 13.9 ($C_5\underline{Me}_5$), -0.7 (SiMe). ^{29}Si NMR (toluene-d_8, 299.9 MHz, 253 K): δ -21.9 (SiH(Me)Ph).

Minor isomer: ^{1}H NMR (toluene-d_8, 299.9 MHz, 253 K): δ 7.61 (2 H, d, ^3J = 7.5 Hz, *o*-C_6H_5), 7.25 (2 H, app. t, app. ^3J = 7.5 Hz, *m*-C_6H_5), 7.18 (1 H, app. t, app. ^3J = 7.5 Hz, *p*-C_6H_5), 5.47 (1 H, q, ^3J = 3.6 Hz, SiH), 4.24 (1 H, app. sept, app. ^3J = 6.9 Hz, NC$\underline{H}_a$MeMe), 3.14 (3 H, s, NN$\underline{Me}$Me), 2.84 (1 H, app. sept, app. ^3J = 6.9 Hz, NC$\underline{H}_b$MeMe), 2.19 (3 H, s, NNMe$\underline{Me}$), 2.15 (15 H, s, C_5Me_5), 1.51 (3 H, s, $MeCN_2$), 1.31 (6 H, m, overlapping NC$H_a$$\underline{MeMe}$), 1.06 (6 H, m, overlapping NC$H_b$$\underline{MeMe}$), 0.58 (3 H, d, ^3J = 3.6 Hz, SiMe). $^{13}C\{^1H\}$ NMR (toluene-d_8, 75.4 MHz, 253 K): δ 169.6 (Me$\underline{C}N_2$), 137.9 (*i*-C_6H_5), 134.5 (*o*-C_6H_5), 129.8 (*p*-C_6H_5), 128.0 (*m*-C_6H_5), 124.9 ($\underline{C}_5Me_5$), 54.6 (NN$\underline{Me}$Me), 50.6 (NNMe$\underline{Me}$), 49.5 (N$\underline{C}H_a$MeMe), 48.1 (N$\underline{C}H_b$MeMe), 23.8 (overlapping NC$H_a$$\underline{MeMe}$), 22.8 (overlapping NC$H_b$$\underline{MeMe}$), 15.1 ($\underline{Me}CN_2$), 14.2 ($C_5\underline{Me}_5$), 0.1 (SiMe). ^{29}Si NMR (toluene-d_8, 299.9 MHz, 253 K): δ -22.6 (SiH(Me)Ph).

NMR tube scale synthesis of Cp*Ti{MeC(N^{i}Pr)$_2$}(Cl){N(NMe$_2$)SiHMe$_2$} (26). To a solution of Cp*Ti{MeC(N^{i}Pr)$_2$}(NNMe$_2$) (17.9 mg, 0.047 mmol) in toluene-d_8 (0.6 mL) in an NMR tube equipped with a J. Young Teflon valve was added Me_2SiHCl (5.20 μL, 0.047 mmol) all at RT. An immediate colour change from dark green to orange was observed and the ^{1}H NMR spectrum recorded immediately showed complete conversion to **26** which was characterised by NMR spectroscopy. ^{1}H NMR (toluene-d_8, 499.9 MHz, 243 K): δ 5.09 (1 H, app. sept, app. ^3J = 3.5 Hz, SiH), 4.30 (1 H, app. sept, app. ^3J = 6.5 Hz, NC$\underline{H}_a$MeMe), 2.95 (3 H, s, NN$\underline{Me}$Me), 2.94 (1 H, app. sept, app. ^3J = 6.5 Hz, NC$\underline{H}_b$MeMe), 2.46 (3 H, s, NNMe$\underline{Me}$), 2.15 (15 H, s, C_5Me_5), 1.56 (3 H, s, $MeCN_2$), 1.35 (3 H, d, ^3J = 6.5 Hz, NC$H_a$$\underline{Me}$Me), 1.33 (3 H, d, ^3J = 6.5 Hz, NCH_aMe$\underline{Me}$), 1.06 (3 H, d, ^3J = 6.5 Hz, NC$H_b$$\underline{Me}$Me), 0.98 (3 H, d, ^3J = 6.5 Hz, NCH_bMe$\underline{Me}$), 0.23 (3 H, d, ^3J = 3.5 Hz, SiH$\underline{Me}$Me), 0.19 (3 H, d, ^3J = 3.5 Hz, SiHMe$\underline{Me}$). $^{13}C\{^1H\}$ NMR (toluene-d_8, 125.7 MHz, 243 K): δ 169.9 (Me$\underline{C}N_2$), 124.5

($\underline{C}_5Me_5$), 55.4 (NN$\underline{Me}$Me), 50.3 (NNMe$\underline{Me}$), 49.4 (N$\underline{C}H_a$MeMe), 48.3 (N$\underline{C}H_b$MeMe), 27.1 (NCH$_b\underline{Me}$Me), 24.1 (NCH$_a$Me$\underline{Me}$), 23.0 (NCH$_b$Me$\underline{Me}$), 22.9 (NCH$_a\underline{Me}$Me), 15.4 ($\underline{Me}CN_2$), 14.1 ($C_5\underline{Me}_5$), 2.9 (SiH$\underline{Me}$Me), 1.1 (SiHMe$\underline{Me}$). ^{29}Si NMR (HMQC ^{1}H-observed, toluene-d_8, 299.9 MHz, 243 K): δ -14.1 ($SiHMe_2$).

NMR tube scale reaction of Cp*Ti{MeC(N^{i}Pr)$_2$}(Cl){N(NMe$_2$)SiH(Me)Ph} (25) with PhSiH$_2$Cl. To a solution of Cp*Ti{MeC(N^{i}Pr)$_2$}(Cl){N(NMe$_2$)SiH(Me)Ph} (**25**, 15.0 mg, 0.028 mmol) in C_6D_6 (0.6 mL) in an NMR tube equipped with a J. Young Teflon valve was added $PhSiH_2Cl$ (3.75 μL, 0.028 mmol) all at RT. The ^{1}H NMR spectrum recorded immediately contained resonances attributed to Cp*Ti{MeC(N^{i}Pr)$_2$}(Cl){N(NMe$_2$)SiH$_2$Ph} (**24**) and Ph(Me)SiHCl.

NMR tube scale reaction of Cp*Ti{MeC(N^{i}Pr)$_2$}(H){N(NMe$_2$)SiH$_2$Ph} (20) with Ph(Me)SiHCl. To a solution of Cp*Ti{MeC(N^{i}Pr)$_2$}(H){N(NMe$_2$)SiH$_2$Ph} (**20**, 15.0 mg, 0.030 mmol) in C_6D_6 (0.6 mL) in an NMR tube equipped with a J. Young Teflon valve was added Ph(Me)SiHCl (4.60 μL, 0.030 mmol) all at RT. The ^{1}H NMR spectrum recorded immediately contained resonances attributed to Cp*Ti{MeC(N^{i}Pr)$_2$}(Cl){N(NMe$_2$)SiH(Me)Ph} (**25**) and $PhSiH_3$.

Cp*Ti{N(NMe$_2$)SiH(Ph)N(^{i}Pr)CMeN^{i}Pr}Cl$_2$ (27). To a stirred solution of Cp*Ti{MeC(N^{i}Pr)$_2$}(NNMe$_2$) (0.305 g, 0.798 mmol) in benzene (20 mL) was added $PhSiHCl_2$ (117.0 μL, 0.798 mmol) all at RT. An immediate colour change from dark green to orange was observed. After 16 h, the volatiles were removed under reduced pressure to give an oily crude product, which was then washed with cold pentane (3 × 10 mL) cooled to -78 ℃ and dried *in vacuo* to afford **27** as an orange solid. Yield: 0.258 g (58%). Diffraction-quality crystals were grown from a saturated diethyl ether solution at -30 ℃. ^{1}H NMR (C_6D_6, 499.9 MHz, 293 K): δ 7.60 (2 H, d, ^3J = 7.5 Hz, *o*-C_6H_5), 7.18 (3 H, m, overlapping *m*- and *p*-C_6H_5), 5.82 (1H, s, SiH), 3.33 (2 H, app. sept, app. ^3J = 6.5 Hz, NC$\underline{H}$MeMe), 3.24 (3 H, s, NN$\underline{Me}$Me), 2.86 (3 H, s, NNMe$\underline{Me}$), 2.06 (15 H, s, C_5Me_5), 1.31 (3 H, s, $MeCN_2$), 0.94 (6 H, overlapping 2 × d, 2 × ^3J = 6.5 Hz, overlapping NCH$\underline{Me}$Me), 0.88 (6 H, overlapping 2 × d, 2 × ^3J = 6.5 Hz, overlapping NCHMe$\underline{Me}$). Cooling an NMR sample in toluene-d_8 to 203 K gave broadening of the resonances but decoalescence was not achieved. ^{13}C{^{1}H} NMR (C_6D_6, 125.7 MHz, 293 K): δ 159.7 (Me$\underline{C}N_2$), 140.6 (*i*-C_6H_5), 133.6 (*o*-C_6H_5), 128.7 (*p*-C_6H_5), 127.9 ($\underline{C}_5Me_5$), 127.8 (*m*-C_6H_5), 54.0 (NNMe$\underline{Me}$), 50.0 (NN$\underline{Me}$Me), 47.4 (N$\underline{C}$HMeMe), 24.4 (NCH$\underline{Me}$Me), 24.1 (NCHMe$\underline{Me}$), 13.5 ($C_5\underline{Me}_5$), 13.1 ($\underline{Me}CN_2$).

^{29}Si NMR (HMQC ^{1}H-observed, C_6D_6, 299.9 MHz, 293 K): δ -45.5 (SiH). IR (NaCl plates, Nujol mull, cm^{-1}): 2183 (w), 1617 (m), 1603 (m), 1427 (m), 1414 (w), 1365 (m), 1320 (m), 1307 (s), 1189 (w), 1174 (w), 1159 (w), 1127 (w), 1108 (m), 1070 (s), 1015 (w), 918 (w), 861 (s), 806 (w), 742 (s), 715 (m), 704 (m), 695 (m), 582 (s). EI-MS: *m/z* = 218 $[Cp^*TiCl]^+$ (50%), 276 $[Cp^*Ti(NNMe_2)Cl]^+$ (35%), 417 $[M - \{MeC(N^iPr)_2\}]^+$ (55%). Anal. found (calcd. for $C_{26}H_{44}Cl_2N_4SiTi$): C, 55.90 (55.81); H, 7.83 (7.93); N, 9.73 (10.01)%.

$Cp^*Ti\{N(NMe_2)SiMe_2N(^iPr)CMeN^iPr\}Cl_2$ (28). To a stirred solution of $Cp^*Ti\{MeC(N^iPr)_2\}(NNMe_2)$ (0.305 g, 0.80 mmol) in benzene (20 mL) was added Me_2SiCl_2 (96.5 μL, 0.80 mmol) all at RT. An immediate colour change from dark green to orange was observed. The volatiles were removed under reduced pressure after 3 h to afford **28** as an orange solid. Yield: 0.169 g (41%). Diffraction-quality crystals were grown from a saturated diethyl ether solution. ^{1}H NMR (toluene-d_8, 499.9 MHz, 223 K): δ 3.87 (1 H, app. sept, app. ^{3}J = 6.5 Hz, NC$\underline{H}_a$MeMe), 3.35 (1 H, app. sept, app. ^{3}J = 6.5 Hz, NC$\underline{H}_b$MeMe), 3.04 (6 H, s, NN$\underline{MeMe}$), 2.00 (15 H, s, $C_5\underline{Me}_5$), 1. 47 (3 H, s, $MeCN_2$), 1.11 (6 H, overlapping 2 × d, 2 × ^{3}J = 6.5 Hz, overlapping NC$H_b\underline{Me}$Me and NCH_bMe$\underline{Me}$), 1.03 (6 H, overlapping 2 × d, 2 × ^{3}J = 6.5 Hz, overlapping NC$H_a\underline{Me}$Me and NCH_aMe$\underline{Me}$), 0.51 (6 H, s, Si$\underline{Me}_2$). ^{13}C{^{1}H} NMR (toluene-d_8, 125.7 MHz, 223 K): δ 158.6 ($Me\underline{C}N_2$), 127.3 ($\underline{C}_5Me_5$), 53.5 (NN$\underline{Me}_2$), 49.2 (N$\underline{C}H_b$MeMe), 45.6 (N$\underline{C}H_a$MeMe), 24.6 (overlapping NC$H_b\underline{Me}$Me and NCH_bMe$\underline{Me}$), 23.3 (overlapping NC$H_a\underline{Me}$Me and NCH_aMe$\underline{Me}$), 16.7 ($\underline{Me}CN_2$) 13.5 ($C_5\underline{Me}_5$), 3.9 (Si$\underline{Me}_2$). ^{29}Si NMR (toluene-d_8, 299.9 MHz, 223 K): δ -12.9 ($SiMe_2$). IR (NaCl plates, Nujol mull, cm^{-1}): 1667 (s), 1457 (s), 1341 (m), 1314 (m), 1204 (m), 1174 (w), 1126 (m), 1092 (m), 1015 (m), 973 (w), 888 (m), 789 (m), 721 (m). EI-MS: *m/z* = 199 $[M - Cp^*TiCl_2NNMe_2]^+$ (90%), 276 $[Cp^*TiClNNMe_2]^+$ (50%), 369 $[M - \{MeC(N^iPr)_2\}]^+$ (100%). Anal. found (calcd. for $C_{22}H_{44}Cl_2N_4SiTi$): C, 51.56 (51.66); H, 8.26 (8.67); N, 10.82 (10.95)%.

NMR tube scale synthesis of $Cp^*Ti\{MeC(N^iPr)_2\}(Br)\{N(NMe_2)SiH_2Ph\}$ (29). To a solution of $Cp^*Ti\{MeC(N^iPr)_2\}(NNMe_2)$ (25.0 mg, 0.065 mmol) in toluene-d_8 (0.6 mL) in an NMR tube equipped with a J. Young Teflon valve was added $PhSiH_2Br$ (12.3 mg, 0.065 mmol) all at RT. An immediate colour change from dark green to brown was observed and the ^{1}H NMR spectrum recorded immediately showed complete conversion to **29** which was characterised by NMR spectroscopy. ^{1}H NMR

(toluene-d_8, 299.9 MHz, 193 K): δ 7.62 (2 H, d, ^3J = 6.6 Hz, *o*-C_6H_5), 7.13 (3 H, m, overlapping *m*- and *p*-C_6H_5), 5.30 (1 H, d, ^2J = 5.7 Hz, Si$\underline{H}_a$H), 5.23 (1 H, d, ^2J = 5.7 Hz, SiH$\underline{H}_b$), 4.72 (1 H, br. s, NC$\underline{H}_a$MeMe), 3.07 (3 H, s, NN$\underline{Me}$Me), 2.71 (1 H, br. s, NC$\underline{H}_b$MeMe), 2.32 (3 H, s, NNMe$\underline{Me}$), 2.13 (15 H, s, C_5Me_5), 1.39 (3 H, s, $MeCN_2$), 1.31 (6 H, m, overlapping NCH$_a\underline{MeMe}$), 0.92 (6 H, m, overlapping NCH$_a\underline{MeMe}$). $^{13}C\{^1H\}$ NMR (toluene-d_8, 75.4 MHz, 193 K): δ 170.0 (Me$\underline{C}N_2$), 137.1 (*i*-C_6H_5), 134.3 (*o*-C_6H_5), 129.1 (*p*-C_6H_5), 128.5 ($\underline{C}_5Me_5$), 128.2 (*m*-C_6H_5), 57.8 (NN$\underline{Me}$Me), 50.7 (N$\underline{C}$H$_a$MeMe), 48.4 (N$\underline{C}$H$_b$MeMe), 47.0 (NNMe$\underline{Me}$), 26.7 (NCH$_b\underline{Me}$Me), 23.8 (NCH$_a$Me$\underline{Me}$), 22.5 (NCH$_a\underline{Me}$Me), 22.1 (NCH$_b$Me$\underline{Me}$), 15.9 ($\underline{Me}CN_2$), 14.3 ($C_5\underline{Me}_5$) ^{29}Si NMR (HMQC ^{1}H-observed, toluene-d_8, 299.9 MHz, 193 K): δ -41.7 (SiH_2Ph). ES^+-MS (sample prepared *in situ* in THF): *m/z* = 489 $[M - Br]^+$ (100%).

NMR tube scale reaction of Cp*Ti{MeC(N^{i}Pr)$_2$}(Cl){N(NMe$_2$)SiH(Me)Ph} (25) with PhSiH$_2$Br. To a solution of Cp*Ti{MeC(N^{i}Pr)$_2$}(Cl){N(NMe$_2$)SiH(Me)Ph} (**25**, 15.0 mg, 0.028 mmol) in C_6D_6 (0.6 mL) in an NMR tube equipped with a J. Young Teflon valve was added $PhSiH_2Br$ (5.21 mg, 0.028 mmol) all at RT. The ^{1}H NMR spectrum recorded immediately contained resonances attributed to Cp*Ti{MeC(N^{i}Pr)$_2$}(Br){N(NMe$_2$)SiH$_2$Ph} (**29**) and Ph(Me)SiHCl.

NMR tube scale reaction of Cp*Ti{MeC(N^{i}Pr)$_2$}(H){N(NMe$_2$)SiH$_2$Ph} (20) or Cp*Ti{MeC(N^{i}Pr)$_2$}(D){N(NMe$_2$)SiD$_2$Ph} (20-*d$_3$*) with PhSiH$_2$Br. To a solution of Cp*Ti{MeC(N^{i}Pr)$_2$}(H){N(NMe$_2$)SiH$_2$Ph} (**20**, 15.0 mg, 0.030 mmol) in C_6D_6 (0.6 mL) in an NMR tube equipped with a J. Young Teflon valve was added $PhSiH_2Br$ (5.72 mg, 0.030 mmol) all at RT. The ^{1}H NMR spectrum recorded immediately contained resonances attributed to Cp*Ti{MeC(N^{i}Pr)$_2$}(Br){N(NMe$_2$)SiH$_2$Ph} (**29**) and $PhSiH_3$. The same reaction was repeated using **20-*d$_3$*** and monitored using ^{2}H NMR spectroscopy.

Cp*Ti{N(NPh$_2$)SiH$_2$Ph}Cl$_2$ (30). To a solution of Cp*Ti{MeC(N^{i}Pr)$_2$}(NNPh$_2$) (0.200 g, 0.395 mmol) in benzene (5 mL) was added $PhSiH_2Cl$ (105.3 μL, 0.790 mmol) in benzene (5 mL) all at RT. A colour change from dark green to brown was observed. After 20 h, the volatiles were reduced under reduced pressure to give a brown oil which contained **30** and the side-product ^{i}PrNC(Me)N(^{i}Pr)SiH_2Ph (**31**) which could not be separated. Combined yield: 0.213 g (83%).

Data for **30**: ^{1}H NMR (C_6D_6, 299.9 MHz, 293 K): δ 7.64 (4 H, d, ^{3}J = 7.5 Hz, *o*-C_6H_5), 7.44 (2 H, d, ^{3}J = 7.5 Hz, *o*-C_6H_5Si), 7.10 (2 H, t, ^{3}J = 7.5 Hz, *m*-C_6H_5Si), 7.05 (1 H, t, ^{3}J = 7.5 Hz, *p*-C_6H_5Si), 6.87 (4 H, t, ^{3}J = 7.5 Hz, *m*-C_6H_5), 6.75 (2 H, t, ^{3}J = 7.5 Hz, *p*-C_6H_5), 5.15 (2 H, s, SiH_2), 1.87 (15 H, s, C_5Me_5). $^{13}C\{^{1}H\}$ NMR (C_6D_6, 75.4 MHz, 293 K): δ 149.9 (*i*-C_6H_5), 136.2 (*o*-C_6H_5Si), 133.7 (*i*-C_6H_5Si), 130.5 (*p*-C_6H_5Si), 130.0 ($\underline{C}_5Me_5$), 128.6 (*m*-C_6H_5), 128.1 (*m*-C_6H_5Si), 126.8 (*p*-C_6H_5), 126.0 (*o*-C_6H_5), 13.2 ($C_5\underline{Me}_5$). ^{29}Si NMR (HMQC ^{1}H-observed, C_6D_6, 299.9 MHz, 293 K): δ -30.6 (SiH_2). IR (NaCl plates, Nujol mull, cm^{-1}): 2152 (s), 1590 (s), 1488 (s), 1452 (s), 1277 (m), 1158 (s), 1058 (s), 1023 (s), 1003 (w), 970 (m), 862 (s), 833 (s), 762 (s), 633 (m), 616 (m), 607 (m). EI-MS: *m/z* = 542 $[M]^+$ (50%), 472 $[M - 2\ Cl]^+$ (50%), 253 $[Cp^*TiCl_2]^+$ (70%). An elemental analysis could not be obtained due to contamination with **31**.

Data for **31**: ^{1}H NMR (C_6D_6, 299.9 MHz, 293 K): δ 7.92 (2 H, d, ^{3}J = 7.5 Hz, *o*-C_6H_5), 7.23 (3 H, app. t, app. ^{3}J = 7.5 Hz, overlapping *m*- and *p*-C_6H_5), 5.33 (2 H, s, SiH_2), 3.38 (2 H, sept, ^{3}J = 6.6 Hz, $NC\underline{H}Me_2$), 1.36 (3 H, s, $MeCN_2$), 1.09 (12 H, d, ^{3}J = 6.6 Hz, $NCH\underline{Me}_2$). $^{13}C\{^{1}H\}$ NMR (C_6D_6, 75.4 MHz, 293 K): δ 159.9 ($Me\underline{C}N_2$), 137.9 (*i*-C_6H_5), 135.2 (*o*-C_6H_5), 129.0 (*m*-C_6H_5), 127.4 (*p*-C_6H_5), 47.3 ($N\underline{C}HMeMe$), 24.7 ($NCH\underline{Me}_2$), 10.7 ($\underline{Me}CN_2$). ^{29}Si NMR (HMQC ^{1}H-observed, C_6D_6, 299.9 MHz, 293 K): δ -58.1 (SiH_2). IR (NaCl plates, Nujol mull, cm^{-1}): 2966 (s), 2931 (s), 2868 (m), 2151 (m), 2107 (m), 1629 (s), 1457 (m), 1428 (s), 1393 (s), 1364 (s), 1323 (s), 1261 (w), 1218 (m), 1176 (w), 1163 (w), 1140 (w), 1129 (w), 1116 (s), 1067 (w), 1019 (m), 975 (s), 900 (s), 874 (s), 808 (m), 737 (m), 699 (s), 656 (w), 638 (m). EI-HRMS: *m/z* found (calcd. for $C_{14}H_{24}N_2Si$, $[M]^+$) 248.1707 (248.1709). An elemental analysis could not be obtained.

Cp*Ti{N(NPh$_2$)SiH(Me)Ph}Cl$_2$ (32). To a solution of Cp*Ti{MeC(N^{i}Pr)$_2$}(NNPh$_2$) (0.203 g, 0.40 mmol) in benzene (5 mL) was added Ph(Me)SiHCl (120.2 μL, 0.80 mmol) in benzene (5 mL) all at RT. After 2 d, the volatiles were removed under reduced pressure to yield a brown oil. Diffraction-quality crystals of **32** were grown by benzene/hexanes layering at 4 ℃. Yield of **32**: 90 mg (40%) The side product ^{i}PrNC(Me)N(^{i}Pr)SiH(Me)Ph (**33**) could not be isolated in a pure form free from **32** and was characterised by spectroscopic methods.

Data for **32**: ^{1}H NMR (C_6D_6, 299.9 MHz, 293 K): δ 7.74 (2 H, d, ^{3}J = 7.5 Hz, o_a-C_6H_5), 7.59 (2 H, d, ^{3}J = 7.5 Hz, o_b-C_6H_5), 7.53 (2 H, d, ^{3}J = 7.5 Hz, *o*-C_6H_5Si), 7.20 (3 H, m, overlapping m_b- and p_b-C_6H_5), 6.89 (2 H, t, ^{3}J = 7.5 Hz, m_a-C_6H_5), 6.82 (3 H,

m, overlapping *m*-C_6H_5Si and p_a-C_6H_5), 6.70 (1 H, app. t, app. ^3J = 7.5 Hz, *p*-C_6H_5Si), 5.43 (1 H, q, ^3J = 3.6 Hz, SiH), 1.86 (15 H, s, C_5Me_5), 0.07 (3 H, d, ^3J = 3.6 Hz, SiMe). $^{13}C\{^1H\}$ NMR (C_6D_6, 75.4 MHz, 293 K): δ 150.6 (i_a-C_6H_5), 150.5 (*i*-C_6H_5Si), 136.5 (i_b-C_6H_5), 135.8 (o_b-C_6H_5), 130.3 (p_b-C_6H_5), 130.0 ($\underline{C}_5Me_5$), 128.7 (*m*-C_6H_5Si), 128.4 (m_a-C_6H_5), 128.2 (m_b-C_6H_5), 127.4 (o_a-C_6H_5), 127.2 (p_a-C_6H_5), 126.4 (*p*-C_6H_5Si), 124.9 (*o*-C_6H_5Si), 13.2 ($C_5\underline{Me}_5$), -4.6 (SiMe). ^{29}Si NMR (HMQC ^{1}H-observed, C_6D_6, 299.9 MHz, 293 K): δ -12.3 (SiH(Me)). IR (NaCl plates, Nujol mull, cm^{-1}): 2154 (s), 1954 (w), 1891 (w), 1586 (s), 1427 (s), 1309 (m), 1257 (s), 1211 (m), 1192 (w), 1167 (w), 1150 (s), 1118 (s), 1086 (w), 1079 (w), 1069 (w), 1041 (s), 1031 (s), 1021 (s), 1001 (m), 985 (w), 970 (w), 914 (w), 878 (s), 861 (s), 812 (s), 760 (s), 741 (s), 731 (s), 701 (s), 690 (s), 628 (w), 617 (w), 606 (w), 590 (m). EI-MS: *m/z* = 421 $[M - Cp^*]^+$ (100%). Anal. found (calcd. for $C_{29}H_{34}Cl_2N_2SiTi$): C, 62.61 (62.48); H, 6.00 (6.15); N, 4.93 (5.03)%.

Data for **33**: ^{1}H NMR (C_6D_6, 299.9 MHz, 293 K): δ 7.84 (2 H, d, ^3J = 7.5 Hz, *o*-C_6H_5), 7.27 (2 H, t, ^3J = 7.5 Hz, *m*-C_6H_5), 7.07 (1 H, t, ^3J = 7.5 Hz, *p*-C_6H_5), 5.16 (1 H, q, ^3J = 3.6 Hz, SiH), 3.38 (2 H, app. sept, app. ^3J = 6.6 Hz, NC$\underline{H}$MeMe), 1.36 (3 H, s, $MeCN_2$), 1.16 (6 H, d, ^3J = 6.6 Hz, NCH$\underline{Me}$Me), 0.97 (6 H, d, ^3J = 6.6 Hz, NCHMe$\underline{Me}$), 0.78 (3 H, d, ^3J = 3.6 Hz, SiMe). $^{13}C\{^1H\}$ NMR (C_6D_6, 75.4 MHz, 293 K): δ 158.7 (Me$\underline{C}N_2$), 140.2 (*i*-C_6H_5), 134.6 (*o*-C_6H_5), 129.5 (*p*-C_6H_5), 127.5 (*m*-C_6H_5), 47.3 (N$\underline{C}$HMeMe), 24.6 (NCH$\underline{Me}$Me), 24.4 (NCHMe$\underline{Me}$), 10.9 ($\underline{Me}CN_2$), -0.5 (SiMe). ^{29}Si NMR (HMQC ^{1}H-observed, C_6D_6, 299.9 MHz, 293 K): δ -35.4 (SiH(Me)). EI-HRMS: *m/z* found (calcd. for $C_{15}H_{26}N_2Si$, $[M]^+$) 262.1870 (262.1865). An elemental analysis could not be obtained.

NMR tube scale synthesis of Cp*Ti{MeC(N^{i}Pr)$_2$}(Cl){N(Tol)SiH$_2$Ph} (34). To a solution of Cp*Ti{MeC(N^{i}Pr)$_2$}(NTol) (15.0 mg, 0.035 mmol) in toluene-d_8 (0.6 mL) in an NMR tube equipped with a J. Young Teflon valve was added $PhSiH_2Cl$ (4.70 μL, 0.035 mmol) all at RT. An immediate colour change from dark green to brown was observed. The product **34** formed quantitatively and was characterised by NMR spectroscopy. ^{1}H NMR data (toluene-d_8, 299.9 MHz, 253 K): δ 7.74 (2 H, d, ^3J = 7.3 Hz, *o*-C_6H_5), 7.06 (3 H, m, overlapping *m*- and *p*-C_6H_5), 6.94 (2 H, d, ^3J = 8.0 Hz, *o*-$C_6\underline{H}_4Me$), 6.78 (2 H, d, ^3J = 8.0 Hz, *m*-$C_6\underline{H}_4Me$), 5.43 (1 H, d, ^2J = 8.7 Hz, Si$\underline{H}_a$H), 5.08 (1 H, d, ^2J = 8.7 Hz, SiH$\underline{H}_b$), 4.50 (1 H, app. sept., app. ^3J = 7.2 Hz, NC$\underline{H}_a$MeMe), 3.70 (1 H, app. sept., app. ^3J = 7.2 Hz, NC$\underline{H}_b$MeMe), 2.09 (3 H, s,

$C_6H_4\underline{Me}$), 1.81 (15 H, s, $C_5\underline{Me}_5$), 1.75 (3 H, s, $\underline{Me}CN_2$), 1.49 (3 H, d, ^3J = 7.2 Hz, $NCH_a\underline{Me}Me$), 1.45 (3 H, d, ^3J = 7.2 Hz, $NCH_b\underline{Me}Me$), 1.24 (3 H, d, 2 × ^3J = 7.2 Hz, $NCH_aMe\underline{Me}$), 1.21 (3 H, d, 2 × ^3J = 7.2 Hz, $NCH_bMe\underline{Me}$). $^{13}C\{^1H\}$ NMR (toluene-d_8, 75.4 MHz, 253 K): δ 170.3 ($Me\underline{C}N_2$), 155.1 (overlapping *i*-C_6H_5 and *i*-$\underline{C}_6H_4Me$), 137.1 (*o*-C_6H_5), 134.0 (*p*-$\underline{C}_6H_4Me$), 132.1(*m*-$\underline{C}_6H_4Me$), 129.6 (*p*-C_6H_5), 128.4 (*o*-$\underline{C}_6H_4Me$), 127.4 ($\underline{C}_5Me_5$), 127.3 (*m*-C_6H_5), 51.1 ($N\underline{C}H_aMeMe$), 49.1 ($N\underline{C}H_bMeMe$), 26.3 ($NCH_bMe\underline{Me}$), 24.3 ($NCH_b\underline{Me}Me$), 23.5 ($NCH_aMe\underline{Me}$), 23.0 ($NCH_a\underline{Me}Me$), 20.9 ($C_6H_4\underline{Me}$), 16.8 ($\underline{Me}CN_2$), 13.0 ($C_5\underline{Me}_5$). ^{29}Si NMR (HMQC ^{1}H-observed, C_6D_6, 299.9 MHz, 253 K): δ -35.7 (SiH_2).

NMR tube scale synthesis of Cp*Ti{MeC(N^{i}Pr)$_2$}(Br){N(Tol)SiH$_2$Ph} (35). To a solution of Cp*Ti{MeC(N^{i}Pr)$_2$}(NTol) (20.0 mg, 0.047 mmol) in toluene-d_8 (0.6 mL) in an NMR tube equipped with a J. Young Teflon valve was added $PhSiH_2Br$ (8.70 mg, 0.047 mmol) all at RT. An immediate colour change from dark green to brown was observed. The product **35** was formed quantitatively and characterised by NMR spectroscopy. ^{1}H NMR data (toluene-d_8, 299.9 MHz, 253 K): δ 7.68 (2 H, d, ^3J = 6.9 Hz, *o*-C_6H_5), 7.04 (3 H, m, overlapping *m*- and *p*-C_6H_5), 6.90 (2 H, d, ^3J = 8.4 Hz, *o*-$C_6\underline{H}_4Me$), 6.69 (2 H, d, ^3J = 8.4 Hz, *m*-$C_6\underline{H}_4Me$), 5.43 (1 H, d, ^2J = 8.7 Hz, $Si\underline{H}_aH$), 5.04 (1 H, d, ^2J = 8.7 Hz, $SiH\underline{H}_b$), 4.66 (1 H, app. sept, app. ^3J = 6.9 Hz, $NC\underline{H}_aMeMe$), 3.66 (1 H, app. sept, app. ^3J = 6.9 Hz, $NC\underline{H}_bMeMe$), 2.10 (3 H, s, $C_6H_4\underline{Me}$), 1.84 (15 H, s, C_5Me_5), 1.75 (3 H, s, $MeCN_2$), 1.51 (3 H, d, ^3J = 6.9 Hz, $NCH_a\underline{Me}Me$), 1.42 (3 H, d, ^3J = 6.9 Hz, $NCH_b\underline{Me}Me$), 1.24 (3 H, d, ^3J = 6.9 Hz, $NCH_aMe\underline{Me}$), 1.17 (3 H, d, ^3J = 6.9 Hz, $NCH_bMe\underline{Me}$). $^{13}C\{^1H\}$ NMR (toluene-d_8, 75.4 MHz, 253 K): δ 170.3 ($Me\underline{C}N_2$), 163.2 (*i*-C_6H_5), 158.6 (*i*-$\underline{C}_6H_4Me$), 137.2 (*o*-C_6H_5), 133.5 (*p*-$\underline{C}_6H_4Me$), 132.4 (*m*-$\underline{C}_6H_4Me$), 129.7 (*p*-C_6H_5), 128.5 (*o*-$\underline{C}_6H_4Me$), 127.7 ($\underline{C}_5Me_5$), 127.3 (*m*-C_6H_5), 52.3 ($N\underline{C}H_aMeMe$), 49.1 ($N\underline{C}H_bMeMe$), 26.7 ($NCH_bMe\underline{Me}$), 24.3 ($NCH_b\underline{Me}Me$), 23.4 ($NCH_aMe\underline{Me}$), 23.3 ($NCH_a\underline{Me}Me$), 20.9 ($C_6H_4\underline{Me}$), 16.8 ($\underline{Me}CN_2$), 13.4 ($C_5\underline{Me}_5$). ^{29}Si NMR (C_6D_6, 299.9 MHz, 253 K): δ -35.5 (SiH_2Ph).

[Cp*Ti{MeC(N^{i}Pr)$_2$}(NNMe$_2$Et)]Br (36-Br). To a stirred solution of Cp*Ti{MeC(N^{i}Pr)$_2$}(NNMe$_2$) (0.300 g, 0.780 mmol) in benzene (10 mL) was added EtBr (58.6 μL, 0.780 mmol) in benzene (10 mL) all at RT. After 2 d, the solution was filtered, and the volatiles were removed under reduced pressure to afford a yellow-brown solid. The crude material was then washed with cold pentane (3 × 10 mL) cooled to -78 ℃, filtered, and dried *in vacuo* to give **36-Br** as a red-brown solid.

Yield: 0.164 g (43%). Diffraction-quality crystals were grown by THF/pentane layering at 4 ℃. ^{1}H NMR (C_6D_6, 299.9 MHz, 293 K): δ 3.83 (2 H, q, ^{3}J = 7.2 Hz, C<u>H</u>$_2$CH$_3$), 3.75 (2 H, sept, ^{3}J = 6.6 Hz, NC<u>H</u>MeMe), 3.41 (6 H, s, NNMe$_2$), 1.98 (15 H, s, C$_5$Me$_5$), 1. 93 (3 H, s, MeCN$_2$), 1.05 (9 H, m, overlapping CH$_2$C<u>H</u>$_3$ and NCH<u>Me</u>Me), 0.98 (6 H, d, ^{3}J = 6.6 Hz, NCHMe<u>Me</u>). ^{13}C{^{1}H} NMR (C_6D_6, 75.4 MHz, 293 K): δ 165.6 (Me<u>C</u>N$_2$), 122.1 (<u>C</u>$_5$Me$_5$), 65.6 (<u>C</u>H$_2$CH$_3$), 57.9 (NNMe$_2$), 49.3 (N<u>C</u>HMeMe), 25.6 (NCH<u>Me</u>Me), 25.1 (NCHMe<u>Me</u>), 14.2 (<u>Me</u>CN$_2$) 13.0 (C$_5$<u>Me</u>$_5$), 9.2 (CH$_2$<u>C</u>H$_3$). IR (NaCl plates, Nujol mull, cm^{-1}): 1457 (s), 1331 (m), 1226 (w), 1206 (m), 1173 (w), 1155 (m), 1119 (w), 1021 (m), 799 (w), 770 (w). ES^{+}-MS (THF): *m/z* = 411 [**36**]$^{+}$ (100%). A satisfactory elemental analysis could not be obtained.

[Cp*Ti{MeC(N^{i}Pr)$_2$}(NNMe$_2$CH$_2$Ph)]Br (37-Br). To a stirred solution of Cp*Ti{MeC(N^{i}Pr)$_2$}(NNMe$_2$) (0.218 g, 0.570 mmol) in benzene (10 mL) was added PhCH$_2$Br (67.7 μL, 0.570 mmol) in benzene (10 mL) all at RT. After 16 h, the resultant brown solution was filtered, and the volatiles were removed under reduced pressure to give a waxy red brown solid. It was then washed with cold pentane (3 × 10 mL) cooled to -78 ℃ and dried *in vacuo* to afford **37-Br** as a red-brown solid. Yield: 0.134 g (43%). ^{1}H NMR (C_6D_6, 499.9 MHz, 293 K): δ 7.33 (2 H, d, ^{3}J = 7.5 Hz, *o*-C$_6$H$_5$), 7.20 (2 H, t, ^{3}J = 7.5 Hz, *m*-C$_6$H$_5$), 7.06 (1 H, t, ^{3}J = 7.5 Hz, *p*-C$_6$H$_5$), 4.74 (2H, s, C<u>H</u>$_2$Ph), 3.78 (2 H, app. sept, app. ^{3}J = 6.5 Hz, NC<u>H</u>MeMe), 2.52 (6 H, s, NNMe$_2$), 2.07 (15 H, s, C$_5$Me$_5$), 1.61 (3 H, s, MeCN$_2$), 1.18 (6 H, d, ^{3}J = 6.5 Hz, NCH<u>Me</u>Me), 1.07 (6 H, d, ^{3}J = 6.5 Hz, NCHMe<u>Me</u>). ^{13}C{^{1}H} NMR (C_6D_6, 125.7 MHz, 293 K): δ 169.0 (Me<u>C</u>N$_2$), 141.9 (*i*-C$_6$H$_5$), 128.5 (overlapping *m*- and *o*-C$_6$H$_5$), 127.2 (*p*-C$_6$H$_5$), 125.0 (<u>C</u>$_5$Me$_5$), 56.6 (<u>C</u>H$_2$Ph), 49.6 (N<u>C</u>HMeMe), 49.0 (NN<u>Me</u>$_2$), 25.5 (NCH<u>Me</u>Me), 24.0 (NCHMe<u>Me</u>), 15.6 (<u>Me</u>CN$_2$), 13.9 (C$_5$<u>Me</u>$_5$). IR (NaCl plates, Nujol mull, cm^{-1}): 1653 (w), 1602 (w), 1457 (s), 1353 (m), 1332 (m), 1200 (m), 1172 (w), 1130 (m), 1076 (w), 1016 (m), 814 (w), 792 (w), 752 (m), 739 (w), 723 (w), 710 (m), 491 (s). ES^{+}-MS (THF): *m/z* = 473 [**37**]$^{+}$ (100%). Anal. found (calcd. for C$_{27}$H$_{45}$BrN$_4$Ti): C, 58.70 (58.59); H, 8.30 (8.20); N, 10.20 (10.12)%.

[Cp*Ti{MeC(N^{i}Pr)$_2$}{N(NMe$_2$)H}][BPh$_4$] (38-BPh$_4$). To a stirred solution of Cp*Ti{MeC(N^{i}Pr)$_2$}(NNMe$_2$) (0.300 g, 0.78 mmol) in THF (10 mL) was added a solution of [Et$_3$NH][BPh$_4$] (0.331 g, 0.78 mmol) in THF (10 mL) all at RT. The resulting red solution was stirred for 1 h. Volatiles were removed under reduced pressure to afford **38-BPh$_4$** as a red solid which was washed with cold pentane (3 ×

10 mL) cooled to -78 ℃, filtered, and dried *in vacuo*. Yield: 0.382 g (61%). Diffraction-quality crystals were grown by THF/pentane layering. ^{1}H NMR (C_6D_5Br, 299.9 MHz, 293 K): δ 7.74 (8 H, br. m, *o*-C_6H_5), 7.11 (8 H, t, ^{3}J = 6.9 Hz, *m*-C_6H_5), 6.96 (4 H, t, ^{3}J = 6.9 Hz, *p*-C_6H_5), 2.94 (2 H, app. sept, app. ^{3}J = 6.6 Hz, NC<u>H</u>MeMe), 1.59 (15 H, s, C_5Me_5), 1.53 (6 H, s, $NNMe_2$), 1.43 (3 H, s, $MeCN_2$), 0.76 (6 H, d, ^{3}J = 6.6 Hz, NCH<u>Me</u>Me), 0.43 (6 H, d, ^{3}J = 6.6 Hz, NCHMe<u>Me</u>). N<u>H</u> resonance not observed in C_6D_5Br but found at 8.94 ppm in THF-d_8. ^{13}C{^{1}H} NMR (C_6D_5Br, 75.4 MHz, 293 K): δ 164.5 (*i*-C_6H_5), 162.5 (Me<u>C</u>N_2), 136.9 (*o*-C_6H_5), 128.3 (<u>C</u>$_5Me_5$), 126.2 (*m*-C_6H_5), 122.4 (*p*-C_6H_5), 50.1 (N<u>C</u>HMeMe), 50.0 (NN<u>Me</u>$_2$), 25.8 (NCH<u>Me</u>Me), 24.2 (NCHMe<u>Me</u>), 13.1 (C_5<u>Me</u>$_5$), 12.7 (<u>Me</u>CN_2). ^{11}B{^{1}H} NMR (C_6D_5Br, 96.2 MHz, 293 K): δ -5.9 (BPh_4). IR (NaCl plates, Nujol mull, cm^{-1}): 3266 (w), 1636 (w), 1580 (m), 1341 (w), 1205 (m), 1172 (w), 1123 (w), 1065 (w), 1032 (m), 1011 (m), 844 (w), 815 (w), 795 (w), 732 (m), 704 (m), 625 (m), 611 (m). ES^{+}-MS (THF): *m/z* = 383 [**38**]$^{+}$ (100%). ES^{-}-MS (THF): *m/z* = 319 $[BPh_4]^{-}$ (100%). Anal. found (calcd. for $C_{48}H_{67B}N_4OTi$ (**38-BPh$_4$**·THF)): C, 74.52 (74.41); H, 8.50 (8.72); N, 7.58 (7.23)%.

NMR tube scale synthesis of [Cp*Ti{MeC(N^{i}Pr)$_2$}{N(NPh$_2$)H}][BPh$_4$] (39-BPh$_4$). To a solution of Cp*Ti{MeC(N^{i}Pr)$_2$}($NNPh_2$) (10.3 mg, 0.020 mmol) in THF-d_8 (0.3 mL) in an NMR tube equipped with a J. Young Teflon valve was added a solution of an excess of [Et_3NH][BPh_4] (17.1 mg, 0.041 mmol) in THF-d_8 (0.3 mL) all at RT. A slow colour change from dark yellow to dark green was observed. The reaction was monitored by ^{1}H NMR spectroscopy. After 16 h, **39-BPh$_4$** had been formed quantitatively (along with Et_3N) and was characterised by NMR spectroscopy. ^{1}H NMR (THF-d_8, 299.9 MHz, 293 K): δ 7.29 (8 H, br. m, *o*-C_6H_5), 6.87 (8 H, t, ^{3}J = 7.5 Hz, *m*-C_6H_5), 6.72 (4 H, t, ^{3}J = 7.5 Hz, *p*-C_6H_5), 3.61 (2 H, app. sept, app. ^{3}J = 6.6 Hz, NC<u>H</u>MeMe), 1.97 (15 H, s, C_5Me_5), 1.76 (3 H, s, $MeCN_2$), 1.13 (12 H, d, ^{3}J = 6.6 Hz, overlapping NCH<u>MeMe</u>). N<u>H</u> not observed and NN<u>Ph</u>$_2$ resonances obscured by [B<u>Ph</u>$_4$]$^{-}$. ^{13}C{^{1}H} NMR (THF-d_8, 75.4 MHz, 293 K): δ 165.1 (*i*-C_6H_5), 163.0 (Me<u>C</u>N_2), 137.4 (*o*-C_6H_5), 126.1 (*m*-C_6H_5), 124.1 (<u>C</u>$_5Me_5$), 122.2 (*p*-C_6H_5), 48.5 (N<u>C</u>H_aMeMe), 45.2 (N<u>C</u>H_bMeMe), 22.9 (NCH<u>Me</u>Me), 21.8 (NCHMe<u>Me</u>), 17.9 (<u>Me</u>CN_2), 11.9 (C_5<u>Me</u>$_5$). NN<u>Ph</u>$_2$ resonances obscured by [B<u>Ph</u>$_4$]$^{-}$. ^{11}B{^{1}H} NMR (THF-d_8, 96.2 MHz, 293 K): δ -6.6 (BPh_4).

NMR tube scale synthesis of [Cp*Ti{MeC(N^{i}Pr)$_2$}{N(H)Tol}][BPh$_4$] (40-BPh$_4$). To a solution of Cp*Ti{MeC(N^{i}Pr)$_2$}(NTol) (10.0 mg, 0.023 mmol) in THF-d_8 (0.3 mL) in an NMR tube equipped with a J. Young Teflon valve was added a solution of an excess of [Et$_3$NH][BPh$_4$] (19.6 mg, 0.047 mmol) in THF-d_8 (0.3 mL) all at RT. An immediate colour change from dark green to brown was observed. The reaction was monitored by ^{1}H NMR spectroscopy. After 20 min, **40-BPh$_4$** had been formed quantitatively (along with Et$_3$N) and was characterised by NMR spectroscopy. ^{1}H NMR (THF-d_8, 299.9 MHz, 293 K): δ 7.29 (8 H, br. m, *o*-C$_6$H$_5$), 6.87 (10 H, m, overlapping *m*-C$_6$H$_5$ and *o*-C$_6$H$_4$Me), 6.73 (4 H, t, ^3J = 7.2 Hz, *p*-C$_6$H$_5$), 6.50 (2 H, d, ^3J = 8.1 Hz, *m*-C$_6$H$_4$Me), 3.60 (2 H, app. sept, app. ^3J = 6.3 Hz, NC<u>H</u>MeMe), 2.21 (3 H, s, 4-C$_6$H$_4$<u>Me</u>), 2.04 (15 H, s, C$_5$Me$_5$), 1.75 (3 H, s, MeCN$_2$), 1.13 (12 H, d, ^3J = 6.3 Hz, overlapping NCH<u>MeMe</u>). N<u>H</u> not observed. ^{13}C{^{1}H} NMR (THF-d_8, 75.4 MHz, 293 K): δ 165.1 (*i*-C$_6$H$_5$), 163.0 (Me<u>C</u>N$_2$), 137.4 (overlapping *o*-C$_6$H$_5$ and *i*-C$_6$H$_4$Me), 129.9 (overlapping *o*-C$_6$H$_4$Me and *p*-C$_6$H$_4$Me) 126.0 (*m*-C$_6$H$_5$), 124.2 (<u>C</u>$_5$Me$_5$), 122.2 (overlapping *p*-C$_6$H$_5$ and *m*-C$_6$H$_4$Me), 48.5 (N<u>C</u>H$_a$MeMe), 45.2 (N<u>C</u>H$_b$MeMe), 22.9 (NCH<u>Me</u>Me), 21.8 (NCHMe<u>Me</u>), 21.3 (4-C$_6$H$_4$<u>Me</u>), 17.9 (<u>Me</u>CN$_2$), 11.7 (C$_5$<u>Me</u>$_5$). ^{11}B{^{1}H} NMR (THF-d_8, 96.2 MHz, 293 K): δ -6.6 (BPh$_4$).

5.5 Experimental details and characterising data for Chapter Four

Cp*Ti{MeC(N^{i}Pr)$_2$}(NNCPh$_2$) (41). To a solution of Cp*Ti{MeC(N^{i}Pr)$_2$}(N^{t}Bu) (2.00 g, 5.06 mmol) in benzene (10 mL) was added Ph$_2$CNNH$_2$ (0.99 g, 5.06 mmol) in benzene (10 mL) all at RT. A colour change from dark red to dark yellow was observed. After 4 h, the solution was filtered, and the volatiles were removed under reduced pressure to afford a brown oil. Pure **41** crystallised following trituration with pentane. The supernatant was filtered away and the product was washed with cold pentane (3 × 10 mL) cooled to -78 ℃, filtered, and dried *in vacuo* to give **41** as a brown powder. Yield: 1.99 g (76%). Diffraction-quality crystals were grown by slow evaporation of a pentane solution. ^{1}H NMR (C$_6$D$_6$, 299.9 MHz, 293 K): δ 7.76 (2 H, d, ^3J = 7.5 Hz, o_a-C$_6$H$_5$), 7.41 (2 H, d, ^3J = 7.5 Hz, o_b-C$_6$H$_5$), 7.13 (4 H, t, ^3J = 7.5 Hz, overlapping m_a- and m_b-C$_6$H$_5$), 7.04 (2 H, app. t, app. ^3J = 7.5 Hz, overlapping p_a- and p_b-C$_6$H$_5$), 3.39 (2 H, app. sept., app. ^3J = 6.6 Hz, NC<u>H</u>MeMe), 2.13 (15 H, s, C$_5$Me$_5$), 1.64 (3 H, s, MeCN$_2$), 0.93 (6 H, d, ^3J = 6.6 Hz, NCH<u>Me</u>Me), 0.73 (6 H, d, ^3J = 6.6 Hz, NCHMe<u>Me</u>). ^{13}C{^{1}H} NMR (C$_6$D$_6$, 75.4 MHz, 293 K): δ 162.1 (Me<u>C</u>N$_2$), 140.0 (N<u>C</u>Ph$_2$), 139.7 (i_a-C$_6$H$_5$), 138.3 (i_b-C$_6$H$_5$), 130.3 (o_b-C$_6$H$_5$), 128.1 (overlapping m_a-

and m_b-C_6H_5), 127.9 (o_a-C_6H_5), 127.3 (p_a-C_6H_5), 127.0 (p_b-C_6H_5), 121.1 ($\underline{C}_5Me_5$), 49.2 (N$\underline{C}$HMeMe), 26.1 (NCH$\underline{Me}$Me), 24.9 (NCHMe$\underline{Me}$), 12.2 ($C_5\underline{Me}_5$), 11.8 ($\underline{Me}CN_2$). IR (NaCl plates, Nujol mull, cm^{-1}): 1595 (m), 1466 (s), 1426 (m), 1378 (s), 1336 (m), 1323 (m), 1313 (m), 1212 (s), 1173 (w), 1155(w), 1123 (s), 1080 (m), 1072 (m), 1061 (m), 1026 (w), 957 (w), 910 (w), 813 (w), 792 (w), 772 (m), 766 (m), 740 (m), 725 (w), 695 (s), 642 (m), 489 (s). EI-MS: *m/z* = 518 $[M]^+$ (100%). Anal. found (calcd. for $C_{31}H_{42}N_4Ti$): C, 71.66 (71.80); H, 7.97 (8.16); N, 10.66 (10.80)%.

NMR tube scale synthesis of Cp*Ti{MeC(N^{i}Pr)$_2$}{N(NCPh$_2$)C(O)O} (42). A solution of Cp*Ti{MeC(N^{i}Pr)$_2$}(NNCPh$_2$) (**41**, 20.0 mg, 0.39 mmol) in toluene-d_8 (0.6 mL) in an NMR tube equipped with a J. Young Teflon valve was freeze-pump-thawed three time. The solution was then exposed to CO_2 at a pressure of *ca.* 1.1 atm at -78 ℃. An immediate colour change from dark yellow to brown was observed. The reaction was monitored by ^{1}H NMR spectroscopy. The reaction was complete almost immediately (5 min). Compound **42** was characterised by NMR spectroscopy. ^{1}H NMR (toluene-d_8, 499.9 MHz, 248 K): δ 7.78 (2 H, d, ^3J = 6.5 Hz, o_a-C_6H_5), 7.45 (2 H, d, ^3J = 6.5 Hz, o_b-C_6H_5), 7.13 (3 H, m, overlapping m_a- and p_a-C_6H_5), 7.08 (3 H, m, overlapping m_b- and p_b-C_6H_5), 3.17 (1 H, app. sept., app. ^3J = 6.5 Hz, NC$\underline{H}_a$MeMe), 3.08 (1 H, app. sept., app. ^3J = 6.5 Hz, NC$\underline{H}_b$MeMe), 2.05 (15 H, s, C_5Me_5), 1.29 (3 H, s, $MeCN_2$), 1.10 (3 H, d, ^3J = 6.5 Hz, NCH$_a\underline{Me}$Me), 1.04 (3 H, d, ^3J = 6.5 Hz, NCH$_b\underline{Me}$Me), 0.99 (6 H, 2 × d, 2 × ^3J = 6.5 Hz, overlapping NCH$_a$Me$\underline{Me}$ and NCH$_b$Me$\underline{Me}$). ^{13}C{^{1}H} NMR (toluene-d_8, 125.7 MHz, 248 K): δ 169.5 (Me$\underline{C}N_2$), 166.1 (OCO), 154.9 (NN$\underline{C}$Ph$_2$), 139.1 (i_a-C_6H_5), 136.4 (i_b-C_6H_5), 129.7 (p_a-C_6H_5), 129.5 (overlapping $\underline{C}_5Me_5$ and o_b-C_6H_5), 129.2 (o_a-C_6H_5), 129.1 (p_b-C_6H_5), 128.2 (m_a-C_6H_5), 127.5 (m_b-C_6H_5), 50.9 (N$\underline{C}$H$_a$MeMe), 50.1 (N$\underline{C}$H$_b$MeMe), 26.5 (NCH$_b$Me$\underline{Me}$), 24.2 (NCH$_b\underline{Me}$Me), 24.0 (NCH$_a\underline{Me}$Me), 23.5 (NCH$_a$Me$\underline{Me}$), 12.6 ($C_5\underline{Me}_5$), 11.3 ($\underline{Me}CN_2$).

[Cp*Ti{MeC(N^{i}Pr)$_2$}{OC(NNCPh$_2$)O}]$_2$ (43). A solution of Cp*Ti{MeC(N^{i}Pr)$_2$}(NNCPh$_2$) (**41**, 0.400 g, 0.77 mmol) in benzene (10 mL) was freeze-pump-thawed three times. The solution was then exposed to CO_2 at a pressure of *ca.* 1.1 atm at RT. An immediate colour change from dark yellow to orange brown was observed. After 24 h, an orange precipitate was formed which was filtered and dried *in vacuo* to give **43** as an orange solid. Yield: 0.125 g (29%). Diffraction-quality crystals were grown from a saturated diethyl ether solution at 4 ℃. ^{1}H NMR (C_6D_6,

499.9 MHz, 293 K): δ 8.08 (4 H, d, ^3J = 7.0 Hz, o_a-C_6H_5), 7.41 (4 H, d, ^3J = 7.0 Hz, o_b-C_6H_5), 7.31 (4 H, t, ^3J = 7.0 Hz, m_b-C_6H_5), 7.29 (4 H, t, ^3J = 7.0 Hz, m_a-C_6H_5), 7.22 (2 H, t, ^3J = 7.0 Hz, p_b-C_6H_5), 7.17 (2 H, t, ^3J = 7.0 Hz, p_a-C_6H_5), 4.97 (2 H, app. sept., app. ^3J = 7.0 Hz, NC$\underline{H}_a$MeMe), 4.08 (2 H, app. sept., app. ^3J = 7.0 Hz, NC$\underline{H}_b$MeMe), 2.05 (30 H, s, C_5Me_5), 1.77 (6 H, s, $MeCN_2$), 1.41 (6 H, d, ^3J = 7.0 Hz, NCH$_a$$\underline{Me}$Me), 1.24 (6 H, d, ^3J = 7.0 Hz, NCH$_a$Me$\underline{Me}$), 1.17 (6 H, d, ^3J = 7.0 Hz, NCH$_b$$\underline{Me}$Me), 1.13 (6 H, d, ^3J = 7.0 Hz, NCH$_b$Me$\underline{Me}$). $^{13}C\{^1H\}$ NMR (C_6D_6, 125.7 MHz, 293 K): δ 169.0 (Me$\underline{C}N_2$), 166.7 (O$\underline{C}$(NNCPh$_2$)O), 154.6 (NN$\underline{C}$Ph$_2$), 141.5 (i_a-C_6H_5), 140.6 (i_b-C_6H_5), 129.9 (o_b-C_6H_5), 128.5 (p_a-C_6H_5), 128.3 ($\underline{C}_5Me_5$), 128.1 (m_a-C_6H_5), 127.9 (m_b-C_6H_5), 127.5 (o_a-C_6H_5), 126.5 (p_b-C_6H_5), 48.6 (N$\underline{C}$H$_b$MeMe), 48.3 (N$\underline{C}$H$_a$MeMe), 24.2 (NCH$_a$$\underline{Me}$Me), 23.9 (NCH$_b$$\underline{Me}$Me), 23.5 (NCH$_bMe\underline{Me}$), 23.0 (NCH$_aMe\underline{Me}$), 18.7 ($\underline{Me}CN_2$), 11.8 ($C_5\underline{Me}_5$). IR (NaCl plates, Nujol mull, cm^{-1}): 2228 (w), 2040 (w), 1644 (w), 1608 (w), 1578 (w), 1547 (s), 1518 (s), 1486 (s), 1464 (s), 1406 (m), 1346 (m), 1316 (m), 1306 (m), 1239 (m), 1204 (m), 1180 (w), 1142 (w), 1128 (m), 1072 (w), 1018 (w), 992 (s), 943 (w), 922 (w), 826 (w), 799 (w), 784 (m), 766 (w), 754 (m), 738 (w), 721 (w), 706 (m), 698 (m), 635 (w), 574 (m). EI-MS: *m/z* = 546 [Cp*Ti{MeC(N^{i}Pr)$_2$}{OCNNCPh$_2$}]$^+$ (60%). Anal. found (calcd. for $C_{64}H_{84}N_8O_4Ti_2$): C, 68.48 (68.32); H, 7.40 (7.53); N, 9.82 (9.96)%.

Cp*Ti{MeC(N^{i}Pr)$_2$}{OC(O)N(NCPh$_2$)C(O)O} (44). A solution of Cp*Ti{MeC(N^{i}Pr)$_2$}(NNCPh$_2$) (**41**, 0.400 g, 0.77 mmol) in benzene (20 mL) was freeze-pump-thawed three times. The solution was then exposed to CO_2 at a pressure of *ca.* 1.1 atm at RT. An immediate colour change from dark yellow to orange brown was observed. After 24 h, an orange precipitate was formed (**43**). After filtration, the mother liquor was evaporated to dryness to give an orange-brown waxy solid. This was redissolved in benzene (15 mL), concentrated and filtered. Crystallisation at 4 ℃ gave **44** as an orange-brown solid. Yield: 0.060 g (13%). Diffraction-quality crystals were grown from a saturated benzene solution at 4 ℃.

Isomer a: ^1H NMR (toluene-d_8, 499.9 MHz, 263 K): δ 8.00 (2 H, d, ^3J = 7.5 Hz, o_a-C_6H_5), 7.49 (2 H, d, ^3J = 7.5 Hz, o_b-C_6H_5), 7.15 (1 H, m, p_a-C_6H_5), 7.09 (1 H, m, p_b-C_6H_5), 7.03 (2 H, m, m_a-C_6H_5), 7.00 (2 H, m, m_b-C_6H_5), 3.35 (2 H, app. sept., app. ^3J = 6.5 Hz, NC$\underline{H}$MeMe) 1.74 (15 H, s, C_5Me_5), 1.27 (3 H, s, $\underline{Me}CN_2$), 0.94 (6 H, d, ^3J = 6.5 Hz, NCH$\underline{Me}$Me), 0.86 (6 H, d, ^3J = 6.5 Hz, NCHMe$\underline{Me}$). $^{13}C\{^1H\}$ NMR (toluene-d_8, 125.7 MHz, 263 K): δ 168.5 (Me$\underline{C}N_2$), 154.5 (OCO), 150.6 (N$\underline{C}$Ph$_2$),

140.5 (overlapping i_a- and i_b-C_6H_5), 130.8 ($\underline{C}_5Me_5$), 129.7 (o_a-C_6H_5), 129.1 (m_a-C_6H_5), 128.6 (p_b-C_6H_5), 128.4 (o_b-C_6H_5), 128.3 (p_a-C_6H_5), 127.5 (m_b-C_6H_5), 50.4 (N$\underline{C}$HMeMe), 23.6 (NCHMe$\underline{Me}$), 23.1 (NCH$\underline{Me}$Me), 14.1($\underline{Me}CN_2$), 12.4 ($C_5\underline{Me}_5$).

Isomer b: ^{1}H NMR (toluene-d_8, 499.9 MHz, 263 K): δ 8.02 (2 H, d, ^3J = 7.5 Hz, o_a-C_6H_5), 7.74 (2 H, d, ^3J = 7.5 Hz, o_b-C_6H_5), 7.34 (1 H, t, ^3J = 7.5 Hz, p_b-C_6H_5), 7.25 (2 H, m, m_b-C_6H_5), 7.15 (1 H, m, p_a-C_6H_5), 7.03 (2 H, m, m_a-C_6H_5), 3.40 (2 H, app. sept., app. ^3J = 6.5 Hz, NC$\underline{H}$MeMe) 1.87 (15 H, s, C_5Me_5), 1.34 (3 H, s, $\underline{Me}CN_2$), 1.06 (6 H, d, ^3J = 6.5 Hz, NCH$\underline{Me}$Me), 1.02 (6 H, d, ^3J = 6.5 Hz, NCHMe$\underline{Me}$). ^{13}C{^{1}H} NMR (toluene-d_8, 125.7 MHz, 263 K): δ 168.7 (Me$\underline{C}N_2$), 154.7 (OCO), 150.8 (N$\underline{C}$Ph$_2$), 141.3 (overlapping i_a- and i_b-C_6H_5), 130.9 ($\underline{C}_5Me_5$), 129.8 (o_a-C_6H_5), 129.1 (m_a-C_6H_5), 128.6 (m_b-C_6H_5), 128.3 (overlapping p_a- and o_b-C_6H_5), 127.5 (p_b-C_6H_5), 50.4 (N$\underline{C}$HMeMe), 24.0 (NCH$\underline{Me}$Me), 23.9 (NCHMe$\underline{Me}$), 14.2($\underline{Me}CN_2$), 12.5 ($C_5\underline{Me}_5$).

Common data: IR (NaCl plates, Nujol mull, cm^{-1}): 1701 (s), 1656 (s), 1566 (m), 1550 (m), 1460 (s), 1351 (s), 1210 (s), 1173 (s), 1149 (s), 1072 (m), 1039 (m), 1022 (m), 974 (w), 940 (w), 885 (w), 822 (m), 801 (s), 783 (m), 766 (s), 730 (w), 701 (s), 676 (w), 621 (m), 594 (w), 581 (w), 564 (w), 530 (m), 485 (m). EI-MS: *m/z* = 465 [*M* – MeC(^{i}Pr)$_2$]$^+$ (20%), 440 [*M* – CPh$_2$]$^+$ (10%), 426 [*M* – NCPh$_2$]$^+$ (40%) Anal. found (calcd. for $C_{33}H_{42}N_4O_4Ti$): C, 65.48 (65.34); H, 7.07 (6.98); N, 9.11 (9.24)%.

Cp*Ti{MeC(N^{i}Pr)$_2$}{N(NCPh$_2$)C(S)S} (45). To a solution of Cp*Ti{MeC(N^{i}Pr)$_2$}(NNCPh$_2$) (**41**, 0.204 g, 0.393 mmol) in benzene (10 mL) was added CS_2 (47.3 μL, 0.787 mmol) in benzene (10 mL) all at RT. A colour change from dark yellow to brown was observed. After 20 h, the brown solution was filtered, and the volatiles were removed under reduced pressure to afford a dark brown solid. This was washed with cold pentane (3 × 10 mL) cooled to -78 ℃, filtered, and dried *in vacuo* to give **45** as a dark brown powder. Yield: 0.140 g (60%). ^{1}H NMR (toluene-d_8, 499.9 MHz, 253 K): δ 8.05 (2 H, d, ^3J = 7.0 Hz, o_a-C_6H_5), 7.43 (2 H, d, ^3J = 7.0 Hz, o_b-C_6H_5), 7.15 (2 H, m, m_b-C_6H_5), 7.08 (3 H, m, overlapping m_a- and p_b-C_6H_5), 7.02 (1 H, m, p_a-C_6H_5), 3.32 (1 H, app. sept., app. ^3J = 6.5 Hz, NC$\underline{H}_a$MeMe), 3.28, (1 H, app. sept., app. ^3J = 6.5 Hz, NC$\underline{H}_b$MeMe), 1.98 (15 H, s, C_5Me_5), 1.47 (3 H, s, $MeCN_2$), 1.08 (3 H, d, ^3J = 6.5 Hz, NCH$_a$$\underline{Me}$Me), 1.04 (3 H, d, ^3J = 6.5 Hz, NCH$_b$$\underline{Me}$Me), 1.02 (3 H, d, ^3J = 6.5 Hz, NCH$_a$Me$\underline{Me}$), 0.98 (3 H, d, ^3J = 6.5 Hz, NCH$_b$Me$\underline{Me}$). ^{13}C{^{1}H} NMR (toluene-d_8, 125.7 MHz, 253 K): δ 166.0 (Me$\underline{C}N_2$), 165.2 (SC(S)N), 159.4 (N$\underline{C}$Ph$_2$), 140.1 (i_a-C_6H_5), 137.0 (i_b-C_6H_5), 130.9 ($\underline{C}_5Me_5$),

130.5 (o_b-C_6H_5), 129.2 (overlapping o_a- and p_a-C_6H_5), 129.1 (p_b-C_6H_5), 127.9 (m_a-C_6H_5), 127.5 (m_b-C_6H_5), 50.8 (overlapping N<u>C</u>H_aMeMe and N<u>C</u>H_bMeMe), 24.6 (NCH_aMe<u>Me</u>), 24.5 (NCH_bMe<u>Me</u>), 24.3 (NCH_a<u>Me</u>Me), 24.1 (NCH_b<u>Me</u>Me), 13.9 (C_5<u>Me</u>$_5$), 13.1 (<u>Me</u>CN_2). IR (NaCl plates, Nujol mull, cm^{-1}): 1546 (w), 1312 (w), 1203 (m), 1170 (w), 1092 (w), 1020 (m), 934 (w), 799 (m), 696 (m), 481 (s). EI-MS: *m/z* = 293 $[M - Cp^* - CPh_2]^+$ (50%). Anal. found (calcd. for $C_{32}H_{42}N_4S_2Ti$): C, 64.50 (64.63); H, 6.89 (7.12); N, 9.24 (9.42)%.

Reaction of Cp*Ti{MeC(N^{i}Pr)$_2$}(NNCPh$_2$) with ^{t}BuNCO. To a solution of Cp*Ti{MeC(N^{i}Pr)$_2$}(NNCPh$_2$) (**41**, 0.300 g, 0.578 mmol) in benzene (10 mL) was added ^{t}BuNCO (66.1 μL, 0.578 mmol) in benzene (5 mL) all at RT. After 6 d, the dark yellow solution was filtered, and the volatiles were removed under reduced pressure to afford a mixture of [Cp*Ti{MeC(N^{i}Pr)$_2$}O]$_2$ and ^{t}BuNCNNCPh$_2$ (**46**). Sublimation (85-90 ℃, 5×10^{-6} mbar) afforded **46** as a white solid. Yield: 36.0 mg (22%). ^{1}H NMR (C_6D_6, 499.9 MHz, 293 K): δ 7.78 (2 H, d, ^3J = 7.5 Hz, o_a-C_6H_5), 7.24 (2 H, d, ^3J = 7.5 Hz, o_b-C_6H_5), 7.10 (3 H, m, overlapping m_b- and p_a-C_6H_5), 7.05 (3 H, m, overlapping m_a- and p_b-C_6H_5), 1.07 (9 H, s, NCMe$_3$). ^{13}C{^{1}H} NMR (C_6D_6, 125.7 MHz, 293 K): δ 166.3 (NN<u>C</u>Ph$_2$), 146.9 (NCNN), 138.2 (i_a-C_6H_5), 136.1 (i_b-C_6H_5), 130.0 (p_a-C_6H_5), 129.5 (o_b-C_6H_5), 129.1 (o_a-C_6H_5), 128.7 (p_b-C_6H_5), 128.2 (m_a-C_6H_5), 127.9 (m_b-C_6H_5), 57.7 (N<u>C</u>Me$_3$), 30.9 (NC<u>Me</u>$_3$). EI-HRMS: *m/z* found (calcd. for $C_{18}H_{19}N_3$, $[M]^+$) 277.1572 (277.1579).

Cp*Ti{MeC(N^{i}Pr)$_2$}{N(NCPh$_2$)C(NAr')O} (47). To a solution of Cp*Ti{MeC(N^{i}Pr)$_2$}(NNCPh$_2$) (**41**, 0.250 g, 0.48 mmol) in benzene (10 mL) was added Ar'NCO (103.1 μL, 0.48 mmol) in benzene (5 mL) all at RT. A colour change from dark yellow to dark brown was observed. After 18 h, the solution was filtered, and the volatiles were removed under reduced pressure to afford **47** as a dark brown solid which was then washed with cold pentane (3 × 10 mL) cooled to -78 ℃, filtered, and dried *in vacuo*. Yield: 0.251 g (72%). ^{1}H NMR (toluene-d_8, 499.9 MHz, 253 K): δ 7.83 (2 H, d, ^3J = 7.5 Hz, o_a-C_6H_5), 7.63 (2 H, d, ^3J = 7.5 Hz, o_b-C_6H_5), 7.24 (4 H, m, overlapping m_b-C_6H_5 and *m*-2,6-C_6H_3(CHMeMe)$_2$), 7.16 (1 H, t, ^3J = 7.5 Hz, p_b-C_6H_5), 7.11 (4 H, m, overlapping m_a- and p_a-C_6H_5 and *p*-2,6-C_6H_3(CHMeMe)$_2$), 3.62 (1 H, app. sept., app. ^3J = 6.5 Hz, NC<u>H</u>$_a$MeMe) 3.46 (2 H, app. sept., app. ^3J = 6.5 Hz, *o*-2,6-C_6H_3(C<u>H</u>MeMe)$_2$), 3.34 (1 H, app. sept., app. ^3J = 6.5 Hz, NC<u>H</u>$_b$MeMe), 1.89 (15 H, s, C_5Me_5), 1.75 (3 H, s, <u>Me</u>CN_2), 1.48 (6 H, d, ^3J = 6.5 Hz, *o*-2,6-

$C_6H_3(CH\underline{Me}Me)_2$), 1.41 (6 H, d, ^3J = 6.5 Hz, *o*-2,6-$C_6H_3(CHMe\underline{Me})_2$), 1.12 (3 H, d, ^3J = 6.5 Hz, $NCH_a\underline{Me}Me$), 1.07 (3 H, d, ^3J = 6.5 Hz, $NCH_aMe\underline{Me}$), 0.84 (6 H, overlapping 2 × d, 2 × ^3J = 6.5 Hz, overlapping $NCH_b\underline{Me}Me$ and $NCH_bMe\underline{Me}$). $^{13}C\{^1H\}$ NMR (toluene-d_8, 125.7 MHz, 253 K): δ 168.4 ($Me\underline{C}N_2$), 165.2 (OCN), 149.0 ($N\underline{C}Ph_2$), 145.1 (i_b-C_6H_5), 140.5 (overlapping i_a-C_6H_5 and *o*-2,6-$C_6H_3(CHMeMe)_2$), 136.6 (*i*-2,6-$C_6H_3(CHMeMe)_2$), 129.8 (o_b-C_6H_5), 129.6 (p_a-C_6H_5), 128.8 (o_a-C_6H_5), 128.7 ($\underline{C}_5Me_5$), 128.4 (p_b-C_6H_5), 128.1 (m_a-C_6H_5) 127.6 (m_b-C_6H_5), 122.2 (*m*-2,6-$C_6H_3(CHMeMe)_2$), 121.5 (*p*-2,6-$C_6H_3(CHMeMe)_2$), 50.1 ($N\underline{C}H_bMeMe$), 49.9 ($N\underline{C}H_aMeMe$), 28.8 (*o*-2,6-$C_6H_3(\underline{C}HMeMe)_2$), 26.3 ($NCH_aMe\underline{Me}$), 25.8 ($NCH_bMe\underline{Me}$), 25.0 ($NCH_a\underline{Me}Me$), 24.1 (*o*-2,6-$C_6H_3(CHMe\underline{Me})_2$), 23.9 (*o*-2,6-$C_6H_3(CH\underline{Me}Me)_2$), 23.3 ($NCH_b\underline{Me}Me$), 12.7 ($C_5\underline{Me}_5$), 12.5 ($\underline{Me}CN_2$). IR (NaCl plates, Nujol mull, cm^{-1}): 2289 (w), 2040 (w), 1618 (s), 1583 (s), 1558 (m), 1507 (m), 1486 (s), 1336 (m), 1314 (m), 1204 (m), 1176 (w), 1073 (w), 1008 (w), 978 (w), 958 (w), 892 (w), 792 (w), 761 (w), 747 (w), 725 (w), 706 (w), 693 (m). EI-MS: *m/z* = 555 [*M* – CPh_2]$^+$ (15%). Anal. found (calcd. for $C_{44}H_{59}N_5OTi$): C, 73.10 (73.21); H, 8.36 (8.24); N, 9.87 (9.70)%.

NMR tube scale synthesis of Cp*Ti{MeC(N^{i}Pr)$_2$}{N(NCPh$_2$)C(NTol)O} (48). To a solution of Cp*Ti{MeC(N^{i}Pr)$_2$}(NNCPh$_2$) (**41**, 20.0 mg, 0.039 mmol) in toluene-d_8 (0.6 mL) in an NMR tube equipped with a J. Young Teflon valve was added TolNCO (4.90 μL, 0.039 mmol) at -78 ℃. An immediate colour change from dark yellow to red was observed. The reaction was monitored by ^1H NMR spectroscopy. The reaction was complete almost immediately (5 min) to give **48** which was characterised by NMR spectroscopy. ^1H NMR (toluene-d_8, 499.9 MHz, 253 K): δ 7.87 (2 H, d, ^3J = 8.0 Hz, *o*-C_6H_4Me), 7.75 (2 H, d, ^3J = 8.0 Hz, o_a-C_6H_5), 7.57 (2 H, d, ^3J = 8.0 Hz, o_b-C_6H_5), 7.19 (2 H, d, ^3J = 8.0 Hz, *m*-C_6H_4Me), 7.14 (3 H, m, overlapping m_a- and p_a-C_6H_5), 7.03 (3 H, m, overlapping m_b- and p_b-C_6H_5), 3.21 (2 H, app. sept., app. ^3J = 6.5 Hz, overlapping $NC\underline{H}_aMeMe$ and $NC\underline{H}_bMeMe$), 2.25 (3 H, s, $C_6H_4\underline{Me}$), 2.08 (15 H, s, C_5Me_5), 1.20 (3 H, d, ^3J = 6.5 Hz, $NCH_a\underline{Me}Me$), 1.13 (3 H, s, $MeCN_2$), 1.06 (3 H, d, ^3J = 6.5 Hz, $NCH_aMe\underline{Me}$), 1.03 (3 H, d, ^3J = 6.5 Hz, $NCH_b\underline{Me}Me$), 0.98 (3 H, d, ^3J = 6.5 Hz, $NCH_bMe\underline{Me}$). $^{13}C\{^1H\}$ NMR (toluene-d_8, 125.7 MHz, 253 K): δ 168.7 ($Me\underline{C}N_2$), 157.2 (OCN), 156.7 ($NN\underline{C}Ph_2$), 147.8 (*i*-C_6H_4Me), 145.3 (i_b-C_6H_5), 141.2 (*p*-C_6H_4Me), 139.2 (i_a-C_6H_5), 129.9 (o_b-C_6H_5), 129.6 (p_a-C_6H_5), 129.5 (o_a-C_6H_5), 129.1 (*m*-C_6H_4Me), 128.6 ($\underline{C}_5Me_5$), 128.3 (p_b-C_6H_5), 128.0 (m_a-C_6H_5), 127.3 (m_b-

C_6H_5), 125.8 (*o*-C_6H_4Me), 50.7 ($NC\underline{C}H_bMeMe$), 50.5 ($NC\underline{C}H_aMeMe$), 26.7 ($NCH_bMe\underline{Me}$), 24.3 ($NCH_aMe\underline{Me}$), 24.0 ($NCH_a\underline{Me}Me$), 23.9 ($NCH_b\underline{Me}Me$), 21.0 ($C_6H_4\underline{Me}$), 12.6 ($C_5\underline{Me}_5$), 10.8 ($\underline{Me}CN_2$).

Cp*Ti{MeC(N^{i}Pr)$_2$}{N(Tol)C(NNCPh$_2$)O} (49). To a solution of Cp*Ti{MeC(N^{i}Pr)$_2$}(NNCPh$_2$) (**41**, 0.160 g, 0.31 mmol) in diethyl ether (5 mL) was added TolNCO (38.9 μL, 0.31 mmol) at -78 ℃. An immediate colour change from dark yellow to red then to brown was observed. After 30 min, the volatiles were removed under reduced pressure at -78 ℃. The crude was then redissolved in benzene and left for 16 h at RT, after which the volatiles were removed under reduced pressure to give **49** as a dark brown solid. Yield: 0.188 g (93%). ^{1}H NMR (C_6D_6, 499.9 MHz, 293 K): δ 8.17 (2 H, d, ^3J = 8.0 Hz, o_a-C_6H_5), 7.58 (2 H, d, ^3J = 8.0 Hz, o_b-C_6H_5), 7.29 (2 H, t, ^3J = 8.0 Hz, m_b-C_6H_5), 7.22 (2 H, d, ^3J = 8.0 Hz, *o*-C_6H_4Me), 7.20 (2 H, t, ^3J = 8.0 Hz, m_a-C_6H_5), 7.15 (1 H, t, ^3J = 8.0 Hz, p_a-C_6H_5), 7.12 (1 H, t, ^3J = 8.0 Hz, p_b-C_6H_5), 6.96 (2 H, d, ^3J = 8.0 Hz, *m*-C_6H_4Me), 3.82 (1 H, app. sept., app. ^3J = 7.0 Hz, $NC\underline{H}_aMeMe$), 3.46 (1 H, app. sept., app. ^3J = 7.0 Hz, $NC\underline{H}_bMeMe$), 2.22 (3 H, s, $C_6H_4\underline{Me}$), 2.03 (15 H, s, C_5Me_5), 1.46 (3 H, s, $MeCN_2$), 1.23 (6 H, d, ^3J = 7.0 Hz, overlapping $NCH_b\underline{Me}Me$ and $NCH_bMe\underline{Me}$), 1.08 (3 H, d, ^3J = 7.0 Hz, $NCH_a\underline{Me}Me$, 0.63 (3 H, d, ^3J = 7.0 Hz $NCH_aMe\underline{Me}$). ^{13}C{^{1}H} NMR (C_6D_6, 125.7 MHz, 293 K): δ 169.1 ($Me\underline{C}N_2$), 157.1 (OCN), 156.8 ($NN\underline{C}Ph_2$), 145.6 (*i*-C_6H_4Me), 141.4 (i_a-C_6H_5), 139.3 (i_b-C_6H_5), 130.7 (o_b-C_6H_5), 130.0 (*p*-C_6H_4Me), 128.6 ($\underline{C}_5Me_5$), 128.5 (o_a-C_6H_5), 128.4 (*m*-C_6H_4Me), 127.8 (p_a-C_6H_5), 127.7 (m_a-C_6H_5), 127.6 (m_b-C_6H_5), 126.9 (p_b-C_6H_5), 122.5 (*o*-C_6H_4Me), 50.7 ($NC\underline{C}H_bMeMe$), 49.4 ($NC\underline{C}H_aMeMe$), 24.2 ($NCH_a\underline{Me}Me$), 24.0 ($NCH_b\underline{Me}Me$), 23.8 ($NCH_bMe\underline{Me}$), 23.7 ($NCH_aMe\underline{Me}$), 20.9 ($C_6H_4\underline{Me}$), 15.3 ($\underline{Me}CN_2$), 12.5 ($C_5\underline{Me}_5$). IR (NaCl plates, Nujol mull, cm^{-1}): 1592 (m), 1554 (s), 1506 (s), 1405 (s), 1338 (m), 1314 (m), 1261 (m), 1228 (m), 1206 (m), 1172 (w), 1119 (w), 1071 (w), 1040 (w), 1024 (m), 1005 (m), 945 (w), 913 (w), 889 (w), 808 (m), 790 (m), 754 (m), 724 (m), 695 (s), 650 (w), 610 (w), 582 (w), 541 (w). EI-MS: *m/z* = 270 [*M* – Cp* – MeC(^{i}Pr)$_2$ – NTol]$^+$ (70%), 221 [*M* – Cp* – MeC(^{i}Pr)$_2$ – 2 Ph]$^+$ (100%). A satisfactory elemental analysis could not be obtained due to contamination by **50**.

Cp*Ti{MeC(N^{i}Pr)$_2$}{OC(NNCPh$_2$)N(Tol)C(NTol)O} (50). To a solution of Cp*Ti{MeC(N^{i}Pr)$_2$}(NNCPh$_2$) (**41**, 0.250 g, 0.48 mmol) in benzene (10 mL) was added TolNCO (121.6 μL, 0.96 mmol) in benzene (10 mL) all at RT. An immediate

colour change from dark yellow to red then to brown was observed. After 5 h, the solution was filtered, and the volatiles were removed under reduced pressure to afford a brown solid which was washed with cold pentane (3 × 10 mL) cooled to -78 ℃, filtered, and dried *in vacuo* to give **50** as a brown solid. Yield: 0.273 g (72%). Diffraction-quality crystals were grown from a saturated benzene solution at 4 ℃. ^{1}H NMR (C_6D_6, 299.9 MHz, 293 K): δ 7.97 (2 H, d, ^{3}J = 7.5 Hz, o_a-C_6H_5), 7.33 (2 H, d, ^{3}J = 7.5 Hz, o_b-C_6H_5), 7.25 (4 H, m, overlapping m_a-C_6H_5 and o_a-C_6H_4Me), 7.07 (5 H, m, overlapping o_b-C_6H_4Me, m_b- and p_b-C_6H_5), 6.98 (5 H, m, overlapping p_a-C_6H_5, m_a- and m_b-C_6H_4Me), 3.76 (1 H, app. sept., app. ^{3}J = 6.6 Hz, NC$\underline{H}_a$MeMe), 3.37 (1 H, app. sept., app. ^{3}J = 6.6 Hz, NC$\underline{H}_b$MeMe), 2.19 (3 H, s, $C_6H_4\underline{Me}_a$), 2.17 (3 H, s, $C_6H_4\underline{Me}_b$), 2.03 (15 H, s, C_5Me_5), 1.43 (3 H, s, $MeCN_2$), 1.25 (3 H, d, ^{3}J = 6.6 Hz, $NCH_a\underline{Me}Me$), 1.20 (3 H, d, ^{3}J = 6.6 Hz, $NCH_aMe\underline{Me}$), 0.90 (3 H, d, ^{3}J = 6.6 Hz, $NCH_b\underline{Me}Me$), 0.84 (3 H, d, ^{3}J = 6.6 Hz, $NCH_bMe\underline{Me}$). ^{13}C{^{1}H} NMR (C_6D_6, 75.4 MHz, 293 K): δ 169.7 ($Me\underline{C}N_2$), 159.1 (OC_aN), 157.7 ($N\underline{C}Ph_2$), 152.5 (OC_bN), 147.7 (i_a-C_6H_4Me), 141.5 (i_a-C_6H_5), 141.0 (i_b-C_6H_4Me), 137.2 (i_b-C_6H_5), 135.2 (p_a-C_6H_4Me), 134.8 (p_b-C_6H_4Me), 130.7 (o_b-C_6H_5), 130.2 ($\underline{C}_5Me_5$), 129.7 (o_a-C_6H_4Me), 129.0 (m_a-C_6H_4Me), 128.7 (o_a-C_6H_5), 128.6 (m_b-C_6H_4Me), 128.1 (m_a-C_6H_5), 127.3 (m_b-C_6H_5), 127.0 (p_b-C_6H_5), 124.6 (p_a-C_6H_5), 124.1 (o_b-C_6H_4Me), 50.5 ($N\underline{C}H_aMeMe$), 49.9 ($N\underline{C}H_bMeMe$), 24.3 ($NCH_aMe\underline{Me}$), 23.9 ($NCH_b\underline{Me}Me$), 23.8 ($NCH_a\underline{Me}Me$), 23.7 ($NCH_bMe\underline{Me}$), 21.2 ($C_6H_4\underline{Me}_a$), 21.0 ($C_6H_4\underline{Me}_b$), 14.8 ($\underline{Me}CN_2$), 12.6 ($C_5\underline{Me}_5$). IR (NaCl plates, Nujol mull, cm^{-1}): 2728 (w), 1623 (s), 1604 (s), 1548 (s), 1516 (s), 1488 (s), 1370 (s), 1344 (m), 1313 (m), 1290 (w), 1254 (m), 1227 (s), 1207 (m), 1168 (m), 1122 (m), 1101 (w), 1072 (w), 1043 (s), 1027 (m), 1004 (m), 947 (w), 929 (w), 917 (w), 894 (w), 876 (w), 822 (m), 809 (s), 787 (s), 774 (m), 733 (m), 723 (m), 692 (s), 668 (w), 652 (m), 601 (m), 589 (s), 542 (s). EI-MS: *m/z* = 643 [*M* – MeC(^{i}Pr)$_2$]$^{+}$ (70%). Anal. found (calcd. for $C_{47}H_{56}N_6O_2Ti$): C, 71.85 (71.92); H, 7.33 (7.19); N, 10.59 (10.71)%.

Cp*Ti{MeC(N^{i}Pr)$_2$}{N(Tol)C(NNCPh$_2$)S} (51). To a solution of Cp*Ti{MeC(N^{i}Pr)$_2$}(NNCPh$_2$) (**41**, 0.220 g, 0.42 mmol) in benzene (10 mL) was added TolNCS (63.3 mg, 0.42 mmol) in benzene (5 mL) all at RT. A colour change from dark yellow to dark brown was observed. After 40 h, the dark brown solution was filtered, and the volatiles were removed under reduced pressure to afford **51** as a dark brown solid which was washed with cold pentane (3 × 10 mL) cooled to -78 ℃, filtered, and dried *in vacuo*. Yield: 0.168 g (59%). Diffraction-quality crystals were

grown from a mixture of saturated diethyl ether and pentane solution at 4 ℃. ^{1}H NMR (toluene-d_8, 499.9 MHz, 253 K): δ 8.21 (2 H, d, ^{3}J = 7.5 Hz, o_a-C_6H_5), 7.39 (2 H, d, ^{3}J = 7.5 Hz, o_b-C_6H_5), 7.27 (2 H, d, ^{3}J = 8.0 Hz, o-C_6H_4Me), 7.18 (2 H, t, ^{3}J = 7.5 Hz, m_b-C_6H_5), 7.16 (2 H, t, ^{3}J = 7.5 Hz, m_a-C_6H_5), 7.11 (2 H, m, overlapping p_a- and p_b-C_6H_5), 6.95 (2 H, d, ^{3}J = 8.0 Hz, m-C_6H_4Me), 3.67 (1 H, app. sept., app. ^{3}J = 6.5 Hz, NC$\underline{H}_a$MeMe), 3.38 (1 H, app. sept., app. ^{3}J = 6.5 Hz, NC$\underline{H}_b$MeMe), 2.24 (3 H, s, $C_6H_4\underline{Me}$), 1.97 (15 H, s, C_5Me_5), 1.48 (3 H, s, $MeCN_2$), 1.10 (3 H, d, ^{3}J = 6.5 Hz, NCH$_b\underline{Me}$Me), 0.99 (3 H, d, ^{3}J = 6.5 Hz, NCH$_a\underline{Me}$Me), 0.98 (3 H, d, ^{3}J = 6.5 Hz, NCH$_b$Me$\underline{Me}$), 0.48 (3 H, d, ^{3}J = 6.5 Hz, NCH$_a$Me$\underline{Me}$). ^{13}C{^{1}H} NMR (toluene-d_8, 125.7 MHz, 253 K): δ 166.8 (Me$\underline{C}N_2$), 160.4 (NCS), 157.2 (N$\underline{C}Ph_2$), 145.3 (i-C_6H_4Me), 140.5 (i_a-C_6H_5), 138.8 (i_b-C_6H_5), 130.6 (p-C_6H_4Me), 130.3 (o_b-C_6H_5), 128.6 (o_a-C_6H_5), 128.3 (m-C_6H_4Me), 128.2 ($\underline{C}_5Me_5$), 127.9 (m_a-C_6H_5), 127.5 (m_b-C_6H_5), 127.0 (p_b-C_6H_5), 125.3 (p_a-C_6H_5), 123.2 (o-C_6H_4Me), 51.9 (N$\underline{C}H_b$MeMe), 49.3 (N$\underline{C}H_a$MeMe), 23.8 (NCH$_b$Me$\underline{Me}$), 23.6 (NCH$_a\underline{Me}$Me), 22.9 (NCH$_b\underline{Me}$Me), 22.8 (NCH$_a$Me$\underline{Me}$), 20.9 ($C_6H_4\underline{Me}$), 17.6 ($\underline{Me}CN_2$), 13.1 ($C_5\underline{Me}_5$). IR (NaCl plates, Nujol mull, cm^{-1}): 1645 (w), 1606 (m), 1501 (s), 1346 (m), 1290 (m), 1208 (m), 1141 (w), 1072 (w), 1027 (w), 958 (m), 871 (w), 801 (w), 771 (w), 695 (m), 659 (w). EI-MS: m/z = 526 [M – MeC(^{i}Pr)$_2$]$^{+}$ (30%), 435 [M – MeC(^{i}Pr)$_2$ – Tol]$^{+}$ (10%), 269 [M – MeC(^{i}Pr)$_2$ – Tol – CPh$_2$]$^{+}$ (40%). Anal. found (calcd. for $C_{39}H_{49}N_5STi$): C, 69.98 (70.15); H, 7.23 (7.40); N, 10.38 (10.49)%.

Cp*Ti{MeC(N^{i}Pr)$_2$}{SC(NNCPh$_2$)N(Tol)C(NTol)O} (52). To a solution of Cp*Ti{MeC(N^{i}Pr)$_2$}{SC(NNCPh$_2$)NTol} (**51**, 0.140 g, 0.31 mmol) in benzene (5 mL) was added TolNCO (26.5 μL, 0.31 mmol) in benzene (5 mL) all at RT. After 40 h, the red brown solution was filtered and the volatiles were removed under reduced pressure to give **52** as a red brown solid. Yield: 0.132 g (79%). ^{1}H NMR (toluene-d_8, 499.9 MHz, 253 K): δ 7.95 (2 H, d, ^{3}J = 8.5 Hz, o_a-C_6H_5), 7.16 (2 H, d, ^{3}J = 8.0 Hz, o_b-C_6H_4Me), 7.10 (4 H, m, overlapping m_b-C_6H_5 and o_a-C_6H_4Me), 7.08 (2 H, m, m_a-C_6H_5), 7.06 (2H, m, p-C_6H_5), 7.00 (2 H, d, ^{3}J = 8.0 Hz, m_a-C_6H_4Me), 6.98 (2H, t, ^{3}J = 8.5 Hz, m_b-C_6H_5), 6.88 (2 H, d, m_b-C_6H_4Me), 3.74 (1 H, app. sept., app. ^{3}J = 7.0 Hz, NC$\underline{H}_a$MeMe), 3.40 (1 H, app. sept., app. ^{3}J = 7.0 Hz, NC$\underline{H}_b$MeMe), 2.20 (3 H, s, $C_6H_4\underline{Me}_a$), 2.14 (3 H, s, $C_6H_4\underline{Me}_b$), 1.96 (15 H, s, C_5Me_5), 1.54 (3 H, s, $MeCN_2$), 1.26 (3 H, d, ^{3}J = 7.0 Hz, NCH$_a\underline{Me}$Me), 1.10 (3 H, d, ^{3}J = 7.0 Hz, NCH$_a$Me$\underline{Me}$), 0.99 (3 H, d, ^{3}J = 7.0 Hz, NCH$_b\underline{Me}$Me), 0.88 (3 H, d, ^{3}J = 7.0 Hz, NCH$_b$Me$\underline{Me}$). ^{13}C{^{1}H} NMR

(toluene-d_8, 125.7 MHz, 253 K): δ 168.4 (Me<u>C</u>N_2), 159.9 (OCN), 159.1 (N<u>C</u>Ph_2), 154.5 (SCN), 147.9 (i_a-C_6H_4Me), 143.4 (i_b-C_6H_4Me), 140.1 (i_a-C_6H_5), 136.7 (i_b-C_6H_5), 134.4 (p_b-C_6H_4Me), 130.0 (m_a-C_6H_5), 129.1 (<u>C</u>$_5$Me$_5$), 129.0 (overlapping o_b- and m_b-C_6H_4Me), 128.9 (o_a-C_6H_5), 128.7 (m_a-C_6H_4Me), 128.6 (p_a-C_6H_4Me), 128.0 (overlapping o_b-C_6H_5 and o_a-C_6H_4Me) 127.4 (m_b-C_6H_5), 123.7 (p-C_6H_5), 50.3 (N<u>C</u>H$_a$MeMe), 49.9 (N<u>C</u>H$_b$MeMe), 24.3 (NCH$_a$Me<u>Me</u>), 23.7 (NCH$_b$<u>Me</u>Me), 23.5 (NCH$_a$<u>Me</u>Me), 23.4 (NCH$_b$Me<u>Me</u>), 21.1 (C_6H_4<u>Me</u>$_b$), 20.9 (C_6H_4<u>Me</u>$_a$), 17.2 (<u>Me</u>CN_2), 12.7 (C_5<u>Me</u>$_5$). IR (NaCl plates, Nujol mull, cm^{-1}): 1614 (m), 1589 (s), 1503 (s), 1330 (s), 1288 (m), 1233 (m), 1208 (m), 1189 (m), 1158 (m), 1141 (m), 1104 (m), 1073 (m), 1073 (w), 1015 (m), 955 (w), 872 (w), 810 (m), 790 (m), 740 (w), 724 (w), 695 (m), 444(s). EI-MS: *m/z* = 659 [*M* – {MeC(^{i}Pr)$_2$}]$^+$ (80%). Anal. found (calcd. for $C_{47}H_{56}N_6OSiTi$): C, 70.58 (70.48); H, 7.13 (7.05); N, 10.57 (10.49)%.

Cp*Ti{MeC(N^{i}Pr)$_2$}{NNCPh$_2$}(CN^{t}Bu) (53). To a solution of Cp*Ti{MeC(N^{i}Pr)$_2$}(NNCPh$_2$) (**41**, 0.200 g, 0.39 mmol) in benzene (5 mL) was added ^{t}BuNC (43.7 μL, 0.39 mmol) all at RT. An immediate colour change from dark yellow to brown was observed. After 4 h, the volatiles were removed under reduced pressure to afford **53** as a brown waxy solid. Yield: 0.171 g (74%). ^{1}H NMR (toluene-d_8, 499.9 MHz, 203 K): δ 7.99 (2 H, d, ^3J = 8.0 Hz, o_a-C_6H_5), 7.71 (2 H, d, ^3J = 8.0 Hz, o_b-C_6H_5), 7.19 (4 H, t, ^3J = 8.0 Hz, overlapping m_a- and m_b-C_6H_5), 7.06 (2 H, t, ^3J = 8.0 Hz, overlapping p_a- and p_b-C_6H_5), 3.60 (1 H, app. sept., app. ^3J = 6.0 Hz, NC<u>H</u>$_a$MeMe), 2.93 (1 H, app. sept., app. ^3J = 6.0 Hz, NC<u>H</u>$_b$MeMe), 2.29 (15 H, s, C_5Me_5), 1.69 (3 H, s, MeCN_2), 1.31 (3 H, d, ^3J = 6.0 Hz, NCH$_a$<u>Me</u>Me), 1.30 (3 H, d, ^3J = 6.0 Hz, NCH$_b$<u>Me</u>Me), 1.17 (3 H, d, ^3J = 6.0 Hz, NCH$_b$Me<u>Me</u>), 1.11 (3 H, d, ^3J = 6.0 Hz, NCH$_a$Me<u>Me</u>), 0.83 (9 H, s, NC<u>Me</u>$_3$). ^{13}C{^{1}H} NMR (toluene-d_8, 125.7 MHz, 203 K): δ 167.5 (Me<u>C</u>N_2), 158.3 (NN<u>C</u>Ph_2), 140.4 (overlapping i_a- and i_b-C_6H_5), 133.9 (<u>C</u>NCMe$_3$), 131.0 (o_b-C_6H_5), 128.2 (overlapping m_a- and m_b-C_6H_5), 127.4 (o_a-C_6H_5), 126.6 (p_b-C_6H_5), 126.4 (p_a-C_6H_5), 115.8 (<u>C</u>$_5$Me$_5$), 55.3 (N<u>C</u>Me$_3$), 49.0 (N<u>C</u>H$_b$MeMe), 48.1 (N<u>C</u>H$_a$MeMe), 29.2 (NC<u>Me</u>$_3$), 27.0 (NCH$_b$<u>Me</u>Me), 26.0 (NCH$_b$Me<u>Me</u>), 25.2 (NCH$_a$Me<u>Me</u>), 24.9 (NCH$_a$<u>Me</u>Me), 12.5 (C_5<u>Me</u>$_5$), 11.7 (<u>Me</u>CN_2) ppm. IR (NaCl plates, Nujol mull, cm^{-1}): 2164 (s), 2041 (w), 1598 (w), 1339 (m), 1315 (m), 1212 (s), 1173 (w), 1122 (m), 1071 (w), 1027 (w), 794 (w), 763 (w), 692 (s), 495 (s). EI-MS: *m/z* = 325 [*M* – Cp* – MeC(^{i}Pr)$_2$]$^+$ (70%). A satisfactory

elemental analysis could not be obtained due to the ready loss of ^{t}BuNC from **53** under vacuum.

Cp*Ti{MeC(N^{i}Pr)$_2$}{NNCPh$_2$}(CNXyl) (54). To a solution of Cp*Ti{MeC(N^{i}Pr)$_2$}(NNCPh$_2$) (**41**, 0.140 g, 0.270 mmol) in benzene (3 mL) was added XylNC (35.4 mg, 0.270 mmol) in benzene (3 mL) all at RT. An immediate colour change from dark yellow to dark brown was observed. After 30 min, the volatiles were removed under reduced pressure to afford **54** as a dark brown solid. Yield: 0.154 g (88%). Diffraction-quality crystals were grown from a saturated benzene solution at 4 ℃. ^{1}H NMR (toluene-d_8, 499.9 MHz, 203 K): δ 7.96 (2 H, d, ^{3}J = 7.5 Hz, o_a-C$_6$H$_5$), 7.65 (2 H, d, ^{3}J = 7.5 Hz, o_b-C$_6$H$_5$), 7.19 (2 H, t, ^{3}J = 7.5 Hz, m_a-C$_6$H$_5$), 7.10 (3 H, m, overlapping m_b- and p_a-C$_6$H$_5$), 7.00 (1 H, t, ^{3}J = 7.5 Hz, p_b-C$_6$H$_5$), 6.66 (1 H, t, ^{3}J = 7.5 Hz, p-C$_6$H$_3$Me$_2$), 6.39 (2 H, d, ^{3}J = 7.5 Hz, m-C$_6$H$_3$Me$_2$), 3.58 (1 H, app. sept., app. ^{3}J = 6.0 Hz, NC<u>H$_a$</u>MeMe), 2.47 (1 H, app. sept., app. ^{3}J = 6.0 Hz, NC<u>H$_b$</u>MeMe), 2.32 (6 H, s, C$_6$H$_3$Me$_2$), 2.28 (15 H, s, C$_5$Me$_5$), 1.60 (3 H, s, MeCN$_2$), 1.41 (3 H, d, ^{3}J = 6.0 Hz, NCH$_a$<u>Me</u>Me), 1.25 (3 H, d, ^{3}J = 6.0 Hz, NCH$_b$<u>Me</u>Me), 1.14 (3 H, d, ^{3}J = 6.0 Hz, NCH$_b$Me<u>Me</u>), 1.10 (3 H, d, ^{3}J = 6.0 Hz, NCH$_a$Me<u>Me</u>). ^{13}C{^{1}H} NMR (toluene-d_8, 125.7 MHz, 203 K): δ 166.3 (Me<u>C</u>N$_2$), 140.1 (i_a-C$_6$H$_5$), 137.5 ((C$_6$H$_3$Me$_2$)N<u>C</u>), 137.1 (i_b-C$_6$H$_5$), 135.3 (overlapping i- and o-C$_6$H$_3$Me$_2$), 134.4 (NN<u>C</u>Ph$_2$), 131.0 (o_b-C$_6$H$_5$), 129.1 (p-C$_6$H$_3$Me$_2$), 128.2 (overlapping m_a- and m-C$_6$H$_3$Me$_2$), 127.5 (o_a-C$_6$H$_5$), 127.4 (m_b-C$_6$H$_5$), 126.7 (p_b-C$_6$H$_5$), 125.3 (p_a-C$_6$H$_5$), 116.3 (<u>C</u>$_5$Me$_5$), 49.0 (N<u>C</u>H$_b$MeMe), 48.3 (N<u>C</u>H$_a$MeMe), 27.6 (NCH$_b$<u>Me</u>Me), 26.4 (NCH$_b$Me<u>Me</u>), 25.5 (NCH$_a$Me<u>Me</u>), 25.4 (NCH$_a$<u>Me</u>Me), 19.6 (C$_6$H$_3$<u>Me</u>$_2$), 12.6 (C$_5$<u>Me</u>$_5$), 11.6 (<u>Me</u>CN$_2$). IR (NaCl plates, Nujol mull, cm^{-1}): 2124 (s), 1654 (w), 1593 (m), 1492 (s), 1404 (m), 1342 (m), 1314 (m), 1230 (m), 1198 (s), 1171 (m), 1120 (s), 1072 (m), 1027 (m) 953 (w), 907 (w), 791 (w), 768 (s), 761 (s), 723 (m), 693 (s), 676 (w), 634 (w), 608 (w), 564 (w). EI-MS: m/z = 469 [M – NCPh$_2$]$^{+}$ (10%). Anal. found (calcd. for C$_{40}$H$_{51}$N$_5$Ti): C, 73.85 (73.94); H, 7.91 (8.03); N, 10.78 (10.66)%.

Cp*Ti{MeC(N^{i}Pr)$_2$}{N(NCPh$_2$)C(Ph)NC(Ph)N} (55). To a solution of Cp*Ti{MeC(N^{i}Pr)$_2$}(NNCPh$_2$) (**41**, 0.300 g, 0.58 mmol) in benzene (10 mL) was added PhCN (179 μL, 1.74 mmol) in benzene (5 mL) all at RT. After stirring for 4 d, the colour had changed from dark yellow to yellow. The volatiles were removed under reduced pressure to afford a sticky yellow oil which was washed with cold pentane (3 × 10 mL) cooled to -78 ℃, filtered, and dried in *vacuo* to give **55** as a

yellow solid. Yield: 0.290 g (69%). Diffraction-quality crystals were grown from a saturated benzene solution at 4 ℃. ^{1}H NMR (C_6D_6, 299.9 MHz, 293 K): δ 8.50 (2 H, d, ^{3}J = 7.5 Hz, o_a-C_6H_5), 7.81 (2 H, d, ^{3}J = 7.5 Hz, o_b-C_6H_5), 7.75 (2 H, d, ^{3}J = 7.5 Hz, o_c-C_6H_5), 7.32 (2 H, t, ^{3}J = 7.5 Hz, m_a-C_6H_5), 7.20 (1 H, t, ^{3}J = 7.5 Hz, p_a-C_6H_5), 7.08 (5 H, m, overlapping m_b-, m_c- and p_c-C_6H_5), 6.95 (1 H, t, ^{3}J = 7.5 Hz, p_b-C_6H_5), 6.85 (3 H, m, overlapping m_d- and p_d-C_6H_5), 6.71 (2 H, d, ^{3}J = 7.5 Hz, o_d-C_6H_5), 4.28 (1 H, app. sept., app. ^{3}J = 6.9 Hz, NC$\underline{H}_a$MeMe), 3.91 (1 H, app. sept., app. ^{3}J = 6.9 Hz, NC$\underline{H}_b$MeMe), 2.12 (15 H, s, C_5Me_5), 1.73 (3 H, s, $MeCN_2$), 1.45 (3 H, d, ^{3}J = 6.9 Hz, NCH$_a$$\underline{Me}$Me), 1.34 (3 H, d, ^{3}J = 6.9 Hz, NCH$_a$Me$\underline{Me}$), 1.10 (3 H, d, ^{3}J = 6.9 Hz, NCH$_b$$\underline{Me}$Me), 0.77 (3 H, d, ^{3}J = 6.9 Hz, NCH$_b$Me$\underline{Me}$). ^{13}C{^{1}H} NMR (C_6D_6, 75.4 MHz, 293 K): δ 171.0 (Me$\underline{C}N_2$), 161.3 (N$\underline{C}_b$(Ph)N), 160.9 (NN$\underline{C}Ph_2$), 159.5 (N$\underline{C}_a$(Ph)N), 139.3 (i_c-C_6H_5), 138.6 (i_b-C_6H_5), 138.2 (i_a-C_6H_5), 134.8 (i_d-C_6H_5), 132.0 (o_b-C_6H_5), 131.7 (o_d-C_6H_5), 129.8 (o_c-C_6H_5), 129.7 (overlapping p_a- and p_c-C_6H_5), 129.3 (o_a-C_6H_5), 128.2 (m_a-C_6H_5), 128.1 (p_b-C_6H_5), 127.9 (m_b-C_6H_5), 127.5 (p_d-C_6H_5), 127.3 (m_d-C_6H_5), 126.7 (m_c-C_6H_5), 122.3 ($\underline{C}_5Me_5$), 51.7 (N$\underline{C}$H$_a$MeMe), 46.9 (N$\underline{C}$H$_b$MeMe), 26.7 (NCH$_b$Me$\underline{Me}$), 25.0 (NCH$_a$Me$\underline{Me}$), 24.0 (NCH$_b$$\underline{Me}$Me), 23.4 (NCH$_a$$\underline{Me}$Me), 18.7 ($\underline{Me}CN_2$), 12.3 ($C_5\underline{Me}_5$). IR (NaCl plates, Nujol mull, cm^{-1}): 3053 (w), 2722 (w), 2041 (w), 1617 (w), 1585 (w), 1558 (w), 1532 (s), 1487 (m), 1345 (w), 1306 (m), 1290 (m), 1277 (m), 1206 (w), 1144 (w), 1117 (w), 1087 (w), 1062 (w), 1025 (w), 1015 (m), 884 (w), 801 (w), 786 (m), 777 (m), 755 (w), 720 (m), 713 (s), 699 (s), 693 (s), 664 (w), 647 (w), 608 (m), 577 (s), 488 (s). EI-MS: *m/z* = 544 [*M* – $NCPh_2$]$^{+}$ (20%), 403 [*M* – MeC(^{i}Pr)$_2$ – $NCPh_2$]$^{+}$ (20%). Anal. found (calcd. for $C_{45}H_{52}N_6Ti$): C, 74.73 (74.57); H, 7.37 (7.23); N, 11.38 (11.59)%.

Cp*Ti{MeC(N^{i}Pr)$_2$}{N(NCPh$_2$)C(Ar^{F5})NC(Ar^{F5})N} (56). To a solution of Cp*Ti{MeC(N^{i}Pr)$_2$}(NNCPh$_2$) (**41**, 0.200 g, 0.39 mmol) in benzene (10 mL) was added C_6F_5CN (97.2 μL, 0.77 mmol) in benzene (10 mL) all at RT. A colour change from dark yellow to yellow was observed. After 16 h, the yellow solution was filtered, and the volatiles were removed under reduced pressure to afford **56** as a yellow solid which was washed with cold pentane (3 × 10 mL) cooled to -78 ℃, filtered, and dried *in vacuo*. Yield: 0.162 g (46%). Diffraction-quality crystals were grown from a saturated benzene solution at 4 ℃. ^{1}H NMR (C_6D_6, 499.9 MHz, 293 K): δ 7.59 (2 H, d, ^{3}J = 6.9 Hz, o_a-C_6H_5), 7.08 (3 H, m, overlapping m_b- and p_b-C_6H_5), 7.02 (3 H, m, overlapping m_a- and p_a-C_6H_5), 6.79 (2 H, d, ^{3}J = 6.9 Hz, o_b-C_6H_5), 3.81 (1 H, app.

sept., app. ^{3}J = 6.3 Hz, NC$\underline{H}_a$MeMe), 3.61 (1 H, app. sept., app. ^{3}J = 6.3 Hz, NC$\underline{H}_b$MeMe), 2.13 (15 H, s, C_5Me_5), 1.64 (3 H, s, $MeCN_2$), 1.32 (3 H, d, ^{3}J = 6.3 Hz, NCH$_a$$\underline{Me}$Me), 1.17 (3 H, d, ^{3}J = 6.3 Hz, NCH$_a$Me$\underline{Me}$), 0.95 (3 H, d, ^{3}J = 6.3 Hz, NCH$_b$$\underline{Me}$Me), 0.86 (3 H, d, ^{3}J = 6.3 Hz, NCH$_b$Me$\underline{Me}$). $^{13}C\{^{1}H\}$ NMR (C_6D_6, 125.7 MHz, 293 K): δ 171.7 (Me$\underline{C}N_2$), 163.3 (N$\underline{C}$Ph$_2$), 148.9 (NCN), 147.8 (NCN), 146.8 (*p*-C_6F_5), 144.4 (*o*-C_6F_5), 143.2 (*p*-C_6F_5), 140.8 (*m*-C_6F_5), 138.5 (i_a-C_6H_5), 137.8 (*m*-C_6F_5), 136.8 (*o*-C_6F_5), 132.6 (i_b-C_6H_5), 131.9 (o_b-C_6H_5), 130.6 (p_a-C_6H_5), 130.3 (o_a-C_6H_5), 130.0 (p_b-C_6H_5), 128.3 (m_b-C_6H_5), 127.9 (m_a-C_6H_5), 125.4 ($\underline{C}_5Me_5$), 115.6 (*i*-C_6F_5), 115.2 (*i*-C_6F_5), 50.8 (N$\underline{C}$H$_a$MeMe), 47.5 (N$\underline{C}$H$_b$MeMe), 25.9 (NCH$_b$Me$\underline{Me}$), 25.1 (NCH$_b$$\underline{Me}$Me), 24.9 (NCH$_aMe\underline{Me}$), 23.5 (NCH$_a$$\underline{Me}$Me), 16.6 ($\underline{Me}CN_2$), 12.6 ($C_5\underline{Me}_5$). ^{19}F NMR (C_6D_6, 470.4 MHz, 293K): -128.2 (1 F, d, ^{3}J = 23 Hz, o_{a1}-C_6F_5), -129.2 (1 F, d, ^{3}J = 23 Hz, o_{a2}-C_6F_5), -136.7 (2 F, d, ^{3}J = 23 Hz, o_b-C_6F_5), -150.7 (1 F, t, ^{3}J = 23 Hz, p_a-C_6F_5), -152.5 (1 F, t, ^{3}J = 23, p_b-C_6F_5), -158.5 (2 F, m, m_a-C_6F_5), -161.2 (2 F, t, ^{3}J = 23 Hz, m_b-C_6F_5). IR (NaCl plates, Nujol mull, cm^{-1}): 2725 (w), 2041 (w), 1651 (m), 1617 (w), 1576 (w), 1552 (s), 1519 (s), 1497 (s), 1418 (m), 1336 (m), 1318 (m), 1219 (m), 1196 (m), 1160 (w), 1127 (w), 1111 (m), 1086 (m), 1019 (w), 994 (s), 961 (w), 946 (w), 891 (m), 812 (m), 795 (s), 770 (m), 758 (m), 722 (m), 706 (m), 697 (s), 686 (w), 666 (w), 627 (w), 602 (m), 574 (s). EI-MS: *m/z* = 765 [*M* – MeC(^{i}Pr)$_2$]$^{+}$ (100%), 518 [*M* – NNCPh$_2$ – C_6F_5CN]$^{+}$ (40%). Anal. found (calcd. for $C_{45}H_{42}F_{10}N_6Ti$): C, 59.80 (59.74); H, 4.84 (4.68); N, 9.15 (9.29)%.

Cp*Ti{MeC(N^{i}Pr)$_2$}{N(NCPh$_2$)C(Ph)NC(Ar^{F5})N} (57). To a solution of Cp*Ti{MeC(N^{i}Pr)$_2$}{N(NCPh$_2$)C(Ph)NC(Ph)N} (**55**, 0.260 g, 0.36 mmol) in benzene (10 mL) was added C_6F_5CN (90.4 μL, 0.72 mmol) in benzene (5 mL) all at RT. A colour change from dark yellow to dark orange was observed. After 16 h, the dark orange solution was filtered, and the volatiles were removed under reduced pressure to afford a waxy red orange solid which was washed with cold pentane (3 × 10 mL) cooled to -78 ℃, filtered, and dried *in vacuo* to give **57** as a red orange solid. Yield: 0.205 g (70%). ^{1}H NMR (C_6D_6, 499.9 MHz, 293 K): δ 7.73 (4 H, 2 × d, 2 × ^{3}J = 7.5 Hz, overlapping o_a-C_6H_5 and o_b-C_6H_5), 7.09 (3 H, m, overlapping m_a-C_6H_5 and p_c-C_6H_5), 7.04 (2 H, m, o_c-C_6H_5), 6.97 (3 H, m, overlapping p_a-C_6H_5 and m_b-C_6H_5), 6.89 (1 H, t, ^{3}J = 7.5 Hz, p_b-C_6H_5), 6.63 (2 H, t, ^{3}J = 7.5 Hz, m_c-C_6H_5), 3.92 (1 H, app. sept., app. ^{3}J = 7.0 Hz, NC$\underline{H}_a$MeMe), 3.80 (1 H, app. sept., app. ^{3}J = 7.0 Hz, NC$\underline{H}_b$MeMe), 2.14 (15 H, s, C_5Me_5), 1.69 (3 H, s, $MeCN_2$), 1.27 (3 H, d, ^{3}J = 7.0 Hz,

NCH_aMeMe), 1.15 (3 H, d, ^3J = 7.0 Hz, NCH_aMeMe), 1.06 (3 H, d, ^3J = 7.0 Hz, NCH_bMeMe), 0.78 (3 H, d, ^3J = 7.0 Hz, NCH_bMeMe). $^{13}C\{^1H\}$ NMR (C_6D_6, 125.7 MHz, 293 K): δ 170.9 ($MeCN_2$), 161.8 (NCN), 161.0 ($NCPh_2$), 149.4 ($NC(C_6F_5)N$, 145.1 (*o*-C_6F_5), 140.6 (*p*-C_6F_5), 138.6 (i_a-C_6H_5), 137.9 (i_b-C_6H_5), 137.8 (*m*-C_6F_5), 134.4 (i_c-C_6H_5), 131.8 (o_a-C_6H_5), 131.5 (m_c-C_6H_5), 130.0 (p_c-C_6H_5), 129.9 (o_b-C_6H_5), 128.8 (p_a-C_6H_5), 128.5 (p_b-C_6H_5), 128.1 (o_c-C_6H_5), 127.9 (m_a-C_6H_5), 126.9(m_b-C_6H_5), 124.0 (C_5Me_5), 115.9 (*i*-C_6F_5), 51.3 (NCH_aMeMe), 46.9 (NCH_bMeMe), 26.5 (NCH_bMeMe), 24.7 (NCH_aMeMe), 24.3 (NCH_bMeMe), 23.2 (NCH_aMeMe), 18.1 ($MeCN_2$), 12.4 (C_5Me_5). ^{19}F NMR (C_6D_6, 282.1 MHz, 293 K): δ -140.9 (2 F, m, *o*-C_6F_5), -157.6 (1 F, t, ^3J = 23 Hz, *p*-C_6F_5), -163.5 (2 F, m, *m*-C_6F_5). IR (NaCl plates, Nujol mull, cm^{-1}): 2228 (w), 2040 (w), 1644 (w), 1608 (w), 1578 (w), 1547 (s), 1518 (s), 1485 (s), 1406 (m), 1346 (m), 1316 (m), 1306 (m), 1239 (m), 1204 (m), 1180 (w), 1142 (m), 1128 (m), 1072 (w), 1018 (w), 992 (s), 943 (w), 922 (w), 826 (w), 799 (w), 784 (m), 754 (m), 738 (w), 721 (w), 706 (m), 698 (m), 675 (w), 666 (w), 635 (w), 594 (w), 583 (w), 574 (m), 548 (w). EI-MS: *m/z* = 519 [*M* – $MeC(^iPr)_2$ – Ph_2]$^+$ (100%), 499 [*M* – Cp* – $NCPh_2$]$^+$ (5%), 479 [*M* – $MeC(^iPr)_2$ – $NNCPh_2$]$^+$ (5%). Anal. found (calcd. for $C_{45}H_{47}F_5N_6Ti$): C, 66.49 (66.34); H, 5.68 (5.81); N, 10.18 (10.31)%.

Cp*Ti{MeC(N^{i}Pr)$_2$}{N(NCPh$_2$)C(Ar^{F_5})C(H)} (59). To a solution of Cp*Ti{MeC(N^{i}Pr)$_2$}($NNCPh_2$) (**41**, 0.300 g, 0.58 mmol) in benzene (5 mL) was added C_6F_5CCH (0.222 g, 1.16 mmol) in benzene (5 mL) all at RT. A colour change from dark yellow to brown was observed. After 23 h, the brown solution was filtered, and the volatiles were removed under reduced pressure to afford **59** as a brown solid which was washed with cold pentane (3 × 10 mL) cooled to -78 ℃, filtered, and dried *in vacuo*. Yield: 0.261 g (63%). ^1H NMR (C_6D_6, 499.9 MHz, 293 K): δ 9.19 (1 H, s, TiC(H)C), 7.76 (2 H, d, ^3J = 8.0 Hz, o_a-C_6H_5), 7.31 (2 H, d, ^3J = 8.0 Hz, o_b-C_6H_5), 7.22 (2 H, t, ^3J = 8.0 Hz, m_b-C_6H_5), 7.14 (2 H, t, ^3J = 8.0 Hz, m_a-C_6H_5), 7.09 (1 H, t, ^3J = 8.0 Hz, p_b-C_6H_5), 7.05 (1 H, t, ^3J = 8.0 Hz, p_a-C_6H_5), 4.31 (1 H, app. sept., app. ^3J = 6.5 Hz, NCH_aMeMe), 3.31 (1 H, app. sept., app. ^3J = 6.5 Hz, NCH_bMeMe), 2.03 (15 H, s, C_5Me_5), 1.90 (3 H, s, $MeCN_2$), 1.61 (3 H, d, ^3J = 6.5 Hz, NCH_aMeMe), 1.46 (3 H, d, ^3J = 6.5 Hz, NCH_aMeMe), 1.07 (3 H, d, ^3J = 6.5 Hz, NCH_bMeMe), 0.97 (3 H, d, ^3J = 6.5 Hz, NCH_bMeMe). $^{13}C\{^1H\}$ NMR (C_6D_6, 125.7 MHz, 293 K): δ 171.6 ($MeCN_2$), 167.8 (TiC(H)C), 147.3 (*o*-C_6F_5), 140.3 (overlapping TiC(H)C and $NCPh_2$), 138.8 (*p*-C_6F_5), 138.3 (i_a-C_6H_5), 137.7 (*m*-C_6F_5), 135.1 (i_b-C_6H_5), 129.7 (m_b-C_6H_5),

129.2 (o_b-C_6H_5), 129.0 (p_b-C_6H_5), 128.3 (m_a-C_6H_5), 127.9 (p_a-C_6H_5), 127.4 (o_a-C_6H_5), 123.9 ($\underline{C}_5Me_5$), 103.9 (i-C_6F_5), 50.6 (N$\underline{C}H_a$MeMe), 48.7 (N$\underline{C}H_b$MeMe), 26.1 (NCH$_b\underline{Me}$Me), 24.6 (NCH$_a\underline{Me}$Me), 24.5 (NCH$_a$Me$\underline{Me}$), 24.0 (NCH$_b$Me$\underline{Me}$), 16.5 ($\underline{Me}CN_2$), 12.9 ($C_5\underline{Me}_5$). ^{19}F NMR (C_6D_6, 282.1 MHz, 293 K): δ -140.4 (2 F, m, ^3J = 22 Hz, o-C_6F_5), -161.5 (1 F, t, ^3J = 22 Hz, p-C_6F_5), -165.2 (2 F, m, m-C_6F_5). IR (NaCl plates, Nujol mull, cm^{-1}): 1653 (w), 1591 (w), 1512 (s), 1493 (s), 1341 (m), 1315 (m), 1203 (m), 1169 (w), 1128 (w), 1063 (m), 1027 (m), 988 (s), 960 (s), 889 (w), 777 (w), 764 (w), 694 (m), 628 (w), 576 (w), 444 (s), 438 (s), 424 (s), 412 (m). EI-MS: *m/z* = 516 [M – NNCPh$_2$]$^+$ (40%), 381 [M – Cp* – NNCPh$_2$]$^+$ (20%). A satisfactory elemental analysis could not be obtained due to slow decomposition of **59**.

Cp*Ti{MeC(N^{i}Pr)$_2$}{N(PhSiH$_2$)N(CHPh$_2$)} (60). To a solution of Cp*Ti{MeC(N^{i}Pr)$_2$}(NNCPh$_2$) (**41**, 0.100 g, 0.19 mmol) in benzene (3 mL) was added PhSiH$_3$ (23.8 μL, 0.19 mmol) in benzene (2 mL) all at RT. A colour change from dark yellow to grey-green was observed. After 18 h, the grey-green solution was filtered, and the volatiles were removed under reduced pressure to afford **60** as a grey-green oil. Yield: 0.108 g (89%). ^{1}H NMR (C_6D_6, 299.9 MHz, 293 K): δ 7.61 (2 H, d, ^3J = 6.9 Hz, o-C_6H_5Si), 7.33 (4 H, d, ^3J = 7.5 Hz, o-C_6H_5), 7.14 (5 H, m, overlapping m-C_6H_5 and p-C_6H_5Si), 7.10 (2 H, t, ^3J = 6.9 Hz, m-C_6H_5Si), 7.06 (2 H, t, ^3J = 7.5 Hz, p-C_6H_5) 5.28 (2 H, s, SiH$_2$), 5.23 (1 H, s, NC$\underline{H}$Ph$_2$), 3.54 (2 H, app. sept., app. ^3J = 6.3 Hz, NC$\underline{H}$MeMe), 2.10 (15 H, s, C_5Me_5), 1.78 (3 H, s, $MeCN_2$), 1.00 (6 H, d, ^3J = 6.3 Hz, NCH$\underline{Me}$Me), 0.82 (6 H, d, ^3J = 6.3 Hz, NCHMe$\underline{Me}$). ^{13}C{^{1}H} NMR (C_6D_6, 75.4 MHz, 293 K): δ 160.5 (Me$\underline{C}N_2$), 143.1 (i-C_6H_5), 135.5 (o-C_6H_5Si), 134.7 (i-C_6H_5Si), 130.1 (p-C_6H_5Si), 129.7 (o-C_6H_5), 127.9 (m-C_6H_5), 126.8 (overlapping m-C_6H_5Si and p-C_6H_5), 119.2 ($\underline{C}_5Me_5$), 70.3 (N$\underline{C}$HPh$_2$), 49.0 (N$\underline{C}$HMeMe), 26.4 (NCH$\underline{Me}$Me), 25.3 (NCHMe$\underline{Me}$), 12.5 ($C_5\underline{Me}_5$), 11.9 ($\underline{Me}CN_2$). ^{29}Si NMR (HMQC ^{1}H-observed, C_6D_6, 299.9 MHz, 293 K): δ -30.0 (SiH$_2$). IR (NaCl plates, Nujol mull, cm^{-1}): 2157 (m), 2119 (m), 1599 (w), 1484 (s), 1335 (m), 1315 (m), 1213 (s), 1173 (m), 1116 (m), 1068 (w), 1029 (w), 940 (m), 918 (w), 897 (s), 863 (s), 812 (w), 774 (w), 754 (w), 736 (m), 698 (s), 674 (w), 651 (w), 629 (w). EI-MS: *m/z* = 491 [*M* – Cp*]$^+$ (70%), 459 [*M* – CHPh$_2$]$^+$ (20%). Anal. found (calcd. for $C_{37}H_{50}N_4SiTi$): C, 70.70 (70.90); H, 7.85 (8.04); N, 8.80 (8.94)%.

NMR tube scale synthesis of Cp*Ti{MeC(N^{i}Pr)$_2$}{N(PhSiD$_2$)N(CDPh$_2$)} (60-*d*$_3$). To a solution of Cp*Ti{MeC(N^{i}Pr)$_2$}(NNCPh$_2$) (**41**, 20.0 mg, 0.038 mmol) in C_6D_6 (0.6 mL) in an NMR tube equipped with a J. Young Teflon valve was added $PhSiD_3$ (4.8 μL, 0.038 mmol) all at RT. The ^1H and $^{13}C\{^1H\}$ NMR spectra recorded after 16 h were the same as for **60** except that the singlets at 5.28 and 5.23 ppm were absent in the ^1H spectrum, while the $^{13}C\{^1H\}$ spectrum showed a triplet ($^1J_{CD}$ = 82 Hz) at 70.0 ppm corresponding to $\underline{C}DPh_2$ of Cp*Ti{MeC(N^{i}Pr)$_2$}{N(PhSiD$_2$)N(CDPh$_2$)} (**60-*d*$_3$**).

Cp*Ti{MeC(N^{i}Pr)$_2$}{N(Ar^{F}SiH$_2$)N(CHPh$_2$)} (61). To a solution of Cp*Ti{MeC(N^{i}Pr)$_2$}(NNCPh$_2$) (**41**, 0.100 g, 0.19 mmol) in benzene (3 mL) was added Ar^{F}SiH$_3$ (Ar^F = 3,5-$C_6H_3(CF_3)_2$) (47.1 mg, 0.19 mmol) in benzene (2 mL) all at RT. A colour change from dark yellow to grey-green was observed. After 16 h, the grey-green solution was filtered, and the volatiles were removed under reduced pressure to afford **61** as a grey-green oil. Yield: 0.126 g (86%).

Major isomer: ^1H NMR (C_6D_6, 299.9 MHz, 293 K): δ 7.76 (3 H, m, overlapping *o*- and *p*-$C_6H_3(CF_3)_2$), 7.16 (6 H, m, overlapping *o*- and *p*-C_6H_5), 7.02 (4 H, t, ^3J = 7.2 Hz, *m*-C_6H_5), 5.48 (1 H, s, NC$\underline{H}$Ph$_2$), 5.06 (2 H, s, SiH$_2$), 3.44 (2 H, app. sept., app. ^3J = 6.6 Hz, NC$\underline{H}$MeMe), 2.05 (15 H, s, C_5Me_5), 1.70 (3 H, s, MeCN$_2$), 0.95 (6 H, d, ^3J = 6.6 Hz, NCH$\underline{Me}$Me), 0.76 (6 H, d, ^3J = 6.6 Hz, NCHMe$\underline{Me}$). $^{13}C\{^1H\}$ NMR (C_6D_6, 75.4 MHz, 293 K): δ 160.7 (Me$\underline{C}$N$_2$), 142.2 (*i*-C_6H_5), 139.4 (*m*-$\underline{C}_6H_3(CF_3)_2$), 134.9 (*o*-$\underline{C}_6H_3(CF_3)_2$), 130.8 ($C_6H_3(\underline{C}F_3)_2$), 129.6 (*o*-$C_6H_5$), 128.2 (*m*-$C_6H_5$), 127.4 (*p*-$C_6H_5$), 126.3 (*i*-$\underline{C}_6H_3(CF_3)_2$), 123.2 (*p*-$\underline{C}_6H_3(CF_3)_2$), 119.5 ($\underline{C}_5Me_5$), 72.6 (N$\underline{C}HPh_2$), 49.0 (N$\underline{C}$HMeMe), 26.3 (NCH$\underline{Me}$Me), 25.2 (NCHMe$\underline{Me}$), 12.4 ($C_5\underline{Me}_5$), 11.7 ($\underline{Me}CN_2$). ^{29}Si NMR (HMQC ^1H-observed, C_6D_6, 299.9 MHz, 293 K): δ -33.0 (SiH$_2$). ^{19}F NMR (C_6D_6, 282.1 MHz, 293 K): δ -62.6 (6F, s, $C_6H_3(CF_3)_2$).

Minor isomer: ^1H NMR (C_6D_6, 499.9 MHz, 293 K): δ 6.95 (4 H, t, ^3J = 7.2 Hz, *m*-C_6H_5), 5.99 (1 H, s, NC$\underline{H}$Ph$_2$), 5.06 (2 H, s, SiH$_2$), 3.06 (2 H, app. sept., app. ^3J = 6.6 Hz, NC$\underline{H}$MeMe), 1.93 (15 H, s, C_5Me_5), 1.61 (3 H, s, MeCN$_2$), 1.03 (6 H, d, ^3J = 6.6 Hz, NCH$\underline{Me}$Me), 0.91 (6 H, d, ^3J = 6.6 Hz, NCHMe$\underline{Me}$). $^{13}C\{^1H\}$ NMR (C_6D_6, 125.7 MHz, 293 K): δ 168.8 (Me$\underline{C}$N$_2$), 145.1 (*i*-C_6H_5), 141.4 (*m*-$\underline{C}_6H_3(CF_3)_2$), 134.6 (*o*-$\underline{C}_6H_3(CF_3)_2$), 130.5 ($C_6H_3(\underline{C}F_3)_2$), 129.4 (*o*-$C_6H_5$), 128.1 (*m*-$C_6H_5$), 127.2 (*p*-$C_6H_5$), 125.4 (*i*-$\underline{C}_6H_3(CF_3)_2$), 122.7 (*p*-$\underline{C}_6H_3(CF_3)_2$), 120.0 ($\underline{C}_5Me_5$), 78.7 (N$\underline{C}HPh_2$), 48.1 (N$\underline{C}$HMeMe), 25.7 (NCH$\underline{Me}$Me), 25.6 (NCHMe$\underline{Me}$), 13.7 ($\underline{Me}CN_2$), 12.8 ($C_5\underline{Me}_5$). ^{29}Si NMR (HMQC ^1H-observed, C_6D_6, 299.9 MHz, 293 K): δ -33.0 (SiH$_2$) ^{19}F NMR

(C_6D_6, 282.1 MHz, 293 K): δ -62.5 (6F, s, $C_6H_3(CF_3)_2$). Other NN$\underline{Ph}_2$ signals are obscured by major isomer.

Common data: IR (NaCl plates, Nujol mull, cm^{-1}): 2165 (w), 2117 (w), 1613 (w), 1598 (w), 1493 (m), 1360 (m), 1338 (w), 1316 (w), 1278 (s), 1212 (w), 1172 (m), 1183 (m), 1137 (s), 1017 (w), 916 (w), 899 (w), 872 (w), 842 (w), 811 (w), 700 (w), 682 (w). EI-MS: *m/z* = 595 $[M - CHPh_2]^+$ (30%), 460 $[M - Cp^* - CHPh_2]^+$ (20%). Anal. found (calcd. for $C_{39}H_{48}N_4F_6SiTi$): C, 61.65 (61.41); H, 6.35 (6.34); N, 7.27 (7.35)%.

Cp*Ti{MeC(N^{i}Pr)$_2$}{N(Ar^{OMe}SiH$_2$)N(CHPh$_2$)} (62). To a solution of Cp*Ti{MeC(N^{i}Pr)$_2$}(NNCPh$_2$) (**41**, 0.100 g, 0.19 mmol) in benzene (3 mL) was added $Ar^{OMe}SiH_3$ (Ar^{OMe} = 4-C_6H_4OMe) (26.7 mg, 0.19 mmol) in benzene (2 mL) all at RT. A colour change from dark yellow to grey-green was observed. After 16 h, the grey-green solution was filtered, and the volatiles were removed under reduced pressure to afford **62** as a grey-green oil. Yield: 0.121 g (96%). ^{1}H NMR (C_6D_6, 299.9 MHz, 293 K): δ 7.56 (2 H, d, ^3J = 8.7 Hz, *o*-C_6H_4OMe), 7.36 (4 H, d, ^3J = 7.2 Hz, *o*-C_6H_5), 7.15 (4 H, t, ^3J = 7.2 Hz, *m*-C_6H_5), 7.07 (2 H, t, ^3J = 7.2 Hz, *p*-C_6H_5), 6.76 (2 H, d, ^3J = 8.7 Hz, *m*-C_6H_4OMe), 5.34 (2 H, s, SiH_2), 5.16 (1 H, s, NC$\underline{H}Ph_2$), 3.57 (2 H, app. sept., app. ^3J = 6.6 Hz, NC$\underline{H}$MeMe), 3.25 (3 H, s, $C_6H_4O\underline{Me}$), 2.12 (15 H, s, C_5Me_5), 1.81 (3 H, s, $MeCN_2$), 1.02 (6 H, d, ^3J = 6.6 Hz, NCH$\underline{Me}$Me), 0.84 (6 H, d, ^3J = 6.6 Hz, NCHMe$\underline{Me}$). ^{13}C{^{1}H} NMR (C_6D_6, 75.4 MHz, 293 K): δ 161.8 (*p*-C_6H_4OMe), 160.4 ($Me\underline{C}N_2$), 143.3 (*i*-C_6H_5), 137.2 (*o*-C_6H_4OMe), 129.8 (*o*-C_6H_5), 127.9 (*m*-C_6H_5), 126.7 (*p*-C_6H_5), 125.3 (*i*-C_6H_4OMe), 119.1 ($\underline{C}_5Me_5$), 114.0 (*m*-C_6H_4OMe), 69.7 (N$\underline{C}HPh_2$), 54.5 ($C_6H_4O\underline{Me}$), 49.0 (N$\underline{C}$HMeMe), 26.4 (NCH$\underline{Me}$Me), 25.4 (NCHMe$\underline{Me}$), 12.5 ($C_5\underline{Me}_5$), 11.9 ($\underline{Me}CN_2$). ^{29}Si NMR (HMQC ^{1}H-observed, C_6D_6, 299.9 MHz, 293 K): δ -29.3 (SiH_2). IR (NaCl plates, Nujol mull, cm^{-1}): 2158 (m), 2109 (m), 1595 (s), 1566 (w), 1501 (s), 1337 (m), 1310 (w), 1281 (m), 1248 (s), 1213 (m), 1180 (m), 1116 (s), 1067 (w), 1014 (w), 1032 (w), 993 (w), 940 (w), 897 (s), 862 (m), 824 (m), 810 (m), 753 (w), 732 (w), 698 (s), 651 (w), 624 (w). EI-MS: *m/z* = 504 $[M - Cp^* - Me - 2\ H]^+$ (100%), 489 $[M - CHPh_2]^+$ (20%). Anal. found (calcd. for $C_{38}H_{52}N_4OSiTi$): C, 69.51 (69.49); H, 7.83 (7.98); N, 8.40 (8.53)%.

Cp*Ti{MeC(N^{i}Pr)$_2$}{N(BuSiH$_2$)N(CHPh$_2$)} (63). To a solution of Cp*Ti{MeC(N^{i}Pr)$_2$}(NNCPh$_2$) (**41**, 0.200 g, 0.39 mmol) in benzene (3 mL) was added BuSiH$_3$ (50.0 μL, 0.39 mmol) in benzene (2 mL) all at RT. A colour change from dark yellow to dark green was observed. After 18 h, the dark green solution was filtered, and the volatiles were removed under reduced pressure to afford **63** as a dark green oil. Yield: 0.215 g (92%). ^{1}H NMR (C$_6$D$_6$, 499.9 MHz, 293 K): δ 7.33 (4 H, d, ^3J = 7.5 Hz, *o*-C$_6$H$_5$), 7.14 (4 H, t, ^3J = 7.5 Hz, *m*-C$_6$H$_5$), 7.07 (2 H, t, ^3J = 7.5 Hz, *p*-C$_6$H$_5$), 5.36 (1 H, s, C<u>H</u>Ph$_2$), 4.71 (2 H, t, ^3J = 3.5 Hz, SiH$_2$), 3.57 (2 H, app. sept., app. ^3J = 6.5 Hz, NC<u>H</u>MeMe), 2.11 (15 H, s, C$_5$Me$_5$), 1.78 (3 H, s, MeCN$_2$), 1.26 (4 H, m, overlapping SiCH$_2$C<u>H$_2$</u>CH$_2$CH$_3$ and SiCH$_2$CH$_2$C<u>H$_2$</u>CH$_3$), 1.02 (6 H, d, ^3J = 6.5 Hz, NCH<u>Me</u>Me), 0.88 (6 H, d, ^3J = 6.5 Hz, NCHMe<u>Me</u>), 0.82 (3 H, t, ^3J = 7.0 Hz, SiCH$_2$C<u>H$_2$</u>CH$_2$C<u>H$_3$</u>), 0.64 (2 H, m, SiC<u>H$_2$</u>CH$_2$CH$_2$CH$_3$). ^{13}C{^{1}H} NMR (C$_6$D$_6$, 125.7 MHz, 293 K): δ 160.5 (Me<u>C</u>N$_2$), 143.2 (*i*-C$_6$H$_5$), 129.7 (*o*-C$_6$H$_5$), 128.3 (*m*-C$_6$H$_5$), 126.9 (*p*-C$_6$H$_5$), 119.0 (<u>C$_5$</u>Me$_5$), 71.5 (<u>C</u>HPh$_2$), 49.0 (N<u>C</u>HMeMe), 26.4 (NCH<u>Me</u>Me), 26.1 (overlapping SiCH$_2$<u>C</u>H$_2$CH$_2$CH$_3$ and SiCH$_2$CH$_2$<u>C</u>H$_2$CH$_3$), 25.4 (NCHMe<u>Me</u>), 14.0 (SiCH$_2$CH$_2$CH$_2$<u>C</u>H$_3$), 13.2 (Si<u>C</u>H$_2$CH$_2$CH$_2$CH$_3$), 12.5 (C$_5$<u>Me$_5$</u>), 11.8 (<u>Me</u>CN$_2$). ^{29}Si NMR (C$_6$D$_6$, 299.9 MHz, 293 K): δ -24.4 (SiH$_2$). IR (NaCl plates, Nujol mull, cm^{-1}): 2152 (m), 2119 (m), 1599 (w), 1492 (s), 1336 (s), 1315 (m), 1213 (s), 1173 (m), 1121 (w), 1071 (m), 1029 (m), 943 (w), 901 (s), 856 (w), 812 (w), 764 (w), 733 (w), 698 (s), 623 (w), 605 (w). EI-MS: *m/z* = 465 [*M* – {MeC(N^{i}Pr)$_2$}]$^+$ (20%), 451 [*M* – 2 Ph – H}]$^+$ (15%). Anal. found (calcd. for C$_{35}$H$_{54}$N$_4$SiTi): C, 69.07 (69.28); H, 8.83 (8.97); N, 9.05 (9.23)%.

Cp*Ti{MeC(N^{i}Pr)$_2$}{N(Ph$_2$SiH)N(CHPh$_2$)} (64). To a solution of Cp*Ti{MeC(N^{i}Pr)$_2$}(NNCPh$_2$) (**41**, 0.200 g, 0.39 mmol) in benzene (3 mL) was added Ph$_2$SiH$_2$ (71.6 μL, 0.39 mmol) in benzene (2 mL) all at RT. A colour change from dark yellow to dark green was observed. After 6 d, the dark green solution was filtered, and the volatiles were removed under reduced pressure to afford **64** as dark green oil. Yield: 0.249 g (92%). ^{1}H NMR data (C$_6$D$_6$, 299.9 MHz, 293 K): δ 7.59 (4 H, d, ^3J = 7.5 Hz, *o*-(C$_6$H$_5$)$_2$Si), 7.42 (4 H, d, ^3J = 7.5 Hz, *o*-(C$_6$H$_5$)$_2$C), 7.14 (12 H, m, overlapping *m*- and *p*-(C$_6$H$_5$)$_2$Si, *m*- and *p*-(C$_6$H$_5$)$_2$C), 5.81 (1 H, s, SiH), 5.30 (1 H, s, C<u>H</u>Ph$_2$), 3.51 (2 H, app. sept., app. ^3J = 6.6 Hz, NC<u>H</u>MeMe), 2.09 (15 H, s, C$_5$Me$_5$), 1.82 (3 H, s, MeCN$_2$), 0.93 (6 H, d, ^3J = 6.6 Hz, NCH<u>Me</u>Me), 0.63 (6 H, d, ^3J = 6.6 Hz, NCHMe<u>Me</u>). ^{13}C{^{1}H} NMR (C$_6$D$_6$, 75.4 MHz, 293 K): δ 160.4 (Me<u>C</u>N$_2$), 143.9

(*i*-(C_6H_5)$_2$C), 136.0 (overlapping *i*- and *o*-(C_6H_5)$_2$Si), 129.8 (*o*-(C_6H_5)$_2$C), 129.7 (*p*-(C_6H_5)$_2$Si), 127.9 (overlapping *m*-(C_6H_5)$_2$C and *m*-(C_6H_5)$_2$Si) 126.7 *p*-(C_6H_5)$_2$C), 119.2 ($\underline{C}_5Me_5$), 69.6 ($\underline{C}HPh_2$), 48.8 (N$\underline{C}$HMeMe), 26.2 (NCH$\underline{Me}$Me), 25.3 (NCHMe$\underline{Me}$), 12.6 ($C_5\underline{Me}_5$), 12.3 ($\underline{Me}CN_2$). ^{29}Si NMR (HMQC ^{1}H-observed, toluene-d_8, 299.9 MHz, 253 K): δ -19.1 (SiH). IR (NaCl plates, Nujol mull, cm^{-1}): 2148 (m), 1600 (m), 1487 (s), 1428 (s), 1333 (m), 1312 (m), 1213 (m), 1173 (w), 1111 (s), 1066 (w), 1029 (w), 962 (w), 939 (w), 897 (w), 843 (m), 815 (s), 792 (s), 753 (w), 732 (s), 698 (s), 648 (w), 624 (w), 608 (w). EI-MS: *m/z* = 490 [*M* – Cp* – Ph]$^+$ (50%), 259 [*M* – Cp* – 4 Ph]$^+$ (10%). Anal. found (calcd. for $C_{43}H_{54}N_4SiTi$): C, 73.37 (73.48); H, 7.63 (7.74); N, 7.86 (7.97)%.

NMR tube scale synthesis of Cp*Ti{MeC(N^{i}Pr)$_2$}(Cl){N(NCPh$_2$)SiH$_2$Ph} (65). To a solution of Cp*Ti{MeC(N^{i}Pr)$_2$}(NNCPh$_2$) (**41**, 20.0 mg, 0.039 mmol) in toluene-d_8 (0.6 mL) in an NMR tube equipped with a J. Young Teflon valve was added PhSiH$_2$Cl (5.2 μL, 0.039 mmol) at RT. An immediate colour change from dark yellow to red was observed. ^{1}H NMR spectrum showed that the reaction went to completion almost immediately (5 min) forming Cp*Ti{MeC(N^{i}Pr)$_2$}(Cl){N(NCPh$_2$)SiH$_2$Ph} (**65**) quantitatively, which was characterised by NMR spectroscopy. ^{1}H NMR data (toluene-d_8, 299.9 MHz, 253 K): δ 7.66 (2 H, d, ^3J = 7.5 Hz, o_a-C_6H_5), 7.43 (2 H, d, ^3J = 7.5 Hz, o_b-C_6H_5), 7.05 (7 H, m, overlapping *o*- and *m*-C_6H_5Si, m_a- and p_a-C_6H_5), 6.94 (3 H, m, overlapping m_b- and p_b-C_6H_5), 6.77 (1 H, t, ^3J = 7.5 Hz, *p*-C_6H_5Si), 5.52 (1 H, d, ^2J = 11.1 Hz, Si$\underline{H}_a$H), 5.17 (1 H, d, ^2J = 11.1 Hz, SiH$\underline{H}_b$), 3.91 (1 H, app. sept., app. ^3J = 6.6 Hz, NC$\underline{H}_a$MeMe), 3.17 (1 H, app. sept., app. ^3J = 6.6 Hz, NC$\underline{H}_b$MeMe), 2.20 (15 H, s, C_5Me_5), 1.46 (3 H, d, ^3J = 6.6 Hz, NCH$_a$$\underline{Me}$Me), 1.16 (6 H, overlapping 2 × d, 2 × ^3J = 6.6 Hz, overlapping NCH$_a$Me$\underline{Me}$ and NCH$_b$$\underline{Me}$Me), 1.11 (3 H, s, $MeCN_2$), 1.05 (3 H, d, ^3J = 6.6 Hz, NCH$_b$Me$\underline{Me}$). ^{13}C{^{1}H} NMR (toluene-d_8, 75.4 MHz, 253 K): δ 168.7 (Me$\underline{C}N_2$), 145.8 (N$\underline{C}$Ph$_2$), 140.5 (i_a-C_6H_5) 137.5 (i_b-C_6H_5), 134.5 (o_b-C_6H_5), 132.9 (*i*-C_6H_5Si), 130.4 (o_a-C_6H_5), 129.3 (p_b-C_6H_5), 128.3 (overlapping p_a-C_6H_5 and *p*-C_6H_5Si), 128.2 (overlapping *o*- and *m*-C_6H_5Si), 127.9 (m_a-C_6H_5), 127.5 (m_b-C_6H_5), 126.8 ($\underline{C}_5Me_5$), 50.0 (N$\underline{C}$H$_a$MeMe), 47.9 (N$\underline{C}$H$_b$MeMe), 26.7 (NCH$_b$Me$\underline{Me}$), 25.6 (NCH$_a$Me$\underline{Me}$), 24.3 (NCH$_a$$\underline{Me}$Me), 24.2 (NCH$_b$$\underline{Me}$Me), 15.4 ($\underline{Me}CN_2$), 13.7 ($C_5\underline{Me}_5$). ^{29}Si NMR (HMQC ^{1}H-observed, toluene-d_8, 299.9 MHz, 253 K): δ -32.1 (SiH_2).

NMR tube scale synthesis of Cp*Ti{MeC(N^{i}Pr)$_2$}(Br){N(NCPh$_2$)SiH$_2$Ph} (66). To a solution of Cp*Ti{MeC(N^{i}Pr)$_2$}(NNCPh$_2$) (**41**, 20.0 mg, 0.039 mmol) in toluene-d_8 (0.6 mL) in an NMR tube equipped with a J. Young Teflon valve was added PhSiH$_2$Br (7.3 mg, 0.039 mmol) at RT. An immediate colour change from dark yellow to red was observed. ^{1}H NMR spectrum showed that the reaction went to completion almost immediately (5 min) forming Cp*Ti{MeC(N^{i}Pr)$_2$}(Br)-{N(NCPh$_2$)SiH$_2$Ph} (**66**) quantitatively, which was characterised by NMR spectroscopy. ^{1}H NMR data (toluene-d_8, 299.9 MHz, 253 K): δ 7.55 (2 H, d, ^3J = 7.5 Hz, o_a-C$_6$H$_5$), 7.44 (2 H, d, ^3J = 7.5 Hz, o_b-C$_6$H$_5$), 7.14 (2 H, m, *o*-C$_6$H$_5$Si) 7.06 (5 H, m, overlapping *m*-C$_6$H$_5$Si, m_a- and p_a-C$_6$H$_5$), 6.97 (3 H, m, overlapping m_b- and p_b-C$_6$H$_5$), 6.69 (1 H, t, ^3J = 7.5 Hz, *p*-C$_6$H$_5$Si), 5.50 (1 H, d, ^2J = 10.5 Hz, Si<u>H$_a$</u>H), 5.14 (1 H, d, ^2J = 10.5 Hz, SiH<u>H$_b$</u>), 4.24 (1 H, app. sept., app. ^3J = 6.9 Hz, NC<u>H$_a$</u>MeMe), 3.21 (1 H, app. sept., app. ^3J = 6.9 Hz, NC<u>H$_b$</u>MeMe), 2.20 (15 H, s, C$_5$Me$_5$), 1.33 (3 H, s, MeCN$_2$), 1.30 (3 H, d, ^3J = 6.9 Hz, NCH$_a$<u>Me</u>Me), 1.15 (3 H, d, ^3J = 6.9 Hz, NCH$_a$Me<u>Me</u>), 1.11 (3 H, d, ^3J = 6.9 Hz, NCH$_b$<u>Me</u>Me), 1.09 (3 H, d, ^3J = 6.9 Hz, NCH$_b$Me<u>Me</u>). ^{13}C{^{1}H} NMR (toluene-d_8, 75.4 MHz, 253 K): δ 168.3 (Me<u>C</u>N$_2$), 147.8 (N<u>C</u>Ph$_2$), 140.4 (i_a-C$_6$H$_5$) 137.6 (i_b-C$_6$H$_5$), 134.6 (o_b-C$_6$H$_5$), 133.1 (*i*-C$_6$H$_5$Si), 130.2 (o_a-C$_6$H$_5$), 129.3 (p_b-C$_6$H$_5$), 128.5 (overlapping *o*-, *m*-, and *p*-C$_6$H$_5$Si), 128.3 (p_a-C$_6$H$_5$), 128.1 (m_a-C$_6$H$_5$), 127.3 (m_b-C$_6$H$_5$), 126.7 (<u>C$_5$</u>Me$_5$), 50.7 (N<u>C</u>H$_a$MeMe), 48.3 (N<u>C</u>H$_b$MeMe), 26.4 (NCH$_b$Me<u>Me</u>), 24.4 (NCH$_a$Me<u>Me</u>), 24.1 (NCH$_a$<u>Me</u>Me), 23.6 (NCH$_b$<u>Me</u>Me), 17.0 (<u>Me</u>CN$_2$), 13.8 (C$_5$<u>Me</u>$_5$). ^{29}Si NMR (HMQC ^{1}H-observed, toluene-d_8, 299.9 MHz, 253 K): δ -31.2 (SiH$_2$).

5.6 X-ray data collection and processing parameters for Chapter Two

Crystal structure determinations for Cp*Ti{MeC(N^{i}Pr)$_2$}{OC(O)N(NPh$_2$)-C(O)O} (3), Cp*Ti{MeC(N^{i}Pr)$_2$}{OC(O)N(NMe$_2$)C(O)O} (4), Cp*Ti{MeC-(N^{i}Pr)$_2$}{N(NPh$_2$)C(NAr')O} (9), Cp*Ti{MeC(N^{i}Pr)$_2$}{N(NPh$_2$)C(NAr')S} (11), N(Me)$_2$NC(NAr')N(Ar')C(O) (15), Cp*Ti{MeC(N^{i}Pr)$_2$}{OC(NNMe$_2$)N(Tol)C-(NTol)O} (16) and [Cp*Ti{MeC(N^{i}Pr)$_2$}(μ-S)]$_2$ (2.16). Crystal data collection and processing parameters are given in Table 5.1. Crystals were mounted on glass fibers using perfluoropolyether oil and cooled rapidly in a stream of cold N_2 using an Oxford Cryosystems Cryostream unit. Diffraction data were measured using an Enraf-Nonius KappaCCD diffractometer. As appropriate, absorption and decay corrections were applied to the data and equivalent reflections merged.[13] The structures were solved by direct methods (SIR92[14]) and further refinements and all other crystallographic calculations were performed using the CRYSTALS program suite.[15] Other details of the structure solution and refinements are given in the Supporting Information (CIF data – see CD Appendix). A full listing of atomic coordinates, bond lengths and angles and displacement parameters for all the structures have been deposited at the Cambridge Crystallographic Data Centre. See Notice to Authors, Issue No. 1.

Table 5.1. X-Ray data collection and processing parameters for Cp*Ti{MeC(N^{i}Pr)$_2$}{OC(O)N(NPh$_2$)C(O)O} (**3**), Cp*Ti{MeC(N-^{i}Pr)$_2$}{OC(O)N(NMe$_2$)C(O)O} (**4**), Cp*Ti{MeC(N^{i}Pr)$_2$}{N(NPh$_2$)C(NAr′)O} (**9**), Cp*Ti{MeC(N^{i}Pr)$_2$}{N(NPh$_2$)C(NAr′)S} (**11**), N(Me)$_2$NC(NAr′)N(Ar′)C(O) (**15**), Cp*Ti{MeC(N^{i}Pr)$_2$}{OC(NNMe$_2$)N(Tol)C(NTol)O} (**16**) and [Cp*Ti{MeC(N^{i}Pr)$_2$}(μ-S)]$_2$ (**2.16**).

compound	**3**	**4**	**9**	**11**
empirical formula	$C_{32}H_{42}N_4O_4Ti$	$C_{22}H_{38}N_4O_4Ti$	$C_{43}H_{59}N_5OTi$	$C_{43}H_{59}N_5STi$
fw	594.61	470.47	709.87	725.94
temp / K	150	150	150	150
wavelength / Å	0.71073	0.71073	0.71073	0.71073
space group	$P2_1/c$	$Pbca$	$P2_12_12_1$	$P2_12_12_1$
a / Å	14.2642(3)	12.1789(2)	11.6533(2)	12.1396(1)
b / Å	13.3667(2)	14.3304(2)	16.8171(3)	15.7202(2)
c / Å	17.0300(4)	27.4288(5)	20.5550(4)	21.3280(2)
α / deg	90	90	90	90
β / deg	109.109(1)	90	90	90
γ / deg	90	90	90	90
V / Å^3	3068.11(11)	4787.11(13)	4028.26(13)	4070.17(7)
Z	4	8	4	4
d (calcd) / Mg m^{-3}	1.287	1.305	1.170	1.185
abs coeff / mm^{-1}	0.321	0.392	0.250	0.297
R indices:[a] R_1 =	0.0511	0.0499	0.0397	0.0461
R_w =	0.0531	0.0531	0.0408	0.0494

[a] $R_1 = \Sigma||F_o|-|F_c|| / \Sigma|F_o|$; $R_w = \sqrt{\{\Sigma w(|F_o|-|F_c|)^2 / \Sigma w|F_o|^2\}}$ for data with I > 3σ(I).

Table 5.1. (Contd.)

compound	**15**	**16**	**2.16**
empirical formula	$C_{28}H_{40}N_4O$	$C_{36}H_{52}N_6O_2Ti$	$C_{36}H_{64}N_4S_2Ti_2$
fw	448.65	648.75	712.86
temp / K	150	150	150
wavelength / Å	0.71073	0.71073	0.71073
space group	$P2_1/n$	$P2_1/n$	$P2_1/m$
a / Å	12.0805(2)	12.3786(4)	12.5737(2)
b / Å	12.7622(3)	20.2596(7)	17.1653(3)
c / Å	17.7166(4)	14.3585(6)	17.5072(3)
α / deg	90	90	90
β / deg	92.8483(9)	102.663(2)	92.5968(12)
γ / deg	90	90	90
V / Å^3	2728.06(10)	3513.3(2)	3774.72(11)
Z	4	4	4
d (calcd) / Mg m^{-3}	1.092	1.226	1.254
abs coeff / mm^{-1}	0.067	0.283	0.563
R indices:[a] R_1 =	0.0468	0.0490	0.0469
R_w =	0.0484	0.0486	0.0450

[a] $R_1 = \Sigma||F_o|-|F_c|| / \Sigma|F_o|$; $R_w = \sqrt{\{\Sigma w(|F_o|-|F_c|)^2 / \Sigma w|F_o|^2\}}$ for data with $I > 3\sigma(I)$.

5.7 X-ray data collection and processing parameters for Chapter Three

Crystal structure determinations for Cp*Ti{MeC(N^{i}Pr)$_2$}(H){N(NMe$_2$)SiH$_2$R} (R = Ph (20), Ar^F (21) or Ar^{OMe} (22)), Cp*Ti{MeC(N^{i}Pr)$_2$}(Cl){N(NMe$_2$)SiH$_2$Ph} (24), Cp*Ti{N(NMe$_2$)SiH(Ph)N(^{i}Pr)CMeN^{i}Pr}Cl$_2$ (27), Cp*Ti{N(NMe$_2$)SiMe$_2$N-(^{i}Pr)CMeN^{i}Pr}Cl$_2$ (28), Cp*Ti{N(NPh$_2$)SiH(Me)Ph}Cl$_2$ (32), [Cp*Ti{MeC-(N^{i}Pr)$_2$}(NNMe$_2$Et)]Br (36-Br) and [Cp*Ti{MeC(N^{i}Pr)$_2$}{N(NMe$_2$)H}][BPh$_4$] (38-BPh$_4$). Crystal data collection and processing parameters are given in Table 5.2. Crystals were mounted on glass fibers using perfluoropolyether oil and cooled rapidly in a stream of cold N_2 using an Oxford Cryosystems Cryostream unit. Diffraction data were measured using an Enraf-Nonius KappaCCD diffractometer. As appropriate, absorption and decay corrections were applied to the data and equivalent reflections merged.[13] The structures were solved by direct methods (SIR92[14]) and further refinements and all other crystallographic calculations were performed using the CRYSTALS program suite.[15] Other details of the structure solution and refinements are given in the Supporting Information (CIF data – see CD Appendix). A full listing of atomic coordinates, bond lengths and angles and displacement parameters for all the structures have been deposited at the Cambridge Crystallographic Data Centre. See Notice to Authors, Issue No. 1.

Table 5.2. X-ray data collection and processing parameters for Cp*Ti{MeC(N^{i}Pr)$_2$}(H){N(NMe$_2$)SiH$_2$R} (R = Ph (**20**), Ar^F (**21**) or Ar^{OMe} (**22**)), Cp*Ti{MeC(N^{i}Pr)$_2$}(Cl){N(NMe$_2$)SiH$_2$Ph} (**24**), Cp*Ti{N(NMe$_2$)SiH(Ph)N(^{i}Pr)CMeN^{i}Pr}Cl$_2$ (**27**), Cp*Ti{N(NMe$_2$)SiMe$_2$N(^{i}Pr)CMeN^{i}Pr}Cl$_2$ (**28**), Cp*Ti{N(NPh$_2$)SiH(Me)Ph}Cl$_2$ (**32**), [Cp*Ti{MeC(N^{i}Pr)$_2$}(NNMe$_2$Et)]Br (**36-Br**) and [Cp*Ti{MeC(N^{i}Pr)$_2$}{N(NMe$_2$)H}][BPh$_4$] (**38-BPh$_4$**).

compound	**20·0.25(C_5H_{12})**	**21**	**22**	**24**
empirical formula	$C_{26}H_{46}N_4SiTi$ 0.25(C_5H_{12})	$C_{28}H_{44}F_6N_4SiTi$	$C_{27}H_{48}N_4OSiTi$	$C_{26}H_{45}ClN_4SiTi$
fw	508.70	626.66	520.69	525.11
temp / K	150	150	150	150
wavelength / Å	0.71073	0.71073	0.71073	0.71073
space group	*P* 2$_1$/*c*	*P*2$_1$/*n*	*P* $\bar{1}$	*P* $\bar{1}$
a / Å	8.5949(2)	8.65520(10)	8.57190(10)	9.8784(2)
b / Å	11.3073(3)	24.6871(3)	9.90560(10)	10.3809(3)
c / Å	31.4337(9)	15.1275(2)	18.2095(2)	15.6151(4)
α / deg	90	90	80.3853(4)	94.6300(11)
β / deg	92.4007(12)	100.2706(5)	87.2553(4)	99.7244(13)
γ / deg	90	90	71.1128(5)	114.5284(13)
V / Å^3	3052.21(14)	3180.53(7)	1442.34(3)	1415.38(6)
Z	4	4	2	2
d (calcd) / Mg m^{-3}	1.107	1.309	1.199	1.232
abs coeff / mm^{-1}	0.340	0.366	0.363	0.460
R indices:[a] R_1 =	0.0637	0.0528	0.0353	0.0481
R_w =	0.0686	0.0618	0.0378	0.0548

[a] $R_1 = \Sigma||F_o|-|F_c|| / \Sigma|F_o|$; $R_w = \sqrt{\{\Sigma w(|F_o|-|F_c|)^2 / \Sigma w|F_o|^2\}}$ for data with I > 3σ(I).

Table 5.2. (Contd.)

compound	**27**	**28**	**32**	**36-Br·0.5(THF)**
empirical formula	$C_{26}H_{44}Cl_2N_4SiTi$	$C_{22}H_{44}Cl_2N_4SiTi$	$C_{29}H_{34}Cl_2N_2SiTi$	$C_{22}H_{43}BrN_4Ti\cdot 0.5(C_4H_8O)$
fw	559.55	511.51	557.49	527.47
temp / K	150	150	150	150
wavelength / Å	0.71073	0.71073	0.71073	0.71073
space group	$P\,2_1/c$	$P\,2_1/c$	$P\,\bar{1}$	$P\,\bar{1}$
a / Å	11.5517(2)	11.5599(3)	8.4930(2)	10.2911(5)
b / Å	14.3261(2)	16.9818(4)	11.6230(3)	16.2599(6)
c / Å	18.0286(3)	13.9465(3)	14.6209(3)	18.4540(9)
α / deg	90	90	95.5060(10)	69.245(2)
β / deg	97.201(1)	91.892(1)	96.0935(9)	78.120(2)
γ / deg	90	90	98.8666(12)	86.849(2)
V / Å^3	2960.0(1)	2736.32(11)	1408.69(6)	2825.2(2)
Z	4	4	2	4
d (calcd) / Mg m^{-3}	1.256	1.242	1.314	1.240
abs coeff / mm^{-1}	0.531	0.568	0.557	1.736
R indices:[a] R_1 =	0.0557	0.0482	0.0525	0.0780
R_w =	0.0598	0.0511	0.0562	0.0737

[a] $R_1 = \Sigma||F_o|-|F_c|| / \Sigma|F_o|$; $R_w = \sqrt{\{\Sigma w(|F_o|-|F_c|)^2 / \Sigma w|F_o|^2\}}$ for data with $I > 3\sigma(I)$.

Table 5.2. (Contd.)

compound	**38-BPh_4**
empirical formula	$C_{44}H_{59}BN_4Ti$
fw	702.69
temp / K	150
wavelength / Å	0.71073
space group	*P n a* 2_1
a / Å	28.0165(4)
b / Å	15.8661(2)
c / Å	8.97260(10)
α / deg	90
β / deg	90
γ / deg	90
V / $Å^3$	3988.43(9)
Z	4
d (calcd) / Mg m^{-3}	1.170
abs coeff / mm^{-1}	0.250
R indices:[a] R_1 =	0.0519
R_w =	0.0576

[a] $R_1 = \Sigma||F_o|-|F_c|| / \Sigma|F_o|$; $R_w = \sqrt{\{\Sigma w(|F_o|-|F_c|)^2 / \Sigma w|F_o|^2\}}$ for data with $I > 3\sigma(I)$.

5.8 X-ray data collection and processing parameters for Chapter Four

Crystal structure determinations for Cp*Ti{MeC(N^{i}Pr)$_2$}(NNCPh$_2$) (41), [Cp*Ti{MeC(N^{i}Pr)$_2$}{μ–OC(NNCPh$_2$)O}]$_2$ (43), Cp*Ti{MeC(N^{i}Pr)$_2$}{OC(O)N-(NCPh$_2$)C(O)O} (44), Cp*Ti{MeC(N^{i}Pr)$_2$}{OC(NNCPh$_2$)N(Tol)C(NTol)O} (50), Cp*Ti{MeC(N^{i}Pr)$_2$}{N(Tol)C(NNCPh$_2$)S} (51), Cp*Ti{MeC(N^{i}Pr)$_2$}(NNCPh$_2$)-(CNXyl) (54), Cp*Ti{MeC(N^{i}Pr)$_2$}{N(NCPh$_2$)C(Ph)NC(Ph)N} (55), Cp*Ti{MeC-(N^{i}Pr)$_2$}{N(NCPh$_2$)C(Ar^{F5})NC(Ar^{F5})N} (56), Ph$_2$CNNC(Ph)NC(Ar^{F5})NH$_2$ (58). Crystal data collection and processing parameters are given in Table 5.3. Crystals were mounted on glass fibers using perfluoropolyether oil and cooled rapidly in a stream of cold N_2 using an Oxford Cryosystems Cryostream unit. Diffraction data were measured using an Enraf-Nonius KappaCCD diffractometer. As appropriate, absorption and decay corrections were applied to the data and equivalent reflections merged.[13] The structures were solved by direct methods (SIR92[14]) and further refinements and all other crystallographic calculations were performed using the CRYSTALS program suite.[15] Other details of the structure solution and refinements are given in the Supporting Information (CIF data – see CD Appendix). A full listing of atomic coordinates, bond lengths and angles and displacement parameters for all the structures have been deposited at the Cambridge Crystallographic Data Centre. See Notice to Authors, Issue No. 1.

Table 5.3. X-ray data collection and processing parameters for Cp*Ti{MeC(N^{i}Pr)$_2$}(NNCPh$_2$) (**41**), [Cp*Ti{MeC(N^{i}Pr)$_2$}{μ–OC(NNCPh$_2$)O}]$_2$ (**43**), Cp*Ti{MeC(N^{i}Pr)$_2$}{OC(O)N(NCPh$_2$)C(O)O} (**44**), Cp*Ti{MeC(N^{i}Pr)$_2$}{OC(NNCPh$_2$)N(Tol)C(NTol)O} (**50**), Cp*Ti{MeC(N^{i}Pr)$_2$}{N-(Tol)C(NNCPh$_2$)S} (**51**), Cp*Ti{MeC(N^{i}Pr)$_2$}(NNCPh$_2$)(CNXyl) (**54**), Cp*Ti{MeC(N^{i}Pr)$_2$}{N(NCPh$_2$)C(Ph)NC(Ph)N} (**55**), Cp*Ti{MeC-(N^{i}Pr)$_2$}{N(NCPh$_2$)C(Ar^{F5})NC(Ar^{F5})N} (**56**), Ph$_2$CNNC(Ph)NC(Ar^{F5})NH$_2$ (**58**)

compound	**41**	**43**	**44**	**50**
empirical formula	$C_{31}H_{42}N_4Ti$	$C_{64}H_{84}N_8O_4Ti_2$	$C_{33}H_{42}N_4O_4Ti$	$C_{47}H_{56}N_6O_2Ti$
fw	518.60	1125.22	606.62	784.90
temp / K	150	150	150	150
wavelength / Å	0.71073	0.71073	0.71073	0.71073
space group	$P\,2_1/c$	$P\,\bar{1}$	$P\,\bar{1}$	$P\,\bar{1}$
a / Å	15.7689(2)	13.6172(3)	11.8397(2)	10.7744(3)
b / Å	10.77690(10)	14.3551(3)	12.1419(2)	14.5856(3)
c / Å	17.3124(2)	17.5551(5)	12.7836(2)	15.2859(4)
α / deg	90	87.0323(9)	62.0554(8)	108.3510(10)
β / deg	99.4312(5)	76.4322(10)	71.6540(6)	101.0820(10)
γ / deg	90	66.3291(11)	79.2076(6)	107.4010(10)
V / Å^3	2902.30(6)	3051.72(13)	1539.20(5)	2064.07(9)
Z	4	2	2	2
d (calcd) / Mg m^{-3}	1.187	1.224	1.309	1.263
abs coeff / mm^{-1}	0.320	0.314	0.321	0.254
R indices:[a] R_1 =	0.0426	0.0584	0.0428	0.0473
R_w =	0.0454	0.0552	0.0456	0.0468

[a] $R_1 = \Sigma||F_o|-|F_c|| / \Sigma|F_o|$; $R_w = \sqrt{\{\Sigma w(|F_o|-|F_c|)^2 / \Sigma w|F_o|^2\}}$ for data with I > 3σ(I).

Table 5.3. (Contd.)

compound	**51**	**54**	**55**	**56·2.5(C_6H_6)**
empirical formula	$C_{39}H_{49}N_5STi$	$C_{40}H_{51}N_5Ti$	$C_{45}H_{52}N_6Ti$	$C_{45}H_{42}F_{10}N_6Ti\cdot 2.5(C_6H_6)$
fw	667.82	649.78	724.85	1100.03
temp / K	150	150	150	150
wavelength / Å	0.71073	0.71073	0.71073	0.71073
space group	$P\bar{1}$	$P\bar{1}$	$P2_1/c$	$P2_1/c$
a / Å	9.20770(10)	8.88330(10)	11.86670(10)	11.3008(2)
b / Å	12.7388(2)	11.5731(2)	17.2265(2)	14.8259(2)
c / Å	15.9765(3)	18.6169(3)	19.5437(2)	32.7390(5)
α / deg	97.6687(6)	80.5720(7)	90	90
β / deg	95.3211(7)	87.3752(7)	99.6815(6)	96.903(1)
γ / deg	106.6660(8)	73.2082(7)	90	90
V / Å^3	1762.17(5)	1807.59(5)	3938.26(7)	5445.48(15)
Z	2	2	4	4
d (calcd) / Mg m^{-3}	1.259	1.194	1.222	1.342
abs coeff / mm^{-1}	0.337	0.271	0.257	0.236
R indices:[a] R_1 =	0.0457	0.0480	0.0446	0.0938
R_w =	0.0451	0.0468	0.0443	0.0947

[a] $R_1 = \Sigma||F_o|-|F_c|| / \Sigma|F_o|$; $R_w = \sqrt{\{\Sigma w(|F_o|-|F_c|)^2 / \Sigma w|F_o|^2\}}$ for data with $I > 3\sigma(I)$.

Table 5.3. (Contd.)

compound	**58**
empirical formula	$C_{27}H_{17}F_5N_4$
fw	492.45
temp / K	150
wavelength / Å	0.71073
space group	$P\ \bar{1}$
a / Å	6.7619(3)
b / Å	12.6505(6)
c / Å	13.8764(7)
α / deg	72.923(2)
β / deg	87.616(2)
γ / deg	80.321(3)
V / Å^3	1118.49(9)
Z	2
d (calcd) / Mg m^{-3}	1.462
abs coeff / mm^{-1}	0.117
R indices:[a] R_1 =	0.0916
R_w =	0.0623

[a] $R_1 = \Sigma||F_o|-|F_c|| / \Sigma|F_o|$; $R_w = \sqrt{\{\Sigma w(|F_o|-|F_c|)^2 / \Sigma w|F_o|^2\}}$ for data with $I > 2\sigma(I)$.

5.9 References

1. A. B. Pangborn, M. A. Giardello, R. H. Grubbs, R. K. Rosen and F. J. Timmers, *Organometallics*, 1996, 15, 1518.
2. A. E. Guiducci, C. L. Boyd and P. Mountford, *Organometallics*, 2006, 25, 1167.
3. J. D. Selby, D.Phil Thesis, University of Oxford, 2009.
4. J. D. Selby, C. D. Manley, M. Feliz, A. D. Schwarz, E. Clot and P. Mountford, *Chem. Commun.*, 2007, 4937.
5. B.-M. Fung and I. Y. Wei, *J. Am. Chem. Soc.*, 1970, 92, 1497.
6. R. A. Benkeser, H. Landesman and D. J. Foster, *J. Am. Chem. Soc.*, 1952, 74, 648.
7. G. A. Molander and C. P. Corrette, *Organometallics*, 1998, 17, 5504.
8. Y. Obora and M. Tanaka, *J. Organomet. Chem.*, 2000, 595, 1.
9. A. Kunai, T. Ochi, A. Iwata and J. Ohshita, *Chem. Lett.*, 2001, 1228.
10. D. Robert, M. Kondracka and J. Okuda, *Dalton Trans.*, 2008, 2667.
11. Y. Zhang and J. Wen, *J. Fluor. Chem.*, 1990, 47, 533.
12. T. Nishikawa, A. Ino and M. Isobe, *Tetrahedron*, 1994, 50, 1449.
13. Z. Otwinowski and W. Minor, *Processing of X-ray Diffraction Data Collected in Oscillation Mode*, Academic press, New York, 1997.
14. A. Altomare, G. Cascarano, G. Giacovazzo, A. Guagliardi, M. C. Burla, G. Polidori and M. Camalli, *J. Appl. Crystallogr.*, 1994, 27, 435.
15. P. W. Betteridge, J. R. Cooper, R. I. Cooper, K. Prout and D. J. Watkin, *J. Appl. Cryst.*, 2003, 36, 1487.